Intermediate Antenna Modeling
A Hands-On Tutorial

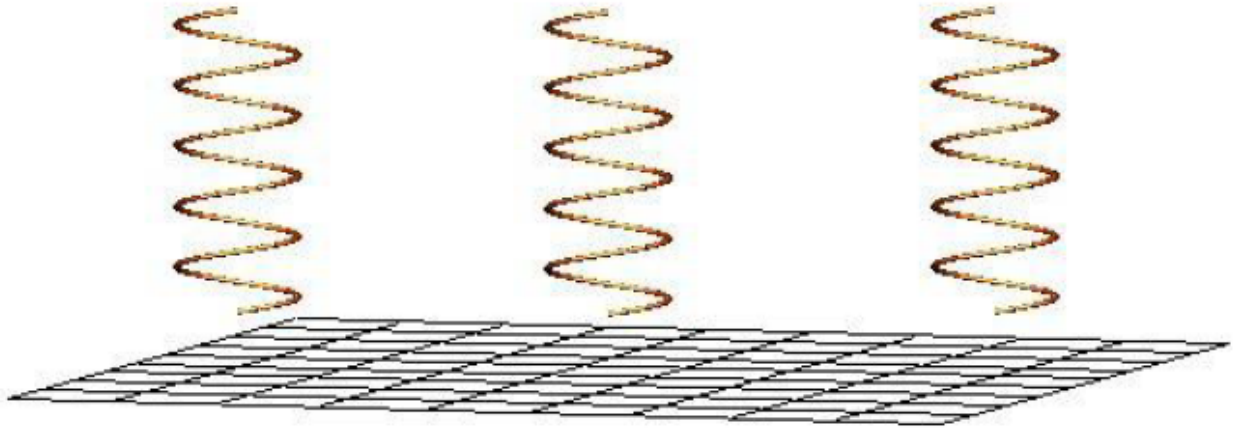

L. B. Cebik

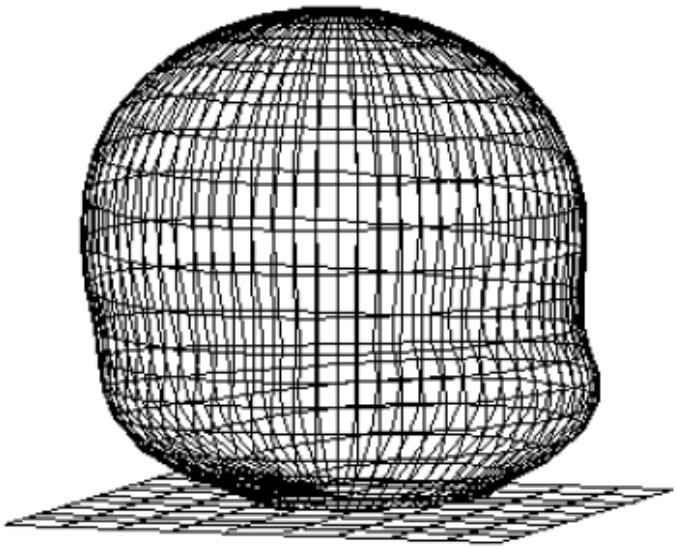

Intermediate Antenna Modeling
A Hands-On Tutorial

L. B. Cebik

Published by
antenneX Online Magazine
http://www.antennex.com/
POB 271229
Corpus Christi, Texas 78427 USA

ISBN: 1-877992-17-8

Dedication

To the memory of my mother, Ella G. Cebik,
who taught me to read avidly and carefully, to think in detail
and deeply, and to serve with honesty and dedication;
indeed, the rarest of moms

Acknowledgments

I would like to thank Joe Finnerty of NSI for his thorough review of a draft of this work. Although he is responsible for innumerable improvements in the volume, I alone am accountable for the remaining shortcomings.

Table of Contents

Important Update & Caveat

Since the initial writing of this book, the Windows OS has gone through several upgrades and thus, the reader should be made aware that any references to Nittany-Scientific, Inc.'s NEC modeling software is known to work up to and including Windows 2000. However, it has issues running under any other new versions of Windows since that version.

It is emphasized that one does not need to use the above-mentioned software as there are other choices on the market and such is further explained in the text of this book.

The reader will find that this book is mainly about the use and application of NEC for antenna modeling and some of the NSI software was used to produce some examples.

This update is written in October 2007 and the plans for any further upgrades of the Nittany-Scientific, Inc.'s software mentioned herein is unclear and doubtful.

Introduction

***Objectives**: In these preliminary notes, you will become familiar with the basic purpose and design of this book on antenna modeling with NEC. You will come to understand why you should go through the exercises carefully with your software as well as reading the principles and techniques portions of each chapter. In addition, you will learn something about the author.*

Antenna modeling with the Numerical Electromagnetics Code (NEC) is well over a quarter century old, but it remains both an art and a science. As a science, it is a craft that requires a thorough understanding of what the computer programs make possible, and as an art, it demands ingenuity born of experience that permits you to overcome some of the program limitations. This guide is designed to advance your understanding of the potentials of NEC beyond the fundamental level covered in *Basic Antenna Modeling: A Hands-On Tutorial*.

At root, NEC employs mathematical algorithms to simulate as closely as possible the performance of antennas, that is, transducers of electrical energy into electromagnetic radiation. In all its forms, NEC is a calculating program using the method of moments supplemented by adjunct algorithms to handle special features of various antenna types. It treats all antenna elements and parts as thin round wires subdivided into many segments. It calculates the mutual impedances among the wire segments, the current on each segment, and (upon call) the near and far fields developed. However, this tiny description only scratches the surface of NEC's capabilities.

NEC has several incarnations. The most common public domain version is NEC-2. It replaced NEC-1 and has itself evolved into NEC-3 and NEC-4, both of which are proprietary programs. All forms of NEC were developed under the leadership of Jerry Burke of the Lawrence Livermore National Laboratory. A similarly named modeling program using different algorithms and initially designed for small desktop personal computers is MININEC, developed by Rockway and Logan.

Modeling in either NEC-2 or NEC-4 is almost identical. Both programs have a FORTRAN origin and allow the use of an ASCII input file that defines both the geometry of the modeled structure and a set of control commands. The control commands subdivide into two types: those that modify the geometry--for example, by loading the structure wires or setting a voltage source on a particular segment--and those that request a specific output, such as a table of near-field values or a table of far-field polar plot values.

Commercial implementations of NEC provide three main adjuncts to the core functions.

1. A good commercial implementation of NEC provides an input interface between the user's antenna design and the formation of a final input file for NEC to process. A good interface will ease the burden of line entry construction by providing a help screen for line data entry, with the line entry following automatically. It may also include ways for transferring a design from a spreadsheet to the input screen. Finally, it may also provide means for simplifying some otherwise complex adjunct functions, such as modeling by equation or setting an indirect current source on a specified wire segment. Additional functions are possible, and some will be sampled

as we proceed.

2. A good commercial implementation of NEC will provide facilities for viewing and testing the antenna structure prior to and after the core performs its calculations (called "running the core"). Checking the geometry of a structure for errors that would either stop the core run or invalidate the results saves considerable time, especially for very large models.

3. A good implementation of NEC provides a variety of output facilities that maximize the modeler's ability to handle and interpret the core output data. The core produces a single massive output file (in keeping with the program's mainframe origins). Commercial implementations may provide specific tabular outputs of part of the data set and change the format for easier reading and use. As well, the implementation can supply a variety of graphical outputs in both polar and rectangular form for easier visualization of the data.

In this volume, we shall use two programs to illustrate the principles of intermediate modeling. Because we shall be surveying the use of almost all of the commands permitted by NEC, we must by-pass the entry-level programs. They tend to use a restricted command set. Even though some may provide alternative means of achieving what NEC allows, they generally do not permit the entry of all commands.

The fullest programs in terms of providing access to all NEC commands are NSI's NEC-Win Pro--for NEC-2 modeling--and GNEC--for both NEC-2 and NEC-4 modeling. In this volume, all exercise models will make use of these programs. We shall have occasion to distinguish between NEC-2 and NEC-4 models, although in many cases, a single model might run on both programs. As well, we shall use the input and output facilities offered by these programs to set up models and view the output.

Although the programs that we shall use to illustrate the provisions of NEC are specific, the principles of modeling involved are perfectly general to NEC. Our goal in this volume is to systematically explore the available commands in NEC in order to facilitate more complex models than we can effectively produce in entry-level programs. Therefore, you may transfer the information to any program that allows the use of NEC's full command structure.

There is one major restriction to this volume. The "intermediate" level of modeling will confine itself to modeling with wires. Surface patches are possible and have numerous applications. However, in order to maintain overall cohesiveness to the chapters and to use models that are capable of clear illustration with the available software, surface patches must await advanced modeling treatment along with many important specialized applications of wire modeling. The need for many exercise models per chapter dictates that we employ simpler models that have multiple applications and allow easy inferences to applications that we do not mention.

The Plan of This Guide

In general, this volume will presume a familiarity with the terms and the fundamentals of modeling with NEC. The first chapter will review some of those fundamentals, but is not a substitute for a certain level of modeling experience that naturalizes the language and parameters of modeling.

Our goal is much more specific: to gain a fundamental mastery of the array of commands of NEC in order to expand our wire-modeling tools. These tools will include both geometry and control commands (as we conventionally divide the full command set). We might also be inclined to subdivide the control commands into those that modify the model geometry and those that request a calculation for an output. However, in surveying the control commands, we shall discover that some modifying and some output commands come in related pairs. Hence, we shall have occasion for some commands to give them a spotlight on their own, while other commands we shall meet in the context of specific information that we wish to derive from a model.

The Overall Plan of the Guide

This guide assumes a broad understanding of antennas as well as knowledge of antenna modeling fundamentals. We shall focus on obtaining a rudimentary mastery of the NEC commands in order to model more effectively. To that end, the volume is divided into 3 parts.

Part A: The Geometry Commands
Part B: Far-Field and General Control Commands
Part C: Special Outputs, Control Commands, and Techniques

Fig. 0-1 illustrates the general division between geometry commands and control commands in a relatively simple model that will run on either NEC-2 or NEC-4. (The model is example *0-1.nec* among the exercise models.)

Part A, on the geometry commands, will open the way to using nearly the full array of geometry commands. This command set allows the modeler to produce compact models of very considerable complexity by allowing the core itself to parse the command and create the required model structure. We shall discover that these commands permit a level of versatility that we may not be able to achieve by creating models such that each straight section requires the entry of an additional wire. At the same time, we shall recognize that being able to compress a model into a small entry file requires exceptional care. The more compact a model, the higher the level of vigilance that we must maintain to ensure that the model is sound and free of error. Hence, we shall stress the use of the "model-adequacy" tests that are built into the core and those made available by the program as important adjunct functions.

Part B bears the general title "far-field and general control commands." In one sense, the division between "general" and "special" control commands is arbitrary. What is special to one modeler is an everyday application to another. For our purposes, the division is functional. Fundamental control commands include the commands that modify a model, such as adding loads, transmission lines, and networks. It also includes commands for outputs that employ the simplest type of source (or excitation). Hence, throughout the chapters devoted to general commands, we shall be interested in far-field outputs, along with related data outputs. (The term "output" simply means the product of NEC calculations. However, we may view these outputs on occasion without looking at the NEC output file itself, using instead the graphical facilities of the programs.)

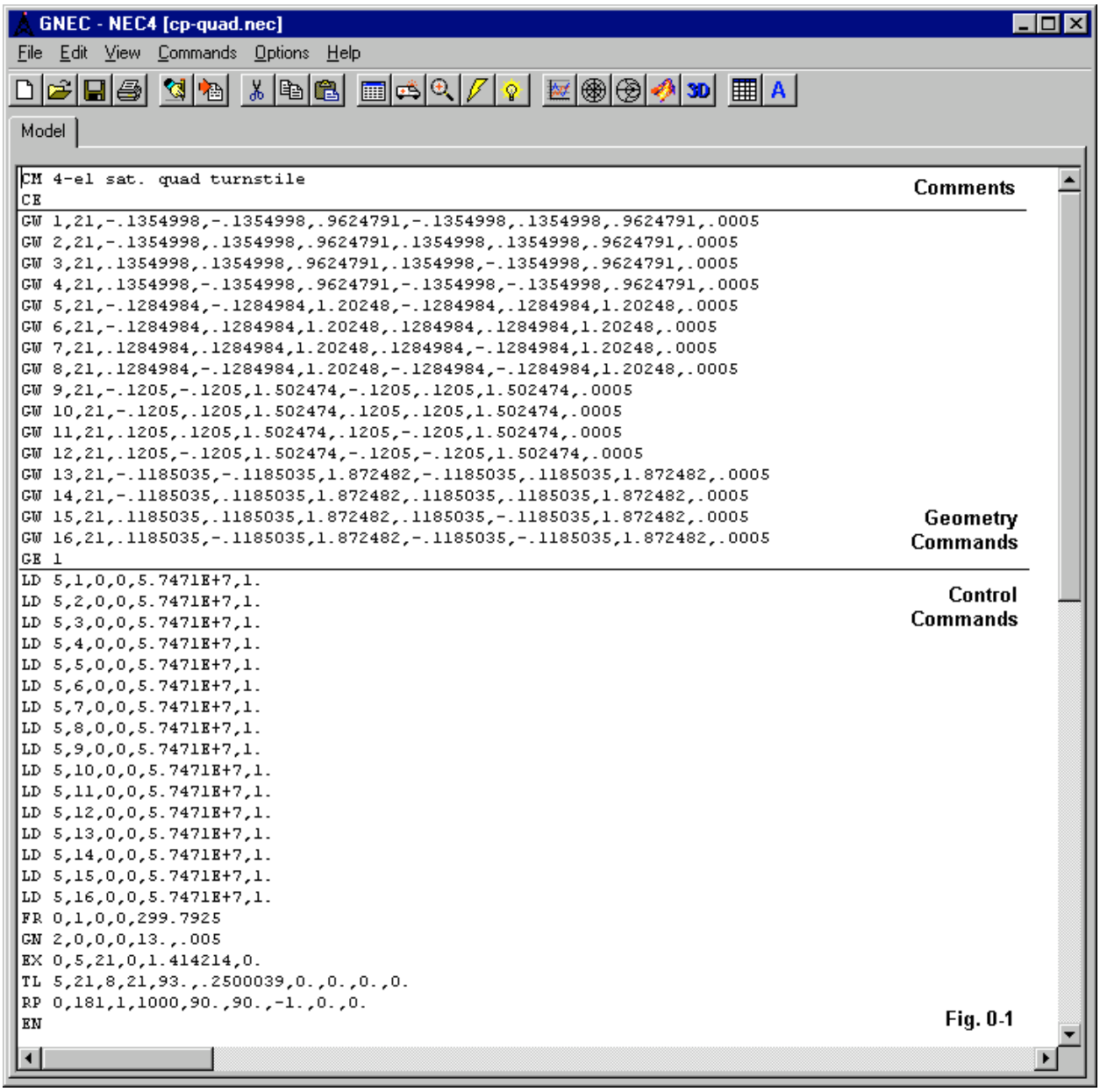

Part C deals with two main types of special commands. One type tends to match excitation sources with certain desired outputs. For example, plane wave excitation generally pairs with receiving and scattering outputs. In addition, there are special outputs for which a standard voltage source is applicable, such as near field and ground wave analysis. As a further complication, there are a number of commands that are unique to either NEC-2 or to NEC-4. We shall explore some of those commands in two ways. First, in some cases, there may be NEC-2 work-arounds for a command unique to NEC-4, for example, the insulated sheath command. Second, we shall want to appreciate the capabilities and the limitations of some of the unique commands, and to understand why the command does not appear in the list for the other core.

In *Basic Antenna Modeling*, I divided each major part into 7 chapters, each focused on an

interrelated cluster of basic or advanced techniques and concepts. Each chapter built upon the preceding one in a graded learning curve. Necessarily, this volume differs. In order to examine as fully as possible the full span of NEC commands, we shall bounce between fundamental and advanced aspects of modeling, as we usually view them after considerable experience. Nevertheless, we shall follow many of the same principles within each chapter of this volume that proved useful in the basic text.

The Plan of Each Chapter

Each chapter is typically subdivided in the following manner (with exceptions for early background information and some late specialized chapters). After a statement of goals, the chapter provides background information on the focal subject. For each major item in the chapter, there is at least one modeling example. The model will appear both in the text and in the collection of exercise models accompanying the volume.

The extensive exercises that model actual antennas are key to the volume. All but a few models will be in .NEC (ASCII) format. There are some special topics that will require the use of formats unique to NSI products. Most of these antennas will be specific to the commands under study and may or may not be suited to physical implementation. All models (except where specifically noted) are contained on the CDROM that accompanies this guide. Since many of the exercises may request the modeler to modify and possibly save the model under a revised name, it is wise to transfer the entire set of exercise models into a file on the hard drive. For ease of location, all models are keyed to the chapters of the guide. For example, the models for chapter 6 have filenames of the form "6-x.NEC," where x is the sequential number of the model in the chapter progression. Because an exercise may involve a sequence of only slightly modified models, expect to find model with suffixes, for example, 6-4a.nec. As well, where we require separate models for each core, the model will add "-nec2" or "-nec4" to the file name.

For each exercise involving a model, the chapter will provide relevant commentary for both the input and output to which the user is directed. Because so many of the antennas are very common, not all will be pictured. The user may always employ the viewing function of the program (Necvu) to examine the configuration of any antenna used as in the exercises. Each chapter closes with a summary of the essential concepts and guidelines developed along the way.

A Note on the Antenna Models Used in this Guide

The basic volume employed classic antenna designs used in amateur and commercial circles in order not only to illustrate the principles of modeling, but as well, to increase the modeler's knowledge of available designs. Because the goal of this volume differs from the basic volume, we shall use a different approach to antennas. The array of modeled antennas will cover a more restricted territory, but will use wherever feasible a common frequency: 299.7925 MHz, where 1 meter = 1 λ. As well, with significant exceptions, we shall provide dimensions in metric form. Using a common base for most of the models will let us focus upon the commands and their uses.

To expand your background of antenna possibilities, there are several sources that you may consult. Compendiums of antenna designs for all frequencies, such as Rothammel's *Antennenbuch* and *The ARRL Antenna Book*, are readily available at reasonable prices. At a

more advanced level, Johnson's *Antenna Engineering Handbook* is an invaluable reference. In addition, a basic college antenna text, such as Kraus, Balanis, or Stutzman and Thiele, is a useful addition to the bookshelf. For some ideas, it may be necessary to consult older texts, such as Laport and Schelkunoff. For matters relating to transmission lines (at differing levels), Kuecken and King may be as useful as more recent texts. Of course, your own main modeling goals may dictate variations in this overly general list, as well as unlimited additions. The nature of our task in this volume will not permit much time or space to pause for antenna fundamentals.

Using This Guide

Like the basic volume, this tutorial is usable by design either as a self-study guide or within a classroom context. Each context opens different possibilities and places different responsibilities on the user.

Using This Guide as a Self-Study Tutorial

The materials in this guide have been structured carefully to develop your skill in modeling. Proceeding step-by-step in order through the chapters and their exercises is in most cases very important to deriving maximum benefit from the work you put into this effort. Although it may be tempting to jump ahead to a problem area in which you may already have an interest, skipping the early chapters can lead to pitfalls, most notably, unreliable models that give misleading results.

A collateral temptation will be to simply skip around, using the volume and its exercise models as reference materials when a particular modeling task calls for a review. This use is certainly valid, but only after working through the volume in the order of presentation. Surveying all of the program possibilities gives you two benefits. One is to provide an overall sense of how the program does its work, which in turn improves your "intuitions" on how to proceed with a special task. The second benefit is to give your long-term memory the full list of NEC commands so that you do not overlook the ones useful to the special task.

This guide can help you develop a good understanding of modeling, but it is not itself a software instruction manual. You will want to have studied the user's manual and worked through a number of the program's sample models before embarking on these exercises. Thoroughly familiarize yourself with how to implement each feature of the program. Keep the user's manual handy for reference along the way. Although the instruction sets for the exercises are keyed to NEC-Win Pro and to GNEC, they do not include detailed instructions regarding the necessary keyboard or mouse operations involved.

If you are using another NEC-2 or NEC-4 software package, you will need to perform another set of tasks in addition to becoming acquainted with how to implement program features. You may need to rewrite the models provided on disk to suit the input requirements of your program. Most advanced packages will provide file-format conversion routines or directly handle .NEC-format files. However, even alternative NEC-4 programs may not be able to convert all of the NEC commands. There may be extensive alternatives for creating the model geometry, but many of the control commands will be absent. Additionally, different software packages may use slightly different values for various constants, including material conductivity and the exact speed of

electro-magnetic radiation.

One final word of caution: different implementations of NEC may yield slightly different numerical results than those you may find on these pages. There may be--especially for models with complex geometric features, differences between NEC-2 and NEC-4 results. In such cases, the NEC-4 results are generally considered the more accurate, although most common antenna types will yield results that differ only insignificantly. Second, different software vendors may use different compilers to convert the original FORTRAN core to PC compatibility and to speed calculations. Again, the differences should be insignificant. Third, there are single-precision and double-precision versions of both cores, with the double-precision core yielding more accurate results, but at the expense of speed. As PCs passed the 1-GHz speed mark, run-time differentials lost their importance for all but the largest models, and precision differentials tend to affect only the most critical modeling situations. Finally, different CPUs may produce very tiny differences in the reported output. Despite the insignificance of the differences in each case, your model run may yield very slightly different numbers than the runs shown in the sample tables. Before concluding that there is an error in the text, analyze the degree of difference to see if it is significant.

Using This Guide in the Classroom

For ease of instruction, this guide is best studied in conjunction with the software used in its development, NEC-Win Pro and/or GNEC. Although other software might be used, significant losses in classroom instruction time may occur, due to continuing questions concerning translating models and instruction sets into the operative procedures used with alternative software.

The chief goals of this volume include bringing together in one place a large, but certainly not exhaustive, collection of practical information on wire modeling with NEC. Moreover, the volume aims to set forth the information and exercises in a progressive development of user understanding, both within chapters and within the guide as a whole. Within the compass of these goals, there remains yet a large potential for customizing the work of a course utilizing these materials. Minimally, any techniques omitted from this manual make very important instructor-based additions to any course.

The chapters comprising this guide offer considerable flexibility in the progression of an introductory course on antenna modeling. There are more chapters than would fit either a 10-week quarter or a 15-week semester, unless multiple classes occur each week. However, for more advanced classes, portions of this guide may be assigned as groups of chapters. Variations on this theme are almost endless, according to the goals and level of the class. In any event, I do not recommend combining the basic volume and this volume into one course.

The background material reported in each chapter by no means exhausts either the theoretical considerations underlying NEC or the practical considerations affecting techniques of modeling. Instead, the background material is designed to focus the student's attention on the relevant considerations for the exercises. There is appreciable room for the instructor to bring additional information to the treatment, information that arises out of the specific goals of a course and out of the instructor's experiences.

Likewise, the graded exercises do not preclude the development of further modeling tasks designed to enlarge either the breadth or the depth of student understanding. Indeed, the assignment of additional variants on the exercises, including more advanced and complex problems of the types on which the chapters focus, is highly recommended. Such problems can minimally increase student abilities in modeling "from scratch," rather than simply modifying supplied models.

Use of this tutorial as a practice-intensive course text is only one of its possibilities. Another is letting it serve in conjunction with other texts on method-of-moments modeling so that the guide and the software become an extended example of the real-world implementation of the fundamental principles and concepts. Alternatively, the guide and the software may be used as adjuncts to, or laboratory materials for, courses on basic antenna principles. The addition of instructor-supplied models to those in the guide is essential in either case.

Although variations on the application of this guide are nearly endless, the work itself may serve in a relatively self-sufficient way to guide students in developing their skills on the road to mastering the craft of antenna modeling.

About the Author

L. B. Cebik

L. B. Cebik retired in 1999 from the University of Tennessee, Knoxville, as professor of philosophy with special interests in formal logic. In addition, he had served the University in past years as Assistant Dean for Research and as Director of Research Compliances. His interests in radio frequency communications arose out of his amateur radio experiences as W1APS, W0JGG, and now W4RNL. He has been a student of electronics and antennas for some 50 years and a teacher for almost 40 years. His writings include about 2 dozen books and over 500 articles and reviews.

Cebik has tested and used almost all of the commercial implementations of NEC and MININEC over the past two decades. In addition, he has written extensively about antennas and antenna modeling at both basic and more advanced levels for many U.S. publications. His writings have included tutorial articles for electronics teachers and regular columns for several publications on various aspects of antenna fundamentals. He also maintains a web site with considerable material from his notebooks (URL: http://www.cebik.com).

Part A
The Geometry Commands

1. The Structure Geometry Input Entries or "Cards:"

Command	*Command Name*	*Notes*
CM, CE	Comment Cards	Not geometry entries
GC	Continuation Data for Tapered Wires	Form differs between NEC-2/NEC-4
CW	Catenary Wire	NEC-4 only
GA	Wire Arc Specification	
GE	End Geometry Input	Form differs between NEC-2/NEC-4
GF	Read Num. Greens Function	
GH	Helix-Spiral Specification	Form differs between NEC-2/NEC-4
GM	Coordinate Transformation	Form differs between NEC-2/NEC-4
GR	Generate Cylindrical Structure	
GS	Scale Structure Dimensions	Form differs between NEC-2/NEC-4
GW	Wire Specification	
GX	Reflection in Coordinate Planes	
SP, SM, SC	Surface Patch(es)	Not covered in this volume

2. The Plan:

Our approach to intermediate wire modeling begins with a review of the parameters and limitations of wire modeling in NEC-2 and NEC-4. The general format of model input files, with the general subdivision of comments, structure geometry commands, and model control commands is common to both cores. Equally common are many of the basic good-modeling practices and practices to avoid. Sources, loads, transmission lines are also common to both cores. The cores differ in the ability to handle subterranean wires and linear tapered-diameter elements. The convergence and average gain tests are applicable to all NEC models. The first chapter partially summarizes information provided in greater detail in *Basic Antenna Modeling: A Hands-On Tutorial*.

The next step in the process involves basic geometry entries, beginning with an understanding of segments, wires, and tags. Geometry entries permit the use of any unit of measure, with the GS command available for scaling to meters, the basic NEC core unit of calculation. However, for many applications, we have alternatives for repetitious entries: separate GW entries or replication via the GM or coordinate transformation command. Using the GM command wisely usually takes some practice. Special wire structure shapes deserves special attention. NEC contains a GW wire continuation card (GC) that allows you to taper either the segment lengths or the wire radius (or both) in multiple ways. A NEC-4-only feature is CW, the catenary wire command to account for wire sag. GA allows you to form wire arcs or circles. What all these commands have in common is that they define the collection of straight segments that simulate a complex shape under a single tag number.

Both NEC-2 and NEC-4 offer commands to form helices and spirals, although NEC-2's GH

command arose as an unofficial addition to the geometry command set. Its format differs quite radically from the NEC-4 version, which reduces some possibilities in order to open others. Unlike the slight variations in commands like GS and GE that let NEC-4 read the NEC-2 version, GH is core specific.

When PC speeds only dreamt of the 100-MHz mark, modelers exploited the possibilities of symmetry to speed the core run times. With current PC speeds exceeding 2 GHz, modelers use the symmetry potentials built into the GX (axis-based) and GR (rotation-based) commands sparingly for the very largest models. Nevertheless, both types of command are worth understanding to allow you to tap into their potentials and to remain within their limitations.

As models attempt to capture ever more complex shapes, we have several options. Curvilinear and irregular shapes often benefit from the use of external geometry synthesizers, although they result in long model descriptions. We may economically capture many regular shapes with simple GM-based models. For complex shapes that require repetitive use, Numerical Green's Functions offer the advantage of saving the matrix calculations to a file (WG) and then recalling the data in a model with additional features (GF).

Finding flaws in the geometry of a model that we have established is as important as creating the entries. Both the cores themselves and the implementing software offer a number of tools for uncovering geometry problems. However, many difficulties--both great and subtle--may require the assistance of the average gain and convergence tests, although these necessary but not sufficient conditions of model adequacy have limitations of their own.

All of the geometry commands appear in a group within the user sections of both the NEC-2 and the NEC-4 manuals. These sections outline the command structure and the meaning of each entry within the command line. What we shall seek is a bit more than the entry meanings. We shall strive for a sufficient understanding of the commands so that we can use them wisely and well. Most of the commands have pitfalls, whether it is the difference between NEC-2 and NEC-4 versions or simple limitations as to what it makes sense to enter. As well, many modelers have limited views of the potentials offered by the commands. At the intermediate level, we cannot hope to master every possibility, but we can make strides in that direction.

1.
A Review of NEC Fundamentals and Limitations

***Objectives**: In this chapter, you will review in a very compressed way the fundamental aspects of NEC models. The exercises will proceed from basic modeling formats and conventions to an enumeration of necessary and recommended modeling procedures. As well, you will review NEC limitations for both NEC-2 and NEC-4 and review basic tests of model adequacy.*

Although it is not possible to compress all of the contents of *Basic Antenna Modeling: A Hands-On* Tutorial in a single chapter, we can review some of the most salient points of modeling in both NEC-2 and NEC-4. In this chapter, the points covered have particular relevance to NEC-Win Pro and GNEC, which use as defaults the basic units in which NEC operates. The programs offer enhanced input and output facilities to ease the process of developing a model and interpreting the output data. However, the core itself tends to determine what counts as fundamental to these programs and what counts as a user enhancement.

The Numerical Electromagnetics Code (NEC) is an outgrowth of a program developed in the 1970s, called the Antenna Modeling Program (AMP). There are at least 4 versions of NEC, with NEC-2 emerging in 1981 and NEC-4 appearing in 1992. NEC-2 is the highest version of the code under public domain. NEC-4 remains proprietary with the Lawrence Livermore National Laboratory and the University of California. It requires a separate license for use, along with the cost of any user interface selected.

NEC in all its forms is a computer code for the analysis of the electromagnetic response of antennas and other metal structures that uses method-of-moments techniques for the numerical solution to integral equations for the currents induced on an antenna structure by sources or by incident fields. The approach has no theoretical limit and may be used for very large arrays or for the very fine subdivision of smaller arrays. However, the matrices involved grow very large very fast, and thus may exceed the capabilities of a given computer.

In fact, NEC was originally developed in FORTRAN for use on large mainframe computers. An alternative method-of-moments program called MININEC emerged of which version 3.13 is the latest public domain level. MININEC was developed specifically to run on small desktop PCs and used compiled BASIC as its language. Limited by early memory constraints and by a slow running pace, the program placed many of the facets of NEC modeling in the hands of a wide range of both amateur and professional antenna designers and analysts.

The increased speed and memory of modern PCs, along with the development of FORTRAN compilers for the PC environment and the release of NEC-2 from security controls, made the higher capabilities of NEC-2 accessible to the desktop computer. Because NEC-2 was itself limited to a rigorous FORTRAN-style input set of "cards," and because the outputs were wholly tabular, several software developers have incorporated NEC-2 (often modified) into a more complete computing environment. On the input side, developers created methods of easing the

burden of entering the data for the antenna structure and other parameters of its operating environment. Fewer inputting errors produced more reliable models more quickly and also permitted more rapid model revision for antenna design development.

The output side saw the conversion of tabular data into a host of graphical outputs that enhanced the interpretation of results. These have included polar plots for far fields, as well as a number of rectangular plots that track such data as gain across a span of radial directions from the antenna or that chart source impedance or SWR across frequency spans. Antenna currents and other data that varies along the antenna structure can be plotted graphically on a representation of the antenna itself.

Model Formats

In the Introduction, we noted two facets of NEC models. First, the basic model uses a simple ASCII or text-only structure. Second, the model stores in a file using the .NEC extension. Hence, one can construct NEC models using any text editor, such as MS Notepad, or even a spreadsheet. Open model *1-1.nec*, which I have reproduced below. (One advantage of the ASCII format is that we can simply insert a model into the text without necessary reference to a graphic. All models and lines extracted from models will use Courier print to distinguish models from the running text.)

```
CM Yagi, 3-el, 6.35 mm (1/4") dia
CM Space separators
CE
GW 1 31 0. -.2434 2. 0. .2434 2. .003175
GW 2 31 .1763 -.2308 2. .1763 .2308 2. .003175
GW 3 31 .3471 -.2134 2. .3471 .2134 2. .003175
GE 1 0 0
FR 0 1 0 0 299.7925 0
GN 2 0 0 0 13.0000 0.0050
EX 0 2 16 0 1. 0.
RP 0 1 361 1000 83 0 1.00000 1.00000 0.
RP 0 181 1 1000 -90 0 1.00000 1.00000 0.
EN
```

Our initial interest in the model is the format of each line. Each line is a separate command. Lines CM through CE are comments. The NEC output report will record these lines, but will not try to parse them or to perform calculations on them. The lines immediately following, through the GE or "End Geometry" command, define the physical structure of the antenna. In this model, we have 3 wires that define a standard Yagi array. Control commands follow and include a frequency specification, a ground specification, an excitation or source specification, and a pair of requests for far-field outputs. EN terminates NEC calculations.

Each line consists of a command identifier followed by a number of numerical entries. A typical command uses up to 4 integer entries, followed by up to 7 floating point entries in NEC-2 and by more in some NEC-4 commands. Perhaps the most basic separator for each entry in the line is a single space. In some cores, added spaces may be treated as zero-entries and result in an error report that a line has too many entries.

NEC-Win Pro and GNEC offer some flexibility for line entries. Compare the GW entries for models *1-1.nec*, *1-1a.nec*, and *1-1b.nec*. Here are the relevant lines.

1-1.nec:
```
GW 1 31 0. -.2434 2. 0. .2434 2. .003175
GW 2 31 .1763 -.2308 2. .1763 .2308 2. .003175
GW 3 31 .3471 -.2134 2. .3471 .2134 2. .003175
```

1-1a.nec
```
GW 1,31,0.,-.2434,2.,0.,.2434,2.,.003175
GW 2,31,.1763,-.2308,2.,.1763,.2308,2.,.003175
GW 3,31,.3471,-.2134,2.,.3471,.2134,2.,.003175
```

1-1b.nec
```
GW 1  31 0.    -.2434   2. 0.    .2434 2. .003175
GW 2  31 .1763 -.2308   2. .1763 .2308 2. .003175
GW 3  31 .3471 -.2134   2. .3471 .2134 2. .003175
```

You may run each model to confirm that all three are the same model, despite the variation in the entry format for each set of 3 wires. In virtually all cores, the comma is equivalent to a space. In the NSI implementations, a tab is also read as a separator, thus easing the transfer of models initially constructed on a spreadsheet into the NEC environment.

The core interprets the difference between the decimal and a separator in terms of U.S. conventions. A decimal is a period (.), while a comma (,) is always a separator.

Some Modeling Conventions

NEC modeling uses scientific and engineering conventions and notations. Hence, you should expect to see some data entries in the NEC output file that express a value as 2.53E03 rather than 2530 or as 6.7245E-02 rather than 0.067245. In some cases, in answer to user requests, the NSI software output tables will convert engineering notation values into more common decimal forms. One prominent example is the report of the source resistance, reactance, magnitude, phase, and any associate VSWR value.

You will construct model wires using Cartesian conventions, outlined in **Fig. 1-1**. Whether you specify free-space (no ground) or one of the ground simulations, the X- and Y-axes are parallel to a presumed flat earth surface. +/-Z records the vertical dimension. In free space, you may use both positive and negative values of Z. With a specified ground, NEC-2 does not permit negative values of Z. However, NEC-4 does permit you to place wires below the ground surface. Note that model *1-1.nec* places the Yagi wires 2 m above ground.

The model also extends the element wires along the +/-Y-axis, with a presumed boom extending along the X-axis. In correlating the model input file to output conventions, the X-axis aligns with a heading of zero degrees on a polar plot. You may offset the model in the X or Y directions with no change of output plot when using free space or a single ground surface. However, if you use multiple ground specifications, the plot may vary according to the antenna position over the inner ground. As well, certain other outputs, for example, near field data, may use coordinates

measured from the coordinate center or origin, and hence, antenna position may become important.

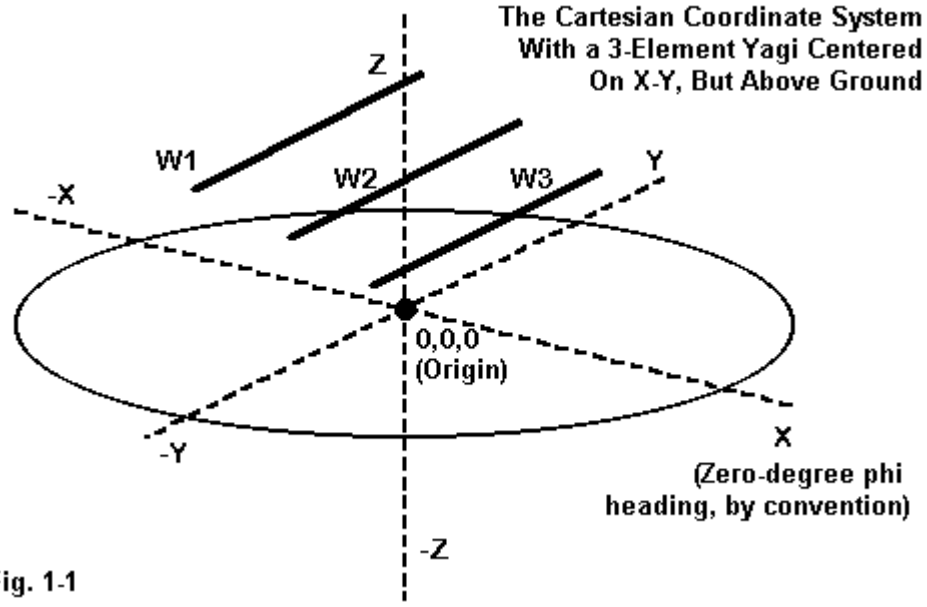

Fig. 1-1

Fig. 1-2 shows the corresponding conventions used by the output data. Inside each circle are the theta (Θ) and phi (Φ) conventions used by the NEC core. Theta counts degrees from the zenith downward toward the horizon. Phi counts degrees in a counterclockwise direction from a starting point that by convention coincides with the +X Cartesian coordinate system. Many field engineers and radio amateurs are more accustomed to using azimuth and elevation as reference systems.

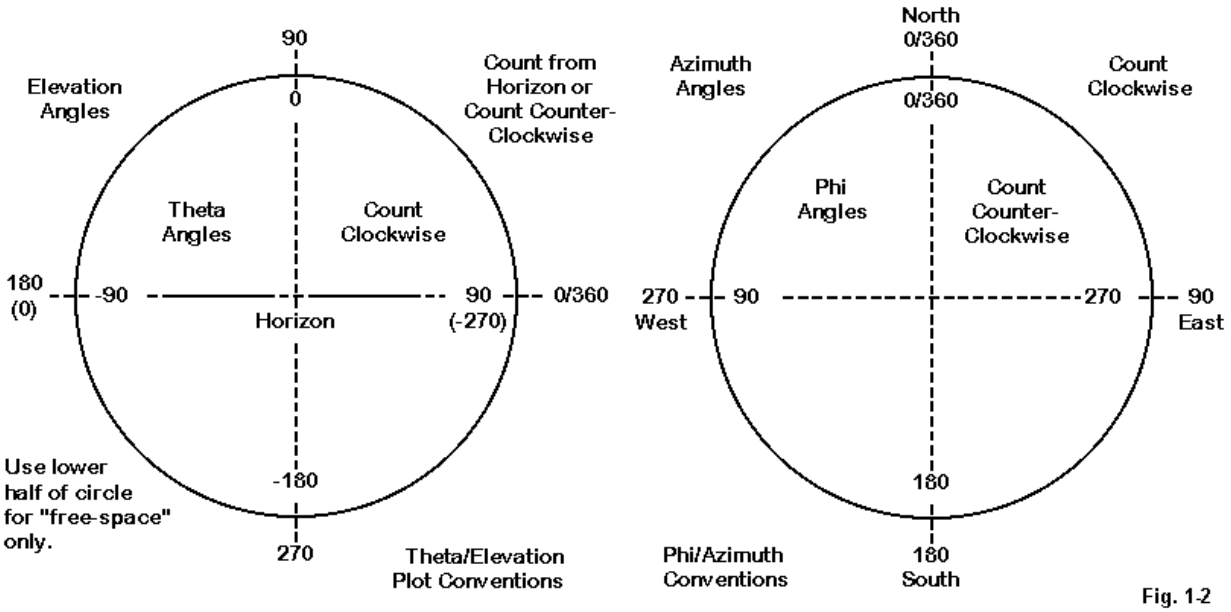

Fig. 1-2

The outside information on the circles in **Fig. 1-2** records the corresponding elevation and azimuth conventions. Elevation counts from the horizon upward, while azimuth counts on a compass rose, that is, in a clockwise direction. NSI polar plots permit either orientation. **Fig. 1-3** shows corresponding theta and elevation plots for the Yagi in model *1-1.nec*. The conversion between theta and elevation angles is simply one form subtracted from 90 degrees. However, as the plots reveal, there are multiple ways of handling elevation angles that pass the zenith or 90° point.

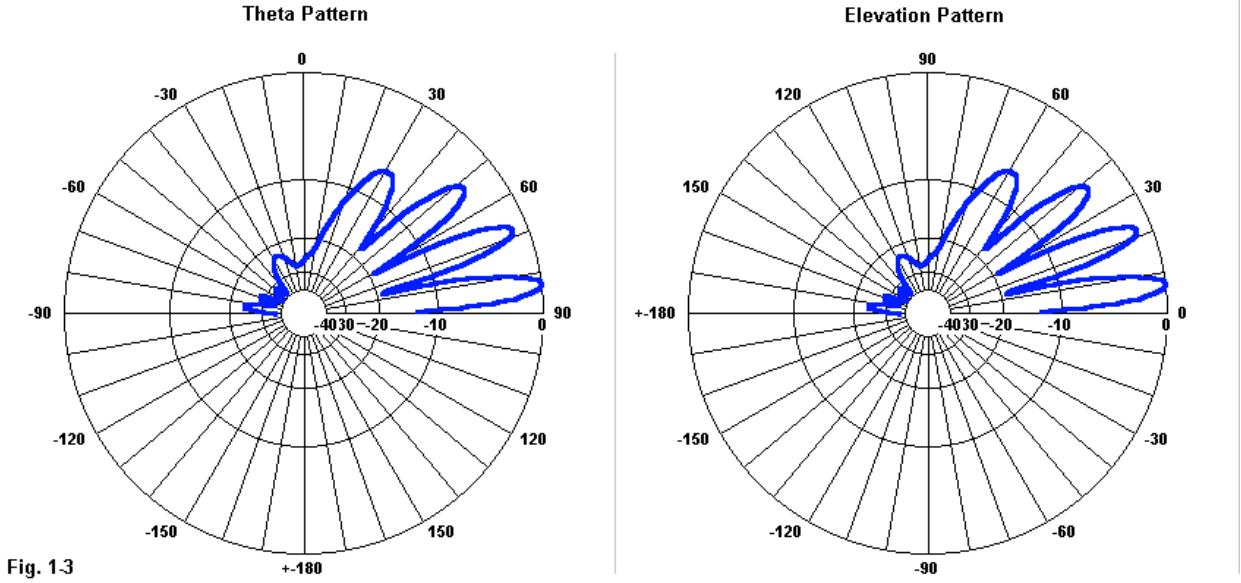

Fig. 1-3

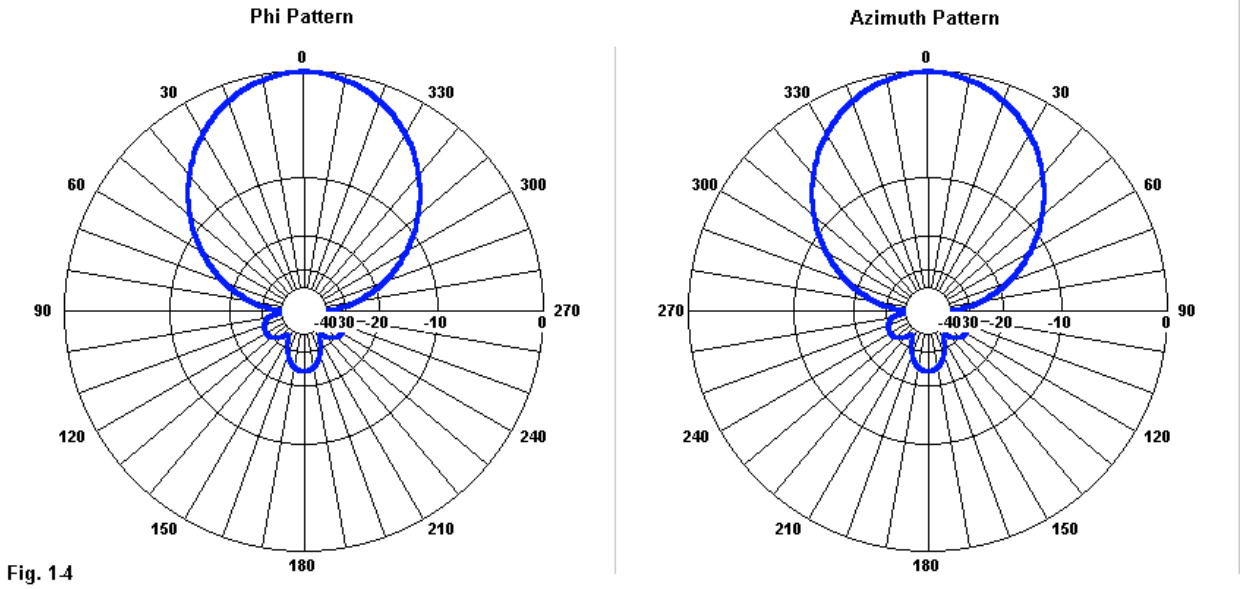

Fig. 1-4

Fig. 1-4 shows corresponding phi and azimuth plots. At present, azimuth plots simply alter the outer ring labels without altering the plot itself. Open model *1-1d.nec* and run it to obtain phi and azimuth patterns. Since the boom is now aligned with the Y-axis, with elements extended in the

+/-X direction, the main pattern lobe on a phi plot will correctly point to 90°. However, the corresponding azimuth plot will point toward 270°.

The sample plots shown so far are "normalized" to set the outer ring at maximum gain. All other plot values appear as reductions from the normalized value. As well, the plots use a "log" scale of gain values. **Fig. 1-5** shows the same values recorded on both a log and a linear scale of gain values. For specific purposes, you may wish to use one or the other option. A log scale generally requires no user selection of the minimum gain value on the plot. However, a linear scale requires careful selection of the maximum and minimum values depending on the pattern detail you wish to enhance without distortion.

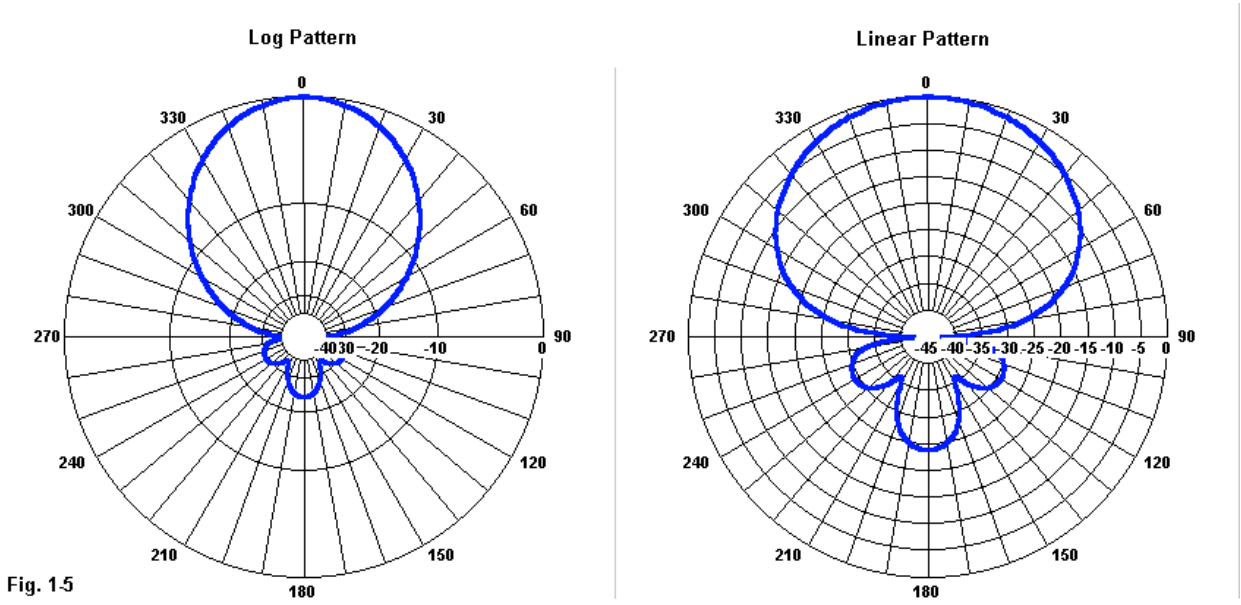

Fig. 1-5

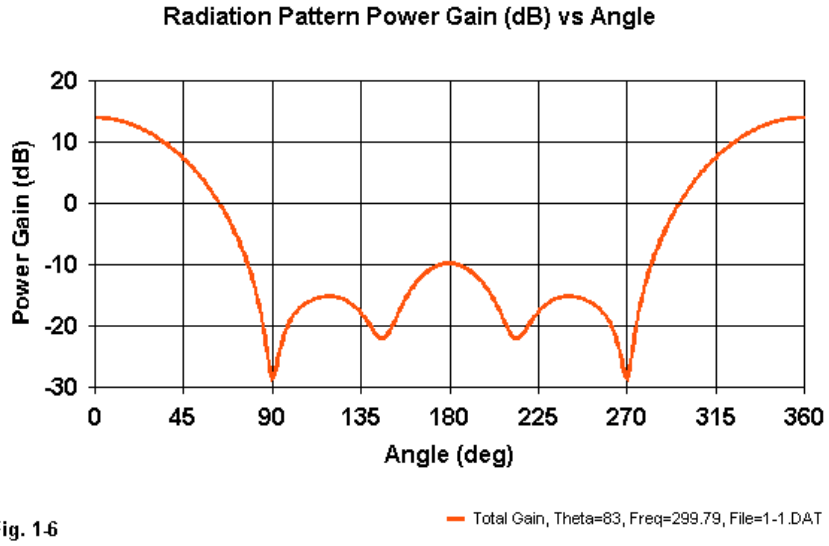

Fig. 1-6

Fig. 1-6 provides a further alternative means to displaying far-field patterns using a rectangular plot of the data. The plot is not normalized and uses a linear Y-axis. Once more, the careful selection of maximum and minimum values is crucial to the fair presentation of the data.

Some Modeling Dos and Don'ts

Both NEC-2 and NEC-4 employ method-of-moments techniques to straight round wires that we subdivide into segments. As a result, there are some rigorous limits to the structure of an adequate model. As well, NEC operates in an environment equivalent to a vacuum or dry air (with one NEC-4 exception). Hence, NEC may not be the best vehicle for modeling wide, thin strip antennas attached to a substrate. Even within the limits of the NEC environment, there are necessary steps, forbidden steps, and recommended steps that you must take to produce an adequate model. In some cases, the transition from definite adequacy to definite inadequacy is not abrupt, which results in some recommended rather than mandated practices.

Those interested in the full background for the modeling dos and don'ts that we shall explore should consult the appropriate manuals for the core used. The NEC-2 manuals are available in 3 volumes in .PDF format and are available at no cost from "The (Unofficial) NEC Archives" web site at http://www.qsl.net/wb6tpu/swindex.html. Although all 3 volumes are useful, perhaps Part 1, which covers the theory behind the NEC-2 core and Part 3, which provides a User's Guide are the more important ones. NEC-4 users will receive a manual containing a user's guide and a theory section when they obtain their licenses. NEC-Win Pro includes the user's guide for NEC-2 in its software manual, while GNEC contains the NEC-4 user's guide. Since GNEC includes both NEC-4 and NEC-2 cores, having the NEC-2 User's guide portion of the manual set will be instructive where commands differ between the 2 cores.

All NEC modeling begins with the straight wire, which the modeler subdivides into segments, as shown in **Fig. 1-7**. All shapes, no matter the curves involved, require synthesis from straight wires or wire segments. Within limits, the shorter the individual wire segment, the more accurately a set of such wires will approximate a curved surface. For most modeling, wires having a voltage source should contain an odd number of segments, especially if the source needs to be centered on the wire. In addition, for greatest accuracy, the source wire should have at least 3 segments so that there are equal-length segments on each side of the source segment. This practice ensures appropriate current levels on each side of the source segment.

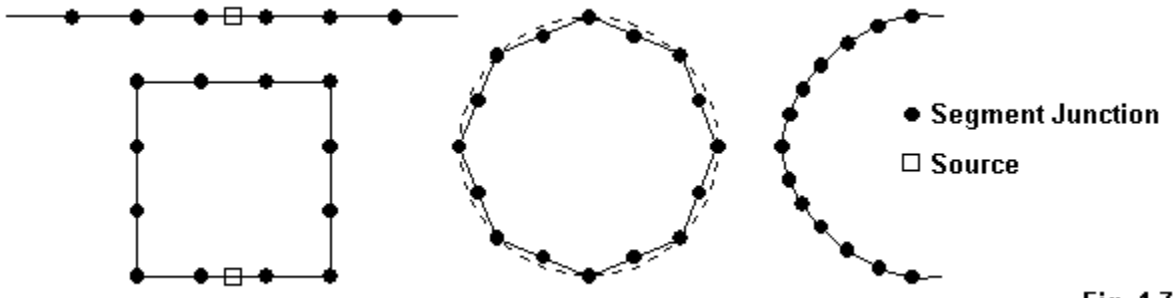

Fig. 1-7

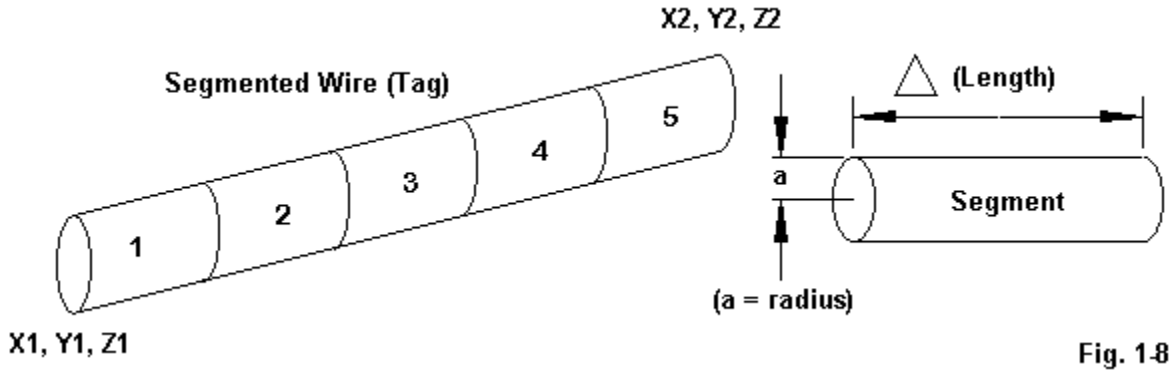

Fig. 1-8

The basic unit within NEC is the segment, which would be any one of the segments marked on the left portion of **Fig. 1-8**. The overall structure of the element shown forms a wire. However, a wire is simply a handy method--external to NEC--for developing and tracking a model's geometry. For beginning modeler's using only a limited number of the NEC geometry commands, keeping track of each new GW entry as a separate wire is exceptionally useful. However, internally, NEC assigns tag numbers that the user specifies within each geometry entry. Tag numbers and the wire numbers assigned by a modeler to a preliminary sketch need not coincide. Indeed, you may assign the same tag number to all of the wires that it might require to synthesize any of the shapes shown in **Fig. 1-7**. We shall grow better acquainted with the wire vs. tag situation as we involve ourselves in the details of the geometry commands.

Segments have both upper and lower limits. At the lower end of the spectrum, Δ (the segment length) should always be greater than $10^{-4}\lambda$. The wire radius, a, should be small relative to both λ and Δ. In general, try to let $a<0.5\Delta$ and $a<0.1\lambda$. At the upper end, there are no rigid rules. However, for greatest accuracy in most cases, Δ should be $<0.1\lambda$, that is, you should use at least 10 segments per λ. In critical regions of complex shapes, $\Delta<0.05\lambda$, that is, use about 20 segments per λ. On very long straight wires, the practical limit for Δ is about 0.2λ or 5 segments per wavelength. (Note: some programs or program facilities may input diameter, which converts to a radius for the core run. The NEC-Win Plus insert in both NEC-Win Pro and GNEC is such a facility.)

Segmentation does make a difference to output accuracy. Open and compare models *1-2.nec* and *1-2a.nec*. Both models are simple dipoles in free space using a lossless wire with a 1-mm radius. Both models place the voltage source at the wire's center segment and request a simple phi (azimuth) pattern. Of course, in free space, an azimuth pattern is actually an E-plane pattern for the dipole in question.

Model 1-2.nec

```
CM Dipole in free space
CE
GW 1 11 0 -.2375 0 0 .2375 0 .001
GE 0 -1 0
EX 0 1 6 0 1 0
FR 0 1 0 0 299.7925 1
RP 0 1 361 1000 90 0 1.00000 1.00000
EN
```

```
Model 1-2a.nec
CM Dipole in free space
CE
GW 1 3 0 -.2375 0 0 .2375 0 .001
GE 0 -1 0
EX 0 1 2 0 1 0
FR 0 1 0 0 299.7925 1
RP 0 1 361 1000 90 0 1.00000 1.00000
EN
```

The two models clearly show the segmentation in the second numerical entry in each GW line: 11 vs. 3. Showing the models also let's me remind you to move the source segment whenever you change the segmentation level so that it maintains a comparable position in both cases. Run both models and record the free-space gain in dBi and the source impedance as R+/-jXΩ. You should obtain the following results.

Model	Number of Segments	Gain dBi	Impedance
1-2	11	2.12	71.7 + j 0.11
1-2a	3	1.95	72.2 - j 4.4

Although the impedance values for the inadequately segmented dipole would not be significantly inaccurate, the gain value is well below the value we anticipate for a dipole. The gain value produced by the more adequate model is still below the theoretic gain of a dipole in free space because the length is well under 0.5λ as a function of the relatively thick wire diameter for the frequency used.

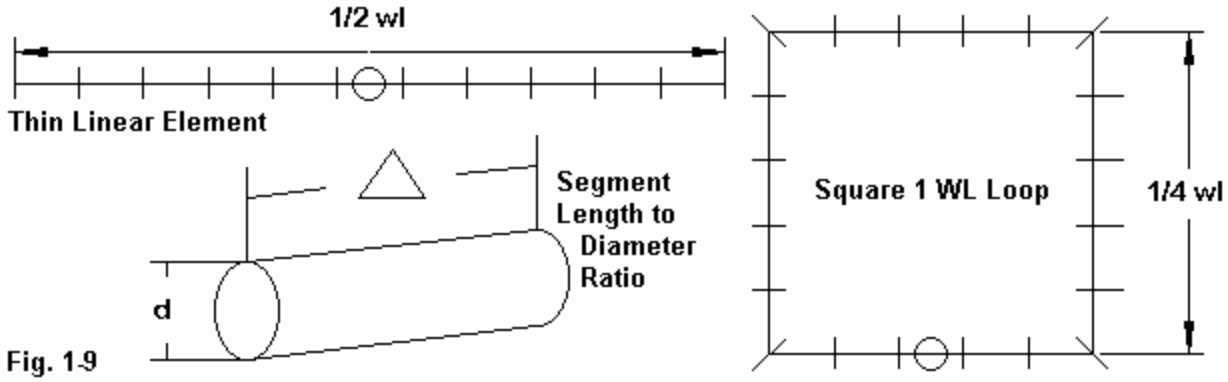

Fig. 1-9

Fig. 1-9 presents some conservative recommendations for beginning modelers to ensure--so far as possible--accurate output data. Thin linear elements that would not approach the radius-to-segment-length limit may use 11 segments per 1/2λ. Square loops and similar shapes that approximate 1λ in circumference should use about 5 segments per ¼-λ side. In NEC-2, it is especially important to keep the segment length about 4 times the wire diameter (8 times the wire radius). You may reduce this value by half by invoking the EK (extended thin-wire kernel) command, which we shall develop in a later chapter. The revised current algorithm in NEC-4 does away with the need for the EK command. Although I normally recommend these practices for beginning modelers, they remain good practice for modelers of any experience level. In all cases, extend these "beginner" limits toward the "absolute" limits in small steps, evaluating the

sensibleness of the output changes along the way.

There are numerous other modeling practices to embrace, as illustrated in **Fig. 1-10**.

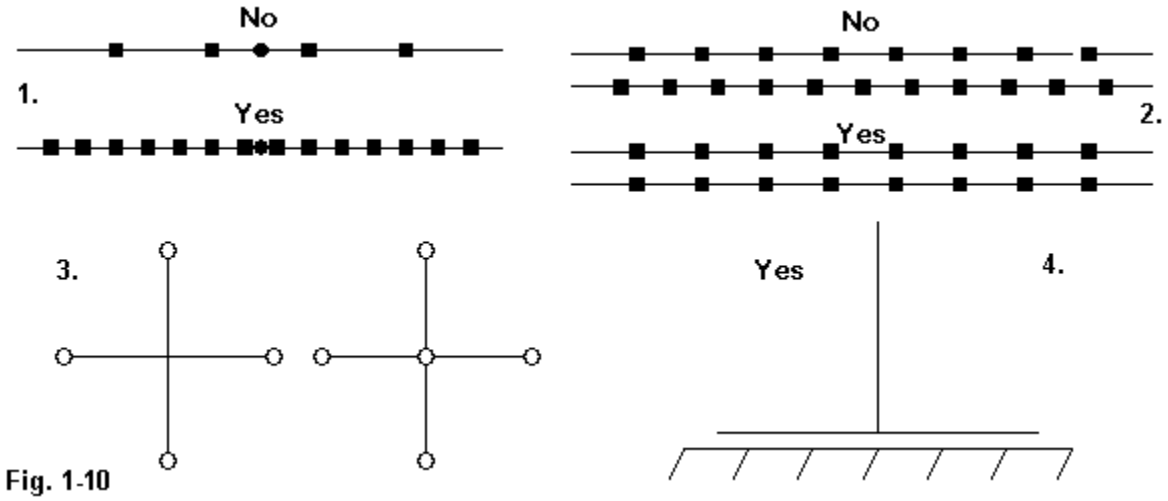

Fig. 1-10

1. Use adequate segmentation (as illustrated by models *1-2* and *1-2a*).

2. For parallel wires, align the segment junctions as closely as the wire lengths permit. The closer the spacing of the wires, the more significant this practice is to obtain accurate results.

3. Although NEC permits a wire to join another at a segment junction, for most cases, the safest and most versatile procedure is to join wires at wire junctions only. We shall explore exceptions to this practice. However, wire-end-to-wire-end junctions tend to create the fewest model errors if one of the wires is altered without altering the joining wire(s).

4. In NEC-2, keep all wires above ground (Z=0), except for a perfect ground. NEC-4 permits subterranean wires, but only with special precautions in model construction.

5. Ideally, connected wires should have the same radius. This practice is critical in NEC-2, which shows large errors if joined wires have different radii. It is less critical in NEC-4, but still good practice, since the NEC-4 improvement in stepped diameter element calculations is not perfect.

6. Plan all models on paper in advance of creating a model file. The basic tutorial presents a very usable form for many types of models. You may copy it or modify it to suit your specific needs.

7. Keep recorded output data in greater than required precision. Truncate or round the values as needed for presentation. For example, a recorded impedance of 52.385 Ω may evolve into 52.4 or even 52 for presentation. But the full value in a series of models may reveal subtle trends that may later turn out to have importance.

Just as there are good modeling practices to embrace, there are poor modeling practices to avoid. **Fig. 1-11** presents a few of the worst.

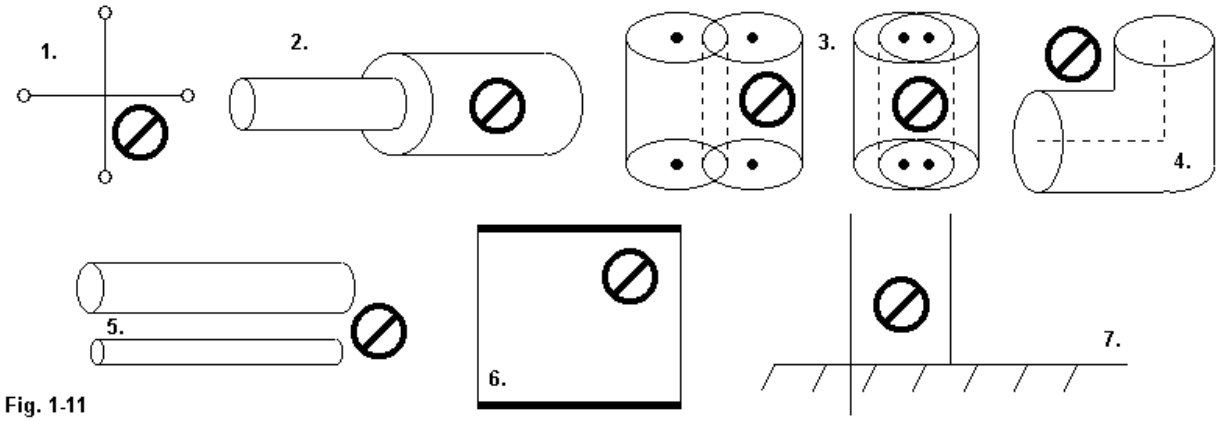

Fig. 1-11

1. Do not let wires cross in the same plane at other than wire or segment junctions. A wire end junction occurs if the coordinates of the end of one wire are the same as those of the end of another wire. If the ends are within about 0.001 segment-length of each other, NEC may presume a connection.

2. Even in NEC-4, avoid large changes of radius. NEC-2 yields large errors, which tend to increase with the size of radius change. NEC-4 overcomes the difficulty to a large degree, but does show error if the change in radius is large enough. See the Basic tutorial, Chapter 9, for hints on the use of Leeson substitute uniform-diameter elements as a work-around.

3. Avoid wires that inter-penetrate. Even if the surface of one wire does not penetrate to the centerline of the other, the situation will trigger warnings in the Necvu error detection system and may stop the core run.

4. When using thick wires, avoid sharp bends where the outer surface of one wire may penetrate into (roughly) the middle third of the other wire.

5. Closely spaced wires having different diameters will tend to yield errors the closer the wires approach each other. This situation holds true even if the wire segment junctions are well aligned. Closely spaced wires of the same diameter should be at least 3 diameters apart, although this value may vary with the segment-length-to-radius ratio.

6. Avoid angular junctions of wires having dissimilar radii. The degree of error is more extreme with NEC-2 than with NEC-4.

7. Except for a perfect ground, do not let model wires touch the ground. Monopoles brought to a real ground rather than to a radial system will show systematic errors. In NEC-4, wires may touch the ground and even penetrate it without registering a program error. However, you must meet specific conditions in NEC-4 for ground penetration.

These brief lists do not include all of the practices to embrace or avoid. Nor do the lists address all of the exceptions. However, as a list of general guidelines, they can serve as a set of cautionary reminders concerning the practical implications of the limitations inherent in the NEC cores. The Basic tutorial contains numerous examples of the limitations and ways to avoid them.

Some Ground Considerations

Any ground, real or perfect, occurs at Z=0. **Fig. 1-12** addresses one limit for NEC models that employ the Sommerfeld-Norton (S-N) ground calculation system.

Fig. 1-12

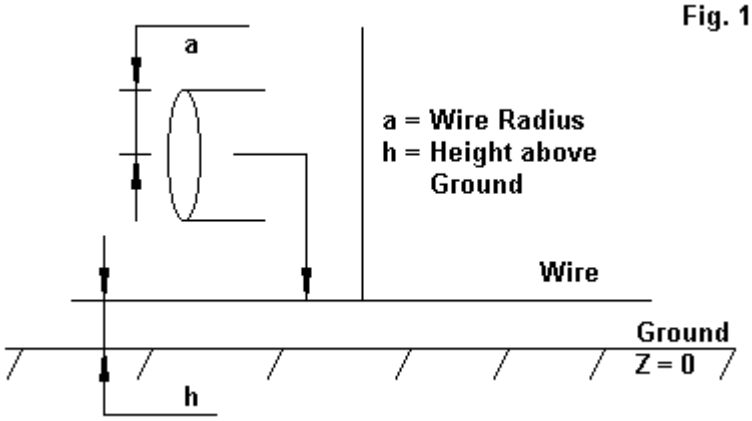

The minimum height for wires above an S-N has two dimensions. The first relates the height above ground limit to the wire radius. The wire height (h) should be several times the wire radius (a), that is, h>~a. As well, the minimum height is related to the wavelength for the frequency in use: $(h^2+a^2)^{1/2}>10^{-6}\lambda$. If a is very small compared to h, the wires may approach $10^{-6}\lambda$ toward ground.

NEC, of course, includes two choices for real ground: the S-N system and the reflection coefficient approximation (RCA). The increased speed of modern PCs has reduced the use of RCA, which calculates somewhat faster than S-N. However, RCA is subject to accuracy limitations for low-level wires. Although you may press the limits judiciously, the general recommendation is that vertical wires should terminate at least 0.1λ to 0.2λ above ground. For greatest accuracy, horizontal wires should be 0.4λ above ground.

Selecting the proper frame of reference for an antenna requires an understanding of the available ground systems. As shown in the upper portion of **Fig. 1-13**, Free space or the "no-ground" condition permits pattern generation in a full sphere. (The simple 2-element antenna sketch simply allows you to remain oriented toward the circles in the figure.) Free space has its most extensive use when doing basic antenna design work. It permits viewing of both the E-plane and the H-plane patterns for desired and undesired conditions. Free space is also useful for comparing series of antennas, all of a similar or relevantly compared type.

The lower portion of **Fig. 1-13** portrays the situation of antennas above ground. With respect to the antenna geometry, you may view the structure at its actual height above ground as defined by the Z-coordinate(s). However, from the perspective of a far-field output, the antenna and its height above ground are insignificant. The effects of height on the pattern are factored into the

output, but the distance from the antenna is so great that the antenna assembly shrinks to a dot at the center of the coordinate system when viewing either a phi/azimuth plot or a theta/elevation plot. NSI's surface plot facility allows a conventionalized rendering of the antenna within the plot, but do not confuse this with how the antenna would appear from the distance used in obtaining pattern information.

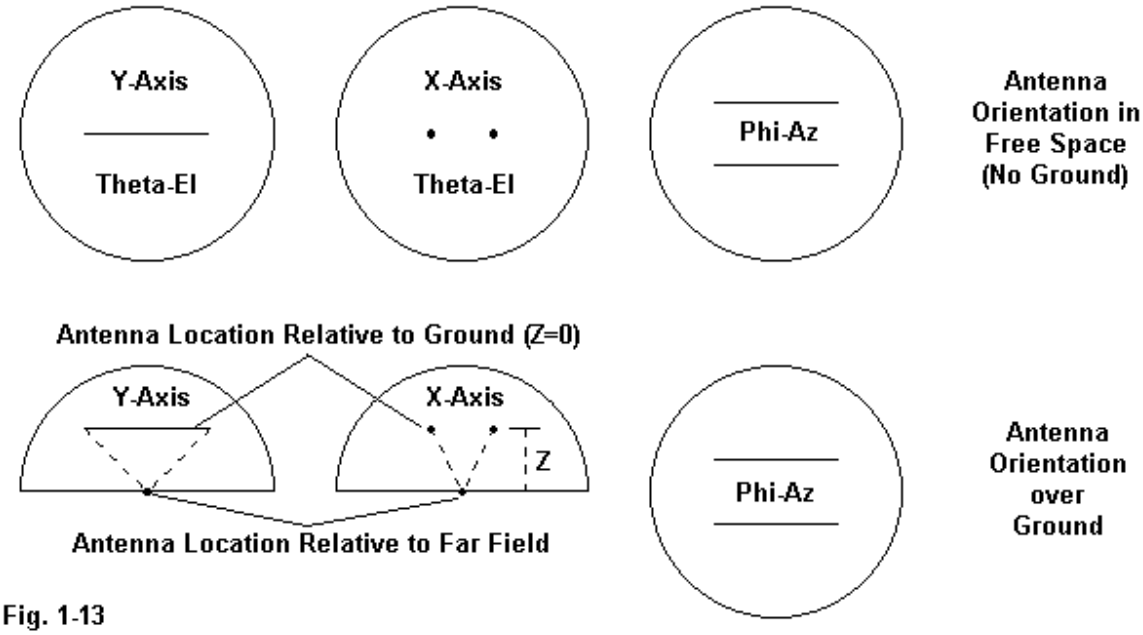

Fig. 1-13

Perfect ground is useful for comparing vertical antennas and arrays without requiring the creation of a set of ground radials. It is also useful for theoretical studies. However, it cannot show the effects of the properties of the ground either in the immediate ("impedance-determining") region or the Fresnel ("far-field ground reflection") region of the array. For reasonably accurate portrayals of these effects, you must construct a relevant above ground radial system in NEC-2 or a properly structured below ground radial system in NEC-4. The Appendix contains information on conventional ground quality values of conductivity and permittivity used by many modelers.

To illustrate the requirements for a NEC-4 buried radial system, let's open model *1-3.nec* and compare it to the sketch shown in **Fig. 1-14**. If you are using NEC-2, you may open the model, but it will not run. The system is a simple monopole that is 25 mm in diameter, with 2-mm diameter radial wires. (Special note: the errors encountered with junctions of wires having dissimilar radii do not occur if one set of wires forms a symmetrical system, such as a radial or a top-hat structure.) The 4 radials are 0.001λ (0.164 m) below ground.

NEC-4 rules require that the passage through the ground surface (Z=0) occur at a wire or segment junction. This requirement calls for a wire segment below ground that is 0.164 m long. The source segment is immediately above ground. For greatest accuracy, the source segment must be the same length as the segments immediately adjacent to it. So the source segment or wire must also be 0.164-m long. As well, it is normally wise to make the segments of wires joining at an angle the same length. Hence, the first segment of each radial must also be about 0.164-m long.

One option open to use is to segment each wire such that every segment in the model is 0.164-m long. However, this option results in a model with over 1000 segments. Alternatively, we can length-taper the radials and the upper part of the monopole and arrive at equally accurate results.

Fig. 1-14

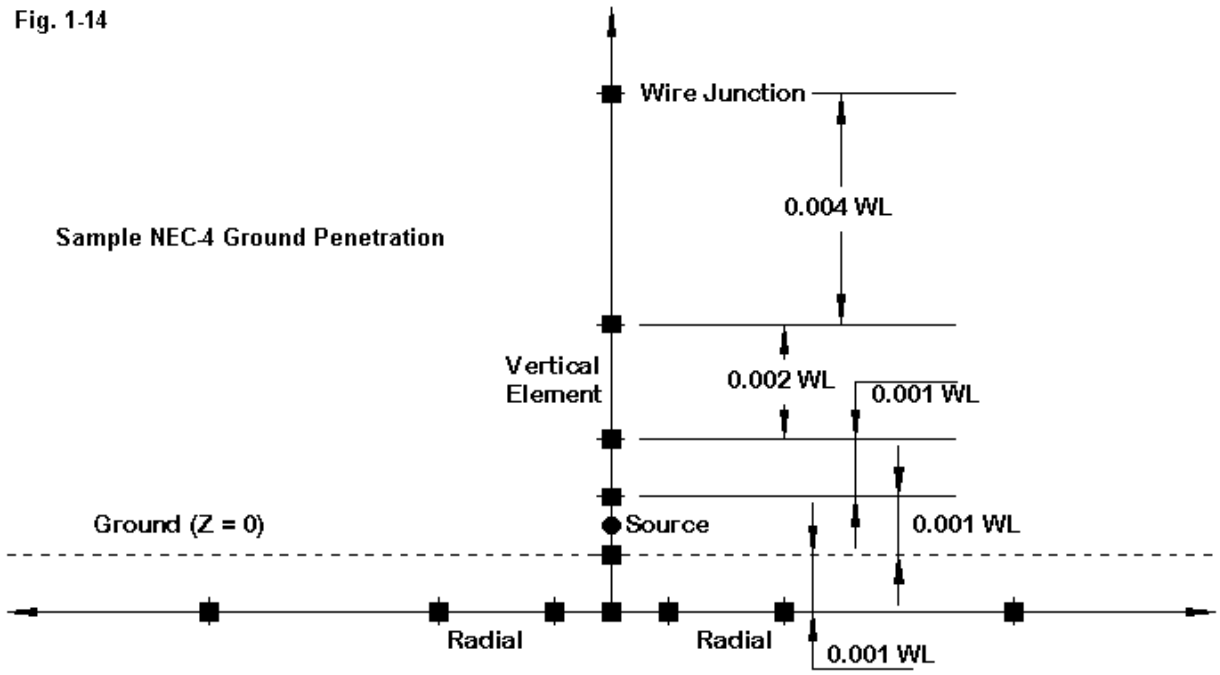

Fig. 1-14 shows the resulting structure. The monopole has a vertical 1-segment wire below ground, with another 1-segment wire above ground to serve as the source segment. The remaining vertical wires are length-tapered (in this case, by an adjunct program) so that the segments begin with a length of 0.164 m and increase until they reach a maximum segment length of a little over 5 m or about 0.03λ. The radials follow the same pattern, but length tapering begins at their junction with the subterranean vertical wire. One might also have length-tapered the wires using the GC command, which we shall encounter in a future chapter. However, the tapering results would not have shown up in the model itself, but only in the NEC output file. The length-tapering techniques result in a model using only 62 segments.

Loads, Transmission Lines, and Sources

The most used control commands that modify the geometry of an antenna are the source or excitation, loads, and transmission lines. These commands have important interrelationships that we should review.

We shall begin with transmission lines as formed by the TL command. As shown in the upper portion of **Fig. 1-15**, a TL entry does not create wires that radiate. Rather, it creates equations that do not participate in the radiation field calculations. TL transmission lines are special forms of networks (NT) that require termination at both ends on different wire segments. The dashed "X" in the left portion of the figure indicates that you may specify a normal or a reversed connection

for the TL entry. Reversed lines are useful for many phased-array applications. The entry allows you also to load either end of the line by assigning conductivity and/or susceptance values. TL entries are especially useful for simulating low-impedance lines, such as coaxial cables, that are normally not feasible to model as wires.

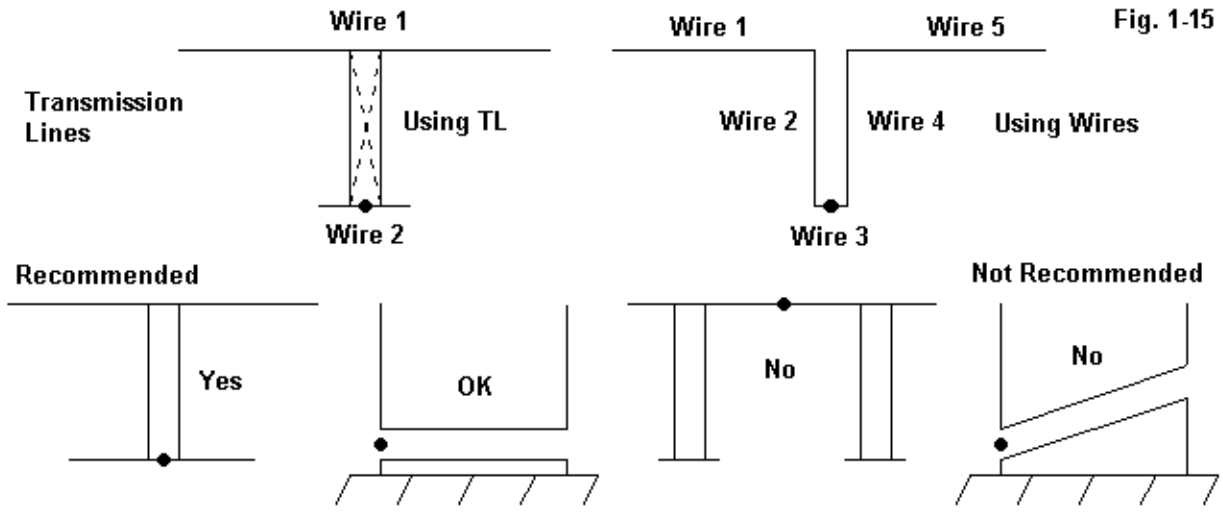

For higher impedance parallel lines, we often have a choice of whether to model a transmission line as a set of wires or using the TL entry. The top right portion of **Fig. 1-15** shows the general scheme for modeling a line with wires. Open and compare models *1-4.nec*, *1-4a.nec*, and *1-4b.nec*. The first model in the sequence is a simple dipole in free space, using 21 segments for the 1-mm radius wire. Run the model, noting both the free-space gain on the phi plot and the source impedance.

For the 'a' and 'b' versions, here are the relevant lines of the models that show how they differ from the basic dipole.

Model 1-4a

```
GW 1 21 0 -10.42 0 0 10.42 0 .001
GW 2 1 0 -.01 -10 0 .01 -10 .0001
GE
GN -1
TL 1 11 2 1 470 21.4138
EX 0 2 1 0 1 0
```

Model 1-4b

```
GW 1 200 0 -10.42 0 0 -.025 0 .001
GW 2 400 0 -.025 0 0 -.025 -21.4138 .001
GW 3 1 0 -.025 -21.4138 0 .025 -21.4138 .001
GW 4 400 0 .025 -21.4138 0 .025 0 .001
GW 5 200 0 .025 0 0 10.42 0 .001
GE 0 -1 0
GN -1
EX 0 3 1 0 1 0
```

1-4a introduces a TL line between the center of the dipole and a new wire (GW2). Since the only function of this wire is to terminate that line and to serve as the new source for the dipole, it is short, thin, and lossless. It may be any distance from the dipole, usually far enough away so that it cannot disturb the radiation pattern. The actual electrical length of the line appears in the TL entry, in this case, 1/2λ at the operating frequency of 7 MHz. Note that the model moves the voltage source excitation (EX) from its former position on wire 1 to the new short wire. Run the model and record the gain and source impedance.

Model 1-4b creates the same situation using wires rather than a TL entry. The line consists of GW2 and GW4, which extend 1/2λ downward from the dipole wires, GW1 and GW5. GW3 is the I-segment source wire that connects the lower ends of the transmission line. The calculated characteristic impedance of the line used is about 470 Ω, based on the 50-mm spacing and 2-mm diameter of the wires. (That impedance value was also assigned to the TL entry of model 1-4a.) Since the source-segment length equals the spacing between the wires, the model assigns that approximate segment length to all wires, resulting in a model with 1201 segments (compared to 22 for the TL version of the model). Run this model and record the gain and impedance reports.

Model	Gain dBi	Impedance R+/-jX Ω
1-4 (simple dipole)	2.14	72.13 + j0.03
1-4a (dipole with TL)	2.14	72.13 - j0.01
1-4b (dipole with wire line)	1.88	75.65 - j3.81

The results might trouble us because the gain of 1-4b is lower and its impedance is higher than the other two models. How we may resolve this matter will appear shortly. For the moment, both methods succeed in modeling a dipole with a 1/2λ transmission line between the antenna and the ultimate source point.

TL-type transmission line entries are subject to restrictions, indicated by the lower portion of **Fig. 1-15**. For highest accuracy, the TL line must be balanced, with equal current levels on the segment on each side of the one to which you attach the line. Balance is most nearly assured when the line attaches to the center of 1/2λ wires, where the current changes slowly from one segment to the next. As the second small graphic suggests, we approximate this condition with monopoles that either touch the ground or a radial system; the current at these positions normally changes slowly from segment to segment. The final two graphics illustrate unbalanced conditions in which the TL version of a line may not yield accurate results. In terms of actual antenna structures, avoid the use of TLs for mid-element stub or linear loading, collinear array inter-element phasing stubs, and off-center-fed doublet feedline simulations. For these and similar situations, construct parallel feedlines with actual wires.

In a later chapter, we shall examine the full array of load or LD entries. However, we note here that spot loads with reactive components (LD0, LD1, and LD4) by which you may load antenna elements on specific segments are subject to the same limitations as TL entries. LD loads are non-radiating equation-based modifications to the model and do not participate in the radiation calculations (although any resistive component will enter into the radiated power calculations and hence the overall gain). They yield the most accurate results when the current is balanced on each side of the loaded segment. Unbalanced current situations yield lesser results. This situation is especially critical to inductive loads. The inductive value inserted as a load presumes

equal currents at the ends of the inductor. Since the current at each inductor end far out on an element is unequal, a real inductor functions partially as a pure inductance and partially as a length of wire that is part of the total antenna element length. An LD entry cannot replicate the latter function. As well, LD4 entries, which use values of resistance and reactance, are fixed and do not change with frequency. When performing frequency sweeps using LD loads, use either LD0 of LD1 loads, which employ values of resistance, inductance, and capacitance. NEC calculates the required reactance for each frequency within the sweep.

The most-used NEC-based excitation applied to a wire segment is the applied E-field voltage source (EX0). Many implementations of NEC provide an indirectly created current source using techniques that we shall examine later. However, the ultimate source remains an EX0 entry. EX0 entries yield the most accurate results when the source segment has a length equal to the length of the segments on either side of it. In many instances of complex geometric antenna structures, you may have to introduce a 3-segment wire to handle the source. In other cases, you may have to carefully segment the wires on either side of a 1-segment source wire so that their segment lengths are the same as the source segment length.

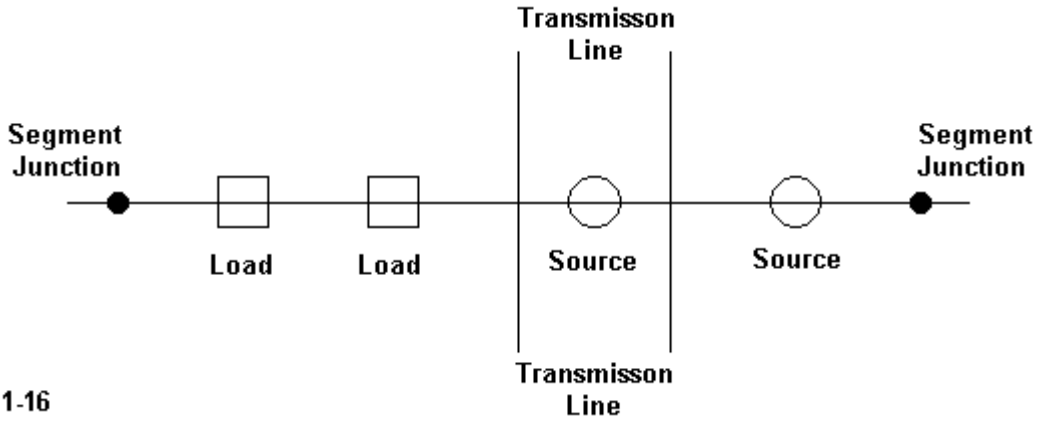

Fig. 1-16

When we place loads, transmission lines, and sources on the same segment, they are related to each other in the general manner indicated by **Fig. 1-16**, although I am not aware of any model requiring the total spread of possibilities to appear on a single segment. Some elements appear in series with other elements, while some appear in parallel. The following table summarizes the relationships, remembering that these relationships apply only when multiple entries appear on the same segment.

	Load (LD0, LD1, LD2)	Source (EX0)	Trans. Line (TL)
Load (LD0, LD1, LD2)	Series	Series	Series
Source (EX0)	Series	Series	Parallel
Trans. Line (TL)	Series	Parallel	Parallel

The table reveals why you cannot load the end wire of a transmission line with an LD value: it appears outside the boundaries of the TL entry and in series on the terminating segment. To load the end of a TL entry, use the conductance and susceptance entries within the TL entry itself.

These notes review only those aspects of source, load, and transmission line commands as we might find in an entry-level NEC program. However, each of these commands has a large number of alternative implementations, many of which lie beyond the scope of entry-level programs. Therefore, we shall give each command set extended treatment.

Convergence and Average Gain Tests

There are two general tests of model adequacy: the convergence test and the average gain test (AGT). Each of these tests is a necessary but not a sufficient condition of adequacy. There are models that may pass both tests and still be inadequate.

Convergence testing derives from a technique first applied to MININEC models. **Fig. 1-17** shows the basic scheme of the test. Although the graphic shows only a single element, the test applies to every element in any antenna at the same time in order to maintain the relationships among the antenna wires and segments.

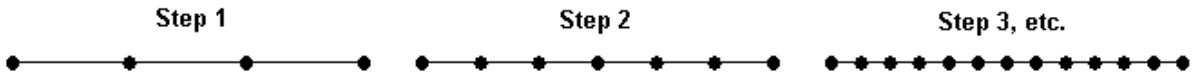

Convergence Testing Fig. 1-17

Beginning with an initial number of segments per wire, we increase the number of segments according to some reasonable scheme. The increment of increase per step of test may range from about 20% to as much as double the total number of segments. The variability of the increment stems from the evaluation of the model. Record the primary performance figures for the model, perhaps gain and source impedance. Within the boundaries of the task specifications that occasion the modeling activity, determine at what level of segmentation the rate of change of reported values reaches a small enough amount between steps. At that level, the model is converged.

Under certain circumstances, the application of the test may yield different types of results between a NEC core and a MININEC core. With a MININEC core, the rate of change may continue decreasing until you reach a segment level that violates length vs. radius limits. In NEC, convergence may not continue, but show a more definite level of segmentation as the most desirable. Open model *1-5.nec*. The model reveals an NBS Yagi using thick elements in a free space environment. Initially, the model uses 11 segments per element. We shall explore convergence in NEC by increasing the number of segments per element in steps of 4, running from the initial 11 up to 35. Remember that each change in the level of segmentation requires you to move the position of the source (EX) to keep it centered on the driver.

To provide a reference to the origins of the convergence test, I also ran the test on a version of MININEC. MININEC places sources at "pulses" which occur at the junctions of segments. Hence, to keep the source centered on the driver, I used an even number of segments for each step in the convergence process.

The tables that follow compare the results. For many purposes, the model might be considered converged at the lowest level of segmentation--or perhaps the level just above the lowest. However, the point of this exercise is to see the numerical trends, not to produce an antenna that we might put into service. Hence, in this--and in many other cases--we should feel free to be overly precise in the numbers that we record. The tables show the free-space gain, the 180° front-to-back ratio, the source impedance, the outcome of the average gain test (AGT), and the average segment length (in meters) and its ratio to the element radius.

NBS Yagi Convergence Tests: NEC-4D Results

# Segments per element	Gain dBi	Front-to-Back Ratio dB	Source Impedance R +/- jX Ω	AGT	Ave. Seg Length	Seg. Len. to Radius Ratio
11	11.20	13.73	17.10 - j1.19	0.9969	0.0401	9.4:1
15	11.22	13.29	17.02 + j0.30	0.9985	0.0294	6.9:1
19	11.22	13.11	17.00 + j0.92	0.9992	0.0232	5.5:1
23	11.22	13.07	17.01 + j1.05	0.9995	0.0192	4.5:1
27	11.22	13.11	17.03 + j0.91	0.9997	0.0163	3.8:1
31	11.22	13.20	17.06 + j0.61	0.9998	0.0142	3.4:1
35	11.22	13.30	17.09 + j0.24	0.9999	0.0129	2.9:1

NBS Yagi Convergence Tests: MININEC Results

# Segments per element	Gain dBi	Front-to-Back Ratio dB	Source Impedance R +/- jX Ω	AGT	Ave. Seg Length	Seg. Len. to Radius Ratio
10	11.14	14.58	17.51 - j2.28	0.9980	0.0401	10.4:1
14	11.17	14.09	17.52 - j0.84	0.9982	0.0315	7.4:1
18	11.18	13.83	17.53 - j0.04	0.9984	0.0245	5.8:1
22	11.18	13.70	17.55 + j0.40	0.9985	0.0201	4.7:1
26	11.19	13.64	17.58 + j0.60	0.9987	0.0167	4.0:1
30	11.19	13.63	17.61 + j0.68	0.9988	0.0147	3.5:1
34	11.19	13.63	17.64 + j0.68	0.9988	0.0130	3.1:1

Although spurious in practical terms, the MININEC model shows convergence at the highest levels of segmentation within the boundaries of the test. However, the NEC-4D model shows convergence between 19 and 23 segments per element, where the values of front-to-back ratio, resistance, and reactance reach either high or low levels and then retreat from those levels. Using NEC, the optimum level of segmentation is not always the maximum level allowable within the limits for the segment length vs. the wire radius.

In the table, I entered the values for the AGT to demonstrate that the numerical progressions for that test do not always coincide with the trends for the convergence test. To perform the average gain test, we must first strip the antenna of all resistive loading and place it either in free space or over a perfect ground (mostly for monopole arrays). If a model is perfectly adequate as a model, then $G_{ave} = k * (P_{rad}/P_{in})$, where G_{ave} is the average power gain of the antenna, P_{rad} is the radiated power, and P_{in} is the input power. For a free-space environment, k = 1, while for perfect ground, k = 2. The test requires that we integrate or average the radiated power (P_{rad}) over a free-space sphere or a perfect-ground hemisphere using sufficient sampling points to arrive at an undistorted average radiated power. The more complex the far-field pattern, the more important it is to use a smaller increment between samples. NEC-Win Pro and GNEC provide a special function button

to allow the user to perform the test. The AGT facility pre-strips the model of resistive loads. It then allows you to select the environment (free space or perfect ground) and to select the angular increment between samples. The smaller the increment, the more accurate the result will be, although the run time for the test will be longer.

The AGT values returned may be higher or lower than perfect values of 1.00 or 2.00, depending upon the environment. As a general guide, NSI provides the following general model evaluations.

AGT Value	Model Evaluation
0.95 to 1.05	Highly accurate
0.85-0.95 and 1.05-1.15	Reasonably accurate and usable
0.80-0.85 and 1.15-1.20	Usable, but can be improved
<0.80 and >1.20	Questionable and requires refinement

The chart is not the final arbiter of the adequacy of a model with respect to the AGT. Instead, just how well a model must score to be adequate is a task-driven judgment of the modeler. For many purposes, you may wish to hold models to a much higher standard than may be implied in the table.

Average gain values are expressed as dimensionless power ratios. We may also express the AGT value in dB simply by multiplying the $\log_{10}$ of the initial AGT value by 10. The result will return a positive value for AGT scores above 1.0 and a negative value for AGT scores below 1.0. We may use this converted AGT score as a means of correcting the reported gain for a model if the initial AGT value is not too far from the ideal. (There is no specific AGT value beyond which the correction does not work, but you likely should limit its use to at least reasonably accurate and usable models.) To illustrate the technique, let's return to models *1-4.nec* through *1-4b.nec*. The table repeats the results we obtained, but adds AGT values to each entry.

Model	Gain dBi	Impedance R+/-jX Ω	AGT	AGT in dB
1-4 (simple dipole)	2.14	72.13 + j0.03	0.9994	-0.0026
1-4a (dipole with TL)	2.14	72.13 - j0.01	0.9994	-0.0026
1-4b (dipole with wire line)	1.88	75.65 - j3.81	0.9513	-0.2170

The AGT values for the first two models in the list indicate that they require no correction. However, the third model that used wires to create the transmission line is correctable. A negative AGT (dB) value indicates that the reported gain is low, and we may increase it accordingly for a more accurate report. The result is a gain of 2.10 dBi. (The remaining difference results from the fact that the theta pattern for the antenna is no longer a perfect circle, as it is for the other models in the sequence.)

We may also correct the resistive component of the source impedance if the reactive component is not large. To arrive at a correct source resistance, simply multiply the basic AGT value times the reported source resistance. For 1-4b, the result is 71.94 Ω. The larger the source reactance, the less reliable that the resistance correction will be.

Because it is possible to automate the process of deriving an AGT value for a model, this test has become the preferred test for model adequacy in NEC. However, like the convergence test, the

AGT is a necessary condition of model adequacy, not a sufficient condition.

The Concept of a Work-Around

Many antenna structures do not permit direct modeling within NEC. In such cases, we may create "work-around" models to analyze the antenna. In the context of review, we shall briefly explore only the concept of a work-around and use only a single example. We shall encounter other examples in future chapters, and the Basic tutorial contains a number of worked examples.

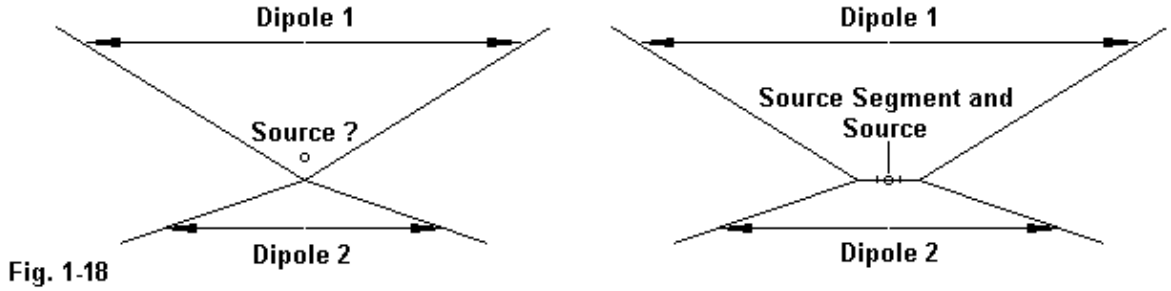

Fig. 1-18

Open model *1-6.nec*. The antenna is a pair of dipoles for amateur use on the narrow 30-meter and 17-meter bands. The question is where one should place the source. The options are the segments closest to the center junction of the wires. But which junction is correct? The initial model uses one placement. Run the model at 10.125 MHz and at 18.108 MHz and record the source impedance values for each seemingly reasonable option.

In fact, none of the options is best. To simulate the 2-band dipoles set, we need to create a model similar to the right-hand sketch in **Fig. 1-18**. Open model *1-6a.nec*. If you examine the wires, you will find an extra wire (GW2) that has 3 segments along its 0.9-meter (3') length. Note that the segment lengths in the remaining wires are close to the segment length in the new central wire. The dipole legs connect on each end to the center wire and we place the source in its center segment. With this arrangement, we obtain the following impedance reports.

Frequency (MHz)	Impedance (R +/-jX Ω)	50-Ω SWR
10.125	60.5 - j1.4	1.2:1
18.108	31.2 - j1.9	1.6:1

The work-around yields very reasonable impedance values and suggests a perfectly satisfactory antenna of its type for amateur use. Nevertheless, the ultimate geometry does not quite coincide with the realities of antenna construction. Even if the antenna has a sizable center insulator, it is not likely to be 3' long. The alternative, however, is being unable to model the antenna at all.

Work-arounds are a fact of life in modeling. For each use, we must evaluate within the task specifications to what degree the work-around produces reasonable results and to what degree it reduces the precision to which it makes sense to carry the numerical reports. In the present example, given the need to adapt the actual antenna to an unspecified environment, we know that the builder would need to do some judicious pruning to resonance. However, the model can

provide very reasonable indications of performance for the final assembly.

Summing Up

In this chapter, we have reviewed many--but by no means all--of the basic parameters within which we shall model in NEC, whether we use NEC-2 or NEC-4. We began with a glimpse at the format that is inherent to the NEC core. If we began our modeling efforts with an entry-level program, we might never have encountered the native ASCII input file for NEC.

We next reviewed the Cartesian conventions that are native to the creation of antenna geometries and how they translate into phi and theta far-field output patterns. We examined alternatives for the patterns, including their translation into azimuth and elevations patterns, the use of log and linear gain scales, normalization, and rectangular plots of the data.

Modeling in NEC has many limitations, beginning with maximum and minimum segment length constraints. Within the absolute limits of the cores, there is a region of recommended practices, not only for beginners, but as well for all modelers. Also, there are a number of practices to avoid, such as wire inter-penetrations and thick-wire corner junctions. Some of the violations of good modeling will result in a core rejection of the model; others will simply yield inaccurate or unreliable output data.

Selecting the right ground or environment for a model is as important as setting up a flawless geometry. We examined the basic difference in the limits of the real ground systems and between NEC-2 and NEC-4 with respect to penetration of the ground or Z=0 level. As well, we explored the parameters for the effective use of segment-specific loads with reactive components, transmission lines, and voltage sources. We also examined the limitations of these three key modifiers of model geometries.

We surveyed the convergence and average gain tests as means of determining the adequacy of our models. We closed the brief review of basic modeling in NEC with the concept of a work-around. Although these notes form a long chapter, they still fall far short of being more than reminders. If the review leaves many aspects of basic modeling opaque, you may wish to review the material in *Basic Antenna Modeling: A Hands-On Tutorial*. However, if you can say that you know all of what has been covered, you are ready to move on.

2.
GW, GM, GS, and GE: Wire Entry Alternatives

***Objectives**: After becoming clear on the distinctions among the concepts of a wire, a segment, and a tag, we shall examine the three most fundamental geometry commands: GW, GS, and GE. Although we can create most antenna structures using only these commands, we shall also observe how the GM command can let us effect significant economies of model formation as well as offer alternative means to the same modeling goals.*

Without a set of defined wires, we can have no antenna model in NEC. Entry-level programs perform virtually all structure modeling using the most basic of all commands, GW, the wire entry command. They supplement that command with a necessary geometry end command, GE, and with a convenience command, GS. GS permits scaling the modeler's preferred wire-entry unit of measure into meters, the unit used by NEC for calculations. In many cases, the entry-level program may not show the actual input file, although NEC-Win Plus provides a view of this file along with its main user-friendly wire entry screen.

However, NEC offers a considerable array of geometry commands that offer added flexibility in model structuring. In this chapter, we shall meet one of the most versatile geometry commands, GM, the coordinate transformation command. However, to use this command effectively, we must begin with more basic geometry concepts used by NEC: the tag, the relative segment, and the absolute segment. To explore these concepts, we shall have to use the GM command before we have dissected it. The sample models, of course, must have some control commands in order to be models that we can run. However, in each model, I shall restrict the control commands to the most common ones and to the minimum number necessary to arrive at a functional output. In general, I shall specify a frequency (FR), a voltage source applied to a specific segment (EX0), and one or two far-field output requests (RP0). All models will terminate with the EN command.

Wires, Tags, Relative Segments, and Absolute Segments

In entry-level programs, each wire specified by a modeler to create an antenna shape, no matter how complex, has a corresponding GW entry, and each new GW entry receives a number that the program entry scheme automatically designates for the user. Although eminently practical within the context of the entry-level program, this practice can obscure the true nature of the numbers that occur both in the GW entry line and the NEC core as it processes the geometry portion of the model. Therefore, let's step back a moment and see what NEC sees with no filtration.

Fig. 2-1 provides two views of the same antenna. The antenna has 3 straight wires for the planned model. 2 of the wires are vertical. Our interest in this antenna extends only to the model-planning wires, which are labeled Wire 1, etc., along with the segments, which are labeled as they progress from End 1 to End 2 of each wire. These are the wires that we shall enter into the

model's geometry section.

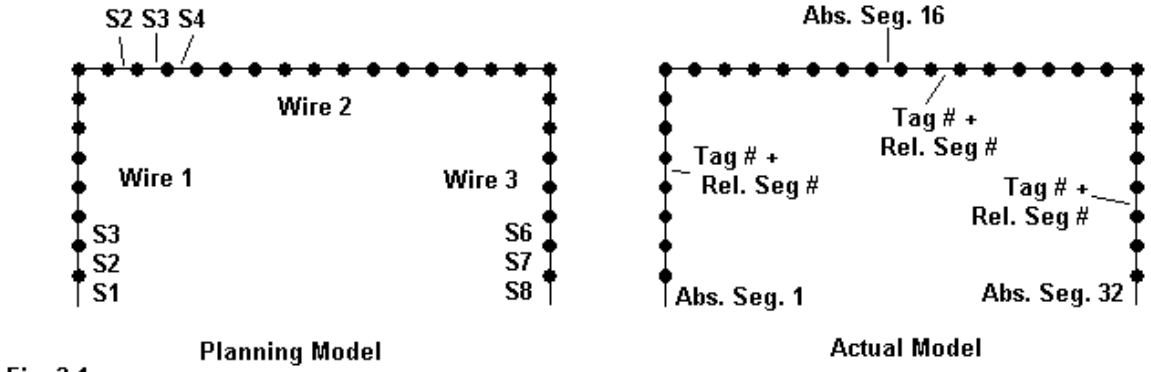

Fig. 2-1

To discover how NEC actually treats our entries, open preliminary model *2-0.nec*. It will show that we have entered the wires according to the paper plan, since we have 3 GW entries, each of which corresponds to the planning version of antenna.

```
CM Inverted-U to sample Tags and Segments
CE
GW 1 8 0 -.125 0 0 -.125 .125 .001
GW 2 16 0 -.125 .125 0 .125 .125 .001
GW 3 8 0 .125 .125 0 .125 0 .001
GE
FR 0 1 0 0 299.7925 1
EX 0 2 8 0 1 0
RP 0 1 361 1000 90 0 1.00000 1.00000
EN
```

We shall run this model solely to examine the geometry portion of the NEC output file. The following lines draw a sample from that file.

```
WIRE                                  NO. OF    FIRST  LAST   TAG
  NO.       X1          RADIUS        SEG.      SEG.   SEG.   NO.
   1    0.00000       0.00100         8          1      8      1
   2    0.00000       0.00100        16          9     24      2
   3    0.00000       0.00100         8         25     32      3
```

The extract omits most of the coordinate entries in order to reveal what happens inside NEC. For every wire that we enter (that is, for each successive GW entry), NEC processes that wire in the order of entry. You may wish to simply use a cut and paste operation to re-order the three GW entries without changing the contents at all and see what emerges in the output file.

The number following the command label, GW, in the model is *not* the Wire No. on the left side of the table. The output file Wire No. is an assigned number based on each successive new wire found in the model. The number following GW in the model geometry entry is the *Tag Number*, found at the far right of each output-file line. NEC assigns the Wire No. but the user assigns the Tag Number.

NEC also counts up the number of segments in each wire entry that it processes and assigns a consecutive number to each one. For each wire entry, the numbers run from the X1, Y1, Z1 end of the wire to the X2, Y2, Z2 end. These are *Absolute Segment Numbers*. The two columns at the right, inboard from the Tag-No. column, register the assigned absolute segment numbers for the wires entered. In addition, NEC assigns to each segment, using the same order, a number specific to the number of segments on the entered wire: these are *Relative Segment Numbers*. Hence, The second wire entered is tag number 2, with absolute segment numbers 9 through 24 and relative segment numbers 1 through 16. If we re-order the lines in the original model without changing their individual content, we shall see the same tag numbers and relative segment numbers, but a different set of absolute segment numbers based on the order of processing.

Remaining clear on these distinctions is crucial to deriving from NEC all of the flexibility available in both the geometry and control commands. As well, it can prevent errors that may not be clearly apparent from the model itself.

Open model *2-1.nec* so that we can sample some of the flexibility. The model uses 5 vertical dipoles in free space at half-wavelength intervals to create an in-phase fed array with the appearance and H-plane (phi) pattern shown in **Fig. 2-2**.

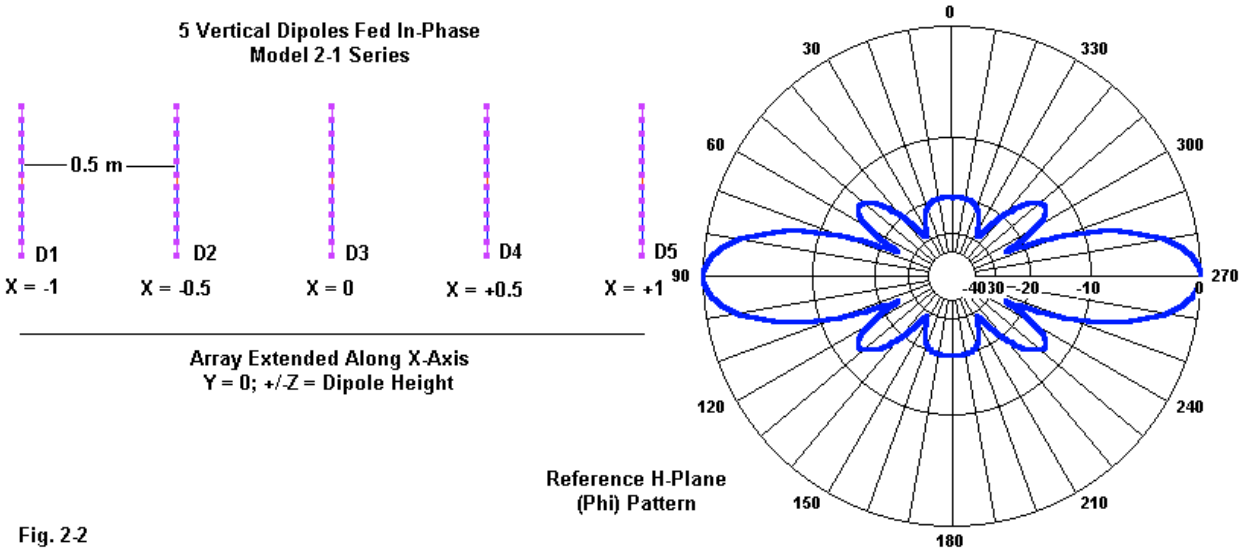

Fig. 2-2

The array has a bi-directional gain of 10.19 dBi with a 22° beamwidth. It produces the following table of source impedances for the 5 feedpoints.

Frequency	Tag	Seg.	Real(Z)	Imag(Z)	Mag(Z)	Phase(Z)	Zo	VSWR
299.790000	1	6	68.519	-0.247	68.519	-0.207	50.000	1.37
299.790000	2	17	50.677	-8.971	51.465	-10.039	50.000	1.20
299.790000	3	28	57.620	-10.937	58.648	-10.748	50.000	1.28
299.790000	4	39	50.677	-8.971	51.465	-10.039	50.000	1.20
299.790000	5	50	68.519	-0.247	68.519	-0.207	50.000	1.37

This data is our reference as we look closely at this model and some equivalent variations. Note

that the impedance data refers to the *tag number* and the *absolute segment number*.

```
CM 5 Vertical Dipoles, spaced 1/2 wl, fed in phase
CM Each Dipole = separate wire
CM EX referred to Tag # and Rel. Seg. #
CE
GW 1 11 -1 0 -.245 -1 0 .245 .001
GW 2 11 -.5 0 -.245 -.5 0 .245 .001
GW 3 11 0 0 -.245 0 0 .245 .001
GW 4 11 .5 0 -.245 .5 0 .245 .001
GW 5 11 1 0 -.245 1 0 .245 .001
GE
EX 0 1 6 0 1 0
EX 0 2 6 0 1 0
EX 0 3 6 0 1 0
EX 0 4 6 0 1 0
EX 0 5 6 0 1 0
FR 0 1 0 0 299.7925 1
RP 0 1 361 1000 90 0 1.00000 1.00000
EN
```

I have reproduced the entire initial model in this sequence to establish the basic geometry and to note that, regardless of the geometry section, each dipole will require its own EX0 entry to establish a source. In this version, the EX0 entries use the tag number and the relative segment number for that tag to place the source at the center of each dipole.

Open model *2-1a.nec* and run it to verify that it returns the same output reports as the initial model. However, notice that this version uses a single tag number throughout. The EX0 entries apply the tag number and increment the relative segment number to obtain positions at the dipole centers. You may use Necvu to confirm that each source has a correct placement.

```
GW 1 11 -1 0 -.245 -1 0 .245 .001
GW 1 11 -.5 0 -.245 -.5 0 .245 .001
GW 1 11 0 0 -.245 0 0 .245 .001
GW 1 11 .5 0 -.245 .5 0 .245 .001
GW 1 11 1 0 -.245 1 0 .245 .001
GE
EX 0 1 6 0 1 0
EX 0 1 17 0 1 0
EX 0 1 28 0 1 0
EX 0 1 39 0 1 0
EX 0 1 50 0 1 0
```

Open model *2-1b.nec* and run it to confirm correct reports.

```
GW 1 11 -1 0 -.245 -1 0 .245 .001
GM 1 4 0 0 0 .5 0 0
GE
EX 0 1 6 0 1 0
EX 0 2 6 0 1 0
EX 0 3 6 0 1 0
EX 0 4 6 0 1 0
EX 0 5 6 0 1 0
```

This new version of the model employs only a single initial GW entry. It then uses the GM entry to replicate the dipole 4 more times at the required 0.5-m spacing. You may use the NEC output report or Necvu's segment locator to confirm the structure. The GM entry increments the tag number by 1 for each replicated dipole. Hence, the excitation section of the model may use the same source-positioning scheme used in the original model, *2-1.nec*.

Finally, open model *2-1c.nec* and confirm its output reports.

```
GW 1 11 -1 0 -.245 -1 0 .245 .001
GM 0 4 0 0 0 .5 0 0
GE
EX 0 0 6 0 1 0
EX 0 0 17 0 1 0
EX 0 0 28 0 1 0
EX 0 0 39 0 1 0
EX 0 0 50 0 1 0
```

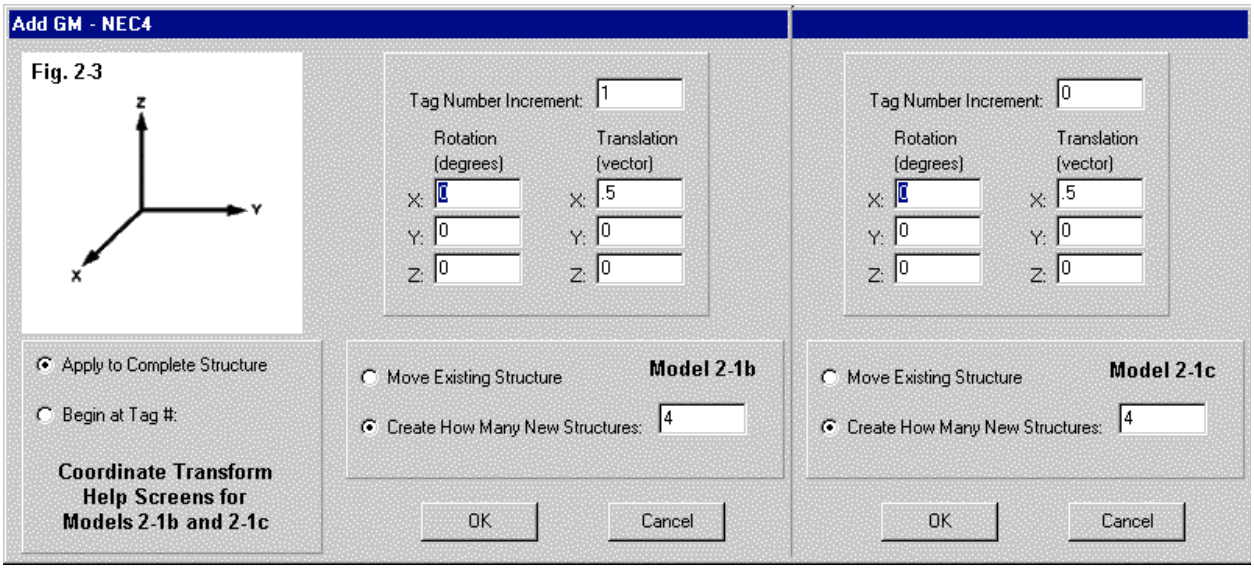

Fig. 2-3 shows the NSI GM assist screen for 2-1b and 2-1c. 2-1b increments the tag numbers of the replicated dipoles. However, 2-1c does not, leaving all dipoles with a tag number 1. In this case, it happens not to matter whether or not the GM entry that replicates the initial wire to yield a total of 5 vertical dipoles increments the tag number. The EX0 entries use a zero for the tag number position, indicating to the core that the source segments will use absolute segment numbers.

Caution: You may use a tag number of zero in some models, but this practice is dangerous. You can easily confuse the resulting segment numbers when applying control commands. Many control commands provide the option of using either absolute segment numbers (usually by assigning a tag number of zero to the control entry) or of using tag numbers plus relative segment numbers. If assigned tags begin at 1, you can easily avoid the potential for confusion.

We have not looked at all of the possible combinations for assigning and using tags. However,

you may check out others while we begin a more detailed examination of the command entries themselves.

The Structure of the GW, GS, and GE Commands

The GW, straight-wire specification command is perhaps the most familiar in all NEC modeling. The structure of the command is identical in both NEC-2 and NEC-4. Open model *2-2.nec*, a simple 1/2λ center-fed dipole. Initially, we shall be interested only in the GW entry for this model, which is longer than resonant to simplify the ultimate dimensions. As well, I have spread the command out across the page to identify the individual numerical entries within it.

```
Cmd   I1    I2       F1    F2       F3    F4    F5       F6    F7
      Tag   No. of   End 1 Coordinates   End 2 Coordinates   Wire
      No.   Segs     X1    Y1       Z1    X2    Y2       Z2    Radius
GW    1     11       0     -.82021  0     0     .82021   0     .003281
```

The top line of the table identifies the integer (In) and the floating decimal (Fn) entries. The next pair of lines specifies the data to input to these slots. The integer entries are used for the assigned tag number and the number of segments into which the core will equally divide the wire. F1 through F3 provide the coordinates for the user specified first end of the wire in X, Y, Z order, while F4 through F6 do the same for end 2. F7 holds the wire radius. **Fig. 2-4** reflects the given GW entry.

Fig. 2-4

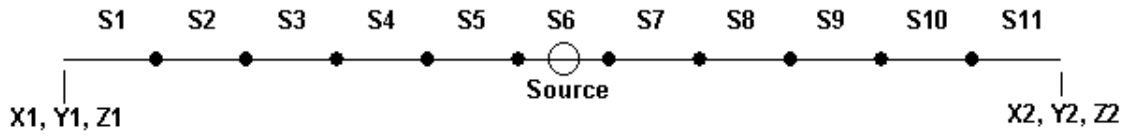

The model does not use meters as the unit of measure. In fact, it is in feet, but any unit of measure will do under the condition that all entries within the geometry section of a model, including the wire radius, use the same unit of measure. Successively open models *2-2a.nec*, *2-2b.nec*, and *2-2c.nec*, and examine the GW lines of these models, all of which are ultimately identical to the initial model.

```
GW 1 11 0 -.82021 0 0 .82021 0 .003281      2-2   Feet
GW 1 11 0 -9.8425 0 0 9.8425 0 .03937       2-2a  Inches
GW 1 11 0 -250 0 0 250 0 1                  2-2b  Millimeters
GW 1 11 0 -.25 0 0 .25 0 .001               2-2c  Meters
```

After running each model, you may check the "Segmentation Data" section of the output file to confirm that all of the models result in the same geometry for the core calculations. (Although many modelers rely upon the graphic and tabular facilities of the implementing program, such as NEC-Win Pro or GNEC, for output data, the basic NEC output file provides a wealth of data, not the least of which is information by which to check the model geometry.)

The means by which NEC converts all geometry dimensions into meters is the GS command. Here, NEC-2 and NEC-4 differ. What the two GS commands have in common appears in the annotated sample line from model 2-2.

```
Cmd   I1 I2 I3
      NU NU Conversion factor
GS    0  0  0.304800
```

NU means that the integer entry is not used and is filled by a place-holding zero. (This reading is the one that appears in the 1992 NEC-4 manual.) The conversion factor, 0.3048, converts feet into meters. The other most common conversion factor converts inches into meters: 0.0254. You will find it useful to keep these in memory.

NEC-4 has a second means of making common conversions from feet and inches into meters. Open model *2-2d.nec*. Examine the GS command,

```
GS 1 0 0
```

In fact, NEC-4 makes use of the I1 position. If the value is 1, then it uses the feet-to-meters conversion factor. If I1 is 2, then it uses the inches-to-meters conversion factor. **Fig. 2-5** illustrates the difference between NEC-2 and NEC-4 by showing the NSI entry assistance screens for both programs. (Although the assistance screens allow you to enter a custom value for the conversion, they will also supply the value for most common conversions.)

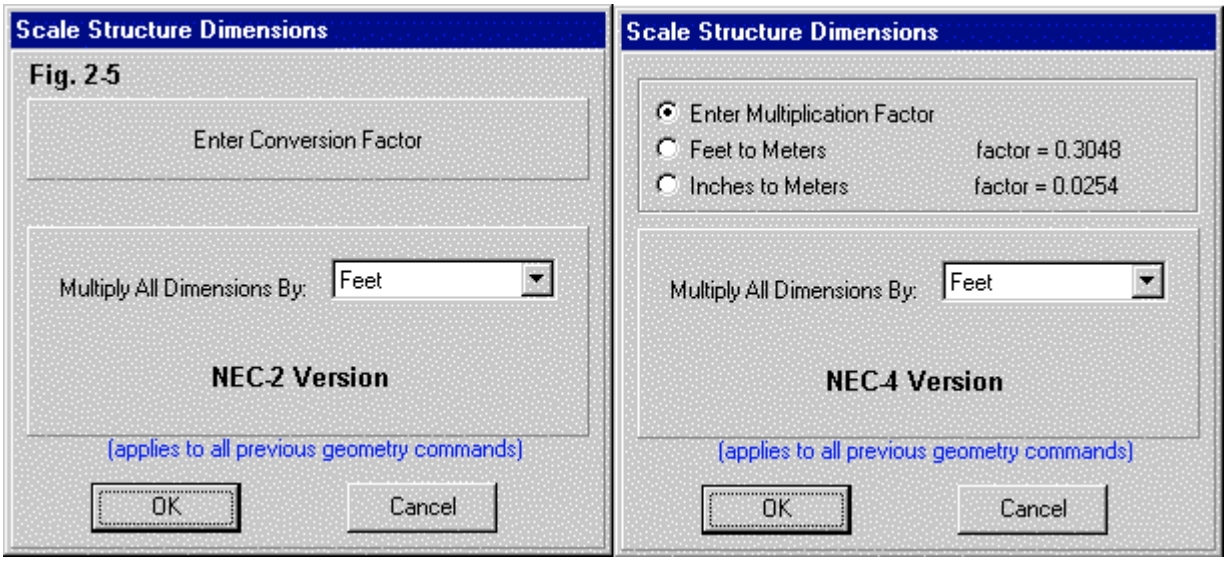

Note that the screens each carry the notation that the conversions apply to all previous geometry commands. There must be at least 1 preceding geometry command to convert, but the GS command need not be the last command preceding the GE, geometry end, command. Open model *2-3.nec* and examine the geometry section.

```
GW 1 11 0 -.82021 0 0 .82021 0 .003281
GW 2 11 -.82021 -.82021 0 -.82021 .82021 0 .003281
GS 0 0 0.304800
```

```
GE
```

The model is a conventional pair of elements, both entered in feet and converted to meters by the GS command. However, the GS command need not be the next-to-last command. Open model *2-3a.nec* and examine the geometry section.

```
GW 1 11 0 -.82021 0 0 .82021 0 .003281
GS 0 0 0.304800
GW 2 11 -.25 -.25 0 -.25 .25 0 .001
GE
```

The first wire is in feet, and the following GS line converts it into meters. The second GW command enters a new wire directly in meters. You may run the models, a rather poor parasitic arrangement of two linear elements, and obtain the same results. The forward gain in free space is about 5.6 dBi, with a 9.3-dB 180° front-to-back ratio. The source impedance is about 94 + j78 Ω. However, you may also confirm that the two alternative geometry entry sets yield the same antenna by examining the Necvu renderings, as shown in **Fig. 2-6**.

Fig. 2-6

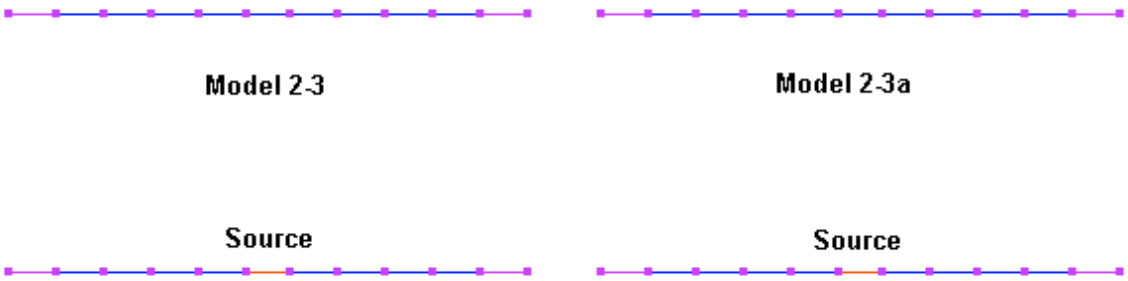

The final entry in the geometry section is always GE, to indicate the end of geometry entries and the beginning of control entries. Both NEC-2 and NEC-4 accept a simple GE entry, which is satisfactory for a free-space environment, such as used in the preceding models. However, NEC-2 GE commands accept a value of 0, 1, or -1 for position I1, the only numeric entry used. 0 indicates that no ground plane is present. 1 indicates that a ground plane is present. The current expansion is modified so that currents on a segment touching the ground in the X-Y plane at Z=0 are interpolated to their images below the ground and the charge at the base is zero. -1 indicates also that a ground is present, but the current expansion is not modified. Hence, currents on segments touching the ground will go to zero at the ground. However, the GE entry does not create a ground. You must use appropriate control commands (such as GD and GN) to specify the ground.

NEC-4 employs a more expansive GE command structure employing up to 3 integer entries. The first entry, I1, is similar to the comparable entry for NEC-2 and specifies whether or not the current expansion is modified. However, use an I1-entry of -1 if you place wires below the ground, or NEC-4 will return an error message. (Re-open model *1-3.nec* and modify the GE entry to a positive value of 1 for the I1 position. Run the model in NEC-4 and check the results.)

I2 gives the user control over the testing performed by the core on the model. An entry of -1 results in no testing of the model. 0, the default setting if you do not enter a value, tests the segments for illegal segment intersections (but not necessarily surface penetrations) and severe violations of the thin-wire approximation. The core produces both error and warning messages. Any error messages will cause the core run to stop, but warning messages will permit the run to continue. An entry of 1 at I2 allows either error or warning messages to stop the run. Entering a 2 in the I2 position tests the segments, but the core continues to run even with errors or warnings.

I3's default value is 0, in which case, no action occurs. Values of 1 or 2 allow the user to save the segment coordinates and currents for plotting in special formats. See the GNEC manual for further information on the formats available and on supplying a file name for the saved data.

In the end, for all but very specific uses, the GE entry depends most upon the I1 entry when wires touch the ground or penetrate the ground (NEC-4). The more complex the NEC-4 entry of GE, the less likely it is that NEC-2 will read it without returning an error. For simple free-space models, GE alone (with no following numerical entries) will handle most cases by presuming the appropriate default entries for the core used.

The GM Command: Replicating and/or Moving One or More Wires

We took a preliminary look at one function of the GM, coordinate transformation command when we replicated vertical dipoles to form an array of 5. I structured that model (the 2-2-series) so that it would read using either NEC-2 or NEC-4 in the NSI software. However, as shown in **Fig. 2-3**, that condition exists only because the command replicates the entirety of the existing structure, that is, all of the preceding GW entries. Mastery of the GM command requires that we attend to its individual numerical entries, as well as certain differences between the NEC-2 and NEC-4 versions of the command.

In order to reveal those differences, let's begin with a fairly simply model. Open model *2-4.nec*.

```
CM Reversible 2-element Yagi
CM Individual wires
CE
GW 1 15 0. .25 0. 0. -.25 0. .001
GW 2 15 .174 .23 0. .174 -.23 0. .001
GW 3 15 -.174 .23 0. -.174 -.23 0. .001
GE 0
FR 0 1 0 0 299.7925 0
GN -1
EX 0 2 8 00  1.00000  0.00000
RP 0 1 361 1000 90. 0. 1.00000 1.00000 0.
EN
```

The antenna is a reversible 2-element Yagi in a free-space environment. GW1 defines the reflector. GW2 defines the active driver, as indicated by the EX0 entry, which specifies tag 2 as the wire on which we have placed the voltage source. GW3 is a second driver, presently inert. However, simply by changing the EX0 entry to specify tag 3, we can reverse the direction of the main forward lobe. **Fig. 2-7** provides the Necvu rendering of the antenna, along with the phi plot

derived from it. The forward gain is about 6.1 dBi, with an 11.2-dB 180° front-to-back ratio, roughly standard for 2-element Yagis. The source impedance is 50.6 + j4.4Ω.

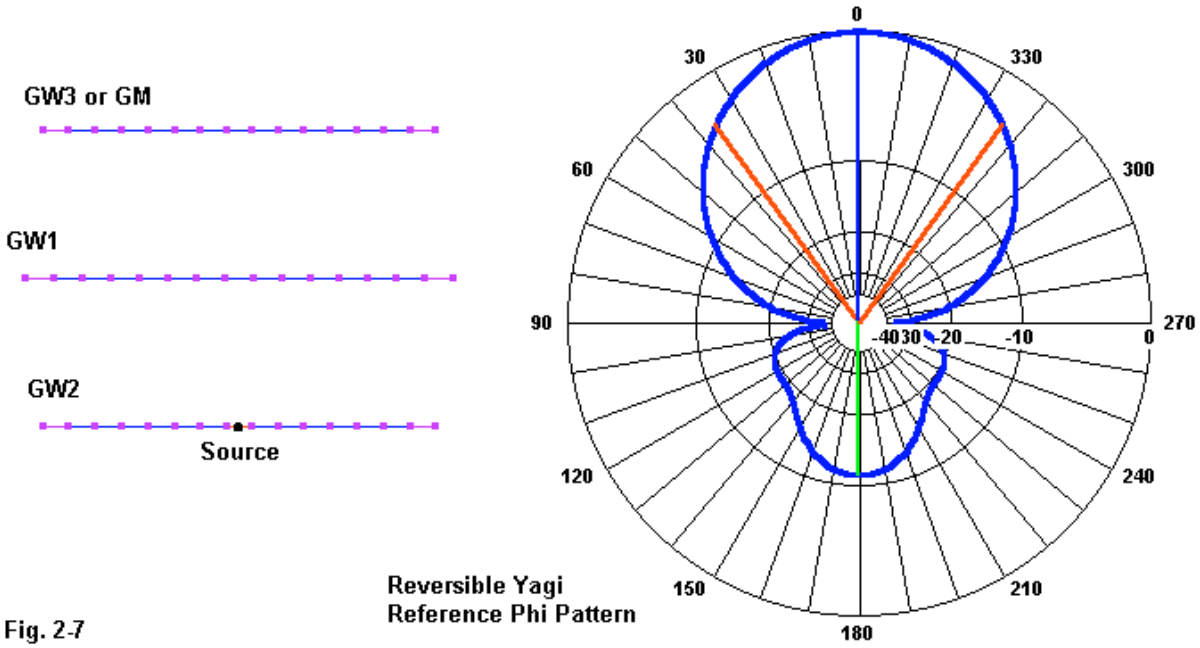

Fig. 2-7

As an exercise, we shall replace GW3 with a GM entry in order to differentiate NEC-2 and NEC-4 versions of the command. Models that the two cores do not read equally well will use a *-necN* suffix on the file name to alert you to that fact. Using NEC-2, open model *2-4a-nec2.nec*. Examine the model in Necvu to confirm that it results in the same set of elements as the original model.

```
GW 1 15 0. .25 0. 0. -.25 0. .001
GW 2 15 .174 .23 0. .174 -.23 0. .001
GM 1 1 0 0 0 -.348 0 0 002.002
GE 0
```

Now let's expand the GM line to see how we used it to create a substitute for the original GW3 entry.

```
Cmd   I1    I2    F1    F2    F3    F4    F5    F6    F7
      ITG1  NRPT  ROX   ROY   ROZ   XS    YS    ZS    IMOV
GM    1     1     0     0     0     -.348 0     0     002.002
```

ITG1: This entry specifies the tag (wire) number increment to be applied either to the present structure or to the created structure. If we leave everything else in the line at zero, we simply increase the tag numbers by the indicated amount.

NRPT: The second integer entry specifies the number of new structures to be generated. If NRPT is zero, then any other instructions apply to the original structure. Since the instructions will either rotate or displace the structure, nothing will remain in its original place. If NRPT is 1 or higher, then the instructions apply to the new structure, and the original structure remains in its

original place.

ROX, **ROY**, **ROZ**: These floating decimal entries specify the angle in degrees through which the structure (new or original, depending on the value of NRPT) will be rotated around the indicated axis. A positive value causes a counterclockwise rotation. Since rotation is around a specified axis, a set of values displaced from a centered position across a given axis will rotate around the axis, not around the center of the structure.

XS, **YS**, **ZS**: These entries specify the amount by which the structure is translated or moved along or parallel to a given axis with respect to the coordinate system.

Note: The order of operation always begins with rotation in the order X, Y, and Z, followed by translation in the order X, Y, and Z. If you wish to move a structure before rotating it, use two GM entries.

IMOV: IMOV is unique to NEC-2 and uses the decimal point to separate two separate integer fields: IMOV1 and IMOV2. IMOV1 indicates the first tag/wire number to which the instructions apply. IMOV2 indicates the ending tag/wire. Early versions of the NEC-2 core used a slightly different entry at this point, but NEC-Win Pro and GNEC use the one shown.

The sample GM line creates one replica of GW 2, with a tag number incremented up by 1, at a distance from the original of -0.348 m, which places the new inert driver on the opposite side of the reflector at the same spacing as the active driver. Run the model and confirm the performance data.

If you have NEC-4, open model *2-4a-nec4.nec*.

```
GW 1 15 0. .25 0. 0. -.25 0. .001
GW 2 15 .174 .23 0. .174 -.23 0. .001
GM 1 1 0 0 0 -.348 0 0
GE 0
```

The GM line has the following parts.

Cmd	I1	I2	F1	F2	F3	F4	F5	F6	F7	F8	F9	F10
	ITG1	NRPT	ROX	ROY	ROZ	XS	YS	ZS	IT1	IS1	IT2	IS2
GM	1	1	0	0	0	-.348	0	0	2	1	2	15

All entries through F6 have the same meaning as in the NEC-2 version of the command. However, in the time between the development of NEC-2 and NEC-4, the limitation on the number of usable floating decimal places relaxed. Hence, NEC-4 is able to use individual entries for the starting and ending segment that the command will manipulate. IT means a tag number, with 1 as the starting tag and 2 as the ending tag. IS1 is the starting (relative) segment on IT1, while IS2 is the ending segment on IT2. In this case, as in most, the specification will include the entirety of one or more wires, but you may choose to replicate or otherwise change only selected segments within a single wire. The restriction on both forms of the GM command is that the tag numbers must be less than the tag number that results from the increment called for in position ITG1. If you have NEC-4, run the model and confirm the performance reports.

In **Fig. 2-3**, we saw that the right-hand side of the assistance screens for NEC-2 and NEC-4 were the same, since they contain the tag-increment, number of replicas, rotations, and translation information that is the same for both versions of the GM command. As shown in **Fig. 2-8**, the left-hand portion of those screens differs according to the NEC-2 limitation on the scope of what you may replicate or alter.

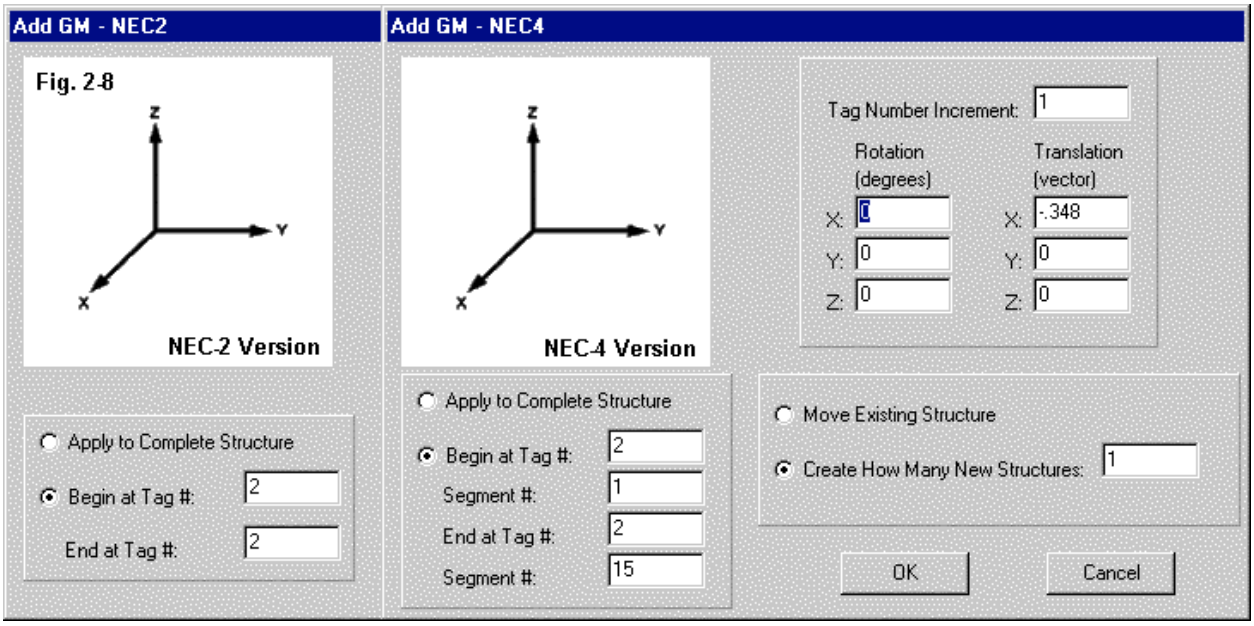

Although the reversible-direction Yagi illustrates the principles for using the tag-selection feature of the GM command, it nets us no savings in the model file. Therefore, let's examine a similar but more extreme case of wire-replication and movement: a planar reflector and dipole driver. The reflector will consist of a wire-grid structure that is 1.2 m per side, using a grid spacing of 0.1-m (or 0.1 λ at the test frequency of 299.7925 MHz). To simulate a solid surface, a wire grid should use wires having a radius that is the segment length or cell size divided by 2*π. In this case, the wire radius is 0.0159155 m. We shall use a 0.436-m dipole extended along the Z-axis using a 0.004-m radius. **Fig. 2-9** portrays the antenna, along with theta (E-plane) and phi (H-plane) patterns. The free-space forward-gain is 9.3 dBi with over 18 dB front-to-back ratio and a source impedance very close to 50 Ω resistive.

Fig. 2-9

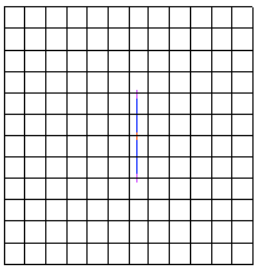

Planar Reflector Wire Grid
Plus Dipole Driver
(View angled to show dipole.)

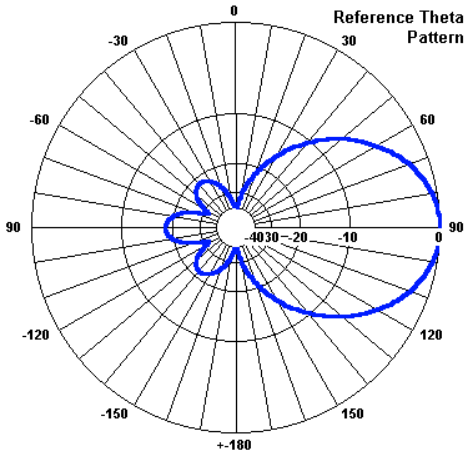

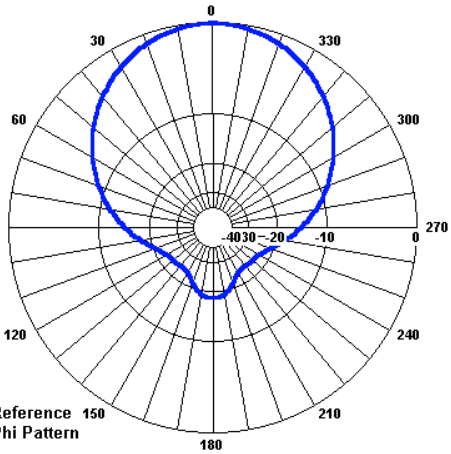

We have two major alternatives for building the model involved. The first way is to construct the wire-grid reflector wire by wire. Open model *2-5.nec* and examine the 313 separate wires, one of which is the dipole. The following listing shows only the first 10 wires of the model.

```
GW 1,11,.18,0.,-.218,.18,0.,.218,.004
GW 2,1,0.,-.6,-.6,0.,-.5,-.6,.0159155
GW 3,1,0.,-.5,-.6,0.,-.4,-.6,.0159155
GW 4,1,0.,-.4,-.6,0.,-.3,-.6,.0159155
GW 5,1,0.,-.3,-.6,0.,-.2,-.6,.0159155
GW 6,1,0.,-.2,-.6,0.,-.1,-.6,.0159155
GW 7,1,0.,-.1,-.6,0.,0.,-.6,.0159155
GW 8,1,0.,0.,-.6,0.,.1,-.6,.0159155
GW 9,1,0.,.1,-.6,0.,.2,-.6,.0159155
GW 10,1,0.,.2,-.6,0.,.3,-.6,.0159155
```

There are numerous entry-level and adjunct programs that will allow you to construct such wire-grids. Run the model and confirm the performance results. You may find slight differences in the NEC-2 and NEC-4 outputs, largely due to the thickness of the dipole relative to its 11 segments.

A simple means of constructing the wire grid makes use of the GM command. Open either model *2-5a-nec2.nec* or model *2-5a-nec4.nec*. The wire section of both models follows for reference.

2-5a-nec2

```
CE
GW 1,11,.18,0.,-.218,.18,0.,.218,.004
GW 2 12 0 -.6 -.6 0 -.6 .6 .0159155
GM 0 12 0 0 0 0 .1 0 002.002
GW 3 12 0 -.6 -.6 0 .6 -.6 .0159155
GM 0 12 0 0 0 0 0 .1 003.003
GE 0
```

2-5a-nec4

```
GW 1,11,.18,0.,-.218,.18,0.,.218,.004
GW 2 12 0 -.6 -.6 0 -.6 .6 .0159155
GM 0 12 0 0 0 0 .1 0 2 1 2 12
GW 3 12 0 -.6 -.6 0 .6 -.6 .0159155
GM 0 12 0 0 0 0 0 .1 3 1 3 12
GE 0
```

The only differences between the two models are those required by the different means of specifying the start and stop tags for the wires. In both cases, we begin below the dipole entry with a wire (GW2) extended along the Z-axis at one edge of the intended grid. Since each side is 1.2-m long, we give the wire 12 segments. Then we use the GM command to repeat the wire 12 times (for a total of 13 wires so that we have a perimeter wire around the construct). Next, we create another wire (GW3) along one edge of the grid space parallel to the Y-axis. We also assign 12 segments to it so that each segment junction will intersect a wire end for the 13 wires we just made. Finally, we invoke the GM command to create 12 more copies of this wire, each one 0.1-m further up the Z-axis. Each segment junction in this wire set will intersect either a segment junction or a wire end of the first set of wires. Note that we were able to use tag numbers 2 and 3 for the initial wires because we did not increment the tag numbers for the GM-created wires.

If you compare the structure specification sections of the initial model and the new ones, you will discover that both versions have 323 total segments. However, the GM-based versions have only 3 tag numbers and only 27 wires. The cost for such economy is that any slight change in the specification of either GW2 or GW3 will throw the entire grid into a morass of illicit intersections of wires at other than wire or segment junctions.

So far, we have not used the GM command to simply move an existing structure. Therefore, let's modify our models one more time by adding a new GM command just above the GE command.

```
GM 0 0 0 0 0 0 0 10
```

The new command applies to the entirety of the structure that we have so far created. Hence, its form will be the same in both NEC-2 and NEC-4, since we need not specify start and end tag numbers. In fact, those floating decimal entries do not appear. As well, we do not increment the tag numbers or make any copies, so the first two numerical entries are both zeroes. The next 3 entries handle rotation, which we have yet to examine. The last three positions handle coordinate transformations, and we have moved the assembly 10 meters in a positive Z direction. The horizontal centerline is now 10 meters above the Z=0 line or 10 meters or wavelengths above ground, should we choose to add a real or perfect ground to the model. We can confirm this fact within Necvu prior to running the model by using the "Identify Segment" function, as shown in **Fig. 2-10**. I have darkened the segment-identification square that corresponds to the entry panel at the left of the graphic.

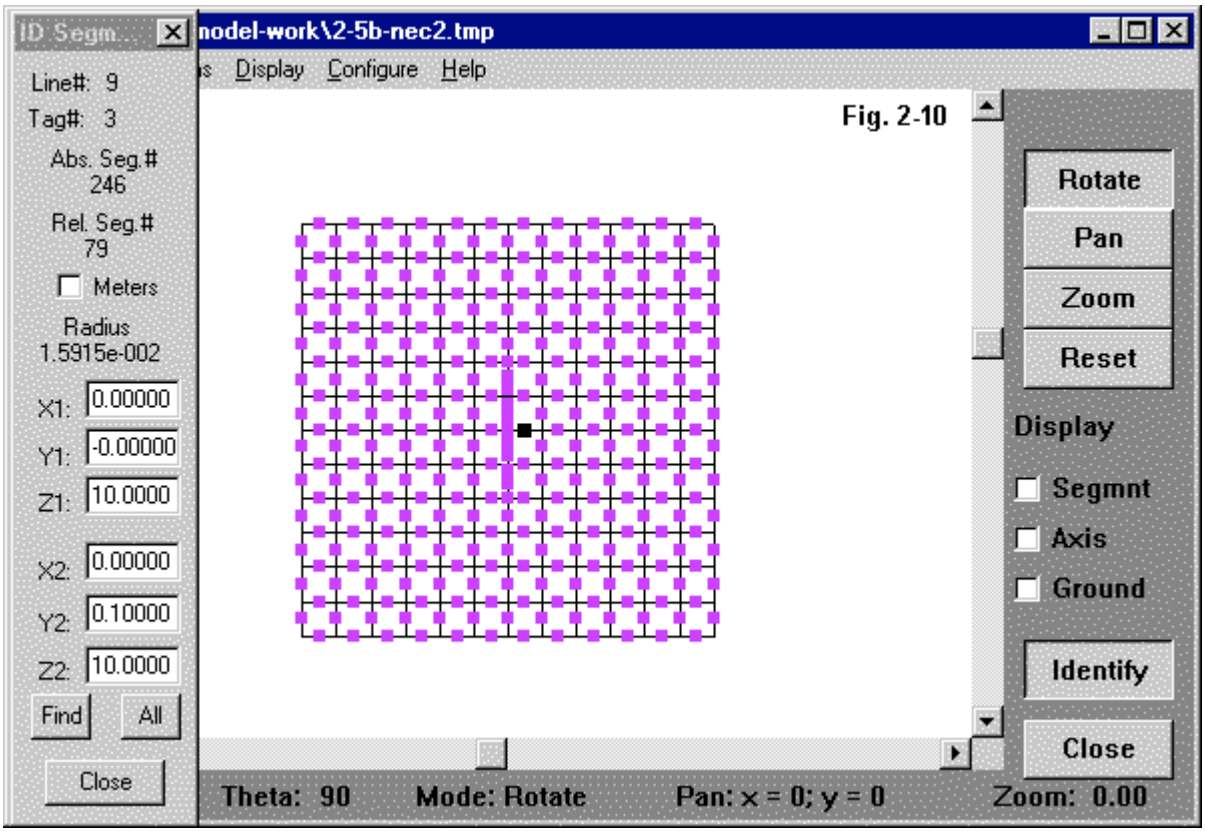

The GM command is very useful when transforming models created within a free-space environment into models over a selected ground system. Very ordinarily, we construct free-space models by centering them at the coordinate system origin. For some models, elevating all parts to an appropriate height above Z=0 for tests using ground can be daunting. However, a single GM command can accomplish the same task very simply.

The GM Command: Rotating One or More Wires

I have saved the rotation feature for this section, because using it requires care. Of course, we can simultaneously rate and move or rotate and replicate--or all together, but only within the rules of progression that attach to the GM command. As noted earlier, the order of operation always begins with rotation in the order X, Y, and Z, followed by translation in the order X, Y, and Z.

Open model *2-6-necN.nec*, where N = 2 or N = 4 according to your core. The models consist of 2 3-element Yagis at different heights above average ground. The NEC-2 geometry section looks like the following lines.

```
GW 1 11 0. -.2434 4. 0. .2434 4. .003175
GW 2 11 .1763 -.2308 4. .1763 .2308 4. .003175
GW 3 11 .3471 -.2134 4. .3471 .2134 4. .003175
GM 0 0 0 0 0 -.17355 0 0
GM 0 0 0 0 45 0 0 0
```

```
GW 4 11 0. -.2434 3. 0. .2434 3. .003175
GW 5 11 .1763 -.2308 3. .1763 .2308 3. .003175
GW 6 11 .3471 -.2134 3. .3471 .2134 3. .003175
GM 0 0 0 0 0 -.17355 0 0 004.006
GE 1 0 0
```

Only the last GM line is different in the NEC-4 version.

```
GM 0 0 0 0 0 -.17355 0 0 4 1 6 11
```

The two 3-element arrays form a stack with each antenna fed in phase. The initial models for each Yagi used X = 0 for the reflector position. Since I wished to rotate the upper antenna, I needed to move the antennas rearward by 0.17355 m along the X-axis so that each is centered at X = 0 and Y = 0. The first GM entry performs the move on the top Yagi (GW1 - GW3). Since this line moves the entire structure, there is no difference between the NEC-2 and NEC-4 versions of the line. However, the last GM entry moves only the lower Yagi (GW4 - GW6). Therefore, the 2 cores require different formats for the tag-specific move.

Only after moving the top Yagi rearward to center it does the rotation command appear in the model--the second GM entry. Since it applies to the entire structure so far defined--the moved top Yagi--we can use the same GM format for both cores. The 45° rotation is entered as a positive angle, moving the antenna in a counterclockwise direction, that is, 45° relative to the Cartesian coordinate and the phi schemes. **Fig. 2-11** shows the Necvu representation of the moved and rotated antennas, as well as reference theta and phi patterns. The phi pattern uses a theta angle of 86°, while the theta pattern uses the composite main forward-lobe heading of 23°, about halfway between the forward headings of the two individual Yagis.

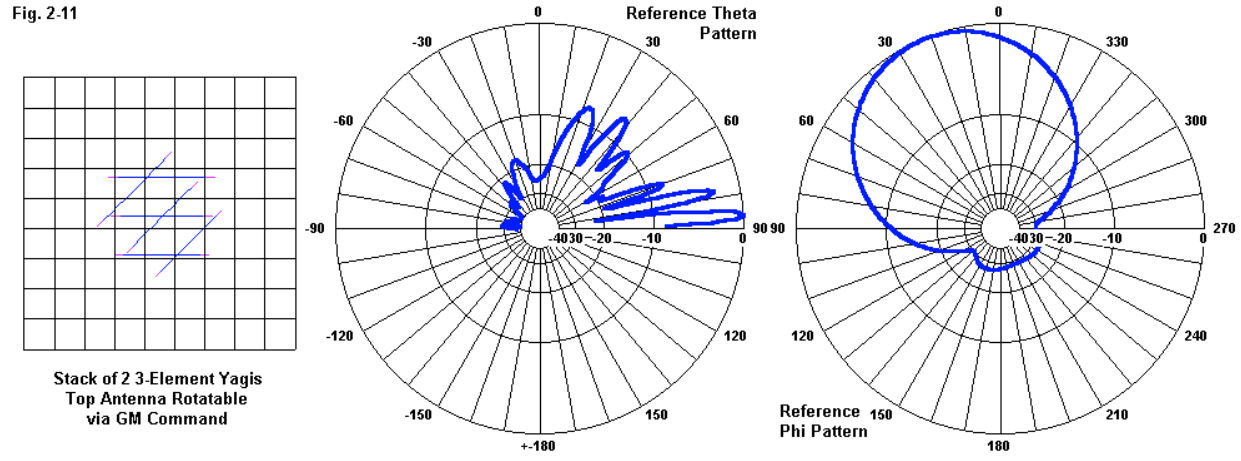

The geometry of this somewhat forced situation illustrates the need in this case to use two separate GM commands to effect the correct translation of coordinates, followed by a rotation. With only a single GM command containing both the rotation and the coordinate transformation, we would have obtained very different results. Open model *2-6a-necN.nec*, where N indicates the core that you are using. The only difference between this version of the model and the preceding one is that the rotation and transformation entries for the top antenna occur in a single GM line.

```
GM 0 0 0 0 45 -.17355 0 0
```

Since the rotation occurs before the movement of the top 3 wires along the X-axis, the two antennas no longer have a common center, as shown in the right portion of **Fig. 2-12**. Just how far off the antenna is becomes clear by comparing the segmentation data in the NEC output reports for the 2 models.

Fig. 2-12

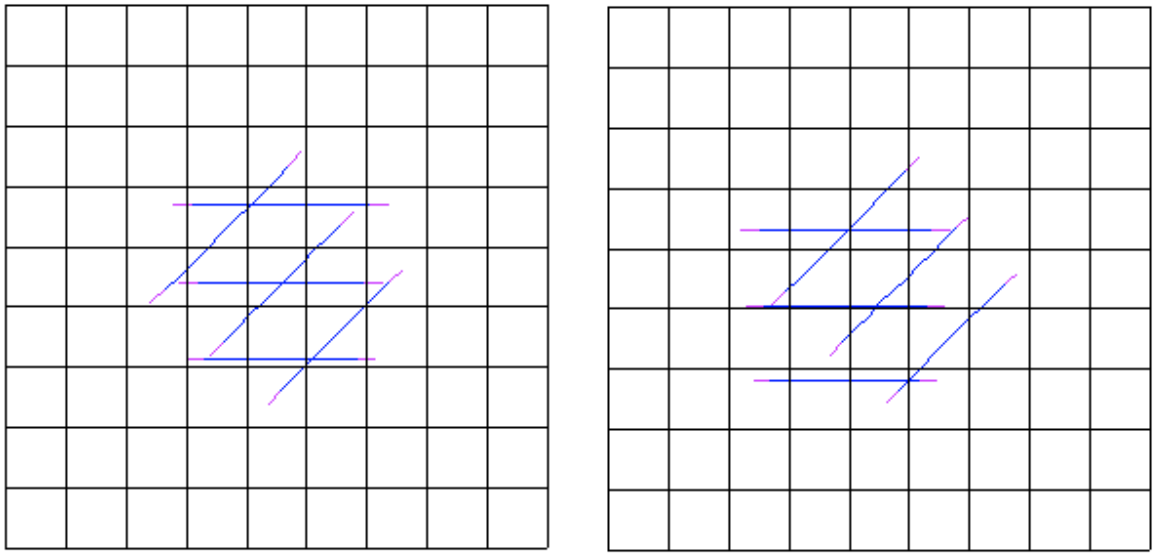

Model 2-6 Model 2-6a

There are numerous occasions for simultaneously rotating and replicating structures. Open model *2-7.nec*. In this instance, the same model is satisfactory for both NEC-2 and NEC-4.

```
GW 1 4 0 0 .125 .05 0 .125 .001
GW 2 4 0 0 .125 0 .05 .125 .001
GW 3 4 0 0 .125 -.05 0 .125 .001
GW 4 4 0 0 .125 0 -.05 .125 .001
GW 5 5 0 0 0 0 0 .125 .001
GE 1 -1 0
```

The geometry section describes 4 top-hat radials (GW1 - GW4) at the top of a vertical monopole (GW5) that reaches down to a perfect ground. The normal order for such a model might well be to begin with the monopole, working from the ground upward, and then to define the top-hat radials from the center outward. Equally one might describe the radials from the outer tips inward to the monopole junction, with the monopole defined from the top down to the ground. Either of these schemes would preserve the current magnitude and phase relationships along the wire segments. Model *2-7.nec* varies from both optimal procedures so that a single version of the GM command works with both cores. Geometrically, this version works I the sense of producing correct pattern and source data. As shown in **Fig. 2-13**, it yields the theta pattern and maximum gain values given. For reference, the source impedance is about 20.1 - j3.8 Ω in NEC-4 and about 20.2 - j2.5 Ω in NEC-2.

Fig. 2-13

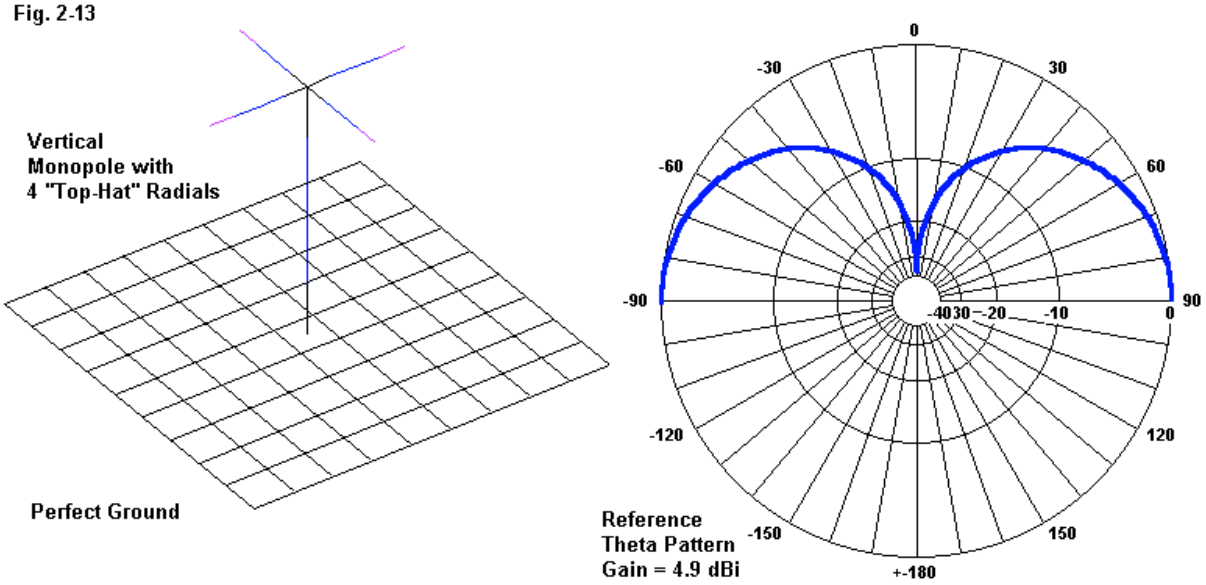

We do not need to use a separate wire for each radial in the top hat. Instead, we may define the first radial and use the GM command to replicate the 3 other copies, rotating each new copy by 90°. Although this action is perhaps trivial in the sample model, most top-hat systems (and ground radial systems) consist of many wires (up to about 120 for broadcast antenna radial systems). Hence, the technique is certainly relevant to numerous modeling applications. To see the format of such a model, open model *2-7a.nec*. We shall examine here only the geometry portion of the full model.

```
GW 1 4 0 0 .125 .05 0 .125 .001
GM 1 3 0 0 90 0 0 0
GW 5 5 0 0 0 0 0 .125 .001
GE 1 -1 0
```

Because the GM command appears before we introduce the monopole, we may apply the command to the entire structure defined so far (even if that structure is only 1 wire). However, we might also have defined the GM command as applying to a specific range of tags (and segments in NEC-4). The GM entry calls for 3 new versions of GW1, each incremented in tag number by 1 relative to the tag assigned. As well each replica is rotated 90° relative to the Z-axis. All rotation occurs relative to the selected axis where the other two values (in this case, for X and Y) are zero. Hence, to use this option requires that we place the center of rotation, which is end 1 of the selected wire (or wires, as we shall see), on the axis of rotation. If the final assembly needs to be somewhere else in the coordinate system, then must move it with a subsequent GM command.

You may examine the completed model using Necvu and run the model to confirm that it yields results identical to those produced by the initial model. As well, examine the NEC output report segmentation data section for both models to confirm that the resulting models are identical from the perspective of the core.

Just as we were able in earlier sample models to move collections of models, we are also able to

rotate multiple wires in a single GM command. Consider an alternative top-hat structure. The original version used 4 radials or spokes, each 0.05-m long at the test frequency. The length required is a function of the monopole length (0.125-m) and the desire for a near-resonant source impedance. As an alternative, we may use 4 shorter spokes and run a perimeter wire from one tip to the next. For near-resonance, the new spokes will be about 0.035-m long. The modeling involved in our simple example does not require that we calculate the length of the perimeter wires, but each one is about 0.0495-m long.

Open model *2-7b.nec* and examine the geometry portion.

```
GW 1 4 0 0 .125 .035 0 .125 .001
GW 2 3 .035 0 .125 0 .035 .125 .001
GM 2 3 0 0 90 0 0 0
GW 9 5 0 0 0 0 0 .125 .001
GE 1 -1 0
```

GW1 and GW2 define the initial pair of wires forming first section of the top-hat system. GW 2 simply creates a wire that runs from the outer tip of the first spoke to a position where the tip of the next spoke should be. However, to create the second spoke (and the remaining spokes), we need to use a GM command. While we are at the task, we might as well include the subsequent perimeter wires.

The GM entry performs the task using the same format as we used in the preceding model, with only one change. To give each new wire a unique tag number, the command specifies that we increment the tag numbers by 2. Hence, the monopole--to preserve its unique tag number--becomes GW9. We need not use unique tag numbers for the assembly to produce the left-hand portion of **Fig. 2-14**, as taken from Necvu. Since NEC calculates using the absolute segment numbers, we might easily have let all of the wires in the top hat system use the same tag number. You will determine whether wires need or do not need unique tag numbers according to the modeling task specifications that guide every real modeling job.

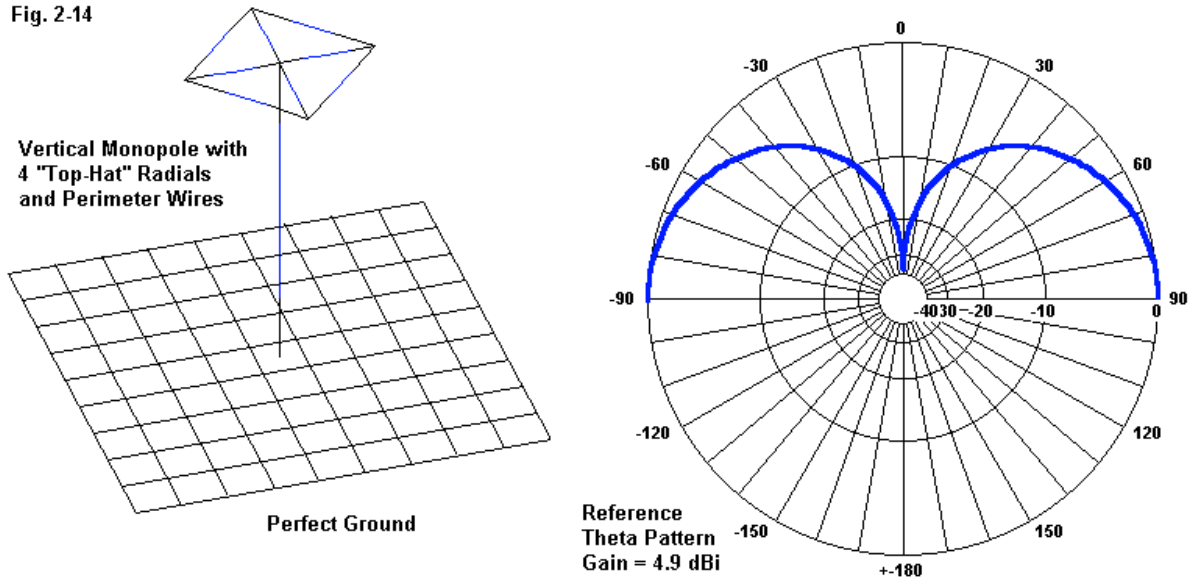

Although incidental to our goals in this chapter, you may run the model and note that the new version of the model has the same gain and just about the same source impedance as the version using only spokes.

Summing Up

In this chapter, we began by sorting out the various terms that we encounter when modeling above the entry-level. Each GW entry is a wire to which we assign a tag number that may be the same as or different from any number we might assign to the wire during planning. The segments within the defined tag are assigned relative segment number, and the entire set of wire segments that form the model have assigned absolute tag numbers. Many control commands allow us to specify either tag numbers and their associated relative segment numbers, or simply absolute segments numbers.

We next explored the structure of the most fundamental geometry commands. GW, the wire specification entry, like all other NEC commands, employs both integer and floating decimal entries to assign a tag number, specify the number of segments in the wire, define end 1 in terms of X, Y, and Z coordinates, define end 2 by X, Y, and Z, and finally enter the wire radius. We may use any unit of measure, so long as we use the same unit throughout the collection of geometry entries that precede a GS command. GS allows us to scale the geometry into meters, the unit of measure used within core calculations. Note that for control commands that may involve measurements, there is no corresponding scaling command, so those commands must be in meters.

GS has slightly different forms in NEC-2 and NEC-4. Hence, small model revisions may be necessary when changing cores. Likewise, GE, the geometry end command has somewhat different forms for each core. Depending upon the complexity of the GE command, a switch in core may or may not require revision of the entry.

In this chapter, we also included one of the most versatile commands in the entire geometry set: GM, the coordinate transformation command. So long as we attend to the restrictions, we may move an existing geometry along any or all of the axes or rotate a specified set of wires. However, rotation precedes translation, and within each action, the order is X, Y, and finally Z. If a single GM entry does not produce the desired transformation, we may always employ successive GM steps. Besides moving an existing structure or partial structure, we may also replicate one or more existing wires and simultaneously rotate or translate them. If a GM entry does not encompass all of the preceding structure, then NEC-2 and NEC-4 have separate command entry forms that are not interchangeable.

Some of the remaining geometry commands that we shall explore in future chapters use fixed frameworks for their initial formation. To place these structures exactly where we need them to be in the final overall structure geometry will require the use of the GM command. Although entry-level programs usually omit this command (and effect wire movements and replications by other means), the step up to more advanced programs requires that we have a firm grasp of what we can and cannot do with the GM command. That is why we have included it among the most fundamental geometry commands available in NEC.

3.
GC, CW, and GA: Special Wire Shapes

***Objectives**: In this chapter, we shall examine 3 commands that yield special structural shapes. GC, a continuation of the GW command, allows both wire length and radius tapering, and has a special format. CW, a NEC-4-only command, permits modeling catenary wire curves. Finally, GA provides the ability to model arcs ranging from a few degrees to a complete circle.*

The three commands that we shall tackle in this exercise set--GC, CW, and GA--have little in common except the fact that they all result in the construction of special shapes for wire structures. Each command has its own special idiosyncrasies. Perhaps that fact gives us a good reason for grouping them together: to explore the range of ways in which the formulators of NEC were able to give the modeler considerable flexibility in creating model structures.

GC: Continuation Data for Tapered Wires

GC is not an independent command. It does not create a new wire. Instead it modifies a preceding existing wire. Hence, it requires attention not only to its own content, but as well to the entries of the GW command just above it. To get a feel for the GC command, let's begin with a standard dipole. Open model *3-0.nec*, a very basic free-space dipole.

```
CM Dipole element continuous
CE
GW 1 19 0 -.237 0 0 .237 0 .001
GE
FR 0 1 0 0 299.7925 1
EX 0 1 10 00 1 0
RP 0 1 361 1000 90 0 1.00000 1.00000
EN
```

The GW entry is most important to us. Note that it must end with the non-zero entry of the wire radius. However, if we wish to use the GC command, we must meet two initial criteria. First, the GW command on which GC rests must enter a zero for the wire radius. Second, without the preceding GW entry, the GC command is meaningless and will result in an error.

The first step in our work will be to explore the ability of the GC command to length-taper the segments of a wire. We normally do not have many occasions on which to taper a simple dipole, but the antenna is handy for illustrating the principles involved without getting lost in more complex geometric structures. However, to create a taper to the length of the segments, we must work outward from the source segment. Therefore, we need one more preliminary step before we come face to face with the GC command. Open model *3-1.nec*.

```
CM Dipole element subdivided
CE
GW 1 23 0 -.237 0 0 -.005 0 .001
GW 2 1 0 -.005 0 0 .005 0 .001
GW 3 23 0 .005 0 0 .237 0 .001
GE
```

The model is identical to 3-0 with two exceptions. First, the dipole now has a total of 47 segments. Second, the segments are divided into 3 wires. Between the two 23-segment wires is a 1-segment source wire. **Fig. 3-1** shows the differences in the top 2 portions of the sketch. Despite the difference in the number of segments, the two models produce very similar results. For example, the 19-segment model shows a source impedance of 71.6 - j1.0 Ω, while the 3-wire version reports the impedance as 71.8 - j0.1 Ω.

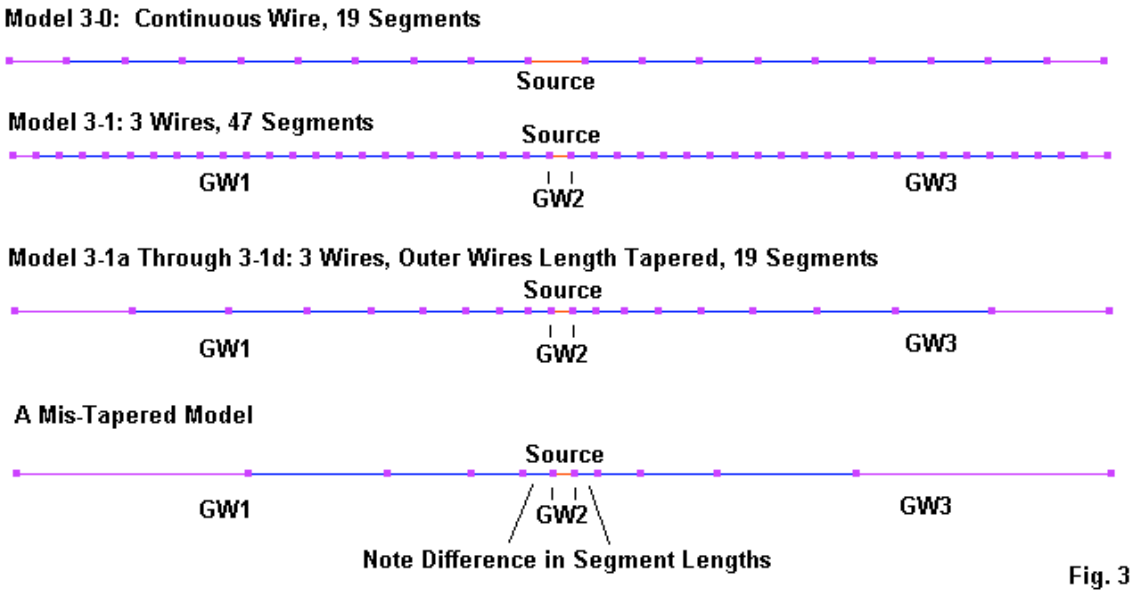

Fig. 3-1

Now we are ready, but only for NEC-2. Open model *3-1a-nec2.nec*.

```
CM Dipole element subdivided
CM NEC-2 GC for length-tapering
CE
GW 1 9 0 -.237 0 0 -.005 0 0
GC 0 0 .8163265 .001 .001
GW 2 1 0 -.005 0 0 .005 0 .001
GW 3 9 0 .005 0 0 .237 0 0
GC 0 0 1.225 .001 .001
GE
```

First notice the structure of the GW line, with the zero entry for the wire radius. Then note the GC lines that follow GW1 and GW3. The NEC-2 structure of the GC line is as follows, using the entry after GW1 as a model.

```
Cmd   I1    I2    F1          F2    F3
      Blank Blank RDEL        RAD1  RAD2
GC    0     0     .8163265    .001  .001
```

The integer entries on the NEC-2 version of the command are always blank, and zeroes indicate that fact to the core. However, the other entries require some explanation.

RDEL is short for the ratio of Δ, the abbreviation for segment length. The value indicates the ratio between a given segment, Δ1 or DEL1, and the next segment, Δ2 or DEL2. As always in NEC, segment counting proceeds from end 1 toward end 2 of a defined wire, in this case, the wire GW1 in the model.

Normally, we use length tapering to gradually increase segment lengths away from a necessarily short segment in order to reduce the total number of segments in a construct and thus shorten the run time. In this case, the short segment that we cannot alter is the source segment. Under some circumstance, we may need a short segment, for example, when we model parallel transmission lines as a parallel pair of physical (GW) wires. The tapering proceeds outward from the short segment in terms of moving from short segments to longer ones. In the model, the GC following GW3 has a ratio greater than 1 because the segments grow longer as we proceed from end1 to end 2 of the wire. For the sample command, the ratio is less than 1 because the wire segments grow shorter as we move from end 1 toward end 2. Because we are creating a symmetrical structure, the two ratios are the inverse of each other.

The lengths of the segments in a length-tapered wire depend upon three factors: the total length of the wire (L), the number of segments (NS) in a wire, as specified in the GW entry, and RDEL. The length of the first segment (Δ1 or DEL1) will be

$$DEL1 = \frac{L(1 - R_{DEL})}{1 - (R_{DEL})^{NS}}$$

In practice, determining the correct number of segments to use in a specific case may require some trial and error mixing of the number of segments and the specified segment-to-segment length ratio. **Fig. 3-1** shows a good selection in the third entry that reveals the length tapering on each side of the source segment. However, the bottom version shows a poor selection, since the last segment of the decreasing section and the first segment of the increasing section have different lengths.

RAD1 and RAD2 have somewhat obvious meanings as the radii of the first and the last segments of the collection. Since we are only tapering the length of the wires, we insert the common radius for all of the wires into these entry positions.

As a matter of passing interest, the source impedance of this NEC-2 length-tapered model of the dipole is 70.9 - j3.1 Ω.

NEC-4 often attempts to expand the options available to the modeler, usually without eliminating the ones available in NEC-2. NEC-4 adds two new ways to length taper a wire to the one that we just explored. If you have NEC-4, open model *3-1a-nec4.nec*. Since the control commands are identical for the entire series of models, we shall examine only the geometry section of the model.

```
GW 1 9 0 -.237 0 0 -.005 0 0
GC 2 0 0 .001 .001 .05 .01
GW 2 1 0 -.005 0 0 .005 0 .001
GW 3 9 0 .005 0 0 .237 0 0
GC 2 0 0 .001 .001 .01 .05
GE
```

We immediately notice the differences in the GC entries. At least one of the integer entries has a non-zero value, and there are 5 floating decimal positions. Let's explore the meanings of the entries by extracting the first NEC-4 GC command below GW1.

```
CMD   I1    I2       F1    F2    F3    F4    F5
      IX    Blank    RDEL  RAD1  RAD2  DEL1  DEL2
GC    2     0        0     .001  .001  .05   .01
```

IX provides the options. If IX=0, then we use the same entries as we did in NEC-2, when the zero was a placeholder for a blank entry. If IX=1, then we specify only the length of the first segment, omitting an entry for the RDEL. The program calculates the remaining segments based on the number of segments specified and the total length of the wire. When X=2, we omit the RDEL entry but specify the length of both the first and the last segments on the wire. The program calculates a value for RDEL:

$$R_{DEL} = \frac{L - DEL1}{L - DEL2}$$

The program also ignores the number of segments specified in the GW line and calculates a new value, N

$$N = 1 + \frac{\log (DEL2 / DEL1)}{\log R_{DEL}}$$

Since the program must round N to an integer, it also re-computes RDEL. The last segment in the sequence may differ slightly from the requested value due to the rounding of N. With too few segments and too high a value for RDEL, we can easily arrive at the mis-modeled situation at the bottom of **Fig. 3-1**.

Essentially, IX option 0 corresponds to the NEC-2 version of the GC command, and NEC-4 can read it. Likewise, most NEC-2 cores can read a NEC-4 GC, option 0. However, as indicated by the collection of NEC-Win Pro and GNEC assistance screens in **Fig. 3-2**, NEC-4 GC option 1 and 2 will contain entries that NEC-2 cannot read correctly.

Under option 2, you can sometimes usefully reverse a descending segment-length wire so that the segment lengths adjacent to the source segment have assured equality. Open *model 3-1b-nec4.nec* for a sample.

```
GW 1 9 0 -.005 0 0 -.237 0 0
GC 2 0 0 .001 .001 .01 .05
```

You may confirm the true symmetry of the model segments structure by examining the segmentation data in the NEC output report. As well, check the source impedance to see the minor excursions created by slightly different segment structures in all of the models.

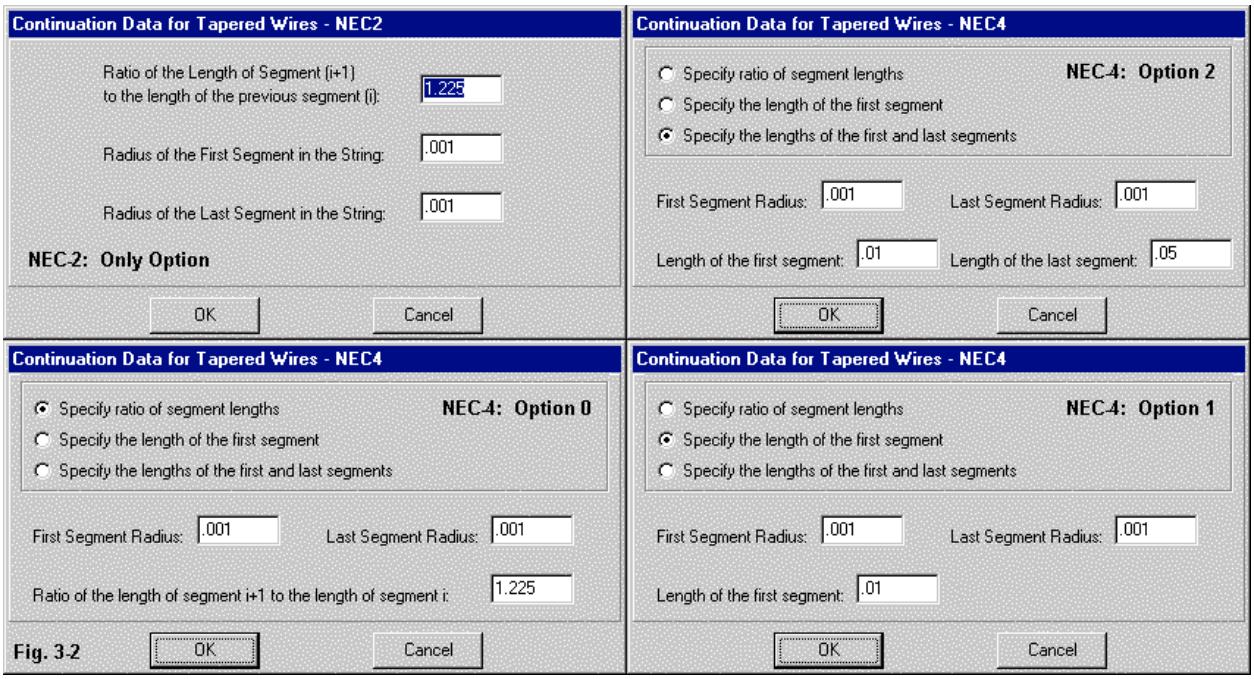

To confirm that option 0 in NEC-4's GC looks like the NEC-2 version of the command line, open model *3-1c-nec4.nec*.

```
GW 1 9 0 -.237 0 0 -.005 0 0
GC 0 0 .8163265 .001 .001
GW 2 1 0 -.005 0 0 .005 0 .001
GW 3 9 0 .005 0 0 .237 0 0
GC 0 0 1.225 .001 .001
```

Note that the NEC-4 line entry only uses the same number of entries as the NEC-2 version of the command. Hence, the line is readable by either core. However, even though limited in the scope of data entry, option 1 results in a NEC-4-only command line. Open model *3-1d-nec4.nec*.

```
GW 1 9 0 -.005 0 0 -.237 0 0
GC 1 0 0 .001 .001 .01
GW 2 1 0 -.005 0 0 .005 0 .001
GW 3 9 0 .005 0 0 .237 0 0
GC 1 0 0 .001 .001 .01
```

Once more, you may compare the segmentation data for each model in the 3-1 series to determine the level of symmetry obtained from each method of length-tapering the segments in a wire.

There are numerous instances where applications may call for length tapering without raising symmetry as an issue. Consider for instance a set of buried radials in a NEC-4 model of a monopole. Open model *3-2.nec*. We initially created the tapered-length monopole and radials in order to reduce the overall segment count of the model without reducing accuracy. Keyed to the shortest 1-segment wires in the model, uniform segment lengths would have required many hundreds of segments in this simple radial system and many thousand in a system with many

radials. Model 3-2 replicates the sample model *1-3.nec*. It consists of 32 GW entries for a vertical monopole and 4 radials. The model, over very good ground, has a maximum reported gain of 2.11 dBi at a theta angle of 73°. However, the AGT value for the model is 1.028 (or +0.119 dB), which yields an adjusted gain of 1.99 dBi.

Now open model *3-2a-nec4.nec*. This model is a GC-version of the same antenna, using option 2 of the command.

```
GW 1,11,0.,0.,40.,0.,0.,.327644,0
GC 2 0 0 .0125 .0125 13 .16328
GW 2,1,0.,0.,.327644,0.,0.,.163821,.0125
GW 3,1,0.,0.,.163821,0.,0.,0.,.0125
GW 4,1,0.,0.,0.,0.,0.,-.163821,.0125
GW 5,12,0.,0.,-.163821,40.9553,0.,-.163821,0
GC 2 0 0 .001 .001 .163281 13.5
GW 6,12,0.,0.,-.163821,0.,40.9553,-.163821,0
GC 2 0 0 .001 .001 .163281 13.5
GW 7,12,0.,0.,-.163821,-40.9553,0.,-.163821,0
GC 2 0 0 .001 .001 .163281 13.5
GW 8,12,0.,0.,-.163821,0.,-40.9553,-.163821,0
GC 2 0 0 .001 .001 .163281 13.5
GE -1
```

The use of the GC command on the radials and the upper portion of the monopole reduces the number of GW entries to 8. The resulting model has, in the most central region, the structure shown in **Fig. 3-3**.

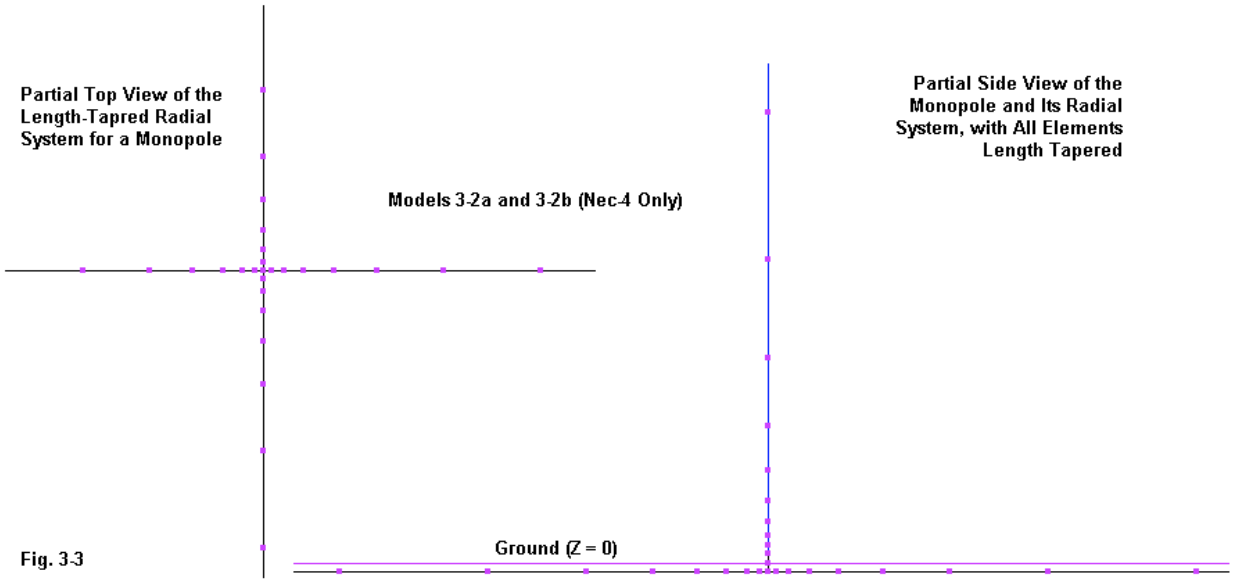

Fig. 3-3

The model reports a gain of 2.07 dBi at a theta angle of 73°. The AGT value is 1.019 (or +0.081 dB), resulting in an adjusted gain figure of 1.99 dBi, the same as in the non-GC-based length-tapered model. Both models report a source impedance of about 47 + j14 Ω.

Of course, there is no good reason why we should have to repeat the GW and GC entries for each radial. We may instead simply define the monopole and one radial. Then we can use the GM command to rotate and replicate the first radial 3 more times (or many more times for a large radial system). Open model *3-2b-nec4.nec* and examine the geometry portion.

```
GW 1,11,0.,0.,40.,0.,0.,.327644,0
GC 2 0 0 .0125 .0125 13 .16328
GW 2,1,0.,0.,.327644,0.,0.,.163821,.0125
GW 3,1,0.,0.,.163821,0.,0.,0.,.0125
GW 4,1,0.,0.,0.,0.,0.,-.163821,.0125
GW 5,12,0.,0.,-.163821,40.9553,0.,-.163821,0
GC 2 0 0 .001 .001 .163281 13.5
GM 1 3 0 0 90 0 0 0 5 1 5 12
```

GW5 defines the radial, while the following GC entry sets up the length tapering. The GM command replicates the other radials at successive 90° angles to the preceding one.

Thus far, we have not examined the other dimension of tapering offered by the GC command: wire radius tapering. If all we wish to do is to taper the radius of a wire via GC, then we may use option 0 in NEC-4 or the equivalent general GC command of NEC-2. Both are the same, and use the same equation to define a radius ratio, RRAD:

$$R_{RAD} = \left(\frac{RAD2}{RAD1} \right)^{1/(NS-1)}$$

The values of RRAD depends on the two values of radius that we insert in all versions of GC, as well as the number of segments in the previous GW command.

To illustrate the idea of radius tapering, let's consider a bi-conical dipole, that is, one that increases in radius as we move away from the center source section. A true bi-conical element would change radius in a smooth continuous manner along its length measured from the center outward. However, since NEC must operate using straight wires such that each segment has the same radius along its length, we must simulate the bi-conical element using a stepped-radius method. **Fig. 3-4** illustrates the process. The radii of the segments immediately adjacent to the source wire/segment should be the same as the radius of that segment--and the length of all 3 center segments should also be the same.

Modeling a Bi-Conical Dipole

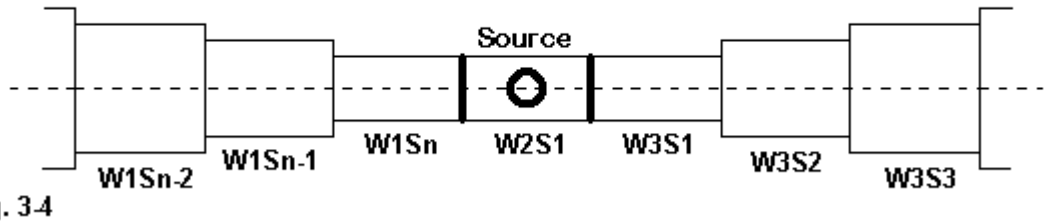

Fig. 3-4

Initially, we shall run the models that create the tapered-radius segments on NEC-4. Open model *3-3.nec*. This model shows a hand-tapered version of the bi-conical elements.

```
GW 1,1,0.,0.,1.7831,0.,0.,1.4589,.152
GW 2,1,0.,0.,1.4589,0.,0.,1.1347,.121
GW 3,1,0.,0.,1.1347,0.,0.,.8105,.0889
GW 4,1,0.,0.,.8105,0.,0.,.4863,.0571
GW 5,1,0.,0.,.4863,0.,0.,.1621,.0254
GW 6,1,0.,0.,.1621,0.,0.,-.1621,.0254
GW 7,1,0.,0.,-.1621,0.,0.,-.4863,.0254
GW 8,1,0.,0.,-.4863,0.,0.,-.8105,.0571
GW 9,1,0.,0.,-.8105,0.,0.,-1.1347,.0889
GW 10,1,0.,0.,-1.1347,0.,0.,-1.4589,.121
GW 11,1,0.,0.,-1.4589,0.,0.,-1.7831,.152
```

The upper end of this vertical dipole has a 6" radius. It tapers at the center to 1" and then increases again to 6" at the bottom. We can shorten the effort and the model description by using 3 wires, with the outer wires radius-tapered. Open model *3-3a.nec*.

```
GW 1 5 0 0 -1.7831 0 0 -0.1024 0
GC 0 0 1 .1514 .0254
GW 2 1 0 0 -0.1024 0 0 0.1024 .0254
GW 3 5 0 0 0.1024 0 0 1.7831 0
GC 0 0 1 .0254 .1514
```

Compare the segmentation data for the two models to determine how closely the GC-tapered version coincides with the hand-tapered model. Finally, we can combine length and radius tapering in one GC step, as illustrated by model *3-3b.nec*.

```
GW 1 5 0 0 -1.7831 0 0 -0.1024 0
GC 0 0 .8 .1514 .0254
GW 2 1 0 0 -0.1024 0 0 0.1024 .0254
GW 3 5 0 0 0.1024 0 0 1.7831 0
GC 0 0 1.25 .0254 .1514
```

In addition to changing the element radius between 1" and 6", we made the fatter segments longer to ensure a satisfactory segment-length-to-radius ratio. Because the GC command attached to GW1 has a descending radius from end 1 to end 2, the segment lengths follow suit, as indicated by option 0 and a length ratio that is less than 1.0. The ratio in the GC command attached to GW3 is the inverse of the first ratio value. If we run all three models, we obtain result close to the ones in the following table. All models use a test frequency of 31.6 MHz.

NEC-4 Results: Bi-Conical Element

Model	Impedance R +/- jX Ω	Reported Gain dBi	AGT	AGT dB	Adjusted Gain dBi
3-3	62.2 - j1.0	1.71	0.927	-0.331	2.04
3-3a	58.0 + j0.9	2.16	1.027	+0.117	2.04
3-3b	62.8 - j0.8	1.67	0.919	-0.365	2.04

Because NEC has a tendency to yield less accurate results when elements have a tapered radius, we automatically performed an average gain test (AGT). Although the raw gain reports show a wide range, the corrected values are all the same. All of the AGT scores fall in the "good" range, but in cases like this--where a close comparison is at stake--"good" may not be good enough without correcting the reports.

The reason that we initially used NEC-4 to obtain our reports is that the later core produces a more accurate report with a radius taper. Compare the NEC-4 table with the following NEC-2 table of results that use the same models.

NEC-2 Results: Bi-Conical Element

Model	Impedance R +/- jX Ω	Reported Gain dBi	AGT	AGT dB	Adjusted Gain dBi
3-3	64.0 - j38.2	1.24	0.832	-0.799	2.04
3-3a	56.8 + j31.9	1.83	0.954	-0.204	2.03
3-3b	65.8 - j24.5	1.15	0.815	-0.888	2.03

Despite the AGT scores that inspire no confidence in the adequacy of the models, the adjusted gain values coincide with each other and with those for the NEC-4 model. Given that the NEC-4 models show impedances values that cluster very close to resonance, we might uncritically give excessive credit to the models as accurate, despite the fact that the AGT scores are simply better than those for the NEC-2 model but still distant from perfect. To test the NEC-4 model reports further, I created a Leeson-corrected uniform-diameter element. Leeson substitute elements calculate both the required length and radius to perform their task as substitutes. Open model *3-3c.nec* to see the resulting model.

```
GW 1,11,0.,0.,2.0687,0.,0.,-2.0687,.11898
GE 0
```

Interestingly, the element produces the following able line (on either core).

NEC-2 Results: Bi-Conical Element

Model	Impedance R +/- jX Ω	Reported Gain dBi	AGT	AGT dB	Adjusted Gain dBi
3-3c	67.1 - j11.1	2.11	1.000	+0.001	2.11

Both cores fall short of the Leeson-element values largely because the radius taper is so great. Even NEC-4 has limitations in how well it can handle radically radius-tapered elements, despite its improvement over uncorrected NEC-2. To illustrate those limitations, let's examine a pair of Yagi antennas that we used in Chapter 9 ("Tapered-Diameter Elements") of *Basic Antenna Modeling*. Our initial use of them employed NEC-2 only. Here, we are dealing with both NEC-2 and NEC-4 and can perform a wider range of comparisons.

The use of Leeson substitute elements is subject to a number of restrictions, as suggested by the enabling and disabling features shown in **Fig. 3-5**. Normally, elements must be straight (without angular bends or corners) and symmetrical with respect to changes in diameter each side of center. The source must be centered, and any loads or transmission lines must also be only at the element center. As well, the corrections are functional only within about +/-15% of the half-wavelength resonant frequency. Programs that implement the correction system usually use a system to disable the system from operating in the presence of violations. The correction system will work on monopoles where one end is in contact with ground. However, such elements must also be straight, with sources, transmission lines, and loads restricted to the lowest segment of the antenna element. The +/-15% frequency rule also applies to monopoles.

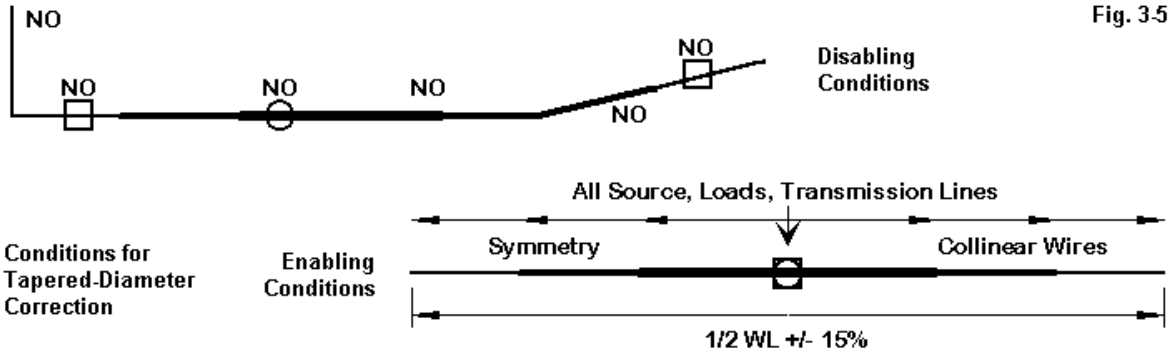

Fig. 3-5

Open model *3-4.nec*, a 5-element Yagi designed for 14.175 MHz. Each element in the array uses a number of wire diameters. The following sample shows only the reflector, since all elements use the same element-tapering scheme and differ only in length.

```
GW 1,5,0.,5.4763,0.,0.,3.9624,0.,.00794
GW 2,3,0.,3.9624,0.,0.,3.048,0.,.00953
GW 3,4,0.,3.048,0.,0.,1.8288,0.,.0111
GW 4,13,0.,1.8288,0.,0.,-1.8288,0.,.0127
GW 5,4,0.,-1.8288,0.,0.,-3.048,0.,.0111
GW 6,3,0.,-3.048,0.,0.,-3.9624,0.,.00953
GW 7,5,0.,-3.9624,0.,0.,-5.47637,0.,.00794
```

The total antenna requires 35 GW entries and 173 segments. In general, the taper that goes from a 1" center diameter to 0.625" at the element ends is gradual, and the center section is long. Under these conditions, we should expect to find no great disparity in reports from the 2 cores. In addition, open model *3-4a.nec*. This model provides the Leeson substitute elements. Each GW entry for this model is a separate array element.

```
GW 1 25 0 -5.3493 0 0 5.3493 0 .01075
GW 2 25 2.0269 -5.1125 0 2.0269 5.1125 0 .0109
GW 3 25 3.9411 -4.9233 0 3.9411 4.9233 0 .01102
GW 4 25 8.5832 -4.8828 0 8.5832 4.8828 0 .01105
GW 5 25 13.4721 -4.7209 0 13.4721 4.7209 0 .01116
```

The results of running the model follow. The Leeson results apply to both cores.

Gently-Tapered Elements

Core/Model	Free-Space Gain dBi	180° Front-to-Back Ratio dB	Impedance R +/- jX Ω
NEC-2/3-4	10.37	26.28	35.1 + j0.0
NEC-4/3-4	10.32	41.79	33.6 - j2.4
Both/3-4a	10.28	44.13	32.6 - j2.3

Given the gentle taper of the elements, none of the cores yields terribly wrong results relative to the Leeson version. However, NEC-4 does come closer to providing a result that coincides with the Leeson report values.

Let's try a more radical element diameter taper. Open model *3-5.nec*. Examine the element structure of this more complex arrangement. The short, fat segment at the center represents a modeling simulation of the effects of connecting the element to the boom. The previous Yagi used a split driver element for a direct feed to coaxial cable. This antenna is designed for use with a gamma match that permits direct element-to-boom contact. Once more, we show only the reflector, since all elements use the same general scheme of element construction.

```
GW 1,10,0.,5.4991,0.,0.,3.5052,0.,.00635
GW 2,6,0.,3.5052,0.,0.,2.4384,0.,.0079375
GW 3,6,0.,2.4384,0.,0.,1.2192,0.,.009525
GW 4,5,0.,1.2192,0.,0.,.1016,0.,.0111125
GW 5,1,0.,.1016,0.,0.,-.1016,0.,.0434213
GW 6,5,0.,-.1016,0.,0.,-1.2192,0.,.0111125
GW 7,6,0.,-1.2192,0.,0.,-2.4384,0.,.009525
GW 8,6,0.,-2.4384,0.,0.,-3.5052,0.,.0079375
GW 9,10,0.,-3.5052,0.,0.,-5.4991,0.,.00635
```

The array model requires 45 wires and 257 segments. However, the Leeson substitute-element version need be no larger than the first substitute model. Open model *3-5a.nec*.

```
GW 1 25 0 -5.3958 0 0 5.3958 0 .008425
GW 2 25 1.8288 -5.0076 0 1.8288 5.0076 0 .0086
GW 3 25 4.064 -4.9644 0 4.064 4.9644 0 .00862
GW 4 25 9.1186 -4.8935 0 9.1186 4.8935 0 .00866
GW 5 25 14.478 -4.715 0 14.478 4.715 0 .008765
```

The table of output report values has a far different look than our earlier table for the gently tapered Yagi.

Radically Tapered Elements

Core/Model	Free-Space Gain dBi	180° Front-to-Back Ratio dB	Impedance R +/- jX Ω
NEC-2/3-4	12.57	37.98	5.0 - j11.3
NEC-4/3-4	11.51	24.19	20.6 - j22.6
Both/3-4a	10.50	22.34	26.8 - j26.4

With the more radically tapered elements of the new Yagi, even NEC-4 is a full dB off the mark in overestimating the gain. Part of the problem lies in the very large element-diameter step that occurs close to the center of the element. This large step creates somewhat of a discontinuity in the current at the region of highest current magnitude. (In contrast, the first diameter step in the gently tapered model occurs at a considerable distance from the element center, and that step is relatively small.) The NEC-2 uncorrected report is only another dB of gain higher than it should be. As well, the impedance report is far off the mark. In contrast, the Leeson impedance report is just what the design calls for as the condition for adding a matching network.

To portray the differences between the consequences of gentle and radical element tapering on the core output reports, **Fig. 3-6** provides comparative E-plane (phi) patterns. Only the NEC-2 and the Leeson patterns appear in each case to reduce the potential confusion of lines. Model 3-4 yields overlapping patterns. However, model 3-5 shows the gain disparity vividly.

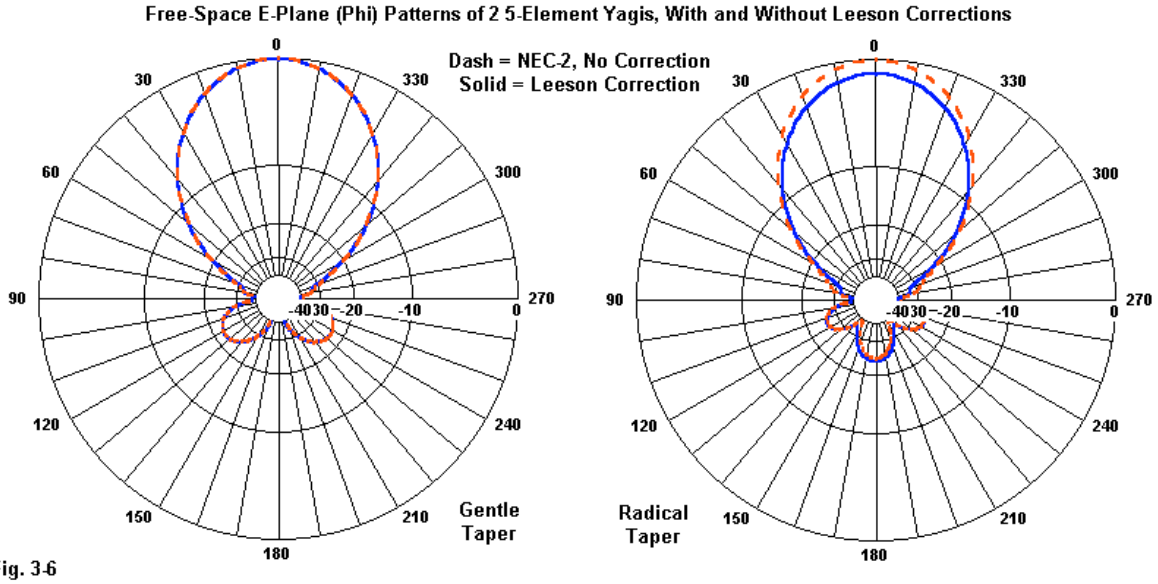

Fig. 3-6

If you see a pattern between the bi-conical element exercise and the Yagi exercise, you would not be mistaken. Normally tapered elements that begin with the largest diameter at the element center tend to produce gain reports that are opposite of those for bi-conically tapered elements with the smallest diameter at the center. Bi-conical elements tend to produce gain value reports that are below those of corrected substitute elements. Normally tapered elements tend to over-estimate the gain. These trends apply whether an element gets its taper from modeling it segment by segment or from invoking the GC command.

CW: Catenary Wire

The GC command expands in NEC-4 relative to its NEC-2 version because NEC-4 is able to use additional floating decimal places beyond the limit used in the earlier core. Those same "extra" floating decimal places also make possible some commands that are unique to NEC-4, for example, CW, the catenary wire command. The basic command line has the following structure.

Cmd	I1	I2	F1	F2	F3	F4	F5	F6	F7	F8	F9	F10
	Tag No.	No. Segs	X1	Y1	Z1	X2	Y2	Z2	Rad.	ICAT	RHM	ZM
CW	1	9	0	-.23	5	0	.23	5	.001	1	.25	4.9

I1, I2, and F1 through F7 are identical to the entries in a standard GW wire entry. We assign the new wire a tag number and prescribe the number of segments within it. We next define each end as X, Y, and Z coordinates. F7 identifies the wire radius. If the line precedes a GS entry, we may use any unit of measure that we can convert into meters before finishing the geometry. Only the final three entries, F8 through F10, require a detailed account. Since F8 will function like an integer entry and have 3 and only 3 possible entries, we likely should pause to set a few catenary relationships, as shown in **Fig. 3-7**.

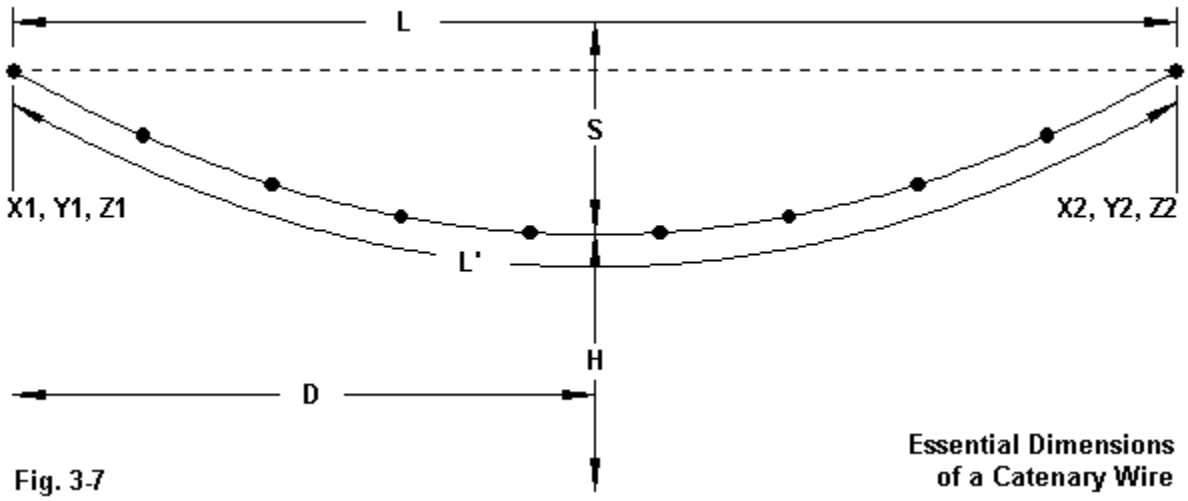

Fig. 3-7 Essential Dimensions of a Catenary Wire

A catenary wire is one that sags due to gravity and its own weight. Virtually all wires supported at their ends show some sag, although in the case of guy wires, careful tensioning of the wire controls the degree of curvature in the hanging cable. The figure shows some of the many ways of viewing a wire supported at its ends. **L** is the horizontal distance between the ends of the cable and would ordinarily determine the entries used for the end coordinates in F1 through F6 in a GW or a CW command. However, a hanging cable will normally have a longer total length, **L'**.

The distance, **D**, is measurable from either end, but in the CW command designates the distance in the chosen unit of measure between end 1 of the wire and the point of maximum sag. For a horizontal wire, this distance is normally half the value of **L**. However, if the wire has a non-conductive support cable at one end or if the wire is not horizontal, the point may be somewhere else along the wire. Because the CW command will divide the catenary wire into equal-length segments, the distance **D**, as used in the command, should not be too close to the wire end.

At the point of maximum sag, we may specify the amount of sag in two equivalent ways. Since coordinates Z1 and Z2 define the height of the wire, we may enter the value of the sag, **S**. If we select this method, we shall use a positive number for the amount of sag. If we enter a negative number, the model will yield an upward curve. Second, we can specify the height above Z = 0 of the point of maximum sag. This number must be less than the end values of Z or else we shall again obtain an upward curve. If Z1 and Z2 are not at the same height, then we can easily calculate the height of a straight wire at the distance **D** and then figure either the height above Z = 0 or the sag.

Before we plug these dimensions into an actual catenary wire, let's open model *3-6.nec*, a simple straight free-space dipole, as indicated by the GW entry.

```
GW 1 9 0 -.2375 5 0 .2375 5 .001
```

The only difference between this and similar dipoles that we have examined is that the model uses a value of 5 m for the Z coordinates. In free space, the Z coordinate makes no difference to the performance, and the resonant dipole has a source impedance of 71.7 - 0.2Ω.

All of our sample models in this series will use the dipole end coordinates and wire radius. For example, open model *3-6a.nec* and examine the CW entry.

```
CW 1 9 0 -.2375 5 0 .2375 5 .001 1 .2375 4.9
```

Through F7, the wire radius, the line is identical to the GW entry in the dipole. However, we have three further entries. F8 bears the label ICAT and may take values of 1, 2, or 3. In this case, the selection is 1, which indicates that we have chosen to specify a height of the point of maximum sag above Z=0. The entry following ICAT is called RHM and is for this option the straight-line distance from end 1 of the wire to the point of maximum sag (**D**). 0.2375 m represents the halfway point along the wire. F10, the last entry, has the label ZM, and for this option represents the height of the point of maximum sag (**H**) above Z=0. In this case, the height is 4.9 m.

For a free-space model only, it is possible to set the straight-line dipole wire at Z=0 or even at a negative value of Z. In such cases, the height value must be a negative value to avoid an upward curve.

Run the model and check the source impedance: 88.6 + 96.6 Ω.

Next, open model *3-6b.nec*. In this version, we shall use option 2 for F8, the ICAT entry.

```
CW 1 9 0 -.2375 5 0 .2375 5 .001 2 .2375 .1
```

When ICAT = 2, we once more use the distance **D** as the value for RHM, that is, for F9. However, instead of entering the height of the point of maximum sag above Z = 0, we enter the sag of the wire (**S**) below the height it would have if the wire were straight in F10, ZM. Although the sag is downward, we enter the amount of sag along the Z-axis as a positive number. (A negative number will yield an upward curve.) Since a sag of 0.1 m results in a height for that point of 4.9 m, we expect to obtain the same source impedance report when we run the model: 88.6 + 96.6 Ω. The model will not disappoint us.

Which version of the catenary wire command we use depends upon the values we might actually measure for a real wire. On some occasions, we may know only the length of wire that we must use to reach from end 1 to end 2 coordinates, and this wire length will be longer than the distance between the terminal coordinates. Under this condition, we may use option 3 for ICAT, as indicated in the CW command for model *3-6c.nec*.

```
CW 1 9 0 -.2375 5 0 .2375 5 .001 3 .52714
```

In this case, there is only one further entry past F8, ICAT. If the value in RHM, F9, is greater than the distance between the terminal coordinates, then the model produces a catenary wire. If the value is the same or less than the distance between the terminal coordinates, then the model produces a straight wire determined by the values of X, Y, and Z in F1 through F6. F10, ZM, is not used in this option and may be either blank or zero. The oddly long value for the length **L'** has a purpose: it yields a source impedance of 88.6 + 96.6 Ω. We now know about how long the wire is in the first two models using the CW command. Since the model fills each increment of the catenary curve with a straight wire, it is inscribed within the actual curve. Hence, the length of the sum of the individual segments will be slightly less than the length of an actual catenary curve.

How much less will be a function of the number of segments used to create the catenary wire model. There will be slight differences in the length of individual segments such that regions with a higher curvature result in shorter segments. The NEC-4 output report supplies both the calculated length of the catenary wire and the sum of the segment lengths in the structure specification portion of the report. For example, our option-1 model produces the following lines.

```
WIRE                                                                    NO. OF  FIRST  LAST   TAG
NO.      X1        Y1        Z1        X2        Y2        Z2      RADIUS   SEG.  SEG.   SEG.   NO.
          THE FOLLOWING WIRE IS A CATENARY,    1 2.37500E-01 4.90000E+00
          Catenary length = 5.27141E-01    Total segment length = 5.26554E-01
 1    0.00000   -0.23750   5.00000   0.00000  0.23750  5.00000  0.00100    9     1      9      1
```

Although our model uses only 9 segments, the total segment length is only about 0.1% short of the true catenary curve length.

GA: Wire Arc Specification

Not all special shapes available in the geometry command set either are unique to NEC-4 or even change their format in the transition from NEC-2 to NEC-4. GA, the wire arc specification, has a common form in both NEC-2 and NEC-4. The GA arc inscribes a series of straight lines (segments) within a calculated arc. The degree to which the GA creation approximates a circle is a function of the number of segments per degree of the selected arc.

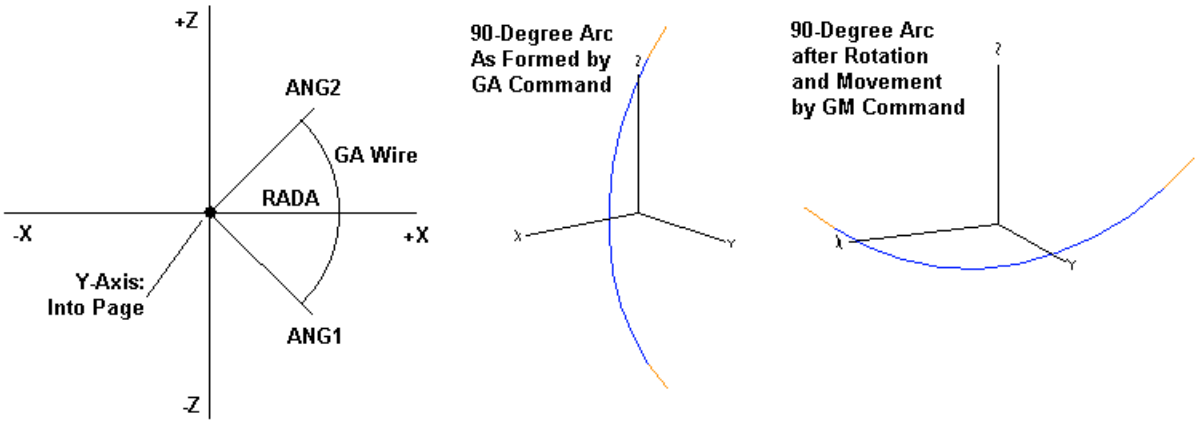

Creating and Positioning an Arc via GA and GM Commands

Fig. 3-8

Let's correlate the elements in the left-most portion of **Fig. 3-8** to an actual GA entry. Open model *3-7.nec* and examine the GA entry. (As usual and unless otherwise specified, the control commands will be simple, with a voltage source (EX0) and a test frequency of 299.7925 MHz.)

```
Cmd    I1     I2     F1       F2     F3     F4
       Tag    No.    RADA     ANG1   ANG2   RAD
       No.    Segs
GA     1      11     .303     -45    45     .001
```

As with virtually all geometry commands, we begin with an assigned tag number and the number

of segments the construct will have. The very last entry (F4, RAD) is the wire radius. The remaining 3 entries define the arc.

All initial arcs revolve around the Y-axis in a counterclockwise rotation with respect to the Z-axis. The initial arc radius is along the +X-axis. In free-space, we may use negative angles that result in an arc that extends below Z = 0. The sample line uses an arc radius (RADA) that is 0.303 m. The initial angle (ANG1) is -45°, which creates a starting point in the -Z region of the coordinate system. The terminating angle (ANG2) is +45°, which creates a final point in the +Z region. The core creates a series of 11 (the number of segments) straight lines inscribed in the calculated arc. To review the segments formed by the command, you have two sources of information. After running the model, you may check the output report segmentation data to find the center points of each segment and their lengths. The segment identification feature of Necvu provides the end coordinates of any selected segment.

The segmentation data provides an interesting glimpse into the process of inscribing straight wires within a calculated arc. Note that the X-coordinate for the center of the 6th segment is 0.30223, although we specified a radius of 0.303. The deficit is due to the fact that segment 6 is a straight wire that cuts off very slightly the curve of a true arc. As the segment length column shows, the command calculates the arc so that all segments have the same length (0.04323 m).

The model radius of 0.303 meters is not accidental. It yields a nearly resonant dipole when fed at segment 6 at the frequency specified in the FR line. In the E-plane, the gain is just under 2 dB, with a source impedance of about 65 Ohms. These values will be sensible to anyone who has modeled an inverted-Vee wire antenna, which brings its ends toward each other, but with straight-line legs.

The orientation of the arc is not especially useful. However, we may move it anywhere we wish via the GM command. Suppose that we wish to point the open side of the arc straight up and bring the bottom of the arc to a ground or Z=0 level. We can do so by using the GM command shown in model *3-7a.nec*.

```
GM 0 0 0 90 0 0 0 .303
```

The GM line specifies that we rotate the arc 90 degrees around the Y-axis so that the wire ends are upward. (Remember that the GM precedence list rotates before moving.) That rotation will bring the bottom of the arc below Z=0, so we may raise it on the Z-axis by the radius of the arc. The resulting segmentation table appears in the model output report. We can see from the table that the ends of the arc are stretched symmetrically across the Y-axis from -X to +X. Segment lengths remain unchanged by the translation and rotation exercise. Note the Z-value for segment 6. Instead of being zero, it is 0.00077. A true arc would rest at Z=0. However, because segment 6 is a straight line, it remains shy of zero by the same amount that the identical position in the first model remained shy of the specified arc radius. For both models, note that the alpha orientation angle increases by 8.18182 degrees with each segment. The right-hand portions of **Fig. 3-8** provide Necvu representations of the pre-GM and post-GM arcs. Note that in the right-most case, the axes are conventionalized to the center of the sketch and do not show the fact that the entire arc is above Z=0.

If you run this version of the model, you will obtain the same gain and source impedance reports.

However, the pattern will differ since we have changed the orientation of the wire with respect to the unchanged phi pattern request.

So far, we have been exercising the GA and GM commands only far enough to orient us to their use to create and position a desired arc. We have not yet built anything interesting. Let's build something. See **Fig. 3-9** and open model *3-7b.nec*.

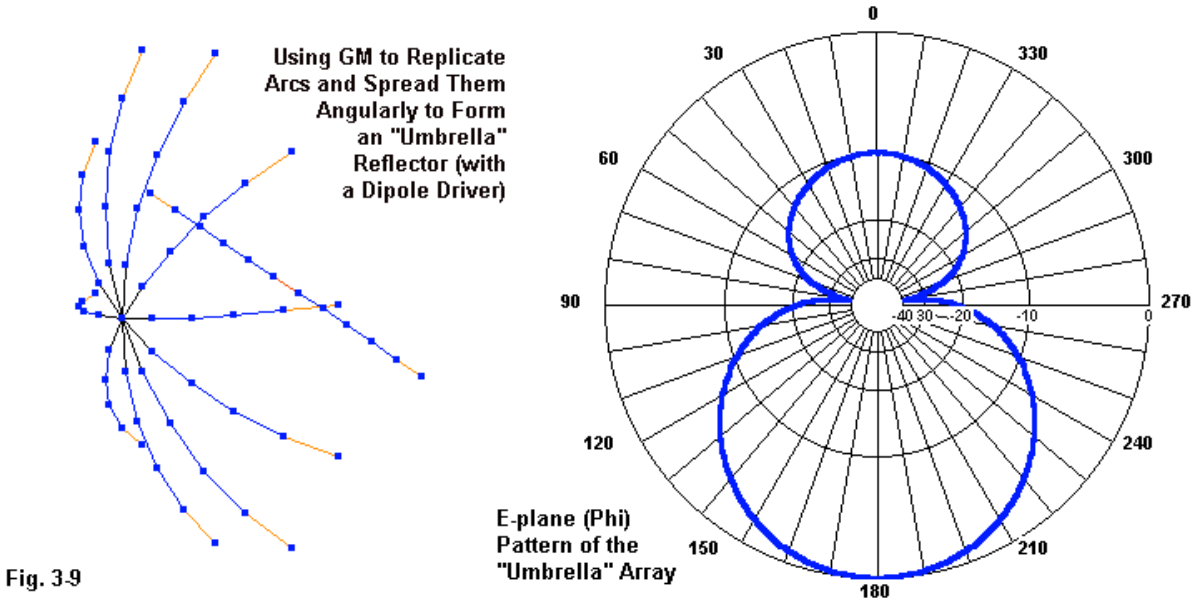

Fig. 3-9

```
GA 1 10 .303 -45 45 .001
GM 1 4 36 0 0 0 0 0
GW 6,11, .15,-.228,0, .15,.228,0, .001
```

The relevant geometry lines show initially that we have created an arc that is like the original with one exception. It has 10 segments so that a segment junction occurs at the very center. The next significant line is the GM command. It specifies that we shall increment the tag numbers by 1 and create 4 new structures identical to the entirety of the first. The third entry in the line specifies a rotation angle of 36 degrees for each new structure around the X-axis. By this means, we can create 5 full arcs or a 10-spoke "umbrella." Since we gave each arc 10 segments, each arc will join at the junction of segments 5 and 6. The left portion of **Fig. 3-9** shows the results of our modeling.

For this model, the umbrella ribs represent a reflector. Hence, the GW line with the tag number of 6 sets a near-resonant dipole ahead of the umbrella. For this exercise, I have not optimized the position of the driver relative to the reflector. Nor have I experimented with optimizing the arc size for maximum performance from the array. Nevertheless, even this rough and ready construct exhibits a reasonable 2-element parasitic beam pattern, as revealed by the pattern in the right-hand portion of **Fig. 3-9**. The free-space gain is 5.1 dBi, with a 9.9-dB front-to-back ratio. The feedpoint impedance is 61 Ohms resistive, since the spacing between the reflector and the driver center is about 0.75λ. You may experiment with the number of umbrella ribs, the size of the arcs, and the spacing of the dipole driver to further optimize performance.

We may use the GA command to create complete circles. Open model *3-8.nec* and look at the GA line.

```
GA 1 90 .169 0 360 .001
```

In this GA line, we specify a full 360-degree arc, that is, a circle. For simplicity, I specified ANG1 as 0 and ANG2 as 360. (Note that we must come full circle to the starting point to produce the last wire segment that closes the circle.) The arc has 90 segments. The number is arbitrary, but intentionally large so that the inscribed polygon will very closely approximate a circle. For many purposes, we may use far fewer segments, but we should be aware of the deficiency in the total circumference for polygons with fewer sides. **Fig. 3-10** provides three samples: a square, an octagon, and a 16-sided polygon, along with the ratio of their circumferences to the circumference of the circle within which they are inscribed.

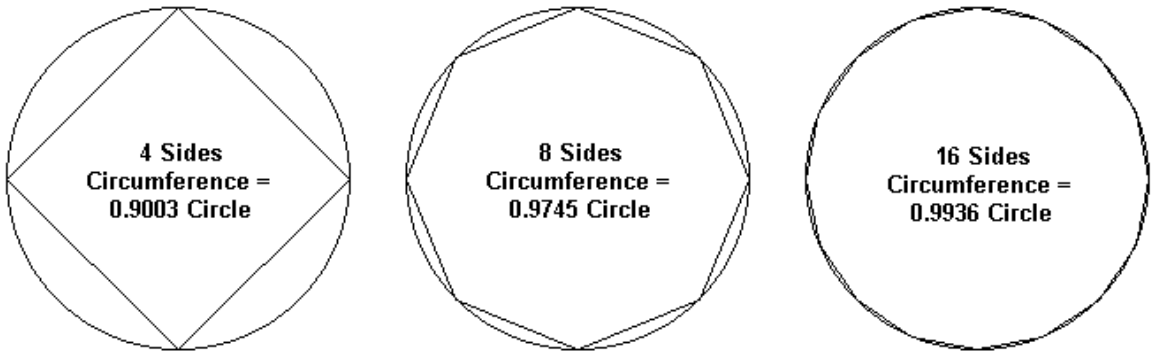

Inscribing Wires Within a Calculated Circle **Fig. 3-10**

An issue often raised by beginning modelers is to what degree a circular loop may outperform a loop with a smaller number of sides. Open model *3-8a.nec* and find a 16-sided polygon with dimensions that achieve resonance (within +/-j1 Ω) at the test frequency. This particular loop uses separate GW entries and gives you a sense of the economy that the GA command achieves, even with far fewer than the 90 segments specified in GA loop. Both models, incidentally, place the source at the bottom-most segment of their respective loops.

Even though a 16-sided loop appears to closely approximate a more completely circular form, there are differences in performance, as the following table reveals.

Model	No. Sides	Free-Space Gain dBi	Feedpoint Impedance R +/- jX Ω
3-8a	16 sides	3.63	140.2 + j 0.9
3-8	90 sides	3.68	142.3 - j 0.8

Given that a square loop shows a gain of about 3.39 dBi with a resonant feedpoint impedance of about 125 Ohms, we see that the closer approximations of a true circle continues the upward progression of values. Just how many segments our models of circles may require will be a task-driven decision.

Single quad loops have applications, but multi-element quad beams are more common, at least for many types of operation. Let's take one final construction step and compare a pair of typical 2-element quad beam models.

One of the models will be a pair of 90-segment loops formed from the GA command and any necessary GM movements. Open model *3-9.nec* to explore the geometry of the model.

```
GA 1 90 .1572 0 360 .001
GA 2 90 .1722 0 360 .001
GM 0 0 0 0 0 0 .1665 0 002.000
```

The loop radii are set to optimize performance for a balance of gain and 180° front-to-back ratio. The GM command moves the second loop 0.1665 m away from the first driven loop. Because the GM command applies only to the segments in GW 2, NEC-4 users will have to revise the command for that core.

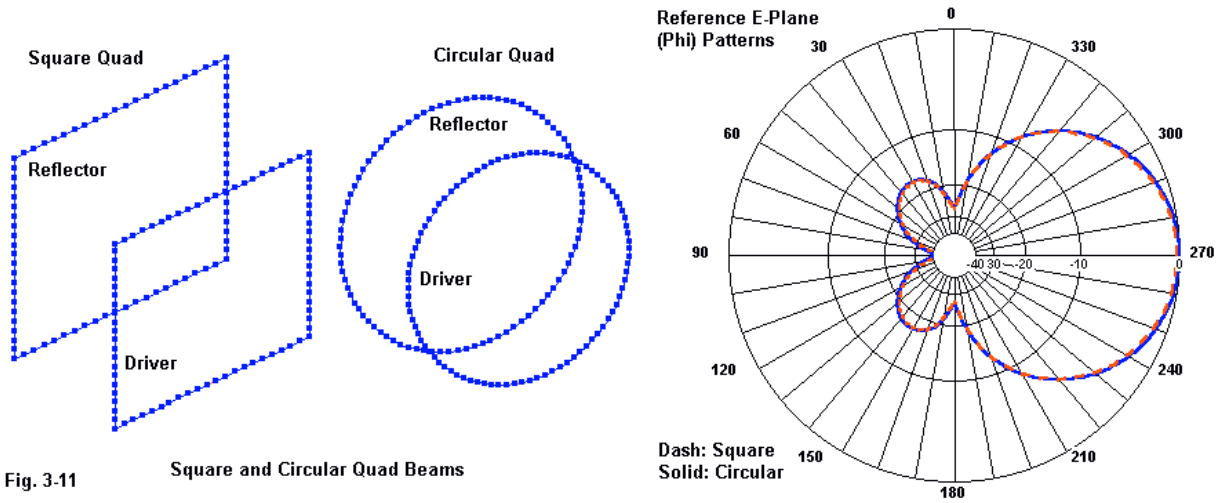

Fig. 3-11 Square and Circular Quad Beams

For comparison, open model *3-9a.nec*. This model provides a comparable and optimized 2-element quad beam using conventional square elements. The shape differences appear in the left portion of **Fig. 3-11**. The high number of digits in each coordinate entry results from the use of a set of optimizing algorithms that we shall explore much later in the chapter on modeling by equation.

```
GW 1 21 -0.12791534 0 -0.12791534 0.12791534 0 -0.12791534 0.001
GW 2 21 0.12791534 0 -0.12791534 0.12791534 0 0.12791534 0.001
GW 3 21 0.12791534 0 0.12791534 -0.12791534 0 0.12791534 0.001
GW 4 21 -0.12791534 0 0.12791534 -0.12791534 0 -0.12791534 0.001
GW 5 21 -0.13948821 0.165675855 -0.13948821 0.13948821 0.165675855 -0.13948821 0.001
GW 6 21 0.13948821 0.165675855 -0.13948821 0.13948821 0.165675855 0.13948821 0.001
GW 7 21 0.13948821 0.165675855 0.13948821 -0.13948821 0.165675855 0.13948821 0.001
GW 8 21 -0.13948821 0.165675855 0.13948821 -0.13948821 0.165675855 -0.13948821 0.001
```

Run both models. The NEC-2 results for the runs appear in the following table. "Cir." means circumference. Gain is referenced to free-space, and the front-to-back ratio is the 180° value. The overlaid E-plane patterns appear on the right in **Fig. 3-11**.

Model	Shape	Driver Cir. Meters	Reflector Cir. meters	Space meters	Gain dBi	Front-Back Ratio dB	Feedpoint Impedance R +/- j X Ω
3-9a	Squ.	1.0233	1.1159	0.1657	7.17	46.25	142.2 - j 1.3
3-9	Cir.	0.9877	1.0820	0.1665	7.37	42.17	160.2 - j 0.4

From a performance perspective, perhaps the difference in source impedance is the most notable factor, even though the circularized version manages about 0.2-dB additional gain. From a design perspective, one might note that perfecting circularization requires not only a change in the loop circumferences, but as well a revision of the element spacing in order to optimize performance. Deciding quad array matters is secondary in this exercise. Our basic premise was that the GA command--especially when combined with the GM command--gives us the ability to construct interesting and potentially useful structures. It does so in a manner that allows easy user control over design modifications, which is always a desirable feature of a model. The umbrella reflector and the 2-element circular quad beam are but two samples that help demonstrate the ease of construction and modification.

Summing Up

We have added to our geometry tools three commands that yield special wire shapes. Each one of the commands in this chapter has its own special characteristics that help us understand the range of command variations to expect.

GC, the wire specification continuation command, is not an independent command, but depends on a preceding GW entry with the wire radius set to zero. By entering a length tapering ratio and both beginning and ending wire radii, we can create segments with tapered lengths or with a changing radius--or both. The NEC-4 version of the command uses the added floating decimal places possible in that core to create options among the ways in which we can specify the tapering of segment lengths.

The CW or catenary wire command is unique to NEC-4 and employs 10 floating decimal places for entries that both create a wire and model its sag. The first portion of the command parallels a standard GW wire entry set. Then we may specify the height of the lowest point in the sage, the amount of sag, or the length of the wire that reaches the defined wire endpoints with the sag included.

Our final command in the collection, GA, allows us to create arcs ranging from small sections to full circles. Unlike the other commands in this chapter, the form is common to both NEC-2 and NEC-4. However, the command has a different unique property. We always create the arc around the Y-axis with the perimeter extending in the X- and Z-axes. If we wish it to have a different position or orientation, we must use the GM command to move the arc after its formation. Like the CW command and unlike the GC command, the GA command creates a new wire with the tag number and the number of segments specified in the command line.

Although each individual command is straightforward in its own structure, the overall set is a good sample of the ways in which NEC creates interesting and useful geometries. None of the remaining geometry commands should offer us any major surprises.

4.
GH in NEC-2 and NEC-4

***Objectives**: This chapter will take a long look at the formation of helices within NEC-2 and NEC-4. In the process, you will learn how the command structures used by each core differ from each other. As well, you will meet not only what the two cores have in common with respect to helix formation, but as well, what unique potentials each version of the command can offer.*

When NEC-2 emerged in the early 1980s, it did not contain a GH or helix-spiral specification command. An unofficial command gradually became a standard part of the geometry command set. When the NEC-4 version of the command emerged with the core program in the 1990s, its form differed considerably from the NEC-2 version. Unlike the GC command, where the differences simply added further capabilities, the newer version of the GH command changed the fundamental basis for forming a helix or a spiral. The commands are so different no NEC-2 helix will run under NEC-4 and no NEC-4 helix will run under NEC-2.

We shall follow the cue offered by the command structures and take up the two different command forms separately. We shall examine what prior calculations we must make in order to create a helix. However, that exercise is only part of our work. Each version of the command offers something unique that we cannot do with the other command. For example, the NEC-2 command offers us the opportunity to create oval as well as circular helices. The NEC-4 version lacks this capability, but offers instead a choice between Archimedes and log spiral structures. Only if we look thoroughly at each command in isolation do we stand much chance of keeping separate the many facets of helix and spiral formation.

Some Helix Basics

A helix is a special case of a spiral structure having a uniform radius from one end to the other and generally having a uniform turn arrangement. Ways of deriving the turn arrangement include counting the number of turns per unit of length or measuring the space between equivalent points on successive turns. If the starting and the ending radii differ, then the helix tends to be labeled a spiral. Unlike the uniform-radius helix that must have an increment of length from one end to the other, a spiral may have either a positive or a zero length. The NEC GH command offers the ability to form either helices or spirals.

Fig. 4-1 shows the basic dimensions of a standard helix, that is, a helix having the same radius or diameter from one end to the other. S is the turn spacing or the linear length of 1 turn of the helix. R is the radius, and 2R the diameter. If we stretch a single turn flat, we obtain the right triangle shown on the right side of the figure. C indicates the circumference of the turn, while L' indicates the length of wire required to obtain a full turn. Angle α is the pitch of the helix. For helices having multiple turns, we shall also be interested in the total helix length.

Fig. 4-1

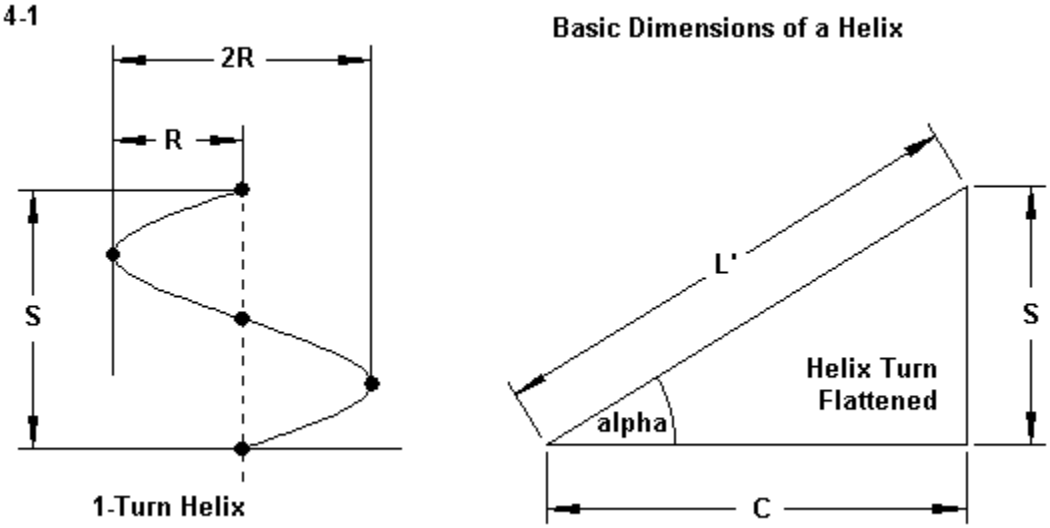

The dimensions are all interrelated by a few trig equations. All dimensions refer to center-to-center distances relative to the wires.

R = radius of the helix, wire-center to wire-center	
C = circumference of the helix	$C = 2 \pi R$
S = spacing between turns	$S = C \tan\alpha$
α = pitch angle	$\alpha = \tan^{-1} (S/C)$
N (or n) = number of turns	
L = axial length of helix	$L = n S$
D = conductor diameter	
L' = Conductor length for a single turn	$L' = SQRT(C^2 + S^2) = C/\cos\alpha = S/\sin\alpha$

There is a special sub-category of helical antennas called axial-mode helices. In order to design an axial-mode helix, we need select only a few of these dimensions and the rest will follow automatically. Perhaps the two most critical dimensions are the pitch angle and the circumference. In fact, basic helix theory tends to restrict axial-mode operation of the helix to pitch angles between 12° and 14°. As well, various texts restrict the circumference to ranges from either 0.8λ to 1.2λ (Kraus) or from 3/4λ to 4/3λ (Balanis). The number of turns in a helix is a builder selection, since gain (for any given pitch and circumference) rises with the number of turns. As well, selection of a wire diameter is also a builder choice, and the conductor size can make a difference to helix performance. If we are not designing an axial mode helix, but only a helix, the same structural rules apply, but we may ignore the constraints regarding pitch angle and circumference.

As with all NEC commands, helix formation involves approximating the continuous curve of the structure by inscribing a set of straight wires along the calculated path. Like the GA command, the GH command allows us to create close approximations of a truly circular form by using many segments per turn without having to calculate the precise positions of each segment. Indeed, we may by-pass the more complex calculations involved in spiral formations altogether and let the program show us the result of providing the command with a limited set of input values. As

always, we have the NEC output report segmentation data table as a reference to see the results of our work.

We shall begin our foray into each GH command version by forming standard helices. However, before we leave each version of the command, we shall sample a number of alternative forms in order to see how their formation within the GH command affects the shape of the resulting structure.

The NEC-2 GH Command

When forming a helix within NEC-2 you will need to make a number of basic decisions about the structure before creating the command. **Fig. 4-2** shows some of the major issues that you face.

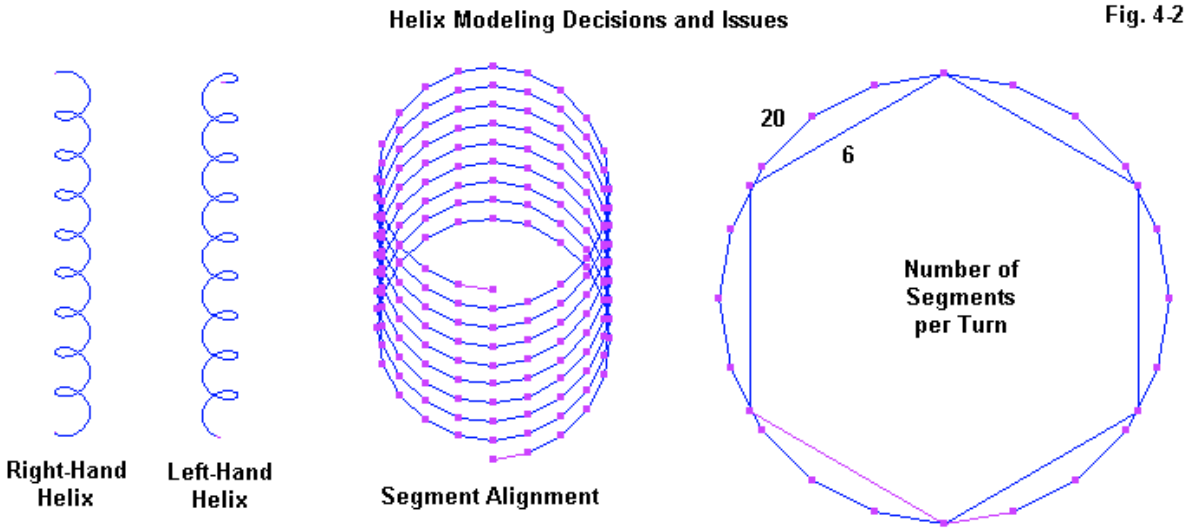

First, do you need a right-hand or a left-hand helical structure? The answer to this question derives from the modeling task specifications.

Second, how well will the segment junctions align? For helices with a large space between turns and a small wire diameter relative to that spacing, segment alignment is less important than for closely spaced fat-wire helices. The fact that helices use a curving structure does not release you from following NEC guidelines for maximum accuracy with close wire spacing.

Third, how many segments will you assign to each turn? As the graphic suggests, a small number of segments per turn may result in a total wire length that is significantly less than the wire length associated with a true circular shape. In general, about a value of 20 segments per turn creates a very reasonable approximation of the circular form, although you may alter that number for many special purposes or circumstance. For example, a dual or quadrifilar helix design may require a different value for the segments/turn value compared to a single helix to obtain the closest alignment of the segment junctions.

To use the NEC-2 GH command effectively, you should pre-calculate the essential dimensions of the helix using the equations that we earlier examined. The command itself asks for only partial data--enough to create a full helix, but often not enough to make obvious all of the relationships between turns or between segments. The following sample line will show what is at stake.

```
Cmd   I1    I2    F1      F2       F3    F4    F5    F6    F7
      Tag   No.   S       HL       A1    B1    A2    B2    RAD
      No.   Segs
GH    1     180   .3048   2.7432   .099  .099  .099  .099  .001
```

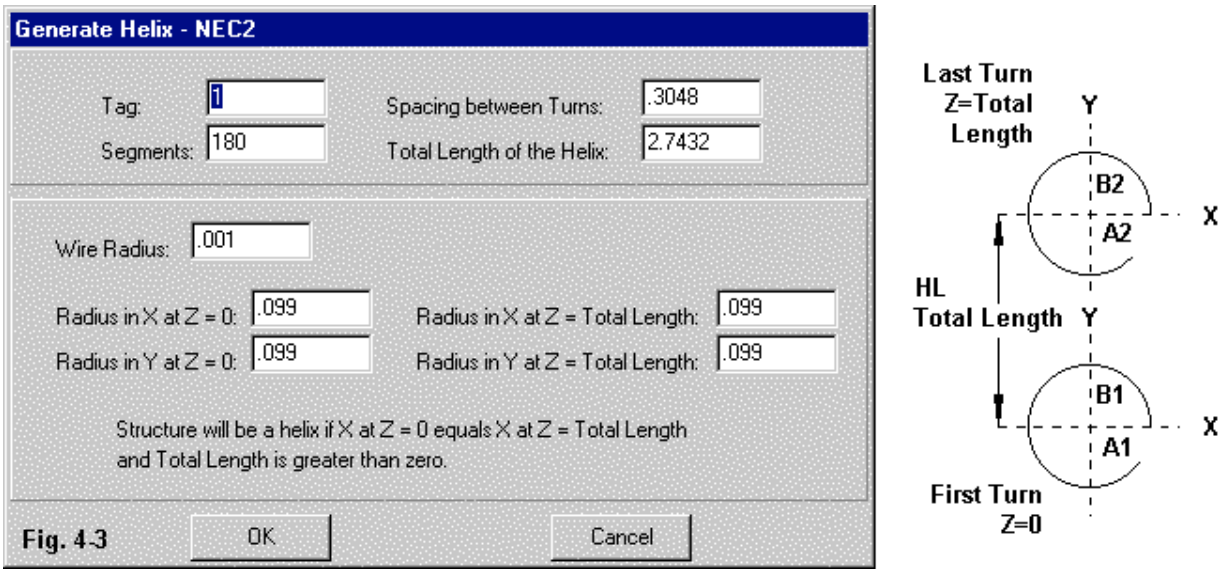

Fig. 4-3 shows how the information in the line appears when entered on the NEC-Win Pro assist screen. The integer entries appear to be standard: I1 carries the assigned tag number, and I2 includes the total number of segments for the entire structure. Prior to entering the I2 value, you must first decide on the number of segments per turn and multiply the number times the number of turns. The number of turns may or may not be an integer. The last entry (RAD) is the wire radius.

NEC-2 uses S, the spacing from one turn to the next, and HL, the total length of the helix, to determine the number of turns in the helix. In many cases, one or both of those numbers may be derivations from an initial set of calculations based upon a pitch angle and a total number of turns. If this or a similar scenario is the case for your modeling, you will have to pre-calculate the turn spacing and total helix length. In general, it is a useful procedure to calculate all of the dimensions of a helix, whether or not the model calls for them.

NEC-2 creates a helix with its starting wire end at Z = 0. The total length of the helix will therefore appear as a positive value of Z at end 2 of the last wire. If you enter HL as a positive number, you will obtain a right-hand helix. If you enter a negative number for HL, the helix will still grow toward a positive Z value, but it will be a left-hand helix.

The right-most portion of **Fig. 4-3** provides the meanings of A and B in the sample line. The centerline of the helix is always X = 0 and Y = 0. A1 and A2 refer to the radius of the helix along

the X-axis at the first and the last turn, respectively. B1 and B2 refer to the radius of the helix along the Y-axis at the first and the last turn, respectively. Together, the radii, the total length, and the turn spacing define the complete helix.

Open model *4-1.nec*, the model from which we have extracted the sample GH entry.

```
CM 28.5-MHz helical dipole-right-hand
CM Radius = 0.099m, Length = 2.7432m, 1-t = 0.3048m, 9 t
CE
GH 1 180 .3048 2.7432 .099 .099 .099 .099 .001
GE 0
EX 0 1 90 00 1.0 0.0
FR 0 1 0 0 28.5 0
RP 0 361 1 1000 -90 0 1  1
EN
```

Unlike many of our exercise models, this one is set for 28.5 MHz and forms a vertically oriented helical dipole. The give-away as to its dipole status is the placement of the source (EX0) at segment 90, the segment closest to the midpoint of the structure. By dividing the total length (2.7432 m) by the spacing between turns (0.3048 m), we may confirm that the helix has 9 turns, each with a uniform radius of 0.99 m. With 180 total segments and 9 turns, the model uses 20 segments per turn. In many cases, we shall already have calculated the pitch angle of the turns. However, the structure specification in the output report also provides that information.

```
THE PITCH ANGLE IS    26.1051
THE LENGTH OF WIRE/TURN IS    0.6927
```

The last value is L' in **Fig. 4-1**. Multiplying the value times the number of turns (9) tells us that we would need 6.2343 m of 2-mm diameter wire to actually construct the helical dipole to the specifications given. Run the model. You should obtain a free-space gain of 1.87 dBi, with a source impedance of 22.6 - j2.7 Ω.

If we wish to have a left-hand helix, in contrast to the right-hand version in model *4-1.nec*, we need to make only one simple change. Open model *4-1a.nec* and examine the GH line.

```
GH 1 180 .3048 -2.7432 .099 .099 .099 .099 .001
```

The only change is the HL entry: the total length is now a negative number to yield a left-hand helix. Compare the two models using the Necvu facility. As well, run the model to confirm that with respect to the total field gain and the source impedance, the two models yield the same reports.

A helical dipole for the 10-meter amateur band might equally require a horizontal position parallel to the earth's surface. We can easily alter the orientation of the model by adding a GM line. Open model *4-1b.nec*.

```
GH 1 180 .3048 2.7432 .099 .099 .099 .099 .001
GM 0 0 -90 0 0 0 0 0 0
```

The new line calls for a -90° rotation around the X-axis, a call that results in the helix now being

extended in a +Y direction from a starting value of Y = 0. Confirm this information by examining the segmentation data section of the NEC output report after running the model. Alternatively, use the segment identification feature of Necvu to determine the end point of the final segment in the model.

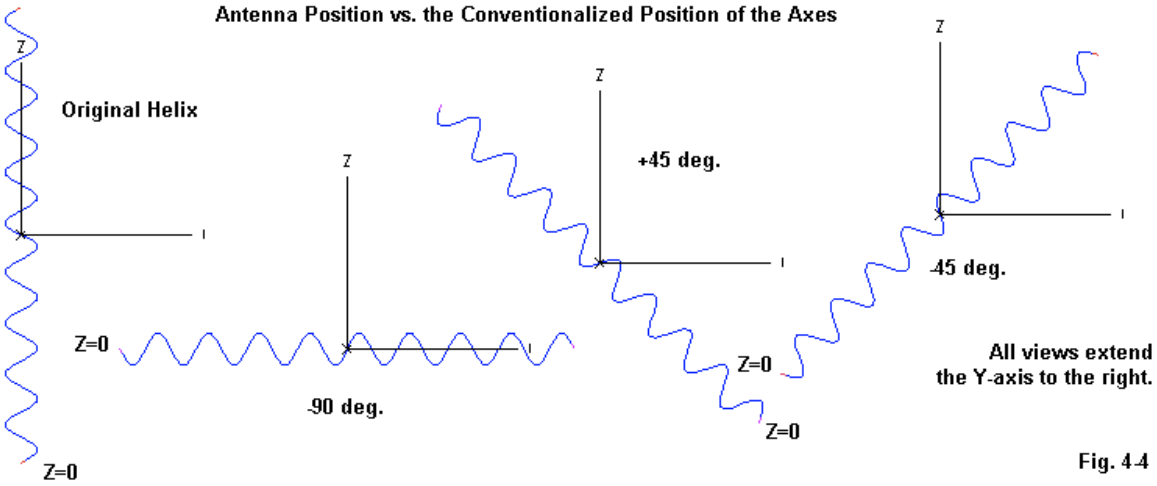

Fig. 4-4 shows why it is important to consult either the segmentation data or the segment identification feature in Necvu. Each sketch past the original shows the rotation used in the GM line X position in degrees. However, without the entry of the "Z=0" starting end value, the conventionalized centering of the background axes would give no clue as to the actual coordinates of the helix. (Note: as you rotate the helix, the starting end wire may depart slightly from a true Z=0 value. In the second case, the -90° rotation of the helix places the centerline of the structure at Z=0.)

Although we shall not remove our sample from free-space, we might as well move the model coordinates to prepare for the entry of a real ground. One useful move is to center the dipole on the X-axis so that it extends equal distances in the +X and -X directions. A second more necessary move is to elevate the antenna to a working height above ground, perhaps 10 meters. Open model *4-1c.nec* to see how we may do this on the same GM entry that we used to rotate the antenna to a horizontal position.

```
GH 1 180 .3048 2.7432 .099 .099 .099 .099 .001
GM 0 0 -90 0 0 0 -1.3716 10 000.000
```

The precedence within the GM command rotates the helix first, followed by a centering movement along the X-axis and then by an increase in the value of Z. Since the order of operations matches what we wish to occur--rotation first, followed by movement along the desired axes--we may include everything in a single command line. The segmentation data of the NEC output report confirms that the helical dipole extends from an end-1 -Y value to an end-2 +Y value. The X and Z values rotate around their centerlines, corresponding to the radius of the helix.

It is a simple matter to create oval helices within the NEC-2 version of the GH command. Indeed, the operation would be a trivial exercise were there not some notable results on the structure.

Therefore, let's go through the process, using as our baseline model 4-1, the initial circular helical dipole. The model yielded a source impedance of 22.6 - j2.7 Ω. We shall alter nothing other than the radii for A and B. The radii for the circular version used a value of 0.099 m. If we double one, we might halve the other to obtain a general similarity of overall structure relative to the original. We shall do so twice, once by doubling the A-values and once by doubling the B-values, as suggested by the centerline views in **Fig. 4-5**.

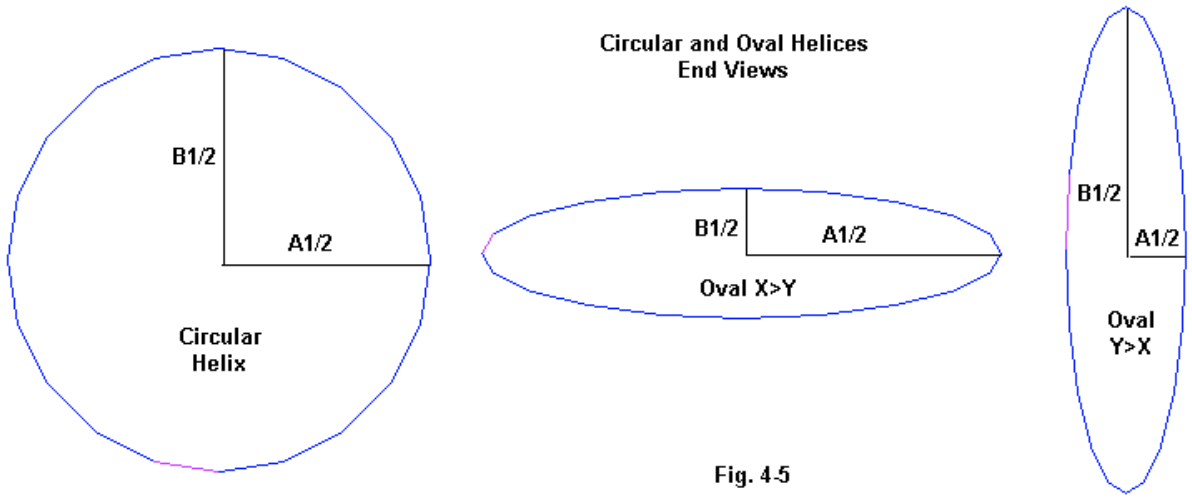

Fig. 4-5

Open model *4-2a.nec* and examine the GH line.

```
GH 1 180 .3048 2.7432 .2 .05 .2 .05 .001
```

The X radii (A1 and A2) are now 0.2 m, while the Y radii (B1 and B2) are 0.05 m. Run the model to confirm a source impedance of 36.2 + j323 Ω.

Next, open model *4-2b.nec* and confirm that the only change is a reversal of the A- and B-values.

```
GH 1 180 .3048 2.7432 .05 .2 .05 .2 .001
```

Run this model to confirm the source impedance of 35.3 + 307 Ω. Although the source impedance values are close, we should wonder why they are not identical, since the ellipses created by the differential in radii are the same and distributed over 9 complete turns. The answer lies partly in the segmentation data for the two models. Examine the length of segment 90, the source segment, for both models. In 4-2a, the length is 0.0238 m, while in 4-2b, the length is nearly 3 times longer, at 0.0637 m. When creating an oval or elliptical helix, NEC-2 uses variable-length segments, longer ones in the "flatter" areas and shorter ones at the peaks, very likely resulting in equal area sections, taking into account the radii at the segment boundaries. The differential in segment length of the two source segments, combined with the difference in the lengths of the adjacent segments for each case, results in a difference in the reported source impedance. There is no significant difference among the gain values for the ovals relative to each other or to the circular version of 4-1.

So far, we have explored the properties of the NEC-2 GH command using a helical dipole. Although this structure may not be the most common form of helix in use, it presents the fewest modeling challenges and gives us unambiguous results. However, we should explore some of the challenges presented by modeling an axial-mode helix, one end of which normally touches ground or a ground-plane structure.

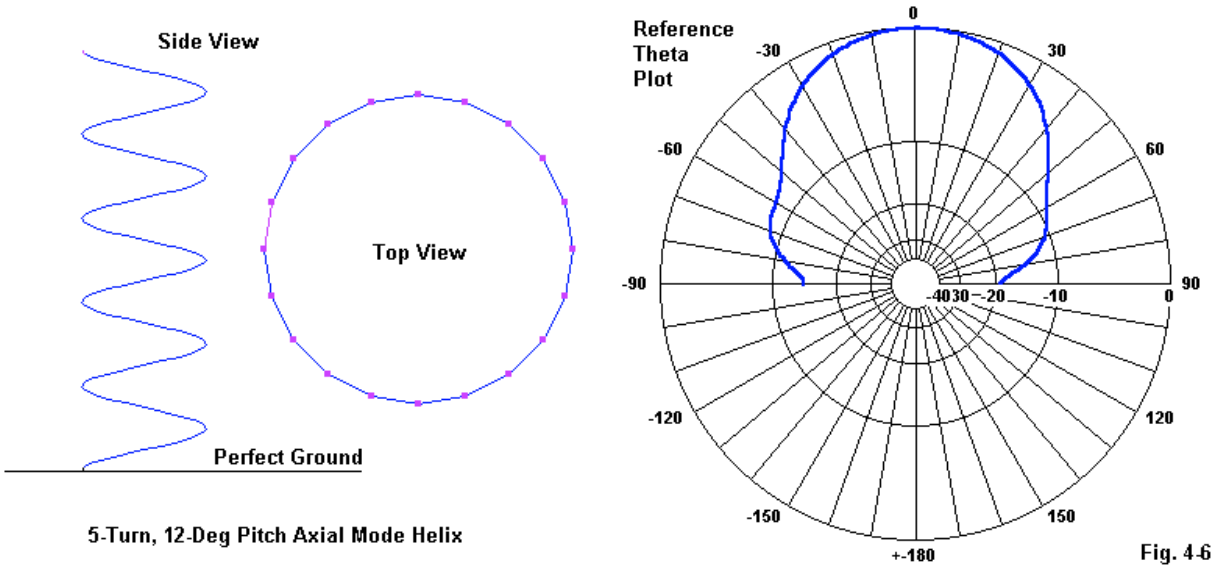

Fig. 4-6

Let's consider the axial-mode helix in **Fig. 4-6**. Initially, we shall model this antenna over a perfect ground so that creating the helix will allow one end to touch ground. Open model *4-3.nec*.

```
GH 1 100 0.2125566 1.0627828 .1591549 .1591549 .1591549 .1591549 .001
GE 1
GN 1
EX 0 1 1 00 1.0 0.0
FR 0 1 0 0 299.7925 0
RP 0 181 1 1000 -90 0 1.00000 1.00000
EN
```

The GN entry indicates that we are using a perfect ground. The GH entry describes the helix itself. In this case, I have selected a 12°-pitch helix using 5 complete turns. Axial-mode helices often use the circumference of their turns as a major reference dimension, and this one has a circumference of 1λ (1 m at 299.7925 MHz). Using the equations at the beginning of the chapter, the radius is 0.1591549 m, the turn spacing is 0.2125566 m, and the total length is 1.0627828 m. This last set of three values defines the helix within the GH entry. The wire radius is 0.001 m (1 mm).

Initially, we shall place the source (EX0) on the very first segment, with a full understanding that this position will not yield the most reliable model. Segment 1 intersects the ground plane at an angle and does not have segments equal in length to itself on either side. Therefore, we shall make the average gain test (AGT) a standard part of the modeling exercise. As noted in previous chapters, the AGT test is automated in NEC-Win Pro. When using it, we shall select

the "perfect ground" option. The test will yield 2 values of interest. First will be the dimensionless average gain, where 2.0 is a "perfect" score, given the use of perfect ground. Second will be the AGT value divided by 2 and converted to a value in dB. This value will permit adjustment of the reported gain value to one that is more nearly correct.

Run model 4-3 and confirm the following output value reports.

Model	Reported Gain dBi	AGT	AGT-dB	Adjusted Gain dBi	Impedance R +/- jX Ω
4-3	8.40	1.819	-0.41	8.81	225 - j40

Although the AGT score is acceptable, it nevertheless results in a gain deficit in the initial report that is significant for many types of modeling tasks. For example, suppose we were surveying 5-turn helices with circumferences that varied in 0.05-λ increments. The AGT value varies from one model to the next and is necessary for obtaining a true gain curve. The resistive portion of the source impedance might also be corrected by multiplying it by half the recorded AGT over perfect ground. Indeed, one reason for using the first segment for the source is to obtain a reasonable idea of the source impedance at the helix end. However, two factors limit our ability to obtain this value. One is the presence of significant reactance in the source impedance, a factor that tends to make the resistance-correction process less reliable. Second, the source position is not at the tip of the helix, but within the first segment itself. As a result, we should use the reported source impedance value--whether raw or corrected--with caution.

Open model *4-3a.nec*. The only change within this model is the position of the source, which moves from segment 1 to segment 2.

```
EX 0 1 2 00 1.0 0.0
```

Run the model and develop a table of values that correlates to the table for model 4-3.

Model	Reported Gain dBi	AGT	AGT-dB	Adjusted Gain dBi	Impedance R +/- jX Ω
4-3a	8.79	1.995	-0.01	8.80	238 + j44

This model reveals several interesting facts about the initial model. First, moving the source to segment 2 places equal length segments on either side. Hence, the AGT score improves to 1.995, so that the gain deficit in the initial report is only 0.01 dB. If our only interest in the axial-mode helix were its gain and pattern shape (sampled in **Fig. 4-6**), we might well use this position for the source for all test models. However, if we also wish to obtain an indication of the source impedance at the end of the helix, the new source position yields a very different value. You may wish to produce further models that move the source position by one segment for each new version.

The axial-mode helices that we have examined so far use only one of two major techniques for modeling these antennas over perfect ground. **Fig. 4-7** shows us another alternative: raising the helix slightly and using a straight vertical wire from the helix tip down to the perfect ground. We shall look at two versions of this technique.

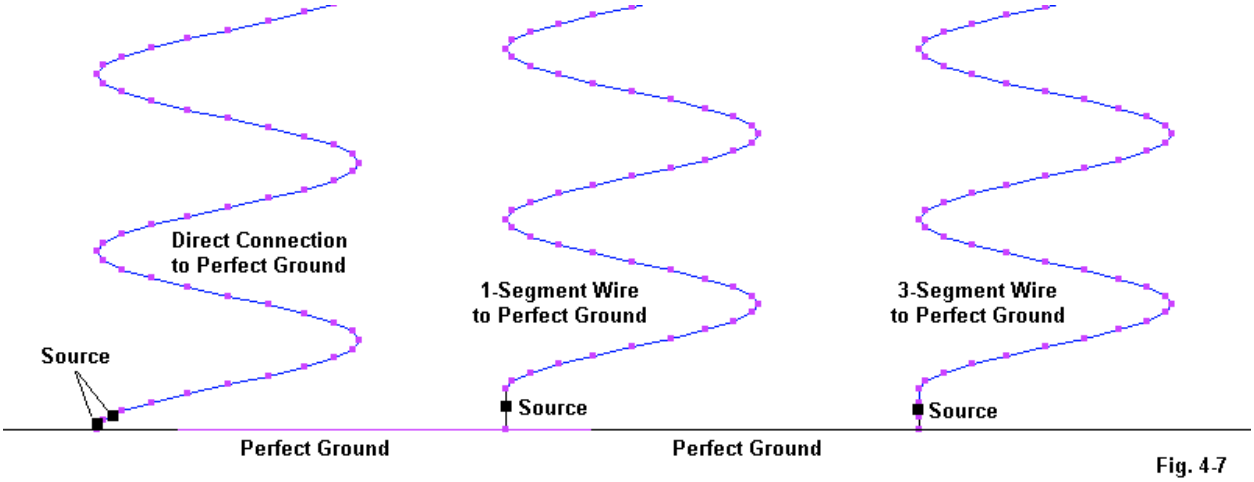

Fig. 4-7

On the left, we see the models we have so far run. The middle sketch reflects the structure of model *4-3b.nec*.

```
GH 1 100 0.2125566 1.0627828 .1591549 .1591549 .1591549 .1591549 .001
GM 0 0 0 0 0 0 0 .05092
GW 2 1 .15915 0 0 .15915 0 .05092 .001
GE 1
GN 1
EX 0 2 1 00 1.0 0.0
FR 0 1 0 0 299.7925 0
RP 0 181 1 1000 -90 0 1.00000 1.00000
EN
```

The model did not change the GH line. However, we inserted a GM line to elevate the entire helix above the ground plane by the length of one helix segment. We obtained that segment length from the segmentation data in either of the two NEC output reports that we developed for our initial axial-mode helix. Next, we added a 1-segment wire (GW2) between the helix tip and ground. We placed the source (EX0) on the new wire. Run the model and obtain the relevant data for a table.

Model	Reported Gain dBi	AGT	AGT-dB	Adjusted Gain dBi	Impedance R +/- jX Ω
4-3b	8.64	1.956	-0.10	8.74	298 + j13

The table gives us several pieces of significant data. First, it appears that even slight separations of the helix from its terminating ground may have an affect on its forward gain. Second, although the AGT value of this model is superior to that of the initial model, it is not perfect, since equal-length segments do not bracket the source segment. Third, the revised model gives us a quite different source impedance relative to the earlier models. Now, open model *4-3c.nec*.

```
GW 2 3 .15915 0 0 .15915 0 .05092 .001
. . .
EX 0 2 2 00 1.0 0.0
```

This model is one final try at developing a near-perfect model of an axial-mode helix over perfect ground. In this model, we changed the segmentation of the new wire to bracket the source segment, but we left the connecting wire length at it initial value. Hence, relative to the helix segments, the new-wire segments are short. Run the model and make a table.

Model	Reported Gain dBi	AGT	AGT-dB	Adjusted Gain dBi	Impedance R +/- jX Ω
4-3c	8.71	1.987	-0.03	8.74	292 - j26

The AGT score improves, and the amount of adjustment that we must make to the reported gain decreases. However, the impedance value differs enough from the previous model to leave some question as to the degree of source-impedance precision that we may obtain from the model. Construction variables associated with both test and production antennas will likely exceed the variation in the modeled impedance values. However, the difference between the first 2 models and the last 2 models suggests that we should use the modeling technique that most closely approximates the anticipated or existing antenna structure.

Modeling over perfect ground is useful as a first approximation of performance of an axial-mode helix. However, most such antennas use a ground plane that functions at some distance above the actual ground. To convert our models requires a few steps of additional work. First, we must elevate the entire model above ground by a desired amount, perhaps 1 m as a start. Then we must establish a real ground. We might use the S-N ground system with average values (conductivity: 0.005 S/m, permittivity: 13). Finally, we must create a ground plane for the model.

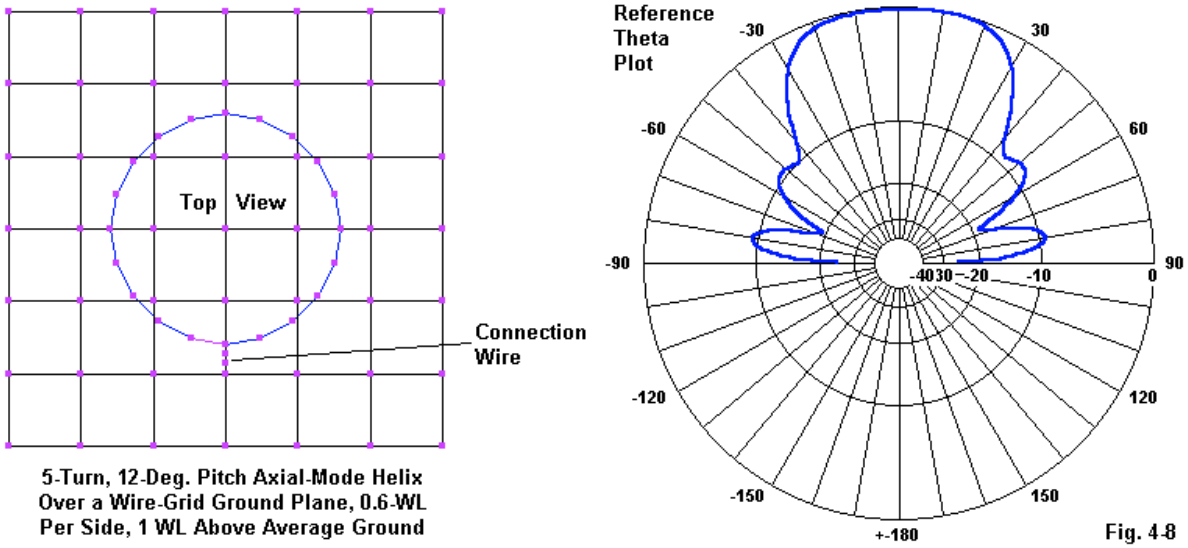

Fig. 4-8

Fig. 4-8 shows the ground-plane structure that we might use: a wire-grid assembly composed of 0.6-λ sides, using wires spaced 0.1λ. A wire grid normally simulates a solid or screen surface when the wire or segment spacing is 0.1λ or less and the wire radius is the segment length divided by 2*π. Hence, the requisite wire radius is about 0.0159 m. Open model *4-4.nec* to see these steps in the evolution of the model from the perfect-ground version.

```
GH 1 100 0.2125566 1.0627828 .1591549 .1591549 .1591549 .1591549 .001
GM 0 0 0 0 0 0 0 .05092
GW 2 1 .2 0 0 .15915 0 .05092 .001
GM 0 0 0 0 0 0 0 1
GW 3 6 -.3 -.3 1 -.3 .3 1 .0159
GM 0 6 0 0 0 .1 0 0 003.003
GW 4 6 -.3 -.3 1 .3 -.3 1 .0159
GM 0 6 0 0 0 0 .1 0 004.004
GE 1
GN 2 0 0 0 13.0000 0.0050
EX 0 2 1 00 1.0 0.0
```

We can recognize GH1 through GW2 as identical to model 4-3b (with one exception that we shall soon note). The next GM line elevates the structure 1 m above the average ground established by the GN entry. The next sets of GW-GM lines establish the first and subsequent wires forming the grid so that each wire intersects a crossing wire at a segment junction. Since the wires have junctions at 0.1-m intervals, the end of the single straight wire from the lower tip of the helix would not intersect a junction if it were vertical. Hence, GW2 moves the lower end of the wire to the nearest wire-grid junction. If it is necessary to maintain the wire more nearly vertical, then you might wish to create the grid using 0.05-λ spacing.

Run the model and create a table like the ones for the variations of model 4-3.

Model	Reported Gain dBi	AGT	AGT-dB	Adjusted Gain dBi	Impedance R +/- jX Ω
4-4	8.47	0.881	-0.55	9.02	328 - j17

Note that the adjusted gain is a bit higher than with a perfect ground. Moreover, as revealed by the right side of **Fig. 4-8**, the theta pattern is more complex with definite sidelobes that do not appear in the perfect-ground version. However, the AGT score is mediocre at best. Perhaps we may use the same technique of segmenting GW2 to increase the score. Open model *4-4a.nec*.

```
GW 2 3 .2 0 0 .15915 0 .05092 .001
```

As before, the re-segmenting of GW2 shortens the length of each segment, since we did not increase the wire length. The only other change made to the model was to move the source segment from 1 to 2. If we run the model, we obtain the following table.

Model	Reported Gain dBi	AGT	AGT-dB	Adjusted Gain dBi	Impedance R +/- jX Ω
4-4a	8.31	0.849	-0.71	9.02	338 - j40

Instead of improving the model, our re-segmentation of the connecting wire made matters worse. To discover why, use the Necvu facility to check the model for errors. You will discover 2 warnings that absolute segment 101 (segment 1 of GW2) is within the volumes of absolute segments 137 and 168, which happen to be the segments at the junction with the lower end of GW2. NEC-2 does not abort its run due to an inter-penetration warning, since inter-penetration of wire surfaces into the middle third of other wires is not a core error. However, the condition

results in outputs that are seriously unreliable. The culprit is the radius of the wires in the wire-grid, which are 15 times fatter than the helix wires. Thus, we have a second reason for using a finer grid for the model, since every reduction in the space between segment junctions results also in a reduction of the wire-grid wire radii.

To complete our survey of NEC-2 GH potentials, let's create some spiral structures. We shall place these models in free space and arbitrarily assign the source to the first segment of the structure. These models serve only to illustrate the shapes that we may create. Open model *4-5.nec*. The Necvu rendition, when rotated, should look like the inward spiral of the left-most sketch in **Fig. 4-9**.

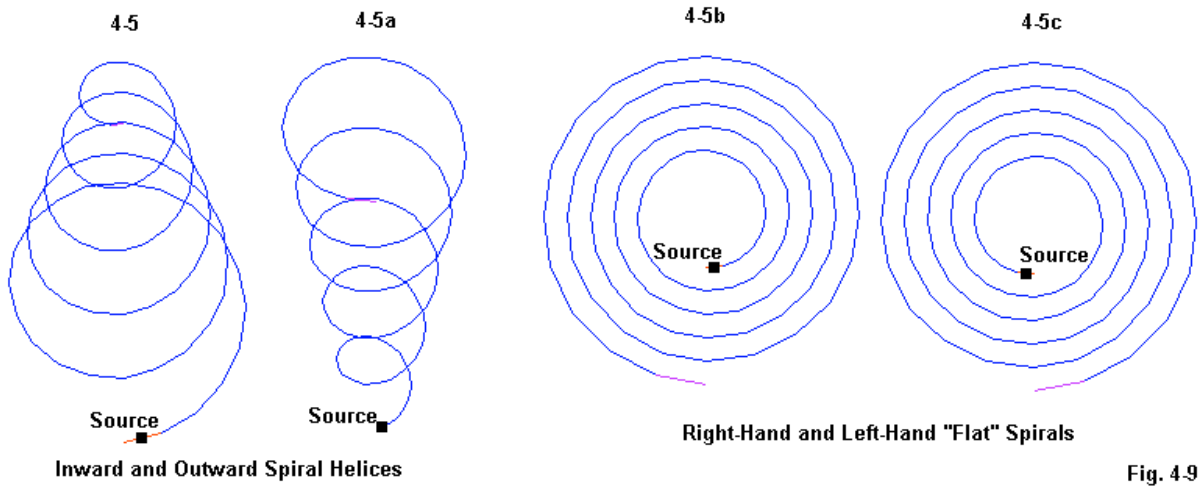

Fig. 4-9

```
GH 1 100 0.2125566 1.0627828 .1591549 .1591549 .05 .05 .001
```

The GH line from the model shows that the A2 and B2 entries have smaller values than originally, yielding a spiral that decreases in radius as it moves away from its origin. To see the opposite effect, open model *4-5a.nec*.

```
GH 1 100 0.2125566 1.0627828 .05 .05 .1591549 .1591549 .001
```

Here, the GH line reduces the values of A1 and B1 to produce a spiral that increases in radius as it progresses.

Most NEC-2 cores will not yield truly flat spirals, although we can produce spirals that are as flat as practical purposes might dictate. Consider model *4-5b.nec*.

```
GH 1 100 .0002 .001 .05 .05 .1591549 .1591549 .001
```

The third numerical entry is the turn spacing, while the fourth is the total length. In a truly flat spiral, the turn spacing would be zero (as would be to total length). Since the command derives the number of turns by dividing the space per turn into the total length, it would have to divide by zero. To eliminate the potential problem, we enter a very small value for the turn spacing (0.0002 m) and multiply that value by the number of planned turns (5) to arrive at the total

length (0.001). The result meets the mathematical needs of the command, but warps the spiral out of true flatness by the radius of the wire. To rotate the spiral in the opposite direction, open model *4-5c.nec*.

```
GH 1 100 .0002 -.001 .05 .05 .1591549 .1591549 .001
```

This version of the model makes the HL (total length) entry negative. The result is the right-most sketch in **Fig. 4-9**. All NEC-2 spirals classify as Archimedes spirals, with a linear or uniform increase (or decrease) in dimensions as the spiral moves from end 1 to end 2. We shall look more closely at spirals as the last step in our examination of NEC-4 GH potentials.

The NEC-4 GH Command

The NEC-4 version of the GH command is so different from its NEC-2 cousin that there are no conditions under which either core can read the other's command. The easiest way to show this is to re-create the initial helical dipole model using the NEC-4 version of GH. Open model *4-6.nec* and examine the GH line. Other than this line, the model is identical to model 4-1. Below are the GH lines from each model.

NEC-2 GH Command (4-1)

Cmd	I1	I2	F1	F2	F3	F4	F5	F6	F7
	Tag No.	No. Segs	S	HL	A1	B1	A2	B2	RAD
GH	1	180	.3048	2.7432	.099	.099	.099	.099	.001

NEC-4 GH Command (4-6)

Cmd	I1	I2	F1	F2	F3	F4	F5	F6	F7
	Tag No.	No. Segs	TURNS	ZLEN	HR1	HR2	WR1	WR2	ISPX
GH	1	180	9	2.7432	.099	.099	.001	.001	0

Both commands begin with the assigned tag number and the specified number of segments in the helix. Whereas NEC-2 derived the number of turns from the turn spacing (S) and the total length (HL), NEC-4 derives the turn spacing from the number of turns (TURNS) and the total length (ZLEN). Also, to produce a left-hand helix in NEC-4, make the number of turns negative. (NEC-2 used the HL entry for this purpose). The value for the number of turns may be fractional, for example, 4.38.

NEC-4 does not allow elliptical helices. Instead, there is one entry only for the starting helix radius (HR1) and only one for the ending radius (HR2). HR1 begins at a positive value of X, with Y and Z set to zero. NEC-4 does allow for the use of wires having a tapering radius from one end to the other (WR1 and WR2). If WR1 and WR2 have different values, then the command scales the radius logarithmically along the wire. If either HR2 or WR2 have zero values, they automatically take on the values of the HR1 or WR1, respectively.

The final NEC-4 entry allows the user to specify one of two possible spiral types: Archimedes (1) or log (0). If HR1 is the same as HR2, then the value inserted in F7 makes no difference to the structure.

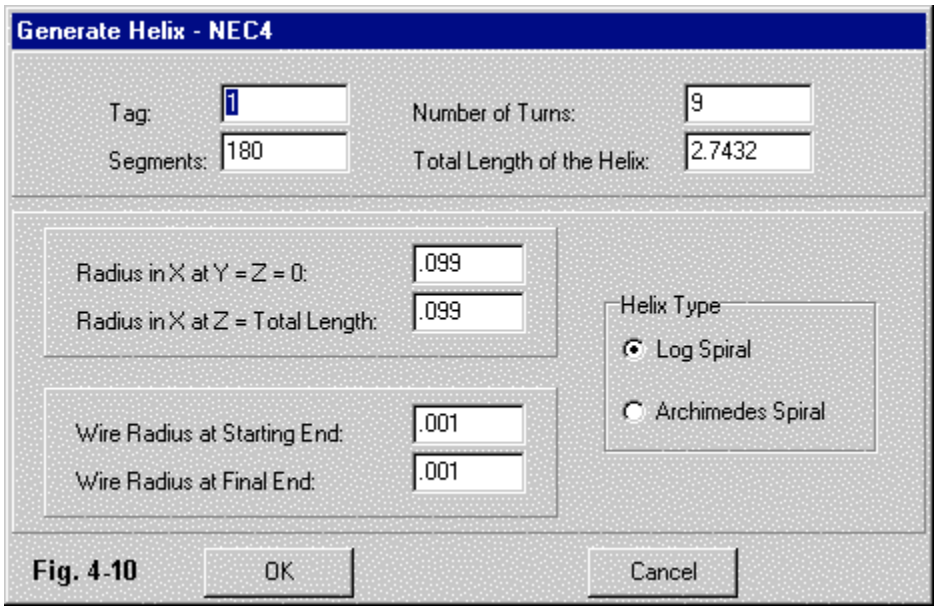

Fig. 4-1, the GNEC GH help screen, will aid you in correlating the line entries with the data that each entry provides to the command. You may determine that model 4-6 produces the same structure as model 4-1 by examining the segment identification data in Necvu or the segmentation data in the NEC output report. The model returns a free-space gain of 1.87 dBi, with a source impedance of 22.6 - j2.9 Ω. Whereas the NEC-2 GH command returns data on the pitch angle and the amount of wire in each turn in the structure specification portion of the NEC output report, the NEC-4 version returns the total length of wire in the helix (6.214 m).

All NEC-4 GH constructs are vertical helices extended along the Z-axis, just as in NEC-2. Therefore, all of the maneuvers applied to variations of model 4-1 also apply to model 4-6. You may directly transfer via copy and paste techniques the lines added to 4-1 in order to rotate it, and to move it to a more desirable position. The one maneuver that requires a change is altering the right-hand default helix into a left-hand helix. Open model *4-6a.nec* and examine the GH line.

```
GH 1 180 -9 2.7432 .099 .099 .001 .001 0
```

The only difference from the previous model is that the entry for the number of turns is negative, the marker for a left-hand helix. Compare the first few lines of the segmentation data in the NEC output report for each model to see the difference. The numerical values of the X and Z coordinates will be the same for both models. However, the Y coordinate values will have the same absolute values, but different signs.

Model 4-6: Right-Hand Helix

SEG. NO.	COORDINATES OF SEG. CENTER X	Y	Z	SEG. LENGTH
1	0.09658	0.01530	0.00762	0.03452
2	0.08712	0.04439	0.02286	0.03452
3	0.06914	0.06914	0.03810	0.03452

Model 4-6a: Left-Hand Helix

```
SEG.   COORDINATES OF SEG. CENTER     SEG.
NO.       X          Y          Z      LENGTH
   1   0.09658  -0.01530   0.00762   0.03452
   2   0.08712  -0.04439   0.02286   0.03452
   3   0.06914  -0.06914   0.03810   0.03452
```

Similar considerations apply to the axial-mode helices that we modeled in the 4-3 and 4-4 series under NEC-2. The only change that we must make to create the NEC-4 equivalent of the model is to re-create the GH entry. For example, the first helix, with its direct connection to the perfect ground appeared in model 4-3. Open model *4-7.nec* and examine the new GH line.

```
GH 1 100 5 1.0627828 .1591549 .1591549 .001 .001 0
```

Most helices tend to give very similar results in both NEC-2 and NEC-4, as the following table of results will attest.

Model	Reported Gain dBi	AGT	AGT-dB	Adjusted Gain dBi	Impedance R +/- jX Ω
4-3 (NEC-2)	8.40	1.819	-0.41	8.81	225 - j40
4-7 (NEC-4)	8.39	1.815	-0.42	8.81	226 - j40

Model 4-3c used a short 3-segment wire to connect the base of the helix to ground. Open model *4-7a.nec*. The GH line remains the same as in 4-7 and all other lines are the same as in 4-3c. The results for the NEC-2 and NEC-4 models are also similar.

Model	Reported Gain dBi	AGT	AGT-dB	Adjusted Gain dBi	Impedance R +/- jX Ω
4-3c (NEC-2)	8.71	1.987	-0.03	8.74	292 - j26
4-7a (NEC-4)	8.70	1.983	-0.04	8.74	292 - j26

We may give the same treatment to the models that use a wire-grid ground plane and are elevated above a real ground. By replacing the GH line alone, model 4-4 becomes model *4-8.nec*.

Model	Reported Gain dBi	AGT	AGT-dB	Adjusted Gain dBi	Impedance R +/- jX Ω
4-4 (NEC-2)	8.47	0.881	-0.55	9.02	328 - j17
4-8 (NEC-4)	8.32	0.851	-0.70	9.02	340 - j20

Here we find a somewhat greater disparity between the results offered by the two cores. However, as we noted in the discussion of the earlier model, both may well undergo considerable refinement before they are highly usable.

Perhaps the most unique aspect of the NEC-4 GH command is its provision for 2 different spirals. Because NEC-4 need not divide the total length by the length of 1 turn to determine the number of turns, NEC-4 can produce true flat spirals simply by entering a zero into the total length position. All spirals are then produced at Z = 0, and GM becomes the means of rotating

and moving them into a final position. However, we need not confine a spiral to a flat antenna. We may create spiral helices and watch their development vertically as well as across the circumference, as suggested in **Fig. 4-11**.

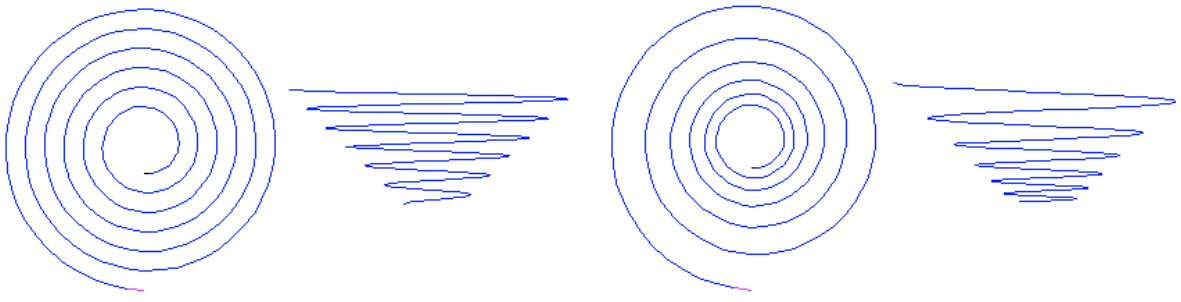

A Comparison of Archimedes and Log Spirals Fig. 4-11

All NEC-2 spirals are the Archimedes type. In NEC-4, an F7 (ISPX) entry of 1 produces an Archimedes spiral, while a 0 yields a log spiral. If we tie the types to a definite model, we may be able to understand the differences more easily. Open model *4-9.nec*.

```
CM General Helix over Perfect Ground
CM Archimedes Spiral
CE
GH 1 100 5 1 1 2 .001 .001 1
GE 1 -1 0
GN 1
EX 0 1 1 0 1 0
FR 0 1 0 0 299.7925 1
RP 0 181 1 1000 -90 90 1.00000 1.00000
RP 0 181 1 1000 -90 0 1.00000 1.00000
EN
```

The model for the log spiral (model *4-9a.nec*) is identical, except that the last entry in the GH line is 0. We have a 5-turn spiral helix over perfect ground. The radius increases from 1 m to 2 m along the 1-m overall length of the helix. The following table lists the radii and the height of the model at each complete turn or every 20 segments for both types of spirals. The NEC output report supplies the information.

Turn	Seg	Archimedes		Log	
No.	No.	X	Z	X	Z
1	1	0.0	0.0	0.0	0.0
1-2	20-21	1.2	0.2	1.14869	0.14869
2-3	40-41	1.4	0.4	1.31950	0.31950
3-4	60-61	1.6	0.6	1.51571	0.51571
4-5	80-81	1.8	0.8	1.74110	0.74110
5	100	2.0	1.0	2.0	1.0

Note that the rise in value along the Z-axis is exactly proportional to the increase in radius. Of course, the two spirals do not have the same electrical properties as radiators. However, the

purpose of our model and its two variations is not to establish a working antenna, but to sample the two types of available spirals.

The simpler spiral is the Archimedes, with its arithmetically regular structure. In an Archimedes spiral, the radius (R) at any wire junction is given by a simple equation:

$$R = Ri + (a * \Theta),$$

R is the radius under consideration, Ri is the initial radius, *a* is a constant, and Θ is an angle. Because the change of radius is uniform, we can formulate values for *a* and Θ in a variety of ways, so long as the product of the two yields a progression of values that steps by an increment of 0.01 per segment in the 100-segment model. (In the model, the units are meters, but the same considerations apply to any system of units.) Let Θ be the segment number of interest within the helix. With 100 segments and a total radius increase of 1.0, along with a total height of 1.0, each segment will increase both the radius and the height by 0.01 of the total. The value of *a* is thus 0.01. If Θ = 40 (the 40th segment), then *a* * Θ becomes 0.01 times 40 segments or 0.4. Since the height begins at zero, the new height is 0.4. Since the radius begins at 1.0, the new height is 1.0 + 0.4, or 1.4. If all that we ever use are Archimedes spirals, then the simplified method of checking coordinates will suffice.

The log spiral formula has an equivalently simple appearance:

$$R = Ri * a^{\Theta},$$

R is the radius under consideration, Ri is the initial radius, *a* is a constant, and Θ is an angle. The constant, *a*, is not the same constant as it is for an Archimedes spiral with its regular or uniform variation along the length of the helix. End 1 of the first segment is at a helix length of zero, and the radius at zero length is Rmin, extended along the +X direction. Therefore, all further segment references apply to end 2 of the segment. Hence, the last segment calculated will yield the final radius and the final height of the spiral. What we are seeking is the radius of the helix (R) and the length of the helix (L) at Θ, the segment of interest, using end 2 of the segment. To calculate these values we need the following data from the model.

Rmax	the maximum radius of the spiral.
Rmin=Ri	the initial or minimum radius of the spiral.
s	the number of segments per turn of the helix.
t	the total number of turns in the helix.
Lt	the total length of the spiral.

Roughly speaking,

$$a = ((Rmax/Rmin)^{(s/t)})^{((1/s)^2)}$$

For the log spiral version on the model that we set up (4-9a), *a* = 1.006956. (Note: I have used a spreadsheet format for the equation because multiple levels of superscripts would be almost impossible to read.) Since Θ is a segment of interest and we know Ri (the same as Rmin), we may use the value of *a* to directly calculate R_{Θ}, the radius at segment Θ. The progression of

helix length is directly proportional to the progression of the radius change. Hence, we may also easily calculate the length of the helix (L_Θ) at the same segment, Θ:

$$L_\Theta = ((R_\Theta - Rmin) * Lt)/(Rmax/Rmin)$$

Finally, we can easily calculate the end-2 coordinates of the segment that we have entered as Θ. First define the angle (A) of the specified segment in radians.

$$A = (2*\pi*\Theta)/s$$

Then the X, Y, and Z coordinates follow.

$$X = R_\Theta \cos(A)$$
$$Y = R_\Theta \sin(A)$$
$$Z = L_\Theta$$

If your work will involve log spiral shapes, you may wish to develop a spreadsheet so that you can pre-calculate what the GH command will create. As well, you may wish to experiment with either 4-9 or 4-9a by using different starting and ending values of the wire radius (WR1 and WR2). Then track the log progression of radii in the segmentation data of the model. Regardless of the type of spiral chosen, the wire radius always follows a log progression.

We have focused on the NEC-4 GH command only where it differs from the NEC-2 version of the same command. The chief areas of difference are the specific data that we need to enter into the command to form a helix and the unique abilities of the command to offer us both Archimedes and log spiral forms. Like its NEC-2 counterpart, the NEC-4 GH command remains dependent on the GM command to rotate and relocate the resulting structure on the coordinate system in the most desirable position.

Summing Up

Helix-creation and spiral-formation are subject to many variations within the scope of programming a GH command. The differences between the NEC-2 and NEC-4 versions of the command do not exhaust the possibilities. Instead, they represent decisions made during the process of the development of the cores. Indeed, the NEC-2 GH command began life as an unofficial addition to the core, but it has become a standard feature of most commercial implementations of NEC-2 that offer the full spectrum of geometry commands. In NEC-4, the GH command is an integral part of the core's capabilities. The differences between the command structures prevent one version being read by the other core.

The NEC-2 version of the command offers uniform helices and Archimedes spiral shapes using a single wire radius throughout the structure. The separation of X-axis and Y-axis radius entries permits the development of elliptical helices and spirals. However, the use of the turn spacing and the total helix length to define the number of turns of the structure prevents us from forming a truly flat spiral, although we may define spirals that are flat enough for most practical modeling purposes.

The corresponding NEC-4 version of the command omits the potential for oval shapes. However, it offers the ability to taper the wire radius along the helix or spiral. As well, the use of the number of turns and the total helix length to define the turn spacing allows the creation of truly flat spirals. As well, the command offers the choice of an Archimedes or a log spiral structure, whether flat or extended into a helix.

Helical dipoles and similar freestanding elements pose no significant modeling problems beyond their formation with the GH command. The modeling of axial-mode helical antennas, however, creates a number of challenges at the intersection of the helical element with its associated ground plane or ground-plane structure. Once you have firmly grasped the GH command, you may then move onward to the task of integrating helices and spirals within even larger structures.

5.
GX and GR: Symmetry

***Objectives**: The seemingly simple symmetry commands require considerable care in order to achieve good results. In this chapter, you will become acquainted with the use of symmetry, first as an alternative means to producing modeled antenna structures, and second as a method of reducing the required run time for the core and reducing the requirements for memory for structures of considerable size.*

When NEC first emerged in the 1980s, computers--both PCs and mainframes--suffered two shortcomings. They had severe limitations on the available memory to allow the complex matrix solutions to the modeling equations to run in-core. An in-core run means that the available memory can run with the dynamic or active memory rather than having to periodically place accumulated data on a storage medium, with the resulting slowing of processes that the transfers require. The second problem involves the limitation in the number of total segments that a model can have and still successfully run.

Contemporary PCs have speeds in excess of 2 GHz, a thousand-fold increase over the 2 MHz speeds of early PCs. As well, available memory has increased within the contemporary Windows environment from a mere 180 KB to about 2 GB of memory available for model processing storage (out of the 4 GB provided by the operating system). Still, the problems of model size and core-run speed persist, simply because designers and analysts wish to create ever-larger models. Some computers with multiple processors have stretched both the size and speed limits, but in the context of 32-bit operating systems using a single processor--the standard at the time of writing--models with over 10,000 segments become problematical. Techniques of controlling the temporary data transfer can increase the segment limit and processing speed, and the promise of 64-bit processors on the horizon will increase the capabilities of NEC modeling in the near future, but there will always be limits. With every increase in the limits, modelers will develop ever more complex models to press them.

One technique that has been a part of NEC since the earliest version is the use of symmetry within the model. Identical parts of a model may not require repetition within the portion of the model that establishes the structure. The core itself can make use of partial data from the first instance of those parts and by-pass portions of the solution routine. Only the results need to be applied to the replicas of the initial parts in order to yield the same results as a full model, but in less time and with less memory.

As we shall see in greater detail, we may establish model symmetry across any one or more of the 3 axes. A model that establishes 1 replica across a single axis has 1 plane of symmetry. We may double the total structures by replicating across 2 planes, that is across two axes, forming essentially a square of structures. The last and perhaps most rare step is to perform a final symmetrical replication across the third axis, forming a cube of structures with 3 planes of symmetry. Under certain conditions, we may interconnect the structures to form a single geometric structure from the entire set that consists of an initial part and a 3-plane call for

symmetry. We should also understand that the core will assign a segment number to each segment created by a symmetry call, although it will not have to perform a complete calculation for replicated segments.

During the core's development of a solution for the currents on each segment of a model, it generates a large number of complex numbers in matrix storage. The number of stored complex numbers is related to the number of segments within a model, N. As well, the core goes through "fill" and "factor" processes that take time (relative to the given speed of a computer), and these times are also related to the number of segments in the model. The use of symmetry can reduce both the required storage space and the run times for the fill and factor processes in rough proportion to the numbers in the following table. 0 planes of symmetry indicates a model that makes no call for symmetry but is otherwise identical in its total size to the other models.

Number of Planes of Symmetry	Matrix Storage Size	Fill Time	Factor Time
0	N^2	N^2	N^3
1	$N^2/2$	$N^2/2$	$N^3/4$
2	$N^2/4$	$N^2/4$	$N^3/16$
3	$N^2/8$	$N^2/8$	$N^3/64$

The timing figures are for optimal conditions when processing large matrices, and somewhat longer times will be the general rule. As well, the core takes time for initial set-up steps prior to entering into these calculations and also does further work in developing the specific output requests that you establish for a model. As a result, you will not realize the indicated time-savings for the entire model. However, the higher the number of segments within a model, the more noticeable the savings.

We shall begin our exploration of the GX command by proceeding through a number of exercises that certainly do not require us to employ it. However, these exercises will acquaint us both with the command structure and with the properties of its use. Then we shall turn to some larger applications and test the savings, learning in the process some of the points that require special care. Finally, we shall turn to the GR command, a very specialized geometry command indeed.

The Basics of GX Models

Fortunately, the GX command is identical in both NEC-2 and NEC-4. Therefore, most of the sample models (but not all of them) that involve GX will run equally well on both cores. The GX command has the official title of "reflection in coordinate planes," a label that indicates the fact that we may use the core to create one or more replicas of a model. The initial model should appear in one of the quadrants of the Cartesian coordinate system using end-1 and end-2 coordinates that do not change sign in the move from one end to the other. That is, the initial wires of the model do not cross the axis that we shall use as a plane of reflection. The wires may cross any axis that we do not intend to use as a plane of reflection.

The input line for the GX command has a deceptively simple appearance. It is one of the few commands to have only two positions for numerical entries, both of which are integers.

```
Cmd      I1            I2
         Tag No.       Plane(s)
         Increment     of Symmetry
GX       2             100
```

Ordinarily (but not always), the GX command will be the last command in the geometry section of a model prior to the GE, geometry end, command. Hence, for the initial structure that we shall replicate, we have all of the tag numbers assigned. The I1 or tag-number increment should be high enough so that any new structure created by the command will not re-use any existing tag numbers. If the structure uses tag number 1-4, then an increment of 4 will ensure that the replica(s) will begin at tag 5. If we call for more than one plane of reflection, each replica will increment by the indicated value of I1.

I2 actually contains 3 independent markers. The first position calls for a reflection along the X-axis if the value is 1 and no reflection if the value is 0. The second position creates or suppresses a reflection along the Y-axis, while the third position does the same relative to the Z-axis. You may call for as many reflections as you wish within a single command. The core creates the replicas in reverse order. If we had entered 111 as the I2 value set, then the core would create the Z-axis replica first. Then it would replicate the 2 existing structures along the Y-axis. Finally, it would create 4 more replicas along the X-axis.

Creating a replica along an axis means that the initial model appears on the other side of the 0-value for that axis. Consider the following two sample GW lines.

```
GW 1 11 -.75 0 -.245 -.75 0 .245 .001
GW 2 11 -.25 0 -.245 -.25 0 .245 .001
```

Each line creates a wire extending above and below Z=0 by an equal amount. Y is uniformly 0. Each wire has a different value of X. If we use the structural sample as our GX call in the next command line, the core will create two new wires, assigning tag numbers that are 2 above the smallest tag number in the GW lines. Hence, the new wires will be tag numbers 3 and 4. The sample call is for reflection along the X-axis only. Therefore, the core will create tag 3 from GW1, simply reversing the sign of the end-1 and end-2 values for X. A GX call will often reverse the left-right, up-down order that we often put into models that we create using only GW entries. In this case, the most positive wire on the X-axis will appear as tag 3, with the positive wire closer to center being assigned tag 4. For many models, this order may make no difference, but we should always be aware of it by checking the segmentation data in the NEC output file. There are some cases in which the replication order can make a big difference.

The GX entry carries with it a list of cautions and warnings. Remember that the destruction of symmetry does not mean that the core will not produce the specified new wires and segments. It will indeed produce those wires, even if they end up in bad positions. Destruction of symmetry means only that the core will not use its faster routines in its calculations.

1. Do not locate segments in the plane (axis-value=0) or crossing the plane around which the reflection occurs. The result will be intersecting or overlapping wire segments, an illicit NEC condition.

2. Do not add a wire or patch after the GX card; that is, do not add on a GW, GH, CW, or SP entry. Such additions will destroy at least one plane of symmetry, and the program will reset to whatever symmetries may exist prior to the ruined one (or more). However, you may add a GW entry if it does not disturb the requested plane of symmetry.

3. Do not use a GM command with a number of new structures greater than zero, or symmetry will be destroyed. As well, a GM command acting on only part of a structure will also destroy symmetry.

4. Avoid second GX entries, since they will negate the symmetry established by the prior GX entry. A following GR (Generate Cylindrical Structure) card will also negate the symmetry of a prior GX command.

5. If the GE command indicates a ground plane by setting I1 to 1 or to -1, then symmetry across the Z-axis (otherwise expressed, symmetry parallel to the X-Y plane) will be destroyed, although any other specified symmetry will be used. As a practical example, if you wish to use symmetry for the square of 4 Yagis, but above a real ground, then the most direct way to accomplish this goal is to set a vertical pair of Yagis either as a pair of GW constructs or a GW + GM construct. Then to use the GX command to create the second pair across (in our examples) the X-axis. A following GM command may be used to rotate a structure about the Z-axis, so long as it includes the entire structure and does not create new structures.

Most of the listed cautions or limitations on the GX entry reset the core to either non-symmetry or to the highest level of symmetry allowable in light of the fault. There are other conditions, such as placing non-symmetrical lumped loads (LD1 through LD4) on the structure, that simply destroy symmetry without any resetting of the core. However, non-radiating networks (NT or TL entries) will not adversely affect a symmetry specification.

Making the GX card the last entry prior to the geometry end (GE) card is perhaps the wisest route. During the learning curve, it may prove useful to develop an over-simplified model having the same essential features as the eventual complex or very large model to ensure that you have introduced no symmetry-destroying features. In fact, our collection of initial models will all be simple. Their only function will be to illustrate properties of the command.

Open model *5-1.nec*. This model will provide us with a baseline for seeing how to create the same model in multiple ways.

```
GW 1 11 -.75 0 -.245 -.75 0 .245 .001
GW 2 11 -.25 0 -.245 -.25 0 .245 .001
GW 3 11 .25 0 -.245 .250 0 .245 .001
GW 4 11 .75 0 -.245 .75 0 .245 .001
GE
EX 0 1 6 0 1 0
EX 0 2 6 0 1 0
EX 0 3 6 0 1 0
EX 0 4 6 0 1 0
```

Each GW entry creates a vertical dipole (with the source assigned in each case to segment 6). The dipoles are equally spaced from the adjacent one(s) and form a symmetrical sequence with X

= 0 as the center of the set. **Fig. 5-1** shows the general layout, as well as providing a reference phi pattern. The array has a bi-directional free-space gain of 9.2 dBi. The outer dipoles have a source impedance of 66 - j1 Ω, while the impedance of the inner pair is 53 - j10 Ω.

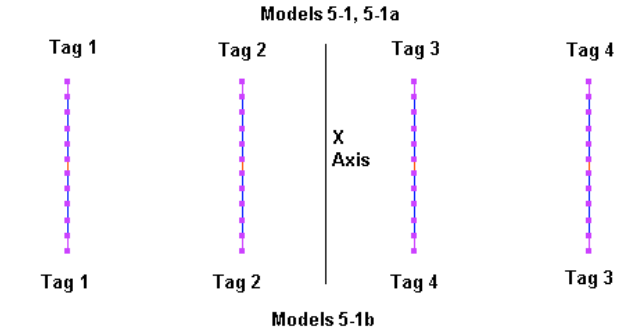

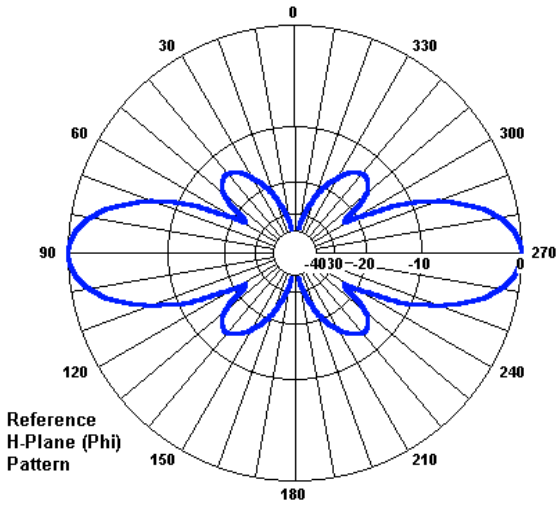

Fig. 5-1

We may create an identical structure by using fewer GW commands and letting the GM command replicate and move the initial dipole. Open *model 5-1a.nec* and examine the geometry section.

```
GW 1 11 -.75 0 -.245 -.75 0 .245 .001
GM 1 3 0 0 0 .5 0 0
```

We start with a single dipole and create 3 copies, each displaced by 0.5 m along the X-axis. Check the segmentation data for the model, comparing it to the comparable data for 5-1. If you run the model, you will arrive at the identical gain and source impedance reports. Now open model *5-1b.nec*.

```
GW 1 11 -.75 0 -.245 -.75 0 .245 .001
GW 2 11 -.25 0 -.245 -.25 0 .245 .001
GX 2 100
```

Here we have the model from which we have extracted parts for the purpose of introducing the command. Run the model and examine the segmentation data. You will discover that tag 3 represents the dipole with the most positive value for X, while tag 4 designates the positive inner dipole. Confirm the phi plot and gain value. Then examine the table of source impedance information (using the NSI program listing for convenience, rather than the NEC output report version).

Model 5-1b

Frequency	Tag	Seg.	Real(Z)	Imag(Z)
299.790000	1	6	65.696	-0.768
299.790000	2	17	52.828	-9.731
299.790000	4	39	52.828	-9.731
299.790000	3	28	65.696	-0.768

The order of sources is arranged to place the inner dipoles next to each other. Compare the tag numbers to those in a similar table for the previous models in this sequence (5-1 and 5-1a).
Models 5-1 and 5-1a

Frequency	Tag	Seg.	Real(Z)	Imag(Z)
299.790000	1	6	65.696	-0.768
299.790000	2	17	52.828	-9.731
299.790000	3	28	52.828	-9.731
299.790000	4	39	65.696	-0.768

Let's alter the project slightly by adding one more dipole, so that there is a wire at X = 0. Refer to **Fig. 5-2** and open model *5-2.nec* to see the standard way of forming this model.

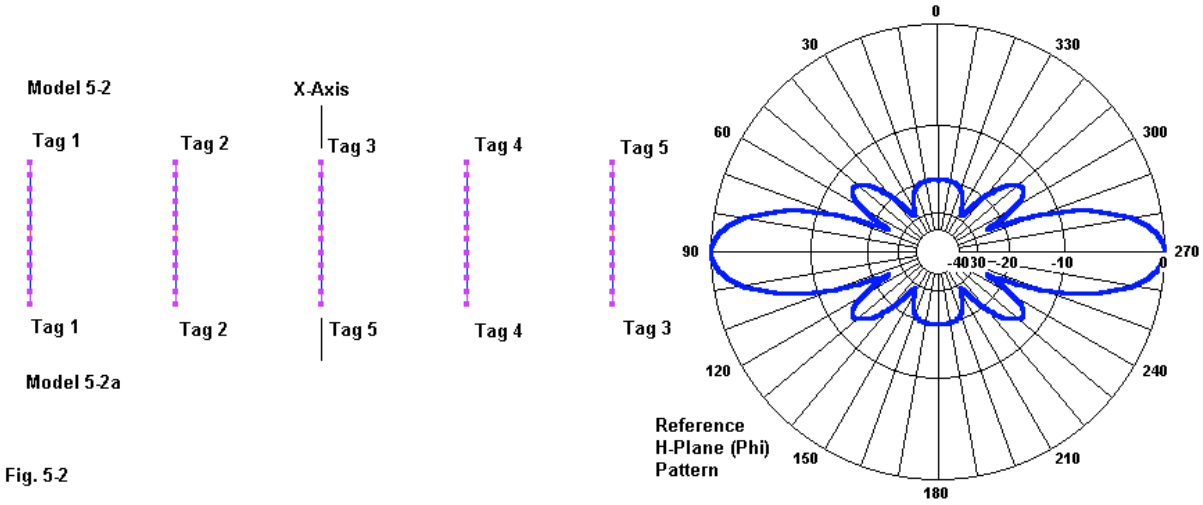

Fig. 5-2

```
GW 1 11 -1 0 -.245 -1 0 .245 .001
GW 2 11 -.5 0 -.245 -.5 0 .245 .001
GW 3 11 0 0 -.245 0 0 .245 .001
GW 4 11 .5 0 -.245 .5 0 .245 .001
GW 5 11 1 0 -.245 1 0 .245 .001
```

For reference, see the phi pattern on the right and run the model. The free-space gain is about 10.2 dBi. From the outer dipole to the center one, the source impedances are 69 - j0 Ω, 51 - j9 Ω, and 58 - j11 Ω.

If we wish to set this model up using the GX command, it will take the form shown in model *5-2a.nec*.

```
GW 1 11 -1 0 -.245 -1 0 .245 .001
GW 2 11 -.5 0 -.245 -.5 0 .245 .001
GX 2 100
GW 5 11 0 0 -.245 0 0 .245 .001
```

The GW entries create the dipoles with negative X-values. The GX command replicates reflections with positive X-values. Finally, the last GW entry (GW5) creates the center dipole. The

question that this model raises is whether the addition of the GW entry destroys symmetry, given the generalized warning associated with the introductory command explanation. The answer appears when you run the model and discover that it produces the same set of reported values as the standard model (5-1).

In fact, we may offset the center dipole (GW5) without disturbing the symmetry of the portion of the array reflected in the X-plane. Open and examine model *5-2b.nec*.

```
GW 1 11 -1 0 -.245 -1 0 .245 .001
GW 2 11 -.5 0 -.245 -.5 0 .245 .001
GX 2 100
GW 5 11 .02 0 -.245 .02 0 .245 .001
```

The center dipole is clearly offset toward the inner reflected dipole. However, if you run this model or examine the segmentation data, you will find that the output file yields sensible results for a 5-dipole array. You may perform other experiments on the center dipole--such as turning it at various angles, to determine under what conditions the core will reset as an indicator that symmetry has been destroyed.

One typical feature of many models has been omitted from the models that we have examined: material loading (LD5). Open model *5-3.nec* and examine the structure and the LD entry.

```
GW 1 11 -.75 0 -.245 -.75 0 .245 .001
GW 2 11 -.25 0 -.245 -.25 0 .245 .001
GW 3 11 .25 0 -.245 .250 0 .245 .001
GW 4 11 .75 0 -.245 .75 0 .245 .001
GE
EX 0 1 6 0 1 0
EX 0 2 6 0 1 0
EX 0 3 6 0 1 0
EX 0 4 6 0 1 0
LD 5 0 0 0 5.8e7 1
```

This standard (GW only) model requires separate excitation entries for each wire. The LD5 entry permits us to cover all of the structure with a single entry using the conductivity and permeability entries for copper. (NEC-2 does not include a permeability entry position, but the NSI cores will read the NEC-4 form.) Run this model. The output reports reflect the very slight loss associated with copper as a less-than-perfect wire: free-space gain is 9.18 dBi, and the two source impedances are 66 - j1 Ω and 53 - 10 Ω. Next, open model *5-3a.nec*, which uses the GX command.

```
GW 1 11 -.75 0 -.245 -.75 0 .245 .001
GW 2 11 -.25 0 -.245 -.25 0 .245 .001
GX 2 100
GE 0
EX 0 1 6 00 1 0
EX 0 2 6 00 1 0
EX 0 4 6 00 1 0
EX 0 3 6 00 1 0
LD 5 0 0 0 5.8e7 1
```

If we run this model, we obtain the same output reports as we received for 5-3. Indeed, also examine the current table for the model to verify that the original (GW) dipoles and the reflected dipoles have corresponding current magnitudes and phase angles. However, the model is ambiguous in terms of how the reflected dipoles receive their material (LD5) loading. So let's modify the model once more to assign separate LD5 values to GW1 and GW2. Open model *5-3b.nec*.

```
GW 1 11 -.75 0 -.245 -.75 0 .245 .001
GW 2 11 -.25 0 -.245 -.25 0 .245 .001
GX 2 100
GE 0
EX 0 1 6 00 1 0
EX 0 2 6 00 1 0
EX 0 4 6 00 1 0
EX 0 3 6 00 1 0
LD 5 1 1 11 5.8e7 1
LD 5 2 1 11 5.8e7 1
```

If you run this model, you will once more obtain the same output reports, including segmentation and current data. Therefore, we have discovered that at least LD5-type loads are fully reflected in a symmetrical structure, although sources are not. The latter require specification for each excited segment, whether original or reflected.

The following models illustrate the fact that we may reflect not only GW entries, but any of the geometry-forming entries, except those that invoke symmetry. If you have NEC-4, open model *5-4.nec*. Also examine **Fig. 5-3**.

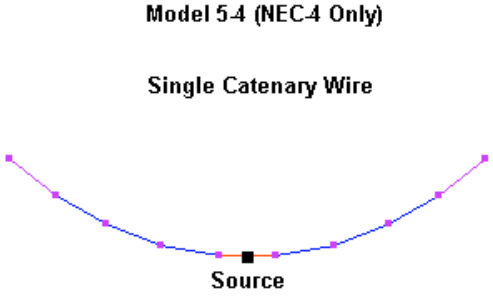

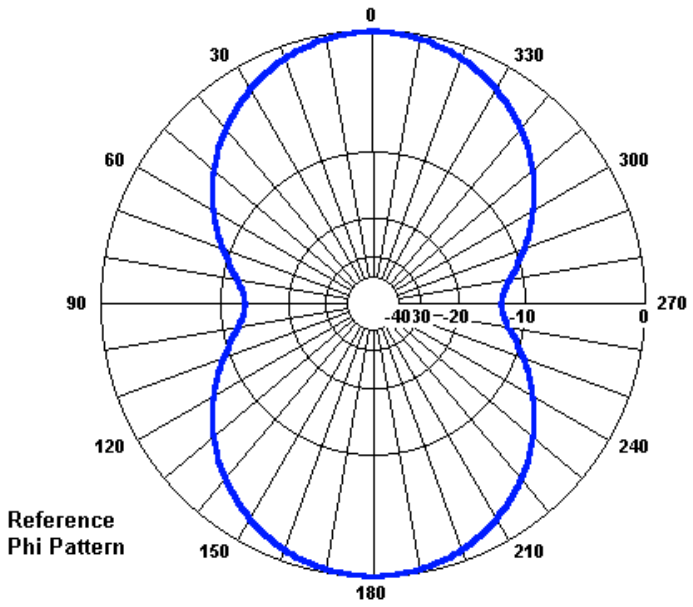

Fig. 5-3

```
CW 1 9 0 -.7125 5 0 -.2375 5 .001 1 .2375 4.9
GE 0 -1 0
EX 0 1 5 0 1 0
```

This model creates a single catenary wire and differs from one of the CW models in an earlier chapter only in the fact that we have shifted the coordinates so that the Y-value is negative at both ends of the wire. Now open model *5-4a.nec*, which attempts to use the GX command to reflect the wire in the X-plane. See **Fig. 5-4**.

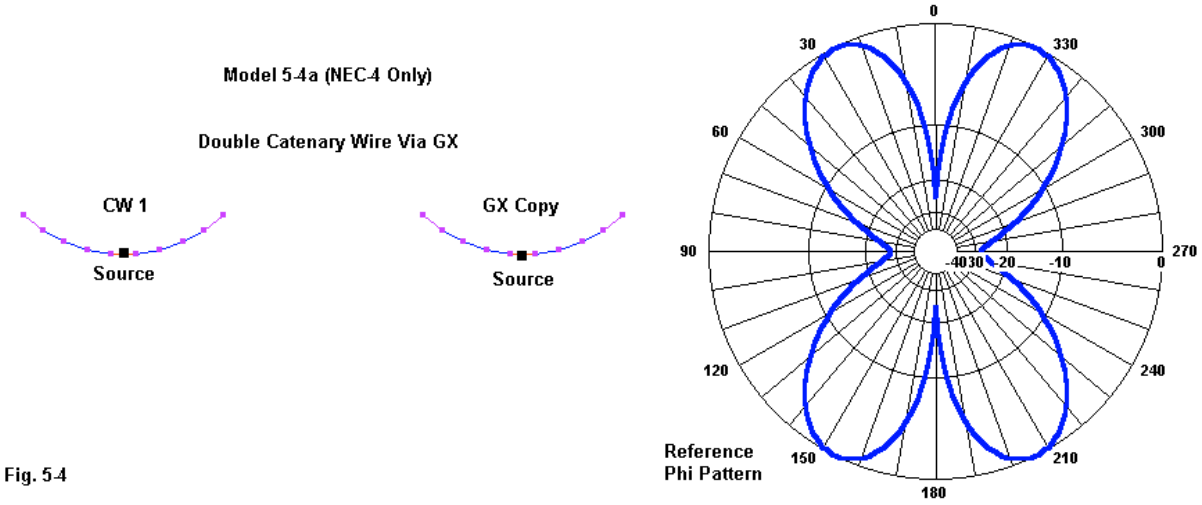

Fig. 5-4

```
CW 1 9 0 -.7125 5 0 -.2375 5 .001 1 .2375 4.9
GX 1 010
GE 0 -1 0
EX 0 1 5 0 1 0
EX 0 2 5 0 1 0
```

The graphic makes clear that the model correctly replicates the catenary wire, although we must remember to create a source for it, if we wish to obtain the pattern shown on the right.

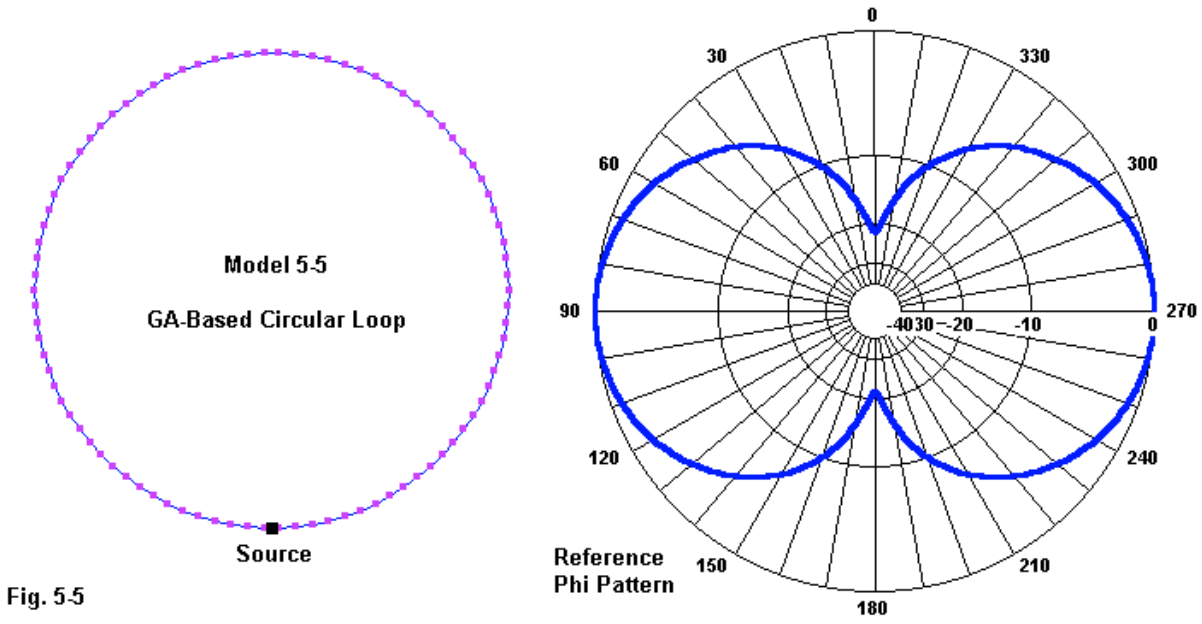

Fig. 5-5

Some geometry commands may require a supplementary GM command to place the construct in a position for reflection. Open model *5-5.nec* and examine **Fig. 5-5**.

```
GA 1 90 .169 0 360 .001
GM 0 0 0 0 0 0 -.1 0
```

This single loop, created with the GA command, initially appears in the X-Z plane at Y = 0. Therefore, the following GM command moves it in the -Y direction by 0.1 m. If we had not moved the loop and still tried to apply symmetry in the Y-plane, the result would have been two loops occupying the same space in the coordinate system, an illicit condition.

The GM movement of the loop allows us to create model *5-5a.nec*, shown in **Fig. 5-6**.

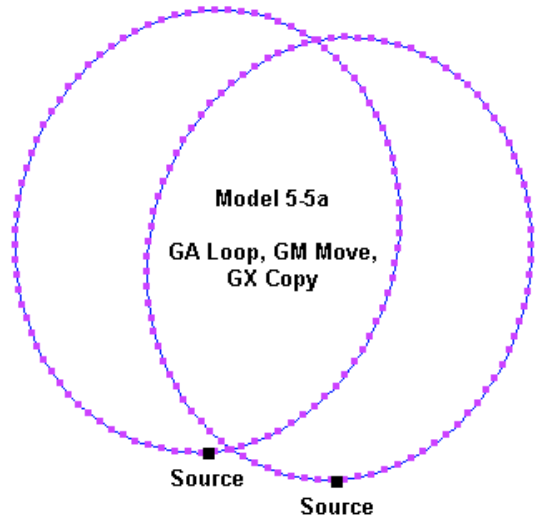

Fig. 5-6

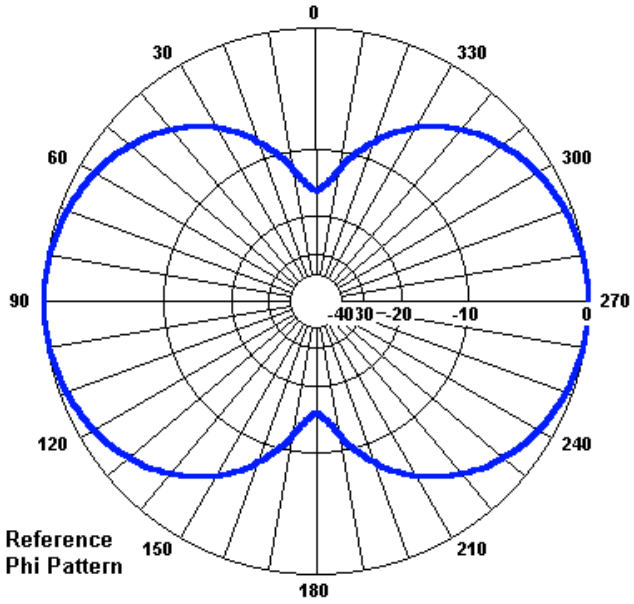


```
GA 1 90 .169 0 360 .001
GM 0 0 0 0 0 0 -.1 0
GX 1 010
```

Run the model and explore the segmentation data. Alternatively, check the coordinates of selected corresponding segments on the two loops that appear in Necvu. In either case, you will find that the GX command has successfully replicated the loop as moved. That is, absolute segments 91 through 180 have Y values of +0.1, in contrast to the -0.1 values for the first 90 segments.

In our catalog of simplified models, we lack perhaps only two items to complete the listing. One is a reflection in the Z-plane. The other is an exploration of what happens to loads other than LD5 material conductivity loads. We may rectify both omissions with a single model: a short (non-resonant) dipole brought to resonance with mid-element loads. We shall begin with a single dipole meeting this description and then move toward doubling it vertically with the GX command.

Open model *5-6.nec* and also examine **Fig. 5-7**.

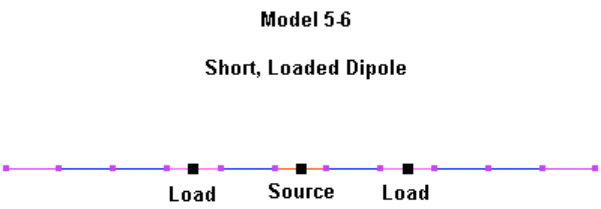

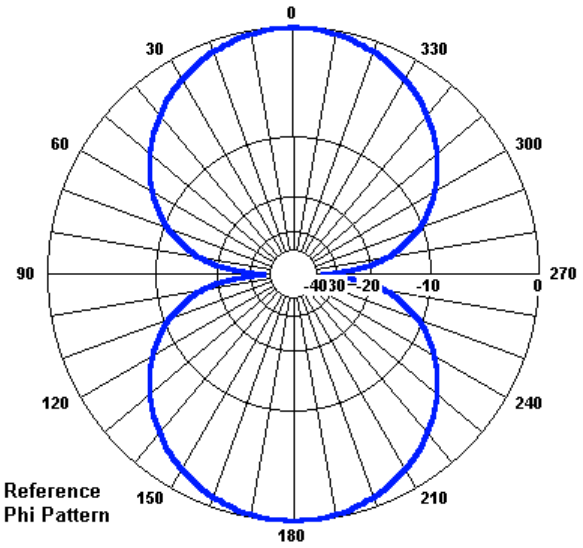

Fig. 5-7

```
GW 1 11 0 -.2 -.25 0 .2 -.25 .001
GE 0 -1 0
EX 0 1 6 0 1 0
LD 4 1 4 4 .1 100
LD 4 1 8 8 .1 100
```

The GW1 entry establishes a wire that is shorter than a resonant dipole for the test frequency, 299.7925 MHz. The wire is 0.25 m below the Z = 0 level, which makes no difference to performance output reports in the free-space environment. On each side of the center of the wire, there is an LD4, a complex or R-X load, consisting of 0.1 + j100 Ω values. The output report records a gain of 2.0 dBi, with a source impedance of 55 + j1 Ω.

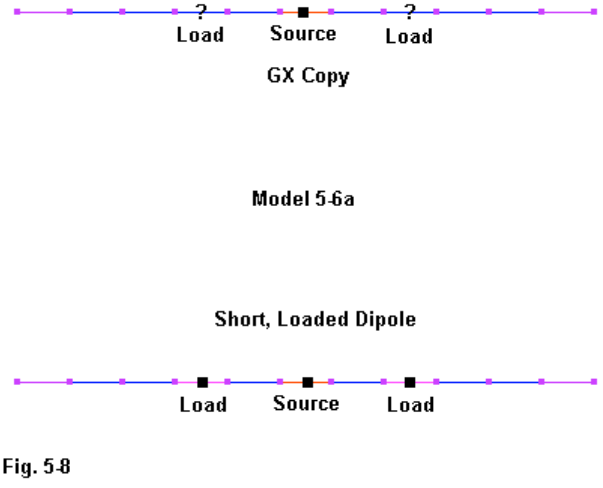

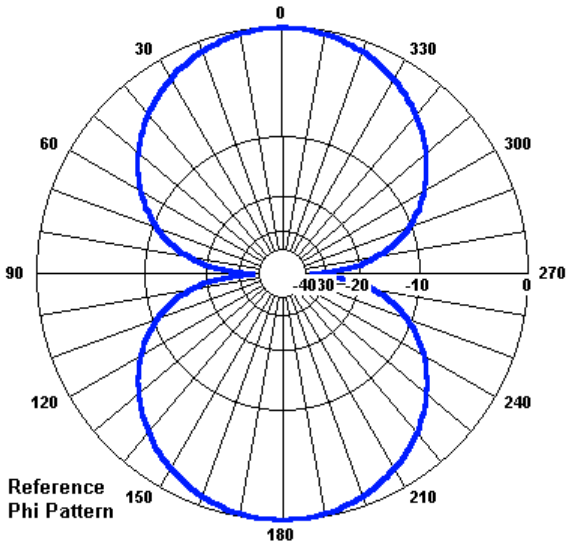

Fig. 5-8

Fig. 5-8 outlines the results of model *5-6a.nec*. The GX entry creates a second dipole at Z =

+0.25 m. However, the Necvu outline in the figure does not show loads at the indicated segments, and the NEC output report nowhere shows such loads. The model does explicitly set a source on the replicated wire, and both Necvu and the output report dutifully record it.

```
GW 1 11 0 -.2 -.25 0 .2 -.25 .001
GX 1 001
GE 0
EX 0 1 6 0 1 0
EX 0 2 6 0 1 0
LD 4 1 4 4 .1 100
LD 4 1 8 8 .1 100
```

How can we tell if the GX command has replicated the loads? We have several ways to find out. First, both sources return impedances of 44.5 - j20.6 Ω, indicating that similar current conditions exist on each element. Second, we can examine the currents along each wire and discover that they are identical on a segment-by-segment basis. Third, we can re-create the model using standard methods and compare its output reports with those of the model that invokes GX. Open model *5-6b.nec*.

```
GW 1 11 0 -.2 -.25 0 .2 -.25 .001
GW 2 11 0 -.2 .25 0 .2 .25 .001
GE 0 -1 0
EX 0 1 6 0 1 0
EX 0 2 6 0 1 0
LD 4 1 4 4 .1 100
LD 4 1 8 8 .1 100
LD 4 2 4 4 .1 100
LD 4 2 8 8 .1 100
```

Run this model and record the performance output values. They are the same as for model 5-6a. As a consequence, even though the NEC output report does not directly show the replication of all loads, we can determine from the data that loads are indeed replicated in the reflected structure. You may replicate the model using LD0 or LD1 R-L-C loads.

This collection of simple models cannot exhaust the possibilities for what happens when we invoke symmetry via the GX command. They should nonetheless provide a reasonable array of expectations. Perhaps we should examine some more challenging uses for the command.

Some Practical GX Models

Let's begin with a simple 6-element Yagi designed for 299.7925 MHz, where 1λ is 1 meter. Open model *5-7.nec* to see the description of the single-bay Yagi. The design uses a single reflector element (GW1), so the driver is GW2, as indicated by the source (EX0) placement. Elements are extended in the -X to +X plane, with the invisible boom extended from Y = 0 toward +Y. We shall stay in free space for this exercise, since eventually we shall want to create a GX version with symmetry relative to the X- and the Z-axes. For simplicity throughout this exercise, we have set the LD5 (material load) line so that it always encompasses all segments, no matter how many wires segments we add to the model by any of the means that we shall explore. A phi-pattern request (RP0) completes the model. See **Fig. 5-9** for the antenna outline and a reference pattern.

```
GW 1 21 -.2506139 0. 0. .2506139 0. 0. .001
GW 2 21 -.2471627 .125307 0. .2471627 .125307 0. .001
GW 3 21 -.2311685 .1771615 0. .2311685 .1771615 0. .001
GW 4 21 -.2245753 .3207017 0. .2245753 .3207017 0. .001
GW 5 21 -.2245753 .4611742 0. .2245753 .4611742 0. .001
GW 6 21 -.2162257 .6706705 0. .2162257 .6706705 0. .001
GE 0
LD 5 0 0 0 2.5E+07
FR 0 1 0 0 299.7925 0
GN -1
EX 0 2 11 00 1 0.
RP 0 1 361 1000 90 0 1.00000 1.00000
```

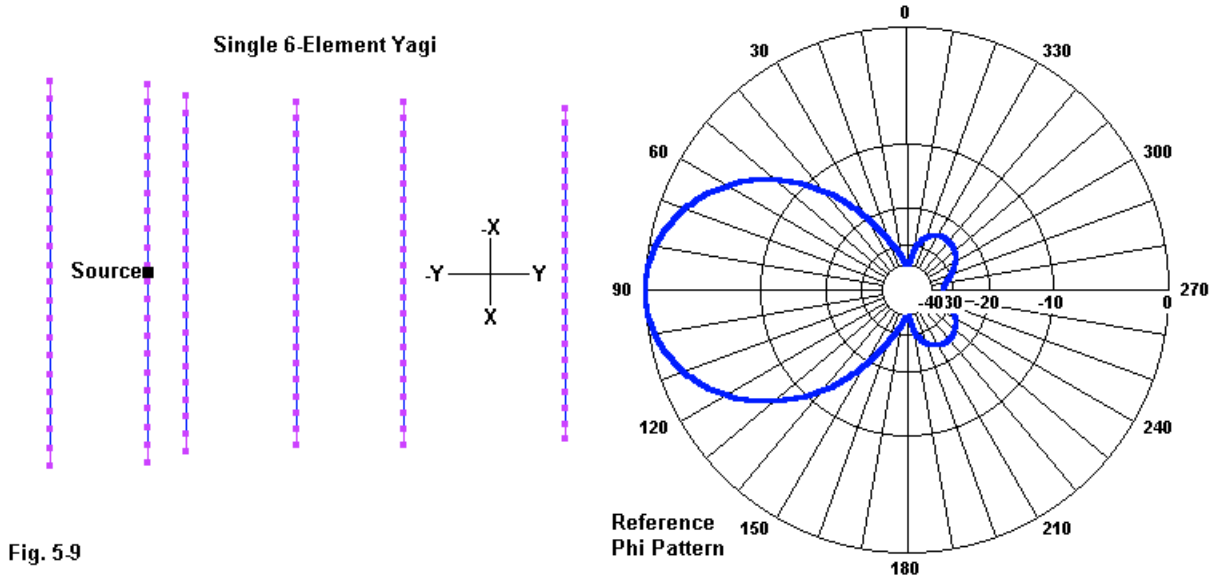

Fig. 5-9

The following table provides some of the significant output data for the model.

Free-Space Gain dBi	180° Front-Back Ratio dB	Source Impedance R +/- jX Ω	Core Run Time Seconds
10.17	33.94	49.5 + j10.6	0.77

The only unusual bit of data in the listing is the core run-time taken from the NEC output report. It encompasses all core operations, which include the modification of values for the conductivity of aluminum and the E-plane or azimuth/phi pattern request as well as the matrix work. Run time is a function of model size and computer speed. This table holds our base-line data against which we shall make comparisons as we modify the model to create a square array of 4 such beams with their booms separated by 1λ in each direction. (We do not here have to concern ourselves as to whether the spacing is optimal, so the convenient measures will work well for us.)

There are at least 3 ways to create our square of Yagi models. The method that is available on entry-level programs is simply to replicate the first Yagi 3 more times and to space each one at the required distances apart to make the square. Using copy and move functions for blocks of GW or wire entries simplifies the process somewhat, but the final model is somewhat large

visually and not too easy to scan rapidly. See **Fig. 5-10** for a sketch of the resulting 4-bay array that results from not only this formation method, but as well from methods to come.

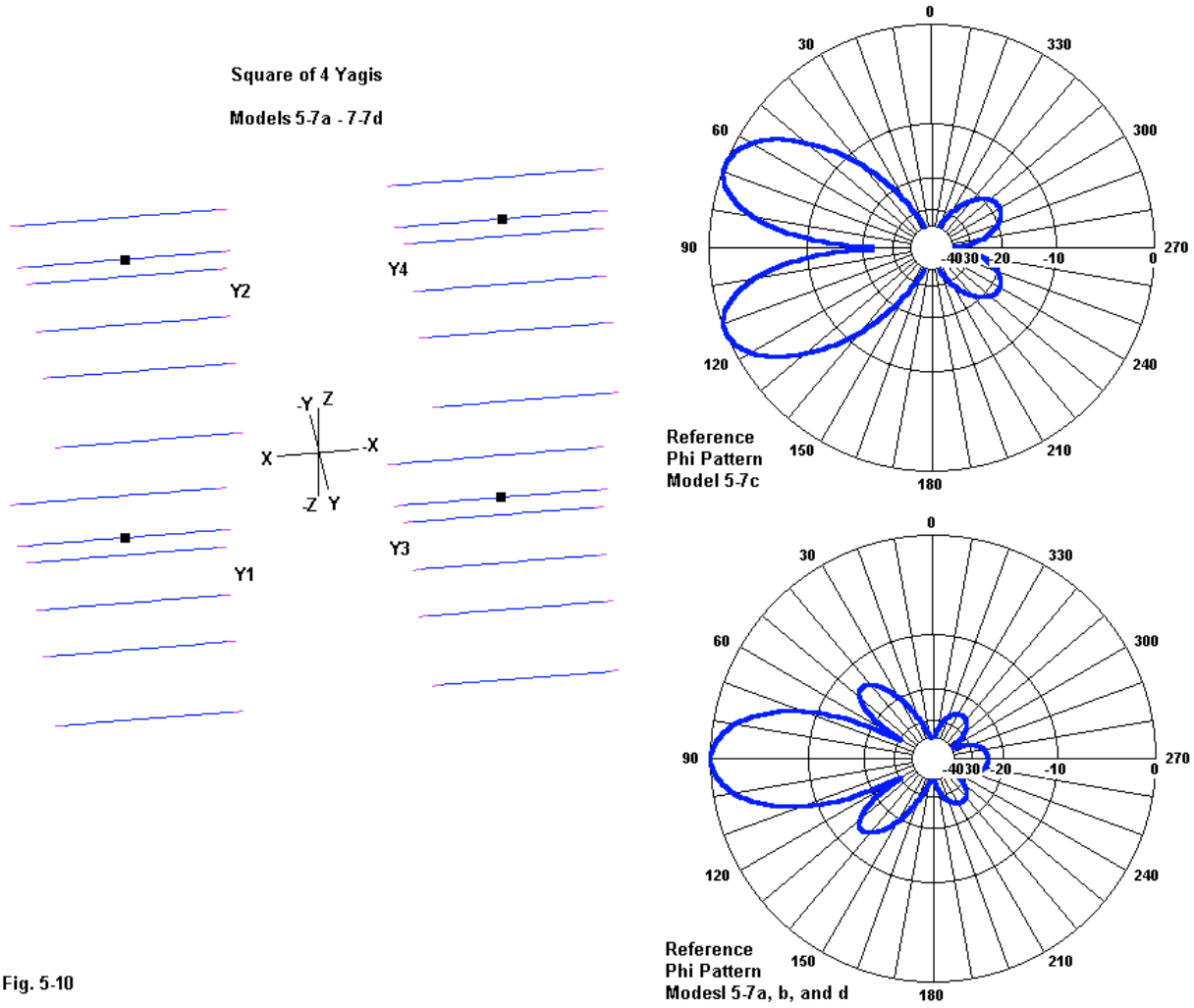

Fig. 5-10

Open model *5-7a.nec* and examine the structure--too long to reproduce here. Note that for at least the first Yagi in the set, you must pre-calculate the end coordinates for each element to assure that the boom is centered. Nevertheless, this somewhat tedious process results in a good model that produces the following results.

Free-Space Gain dBi	180° Front-Back Ratio dB	Source Impedance R +/- jX Ω	Core Run Time Seconds
16.20	24.06	51.3 + j8.5 (X4)	5.60

Quadrupling the number of segments and tags in the model has increased the run time by a factor of over 7.25. The run-time ratio would be higher for larger models multiplied by 4, since the output request overhead processing time remains about the same for the single Yagi and for the square of 4 Yagis.

A second formation technique employs the GM or Coordinate Transformation command. So let's reuse our 6 GW lines for a single Yagi and then make the moves indicated by the GM lines that follow in model *5-7b.nec*.

```
GW 1 21 -.2506139 0. 0. .2506139 0. 0. .001
GW 2 21 -.2471627 .125307 0. .2471627 .125307 0. .001
GW 3 21 -.2311685 .1771615 0. .2311685 .1771615 0. .001
GW 4 21 -.2245753 .3207017 0. .2245753 .3207017 0. .001
GW 5 21 -.2245753 .4611742 0. .2245753 .4611742 0. .001
GW 6 21 -.2162257 .6706705 0. .2162257 .6706705 0. .001
GM 0 0 0 0 0 -.5 0 -.5
GM 6 1 0 0 0 0 0 1
GM 12 1 0 0 0 1 0 0
GE 0
```

The first GM line moves the existing Yagi into the -X and -Z region. The amount of each move is 0.5λ. This move will simplify the required moves for both this and the third alternative square of Yagis. The second GM line creates a second Yagi 1λ above the first one and assigns it tag numbers 7-12. The third GM line creates a new pair of Yagis 1λ in the +X direction and assigns them the tag numbers 13-24. We end up with the same square of Yagis that we viewed in **Fig. 5-10**. The output report appears in the following table.

Free-Space Gain dBi	180° Front-Back Ratio dB	Source Impedance R +/- jX Ω	Core Run Time Seconds
16.20	24.06	51.3 + j8.5 (X4)	5.71

The only difference in the reported data is the run-time. In this instance, it is 0.11 seconds longer than the run-time for the GW construct. However, run times will vary slightly from one run to the next. So we may view the times for the two formulations of the 4-bay array as essentially the same. GM allows us to scan the model more easily, but it does not save any run time.

Now let's create the same models with the GX reflection input. We shall add a GM card to move the initial single Yagi into the same -X, -Z position that we used with the GM construct. However, this time, we shall create the other 3 Yagis with a single GX line, as shown in model *5-7c.nec*.

```
GW 1 21 -.2506139 0. 0. .2506139 0. 0. .001
GW 2 21 -.2471627 .125307 0. .2471627 .125307 0. .001
GW 3 21 -.2311685 .1771615 0. .2311685 .1771615 0. .001
GW 4 21 -.2245753 .3207017 0. .2245753 .3207017 0. .001
GW 5 21 -.2245753 .4611742 0. .2245753 .4611742 0. .001
GW 6 21 -.2162257 .6706705 0. .2162257 .6706705 0. .001
GM 0 0 0 0 0 -.5 0 -.5
GX 6 101
```

Note that by incrementing the tag numbers by 6, we shall create a total of 24 tags. The GX line indicates replication across the Z-axis and then total replication across the X-axis. The Necvu result is identical to the square of Yagis shown in **Fig. 5-10**. We also have added the EX lines to make sure that we have a source for each reflection. So why does the resulting pattern emerge as shown in the upper right portion of **Fig. 5-10**? And why do we obtain a table of performance results like the following one?

Free-Space Gain dBi	180° Front-Back Ratio dB	Source Impedance R +/- jX Ω	Core Run Time Seconds
13.71	19.22	58.9 - j9.5 (X4)	2.53

The answer lies in how NEC creates reflections in coordinate planes. The new structures are indeed mirror images. The following abbreviated table compares the first and last segments of each of the 4 reflector wires from the GM construct (which is identical to the GW construct) and from the GX construct, as recorded in the segmentation data in the NEC output file.

Partial Segmentation Tables From NEC-4 Output Files

5-7b: GM Construct

SEG. NO.	COORDINATES OF SEG. CENTER X	Y	Z	LENGTH
1	-0.73868	0.00000	-0.50000	0.02387
21	-0.26132	0.00000	-0.50000	0.02387
127	-0.73868	0.00000	0.50000	0.02387
147	-0.26132	0.00000	0.50000	0.02387
253	0.26132	0.00000	-0.50000	0.02387*
273	0.73868	0.00000	-0.50000	0.02387*
379	0.26132	0.00000	0.50000	0.02387*
399	0.73868	0.00000	0.50000	0.02387*

5-7c: GX Construct

SEG. NO.	COORDINATES OF SEG. CENTER X	Y	Z	LENGTH
1	-0.73868	0.00000	-0.50000	0.02387
21	-0.26132	0.00000	-0.50000	0.02387
127	-0.73868	0.00000	0.50000	0.02387
147	-0.26132	0.00000	0.50000	0.02387
253	0.73868	0.00000	-0.50000	0.02387*
273	0.26132	0.00000	-0.50000	0.02387*
379	0.73868	0.00000	0.50000	0.02387*
399	0.26132	0.00000	0.50000	0.02387*

If we compare the entries for the 3rd and 4th reflectors, which emerge from translations or from reflections across the X-axis, we can see that the order from first to last segment is reversed in the GX construct. (As well, the beta orientation angle is not 0, but 180 degrees.) However, if we return to the model description and examine the EX lines, we set up all four sources with the same phase angles: 1 real and 0 volts imaginary. The result is a square of four Yagis with the left pair fed out of phase with the right pair. To restore the in-phase feed for the two pair of Yagis, we need to reverse the phase of the right-most beam sources or EX entries (or, alternatively, of the left-most pair). We achieve this simply by adding a minus sign to the real component of the voltage at the source, as shown in model *5-7d.nec*.

```
EX 0 2 11 00 1 0.
EX 0 8 11 00 1 0.
EX 0 14 11 00 -1 0.
EX 0 20 11 00 -1 0.
```

When we make the change, the following data emerge from the model after running the core.

Free-Space Gain dBi	180° Front-Back Ratio dB	Source Impedance R +/- jX Ω	Core Run Time Seconds
16.20	24.06	51.3 + j8.5 (X4)	2.52

Obviously, almost nothing changes relative to the GW and GM constructions, except for the run-time. In this trivial-sized model, the run-time is less than half that of the other two models, and most of that time is taken up in pre- and post-matrix calculations and file generation. A truly large model would show a far greater reduction in core run-time.

A second type of example may better illustrate the run-time savings that symmetry yields. We shall develop a simple doublet at 15 MHz, where a wavelength is close to 20 meters. We shall use segments close to 1-m long so that there are about 20 segments per wavelength. We shall employ 2 construction methods for the model, as illustrated by **Fig. 5-11**.

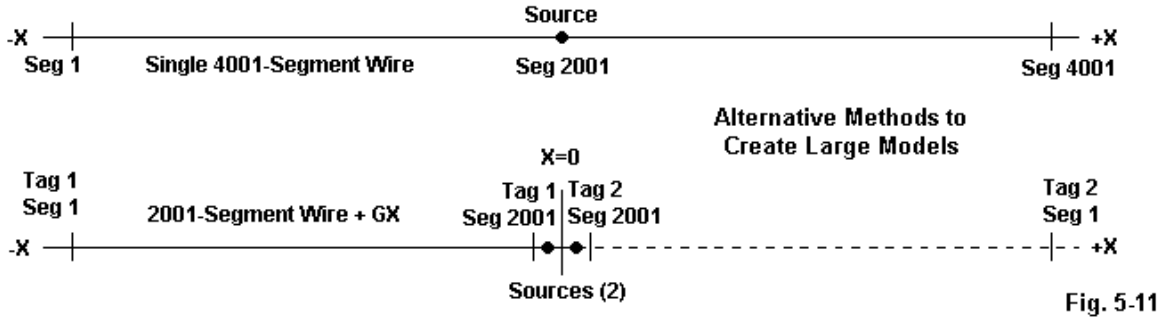

Fig. 5-11

Open model *5-8.nec*, which uses standard GW methods.

```
GW 1 4001 0 0 0 0 4000 0 0.000005
```

The second model (model *5-8a.nec*) uses a GW1 entry with 2001 segments, each with the same length as in the first model. However, we set the 2001 segments from a position of Y=-2000 to Y=0. Then we set the GX input as shown in the model description.

```
GW 1 2001 0 -2000 0 0 0 0 0.000005
GX 1 010
```

This entry creates a reflection across the Y-axis. The reflection runs from Y=+2000 to Y=0. The result is a single continuous wire-pair running 2000 meters each side of Y=0. To center the source, we create two EX lines, each in the segment closest to Y=0. The sum of the two source impedance reports should equal the impedance we would achieve in the 4001-segment model at the same overall length (4000 m). The values will not be precisely the same, because the sources are located in a low current, high voltage region of the antenna, where the impedance

changes rapidly in a very small distance. However, we are here less interested in the output reports for the models--except to ensure that each model is accurately constructed--and more interested in the run times. Model *5-8b.nec* is a simple 2000-m, 2001-segment doublet used only to compare run times.

Model	Run-Time (sec)
5-8 (1-wire, 4001 segments)	777.31
5-8a (2001 segment wire + GX)	238.05
5-8b (1-wire, 2001 segments)	119.90

The models are perhaps medium-size and simple enough not to require excessive run-times regardless of the method of construction. However, they are large enough that the overhead becomes insignificant compared to the matrix time. Hence, their relative times are useful in developing an expectation of run times on models of this size and larger. A single reflection requires about twice the run-time of virtually the same 2001-segment model without the reflection. However, the GW-only version of the large doublet requires over 3.2 times the run-time of the GX version of the same wire antenna.

Doubling of the number of segments in the two GW-only models results in a nearly 6.5 increase in run-time. Reducing that time to merely double the smaller-model run-time represents a considerable saving, especially when extrapolated (roughly) to still larger models. Since I did not exclude to the degree possible all overhead time, these numbers will be imprecise relative to all of the possible variations in model construction. But they do provide an indication of the orders of saving possible whenever a GX input is relevant to a large model.

Run-times are not the only notable feature of the model. The ability to bring a wire to a zero value, that is, to a position on an axis, can be multiplied indefinitely within the limits of array dimensions allowed by the core and the operating system. Hence, one might build 1/2 of a wire-grid ship, plane, or ground vehicle and create the other half via the GX entry. Similarly, a free-space sphere may begin with 1/8th of the structure and reach completion via the GX entry specifying reflection in all three planes. An oval may require only ¼ of the structure for completion in two reflections.

The GR or Generate Cylindrical Structure Command

The GR command is a specialized rotational device that invokes symmetry for rapid replication of an initial structure. View the initial structure as vertical and offset from the center (X = 0, Y = 0) position. Invoking the GR command will then create rotated versions of the initial structure the number of times (NR) specified by the command with each new version rotated around the Z-axis by 360°/NR. The result is a cylindrical structure with the added property of running much faster than a similar structure produced by the GM command due to the use of symmetry.

Like the GX command, GR is deceptively simple, since it employs only the first two integer positions on the command line. It does not use any of the floating decimal positions. Due to its simplicity, the command carries with it a host of restrictions, some of which have led modelers to by-pass the command in favor of others. Like GX, GR is identical in both NEC-2 and NEC-4.

```
Cmd   I1          I2
      Tag No.     Total No.
      Increment   of Occurrences
GR    1           6
```

Like GX, the I1 entry should specify an increment such that each new occurrence of the initial structure takes on a previously unused tag number. In some commands, such as GM, you will specify the number of new structures beyond the initial structure. However, in GR, you specify the total number of structures, including the initial structure. Now let's sample the restriction list.

1. Avoid using GR when segments lie on or cross (at other than junctions) the Z-axis to prevent the occurrence of overlapping segments.

2. Avoid adding a GW entry following GR or symmetry may be destroyed.

3. Use a following GM command only if the number of new structures is set to zero and if the command acts only on the entire structure. Also avoid rotating the structure with GM around the X- or Y-axis when a ground is specified.

4. A following GX or GR entry will destroy the previously established symmetry.

5. Avoid non-symmetrical lumped loads. However, non-radiating networks and sources will not affect symmetry.

We shall sample the formation of GR structures using the simplest possible structures. **Fig. 5-12** shows the structures that result from the sample models. Note that destruction of symmetry does not mean a failure to create the specified wires. Destruction of symmetry means only that the core will not use the symmetry routines for calculating.

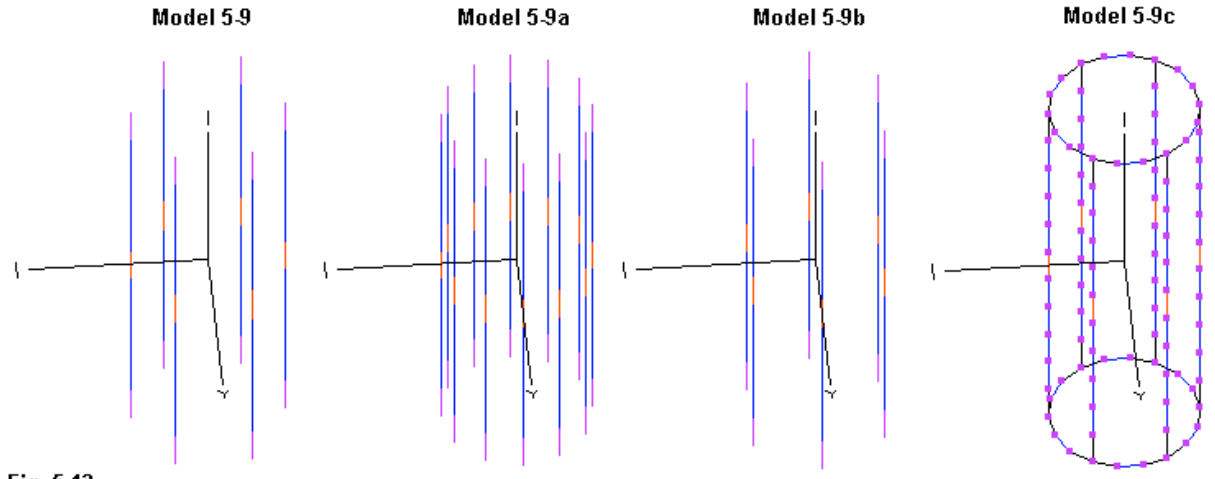

Fig. 5-12

Despite the seeming complexity of some of the structures, formation is very straightforward. Begin by opening model *5-9.nec*. To create the set of 6 vertical dipoles in the left-most portion of **Fig. 5-12**, we need only 2 geometry commands (plus the obligatory GE command to terminate the

geometry portion of the model).

```
GW 1 11 -.1 0 -.280 -.1 0 .280 .001
GR 1 6
```

GW1 sets up a vertical dipole in this free-space model. It extends equally above and below the Z = 0 level. As well, the dipole is displaced -0.1 m along the X-axis. However, a starting structure may begin with any values of X and Y so long as they are not both zero. Since we have only one tag number, we need increment it only by 1 in the GR line. Then we specify 6 total structures to form the cylinder at the left in **Fig. 5-12**.

```
WIRE
  NO.       X1          Y1          Z1          X2         Y2        Z2
   1   -0.10000    0.00000   -0.28000   -0.10000   0.00000  0.28000
                        NO. OF    FIRST  LAST     TAG
            RADIUS      SEG.      SEG.   SEG.     NO.
            0.00100      11        1     11        1
STRUCTURE ROTATED ABOUT Z-AXIS  6 TIMES.  LABELS INCREMENTED BY   1

TOTAL SEGMENTS USED= 66, NO. SEG. IN A SYMMETRIC CELL= 11, SYMMETRY FLAG= -1
   STRUCTURE HAS 6 FOLD ROTATIONAL SYMMETRY
```

The sample structure specification portion of the output file for model 5-9 shows how the core sets up the GR command. The segmentation data provides a full set of the 66 segments within the overall cylinder of wires. Note that in the original model, there is an EX0 entry for each wire. In the source impedance report, the actual value is not especially meaningful to any real antenna structure. However, observing that all the values are the same is good modeler evidence that the geometry has a correct set-up.

We may easily change the number of wires in the model by altering only the GR line of the model. Open model *5-9a.nec* and look at the GR line.

```
GR 1 12
```

The new version of the model produces the structure in **Fig. 5-12** just left of center. The command automatically recalculates the proper angular displacement for the 12-wire cylinder. Note also in the model that there are now 12 EX0 entries to make this model comparable to the first one. One caution to observe when increasing the number of occurrences of the initial structure is not to add so many that the individual wires are too close together. Although not a problem with our standard 0.001-m radius wire, inaccuracies may result if the individual wire radii are too large for the spacing between them.

Open model *5-9b.nec*. This model adds an allowable post-symmetry rotation and movement of the 6-wire structure in 5-9.

```
GW 1 11 -.1 0 -.280 -.1 0 .280 .001
GR 1 6
GM 0 0 0 0 30 0 0 .280
```

Since the GM entry affects the entire structure, it will run on both NEC-2 and NEC-4. The first motion entry in the command rotates the structure 30°. You can see the rotation by referencing

the Y-axis line in the inner right-of-center view in **Fig. 5-12**. Compare its orientation to the un-rotated left-most view within the figure. The second maneuver within the GM command elevates the entire cylinder 0.28-m along the Z-axis. Since neither motion disturbs the symmetry of the structure, the moves show up correctly in the segmentation data of the output report. Compare the data--especially the Z-axis values--for this model with the comparable values in the report for model 5-9. The GR command creates the new wires, but does not invoke symmetry, since a geometry command follows the GR entry.

The right-most view in **Fig. 5-12** shows a 6-wire cylinder that is closed top and bottom by circular structures. Open model *5-9c.nec* to see how we can perform the operation. Because the structure development involves GM commands that affect individual tags and not the entire structure, there are separate NEC-2 and NEC-4 versions of the model.

```
GW 1 11 -.1 0 -.280 -.1 0 .280 .001
GA 2 3 .1 0 60 .001
GM 0 0 90 0 0 0 0 .28 002.002
GA 3 3 .1 0 60 .001
GM 0 0 90 0 0 0 0 -.28 003.003
GR 3 6
```

After creating the initial vertical wire, we enter two separate GA commands to create 60° arcs, the angular distance between the wires in the ultimate set. However, GA initially creates each arc vertically, so we must rotate each one by 90°, while moving it to the proper end of the initial wire. The result is an initial structure consisting of a vertical wire with an arced wire attached to each end. The GR command finishes the full cylinder with its closed top and bottom ends.

By locating the coordinates of each segment junction in the original wire, you may add arcs at each junction and create a cylinder that is closed at all available intermediate points. Note in the sample model that the 6 EX0 entries now use new tag numbers to reflect the 3-tag initial structure. When creating structures by symmetry, it is useful to keep track of the ways that geometry modifications will affect other parts of the total model. If a scratch pad will not suffice, you may consult the Necvu segment identification feature or the segmentation data to track these affects.

Even though these small sample models do not fairly show the core-run timesaving, the largest model (132 segments) required less than twice the time of the smallest (66 segments). Wire cylinders also offer some advantages when modeling large diameter tubular structures, since the radii of the individual wires forming them via GR may have the same size as wire attached to them (so long as those wires do not destroy the symmetry). A disadvantage is that GR-formed cylinders are not suitable for antennas such as slotted cylinders, since there is no way to remove selected wires from the finished product.

A simple but practical example of a good use for the GR command is the generation of radials for a monopole situated at X = Y = 0. It serves as an alternative to the use of the GM command, so let's begin with a model that generates all but the first radial with GM. Our model will place 32 radials 0.001 m above average ground. The radials will be 0.25 m long with a monopole projecting upward to a length that yields near resonance. The test frequency is 299.7925 MHz.

Open model *5-10.nec*.

```
GW 1 10 0 0 .001 .25 0 .001 .001
GM 1 35 0 0 10 0 0 0
GW 37 10 0 0 .001 0 0 .24 .001
GE
GN 2 0 0 0 13.0000 0.0050
FR 0 1 0 0 299.7925 1
EX 0 37 1 00 1 0
RP 0 181 1 1000 -90 90 1.00000 1.00000
EN
```

GW1 defines the first radial. The following GM command replicates the radial 35 times, with each new structure rotated 10° around the Z-axis. Since each new structure increments the tag number by 1, we end up with 36 tags. The monopole itself receives tag number 37. Run the model to confirm a source impedance of 32.3 - j 0.4 Ω, and a gain (from the theta plot) of 0.63 dBi at a take-off angle of 62°. **Fig. 5-13** shows the model outline with a reference theta pattern.

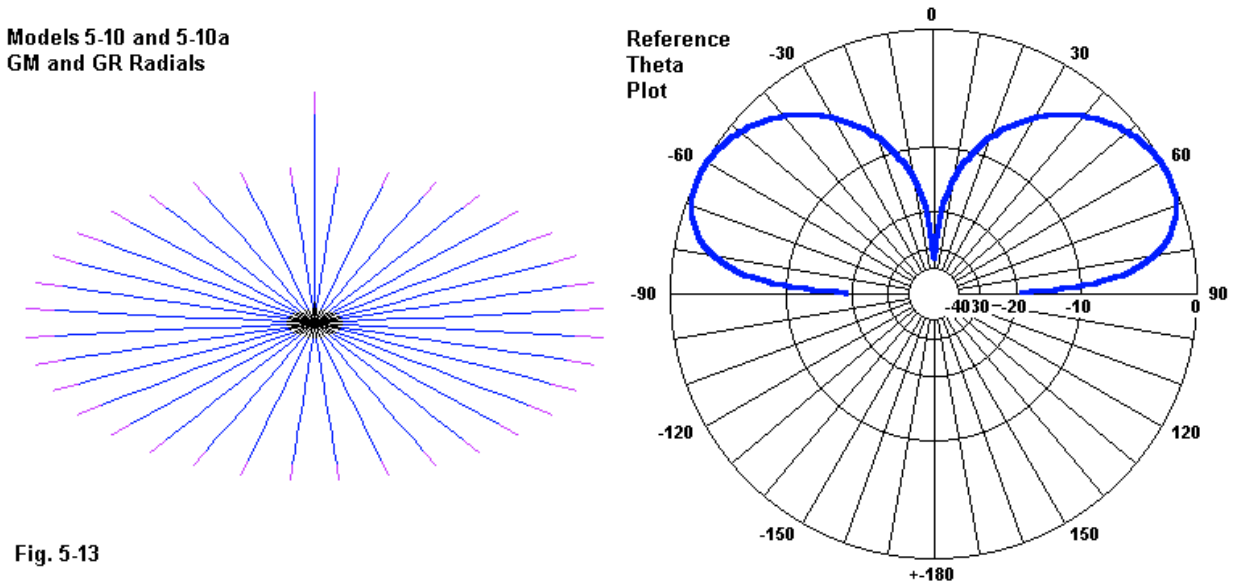

Fig. 5-13

Open model *5-10a.nec*.

```
GW 1 10 0 0 .001 .25 0 .001 .001
GR 1 36
GW 37 10 0 0 .001 0 0 .24 .001
GE
GN 2 0 0 0 13.0000 0.0050
FR 0 1 0 0 299.7925 1
EX 0 37 1 00 1 0
RP 0 181 1 1000 -90 90 1.00000 1.00000
EN
```

The only difference between model 5-10 and model 5-10a is the second geometry line. The GM line is gone, replaced by a GR command. The line specifies a tag increment of 1 with 36 total

structures within the 360° limit of rotational symmetry. The monopole (GW37) remains unchanged. If you examine the model outline in Necvu, you will see that the result is identical to the GM version of the antenna. Because a GW follows the GR command, we obtain the new radial wires, but symmetry shortcuts in calculation do not occur.

Run the model and obtain the normal output values for this GR version of the monopole and its radials. Like the structure, these values will be the same as for the GM version of the model. In the present context where the GW command follows the GR command, the symmetry command will not effect any noticeable time or file size savings. However, for large radial systems, the savings can be considerable. Consider the typical AM broadcast monopole that uses 120 radials, as outlined in **Fig. 5-14**.

A 120-Radial Monopole System Fig. 5-14

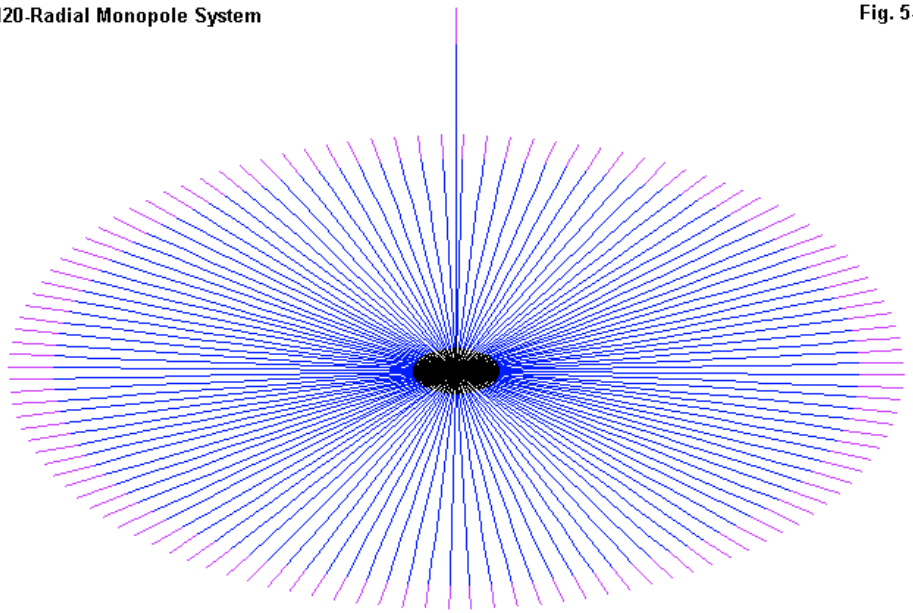

First, we must insert a caution about the tightness of the angle (3°) between wires. In many instances, unless segment lengths are long and/or the wires are very thin as a fraction of a wavelength, the wires at the hub will interpenetrate, although the symmetry of the system will largely eliminate the errors that accompany that situation. The technique is most apt to NEC-4 modeling of buried radial wires, where the set of radials becomes part of a Numerical Green's Function (.NGF file), with the monopole and its connections to the hub becoming part of a second model that calls up the NGF file. Chapter 17 contains several examples of combining the GR command and the commands for writing and calling Green's files (see next chapter) into a time- and space-saving combination.

Summing Up

In this set of exercises, we have taken a long look at both the GX and GR command. We focused more intensely on the GX command because it is used more regularly than the GR command. In some ways, the GX command more easily shows the ability of the symmetry commands to

replicate structures produced by any of the geometry commands, such as GW, GC, GA, GH, and CW. Nevertheless, either command would have sufficed as an introduction to symmetry as a useful working tool within the NEC-2 and NEC-4 commands. As well, both commands share a convenient property: they are the same in both the NEC-2 and NEC-4 cores.

Although the two commands are comparable in many ways and subject to the same restrictions and limitations, the GR command differs from the corresponding GX command in several important ways, even though both make use of symmetry during the core run. First, GX allows symmetry in all 3 planes--X, Y, and Z--and the modeler can select from 1 to 3 planes of symmetry for any model. In contrast, the GR command applies symmetry around the Z-axis only.

Second, the GX command applies symmetry once per option, although with multiple planes of symmetry, we may end up with up to 8 total objects. One is the original and the other 7 are replications created in a cube if we select the maximum level of symmetry available in a free-space environment. The GR command uses symmetry rotationally relative to the original structure. Hence, in principle, there is no limit to the number of replications (one less than the total number of occurrences that we specify within the command itself). However, there are very practical limitations on the number of successful replications we may have. That number depends upon the X-Y dimensions of the original structure. Specifying too many occurrences will result in overlapping or inter-penetrating structures that yield a defective model.

Third, the reflections in the GX command are essentially linear across a specified plane of reflection. For the plane in question, we arrive at the same absolute values for the coordinates, but with the signs reversed. The GR command uses symmetry rotationally, separating each occurrence of the structure by an angular distance, but at the same radius from X = 0 and Y = 0 as the original structure.

For very large models, both GX and GR (but not in the same model) can speed core runs. Although the sample models are small in order to make them clear, symmetry's true home is the model that otherwise would press the core in terms of required matrix space or the time it takes a PC to process the model.

6.
WG and GF: Numerical Green's Functions and Wire Grids

***Objectives**: This set of exercises will introduce some methods of handling complex geometries, ranging from the importation of externally synthesized files to wire-grid fabrication. Related to such geometries are methods of saving core-run time, particularly the use of Numerical Green's files. You will learn how to both write and then recall such files.*

At what point antenna geometry becomes "complex" is always a user judgment. Most often, the transition from simple or straightforward to complex gradually shifts as you increase your modeling experience and expertise. Indeed, few of the models in this chapter will qualify as truly complex, although they will generally be more complex than the illustrative models in past chapters. Hence, they will suffice to show what is different about the "complex."

Complexity does not automatically imply the use of wire-grid techniques for construction. There are many structures that are only mathematically complex, but not true wire-grid structures. Complex curvatures, for example, may benefit from automated or semi-automated synthesis procedures. However, such procedures tend to have limitations as well as benefits with respect to either model or model-description size. In some cases, the features internal to NEC may be more powerful for various purposes than externally synthesized equivalents.

When structures reach a certain size, they may press the segmentation limit for the program or simply require more run time than we wish. The latter fact is especially true of cases in which we wish to repetitively use parts of a model while modifying other parts for each new run. For these situations, NEC contains two exceptionally useful commands: WG and GF. Both relate to Numerical Green's Functions (NGF). WG writes to file a partial calculation of the matrix functions. GF reads these results into another model that contains the remaining portions of a complete model structure and its associated control commands.

External Geometry Synthesis

Complex structures--whatever the basis of the complexity--normally require considerable external calculation prior to entering the appropriate geometry commands into a NEC model. One handy technique for constructing geometric shapes on the basis of equations is to use a spreadsheet facility, either the one that is part of the NEC-Win Plus insert within NEC-Win Pro or GNEC or an external spreadsheet. In either case, the program-input side has methods of aiding the importation process and the cores used in the programs will read the standard spreadsheet "tab" separator directly.

Alternative to this method is the use of a geometry synthesizer, such as NEC-Win Synth. Such programs contain a collection of preset shapes for which you provide dimensions, segmentation information, and a test frequency. As well, most programs also permit you to create additions to

the structure or additional structures. **Fig. 6-1** shows the dual construction page for the program.

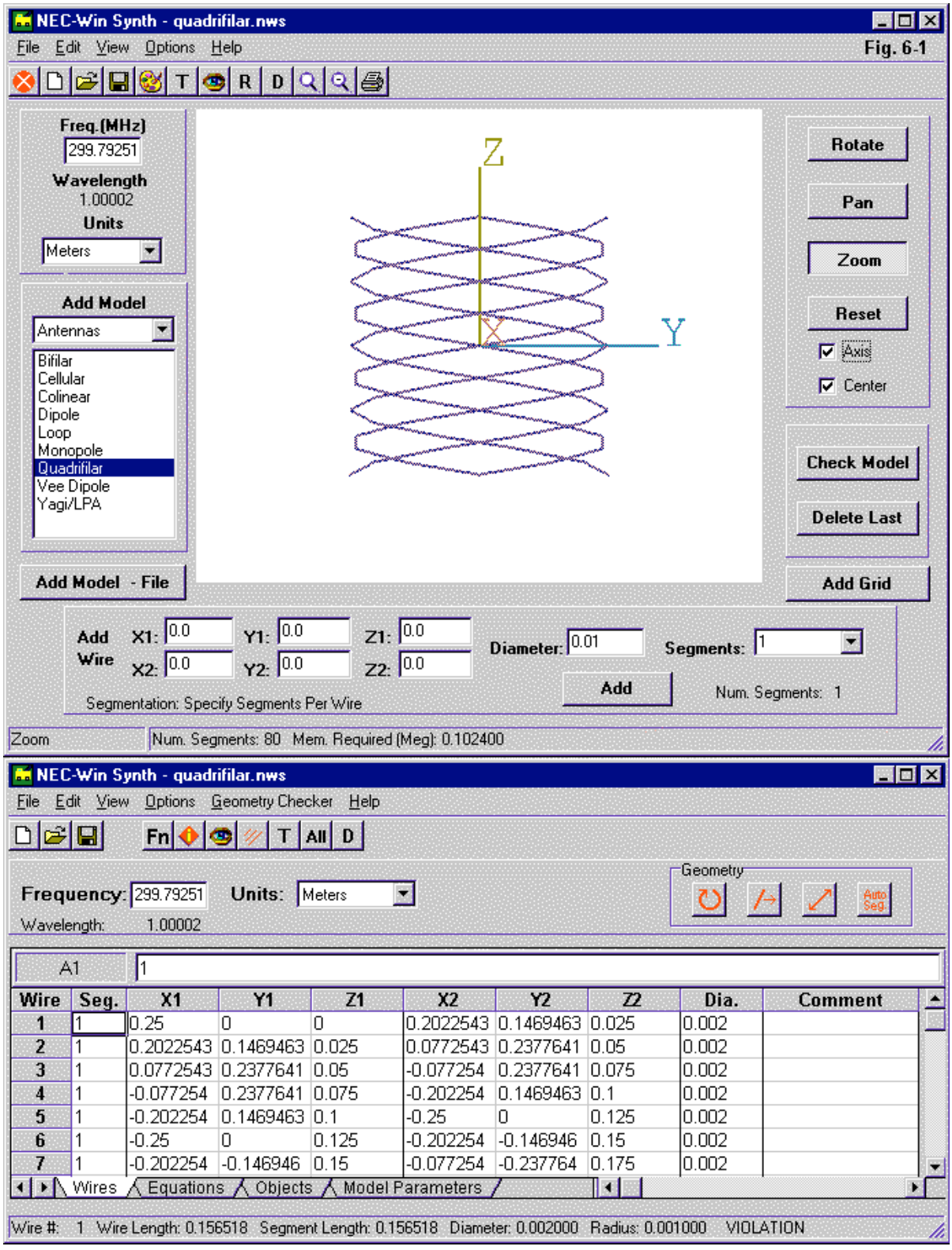

The upper portion of the graphic shows the program's basic selection and viewing areas. The page also includes the test frequency, the unit of measure, and the ability to create additional wires (GW entries) for the synthesized structure. As the highlighted "Add Model" entry suggests and the viewing area confirms, the construction of a quadrifilar model is underway. The lower portion of the figure shows part of the second screen, the wire entries composing the model geometry. You may save compositions in either the native format of the synthesizer or as .NEC (ASCII) files for importation into a NEC program.

Synthesizing a geometry for a model is not wholly automatic. You must still know the relevant dimensions and the level of segmentation. Consider the quadrifilar structure. Then refer to **Fig. 6-2**.

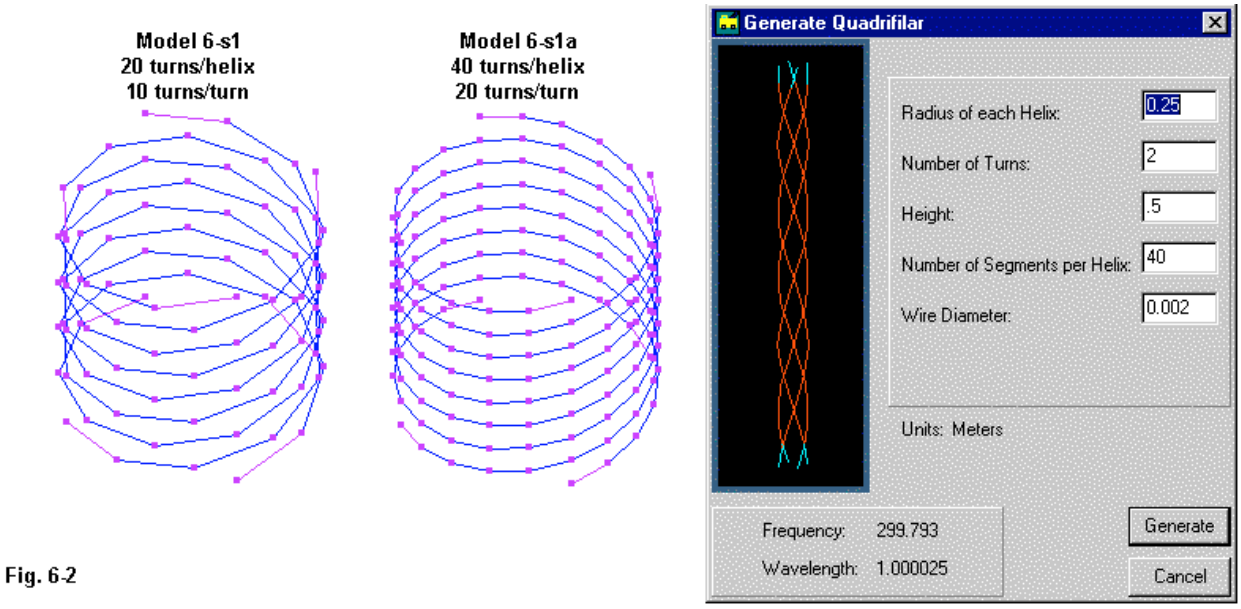

Fig. 6-2

The box to the right provides spaces for entering critical data, including the helix radii, the number of turns, the overall height, the number of segments per helix, and the wire diameter (or radius as an option). The initial trial specified 20 segments per helix and resulted in model *6-s1.nec* (where the "s" indicates synthesized model geometry).

```
CM Generated by NEC-Win Synth 1.0
CM quadrifilar: helix radius 0.25m, helix height 0.5m
CM no. turns 2, segments/helix 20, total tags 80
CE
GW 1 1 0.25000 0.00000 0.00000 0.20225 0.14695 0.02500 0.00100
GW 2 1 0.20225 0.14695 0.02500 0.07725 0.23776 0.05000 0.00100
GW 3 1 0.07725 0.23776 0.05000 -0.07725 0.23776 0.07500 0.00100
GW 4 1 -0.07725 0.23776 0.07500 -0.20225 0.14695 0.10000 0.00100
```

The first few lines of the model show the individual wires created for the 4 helices, plus the model data added to the comment section of the file. However, the Necvu rendition of the model on the far left of the figure shows it to be malformed, since the segment junctions do not closely align. 10 segments per helix turn does not allow segment alignment with 4 helices, each leg of which is 90°

separated from adjacent legs. Therefore, let's try again, this time using 20 segments per helix turn or 40 total segments for each helix in the construct. Open model *6-s1a.nec*.

```
GW 1 1 0.25000 0.00000 0.00000 0.23776 0.07725 0.01250 0.00100
GW 2 1 0.23776 0.07725 0.01250 0.20225 0.14695 0.02500 0.00100
GW 3 1 0.20225 0.14695 0.02500 0.14695 0.20225 0.03750 0.00100
GW 4 1 0.14695 0.20225 0.03750 0.07725 0.23776 0.05000 0.00100
GW 5 1 0.07725 0.23776 0.05000 0.00000 0.25000 0.06250 0.00100
GW 6 1 0.00000 0.25000 0.06250 -0.07725 0.23776 0.07500 0.00100
GW 7 1 -0.07725 0.23776 0.07500 -0.14695 0.20225 0.08750 0.00100
GW 8 1 -0.14695 0.20225 0.08750 -0.20225 0.14695 0.10000 0.00100
```

It takes twice as many entries for the new version to reach a Z value of 1.0, and the total helix has 160 wires. The segments, as shown in the center of **Fig. 6-2**, are now well aligned. However, the work is not finished. First, most quadrifilar structures are closed at the top, requiring additional wires in the model. Second, examine the end of the model as transferred from the synthesizer to the NEC program.

```
GW 158 1 -0.20225 -0.14695 0.46250 -0.14695 -0.20225 0.47500 0.00100
GW 159 1 -0.14695 -0.20225 0.47500 -0.07725 -0.23776 0.48750 0.00100
GW 160 1 -0.07725 -0.23776 0.48750 0.00000 -0.25000 0.50000 0.00100
GS 0 0 1.000000
GE
FR 0 1 0 0 299.7925 1
```

The synthesized structure requires a number of control command additions before it becomes a complete NEC model. The wire is perfect and may require the addition of a material load (LD5). There is no excitation, either direct or plane wave. The model presumes free space as the environment and may require revision for the addition of a ground. Finally, the model makes no request for an output. If you run the model in its present state, you will obtain only the structure and segmentation data.

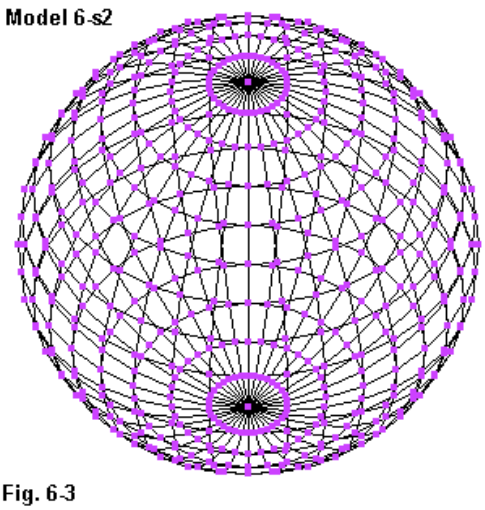

Fig. 6-3

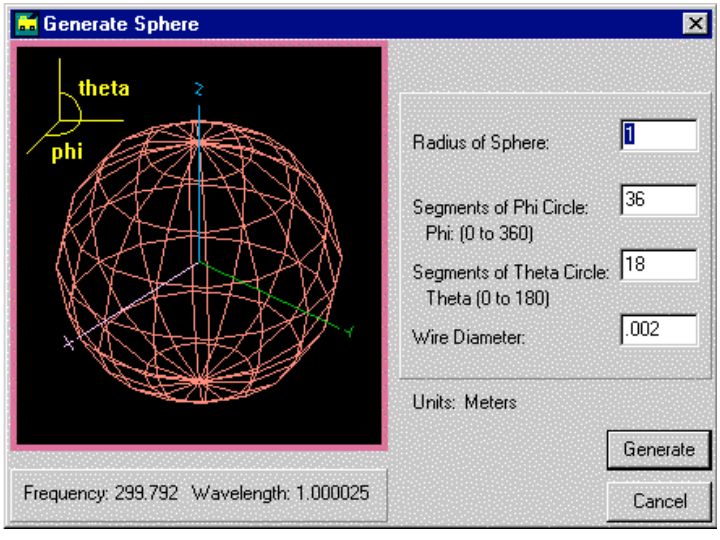

Some synthesized models, such as model *6-s2.nec*, create very large files, even with sparse line

structures. The right side of **Fig. 6-3** shows the modest specifications for a sphere: 36 segments per circle in the phi or horizontal plane and 18 in the theta or vertical hemispheric plane. The result is a model with 1280 individual wires, of which the following lines are only a meager sample.

```
CM Generated by NEC-Win Synth 1.0
CM Sphere: radius 1m, wire radius 0.001m
CM Segments/phi 36, segments/theta 18
CE
GW 1 1 0.17101 0.03015 0.98481 0.16318 0.05939 0.98481 0.00100
GW 2 1 0.16318 0.05939 0.98481 0.15038 0.08682 0.98481 0.00100
GW 3 1 0.15038 0.08682 0.98481 0.13302 0.11162 0.98481 0.00100
GW 4 1 0.13302 0.11162 0.98481 0.11162 0.13302 0.98481 0.00100
```

Synthesizers usually employ one and only one way of creating a geometric structure. In this case, the result is equal-length longitudinal segments, but highly variable latitudinal segment lengths. You must judge whether such a way of forming the sphere will yield satisfactory results in the context of the total model. The sphere is a sample of a full wire-grid structure. You may place an excited antenna outside the sphere to illuminate its surface or within the sphere to achieve relatively complete reflection. You may wish to try a simple dipole within the sphere and add a suitable RP0 request to check the resulting pattern. The results may tell you whether or not you need to increase the segmentation density in the model.

Synthesizers generally make available pre-set shapes that are useful in antenna work. They may include vehicle shapes to check mobile antenna installations or common UHF geometries. NEC-Win Synth is no exception, as illustrated by the parabolic shape in model *6-s3.nec*.

```
CM Generated by NEC-Win Synth 1.0
CM Parabola: Height 1m; Radius X 4m, Radius Y 4m
CM Segments/circle 12, Segments/side 6
CE
GW 1 1 1.63299 0.00000 0.16667 1.41421 0.81650 0.16667 0.00100
GW 2 1 1.41421 0.81650 0.16667 0.81650 1.41421 0.16667 0.00100
GW 3 1 0.81650 1.41421 0.16667 0.00000 1.63299 0.16667 0.00100
GW 4 1 0.00000 1.63299 0.16667 -0.81650 1.41421 0.16667 0.00100
```

The comments contain the same information as the formation screen. We can form oval parabolas by choosing different radii for the X and Y coordinates in this version that points straight up. (We could have chosen another pair of axes for creating the parabola or we might simply rotate the structure via the GM command.) The height of the parabola from its center to the lip is 1 meter. For the illustration, all dimensions are arbitrary.

The model uses 12 segments per circle and 6 segments per radial line. Because we have a curvature to approximate with straight wires, the model produces an individual wire for each 1-segment section of the structure. The simplified parabola created here uses 144 GW entries to complete the structure. The result appears at the left in **Fig. 6-4**.

The parabola gives us the opportunity to complete the model. Open model *6-s3a.nec* and examine the lines at the bottom. The model adds an 11-segment dipole (GW145) about 0.2 m above the base of the parabola and gives it a voltage source (EX0). The model also requests a pair of theta patterns. The center of **Fig. 6-4** shows the final result, along with a sample pattern.

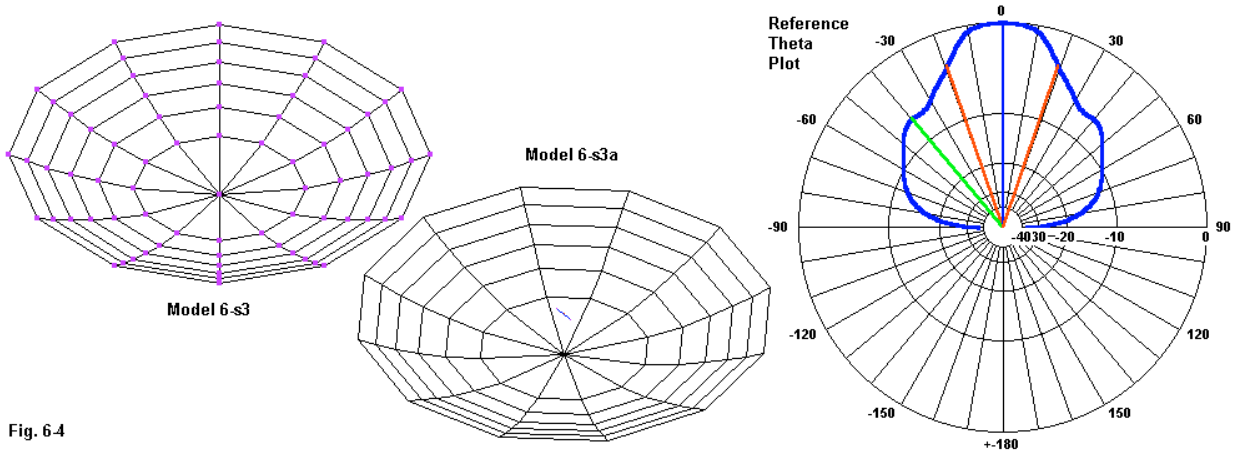

Fig. 6-4

```
GW 143 1 1.82574 -3.16228 0.83333 2.00000 -3.46410 1.00000 0.00100
GW 144 1 3.16228 -1.82574 0.83333 3.46410 -2.00000 1.00000 0.00100
GW 145 11 0 -.2375 .2 0 .2375 .2 .001
GS 0 0 1.000000
GE
FR 0 1 0 0 299.7925 1
EX 0 145 6 00 1 0
RP 0 181 1 1000 -90 90 1.00000 1.00000
RP 0 181 1 1000 -90 0 1.00000 1.00000
EN
```

In place of GW145, you may wish to install any other form of signal source assembly for the parabola--of course, after reshaping the sample reflector to dimensions suitable for some given task.

To Synthesize or Not to Synthesize

Not all complex structures require synthesis. Indeed, some structures may benefit from direct construction within NEC itself. Let's consider a planar reflector that uses a simple dipole to create a directional array. One way to create the reflector is to make a series of 1-segment wires. We only need 312 of them. Alternatively, we may manually create 26 wires--13 verticals and 13 horizontals--each with 12 segments, and let the wires intersect at segment junctions. Either procedure will work. But not only is the procedure tedious, it is subject to typographical errors during entry. A third alternative is to use the synthesizer to create a parallelogram, of which rectangles and squares are special cases using 90° angles at the corners.

At the far left in **Fig. 6-5** is the 1.2m by 1.2m reflector with its dipole exciter. As with all wire-grid structures that simulate a solid surface or a closely spaced screen, the spacing between wires is no greater than 0.1λ. The wire diameter is the wire length divided by π, or about 0.0318 m. (The wire radius, of course, is half this value or 0.0159 m.) The reflector alone, shown in model *6-s4.nec* requires 26 wires and 312 segments. Note that in this particular case, the wire-grid junctions occur at segment junction and not at the junction of individual wires, except at the edges of the screen.

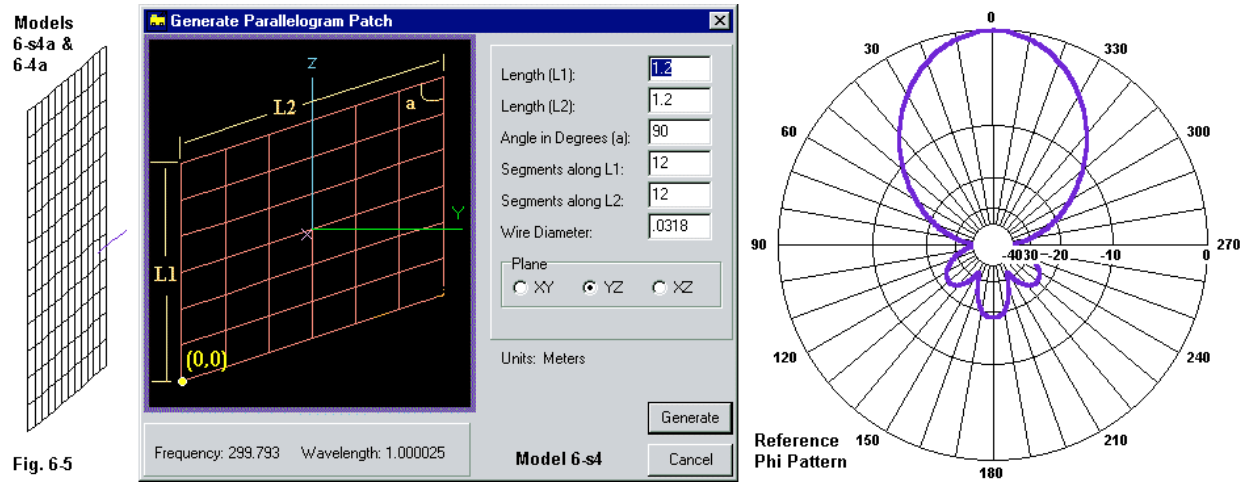

Fig. 6-5

```
CM Generated by NEC-Win Synth 1.0
CM Parallelogram: Vert 1.2m, Hor 1.2 m, Angle 90 deg
CM Segments/side 12, wire radius 0.0159
CE
GW 1 12 0.00000 0.00000 0.00000 0.00000 1.20000 0.00000 0.01590
GW 2 12 0.00000 0.00000 0.00000 0.00000 0.00000 1.20000 0.01590
GW 3 12 0.00000 0.00000 1.20000 0.00000 1.20000 1.20000 0.01590
GW 4 12 0.00000 1.20000 1.20000 0.00000 1.20000 0.00000 0.01590
```

Model *6-s4a.nec* adds the dipole to the model and provides a voltage source and an output request.

```
GW 25 12 0.00000 0.00000 1.00000 0.00000 1.20000 1.00000 0.01590
GW 26 12 0.00000 0.00000 1.10000 0.00000 1.20000 1.10000 0.01590
GM 0 0 0 0 0 0 -.6 -.6
GW 27 11 .1753 -.2183 0 .1753 .2183 0 .004
GS 0 0 1.000000
GE
FR 0 1 0 0 299.7925 1
EX 0 27 6 00 1 0
RP 0 361 1 1000 -90 0 1.00000 1.00000
RP 0 1 361 1000 90 0 1.00000 1.00000
EN
```

In fact, it does more. Because the wire-grid square has one corner at Y = 0 and Z = 0, we had to add a GM entry to move the first 26 wires down and over to center the screen at the origin of the Cartesian coordinate system. Because the GM line moves the entire preceding structure, the model will run on either NEC-2 or NEC-4. The result of the run is the phi (E-plane) pattern to the right in **Fig. 6-5**. The free-space gain is 9.3, the 180° and worst-case front-to-back ratios are 18.6 dB, and the source impedance is 50.0 + j0.0 Ω.

If you are using an entry-level program that lacks access to the GM command, then the synthesized reflector is handy. However, for implementations of NEC that permit the use of GM, consider model *6-4.nec*, where the absence of the "s" marker indicates a model created within NEC itself. Model 6-4 replicates 6-s4 as a wire-grid-only structure.

```
CM Planar reflector via GM
CE 1.2m by 1.2m
GW 1 12 0 -.6 -.6 0 -.6 .6 .0159
GM 0 12 0 0 0 0 .1 0 001.001
GW 2 12 0 -.6 -.6 0 .6 -.6 .0159
GM 0 12 0 0 0 0 0 .1 002.002
GS 0 0 1.000000
GE
FR 0 1 0 0 299.792500 1
```

In 4 entries, the model creates the entire wire grid. GW1 creates a vertical edge wire and the following GM line replicates it 12 more times. GW 2 creates an edge horizontal wire, and the subsequent GM line creates 12 more properly spaced copies. By specifying 12 segments per wire, the wires all intersect at segment junctions. The result, however, is the same 312 segments that the synthesized version produced. You may wish to check the segmentation data on the respective NEC output reports, although the segments may not all appear on the same lines. As well, the version in model 6-4 uses only 2 tag numbers. Incidentally, as the GM lines indicate, this is a NEC-2-only model. If you use NEC-4, revise the two GM lines.

To complete the work, open model *6-4a.nec*. This version adds the dipole as GW3 in the same place as in the synthesized version.

```
GW 3 11 .1753 -.2183 0 .1753 .2183 0 .004
GS 0 0 1.000000
GE
FR 0 1 0 0 299.7925 1
EX 0 3 6 00 1 0
RP 0 361 1 1000 -90 0 1.00000 1.00000
RP 0 1 361 1000 90 0 1.00000 1.00000
EN
```

Since the two reflectors are the same, even though constructed by different means, and since the dipole is the same, the results are the same. This is, the pattern in **Fig. 6-5** holds true, and the other data is identical to the values already reported.

For some models, direct modeling within NEC may prove more versatile. Let's reconsider a model discussed in Chapter 4 (model 4-4), a helix over a wire-grid ground plane surface. Open model *6-5.nec*.

```
GH 1 100 0.2125566 1.0627828 .1591549 .1591549 .1591549 .1591549 .001
GM 0 0 0 0 0 0 0 .05092
GW 2 1 .2 0 0 .15915 0 .05092 .001
GM 0 0 0 0 0 0 0 1
GW 3 6 -.3 -.3 1 -.3 .3 1 .0159
GM 0 6 0 0 0 .1 0 0 003.003
GW 4 6 -.3 -.3 1 .3 -.3 1 .0159
GM 0 6 0 0 0 0 .1 0 004.004
```

This model describes--in NEC-2 terms--a 100-segment helix that has 5 turns. It connects to the elevated ground plane surface via GW 2, a 1-segment wire that must angle considerably to meet a junction in the wire-grid below it. The wire-grid (GW3 and GW4, plus following GM lines) uses

0.1 m (or 0.1λ) wire lengths, corresponding to the left grid in **Fig. 6-6**.

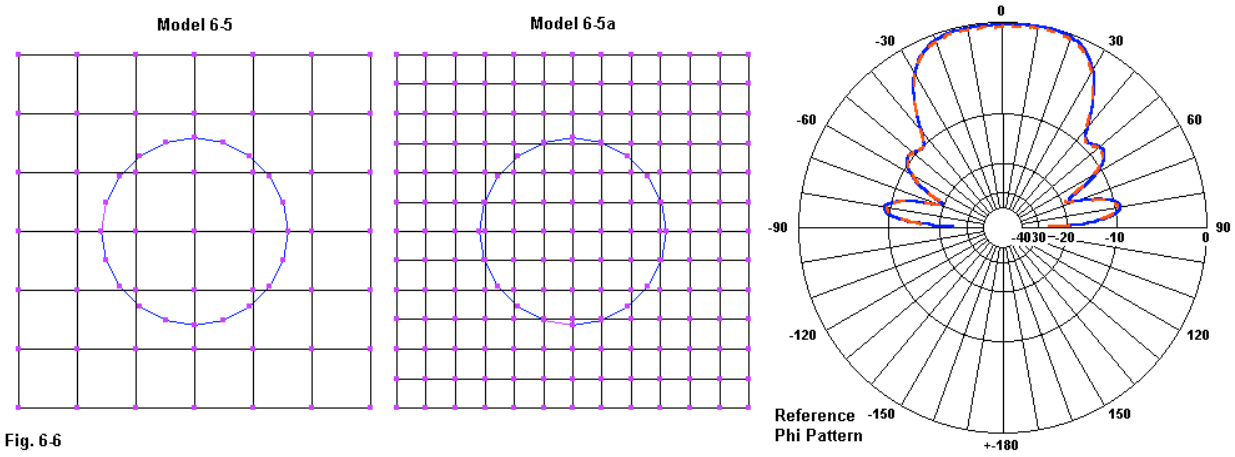

Fig. 6-6

If you re-run the model, you will obtain the following results.

Model	Reported Gain dBi	AGT	AGT-dB	Adjusted Gain dBi	Impedance R +/- jX Ω
6-5	8.47	0.881	-0.55	9.02	328 - j17

By making two small changes to model 6-5, we can obtain model *6-5a.nec*, which uses 0.05λ wires, with the wire radii also halved.

```
GW 3 12 -.3 -.3 1 -.3 .3 1 .00796
GM 0 12 0 0 0 .05 0 0 003.003
GW 4 12 -.3 -.3 1 .3 -.3 1 .00796
GM 0 12 0 0 0 0 .05 0 004.004
```

Essentially, the wire-grid formation-lines double the number of segments in GW3 and GW4, and the GM entries create 12 copies of each wire rather than just 6. The result is the wire grid in the center part of **Fig. 6-6**. We also make one other change: we straighten (almost) GW2 by connecting it at a closer junction (+0.15 instead of +0.2). Running this model, we obtain different report results.

Model	Reported Gain dBi	AGT	AGT-dB	Adjusted Gain dBi	Impedance R +/- jX Ω
6-5a	8.65	0.913	-0.40	9.05	314 - j19

The improvement in AGT values tends to lend more confidence to the model, although the actual performance has not changed perceptibly. The overlapping patterns at the right in **Fig. 6-6** shown the degree of performance coincidence.

To obtain the full versatility of the GM command in NEC sometimes requires slightly different tactics in NEC-2 and NEC-4. Consider a corner reflector that uses a simple dipole driver, as suggested by **Fig. 6-7**.

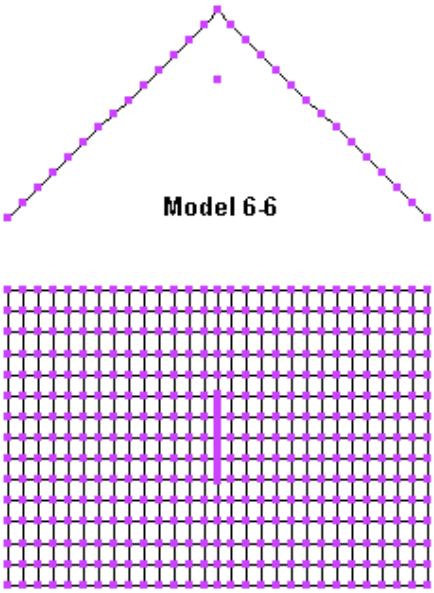

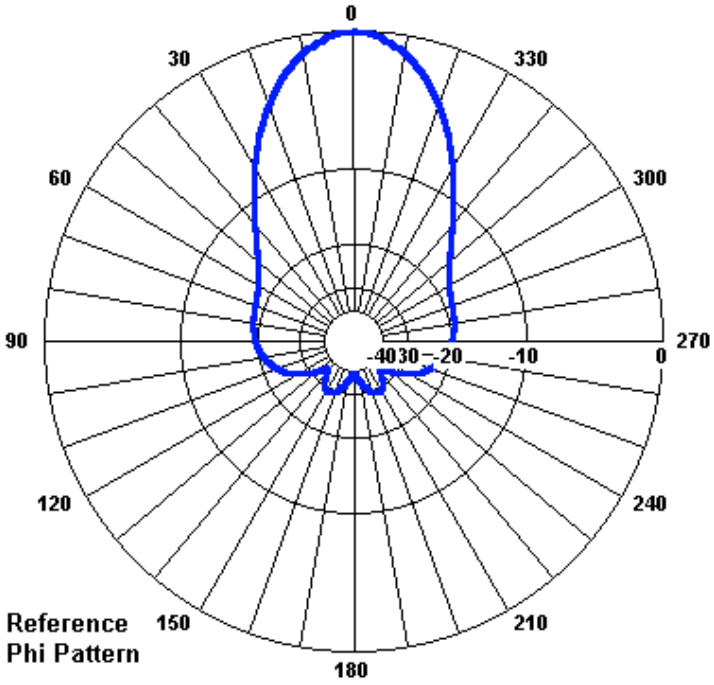

Fig. 6-7

The reflector is vertical (as is the dipole) with a height of 1.4 m. Each side is 1.4-m long horizontally. Because the GM command forming the sides differs between the cores, we shall begin with the NEC-4 version. Open model *6-6-nec4.nec*.

```
GW 1 14 0 0 -.7 0 0 .7 .0159
GW 2 14 0 -.1 -.7 0 -.1 .7 .0159
GM 0 13 0 0 0 0 -.1 0 2 1 2 14
GW 3 14 0 0 0 0 -1.4 0 .0159
GM 0 7 0 0 0 0 0 -.1 3 1 3 14
GM 0 7 0 0 0 0 0 .1 3 1 3 14
GM 0 0 0 0 45 0 0 0 2 1 0 0
GW 4 14 0 .1 -.7 0 .1 .7 .0159
GM 0 13 0 0 0 0 .1 0 4 1 4 14
GW 5 14 0 0 0 0 1.4 0 .0159
GM 0 7 0 0 0 0 0 -.1 5 1 5 14
GM 0 7 0 0 0 0 0 .1 5 1 5 14
GM 0 0 0 0 -45 0 0 0 4 1 0 0
GW 101 11 .326 0 -.2119 .326 0 .2119 .004
```

GW101 simply places the dipole in front of the reflector. The lines above it form the reflector itself, beginning with the vertical center wire (GW1). GW2 and the following GM line finish the required vertical wires for one side of the reflector. GW3 creates a centered (Z = 0) horizontal wire. The following 2 GM lines create 7 copies below and 7 copies above the center horizontal wire. We can use this process without increasing the tag number because NEC-4 allows its GM command to specify both the starting and ending tag numbers and relative segment numbers. The last GM line above GW4 rotates the structure 45°. The GW lines from GW4 to just above GW101 perform the same task on the other side of the center vertical wire, eventually rotating this grid by -45° so that it will create the ultimate 90° corner.

In NEC-2, we must alter the procedure somewhat. Open model *6-6-nec2.nec*,

```
GW 1 14 0 0 -.7 0 0 .7 .0159
GW 2 14 0 -.1 -.7 0 -.1 .7 .0159
GM 0 13 0 0 0 0 -.1 0 002.002
GW 3 14 0 0 -.7 0 -1.4 -.7 .0159
GM 0 14 0 0 0 0 0 .1 003.003
GM 0 0 0 0 45 0 0 0 002.003
GW 4 14 0 .1 -.7 0 .1 .7 .0159
GM 0 13 0 0 0 0 .1 0 004.004
GW 5 14 0 0 -.7 0 1.4 -.7 .0159
GM 0 14 0 0 0 0 0 .1 005.005
GM 0 0 0 0 -45 0 0 0 004.005
GW 101 11 .326 0 -.2119 .326 0 .2119 .004
```

Because the NEC-2 GM command only allows specification of the starting and ending tag numbers--without segment identification--we face a choice. If we do not use an increase in the tag number in the horizontal GM lines, then we must start the horizontals--as in the model--at the bottom and create an entire sequence with 1 GM entry per side. Had we used the NEC-4 technique, then the second horizontal entry would have replicated not only the GW wire but also all of the wires in the first GM command of the pair.

An alternative procedure would have been to increment the tag numbers within the GM command and then to increase the tag numbers on subsequent GW entries so that there is no overlap. That, in turn, would force us to carefully track the tag numbers so that the rotation commands encompassed all, but only the proper tag numbers for each side.

You may confirm from the segmentation data that the two models shown produce identical models. Further evidence shows up in the performance reports that underlie the reference pattern in **Fig. 6-7**.

Model	Free-Space Gain dBi	180° Front-to-Back Ratio dB	Source Impedance R +/- jX Ω
6-6-nec4	12.99	39.14	50.2 - j1.6
6-6-nec2	12.99	38.51	50.5 - j1.2

The NEC-4 procedure has an interesting advantage. Suppose that you were making a study of corner reflectors, each with a different vertical dimension and a different horizontal dimension. Each dimension change requires a change in the length of and number of segments in the baseline wire, followed by changes in the number of copies in the appropriate GM line or lines. In a fairly short period, you could create a range of reflector sizes from small to large heights and from short to long sides. Then you might run each of the models to check for performance changes that might be a function of the reflector size. In addition, you might change the angle of the reflector by altering each of the rotation GM entries. In this manner, you might determine what angle yields the highest gain, cleanest pattern, or other valuable information. You might even test the collection of corner reflectors with a collinear pair of in-line dipoles at various end-to-end spacing. This last step calls for repetitions of running some corner reflectors having up to thousands of segments. This task is well suited to the use of the Numerical Green's Function.

Numerical Green's Functions: WG and GF

The use of Numerical Green's Functions (NGF) is a two step process involving a control command (WG or write an NGF file) and in a separate model a geometry command (GF or read a previously saved NGF file). The initial model that writes the file performs the matrix portions of the calculation as they pertain to the geometry structure recorded in the model. In the new model, which may add to the geometry and provide other control commands and output requests, the core calls up the results of the previous calculation and needs only to apply them to the additions in the current model. The process can be used in part to split a model that might be too big for the PC on hand to complete within a reasonable time (or at all). We shall focus on the time saving dimension of the process.

The WG Command

The WG or Write NGF File command appears at or near the end of the model whose results we wish to store. It consists simply of a command identifier and file name that we assign, with the extension .NGF or .WGF. (Actually, raw NEC-4 will write a file with the extension .NEC, but this can lead to confusion with input files having the same extension. Hence, the NSI cores provide for selecting the extension as well as the file name. Virtually any extension not already in use by other stored output files will work. Since these may not be well known, using .NGF is recommended by NSI manuals, while .WGF also works and is used in the examples. Whatever the extension, it should clearly indicate the command involved or the NGF function in general.)

```
WG filename.WGF
```

Early versions of NEC-2 did not contain provision for writing the NGF information to a specific file. Hence, NEC-2 output reports will show the lines that follow.

```
****NUMERICAL GREEN'S FUNCTION FILE ON TAPE 20****,
     MATRIX STORAGE - 682276 COMPLEX NUMBERS
```

The NSI NEC-2 core has added the ability to specify a filename, so that the information no longer needs to be stored on "tape 20." The NEC-4 output report carries the correct file name.

```
****NUMERICAL GREEN'S FUNCTION WRITTEN ON FILE C-V14-H14.WGF
     MATRIX STORAGE - 682276 COMPLEX NUMBERS
```

The matrix storage values for the two files are the same, since both entries represent the same corner reflector that we saw in model 6-6. Stored NGF files will be very large and require preplanning for the required hard drive space in the same directory as the model and NEC output files. The present model uses almost 11 MB for the NEC-2 and NEC-4 NGF files on the 826-segment model. However, for comparable NEC-2 and NEC-4 NGF files, the required storage space will not always be the same.

To sample an actual model using the WG command, open model *6-7-nec-2.nec*, the NEC-2 version of just the corner reflector in model 6-6. We need to examine just what we might or

must include in a file with a WG command.

```
GW 1 14 0 0 -.7 0 0 .7 .0159
GW 2 14 0 -.1 -.7 0 -.1 .7 .0159
GM 0 13 0 0 0 0 -.1 0 002.002
GW 3 14 0 0 -.7 0 -1.4 -.7 .0159
GM 0 14 0 0 0 0 0 .1 003.003
GM 0 0 0 0 45 0 0 0 002.003
GW 4 14 0 .1 -.7 0 .1 .7 .0159
GM 0 13 0 0 0 0 .1 0 004.004
GW 5 14 0 0 -.7 0 1.4 -.7 .0159
GM 0 14 0 0 0 0 0 .1 005.005
GM 0 0 0 0 -45 0 0 0 004.005
GE 0 -1 0
FR 0 1 0 0 299.7925 1
GN -1
WG c2-v14-h14.WGF
```

The most essential part of the NGF file will be the portion of the geometry that we later wish to call up in another file. As well, the FR (frequency) information and the GN (ground information) must be included here and excluded from the subsequent model that makes use of the NGF file. In addition, any loads (LD) applying to the tags specified in the geometry section must be included, although there are none in the sample. For an initial run with this model, you may also include other control commands below the WG command. For example, you may add excitation specifications and output requests. They will not affect the data stored in the NGF file specified by the preceding WG command. If you plan to use the output in a sequence of data, it is likely better to save such model modifications and output requests for a separate file, since a re-run of this file to obtain the data will require re-running the entire matrix and a re-filing of the data.

Open model *6-7-nec4.nec*. This model uses the comparable set of lines describing the reflector with the omission of the dipole. The only line to note especially is the WG command.

```
WG c-v14-h14.WGF
```

For these exercises, all NEC-2 NGF file names add the number "2" after the first character of the file name. Hence, NEC-2 and NEC-4 NGF files will not interfere with each other.

The GF Command

Like its writing counterpart, the reading command, GF is simplicity itself.

```
Cmd     I1           S
        End Table    File Name and Extension
GF      0            c-v14-h14.WGF
```

The default value for the only integer position is 0. However, for some models where the added geometry parts may contact the part stored in the NGF file, you may wish to have a list of wire end coordinates. The output report will print this list if I1 is any value other than zero. The remaining part of the command is the file name and extension of the stored NGF file.

Open model *6-8-nec2.nec*.

```
CM Dipole .326 m from planar reflector
CE
GF 0 c2-v14-h14.WGF
GW 101 11 .326 0 -.2119 .326 0 .2119 .004
GE 0
EX 0 101 6 0 1 0
RP 0 361 1 1000 -90 0 1.00000 1.00000
RP 0 1 361 1000 90 0 1.00000 1.00000
EN
```

The first command opens the NGF file for the reflector. Then we add the dipole driver element, using an arbitrarily high tag number to ensure that the tag number will not overlap with any tag used in the NGF file. If you run the model and examine the segmentation data for the model, you will find all 837 segments listed, although only 11 are a function of the new GW101 line. The new model must also add the excitation assignment, any new loads, and any output requests. If you use the LD5 shortcut of assigning the same material loading to all segments of the model here, it will apply only to the new segments added by this model.

Open model *6-8-nec4.nec*. The only difference between the NEC-2 and NEC-4 versions of the model is the file name called up by the GF command

```
GF 0 c-v14-h14.WGF
```

You may run both models and confirm that they produce outputs identical to those yielded by model 6-6 for each core.

Model	Free-Space Gain dBi	180° Front-to-Back Ratio dB	Source Impedance R +/- jX Ω
6-6-nec4	12.99	39.14	50.2 - j1.6
6-6-nec2	12.99	38.51	50.5 - j1.2

Since these are essentially small models, the run time differences will be small between a full model and the new version that calls up an NGF file, perhaps by a factor of 2. The absence of significant saving is a function of the fact that overhead uses most of the time.

There are numerous uses for NGF files. For example, if only part of a model is symmetrically structured, you may set up an NGF file to calculate the symmetrical portion and then place the remaining structure in an additional file that uses the GF command. Perhaps the most common NGF applications involve repetitive uses of a structure (or of many structures, each with its own NGF file). Let's create a planar reflector that is larger than the earlier one, 1.4 m high by 1.8 m wide. Then we can try different driving systems with the same wire-grid surface.

Open model *6-9-nec2.nec*. This version of the reflector begins with edge wires (GW1 and GW2) and enters GM commands to copy those wires enough times to form a rectangle. The wire length for each segment is 0.1λ or 0.1 m, and the wire radius is 0.0159 m. Free space is the environment, and the test frequency, as usual, is 299.7925 MHz. A WG command completes the model.

```
GW 1 18 0 -.9 -.7 0 .9 -.7 .0159
GM 0 14 0 0 0 0 0 .1 001.001
GW 2 14 0 -.9 -.7 0 -.9 .7 .0159
GM 0 18 0 0 0 0 .1 0 002.002
GE 0
FR 0 1 0 0 299.7925 1
GN -1
WG R2-H18-V14.WGF
```

Open the model *6-9-nec4.nec*.

```
GW 1 18 0 -.9 0 0 .9 0 .0159
GM 0 7 0 0 0 0 0 -.1 1 1 1 18
GM 0 7 0 0 0 0 0 .1 1 1 1 18
GW 2 14 0 0 -.7 0 0 .7 .0159
GM 0 9 0 0 0 0 -.1 0 2 1 2 14
GM 0 9 0 0 0 0 .1 0 2 1 2 14
GE 0 -1 0
FR 0 1 0 0 299.7925 1
GN -1
WG R-H18-V14.WGF
```

The NEC-4 version of the reflector sets up center wires, followed by separate GM commands to place wires on each side of center. Otherwise, the final wire grid is the same, with only a slight change of file name to make it unique.

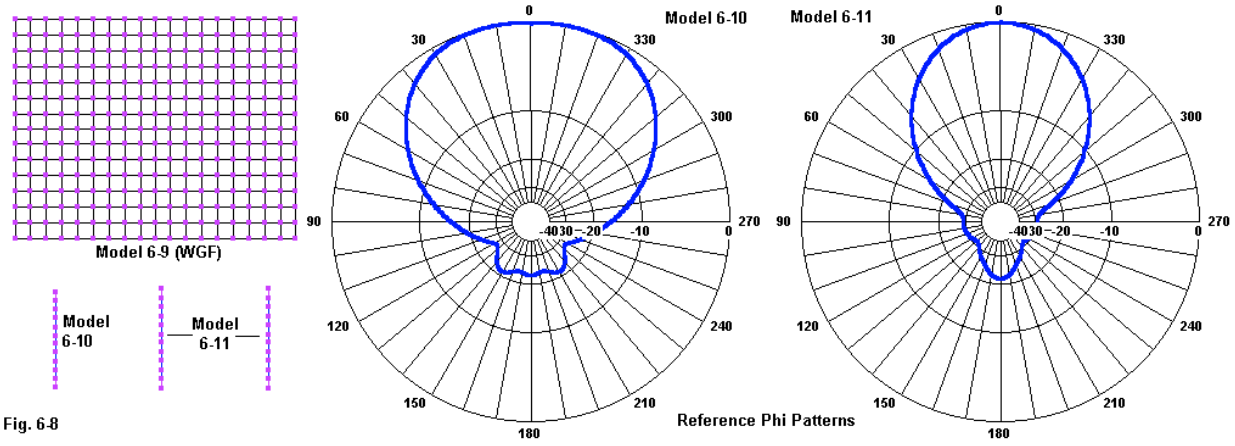

Fig. 6-8 shows the rectangular reflector plus the two driver systems that go in front of the surface. Open model *6-10-nec-2.nec*.

```
GF 0 R2-H18-V14.WGF
GW 24 11 .175 0 -.218 .175 0 .218 .004
GE 0 -1 0
EX 0 24 6 0 1 0
RP 0 361 1 1000 -90 0 1.00000 1.00000
RP 0 1 361 1000 90 0 1.00000 1.00000
EN
```

If you open model *6-10-nec4.nec*, you will discover that it is identical to the nec-2 version except for the file name in the GF entry. Run both models, if possible.

Model	Free-Space Gain dBi	180° Front-to-Back Ratio dB	Source Impedance R +/- jX Ω
6-10-nec4	8.70	22.53	49.2 - j0.6
6-10-nec2	8.77	22.56	49.0 - j1.0

Next, open model *6-11-nec2.nec*.

```
GF 0 R2-H18-V14.WGF
GW 24 11 .25 -.25 -.233 .25 -.25 .233 .004
GW 25 11 .25 .25 -.233 .25 .25 .233 .004
GE 0 -1 0
EX 0 24 6 0 1 0
EX 0 25 6 0 1 0
RP 0 361 1 1000 -90 0 1.00000 1.00000
RP 0 1 361 1000 90 0 1.00000 1.00000
EN
```

Like model 6-10, the new model calls upon R2-H18-V14.WGF in the GF command. However, it sets up 2 dipoles spaced 0.5λ apart and feeds the two drivers in phase. If you open model *6-11-nec4.nec*, you will find that it sets up the same situation, but calls on R-H18-V14.WGF in the GF command. Running the models produces the following reports.

Model	Free-Space Gain dBi	180° Front-to-Back Ratio dB	Source Impedance R +/- jX Ω
6-11-nec4	10.54	21.50	96.9 - j0.9 (x2)
6-11-nec2	10.61	21.15	96.6 - j1.1 (x2)

Using a single reflector size, neither driver system is working with an optimal size reflector. As a result, one might well explore a whole collection of planar reflectors in search for the best dimension for each driver type. As well, there are other driver assemblies--such as rectangles, half squares, and dual-diamond quads--that deserve to be run through the reflector collection. The result might well be a considerable collection of NGF files (and their required storage space on the hard drive) and an equally considerable number of driver models. Once the NGF files are run a single time apiece, using them to test a given driver takes between 4 to 6 seconds on a slow computer for each run. Full models of each might take 2 to 4 times as long.

As a final exercise, let's explore the principle of using symmetry in the NGF file. We need not create a phenomenally large structure just to see how it works. In fact, we can rewrite the reflector files to incorporate symmetry. We shall not acquire any significant run-time improvements by using such small models, but we shall be able to see clearly how the model geometry goes together.

Open model *6-12-nec-2.nec*. In this model, we create -Y versions of a half reflector, minus the center vertical wire. This process involves as many GW and GM entries as the earlier version of the reflector (model 6-10), but less than half the segments. Next, we introduce a GX command to order a mirrored replication of the initial structure, and we increment the tag

numbers by 2 to avoid overlapping tags. Because the result lacks a center vertical wire, we add one, GW5. Finally, we alter the NGF file name.

```
GW 1 9 0 -.9 -.7 0 0 -.7 .0159
GM 0 14 0 0 0 0 0 .1 001.001
GW 2 14 0 -.9 -.7 0 -.9 .7 .0159
GM 0 8 0 0 0 0 .1 0 002.002
GX 2 010
GW 5 14 0 0 -.7 0 0 .7 .0159
GE 0
FR 0 1 0 0 299.7925 1
GN -1
WG R2-H18-V14-GX.WGF
EN
```

The NGF file requires about half the hard-drive storage space of the full reflector NGF file for model 6-10-nec2.

The procedure for model *6-12-nec4.nec* is quite similar. The NEC-4 models originally used a center wire plus -Y and +Y GM commands. In the version employing the GX command, we omit the +Y GM command, while altering all other commands to create only -Y values. The GX command is identical to the NEC-2 version of the model, as is the final GW entry of a center vertical wire. Once more, we create a unique file name for the NGF file.

```
GW 1 9 0 -.9 0 0 0 0 .0159
GM 0 7 0 0 0 0 0 -.1 1 1 1 9
GM 0 7 0 0 0 0 0 .1 1 1 1 9
GW 2 14 0 -.1 -.7 0 -.1 .7 .0159
GM 0 8 0 0 0 0 -.1 0 2 1 2 14
GX 2 010
GW 5 14 0 0 -.7 0 0 .7 .0159
GE 0 -1 0
FR 0 1 0 0 299.7925 1
GN -1
WG R-H18-V14-GX.WGF
EN
```

Models *6-13-nec2.nec*, *6-13-nec4.nec*, *6-14-nec2.nec*, and *6-14-nec4.nec* replicate the single and double driver systems of models 6-10 and 6-11, but call up in their GF commands the appropriate NGF files based upon the introduction of symmetry into them. You will find that all of the elements of **Fig. 6-8** and the previous output report tables apply to these new versions.

Except for the NGF file storage space, we cannot in these small models demonstrate any significant improvements in performance of the core for the use of symmetry. Faster run times with NGF files abetted by the use of symmetry more clearly emerge in large files. Ships, planes, helicopters, and motor vehicles usually show clear benefits of adding symmetry to the NGF file, depending upon the level of detail required in the model. Repetitious use of reflector and similar structures shows the advantages of using NGF files, even if none of those files is exceedingly large.

Summing Up

In this set of exercises, we have explored various ways of handling complex structures, including the use of external shape-synthesizers, wire-grid structures, and Numerical Green's Functions. Our exercise models were sized to be just large enough to illustrate the principles involved, but not so large as to reveal fully the extent of improvement that we might make to the total usable model segment count or to the core run-times.

External synthesizers prove to be very useful in setting up the wires for complex shapes where the manual calculation of each wire or segment would be tedious and error prone. For irregular or constantly changing shapes, such as curved lines and surfaces, synthesizers tend to produce a large collection of 1-segment GW entries. For regular polygons, they can produce fewer wires by allowing wire intersections to occur at segment junctions. In either case, the NEC input model tends to be large, which may be a hindrance to error detection by visual scanning. As well, any revisions to even a single aspect of the synthesized geometry tend to require creating a new or substitute model. Finally, synthesized models require completion in terms of adding necessary control commands, including output requests.

Wire-grid structures having regular features are amenable to construction by either synthesis or by the economical use of combinations of GW and GM entries. Such models can produce very large structures in only a few command lines. The techniques are especially apt to rectangular structures and to volumes composed of rectangles. Although we used planar and corner reflectors in the examples, we might easily form boxes of various sizes. An added advantage of the rectangular wire grid is that we may easily modify the line spacing and segment density without altering the number of lines in the NEC input file.

For some types of modeling work, Numerical Green's Functions are highly serviceable. We explored both the writing of NGF files (WG) and the reading of them (GF), including taking note of what goes into the NGF file and what remains for the model that reads it. For repeated use of a structure, the NGF file is invaluable. For very large files, the NGF model can make use of symmetry to speed its run, leaving non-symmetrical elements for the file that uses the NGF data.

Although we have not explored every nuance of large-model formation in this brief chapter, perhaps there are enough techniques at hand to permit some eventual creative modeling.

7.
Finding Geometry Limitations in a Model

***Objectives**: In the final exercise on model geometry, you will meet in a concentrated dose many of the limitations associated with setting up a model using those commands. In addition, you will become acquainted with some of the tools available both in the NEC cores and in the overall program for detecting geometry error and warning conditions, along with ways of correcting them.*

The exercise models that we have encountered in Part A focus upon the correct ways of using each command. However, errors that range from simple typographical slips to misunderstandings of commands do occur when we convert a physical structure into a set of Cartesian coordinates. Some errors are large and trigger every error detection system within both the NEC core and the program interface modules. Other errors are subtler, allowing the core to run as if the geometric set-up were correct. In some cases, the results may not differ significantly from those derived from a geometrically correct model. However, the flawed geometry makes those results unreliable unless we have a corrected model with which to compare them.

In this chapter, we shall survey a considerable number of large and small, blatant and subtle geometry flaws. We shall ultimately probe into errors and limitations that may not show up in the tools available for detection. However, the first step is to become acquainted thoroughly with the tools provided by the NEC cores and by NEC-Win Pro and GNEC for detecting errors. In these exercises, virtually all models--except the very first--will run on both the NEC-2 and NEC-4 cores. In some cases, we may obtain different results, depending on the error or limitation under study.

Our work in these exercises will focus only on errors and limitations associated directly with the geometry commands. In succeeding sections of this volume, we shall encounter difficulties related to various control commands. In addition, we shall also by-pass some of the most obvious faults that we can pack into a model, such as using a wire radius that exceeds the segment length or giving 2 wires the very same set of coordinates for both end 1 and end 2. A review of Chapter 1 will provide enough caution for us to avoid these obvious problems.

Error Detection Tools

Both the NEC cores themselves and the programs that encase them provide a large but not exhaustive number of tools for finding model geometry flaws. Many of the tools are available for use while we set up a model. However, there is a fundamental rule that applies to virtually all trouble-shooting activities. The ailing patient is the best indicator of the problem. If we understand the antenna structure that we are modeling, then flawed results will help us find the source of the problem and indicate its cure.

Open reference model *7-0.nec*. This model contains intentionally large flaws to help us catalog the contents of our tool kit. Since it involves an axial-mode helical antenna, we must use NEC-2

to run the model, since the GH command changes radically between NEC-2 and NEC-4. The model consists of a helix with a single connecting wire from its lower tip to a perfect ground.

```
CM Helix on perfect ground
CM Example of clues to 1 or more geometry flaws
CE
GH 1 200 .238 2.38 .171 .171 .171 .171 .225
GM 0 0 0 0 0 0 0 .115
GW 2 5 .171 0 0 .171 0 .115 .005
GE 1 0 0
GN 1
FR 0 0 0 0 299.7925 1
EX 0 2 1 00 1 0
RP 0 181 1 1000 -90 0 1.00000 1.00000
EN
```

Run the model and examine the output data, some of which appears in **Fig. 7-1**.

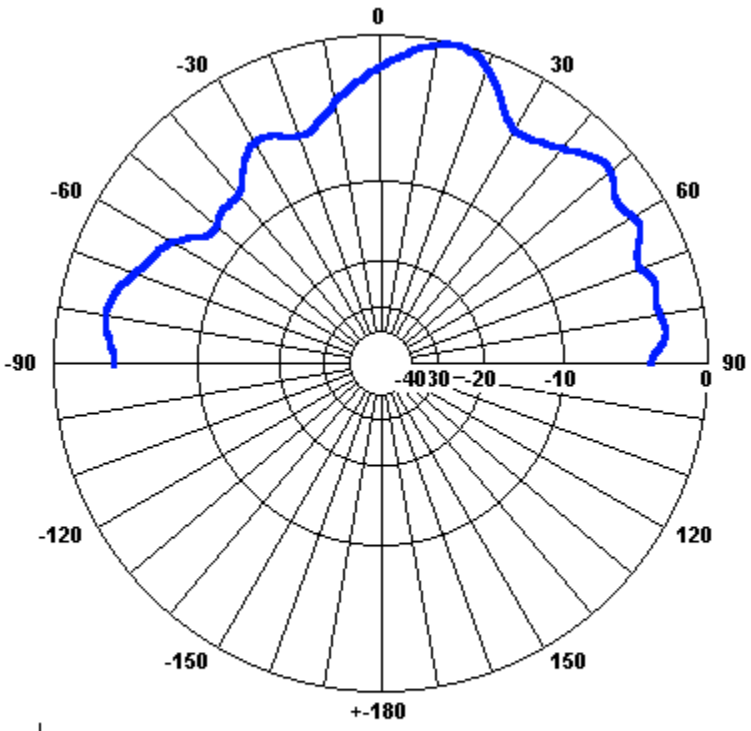

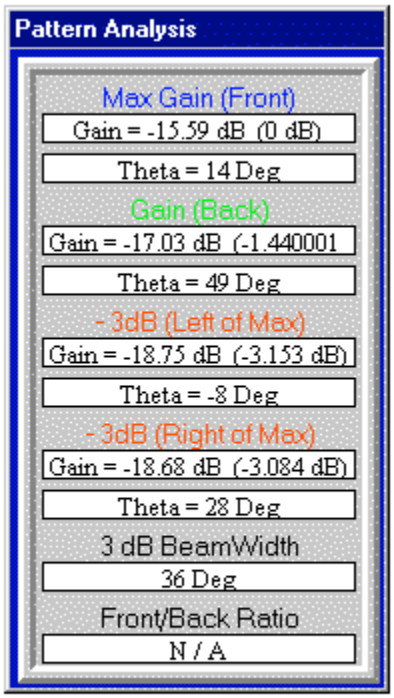

Input Impedance and VSWR

Frequency	Tag	Seg.	Real(Z)	Imag(Z)
299.790000	2	201	24.905	-383.023

Fig. 7-1

All of the data is way off the mark for axial-mode helices, even if somewhat badly designed. The pattern shape is wholly unexpected. The gain report is unrealistically low, and the source impedance report is completely atypical of an axial-mode helix. There are clues to the problem in the NEC-2 output report, specifically in the segmentation data. **Fig. 7-2** provides a partial listing in order to highlight relevant details.

- - - - SEGMENTATION DATA - - - -

COORDINATES IN METERS

I+ AND I- INDICATE THE SEGMENTS BEFORE AND AFTER I

SEG. NO.	COORDINATES OF SEG. CENTER X	Y	Z	SEG. LENGTH	ORIENTATION ANGLES ALPHA	BETA	WIRE RADIUS	CONNECTION DATA I-	I	I+	TAG NO.
1	0.16682	0.02642	0.12095	0.05481	12.54001	99.00000	0.22500	205	1	2	1
2	0.15049	0.07668	0.13285	0.05481	12.54001	117.00000	0.22500	1	2	3	1
3	0.11943	0.11943	0.14475	0.05481	12.54001	135.00000	0.22500	2	3	4	1
4	0.07668	0.15049	0.15665	0.05481	12.54001	153.00000	0.22500	3	4	5	1
198	0.11943	-0.11943	2.46525	0.05481	12.54001	44.99994	0.22500	197	198	199	1
199	0.15049	-0.07668	2.47715	0.05481	12.54001	62.99994	0.22500	198	199	200	1
200	0.16682	-0.02642	2.48905	■0.05481	12.54001	80.99994	■0.22500	199	200	0	1
201	0.17100	0.00000	0.01150	■0.02300	90.00000	0.00000	■0.00500	201	201	202	2
202	0.17100	0.00000	0.03450	0.02300	90.00000	0.00000	0.00500	201	202	203	2
203	0.17100	0.00000	0.05750	0.02300	90.00000	0.00000	0.00500	202	203	204	2
204	0.17100	0.00000	0.08050	0.02300	90.00000	0.00000	0.00500	203	204	205	2
205	0.17100	0.00000	0.10350	0.02300	90.00000	0.00000	0.00500	204	205	1	2

Fig. 7-2

The markers that I added call attention to some potential difficulties. At the transition from the helix to the straight wire, the segment length changes by nearly a 2.5:1 ratio. At that same point, we also find an even more radical change in the wire radius. Here, the difference--although important--is less significant than the wire radius within the helical portion of the model. It is simply too large for any real helix.

The program also provides a number of tools to pinpoint the errors in this model. See **Fig. 7-3** for a potpourri of indicators.

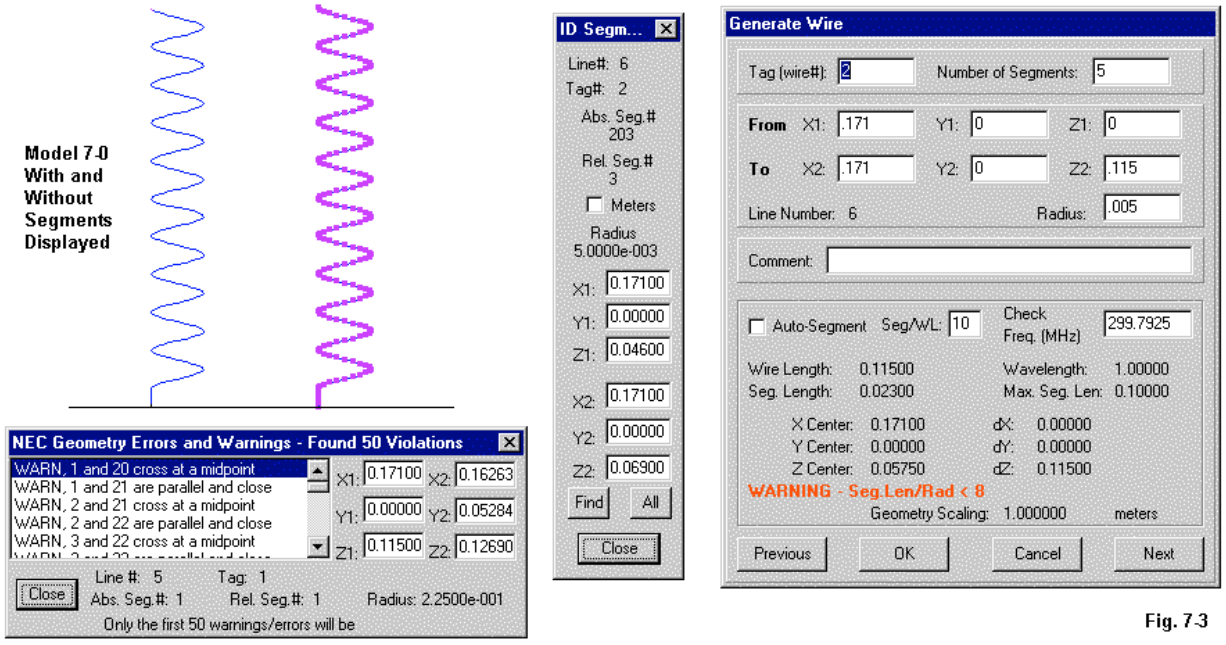

Fig. 7-3

Displaying the segments in Necvu can often tell us that something may be amiss. The segments

in the connecting wire appear shorter than those in the helix itself. Necvu contains a segment-identification feature that can provide the end coordinates of any selected segment. However, warnings appear even earlier in model development. If we double-click on the GW entry, we obtain the screen at the right in the figure. Note that it warns us that the segment length is less than 8 times the radius, a condition in NEC-2 that (by conservative modeling standards) would ordinarily be a sign to invoke the EK command that we shall meet in Part C. (The revised current algorithm in NEC-4 encompasses what the EK command does for NEC-2 and so the command was dropped from the NEC-4 control command list.)

However, the main diagnostic tool appears in the lower left corner of **Fig. 7-3**. Necvu runs the geometry section of the model and applies modeling standards to it. The result is an error list--at least through the first 50 errors. Note that the errors include wires that are too close together and wires that cross a midpoints. Our first indicator that the helix wires had too large a radius is confirmed graphically.

```
GH 1 200 .238 2.38 .171 .171 .171 .171 .225
```

In the NEC-2 GH command, the wire radius appears in the last position. In a 300-MHz axial-mode helix, a value ranging from 0.001 to perhaps 0.005 might be more reasonable. While you are revising the model to re-check it, you might make the wire radii of the helix and the straight wire the same and perhaps reduce the number of segments in the connecting wire to 3.

One test that we did not show is the Average Gain Test (AGT). If we perform this test on the unmodified model, we obtain a value over perfect ground of 0.0129 or -21.91 dB, indicating a very unreliable model indeed. The values that you obtain after modifying the model will depend on the precise corrections that you make.

With these tools at our disposal, we might too easily believe that either the core or the program will uncover everything that we might do wrong initially. However, as we shall see from some of our exercise models, the modeler's vigilance remains the key element in error detection. One obvious illicit condition is to have two wires cross at other than a segment or a tag junction. However, the existence of that condition does not necessarily prevent the core from running a model and reporting seemingly sensible results. Open model *7-1.nec*.

```
CM Illicit wire junction
CE
GW 1 11 0 -.2375 0 0 .2375 0 .001
GW 2 11 0 -.2375 0 .2 .005 0 .001
GW 3 11 0 .2375 0 .2 -.005 0 .001
GE 0 1 0
EX 0 1 6 0 1 0
FR 0 1 0 0 299.7925 1
RP 0 1 361 1000 90 0 1.00000 1.00000
EN
```

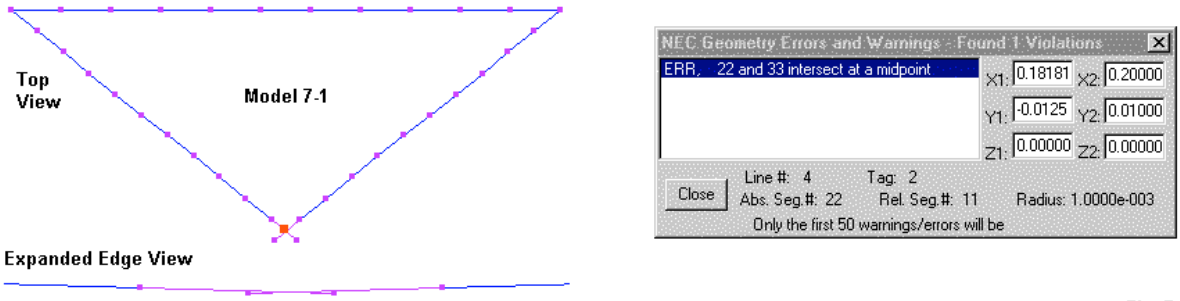

Fig. 7-4

Although not immediately self-evident from the model description, the segments at the extreme ends of the triangle legs cross at mid-segment. **Fig. 7-4** uses two views of the triangle to establish the error, with a report from Necvu on the right. Under these conditions, NEC-2 will execute, returning a maximum free-space gain of 2.07 dBi, with a source impedance of 269 - j337 Ω. The reported AGT value is 0.9949, erroneously indicating an excellent model. (As noted earlier, the AGT is a necessary but not a sufficient condition of model adequacy.)

What NEC-4 does with the model depends upon the settings in the center numerical entry of the GE command. (NEC-2 reads only the first numerical entry to establish the presence or non-presence of a ground plane.) By way of review, the following list summarizes the values of I2 for the GE command:

-1	Tests of illegal segment intersections or severe violations of the thin-wire approximations not performed.
0 (default)	Segments tested and reported; only "errors" cause the code to stop.
1	Both error and warning messages cause the code to stop.
2	Segments tested, but code runs, even with errors or warnings.

Since model 7-1 uses a value of 1, it stops the core. In the output file, we find the following line.

```
SEGCHK: ERROR - SEGMENTS  22 AND  33 INTERSECT AT A MIDPOINT
```

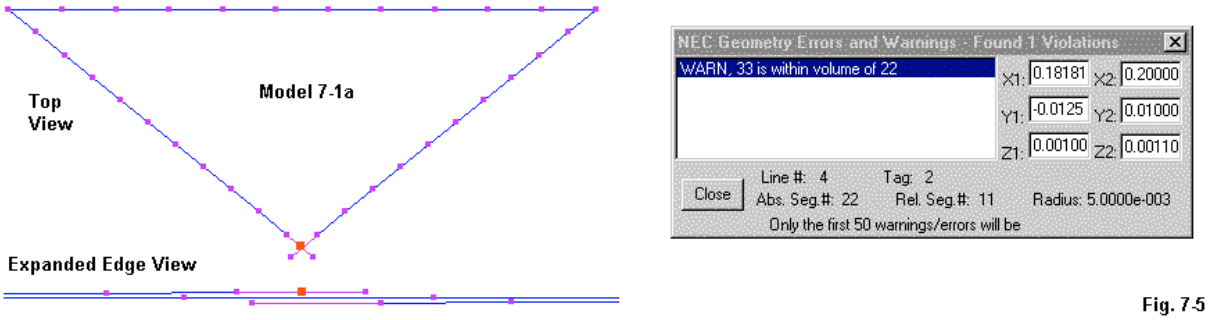

Fig. 7-5

Fig. 7-5 displays a slightly different condition that appears in model *7-1a.nec*. Since Necvu shows only the centerline of the wires and not their full thickness, the legs of the triangle appear to pass each other. However, the error report screen warns of a wire being within the volume of another, the condition that we have called inter-penetration. You may estimate the penetration from the GW lines of the model.

```
GW 1 11 0 -.2375 0 0 .2375 0 .005
GW 2 11 0 -.2375 0 .2 .01 .0011 .005
GW 3 11 0 .2375 0 .2 -.01 -.0011 .005
```

From the end-2 Z values of 0.0011 and -0.0011, with a wire radius of 0.005, the surfaces will just touch slightly short of the wire ends. Although Necvu warns of the inter-penetration, it returns a maximum free-space gain of 2.35 dBi with a source impedance of 242 - j 185 Ω. The AGT is 0.9733, making this test unreliable as an indicator of the flaw. In contrast, NEC-4 (using a value of 1 for I2 in the GE command) stops the run and returns a complete set of warnings.

```
 SEGCHK: WARNING - SEGMENTS  22 AND  33 CROSS AT A MIDPOINT WITH
SEPARATION LESS THAN THE SUM OF THEIR RADII
 SEGCHK: WARNING - THE CENTER OF SEGMENT  22 IS WITHIN THE VOLUME OF
SEGMENT  33
 SEGCHK: WARNING - THE CENTER OF SEGMENT  33 IS WITHIN THE VOLUME OF
SEGMENT  22
```

We might wish to believe that the reason for the failure of the AGT to show the error by returning a value that is far from ideal is that the segment crossing occurs far from the high current region of the antenna elements. So let's repeat the process using a turnstiled pair of dipoles, that is, a pair of dipoles that cross at their centers, normally without touching. Each dipole is fed 90° out of phase with the other. See **Fig. 7-6** for the options that we shall explore.

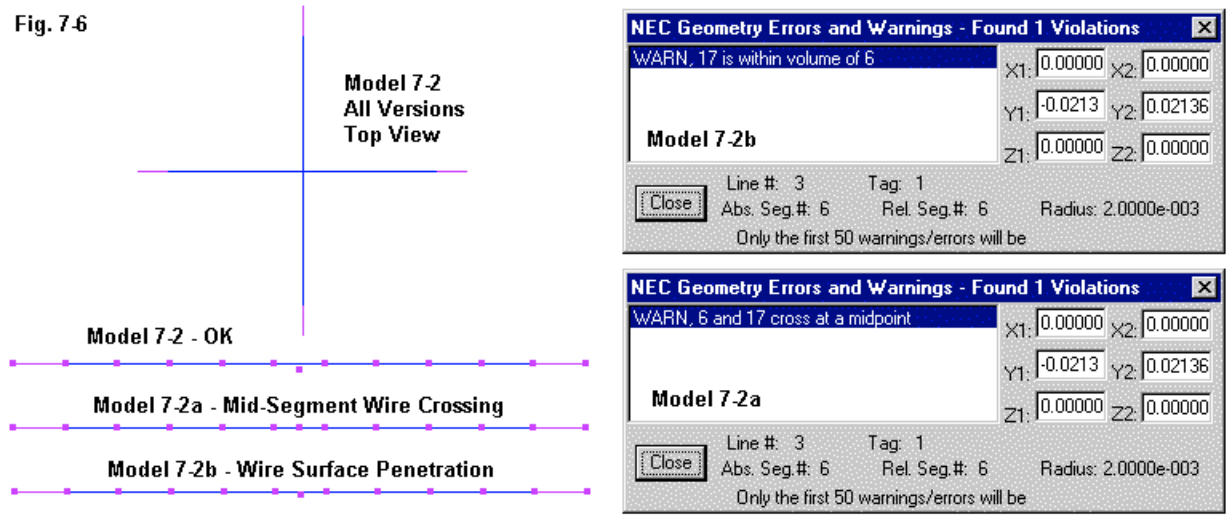

Open model *7-2.nec*. Note the separation of the dipoles at their center points.

```
GW 1 11 0 -.235 0 0 .235 0 .002
GW 2 11 -.235 0 .006 .235 0 .006 .002
```

The separation is 0.006 m, more than the sum of the radii of the two wires (0.004 m). Therefore both cores run and return essentially the same reports: a maximum free-space gain for the nearly circular patterns of -0.89 dBi, with two source impedances of 71.8 + 0.3 Ω. The AGT value is 0.9974.

Next open model *7-2a.nec* and check the Z coordinates of the two wires.

```
GW 1 11 0 -.235 0 0 .235 0 .002
GW 2 11 -.235 0 0 .235 0 0 .002
```

These wires intersect at mid-segment. However, NEC-2 returns the very same set of values as the model with adequate clearance. NEC-4 would also return these values if we had not set it to stop the run in the event of errors or warnings. It sends back the following error report.

```
 SEGCHK: ERROR - SEGMENTS   6 AND  17 INTERSECT AT A MIDPOINT
 SEGCHK: WARNING - THE CENTER OF SEGMENT   6 IS WITHIN THE VOLUME OF
SEGMENT  17
 SEGCHK: WARNING - THE CENTER OF SEGMENT  17 IS WITHIN THE VOLUME OF
SEGMENT   6
```

Finally, open model *7-2b.nec*. From the Z coordinates of the two wires, you may surmise that the wires inter-penetrate, but do not intersect at their centerlines.

```
GW 1 11 0 -.235 0 0 .235 0 .002
GW 2 11 -.235 0 .0039 .235 0 .0039 .002
```

Once more, NEC-2 returns the same set of values as for the first 2 versions of the model. However, NEC-4 stops and returns the following warning message.

```
 SEGCHK: WARNING - SEGMENTS    6 AND   17 CROSS AT A MIDPOINT WITH
SEPARATION LESS THAN THE SUM OF THEIR RADII
```

First, we have learned that illicit wire intersections and inter-penetrations do not necessarily lead to poor AGT values, even when they occur in high current regions of a modeled antenna. Second, we have seen that the use in NEC-4 of a GE I2 value of 1 is very useful, since it alerts us to errors and warnings, even if we fail initially to check the geometry via the Necvu feature. Third, we have seen that NEC-2 lacks a core-stopping feature, which makes us more dependent upon the Necvu error detection system, as well as our own careful scrutiny of the models that we construct.

Wire inter-penetrations may occur at the corners of model geometries. Consider the structure and wire radii of model *7-3.nec*.

```
GW 1 11 0 -.13 -.13 0 .13 -.13 .02
GW 2 11 0 .13 -.13 0 0 .1 .02
GW 3 11 0 0 .1 0 -.13 -.13 .02
```

The model creates an equilateral triangle using 11 segments per leg and 20-mm radius wires. Each segment is 0.02364-m long, so that even a right-angle junction would place the surface of one wire very close to the center point of the one to which it joins. With a 60° angle at the corners, the penetration goes even further into the center region of the mating wire. The Necvu error report box in **Fig. 7-7** shows the error that repeats itself at each of the triangle's corners.

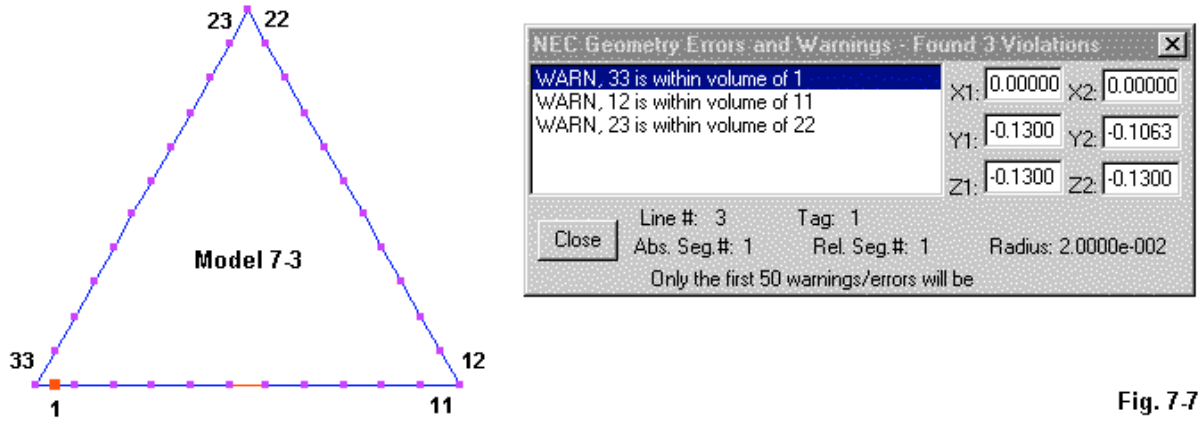

Fig. 7-7

Despite these geometry errors, NEC-2 returns an initially plausible report that shows a maximum free-space gain of 1.85 dBi, a source impedance of 36 - j167 Ω, and an AGT score of 1.0091. With the core-stopping GE code in place, NEC-4 returns a set of warnings.

```
 SEGCHK: WARNING - THE CENTER OF SEGMENT   1 IS WITHIN THE VOLUME OF
SEGMENT  33
 SEGCHK: WARNING - THE CENTER OF SEGMENT  33 IS WITHIN THE VOLUME OF
SEGMENT   1
 SEGCHK: WARNING - THE CENTER OF SEGMENT  11 IS WITHIN THE VOLUME OF
SEGMENT  12
 SEGCHK: WARNING - THE CENTER OF SEGMENT  12 IS WITHIN THE VOLUME OF
SEGMENT  11
 SEGCHK: WARNING - THE CENTER OF SEGMENT  22 IS WITHIN THE VOLUME OF
SEGMENT  23
 SEGCHK: WARNING - THE CENTER OF SEGMENT  23 IS WITHIN THE VOLUME OF
SEGMENT  22
```

Note that the warnings are the same as those in the Necvu error check system, except that Necvu eliminates the redundant entries.

A further way to check the sensibleness of the NEC-2 report for model 7-3 is to reset the wire radii to values that fall well within specifications. Open model *7-3a.nec* and note the new wire radius for each tag: 0.001 m.

```
GW 1 11 0 -.13 -.13 0 .13 -.13 .001
GW 2 11 0 .13 -.13 0 0 .1 .001
GW 3 11 0 0 .1 0 -.13 -.13 .001
```

If you run the model on either core, you will obtain the following results: a maximum free-space gain of 2.11 dBi, a source impedance of 97 - j622 Ω, and an AGT score of 1.005. You may modify model 7-3a by gradually increasing the wire radius to 0.005 and then upwards in steps of 0.005. (At and above a radius of 0.015 m, only NEC-2 will complete the core run with the GE command set to stop NEC-4 if there is a segment-check warning or error.) Note the rapid change in both source resistance and reactance as the radius increases beyond 0.01 m.

Not all geometry difficulties occur as a function of wire intersections and inter-penetrations. Some

arise when there are no warnings at all. For example, as we press the limits of the recommended separation of wires, we shall discover growing errors in the output reports. These may occur even if we rigorously adhere to the injunction to keep the segment junctions of closely spaced wires well aligned. Open model *7-4.nec*. In this model, we place a source at the center of GW 1. GW2 is a closely spaced shorter wire that--for illustrative purposes--has a length that results in segments of just about the same length as those in the longer wire. The pattern request (RP0) is at right angles to the wire pair, since there will be a very small difference in gain values in the plane of the wires. **Fig. 7-8** sets up the situation visually.

```
GW 1 11 0 -.243 0 0 .243 0 .01
GW 2 7 0 -.152 .04 0 .152 .04 .01
```

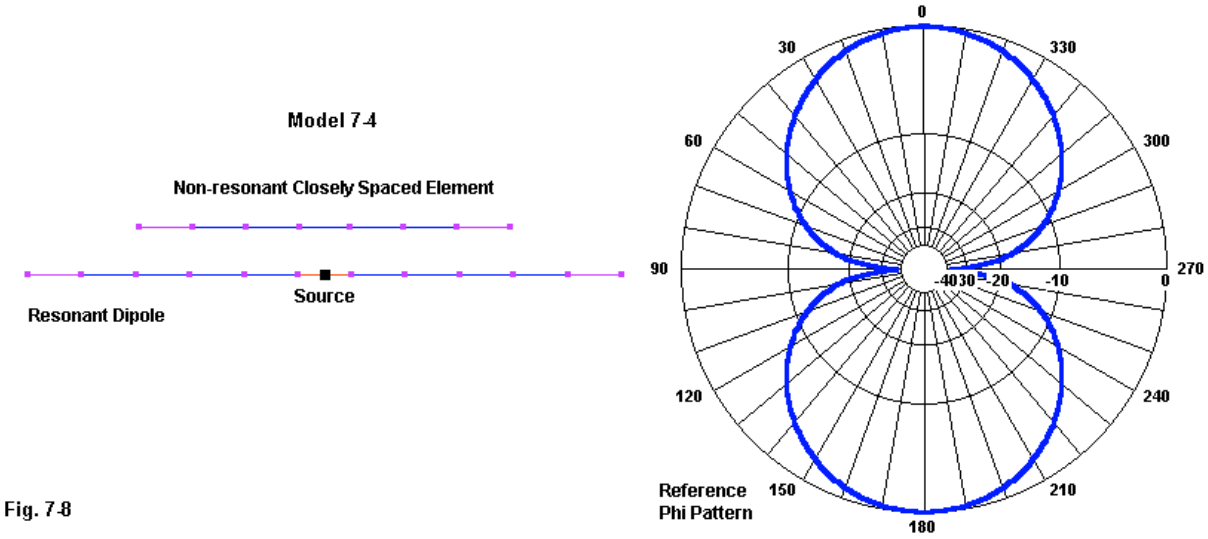

Fig. 7-8

Our goal here is to gradually reduce the spacing between the wires and watch what happens to the output reports. Due to the wire radii, 0.020 m is the closest we dare space the wires. The following table uses NEC-2 values for the exercise. Run the exercise to confirm the values shown.

Spacing Meters	Free-Space Gain dBi	Source Impedance R +/- jX Ω	AGT	AGT-dB	Corrected Gain dBi	Corrected Resistance
0.040	2.19	92.12 - j0.11	1.0021	+0.009	2.18	92.32
0.035	2.21	92.08 - j3.59	1.0062	+0.027	2.18	92.65
0.030	2.25	91.24 - j8.08	1.0150	+0.065	2.18	92.61
0.025	2.33	88.66 - j13.88*	1.0349	+0.149	2.18	91.75*
0.020	2.52	82.37 - j21.00*	1.0814	+0.340	2.18	89.07*

We obtain corrected gain figures by subtracting positive AGT-dB values from the reported gain. The result is a uniform gain value. We obtain corrected source resistance values by multiplying the basic AGT value times the reported resistance value. However, this second correction is only reliable if the source reactance is very small. In the last two lines of the table, the reactance value has reached a level that makes the correction only useful as an indicator, but not reliable as a corrected value.

In most models, the values for a NEC-2 and NEC-4 run will be very similar. In this instance, that similarity holds--except for the fact that we are exploring fine shades of differences and their correction via the AGT score. Therefore, the following values are the NEC-4 reports for the same model and situation.

Spacing Meters	Free-Space Gain dBi	Source Impedance R +/- jX Ω	AGT	AGT-dB	Corrected Gain dBi	Corrected Resistance
0.040	2.20	90.98 - j0.35	1.0039	+0.017	2.18	91.33
0.035	2.22	90.85 - j3.65	1.0088	+0.038	2.18	91.65
0.030	2.26	89.89 - j7.87	1.0192	+0.083	2.18	91.62
0.025	2.36	87.17 - j13.26*	1.0424	+0.180	2.18	90.87*
0.020	2.58	80.77 - j19.72*	1.0960	+0.398	2.18	88.52*

In the gain report column, we can notice that the NEC-4 curve grows steeper at the closest spacing levels than the corresponding NEC-2 curve. As well, the source resistance reported by NEC-4 is a bit lower at every spacing level, although the reactance has a close correlation to NEC-2 values. Nevertheless, the gain values all return to 2.18 dBi when corrected by the AGT-dB value. As well, the source resistance values show the same pattern of correction, with higher report reactance values making the corrected resistance values less reliable. The repetition of the exercise using the two cores gives us a small insight into how the revised algorithms affect critical results.

More significantly, the exercise reveals that not all geometry problems show up as errors and warnings. Some are subtler as we press the limits of the cores. In many of these cases, we may use the average gain test to correct the reported results and thereby obtain truer performance curves. Whether this operation is mandated depends upon the overall task specifications for a given set of models. Whether or not mandated, performing an AGT is a wise precaution, even if--as we have seen--there are many cases in which it will not reveal a geometry flaw.

Mixed Wire Limitations

There are a number of situations that press NEC to its limits or take the core beyond its limits, but they do not appear on any error checking system within the core itself or within the implementing program. **Fig. 7-9** illustrates one of them: an angular junction of 2 wires having different radii. Open model *7-5.nec*.

```
GW 1 5 0 0 0 0 0 .125 .01
GW 2 5 0 0 .125 0 .125 .125 .001
GE 1
GN 1
EX 0 1 1 0 1 0
```

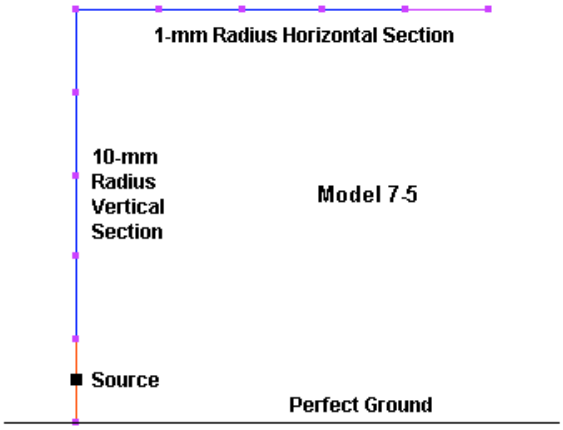

Fig. 7-9

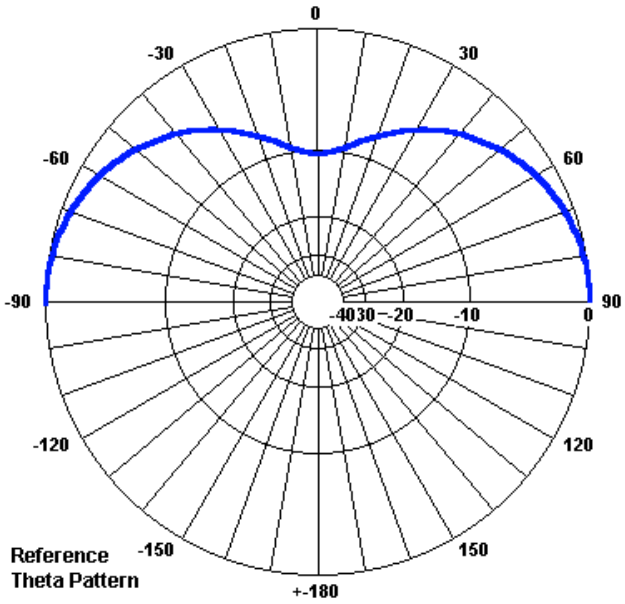

The antenna is a common "inverted-L" consisting of a fat (10-mm radius) vertical section and a thin (1-mm radius) horizontal section. The current algorithm for NEC-4 improves the ability of the core to handle (within limits) all junctions of wires having dissimilar radii. Compare the following table of values drawn from the present model and two others in the series: *7-5a.nec* and *7-5b.nec*. The supplementary models simply increase the segmentation on each leg in increments of 5 segments per wire. AGT values approach 2.0 since the antenna is over a perfect ground.

Core	Model	Segments/ Wire	Free-Space Gain dBi	Source Impedance R +/- jX Ω	AGT
NEC-2	7-5	5	4.68	19.3 - j15.0	1.998
	7-5a	10	4.60	21.7 - j 1.3	1.977
	7-5b	15	4.55	23.8 + j 5.6	1.965
NEC-4	7-5	5	4.75	17.2 - j28.0	2.019
	7-5a	10	4.72	15.6 - j30.7	1.996
	7-5b	15	4.72	15.0 - j28.2	1.999

The NEC-4 results are reasonably stable for this simple structure. The progression of source resistance values is sensible, since with shorter segments, the source point draws ever closer to the ground. In contrast, the weaker ability of NEC-2 to handle wire junctions where the radii are quite different shows up in almost all of the report categories. The gain descends noticeably, but the AGT correction is insufficient to bring it to a stable value. As we add more segments per wire, the source impedance rises, and the source reactance changes with each level of segmentation. The result is an untrustworthy set of report values, despite the AGT scores. How untrustworthy the scores are depends on the task specifications brought to the modeling exercise.

Even the NEC-4 results have limits. However, we cannot know internally to the pair of cores just what those limits are. There are two general methods of determining the limits. One method is to compare NEC (-2 or -4) results against a set of carefully refined experiments. The other technique employs an alternative core, one that uses algorithms that do not have the potential

junction dysfunction. MININEC, when well corrected for its own limitations, is one such core. Indeed, the original Leeson correction factors that use substitute uniform-diameter elements for stepped-diameter elements took their calibration from MININEC.

More dramatic than the simple inverted-L model are folded dipoles that employ wires having different diameters. Both NEC-2 and NEC-4 model standard folded dipoles--where the radius of both wires is the same--very well indeed. Consider some folded dipoles for 28.5 MHz. To preclude very-close wire problems, we shall space the long wires 3" apart. As a reference point, we know that a standard folded dipole should have a resonant impedance close to 4 times that of a single-wire dipole. Hence, the source impedance of a standard folded dipole should be in the range of 280 to 290 Ω.

Open model *7-6.nec*. The dimensions are in feet, as the GS line indicates. The wire diameter is 0.5".

```
GW 1 67 -8.05 0 0 8.05 0 0 .02085
GW 2 1 8.05 0 0 8.05 .25 0 .02085
GW 3 67 8.05 .25 0 -8.05 .25 0 .02085
GW 4 1 -8.05 .25 0 -8.05 0 0 .02085
GS 0 0 .3048
```

For this model both NEC-2 and NEC-4 return a free-space gain of 2.22 dBi, with a source impedance of 286 + j4 Ω. The AGT score is too close to a perfect 1.0 to require any gain or source resistance correction. Now open model *7-6a.nec*, a resonant folded dipole for the same frequency and the same wire spacing, but with AWG #12 wire (0.0808" diameter). As well, the model uses the same segmentation as 7-6, but with a length adjustment to bring the antenna to near resonance.

```
GW 1 67 -8.14 0 0 8.14 0 0 3.36778E-03
GW 2 1 8.14 0 0 8.14 .25 0 3.36778E-03
GW 3 67 8.14 .25 0 -8.14 .25 0 3.36778E-03
GW 4 1 -8.14 .25 0 -8.14 0 0 3.36778E-03
GS 0 0 .3048
```

Once more, both NEC-2 and NEC-4 return very nearly identical results: a free-space gain of 2.19 dBi, a source impedance of 286 + j1.1 Ω, and an AGT value too close to perfect to require corrections of the reports.

These two models set us up for model *7-6b.nec*.

```
GW 1 67 -8.1 0 0 8.1 0 0 3.36778E-03
GW 2 1 8.1 0 0 8.1 .25 0 3.36778E-03
GW 3 67 8.1 .25 0 -8.1 .25 0 .02085
GW 4 1 -8.1 .25 0 -8.1 0 0 3.36778E-03
GS 0 0 .3048
```

The only difference between this model and the preceding ones is that the wire holding the source is AWG #12, while the other long wire has a diameter of 0.5". The short connecting wires at the ends are #12 in this model, but making them any diameter from the small #12 value to 0.5" will change nothing critical to the model. **Fig. 7-10** presents the model in graphic form, with a

reference phi pattern that applies to all three folded-dipole models. For this version of a folded dipole, NEC-2 and NEC-4 return very different reports, as revealed in the brief table that follows the graphic.

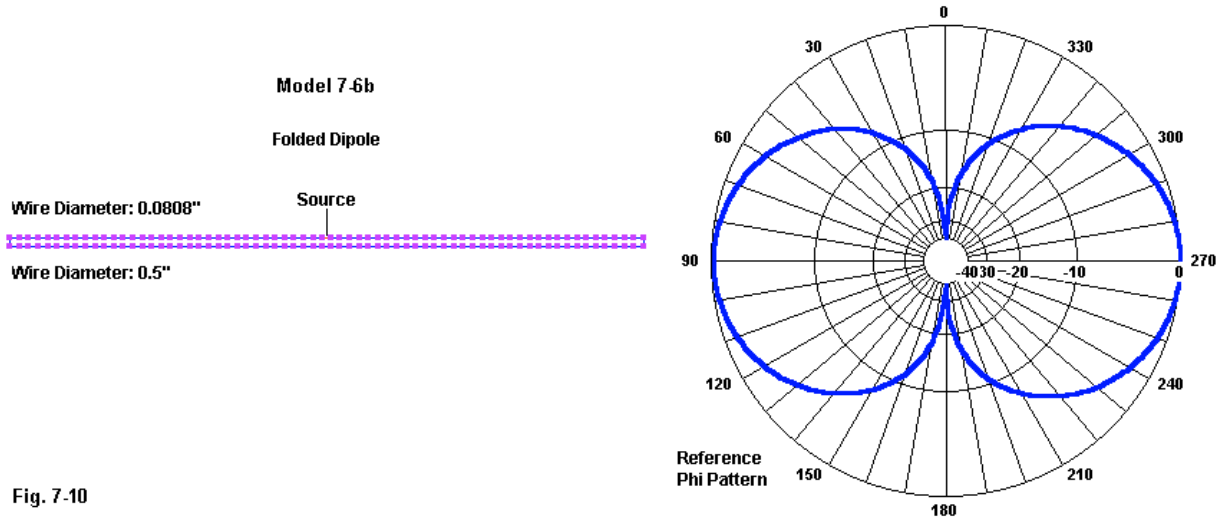

Fig. 7-10

Core	Free-Space Gain dBi	Source Impedance R +/- jX Ω	AGT	AGT-dB	Corrected Gain dBi
NEC-2	0.98	398.8 + j23.7	0.7493	-1.254	2.23
NEC-4	1.72	474.7 + j16.1	0.8898	-0.507	2.23

Because the source impedance report contains considerable reactance, a correction factor for the source resistance is omitted. In addition, multiplying the report values by an AGT of less than 1.0 would reduce the source impedance. In fact, the error is in the opposite direction. The classical equation for calculating the resistive transformation of a folded dipole having different diameter wires has the following form.

$$R = \left(1 + \frac{\log\frac{2s}{d_1}}{\log\frac{2s}{d_2}}\right)^2$$

R is the impedance transformation ratio, s is the center-to-center wire spacing, d_1 is the diameter of the fed wire, and d_2 is the diameter of the second wire. The terms s, d_1, and d_2 are given in the same units. It should be clear that for equal diameter wires of any reasonable spacing, the transformation ratio will be 4. For a spacing of 3", a fed wire diameter of 0.0808", and a second wire diameter of 0.5", the resultant transformation ratio is about 7.47. For a linear-dipole impedance between 70 and 72 Ω, the anticipated folded-dipole impedance would be between 523 and 538 Ω. We might expect some variation, since the equation does not account for the length or diameter of the connecting wires, which are AWG #12 in this model. However, that variation should be slight. The source impedance value of a MININEC model falls squarely within the range of anticipated source impedances for the model folded dipole. Although the NEC-4 model shows a value closer to the calculated value, it remains unreliable, although less obviously so than the NEC-2 model.

There are subtler cases that relate to the folded dipole, but without the impedance transformation factor that we can pre-calculate as a reference. Consider, for example, the dual-material square loop shown in **Fig. 7-11**.

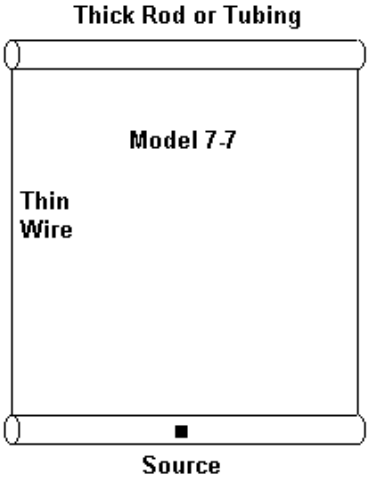

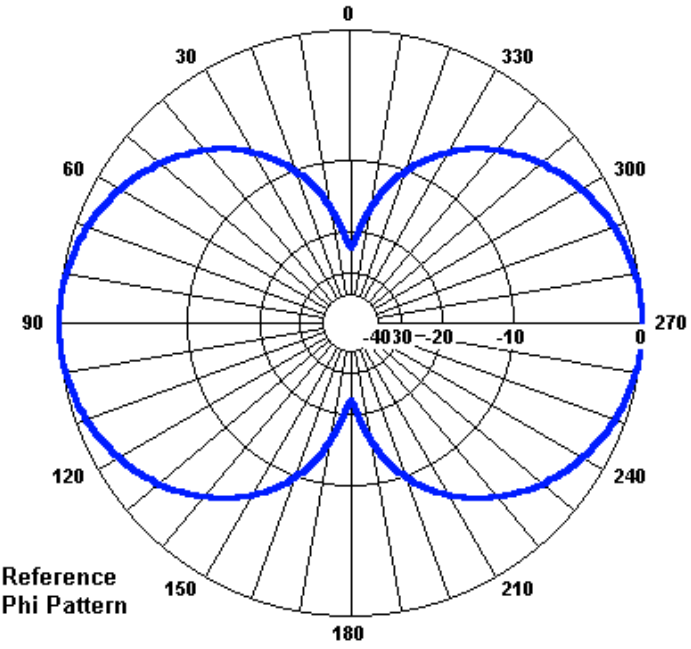

Fig. 7-11

Now open model *7-7.nec*. The 28.5-MHz loop uses 0.5" diameter aluminum rods for the horizontal sections and AWG #12 wire for the side sections. Dimensions are once more in feet, as indicated by the GS entry.

```
GW 1 61 -5.075 0 -5.075 5.075 0 -5.075 .02085
GW 2 61 5.075 0 -5.075 5.075 0 5.075 3.36778E-03
GW 3 61 5.075 0 5.075 -5.075 0 5.075 .02085
GW 4 61 -5.075 0 5.075 -5.075 0 -5.075 3.36778E-03
GS 0 0 .3048
```

Our question might be what sort of performance we should expect from the loop in its free-space environment. The following short table gives the NEC-2 and NEC-4 results.

Core	Free-Space Gain dBi	Source Impedance R +/- jX Ω	AGT	AGT-dB	Corrected Gain dBi
NEC-2	3.59	170.4 + j122.2	0.9915	-0.037	3.63
NEC-4	3.62	149.8 + j43.9	0.9970	-0.005	3.63

In this case, we have no initial guidance as to what the source impedance should be, although the AGT-corrected gain values coincide--a normally good sign that the result is accurate in that category. Open and run models *7-7a.nec* and *7-7b.nec*. Each of these models is a loop created from a single wire diameter: 7-7a uses 0.5" elements, while 7-7b uses AWG #12 elements. For both cores, 7-1a produces a 3.37-dBi gain and a 129 - j0.4 Ω impedance, with AGT scores too close to 1.0 to require any correction. Likewise, 7-1b yields a gain of 3.30 dBi

and an impedance of 126 - j2 Ω, again with nearly perfect AGT scores. However, both models suggest that the reported and corrected gain values of the original model are too high.

In fact, the correct gain value of model 7-7 is roughly correct. The models using a single wire size throughout do not account for the higher current near the ends of the horizontal sections of the mix-wire model. Once more, we require an external source of information to establish this situation. Careful experimental measurements are one route to the data. A well-corrected version of MININEC--which does not have the NEC weakness related to junctions of wires with dissimilar radii--can offer some guidance. For model 7-7, MININEC returns a gain of 3.63 dBi using the same dimensions. However, its source impedance is 137 - j5 Ω, which is distant from either NEC report. The AGT correction for source resistance does not come close to the MININEC value, once more suggesting that the NEC impedance reports have gone past the core limits.

Convergence Failures

The model samples that we have so far examined have used the average gain test as one key to detection. We have seen that the AGT score sometimes provides excellent corrections, sometimes partial corrections, and some times no correction at all. The alternative test is the convergence test. Like the AGT, it is a necessary but not a sufficient condition of model adequacy. Unfortunately, there are models that will not converge when using a NEC core. As modelers, we need to understand why.

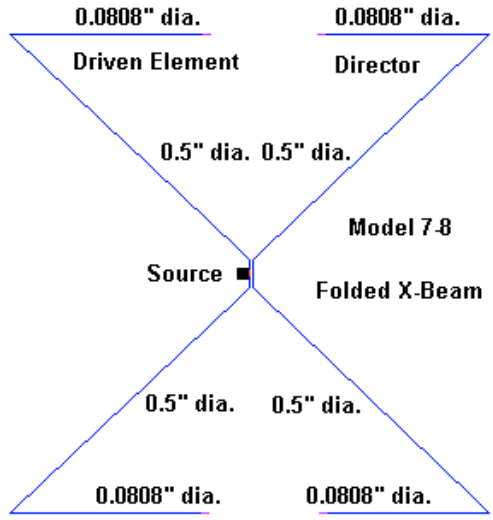

Fig. 7-12

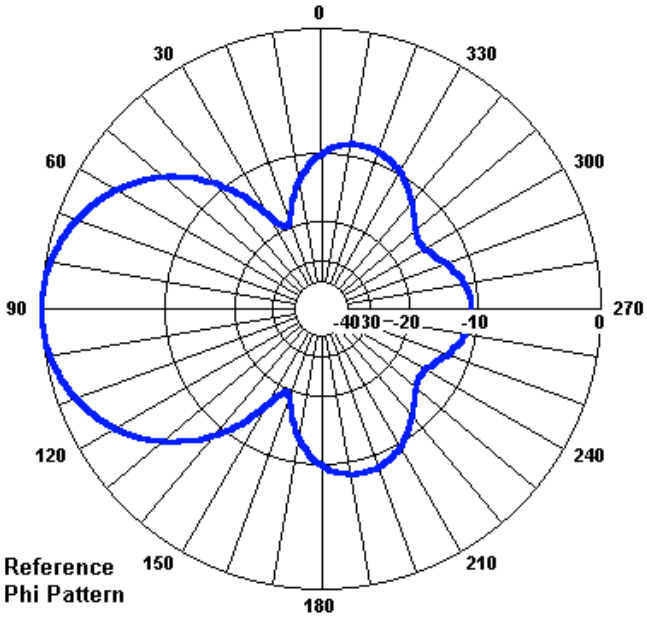

Fig. 7-12 shows a folded X-beam for 28.5 MHz. It consists of two elements, a driver and a director. For maximum accuracy, the very center of each element consists of a short wire so that the source segment is the same length as the adjacent segments. Normal construction of the beam would use aluminum tubing for the X portion of the array to support lightweight wire

tails. As we have done with some past models, we shall use 0.5" diameter arms and AWG #8 tails.

Open model *7-8.nec*. The dimensions are in feet. The LD entries specify two different material losses to reflect the combination of aluminum and copper construction.

```
GW 1 20 -4.893 -.8 35 -4.893 -4.893 35 1.67979002624672E-03
GW 2 33 -4.893 -4.893 35 -.3 0 35 .02085
GW 3 3 -.3 0 35 .3 0 35 .02085
GW 4 33 .3 0 35 4.893 -4.893 35 .02085
GW 5 20 4.893 -4.893 35 4.893 -.8 35 1.67979002624672E-03
GW 6 20 -4.893 1.4 35 -4.893 4.893 35 1.67979002624672E-03
GW 7 33 -4.893 4.893 35 -.3 .08 35 .02085
GW 8 3 -.3 .08 35 .3 .08 35 .02085
GW 9 33 .3 .08 35 4.893 4.893 35 .02085
GW 10 20 4.893 4.893 35 4.893 1.4 35 1.67979002624672E-03
GS 0 0 .3048
```

The version of the model shown uses a high segment density. If you systematically reduce the segmentation and maintain about a 5:8 ratio of tail segments to arm segments, you will discover that the gain value and source impedance change for every level. In its present form, the array returns very disparate NEC-2 and NEC-4 results.

Core	Free-Space Gain dBi	Source Impedance R +/- jX Ω	AGT	AGT-dB	Corrected Gain dBi
NEC-2	6.58	33.0 + j58.7	1.1124	+0.463	6.12*
NEC-4	4.47	86.6 + j36.5	1.0319	+0.136	4.33*

Note that the usually reliable AGT correction does not bring the two gain values any closer to similar values, even though the AGT scores appear to be reasonably good. Although the model appears to pass one necessary condition of being a reliable model, it fails the other test, the convergence test. In fact, the folded X-beam, which is modeled using different wire diameters for adjacent sections of the elements, simply will not converge. The problem lies in the very tight angles formed by the arm-to-tail junctions. Even though the arm and tail segment lengths are similar and the wires do not raise any error or warning flags (not even in NEC-4), the angles are too acute for dissimilar diameter materials to yield accurate results. In fact, the pattern in **Fig. 7-12** is the NEC-2 pattern; the NEC-4 pattern is slightly different. Neither pattern is reliable.

Convergence difficulties do not always require angular junctions of wires having dissimilar diameters. Consider a right triangle, all AWG #12 wire, as shown in **Fig. 7-13**. The antenna is about 50' long at the top and 30' high vertically, with the hypotenuse being about 62.6' long. Open model *7-9.nec*, a free-space version of the antenna.

```
GW 1 20 -27.5 0 30 -27.5 0 60 3.3677E-03
GW 2 40 -27.5 0 60 27.5 0 60 3.3677E-03
GW 3 45 27.5 0 60 -27.5 0 30 3.3677E-03
GS 0 0 .3048
```

The Z coordinates show a positive set of values, which make a difference only to the version of the antenna above ground. Examine the GE and GN entries for this version and for model *7-*

9a.nec. However, the existence of a ground beneath the antenna does not affect the fact that this model does not fully converge, even with a very high segmentation density. The key performance parameter is the source impedance. Note in **Fig. 7-13** that the antenna uses a "split source."

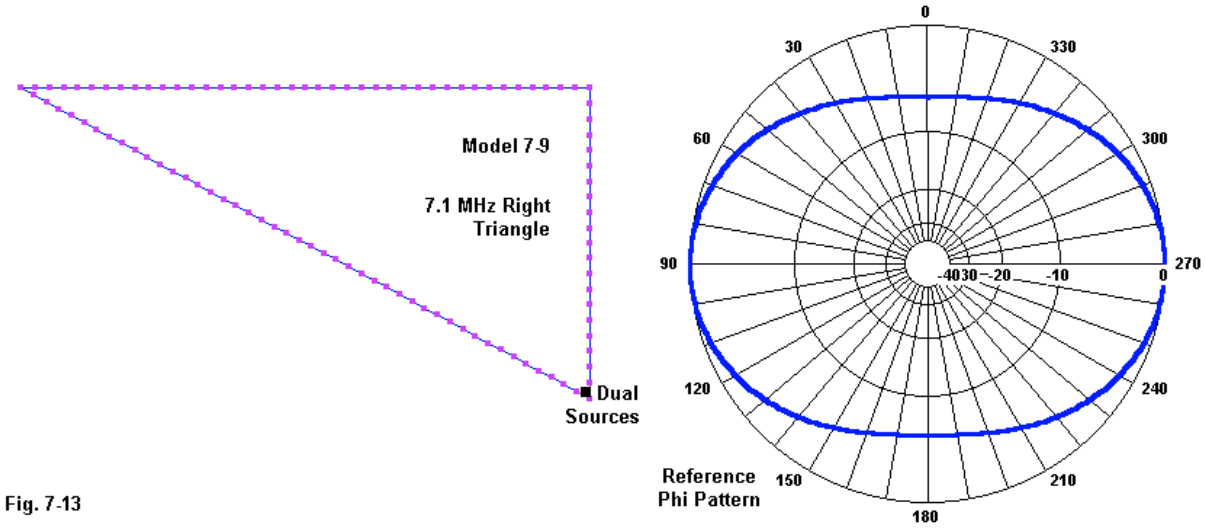

Fig. 7-13

```
EX 0 3 45 00 1 0
EX 0 1 1 0 1 0
```

The EX0 entries place a source on adjacent segments, a common set-up for sources that technically belong exactly on a point in the model's geometry. The series sum of the two source values provides a very close approximation of the actual source impedance on the point.

Using the NEC-2 reports, the two sources return 20.8 + j6.6 Ω and 20.3 + j6.5 Ω. The sum is 41.1 + j13.1 Ω. However, the key fact is the slight difference between the two values. Because the two wires leading to (or from) the source(s) have different lengths and depart the sources at different angles relative to the third wire, the mutual interactions among the segments will always yield different source impedances on the corner segments. No segmentation density (large or small) will yield identical source impedances on the corner source segments. Using indirect current sources (a subject for a future chapter), the differential and the individual values will vary from the values obtained from using standard voltage (EX0) sources. In this case, the values obtained provide reasonable approximations for general work, but are not of the precision required for many modeling tasks.

Core-Related Limitations

The core itself sets some limitations that range from fundamental to procedural. We shall sample one from each end of the spectrum on the premise that a complete catalog is not likely to fit into a single chapter.

Both the NEC-2 and NEC-4 manuals clearly note that the algorithm used to calculate current takes into account only axial currents, that is, currents along the centerline of the wire segment.

One consequence of this restriction is that so-called "boom effects" upon the elements that they support at right angles will not show up in the output reports. Boom effects are real, and have been calculated for VHF and UHF through-boom insulated elements as well as for elements that make direct contact with conductive booms. We can sample the absence of these effects with a series of 3-element Yagis designed the 144-148-MHz range. Indeed, we shall look at the Yagis outline in **Fig. 7-14**.

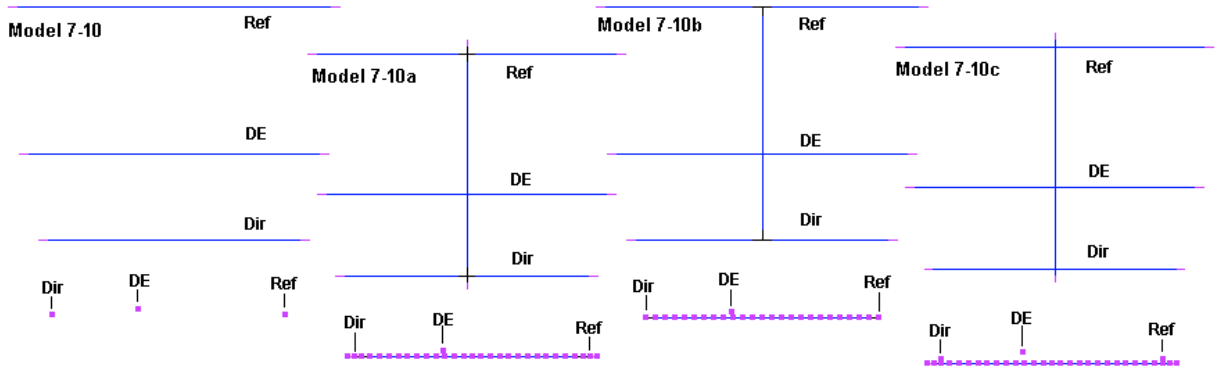

Fig. 7-14

Model *7-10.nec* uses the normal method of modeling a parasitic beam, that is, without modeling the boom. Such models presume that the elements use a non-conductive boom or are at least well insulated and isolated from a conductive boom. The elements have radii of 0.00635 m or 0.25".

```
CM 146 MHz Yagi: no boom, split parasitic elements
CE
GW 1 17 0. -.519684 0. 0. 0. 0. .00635
GW 2 17 0. 0. 0. 0. .519684 0. .00635
GW 3 33 .45974 -.48641 .0254 .45974 .48641 .0254 .00635
GW 4 14 .72644 -.42672 0. .72644 0. 0. .00635
GW 5 14 .72644 0. 0. .72644 .42672 0. .00635
GE 0
LD 5 0 0 0 2.5E+07
FR 0 3 0 0 144 2
```

In anticipation of models to follow, the parasitic elements are composed of two halves. The driven element is a single GW entry, but elevated slightly above the plane of the other elements, since we shall be adding a boom in subsequent variations. Since this model and the ones to follow press no core limitations likely to show warning or error flags, both NEC-2 and NEC-4 give us essentially the same results. The following table provides samples at 144, 146, and 148 MHz for both cores.

Core	Frequency MHz	Free-Space Gain dBi	180° Front-Back Ratio dB	Source Impedance R +/- jX Ω	50-Ω SWR
NEC-2	144	7.04	20.02	52.4 - j7.3	1.16
	146	7.14	23.49	49.7 - j0.1	1.01
	148	7.31	26.42	46.0 + j8.3	1.21

NEC-4	144	7.04	19.85	52.6 - j7.7	1.17
	146	7.14	23.26	49.9 - j0.6	1.01
	148	7.30	26.32	46.3 + j7.8	1.20

The slight but systematic offset of one set of values from the other has its likely source in the fact that the high segmentation density combined with the relatively fat elements presses NEC-2 a bit, since the segment-length-to-radius ratio is less than 8:1. Nonetheless, the differential is too minor to call for invoking the EK command in NEC-2. **Fig. 7-15** shows free-space E-plane (phi) patterns at the sampled frequencies.

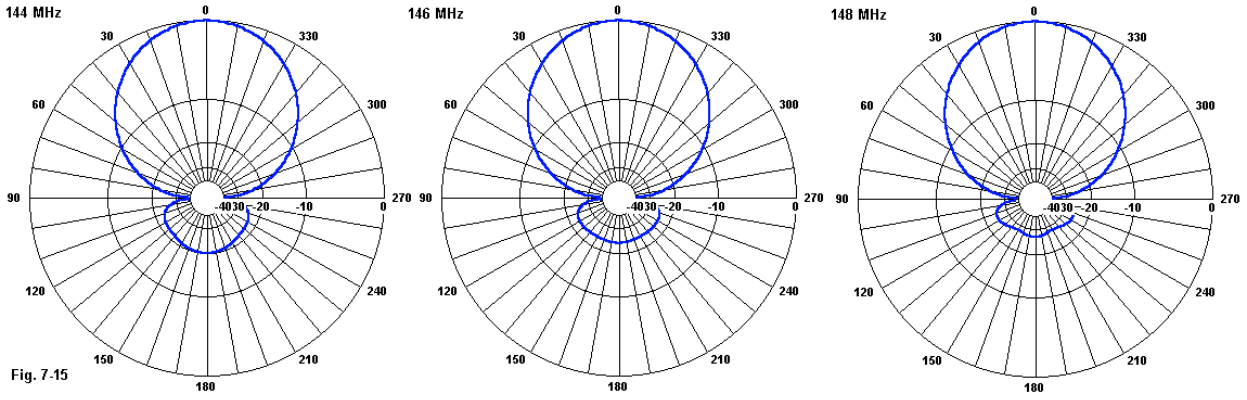

Fig. 7-15

Open model *7-10a.nec*. This version of the array adds a boom. Due to the weakness of NEC with angular junctions of wires having dissimilar diameters, the boom radius is the same as that of the elements: 0.25". In addition to a section of boom that connects the parasitic reflector and the parasitic director, the model places short extensions aft of the reflector and forward of the director to reflect actual building practices. The control commands remain unaltered relative to model 7-10.

```
GW 1 17 0. -.519684 0. 0. 0. 0. .00635
GW 2 17 0. 0. 0. 0. .519684 0. .00635
GW 3 33 .45974 -.48641 .0254 .45974 .48641 .0254 .00635
GW 4 14 .72644 -.42672 0. .72644 0. 0. .00635
GW 5 14 .72644 0. 0. .72644 .42672 0. .00635
GW 6 24 0. 0. 0. .72644 0. 0. .00635
GW 7 2 -.04318 0. 0. 0. 0. 0. .00635
GW 8 2 .72644 0. 0. .76962 0. 0. .00635
```

Open model *7-10b.nec*. This version is identical to the preceding model, except that it removes the boom extensions. All control commands remain unchanged from those used in models 7-10 and 7-10a, including the 3-step frequency (FR) command.

```
GW 1 17 0. -.519684 0. 0. 0. 0. .00635
GW 2 17 0. 0. 0. 0. .519684 0. .00635
GW 3 33 .45974 -.48641 .0254 .45974 .48641 .0254 .00635
GW 4 14 .72644 -.42672 0. .72644 0. 0. .00635
GW 5 14 .72644 0. 0. .72644 .42672 0. .00635
GW 6 24 0. 0. 0. .72644 0. 0. .00635
```

Finally, open model *7-10c.nec*. This last version of the model places the elements in very close proximity to the boom without actual contact. This model uses the boom extensions that make the overall boom longer than the distance from the reflector to the director.

```
GW 1 17 0. -.519684 0. 0. 0. 0. .00635
GW 2 17 0. 0. 0. 0. .519684 0. .00635
GW 3 33 .45974 -.48641 .0254 .45974 .48641 .0254 .00635
GW 4 14 .72644 -.42672 0. .72644 0. 0. .00635
GW 5 14 .72644 0. 0. .72644 .42672 0. .00635
GW 6 24 0. 0. -.012954 .72644 0. -.012954 .00635
GW 7 2 -.04318 0. -.012954 0. 0. -.012954 .00635
GW 8 2 .72644 0. -.012954 .76962 0. -.012954 .00635
```

Run all three additional versions of the model and you will obtain the very same table of output reports recorded for model 7-10. If you examine the table of currents in the NEC output report, you will understand in part why the output reports do not change with the various booms in place. The following NEC-4 sample comes from model 7-1a. Absolute segments 17 and 18 represent the center region of the reflector. The current magnitude on the segments on each side of center is 6.9E-3. Absolute segments 96 and 121 are the boom segments that connect to the reflector junction. Their current magnitudes are 1.8E-17 and 1.6E-18, respectively. These current levels are too small to play a role in any of the performance reports. The NEC-4 values are also far smaller than found in the boom-to-element region in actual antennas.

```
SEG.  TAG    COORD. OF SEG. CENTER   SEG.             - - - CURRENT (AMPS) - - -
NO.   NO.    X         Y        Z     LENGTH      REAL          IMAG.        MAG.        PHASE

17    1   0.0000  -0.0073   0.0000  0.01468   -1.8320E-03   5.6873E-03   5.9751E-03  107.855
18    2   0.0000   0.0073   0.0000  0.01468   -1.8320E-03   5.6873E-03   5.9751E-03  107.855

96    6   0.0073   0.0000   0.0000  0.01454   -1.7524E-17  -1.3737E-18   1.7578E-17 -175.518
121   7  -0.0052   0.0000   0.0000  0.01037    3.9832E-19  -1.5507E-18   1.6010E-18  -75.594
```

Far distant from the fundamental core formulations that control the results for model 7-10 are the strictly procedural conventions and rules that yield what we derive from model *7-11.nec*. For many modeling purposes, especially those involving only a single source, the order in which we model the wires of an antenna makes no difference to the reported gain or source impedance. However, when we have multiple sources and wish to intentionally feed an array either in-phase or out-of-phase, the order of modeling wires and the direction of those wires on the Cartesian coordinate system can make a considerable difference.

```
GW 1 11 -0.1939 0 0 0 0 -0.1939 0.001
GW 2 11 0 0 -0.1939 0.1939 0 0 0.001
GW 3 11 0.1939 0 0 0 0 0.1939 0.001
GW 4 11 0 0 0.1939 -0.1939 0 0 0.001
GS 0 0 1
GE 0
EX 0 1 11 0 1 0
EX 0 2 1 0 1 0
EX 0 3 11 0 1 0
EX 0 4 1 0 1 0
```

One convention that many modelers follow when modeling a 1-λ loop is to let end 2 of each preceding wire become end 1 of the next wire. The result is a continuous loop, in this case

modeled counterclockwise. The loop forms a diamond, and the feedpoints are top and bottom. To feed the loop at these positions, we create dual sources, for a total of 4 source segments. The final model, 7-11, has the appearance of the left part of **Fig. 7-16**. Unfortunately, the pattern is the version in the center of the figure.

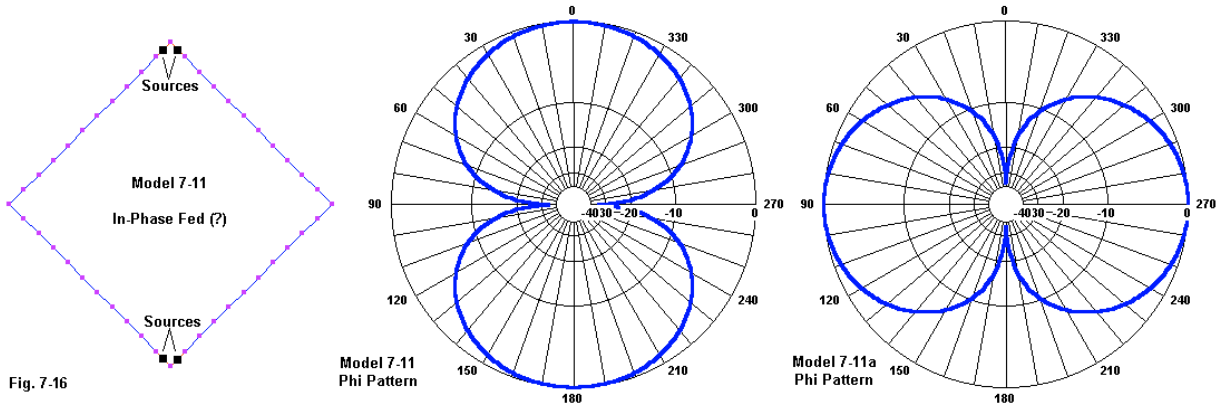

The pattern is off the edges of the loop, indicating that the attempt at in-phase feeding has failed. Rather, the top and bottom halves of the diamond are fed out-of-phase, resulting in gain off the edges of the loop, rather than broadside to it. Compare the GW entries of model 7-11 to those of model *7-11a.nec*.

```
GW 1 11 -0.1939 0 0 0 0 -0.1939 0.001
GW 2 11 0 0 -0.1939 0.1939 0 0 0.001
GW 3 11 -0.1939 0 0 0 0 0.1939 0.001
GW 4 11 0 0 0.1939 0.1939 0 0 0.001
```

Run this version of the model to obtain the correct broadside pattern shown at the right in **Fig. 7-16**. You may also compare the 4 source impedance reports for each model: 300 - j1511 Ω for the mis-modeled version and 34 + j1 Ω for the correctly modeled version.

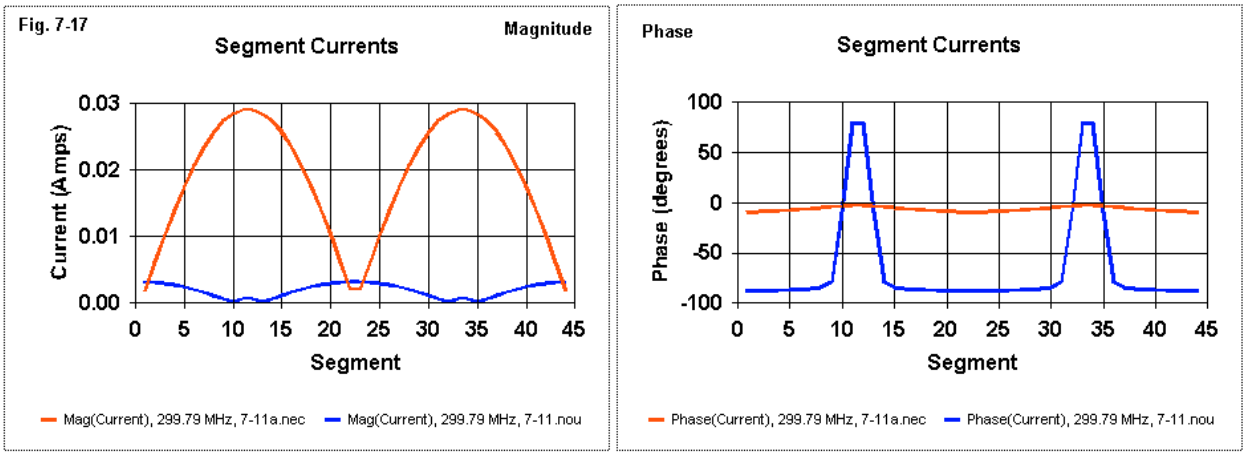

The order of entry also makes a difference to the registration of current magnitudes and phase angles. As suggested by **Fig. 7-17**, in a continuous sweep of the current values, both the NEC output report tables and rectangular plot functions within the program make use of the absolute

segment numbers. The red lines (the lines with higher average values) for model 7-11a count from left to right, first the lower half of the diamond, then the upper half. The blue lines (the lines with lower average values, despite the spikes in the phase graph), from model 7-11 count left to right for the lower half and then right to left for the upper half. In many models, the reversal of direction--reflecting a reversal of coordinate entry--may result in a phase angle that is 180° reversed from a value obtained by an external calculation. Wherever you need the current magnitude and phase to coincide with normal calculations--which normally presume that all elements run in the same direction--you must handle the wire entry with great care.

Summing Up

In these exercises, we have taken a highly compressed look at many--but not all--of the ways in which we can create geometry flaws in our models. The first step in the process involved finding the tools at hand to detect flaws, and we discovered three types: symptoms revealed in output reports, NEC output report error and warning flags, and Necvu error checking routines within the implementation programs. Although these checking systems will turn up many of the faults we might slip into models, they do not cover all of them. The average gain test proves to be an invaluable but not flawless test for detecting conditions that press the limits of the core and of correcting at least some of the gain and source resistance values.

Junctions of wires having dissimilar diameters provide interesting models that prove unreliable unless supplemented by outside standards. In some cases, such as folded dipoles, we may have a means of calculating the anticipated result. However, for many other cases, only experimental results or the use of a modeling core that does not suffer shortcomings in precisely the same places as NEC will reveal the reliability of a model. Even the convergence test, the second necessary but not sufficient condition of model adequacy, fails to reveal the adequacy of some models with very specific geometric shapes.

The NEC core presents limitations on what we may effectively model, and some phenomena may not model at all due to the fundamental algorithms that NEC employs. At the opposite extreme, the conventions required to record and organize the geometry of the model require careful entry of the structure if we wish to achieve a complete and organized progression of output data. For simple goals, we may overlook some of the entry constraints--a temptation toward bad habits that may beset us when we need everything that the modeling program can tell us, and we need it in good order.

Part B
Far-Field and General Control Commands

1. The Control Command Input Entries or "Cards" introduced in this Part:

Command	*Command Name*	*Notes*
EN	End of Run	
EX*	Structure Excitation	
FR	Set Frequencies	
GD	Additional Ground Parameters	
GN	Ground Parameters	Form differs between NEC-2/NEC-4
LD*	Impedance Loading	
NT	Non-Radiating Networks	
NX	Next Structure	Conditions differ slightly in NEC-2/-4
RP*	Radiation Pattern	Form differs between NEC-2/NEC-4
TL	Transmission Line	
XQ	Execute	NEC-4 only

A star (*) indicate that in this Part, the command will receive partial coverage as may be relevant to far-field analysis. The command will receive further coverage in Part C.

2. The Plan:

The complete set of control commands is simply too large for us to master in a single set of chapters. As well, many commands have variable structures according to what use we wish to make of them. Mastering the control commands may benefit from seeing how they work with respect to one of the primary overall uses to which we put NEC: far-field analysis. This form of analysis provides some of the most fundamental data sets about the performance of an antenna or antenna system under analysis. As well, it involves many of the control commands that refine the geometry structures set up in Part A. The restriction that far-field analysis places on us is to allow only partial coverage of certain control commands, specifically excitation (EX), loading (LD), and radiation pattern requests (RP). Part C will complete our coverage of these commands.

The fundamental output of the NEC core run is a long table of results. The first step in the process of mastering control commands is to understand both the table contents and how commands produce the tables. Some commands force execution of the calculations, while others require a separate execution command (XQ). Still other commands either separate multiple runs in a single model (NX) or simply mark the end of a run (EN).

The request for a radiation pattern (RP) is basic to far-field analysis, but the command has so much versatility that we shall confine ourselves only to far-field pattern functions. Mastering XNDA, and obtaining an orderly set of output pattern data for various antenna types requires careful structuring of the command. We shall sample other uses of RP in Part C.

Far-field analysis normally requires that we provide the antenna with an "internal" excitation

source (EX0). Incident plane wave excitation of the structure appears in Part C. However, we can provide not only a direct voltage source, but as well, an indirect current source. In conjunction with the excitation, we must also provide a test frequency or set of frequencies (FR). The latter "frequency sweep" option has both linear and multiplicative options to consider.

Since not all far-field analyses involve the free-space environment, we must take a long look at the ground options available to use (GN, GD). Not only do we need to examine the range of options and how well each suits a given modeling task, but we must also consider the differences in the NEC-2 and NEC-4 ways of setting up grounds, especially multiple ground areas.

NEC provides a series of non-radiating additions to models, that is, equation-based constructs that do not themselves enter into the wire structure, but which modify the performance of the antenna in accord with the terms of the addition. We shall begin with transmission lines (TL), a special form of network that allows the simulation of lossless lines. We shall expand our study to include the construction and behavior of lines constructed--where possible--from wires that do enter into the overall wire structure. We shall even find a way to include (in NEC-4) the transmission line velocity factor into the wire line construct.

An additional non-radiating facility in NEC is the impedance load, either lumped in specifically designated wire segments or distributed over a full wire in terms of impedance per unit measure. We shall explore the former, that is, spot loads (LD0 and LD1). These loads include both series and parallel R-L-C circuits. In addition, we may use LD4, R-X complex impedance loads. We shall learn which loads are frequency nimble and which are frequency static--and why the distinction is significant.

A TL line is a special form of network (NT). We shall examine the basic structure of the NT command and sample some the applications of 2-port admittance parameter networks in simulating common passive circuitry associated with antennas. We shall also examine an alternative simulation technique that is frequency nimble.

Obviously, the plan to deal in this Part only with commands fitting far-field analysis, while saving others for Part C, is imperfect. Nevertheless, the plan is serviceable. More significantly, it will provide us with an improved mastery of the most basic and most used control commands in NEC.

8.
Output Tables and Graphics

***Objectives**: The first step in mastering the control commands is to become familiar with the structure and content of the NEC output file contents under various command conditions. Then, we may proceed to understand how implementing programs translate the tabular calculation results into a large variety of graphic presentations to enhance data comprehension.*

Both NEC-2 and NEC-4 produce the results of their calculations in the form of a single large output file that reflects the Fortran origins of the cores. Although implementing programs provide the user with numerous easy ways of viewing the data through graphics, all graphics derive their data from the output file. Hence, the NEC output file is the proper starting point for exploring the function of the control commands. In fact, very few of the commands cause the core to execute calculations beyond the set-up analysis of the structure geometry.

Our first stop on the expedition through control commands will be the output file and all of its tabular data. The file uses nothing more than ASCII coding, with spaces between data columns. NSI software stores the output file using the same file name that you assign to the model itself. Whereas the model description uses the extension .NEC, the output file uses the extension .NOU. (Other implementing programs may assign different extensions to the output file, and some may not save the file at all after its use as the foundation for the generation of some specific tables and graphics.)

If we wish to obtain calculations beyond the structure analysis, that is, if we wish the core to process the interaction matrix and generate current values for the wire segments, we must provide the model with at least one "execution" command. As we shall discover, some output requests automatically place the core into execution mode, while others need a supplementary command. A few output requests require special treatment if the frequency command (FR) specifies more than 1 frequency.

Once we become familiar with the output file contents under various conditions, we can then turn to the interface between the output file and some of the ways implementing programs allow us to examine and present data. At the bottom line, implementing programs, such as NEC-Win Pro and GNEC, can provide an array of graphics covering the most used data. But, there will always be a need for us to sometimes transfer partial output data tables to other software in order to generate specific graphics for special analyses or presentations.

Output Files and the Execution Commands

Our first work involves looking at the NEC output file. This file is always accessible in GNEC and NEC-Win Pro via the list of tabular outputs. Those outputs also provide direct access to portions of the file data that may be of special interest. A few, such as the impedance and VSWR table

option perform additional calculations and reformat the information for easier viewing. However, the original information and format are always available.

To examine the table, we need only the simplest of models. Therefore, we shall return to a fundamental free-space dipole at the test frequency of 299.7925 MHz. Open model *8-1.nec*. The dipole will have the shape shown in **Fig. 8-1**, but it will not yet produce the pattern shown at the right of the graphic.

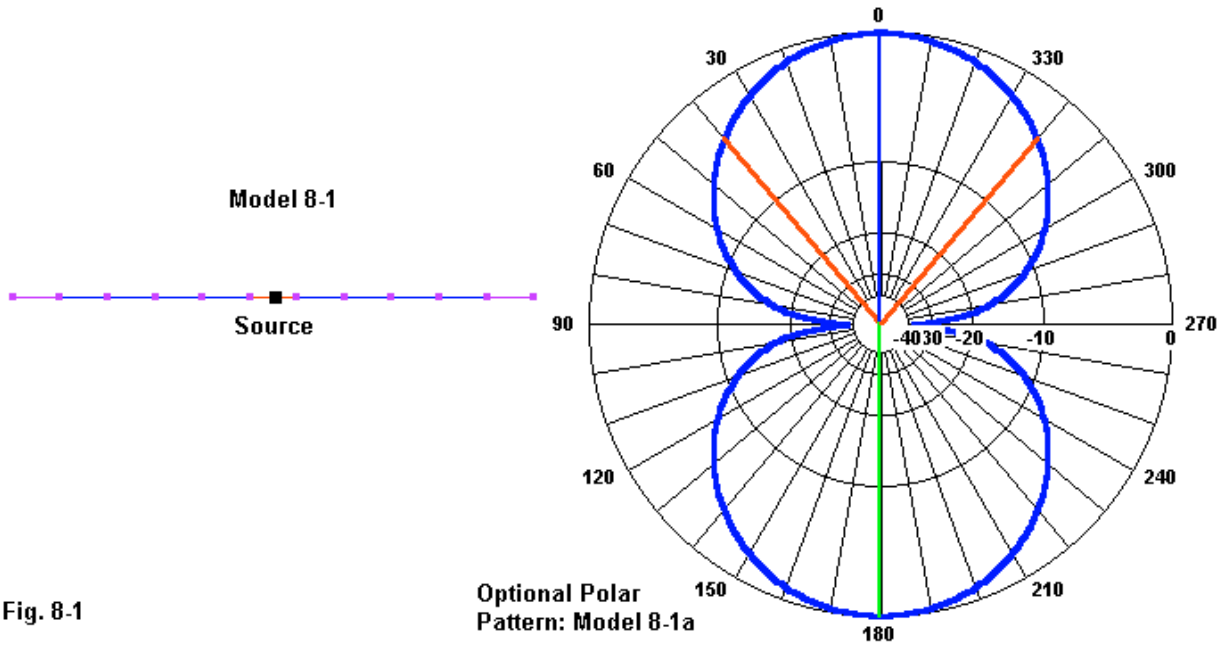

Fig. 8-1

```
CM No executable command
CE
GW 1 11 0 -.2375 0 0 .2375 0 .001
GE
FR 0 1 0 0 299.7925 1
EX 0 1 6 00 1 0
EN
```

The first control command to notice is EN, the end-of-run command. It simply signals the completion of the model and belongs at the end of each model, even if the core will execute without it. In addition to the geometry, the model also provides the antenna with a source (EX) and a frequency (FR). Run the model and examine the output file.

```
- - - - COMMENTS - - - -
- - - STRUCTURE SPECIFICATION - - -
- - - - SEGMENTATION DATA - - - -
RUN TIME =     0.160
```

The extracted list provides the headings for the output report, as the present model generates it. All NEC does is to analyze the structure and the segmentation that emerges, nothing more. However, this step is useful, since we may use the data to evaluate a model prior to setting NEC

into a time consuming full calculation run. The Necvu error checking routines are fully functional with just this much information.

For a more familiar form of the model, open model *8-1a.nec*.

```
CM Single RP command
CE
GW 1 11 0 -.2375 0 0 .2375 0 .001
GE
FR 0 1 0 0 299.7925 1
EX 0 1 6 00 1 0
RP 0 1 361 1000 90 0 1.00000 1.00000
EN
```

The only addition to the model is the request for a single phi pattern. However, if we now run the model, the output report suddenly becomes much longer, as suggested by the following list of data headings. Although we shall later take a longer look at the data under most of the headings as we develop the control command functions, you may wish to begin familiarizing yourself with the column headings and the format that NEC uses for individual entries. A number of headings have no data for this simple model. However, you may wish to find the antenna source impedance in the listing for antenna input parameters. Under the radiation pattern heading, you may also wish to correlate the phi plot in **Fig. 8-1** to the data in terms of the headings for maximum and minimum gain.

```
- - - - COMMENTS - - - -
- - - STRUCTURE SPECIFICATION - - -
- - - - SEGMENTATION DATA - - - -
- - - - - - - FREQUENCY - - - - - -
- - - STRUCTURE IMPEDANCE LOADING - - -
- - - ANTENNA ENVIRONMENT - - -
- - - MATRIX TIMING - - -
- - - ANTENNA INPUT PARAMETERS - - -
- - - CURRENTS AND LOCATION - - -
- - - POWER BUDGET - - -
- - - RADIATION PATTERNS - - -
RUN TIME =     0.330
```

The output report headings provide the data categories developed by NEC for virtually any far-field request. *The RP command automatically sets the core into execution mode*.

Suppose that we wish the core to execute its calculations, but do not wish to add a pattern request. Open model *8-1b.nec*,

```
CM XQ command
CE
GW 1 11 0 -.2375 0 0 .2375 0 .001
GE
FR 0 1 0 0 299.7925 1
EX 0 1 6 00 1 0
XQ
EN
```

The model down through the EX command will not set the core into execution mode, that is, cause it to stop reading data and start performing calculations. Since we only wish the core to calculate the impedances and currents, along with data immediately derived from them, we must use the XQ or "execute" command. Run this model and examine the output file. The file contains all of the information also contained in the file for model 8-1a except for the radiation pattern data. You may compare the two files to confirm that the information is identical.

Normally, modelers use the XQ command as shown, with no following numerical entries. In fact, the command has a single I1 entry that defaults to zero if there is no entry. If I1 = 0, then the command makes no pattern request. However, we may also specify values of 1, 2, or 3 for the I1 position. Each of the entries produces a theta-based radiation pattern where theta varies from 0° (zenith) to 90° (horizon). If I1 = 1, then the pattern is in the XZ plane, that is, phi = 0°. If I1 = 2, then the pattern is in the YZ plane, that is, phi = 90°. If I1 = 3, then the core produces both patterns. All patterns use 1° increments.

In most instances, you will wish to exert more specific control over the pattern produced by using an RP command. However, as an experiment, open model *8-1c.nec* and run the model.

```
CM XQ command
CE
GW 1 11 0 -.2375 0 0 .2375 0 .001
GE
FR 0 1 0 0 299.7925 1
EX 0 1 6 00 1 0
XQ 3
EN
```

In the output report, note the re-appearance of the "radiation patterns" category. Within the category, you will find that the two plots follow each other without separation. You will not be able to view the data graphically, because NSI software keys on the RP command to allow reading of the radiation pattern data for polar and rectangular plots.

When NEC was strictly a mainframe Fortran program, it initially required the usual submission to a central computer for running when time was available according to whatever queuing priorities might have applied. Compacting multiple models into a single model file seemed far more attractive than it is today, when the program runs on an individual PC. (It is unclear whether the widespread use of administratively controlled computers with present-day Windows operating systems within various companies and institutions will cause a reversion to the older practice.) To accomplish the desired run of multiple models in a single model file, we may use the NX or "next structure" command between the models within the input file.

NX has no numerical entries, but the conditions of use differ slightly between NEC-2 and NEC-4. In NEC-2, NX must be followed by a comment entry, either CM or CE. As the sample file will show, we may use text on a CE line, although as a visual marker, we usually leave the CE line empty. In contrast, NEC-4 may use the NX command and follow it wither by a comment entry or by the geometry structure entry, that is, by any of the commands that we met in Part A. So that the sample will run on both cores, it follows the NEC-2 convention.

Open model *8-2.nec* and identify the two models within it.

```
CM Multiple models
CE First model structure
GW 1 11 0 -.2375 0 0 .2375 0 .001
GE
FR 0 1 0 0 299.7925 1
EX 0 1 6 00 1 0
RP 0 1 361 1000 90 0 1.00000 1.00000
NX
CE Second model structure
GW 1 11 0 0 -.2375 0 0 .2375 .001
GE
FR 0 1 0 0 299.7925 1
EX 0 1 6 00 1 0
RP 0 1 361 1000 90 0 1.00000 1.00000
EN
```

The sample files contains, first, the "horizontal" dipole with a single phi pattern request. The second model is the same dipole, oriented "vertically." (The terms "horizontal" and "vertical" are in quotes because the antenna environment is free-space. The antennas are only horizontal or vertical by reference to the conventions governing the X, Y, and Z planes of the NEC Cartesian coordinate system.) Run the model and view the resulting patterns using the polar plot facility. The figure-8 for the E-plane pattern and the circle for the H-plane pattern should be very familiar by now. More importantly, examine the NEC output file.

Note that the output file consists of 2 complete and independent core runs. Each run begins at the beginning with a listing of the core-run parameters. The parameter values may differ depending upon whether you are using an "auto-dma" or auto-dimensioning version of the core or a version for which you have specified parameter limits. Each run provides the full list of data applicable to the model for which the core makes its calculations. The only combined function is the core-run time value, which covers both models. As a result, you must provide each model within the combined input file with its own execution command, whether in the form of an automatically executing command like RP or a "forced" execution command like XQ. Otherwise, you may end up with only structure and segmentation information on one of the models.

RP and XQ are not the only control commands that cause the core program to begin its calculations. Let's leap ahead in our coverage of control commands to take a brief look at how near-field requests operate. The relevant commands are NE, a request near electric fields, and NH, a request for near magnetic fields. We may use either command alone or--what is most usual--as a pair. Open model *8-3.nec*. We shall explore the contents of the entries in Part C.

```
CM NE/NH single frequency
CE
GW 1 11 0 -.2375 0 0 .2375 0 .001
GE
FR 0 1 0 0 299.7925 1
EX 0 1 6 00 1 0
NE 0 11 1 1 -5.0 0 0.0 1.0 1.0 1.0
NH 0 11 1 1 -5.0 0 0.0 1.0 1.0 1.0
EN
```

Run the file and examine the NEC output report heading.

```
- - - NEAR ELECTRIC FIELDS - - -
- - - NEAR MAGNETIC FIELDS - - -
```

Following the power budget, we do not find a heading for radiation patterns, because we did not request them. Instead, we find data on near electric and magnetic fields, indicating that the near-field commands are--like the RP command--self-executing. Let's also store the fact that the FR command contains only a single frequency. Now open model *8-3a.nec*.

```
CM NE/NH 3 frequencies
CE
GW 1 11 0 -.2375 0 0 .2375 0 .001
GE
FR 0 3 0 0 290 10
EX 0 1 6 00 1 0
NE 0 11 1 1 -5.0 0 0.0 1.0 1.0 1.0
NH 0 11 1 1 -5.0 0 0.0 1.0 1.0 1.0
EN
```

The only difference between this model and the preceding one is the request for a sweep of 3 frequencies. Run the model and examine the end of the NEC output file. There is no listing of either field, but only a notice.

```
WHEN MULTIPLE FREQUENCIES ARE REQUESTED, ONLY ONE NEAR FIELD CARD CAN
BE USED - LAST CARD READ IS USED
```

The last card is EN, so no near-field calculations occur. Let's reduce the request to a single near field, arbitrarily, the electric field. Open model *8-3b.nec*.

```
CM NE only 3 frequencies
CE
GW 1 11 0 -.2375 0 0 .2375 0 .001
GE
FR 0 3 0 0 290 10
EX 0 1 6 00 1 0
NE 0 11 1 1 -5.0 0 0.0 1.0 1.0 1.0
EN
```

The frequency sweep remains, but for only one near-field request. Run the model and examine the output report. You will find no electric field data at all. The existence of a multiple frequency request requires an external execution command, as found in model *8-3c.nec*.

```
CM NE/NH + XQ 3 frequencies
CE
GW 1 11 0 -.2375 0 0 .2375 0 .001
GE
EX 0 1 6 00 1 0
FR 0 3 0 0 290 10
NE 0 11 1 1 -5.0 0 0.0 1.0 1.0 1.0
XQ
NH 0 11 1 1 -5.0 0 0.0 1.0 1.0 1.0
XQ
EN
```

The model restores the dual request and places an XQ command after each request. Surely the model will give us near-field data for all three frequencies. The output report will tell us in short order.

```
- - - - - - FREQUENCY - - - - - -
- - - STRUCTURE IMPEDANCE LOADING - - -
- - - ANTENNA ENVIRONMENT - - -
- - - MATRIX TIMING - - -
- - - ANTENNA INPUT PARAMETERS - - -
- - - CURRENTS AND LOCATION - - -
- - - POWER BUDGET - - -
- - - NEAR ELECTRIC FIELDS - - -
```

We find for each individual frequency a listing of all data headings (and their data) for the categories shown. However, only after the last set of electric near fields for 310 MHz do we find the following heading:

```
- - - NEAR MAGNETIC FIELDS - - -
```

The missing magnetic field reports result from the fact that frequency sweeps form a loop. Essentially, after any execution command, the loop runs its course and remains at its last value for any subsequent execution commands. Hence, after executing calculations for the set of 3 near electric fields requested, the magnetic fields provide data only for the last frequency in the loop. To resolve the problem is simple. Open model *8-3d.nec*.

```
CM NE/NH + XQ 3 frequencies
CE
GW 1 11 0 -.2375 0 0 .2375 0 .001
GE
EX 0 1 6 00 1 0
FR 0 3 0 0 290 10
NE 0 11 1 1 -5.0 0 0.0 1.0 1.0 1.0
XQ
FR 0 3 0 0 290 10
NH 0 11 1 1 -5.0 0 0.0 1.0 1.0 1.0
XQ
EN
```

To create the missing reports, we need only insert a copy of the FR entry prior to each of the near-field requests. You may confirm the presence of all data via the output report. At this point, your familiarity with the whole output file may be great enough to let you use the short-cut of requesting the near-field data (only) from the list of specific tabular data provided in the implementing program.

NEC-4 introduces two additional near-field requests: LE and LH, that is, near fields along a line. The output requests operate in the same manner and with the same restrictions as the NE and NH commands.

Frequency sweeping limits the RP command in a somewhat different manner than the near-field requests. Open model *8-4.nec*.

```
CM Multiple RPs and frequencies
CE
GW 1 11 0 -.2375 0 0 .2375 0 .001
GE
EX 0 1 6 00 1 0
FR 0 3 0 0 200 100
RP 0 1 361 1000 90 0 1.00000 1.00000
RP 0 361 1 1000 -90 0 1.00000 1.00000
EN
```

In this model, we have two radiation pattern requests and a request for 3 frequencies. If you examine the output file, you will find all 3 patterns tables for the first RP (phi) request, but only a single table at the highest frequency for the second RP (theta) request. Moreover, we did not receive the patterns shown in **Fig. 8-2**, which shows composites of the 3 phi and 3 theta patterns.

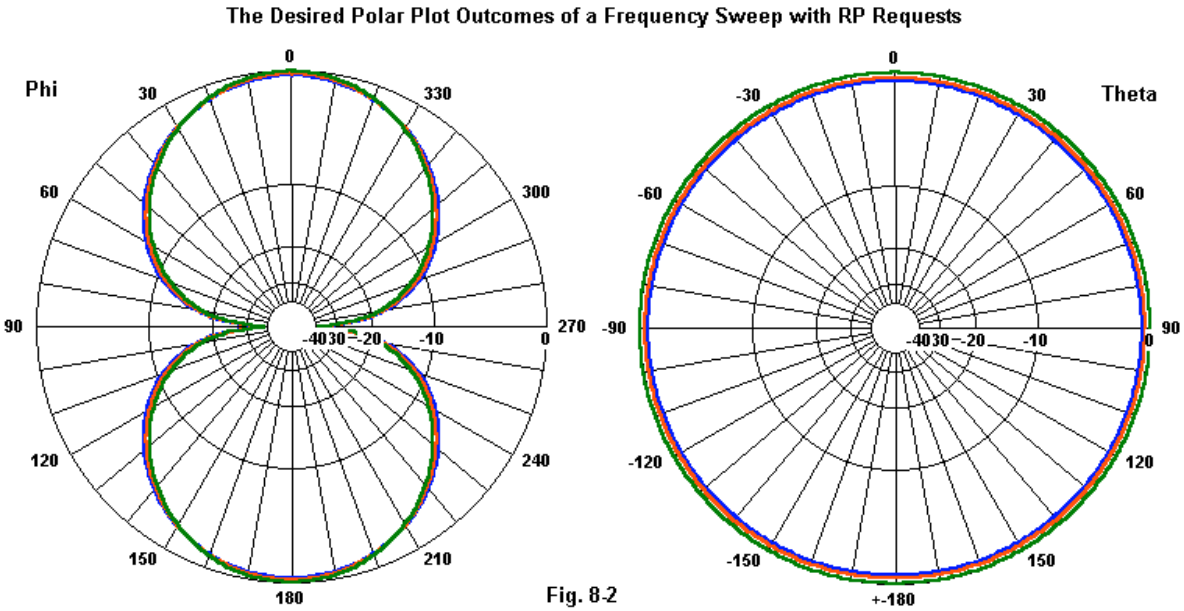

Fig. 8-2

RP does not require an XQ command to run a sweep, but it is otherwise subject to the FR loop conventions. To resolve the problem and obtain the entire set of tables, we need to revise the model. Open model *8-4a.nec*.

```
CM Multiple RPs and frequencies
CE
GW 1 11 0 -.2375 0 0 .2375 0 .001
GE
EX 0 1 6 00 1 0
FR 0 3 0 0 250 50
RP 0 1 361 1000 90 0 1.00000 1.00000
FR 0 3 0 0 200 100
RP 0 361 1 1000 -90 0 1.00000 1.00000
EN
```

Repeating the FR command prior to each RP request produces all of the desired radiation pattern

tables. You may confirm this from the output report or take a short cut and look at the available polar plots for the model. Model 8-4 produced 4 patterns, while 8-4a yielded 6.

We have not looked at all of the commands that require care when using multiple frequency requests or that require an XQ or execution command. We shall alert you to such requirements as we examine each command in its proper place in this sequence. For now, we have surveyed enough output files to understand their overall structure. As well, we have learned the main self-executing commands and their restrictions. Finally, we have learned how to separate within a single file either whole models (with the NX command) or parts of modeling output requests that need special treatment.

Tabular and Other Methods of Viewing NEC Output Data

The NEC output report is the final arbiter of the results calculated by the core. However, it is a long, densely packed, and often repetitive document. The NEC manuals list a number of techniques for ordering operations to reduce the amount of re-calculation performed by the core. However, implementing software often provides easier ways of viewing the data, both tabularly and graphically.

Open model *8-5.nec*. The 6-element Yagi of the geometry section is in free space and requests a single phi pattern, but over 5 frequencies in a sweep, with the sweep centered at 300 MHz.

```
CM FR sweep rectangular plots
CM 6-element Yagi
CE
GW 1 21 0 0.2506 0 0 -0.2506 0 0.001
GW 2 21 0.1253 0.2472 0 0.1253 -0.2472 0 0.001
GW 3 21 0.1772 0.2312 0 0.1772 -0.2312 0 0.001
GW 4 21 0.3207 0.2246 0 0.3207 -0.2246 0 0.001
GW 5 21 0.4612 0.2246 0 0.4612 -0.2246 0 0.001
GW 6 21 0.6707 0.2162 0 0.6707 -0.2162 0 0.001
GS 0 0 1
GE 0
EX 0 2 11 0 1 0
FR 0 5 0 0 295 2.5
RP 0 1 361 1000 90 0 1 1
EN
```

Fig. 8-3 shows the outline of the antenna as well as a composite of the phi pattern produced for each of the swept frequencies. Indeed, the polar plot facility in NSI software permits a variety of plot styles. For example, the scale may be linear or log, and the patterns may be normalized to the plot maximum value or it may use maximum and minimum values set by the user. Like most polar plot facilities, there are a number of user options for colors, for line thickness and style, and the fonts used for the labels and titles. In addition, analytical data, such as the maximum gain, 3-dB beamwidth, and front-to-back ratio, are also available. Finally, you may select from 2 measures of front-to-back ratio and also opt for azimuth-elevation vs. phi-theta conventions of labeling the outer ring of the pattern. You may even import patterns from other models to composite with the pattern or patterns from the present model.

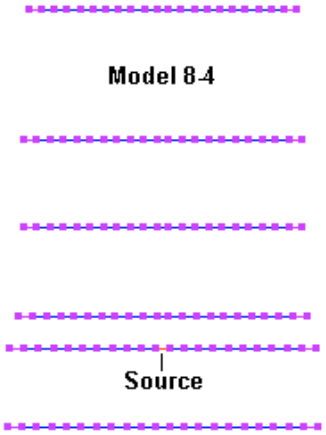

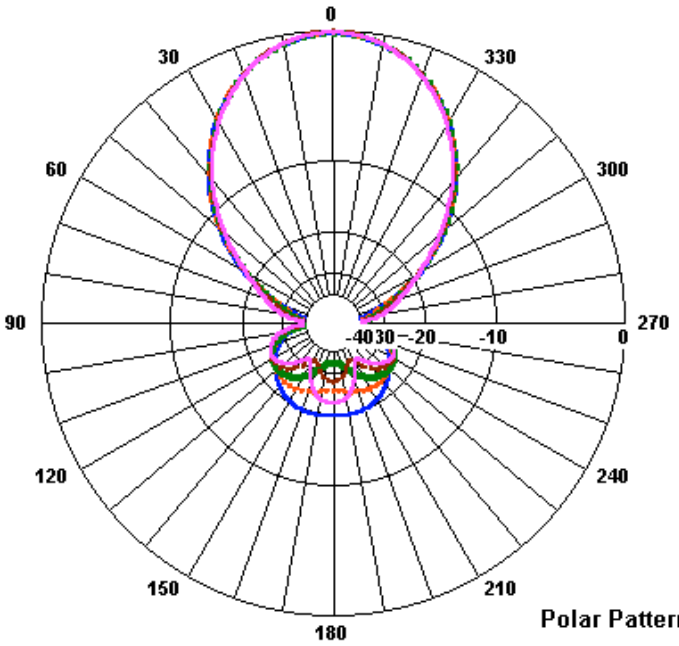

Fig. 8-3 Polar Patterns

The radiation pattern data is also available in rectangular format, as shown in **Fig. 8-4**. Note that the rectangular plot centers at 180 degrees. For presentation purposes, you might wish to reset the geometry so the maximum gain occurs on this heading.

Fig. 8-4

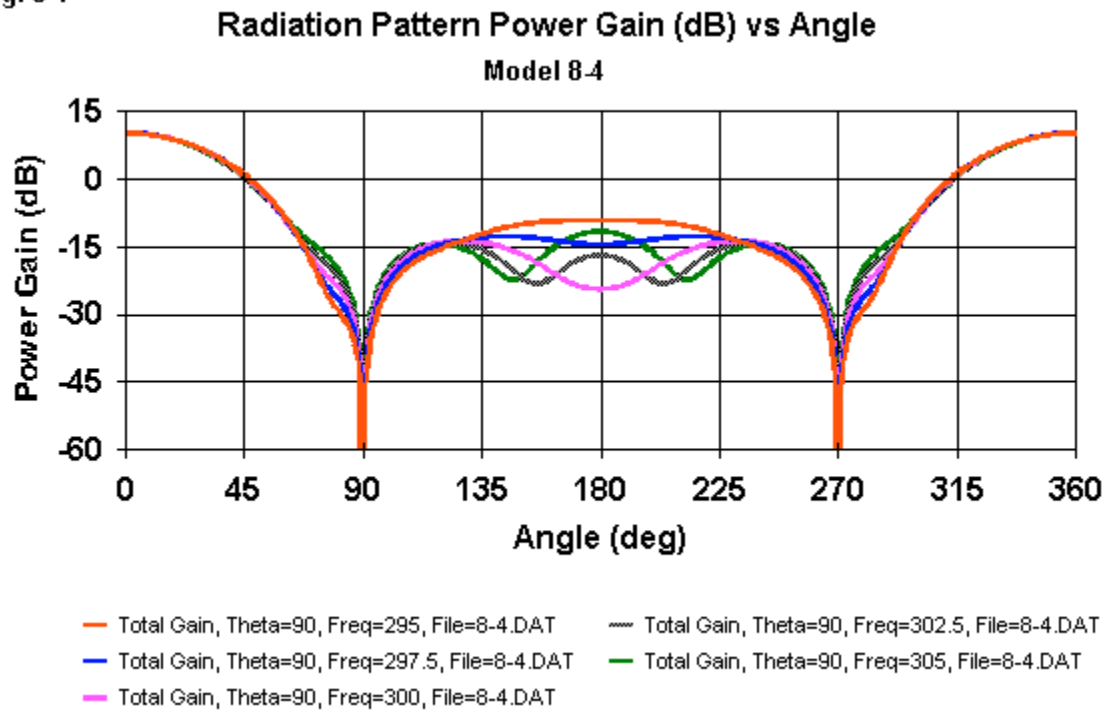

Current data is available in the main NEC output report or in the specific report listed under tabular data. The following extract from the output report shows the completeness of the data available--at least for the first few segments and at the lowest frequency swept.

```
                        - - - CURRENTS AND LOCATION - - -
SEG.  TAG    COORD. OF SEG. CENTER     SEG.            - - - CURRENT (AMPS) - - -
 NO.   NO.      X        Y        Z      LENGTH     REAL        IMAG.       MAG.        PHASE
    1    1   0.0000   0.2348   0.0000  0.02348  -3.2283E-04  1.2590E-03  1.2997E-03  104.382
    2    1   0.0000   0.2114   0.0000  0.02348  -8.3889E-04  3.1967E-03  3.3050E-03  104.704
    3    1   0.0000   0.1879   0.0000  0.02348  -1.3176E-03  4.9171E-03  5.0905E-03  105.001
    4    1   0.0000   0.1644   0.0000  0.02348  -1.7729E-03  6.4994E-03  6.7369E-03  105.258
    5    1   0.0000   0.1409   0.0000  0.02348  -2.1959E-03  7.9315E-03  8.2298E-03  105.475
    6    1   0.0000   0.1174   0.0000  0.02348  -2.5755E-03  9.1919E-03  9.5459E-03  105.653
    7    1   0.0000   0.0939   0.0000  0.02348  -2.9014E-03  1.0258E-02  1.0660E-02  105.793
    8    1   0.0000   0.0705   0.0000  0.02348  -3.1646E-03  1.1110E-02  1.1552E-02  105.900
```

Of course, the current values are in peak amps, just as the source voltage input is in peak volts. The data is available as both real and imaginary values and as a magnitude and phase angle. Although such data is complete, sorting it out can be daunting. Therefore, a rectangular plot of part of the data may be more informative. For example, consider **Fig. 8-5** and **Fig. 8-6**, which present the current magnitude and the current phase angle for each element at one of the swept frequencies. The gray scale of the reproductions may preclude sorting out the individual curves. On screen, color selection will clarify each curve and the element to which it belongs. When making such identifications, do not presume anything. For example, in most Yagi designs, the driver (tag 2) would have the highest current. However, in this case, at the frequency selected for viewing, the first director carries higher peak current, with the driver in second place. More normally, the reflector carries the least current.

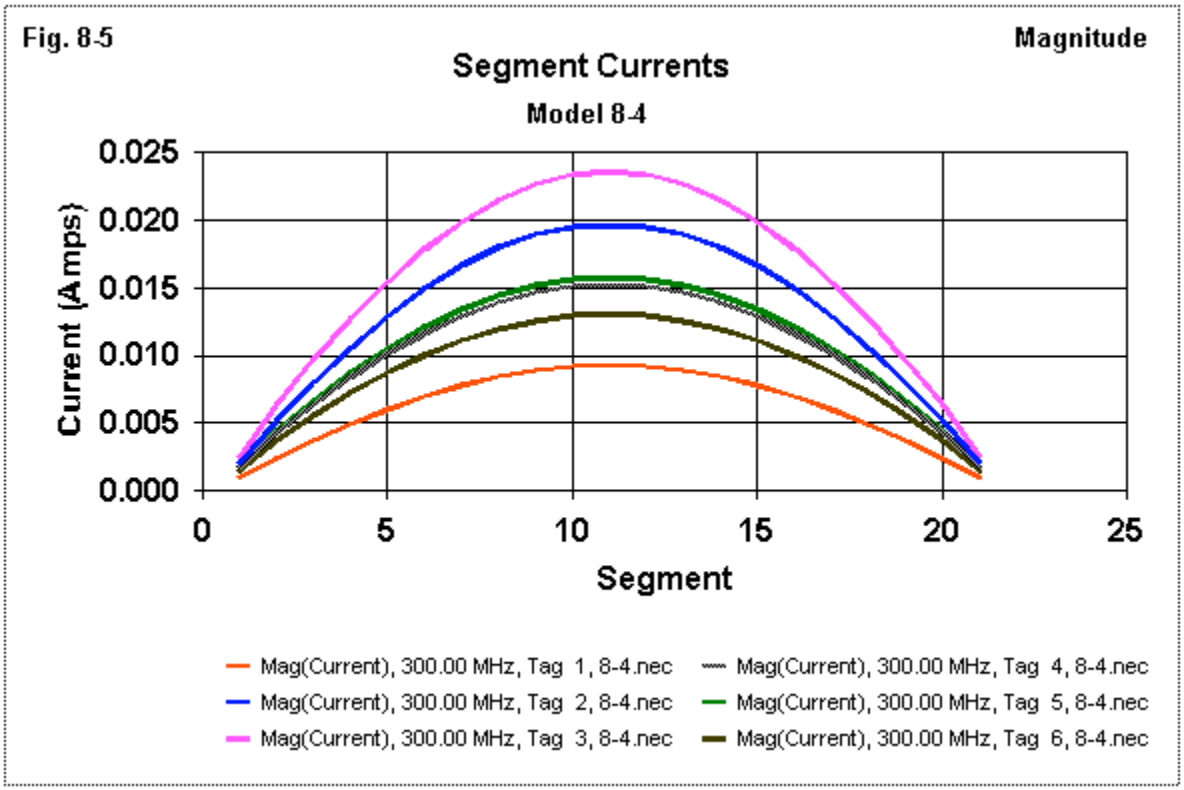

Fig. 8-6 Phase Angle

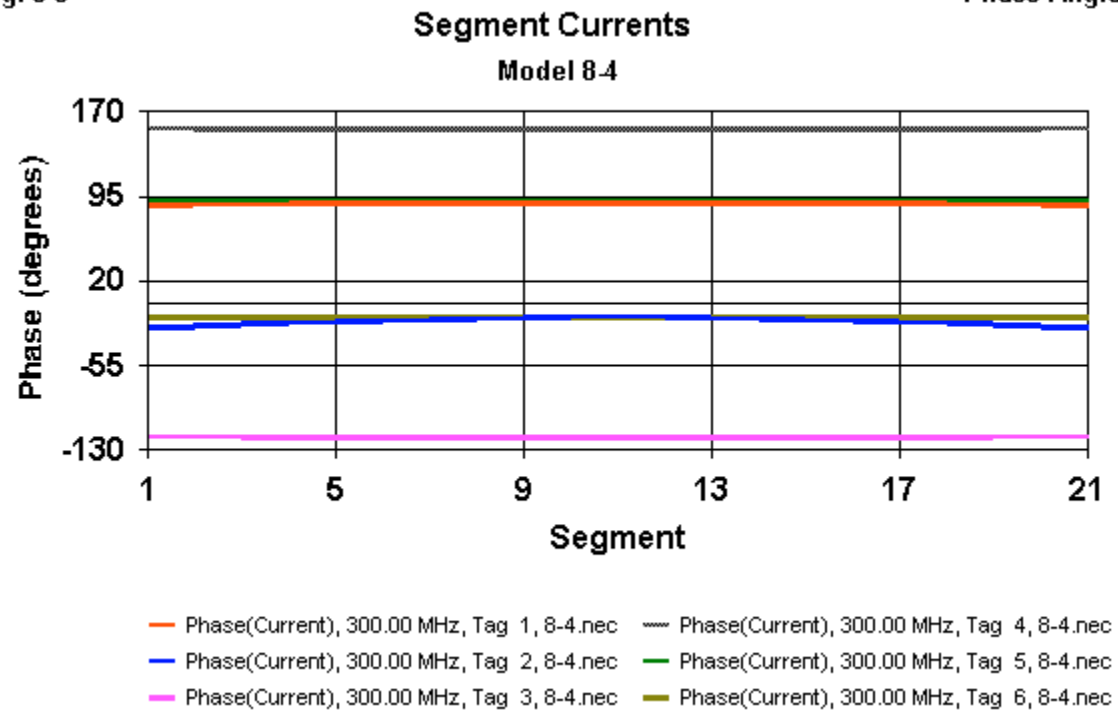

The phase graph shows another useful feature of plotting systems. The X- and Y-axis values have been adjusted for best viewing of the data. The elements all have 21 segments, and thus, the X-axis values run between 1 and 21. Contrast the graph to the current magnitude plot, where the automated X-axis values of 0 to 25 remain in place. The lesson is more than idle: data interpretation and presentation require great care in setting up the plot configuration.

Some tabular data is not suited for direct presentation or easy reading. Consider as an example the report of the source impedance for the present model. As the data emerges from the NEC output report, it has the following appearance for 300 MHz.

```
- - - ANTENNA INPUT PARAMETERS - - -

TAG    SEG.     VOLTAGE (VOLTS)          CURRENT (AMPS)
NO.    NO.     REAL         IMAG.       REAL         IMAG.
  2     32 1.00000E+00 0.00000E+00 1.92647E-02-4.03776E-03

          IMPEDANCE (OHMS)         ADMITTANCE (MHOS)       POWER
          REAL         IMAG.       REAL         IMAG.     (WATTS)
        4.97241E+01 1.04219E+01 1.92647E-02-4.03776E-03 9.63235E-03
```

I have broken up the line into two parts in order to enlarge the entries for easier viewing. At 300 MHz, the impedance is 4.972E+01 + j1.042E+01 Ω. We may translate this value into more conventional terms: 49.72 + j10.42 Ω. As a side note, remember that all voltage and current values in NEC are peak. Hence, calculating the power from the listed values requires a bit of calculator work. Find the current magnitude from the listed values for the real and imaginary components. Square that value and then take half of it to account for the transition from peak to

RMS values. Finally, multiply the result by the resistive component of the impedance to arrive at the reported power level in watts.

Although source impedance is a useful value to know, most implementing software for NEC calculates the VSWR after the core run. Such calculations use a reference (resistive) impedance value provided or selected by the user. As a result, tabular impedance tables extracted from the NEC output report ordinarily use a custom format, as indicated by the following table for the present model. The reference impedance is 50 Ω.

Input Impedance and VSWR

Frequency	Tag	Seg.	Real(Z)	Imag(Z)	Mag(Z)	Phase(Z)	Zo	VSWR
295.000000	2	32	44.642	6.628	45.131	8.445	50.000	1.20
297.500000	2	32	46.962	9.356	47.885	11.267	50.000	1.22
300.000000	2	32	49.724	10.422	50.805	11.838	50.000	1.23
302.500000	2	32	50.756	6.512	51.172	7.311	50.000	1.14
305.000000	2	32	41.157	-0.643	41.162	-0.895	50.000	1.22

Besides changing the engineering notation to decimal notation, the table calculates the impedances in terms of magnitude and phase. Of course, the right hand column provides the 50-Ω SWR at each frequency. An added bonus is that the entire data set appears together, rather than as separate and widely separated reports for each frequency.

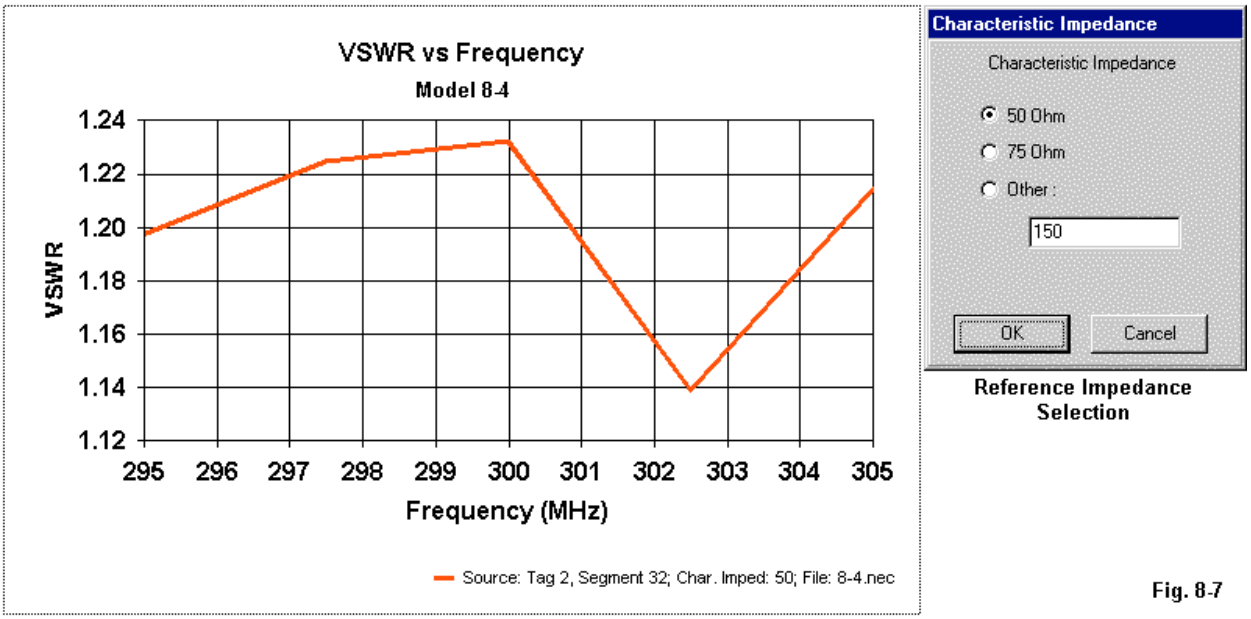

Fig. 8-7

Once calculated, the VSWR data becomes a part of the model's overall data set. Hence, it is eligible for plotting, as shown in **Fig. 8-7**. The curve will be as smooth or as angled as the number of data point permits. With only 5 data points, each separated by 2.5 MHz, the curve presents very sharp transitions from some values to others. However, note also the values in the Y-axis. The automated plot formation function uses terminal values just above and just below the highest and lowest data values. Often, you will need to override such functions to set curves in a format more suited for either interpretation or presentation. A minimum value of 1.0 would likely be the

best value for the curve, while some standard maximum value--such as 2.0--might be useful at the upper end. Under these conditions, even with only 5 data points, the curve transitions would appear less extreme. The figure also makes evident the user selection of a specific reference impedance for the plot.

The SWR graph is a sample of plots that require multiple frequencies in order to be possible. The plotting system also permits us to plot the impedance either in terms of magnitude and phase angle or in terms of real (resistive) and imaginary (reactive) components. When plotting magnitude and phase angle, separate plots are more useful, since the values are normally sufficiently far apart to obscure small changes in each one. However, in many cases, we may successfully plot the resistance and reactance on the same plotting frame. See **Fig. 8-8** for the plots for model 8-4. In particular, the slow rates of change of each value combine with their relative closeness to produce a very usable composite graph. Wherever you may need to see or to present finer detail for each curve, you may, of course, separately plot them. As well, the tabular data is always available to supplement any rectangular plot that you create.

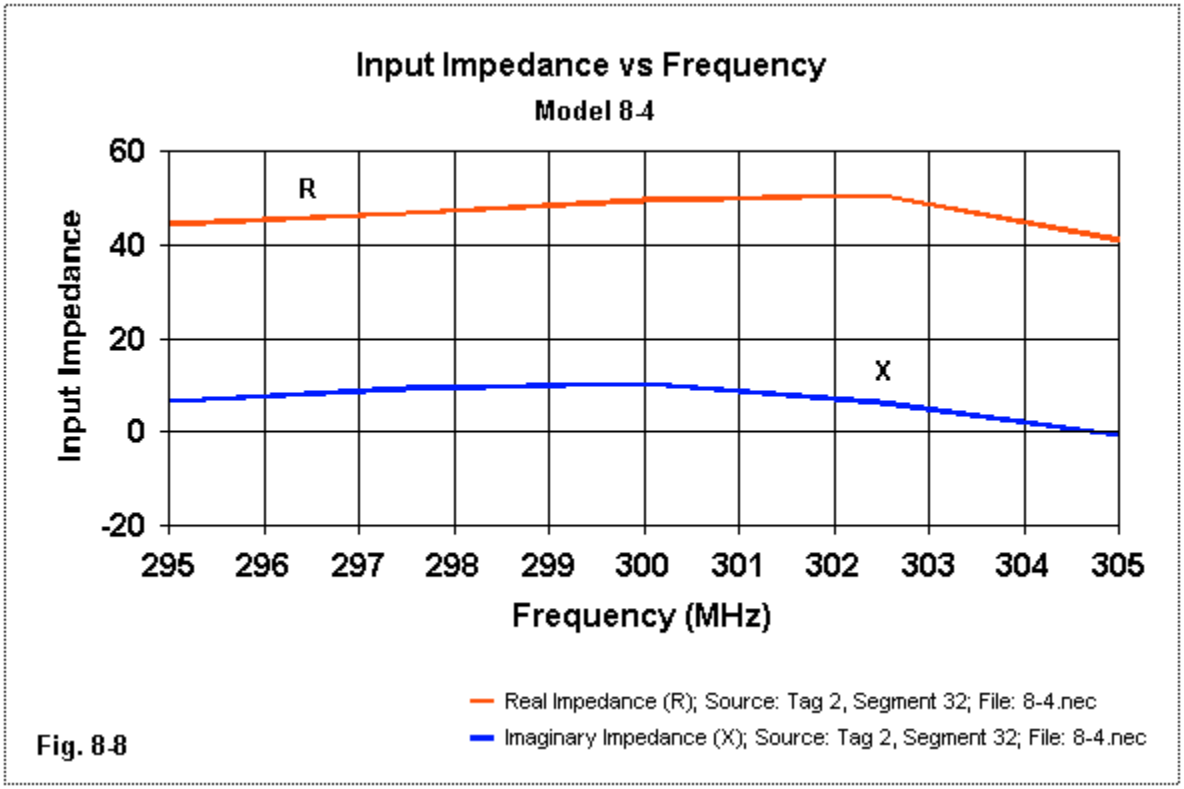

Fig. 8-8

There are a number of other possibilities for rectangular plots that we have not sampled here. Some of them are unavailable for the present model because it lacks the appropriate output requests to produce the necessary data. In the following list, these plotting potentials have a parenthesized indicator of the required output request. I have omitted a second group of plotting possibilities for modeling reasons. In one case, the plot would be irrelevant to the linear-element antenna under our cursory scrutiny. In another case, making sense of the plot will require some detailed attention to the data stream for RP requests, the main subject of the next chapter in this part of our work.

Omitted Graph	*Comment*
Radiated E Fields (RP1)	Requires a ground-wave request
Electric Field vs. Angle	Requires orientation to electrical field in far-field analysis
Polarization	Not relevant to a wholly linear antenna array
Near Fields (NE/NH)	Requires one or more near-field requests
Receive Patterns (PT1)	Requires an incident plane wave form of excitation
Normalized Receive Patterns (PT2)	Requires an incident plane wave form of excitation

A useful form of graphing impedances or admittances is against a Smith Chart. To illustrate the potential, let's revise the frequency sweep entry of the model to extend from 275 to 325 MHz. Open and run model *8-5a.nec*, and then invoke the Smith chart.

```
EX 0 2 11 0 1 0
FR 0 9 0 0 275 5
RP 0 1 361 1000 90 0 1 1
```

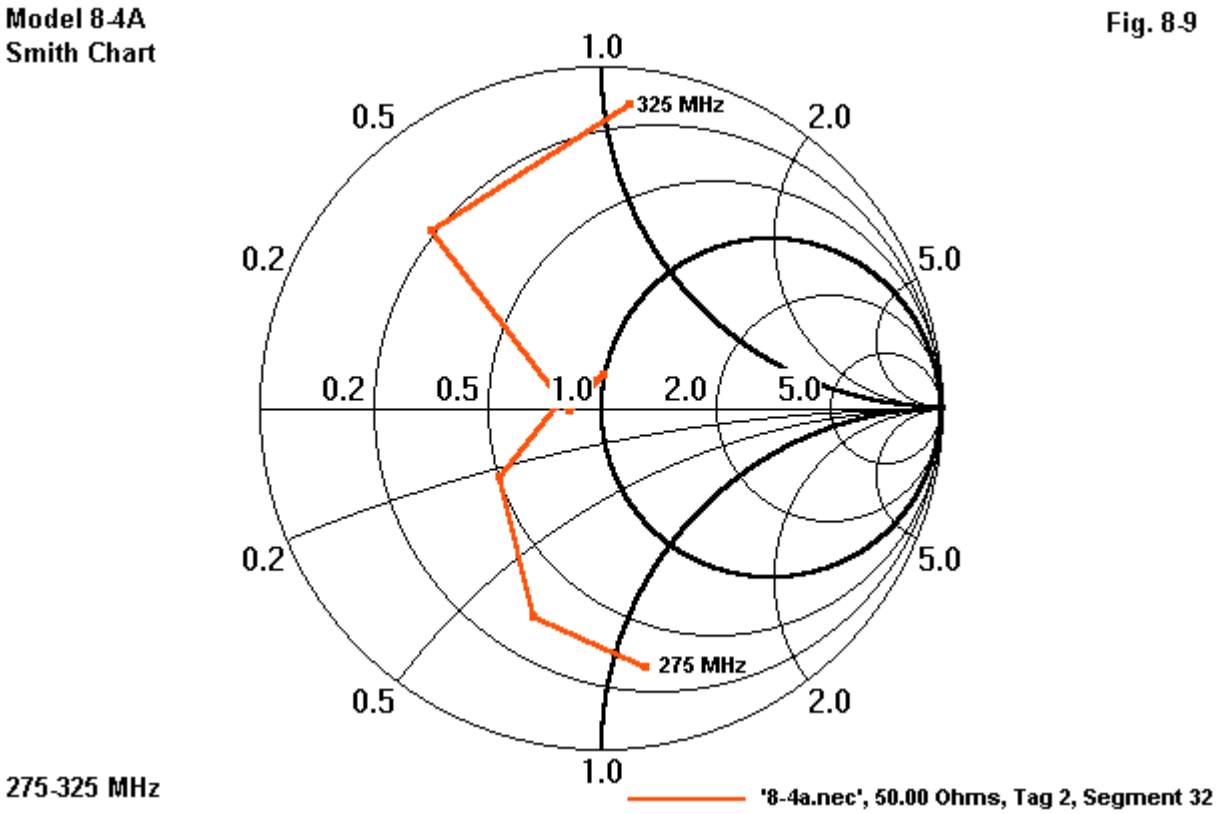

Within the original sweep, the impedance points would have been too tightly grouped to separate. For antenna design, that condition is desirable, but for illustrating a graphing possibility, it would have resulted in an invisible curve. The use of Smith Charts lies outside of the scope of our work here, but a number of texts are available to understand and master this analytical tool. In fact, Smith's original work on the subject was republished a few years back.

A productive graphing potential within the NSI implementing software is the surface or 3-

dimensional plot of the far-field pattern, as illustrated by **Fig. 8-10**. The figure includes both the plot and the set-up screen.

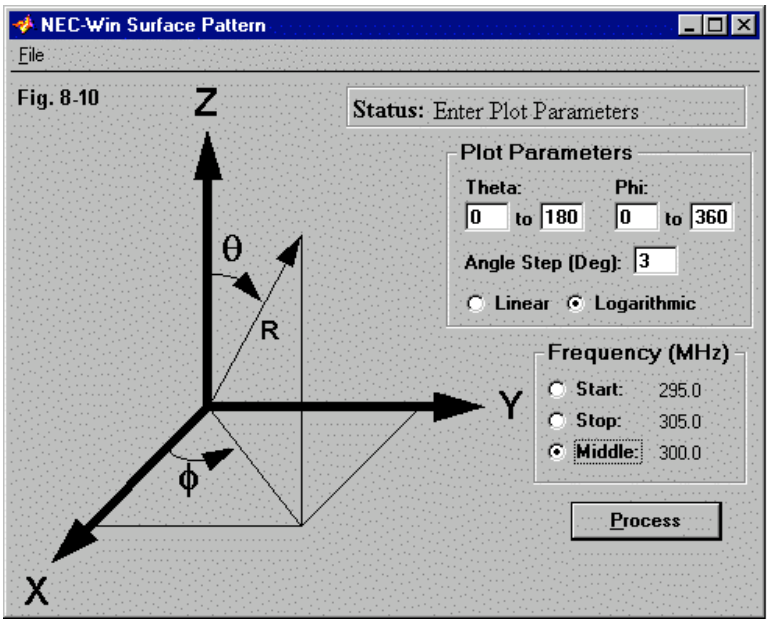

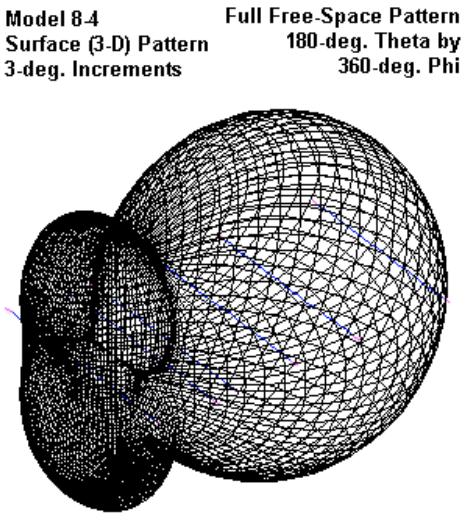

Surface plots in free space require a 180° theta range to produce a full pattern. Over ground, a theta range of 90° is adequate, since none of the pattern appears below ground. To coincide with the 2-dimensional polar plots viewed earlier, the pattern specifies a logarithmic plot, that is, a plot in which the relative gain values diminish logarithmically toward the plot center, which is the ostensible antenna position.

The creation of this plot requires data points at uniform angular increments for the full sphere surrounding the antenna position or origin of the plotting system. If the increment is too large (approaching 10° perhaps), the smooth lines that outline the pattern turn into angular junctions capable of losing important detail in some plots. If the increment is too small (perhaps approaching 1°, the lines will close into an unreadable blob. For most purposes, 3° to 5° is a good range to use for 3-dimensional surface plots.

NSI software includes a special graphical but not graphing capability, the plot button labeled "3D." The function has no analytical purpose, but does provide a considerable presentational capability. It can model the antenna structure as a set of wires or a set of tubes. For the present antenna, tubes are the proper choice. In addition, you can choose the color, using either solid or metallic colors. The latter have highlight regions to simulate a distant light source. Of course, you may move the antenna image around and change its size to suit the desired presentation. Finally, you may select a suitable background for the antenna in accord with presentational needs.

For a sample, I have given model 8-4 tubular dimensions combined with a highlighted copper finish. The highlights show well against the sky portion of a background called "dusk." The result is the image in **Fig. 8-11**. Even in the grayscale of monochromatic reproduction, the main elements of the color version show through.

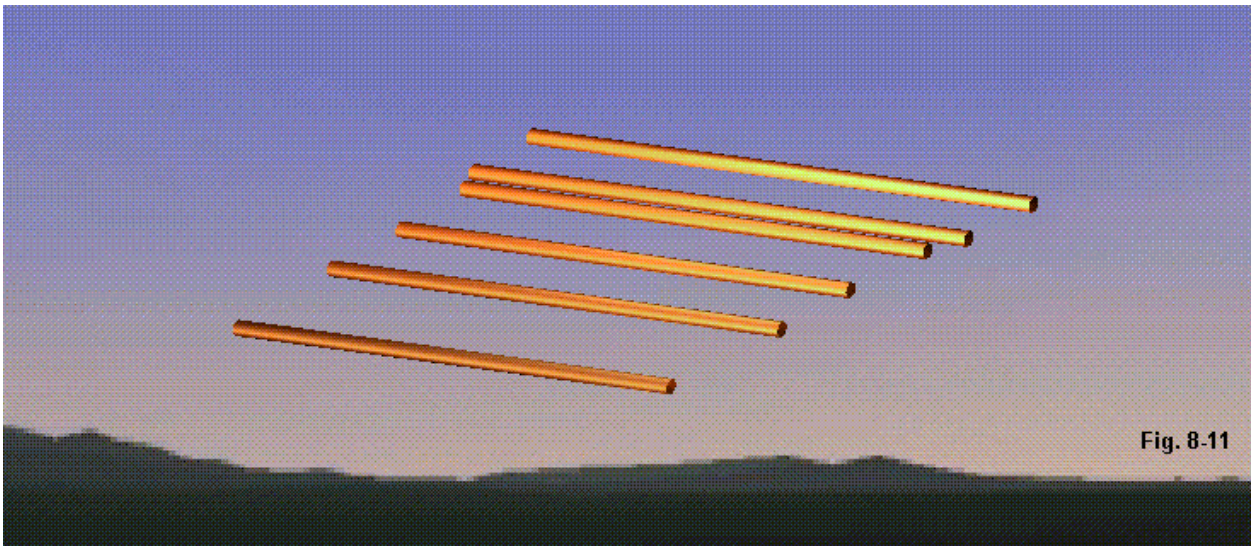

The main purpose of this review of graphing potentials for tabular data has not been to teach the NSI software, although something of that effort is unavoidable. Instead, the goal has been to develop an awareness of the relationship between the plots and the NEC output report tabular data on which the plots rest and the advantages of plotting (in many instances) for presenting information clearly.

Before we conclude our introductory studies of the NEC output report, we should note some areas that have so far drawn blanks. That is, the headings either have had no content or have had absolutely constant content. The antenna environment has been free-space throughout, giving us no clue as to what the entry might look like with a ground specification. The antenna wire has been perfect or lossless, requiring no entry of material loading. With no loads, the power budget has shown 100% power efficiency.

Let's modify the 6- element Yagi. Open model *8-6.nec*.

```
CM Adding ground and material loads
CM 6-element Yagi
CE
GW 1 21 0 0.2506 0 0 -0.2506 0 0.001
GW 2 21 0.1253 0.2472 0 0.1253 -0.2472 0 0.001
GW 3 21 0.1772 0.2312 0 0.1772 -0.2312 0 0.001
GW 4 21 0.3207 0.2246 0 0.3207 -0.2246 0 0.001
GW 5 21 0.4612 0.2246 0 0.4612 -0.2246 0 0.001
GW 6 21 0.6707 0.2162 0 0.6707 -0.2162 0 0.001
GM 0 0 0 0 0 0 0 2
GS 0 0 1
GE 1
GN 2 0 0 0 13.0000 0.0050
EX 0 2 11 0 1 0
LD 5 0 0 0 3.1e7
FR 0 1 0 0 299.7925 1
RP 0 181 1 1000 -90 0 1.00000 1.00000
RP 0 1 361 1000 83 0 1.00000 1.00000
EN
```

The first maneuver is to introduce a GM command to elevate the antenna 2 m (2λ) above Z = 0. Next, we set the GE command for a ground plane and introduce the GN ground specification entry. The selected ground is average, that is, has a conductivity of 0.005 S/m and a permittivity or relative dielectric constant of 13. The final modification is the LD5 entry that specifies a material conductivity to all segments in the model of 3.1E7 S/m, about the value of aluminum. **Fig. 8-12** presents the polar plots of the resulting model.

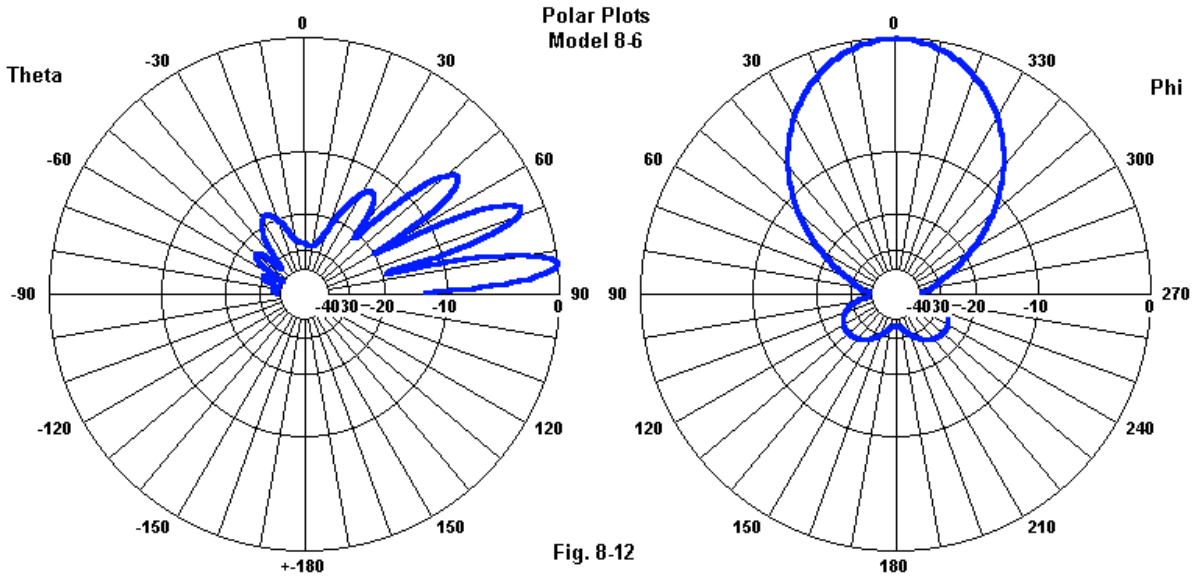

Fig. 8-12

The reported gain is 15.8 dBi at a theta angle of 83°. The 180° front-to-back ratio is almost 36 dB, with a source impedance of 50 + j10 Ω. More important than the numbers are the interesting changes in the output report from the core.

```
- - - STRUCTURE IMPEDANCE LOADING - - -

  LOCATION       RESISTANCE INDUCTANCE CAPACITANCE   IMPEDANCE (OHMS)  CONDUCTIVITY    TYPE
ITAG FROM THRU     OHMS        HENRYS     FARADS    REAL      IMAGINARY  MHOS/METER
ALL                                                                     3.1000E+07    WIRE
```

The structure impedance loading shows the introduction of the LD5 command that applies the conductivity value to all segments of the elements. Had we introduced a different type of load, the last entry called "type" would change its content, a marker to change the way in which the core handles the numbers under each of the column headings.

```
- - - ANTENNA ENVIRONMENT - - -

FINITE GROUND.  SOMMERFELD SOLUTION
RELATIVE DIELECTRIC CONST.= 13.000
CONDUCTIVITY= 5.000E-03 MHOS/METER
COMPLEX DIELECTRIC CONSTANT= 1.30000E+01-2.99807E-01
```

The antenna environment heading no longer has a simple label beneath it. Instead, it records the conductivity and permittivity values that we entered in the GN command, as well as recording the

fact that we selected the Sommerfeld-Norton ground calculating system. The core also calculates from the entered values a complex dielectric constant, which is the value used in calculating the radiation pattern values.

```
- - - POWER BUDGET - - -

INPUT POWER   = 9.6445E-03 WATTS
RADIATED POWER= 9.4448E-03 WATTS
STRUCTURE LOSS= 1.9970E-04 WATTS
NETWORK LOSS  = 0.0000E+00 WATTS
EFFICIENCY    =  97.93 PERCENT
```

The power budget shows the last interesting change in the NEC output report (at least among the entries that are heavily tabular). Whereas all the other models in the exercises in this chapter had shown 100% efficiency, the more realistic construction of the present model shows an efficiency just shy of 98%. (You may wish to return the power efficiency to 100% by deleting the LD5 entry to see whether the maneuver changes any of the reported performance figures.) Note that this value is a power efficiency based on the supplied power minus any losses in the structure of the antenna. In a later chapter, we shall delve into the difference between power efficiency and radiation efficiency and show how to calculate the latter with the right RP command entries.

If there is any conclusion that we can draw from the new version of the 6-element Yagi, it is that there is no portion of the NEC output file that deserves to be overlooked.

Summing Up

A "standard" far-field model having only a single RP request will produce an output file with information in each of the following categories.

Comments
Structure Specification
Segmentation Data
Frequency
Structure Impedance Loading
Antenna Environment
Matrix Timing
Antenna Input Parameters
Currents and Locations
Power Budget
Radiation Patterns
Run Time

If a model has no command causing the core to perform its calculations, the file will end with the segmentation data. If the output request is for something other than a far field pattern, then the later entries of the file will differ. As well, if the model performs a frequency sweep, then some entries after the matrix timing will occur more than once.

RP, the radiation pattern command, will self-execute. However, if there are multiple frequencies and multiple pattern requests, the frequency command must be repeated before each pattern request to obtain a complete set of patterns. NE and NH, the near field requests, also self-execute, but only if there is a single frequency specified. If the FR command specifies multiple frequencies, then NE or NH require the use of XQ, the execute command. As well, when specifying multiple frequencies, the FR command must precede each NE or NH command, and each such command must have a following XQ command.

Input files may include multiple models if each one is complete in its command requests, and if the NX or next structure command occurs between the models. In NEC-2, models past the first one must begin with a comment (CM or CE) entry, although NEC-4 allows the first entry to be a geometry command.

NSI software packages--NEC-Win Pro and GNEC--provide the user with many ways of presenting the output file data. Besides giving access to the complete file, the programs have options to request viewing of specific data sets, such as currents, near-field information, or source impedances. These tables coalesce data that may be in widely distant parts of the output file, especially when multiple frequencies are requested. Where tabulated information involves post-core-run calculations--for example, for VSWR--the table format may alter the NEC output style of presentation for easier reading.

In addition, the implementing program provides a wide variety of graphical plotting facilities, some of which allow multiple ways of showing the same data, For example, radiation pattern data can appear in polar or rectangular plots, each with options for setting up the graphics. Source impedance data across multiple frequencies can appear on rectangular plots or on a Smith chart. Plotting facilities can show Impedance and current values as real and imaginary components or as magnitudes and phase angles.

Effective use of advanced NEC software with access to the complete command set demands a full appreciation and understanding of the output file produced by the core. As well, you should also understand the relationship between the core output file information and the many ways in which an implementing program allows its display.

9.
Far-Field Radiation Pattern Requests

***Objectives**: The radiation-pattern request command is central to NEC calculations and is more flexible than most modelers imagine. In this first set of RP exercises, you will examine the space wave options available and what they can tell you about the performance of different types of antennas that you may model. As well, you will learn several cautions to observe when using the command.*

The radiation pattern or RP command is the most common output request for NEC models. Following the calculation of currents on the segments of the model's wires, the core calculates over a specified set of spherical coordinates the electrical fields at either a specified distance from the coordinate center or at an indefinitely large distance. These fields result in a number of useful gain values, for example, the power gain or the directive gain. As well, the core calculates the vertical, horizontal, and total field gain or, as an alternative, the major axis, minor axis, and total field gain. These outputs only sample what is possible within the command.

The RP command offers a number of options, of which the space wave and the ground wave are common to both NEC-2 and NEC-4. We shall examine ground wave analysis in a future chapter. This set of exercises will focus on space wave functions. NEC-2 includes a number of special options that depend upon the ground data selected for the model. We shall explore those options when we examine the ground commands more closely. However, even restricting ourselves to the "RP0" option within the radiation pattern command, we shall have a large number of alternatives to find and learn how to use effectively.

To use the RP command well requires that we understand each of the options available for each of the numerical positions within the command. Some call for normal integer or floating decimal entries. Others require an understanding of how to set up spherical coordinates to obtain a pattern covering the desired segment of the overall pattern. Still others have special functions, and the unpronounceable "XNDA" will become very familiar to us.

The Structure of the RP Command

We have on numerous occasions used the RP command for most of the models that illustrated the geometry commands. Entry level modeling programs tend to hide the full structure of the command from us. They offer simplified entry systems for 2-dimensional slices of the radiation sphere (in free space) or hemisphere (over ground). Hence, we learn to set starting and ending values for a phi or azimuth pattern. If there is a "3-D" pattern system, its entries are either partially or completely automated. Hence, the modeler often does not know that each of these outputs is a version of an RP request. When we employ software that requires us to handle the RP command directly, we often fall back on settings that give us only those patterns with which we are familiar and do not tap the full potential of the command.

Let's begin with the familiar. Open model *9-1.nec*, another version of the standard free-space dipole at 299.7925 MHz.

```
GW 1 11 0 -.2375 0 0 .2375 0 .001
GE
FR 0 1 0 0 299.7925 1
EX 0 1 6 00 1 0
RP 0 361 1 1000 -90 0 1.00000 1.00000
RP 0 1 361 1000 90 0 1.00000 1.00000
```

The two RP commands produce two different polar plot patterns, once an external module translates the data into graphical form. **Fig. 9-1** shows the results.

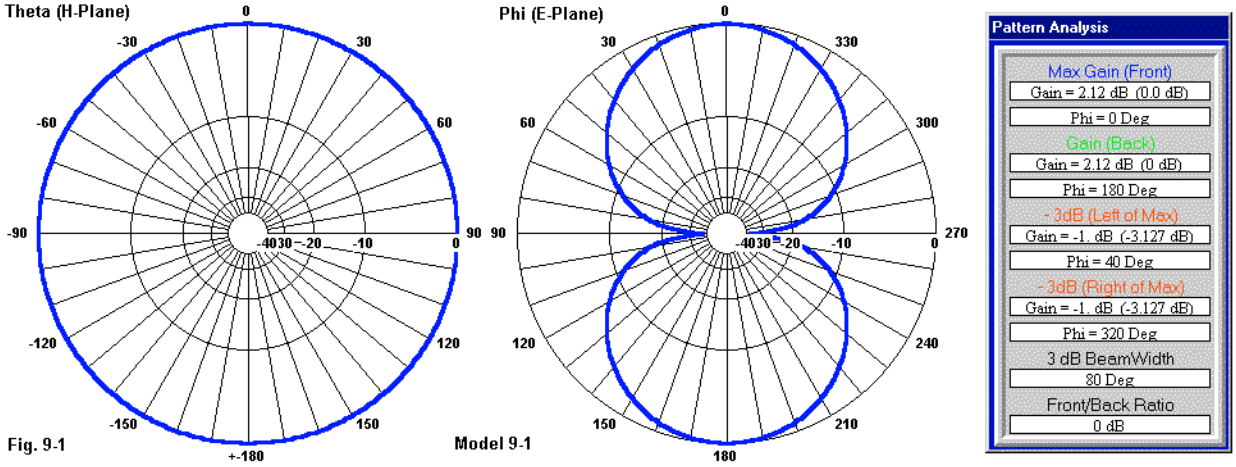

The external module may also scan the NEC output file pattern data and select various values, for example, the maximum gain value reported. It may also select associated data, such as the angle at which the maximum gain occurs. Finally, it may perform calculations to arrive at information, such as the 3-dB beamwidth of the lobe in which maximum gain occurs, that is, the angular spread between points at which the gain is 3 dB lower than the maximum gain. The "pattern analysis" table in **Fig. 9-1** illustrates some of those post-run capabilities.

The command itself consists of 4 integer positions and 6 floating decimal positions. The following lines provide an outline of the command structure, using the second RP request in the model as a sample.

```
Cmd   I1    I2    I3    I4    F1      F2    F3    F4    F5    F6
      I1    NTH   NPH   XNDA  THETS   PHIS  DTH   DPH   RFLD  GNOR
RP    0     1     361   1000  90      0     1.00  1.00  (NU)  (NU)
```

Because early Fortran had limited entry potentials, the RP command separates some information that goes together. I2 and I3 combine with F1 through F4 to define the radiation pattern coverage under the condition where I1 = 0. In the sample command entry, F5 and F6 have no entries, and NU = not used. However, under certain conditions, we might well make use of these entries. To get a grasp on the command, we must start at the beginning, but we need not handle everything in the exact order of command entry.

I1: The first entry specifies whether we wish a space wave (0) or a ground wave (1) in both NEC-2 and NEC-4. As noted, the RP1 request will be the subject of a future exercise. Hence, all of our models in this chapter will make RP0 requests. In NEC-2, there is a close relationship between the ground specification commands (GD, GN) and the RP command. Hence, the NEC-2 version contains a total of 7 entries, the last 5 of which pertain to the use of special ground conditions. The models in this chapter will not invoke any of those conditions, so we can defer discussion of them until we tackle the ground conditions themselves. **Fig. 9-2** illustrates the NEC-2 options, while serving as an aid to the explanation of the other entries in the RP command system. The "Radiated Fields" entries show all 7 options. I have enlarged the NEC-Win Pro assistance screen to show the upper right portion under requests for a theta, phi, and custom pattern.

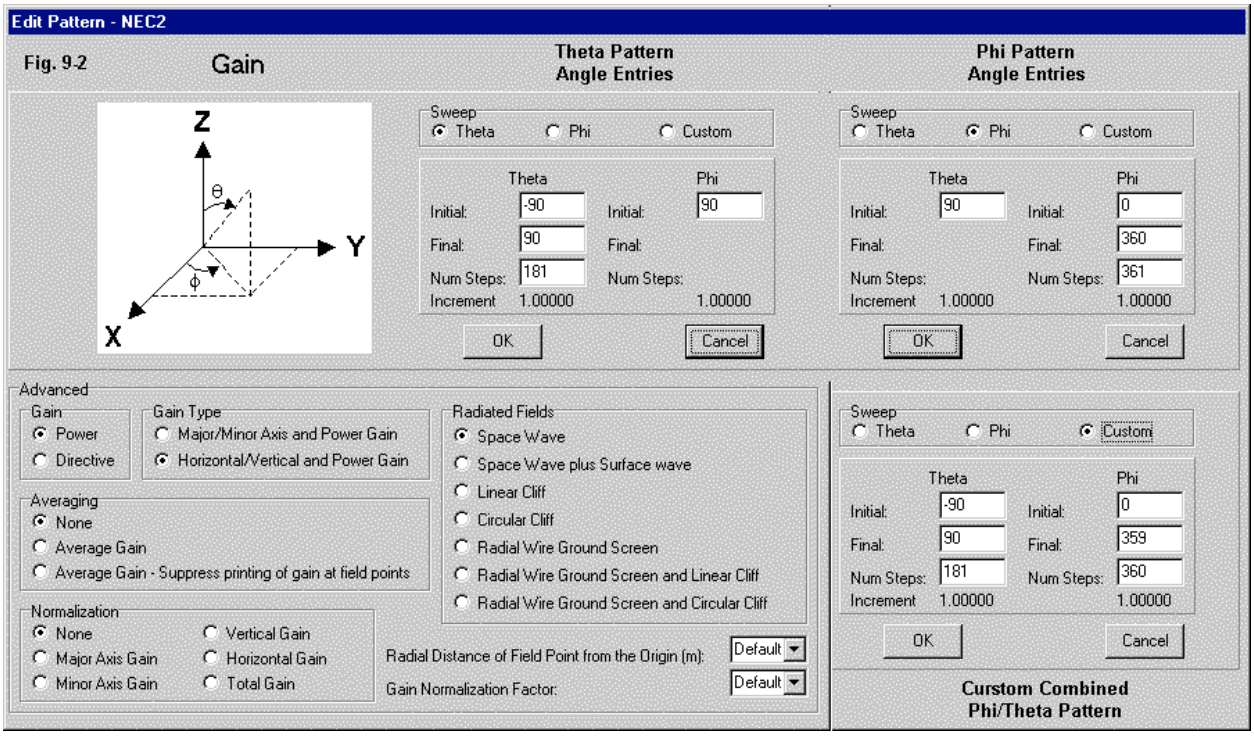

I2, **I3**, **F1**, **F2**, **F3**, **F4**: The indicated entries define the segment of the radiation sphere to be sampled. To define a sphere section, we need both phi (I3, F2, F4) and theta coordinates.(I2, F1, F3). We first need a starting angle: F1 for theta and F2 for Phi. Next, we need the increment between each angle to sample after the starting angle: F3 for theta and F4 for phi. Finally, we need the total number of angles to sample (including the starting angle): I2 for theta and I3 for phi. In order not to develop any confusion between coordinate systems, we shall with rare exception use the phi-theta system that is inherent to the NEC cores.

A request for a 2-dimensional pattern--either theta or phi--must contain entries for all 6 of the entry positions. A theta pattern--with its starting angle, increments, and number of steps--must always be at some phi angle as defined by a starting angle value. However, the increment for phi may be any value, since the number of steps will be 1. Similarly, a phi pattern's full data must be accompanied by a starting angle for theta and the specification of 1 step, with the value of the increment being optional. In NEC-2, theta angles greater than 90° from zenith are not valid.

If you wish to sample a full phi circle, then enter onto the assistance screen equivalent start and final angles, such as 0° and 360°. The number of steps should then add one more (361) both to close the circle and to arrive at an increment (1°) that you desire for the F4 increment. In free space, you may perform a similar entry routine for a theta circle, but starting at -90° and ending at 270°. For a hemisphere over ground, you may specify a range of -90° to +90°, with 181 steps if you wish an increment of 1° per step. As we shall see, there are occasions to use less than 1° increments, especially in theta patterns over ground.

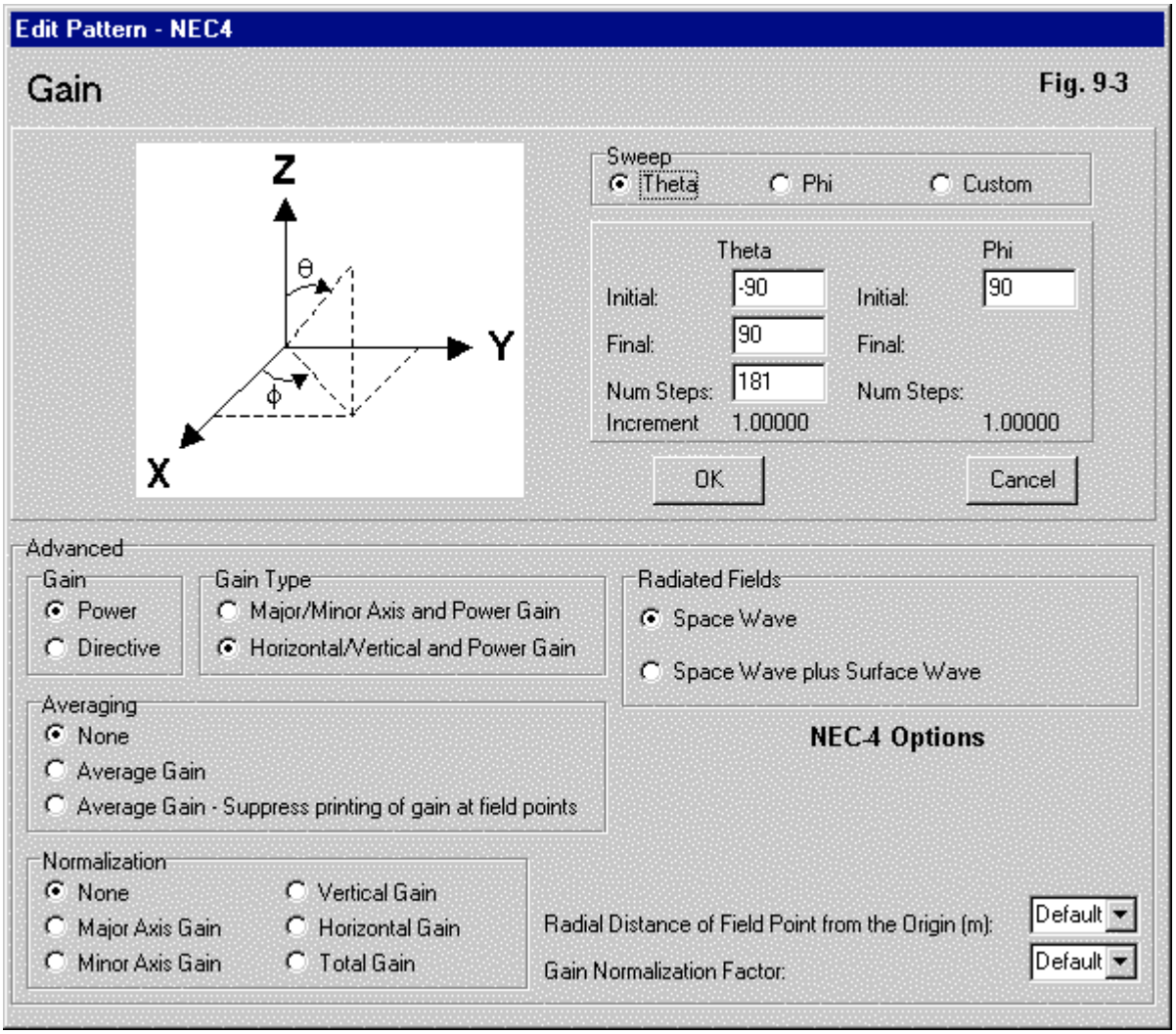

Fig. 9-3 shows that the pattern specification system is the same in both NEC-2 and NEC-4. The only difference between the assistance screens for the two cores is that NEC-4 does not tie the ground condition specifications to the radiation pattern request. Nothing in either core rules out the specification of a broad section of the radiation sphere through a custom RP entry. In this case, both phi and theta will contain starting angles, increments and numbers of steps greater than 1. However, use this option with great caution. If you wish to obtain a series of 2-dimensional theta or phi patterns, it is usually good practice to provide a separate RP entry for each one in order to keep track of them. The polar plot and rectangular post-run modules have

limitations on the number of plots that each can handle. If you create a custom pattern request with numerous theta and phi angles for sampling, the number of potential theta and phi patterns can easily overrun the plotting module capabilities. Nonetheless, you will have considerable occasion to set up custom plots that cover the entire radiation sphere.

F5: The RFLD entry position has separate meanings, depending on the setting of I1. When I1 = 0, a request for a space wave, RFLD specifies a radial distance in meters from the coordinate system origin. If you enter a value for RFLD, it must be in the far field, since the space wave calculations do not include near field components. Classically, the distance from the antenna to the far field (or the Rayleigh distance) is $2D^2/\lambda$, where D is the maximum dimension of the antenna and λ is a wavelength in the same unit of measure. However, the distance should be much greater than both D and λ. The entry of a value for RFLD is significant only if you wish to have a calculated value for the electrical field at the specified distance. You may leave the entry blank if you need only gain values within the pattern that you request.

F6: The last entry in the RP sequence is called GNOR or gain normalization. There is a switch in another entry under RP that requests normalization, and only if this normalization is switched on do you need an entry for F6. If the entry is zero, normalization is to the maximum gain value in the table. If F6 is other than zero, then normalization is to the value of the entry. In most cases, you will not need to activate normalization within the RP command because the post-run plotting module will make provision for normalizing a requested plot. By letting the external module perform the normalization, you can retain the basic gain values in the NEC output report.

I4: The I4 entry is not a single integer entry, but a 4-place combination of entries. Each of the 4 digits within this integer position has a designation: XNDA (running from left to right). In turn, each of those places has a range of allowable values, and each one of those has a special meaning.

X: The first place of column controls the output format of the output table of values. If X = 0, then the table prints the major axis, the minor axis, and the total field gain. If X = 1 (the most usual case), the table prints of vertical, horizontal, and total gain. As we shall see, the table contains other values as well.

N: The second place or column controls normalization of the values in the tabular output for the radiation pattern. Normally, N = 0, meaning that there is no normalization. If N > 0, then the gain normalized to the value specified in F6 is as follows:

N	Normalized Gain	N	Normalized Gain	N	Normalized Gain
1	Major axis	2	Minor axis	3	Vertical axis
4	Horizontal axis	5	Total gain		

D: The third place or column determines whether the gain is reported as a power gain or as directive gain. D = 0 yields power gain in dBi or decibels relative to an isotropic source. D = 1 yields directive gain, also in dB. The distinction applies to antenna structures containing a source assigned to one or more segments. If the source is an incident plane wave, then the output report prints the scattering cross section, although the column heading will read as the value of D dictates.

A: The final place or column controls gain-averaging computations. If A = 0, the core does not

compute an average gain. If A = 1, the core computes the average gain in addition to producing the table of individual gain and field values. This option is useful under certain circumstances for determining the radiation efficiency of an antenna. If A = 2, the core calculates the average gain, but suppresses printing the individual gain and field values. This last option is required for the Average Gain Test (AGT). Gain averaging generally is sensible only if the sampling field is the entire radiation sphere in free space or the entire hemisphere over a specified ground.

Theoretically, all combinations of XNDA values are possible. However, some combinations make no sense. For example, if X = 0 to yield a printing of the major and minor axis values, then setting N to either 3 or 4 to normalize either the vertical or horizontal axis gain values will be senseless. The most common value set for XNDA is 1000, requesting the gain in the vertical and horizontal axes, suppressing normalization, selecting power gain, and omitting an average gain calculation. This set applies generally to requests for 2-dimensional radiation patterns that post-run modules may convert to polar plots.

```
- - - RADIATION PATTERNS - - -

- - ANGLES - -           - POWER GAINS -       - - - POLARIZATION - - -
THETA     PHI         VERT.    HOR.     TOTAL      AXIAL      TILT   SENSE
DEGREES   DEGREES       DB       DB       DB        RATIO      DEG.
  90.00     0.00   -999.99     2.12     2.122    0.00000    -90.00  LINEAR

                                    - - - E(THETA) - - -    - - - E(PHI) - - -
                                      MAGNITUDE    PHASE      MAGNITUDE    PHASE
                                      VOLTS/M    DEGREES      VOLTS/M    DEGREES
                                   0.00000E+00     0.00    8.25172E-01   -93.09
```

To illustrate the tabular output of a typical radiation pattern report, I have reproduced the headings and only the first data line of the phi-pattern request in model 9-1. Because the report packs data tightly across what was once standard wide computer paper, I have had to break the single line into two parts for reproduction here. The first two columns record the sampling position in terms of theta and phi angles. Since XNDA was 1000, the power gains record values for the vertical, horizontal, and total field. For an antenna oriented in the X-Y plane only, the total gain and the horizontal (or E-plane) gain will be equal. The vertical (or H-plane) gain will be negligible, which NEC reports as -999.99 dBi. If you open and run model *9-1a.nec*, you will discover the same figures, since this is a simple bi-directional antenna with equal lobes on each side of a line running along the antenna wire.

If you wish to know the relative power gain (A), you may start with any tabulated gain value in dBi. Then $A = \log^{-1}(\text{gain}_{dBi}/10)$. If the total field gain is 2.122 dBi, then A = 1.63. Moving back and forth between relative power gain and the gain expressed in dB above an isotropic source will prove useful from time to time. For example, the AGT value makes use of relative gain in its primary form and requires conversion to dB to provide a gain report correction.

The remaining figures in the table have minimal value for the present sample antenna, but they do acquire significance under the proper conditions. The polarization data is more relevant to patterns produced by circularly or elliptically polarized antennas. For the dipole, the data simply confirm that the antenna is linearly polarized. The electric field data in the theta and phi planes has value only as a relative field strength (vs. angular heading) indicator in the absence of an entry for F5, RFLD.

Some Common Pattern Requests and Cautions

The theta pattern of a dipole in free space is the common circle. However, the theta pattern becomes far more significant once we specify a ground for the antenna. Open model *9-2a.nec*.

```
CM Dipole phi/theta patterns
CE 1 m (wl) above Average Ground
GW 1 11 0 -.2375 0 0 .2375 0 .001
GM 0 0 0 0 0 0 0 1
GE
GN 2 0 0 0 13.0000 0.0050
FR 0 1 0 0 299.7925 1
EX 0 1 6 00 1 0
RP 0 181 1 1000 -90 0 1.00000 1.00000
RP 0 1 361 1000 76 0 1.00000 1.00000
EN
```

To use a ground, we must elevate the antenna above Z = 0. The GM entry places the dipole at 1 m (1λ) above ground. The GN command specifies a Sommerfeld-Norton (SN) ground with "average" (by convention) values. The model still requests both theta and phi patterns, but with modifications from the free-space versions. The first RP entry requests a theta pattern covering only the hemisphere above ground--in 1° increments. The phi pattern also uses 1° increments for a full circle. However, the theta angle for this pattern is no longer 90°. Instead, it is a value above the horizon, specifically, 76°. Run the model and confirm the patterns shown in **Fig. 9-4**. Note also the reported gain of the dipole: 7.6 dBi, a value that accounts for the ground reflection at the theta angle of maximum radiation, otherwise known as the "take-off" angle. Finally, compare the phi pattern with the one in **Fig. 9-1**. The nulls of the dipole ends remain prominent, but have less depth than in the free-space model. Ground reflection is also the source of this change.

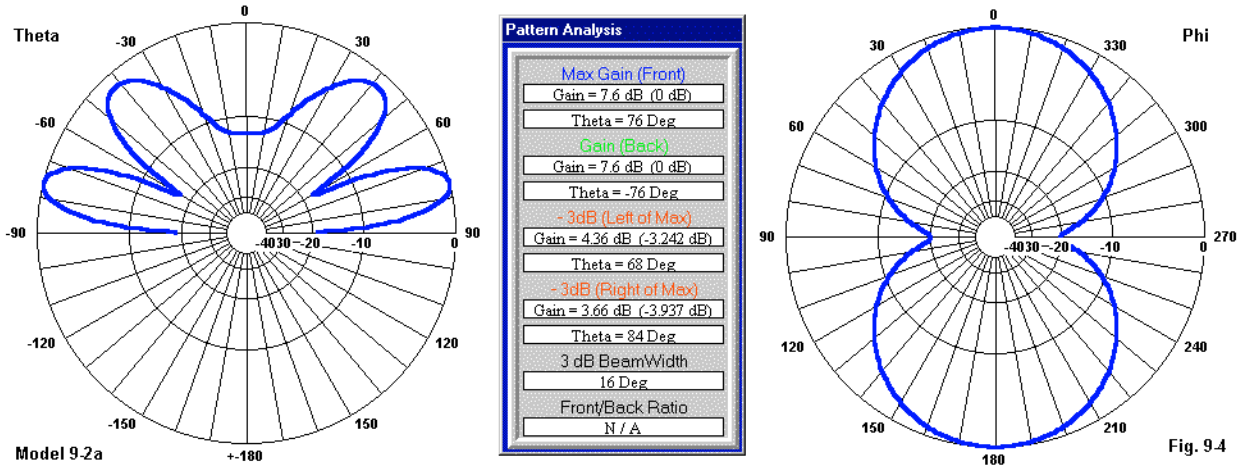

The concept of a take-off (TO) angle is useful where there are no overriding reasons to use another angle for the phi patterns. The theta pattern, when aligned to the phi heading for

maximum gain, will report the TO angle, as it did in the analysis shown in **Fig. 9-4**. However, you may also estimate the TO angle and the lobe angles for any horizontally polarized antenna that lies in an X-Y plane with no Z-plane extension. (A dipole and a Yagi are examples of such 2-dimensional antennas. A quad beam and a stack of two or more Yagis are examples of antennas having Z extensions. For them, determination of the TO angle and overall elevation lobe structure is more complex.) The classical equation for estimating the angle of lobes employs the elevation convention counting upward from the horizon.

$$A_{LN} = \arcsin\frac{N}{4h}$$

A_{LN} is the angle of a lobe or null. N is the number of the null or lobe counting upward. The horizon null is 0, the first lobe is 1, the next null is 2, the next lobe is 3, etc. Odd values of N represent lobes or headings of maximum strength, while even values designate nulls or headings of minimum strength. The antenna height in wavelengths or fractions thereof is h. For the present example, the lowest lobe in the theta pattern is the strongest and provides the TO angle. Since N = 1 and the height is 1λ, then A_{LN} = 14.4° elevation or a theta angle of 76°.

In all theta and phi pattern requests so far, we have used an increment of 1°. For most phi patterns, this increment is sufficient to reveal critical pattern detail without undue length to the radiation table in the NEC output report. However, under certain conditions, that increment will fail us when requesting theta patterns for antennas above ground. The dipole in model 9-2a is 1λ above ground. As you increase the height above 5λ, the theta pattern resolution begins to fail using a 1° increment. Open model *9-2b.nec*.

```
GM 0 0 0 0 0 0 0 10

RP 0 181 1 1000 -90 0 1.00000 1.00000
```

The lines from the model show only the changes. The GM command now raises the dipole to 10m (10λ) above ground. However, the RP command requests a theta pattern using 1° increments. Compare this model to model *9-2c.nec*.

```
GM 0 0 0 0 0 0 0 10

RP 0 1801 1 1000 -90 0 0.10000 1.00000
```

The antenna remains 10m above ground, but the theta pattern request has decreased the increment between steps to 0.1°. For a complete theta pattern that covers the entire hemisphere, we need 1801 steps. In most cases, the thought of such a long table of pattern values is forbidding. However, a glance at **Fig. 9-5** shows the wisdom of obtaining a pattern using smaller increments. For the pattern on the left, analysis reports a maximum gain of 7.69 dBi at a theta angle of 80°, which corresponds with the 4th lobe. The tighter pattern on the right reports a maximum gain of 8.08 dBi at a theta angle of 88.6°, the angle of the lowest lobe.

NEC correctly reports the gain at each of the 1° intervals. But the maximum strength of the many lobes in the theta pattern does not match up with 1° headings. A second indicator of the inadequacy of the plot that uses 1° intervals appears in the pattern of nulls. On the left, the pattern of null points is exceptionally ragged, an indicator that the model uses too large an increment between sampling points. The smooth circular ring on the right suggests adequate

sampling. The conclusion is that the higher the antenna as a function of a wavelength, the smaller the angular increments must be to arrive at an accurate theta radiation pattern.

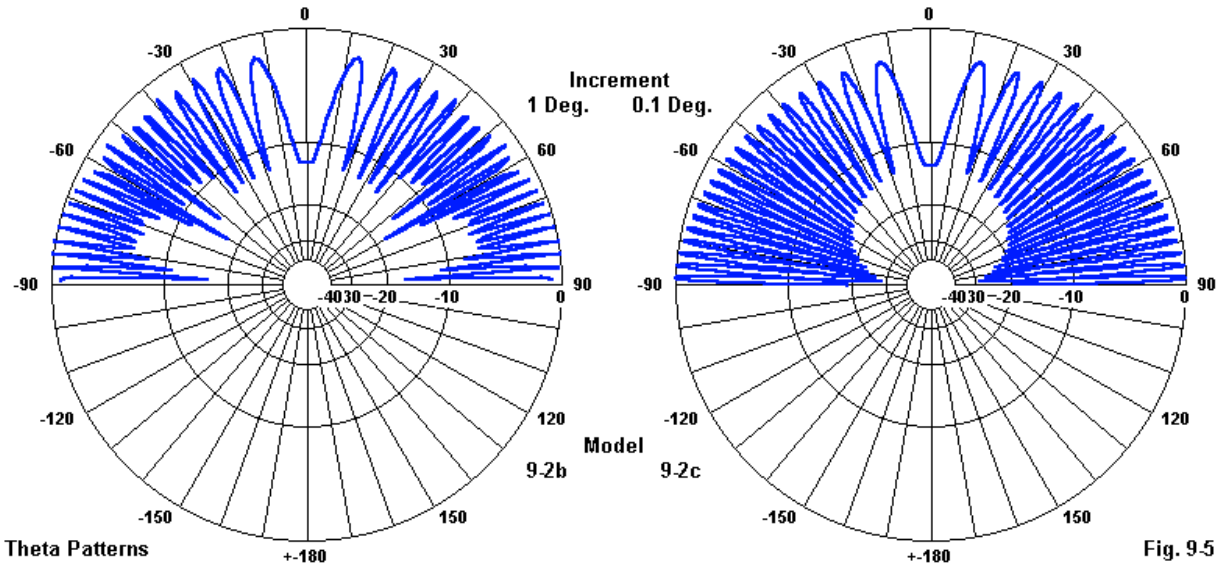

Although the general rule concerning the required angular increment of theta patterns applies equally to vertically polarized antennas as we elevate them, the tool that we used to estimate the TO angle does not. Let's briefly examine what happens to the theta pattern of a vertical antenna by using a 1/4λ monopole with 4 sloping radials. We shall raise the antenna 1λ (1 m) above average ground. The reference point in the antenna structure for the determination of height will be the junction of the vertical element with the four 45°-angle radials. Open model *9-3a.nec*.

```
CM Monopole with 4 radials
CM Radials angles at 45 degrees
CM Height 1 wl
CE
GW 1 11 0. 0. 1 0. 0. 1.23 .0015
GW 2 11 .162 0. .84 0. 0. 1 .0015
GW 3 11 0. .162 .84 0. 0. 1 .0015
GW 4 11 -.162 0. .84 0. 0. 1 .0015
GW 5 11 0. -.162 .84 0. 0. 1 .0015
GE 1
FR 0 1 0 0 299.7925 1
GN 2 0 0 0 13. .005
EX 0 1 1 00 1 0
RP 0 181 1 1000 -90 0 1.00000 1.00000
EN
```

This model begins with the height above ground built into the 5 GW commands. Because the antenna is relatively close to the ground, the RP command requests a "standard" 1°-increment theta pattern. Run the model and either save or print the theta pattern. For later reference, the gain at the TO angle of 80° is about 3.3 dBi, and the source impedance is 46.8 - j3.4 Ω. Next, open model *3-9b.nec*.

```
GM 0 0 0 0 0 0 0 9

RP 0 1801 1 1000 -90 0 0.10000 1.00000
```

The two lines shown represent changes to the original model. The GM entry raises the antenna structure 9m for a total height of 10λ above ground at the element junction point. The RP command uses an increment of 0.1° and hence requests 1801 steps to the radiation table. If you run this model, you will discover a maximum gain of 7.5 dBi at a TO angle of 88.6°. Save or print the theta pattern and compare it with the earlier one. Or else, examine **Fig. 9-6**.

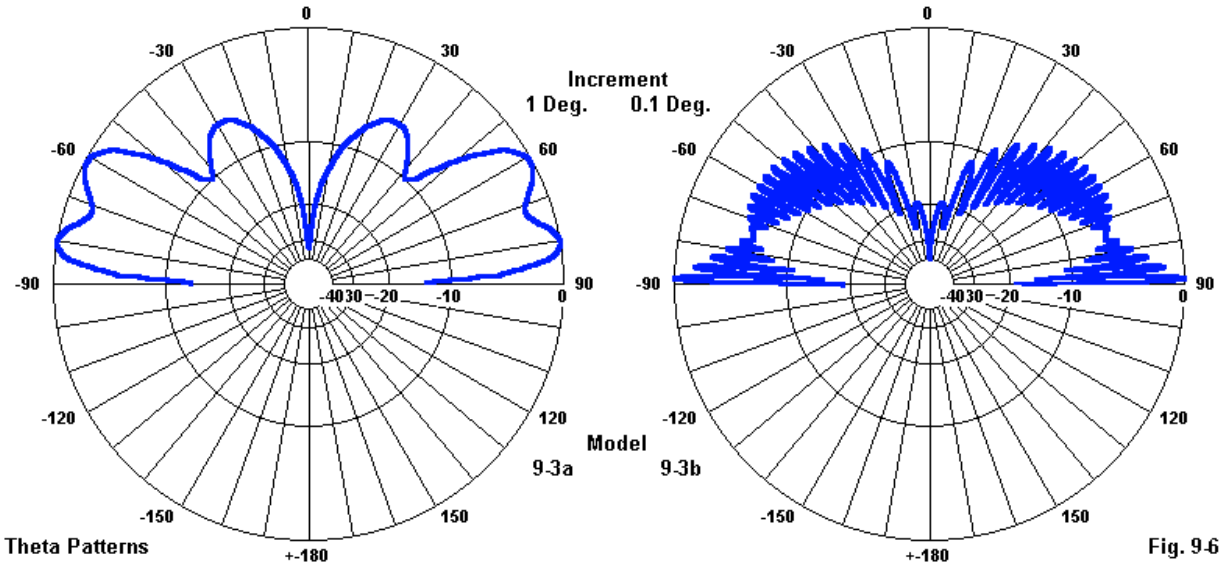

Although the monopole at 10λ above ground has a TO angle that is the same as for the horizontal antenna, the TO angle of the lower monopole differs considerably from its horizontal counterpart. The monopole has a higher TO angle and shows 3 rather than just 2 lobes on each side of the line up to the zenith point. Even though the higher monopole has the same TO angle as the corresponding dipole, the lobe development differs considerably above that angle. Compare **Fig. 9-6** with **Fig. 9-5**. Additionally, the gain differential between low and high dipoles is small, especially compared to the corresponding gain differences for the monopoles. The interactions between the antennas and the ground clearly differ. We shall have occasion to return to these models in a later chapter.

Although we have illustrated the required procedures for obtaining multiple patterns from frequency sweeps in the previous chapter, the matter deserves a second look in the present context. Let's suppose that we wish to use the dipole at 1λ above average ground at a number of frequencies between 290 and 310 MHz. Open model *9-4.nec*. This model returns to our horizontal dipole that is 1λ above average ground. In this case, we wish to obtain both phi and theta patterns for each of the three frequencies in the simplified sweep. The question we must now pose is whether the model that we have created will produce all 6 of the required radiation patterns. If we recall the notes from Chapter 8, we should arrive at a negative conclusion. Of course, the straightforward test of this result receives confirmation by running the model and counting radiation pattern tables in the NEC output file.

```
CM Dipole phi/theta patterns: frequency sweep
CE 1 m (wl) above Average Ground
GW 1 11 0 -.2375 0 0 .2375 0 .001
GM 0 0 0 0 0 0 0 1
GE
GN 2 0 0 0 13.0000 0.0050
FR 0 3 0 0 290 10
EX 0 1 6 00 1 0
RP 0 181 1 1000 -90 0 1.00000 1.00000
RP 0 1 361 1000 76 0 1.00000 1.00000
EN
```

The clue to our failure lies in the successive RP commands. Because the request for multiple frequencies creates a loop function, the second RP command executes only for the final frequency in the loop. Hence, we have 3 theta patterns but only 1 phi pattern, and it is for the highest frequency in the progression. The solution is simply to insert the FR command again between the RP commands. Open model *9-4a.nec*.

```
FR 0 3 0 0 290 10
EX 0 1 6 00 1 0
RP 0 181 1 1000 -90 0 1.00000 1.00000
FR 0 3 0 0 290 10
RP 0 1 361 1000 76 0 1.00000 1.00000
EN
```

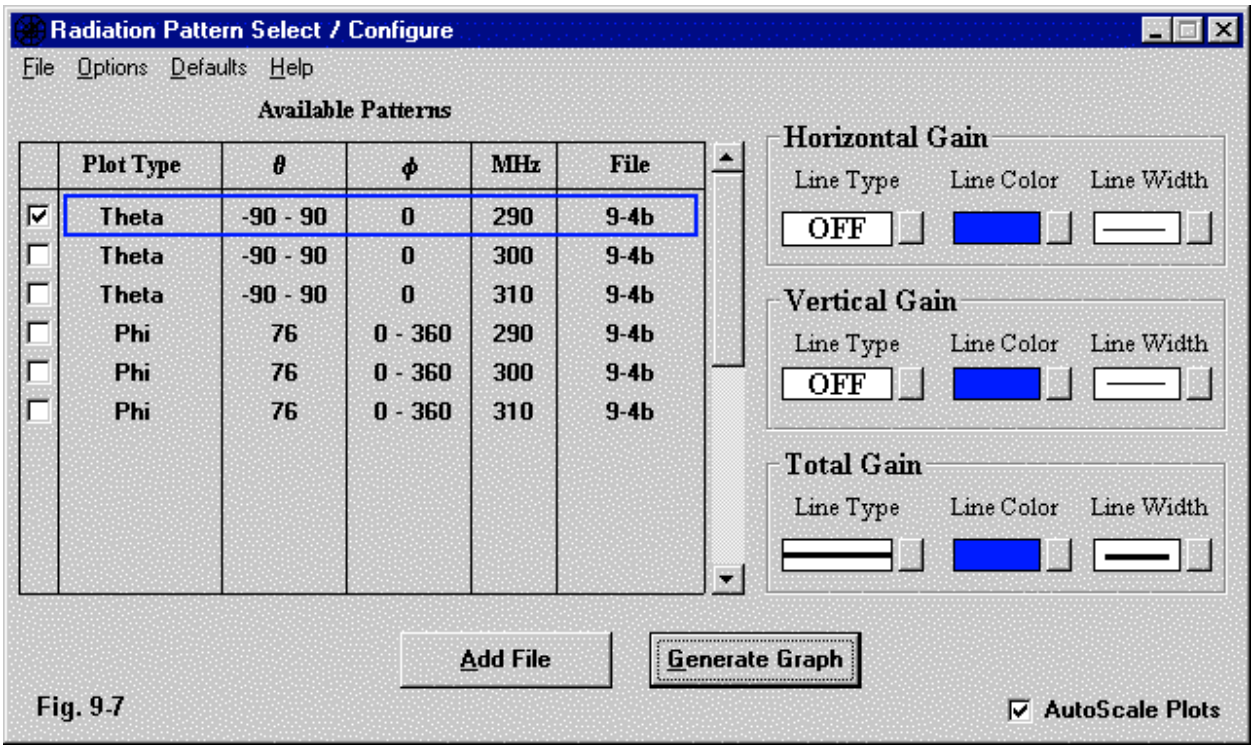

Fig. 9-7

As shown in **Fig. 9-7**, we can take a shortcut in the process of counting patterns to verify that all are present. The polar plot facility lists the radiation patterns for our selection. However, the use of the frequency sweep for both the theta and the phi plots raises another question. Open

each theta plot and opt for analysis for each frequency in the sweep. You should discover that the TO angle for each frequency is not the same. The lowest frequency shows a 75° TO angle, rather than the 76° angle for the other two frequencies. However, all three phi plots use a theta angle of 76°. Whether the differential makes a difference to the results of the work depends, of course, on the task specifications brought to the modeling enterprise.

There is one more facet to the frequency sweep that most modelers overlook. Reinserting the FR command to produce all 6 patterns also gives us 3 extra copies of the current tables. Although the 11-segment dipole does not use much space for its current tables, we anticipate creating frequency sweeps on much larger geometric structures, some having thousands of segments. As well, we may have dozens of frequencies within the sweep range. Hence, the NEC output file can grow to a very large size. For model 9-4a, the file requires 221 KB of storage space, mostly occupied by the radiation pattern tables. However, we can easily omit the unneeded replications of the current tables. Open model *9-4b.nec*.

```
FR 0 3 0 0 290 10
EX 0 1 6 00 1 0
RP 0 181 1 1000 -90 0 1.00000 1.00000
FR 0 3 0 0 290 10
PT -1
RP 0 1 361 1000 76 0 1.00000 1.00000
EN
```

The control command section of the new version of the dipole has only one difference from the previous version. After the added FR command, the model inserts PT -1 as a new command. Although it is too early in our work to explore the full dimensions of the PT command, control commands interact with other commands too thoroughly for us to by-pass it in this instance. The PT command, when given a value of -1, suppresses the printing of current tables. Since the first RP command has already executed, its current tables appear. However, the set produced for the second RP request does not appear in the output file. You may run the model and confirm this fact by examining the output file. For our simple dipole, the suppression of unnecessary replications of the current tables only saves us about 4 KB of storage space. The savings for large models can be very much greater.

Our RP commands so far have all used a XNDA setting of 1000. Before altering that setting, let's examine one more model: *9-5.nec*.

```
CM Free-space turnstile
CE V, H, and total patterns
GW 1 11 0 -.2375 0 0 .2375 0 .001
GW 2 11 -.2375 0 .005 .2375 0 .005 .001
GE
FR 0 1 0 0 299.7925 1
EX 0 1 6 00 1 0
EX 0 2 6 00 0 1
RP 0 361 1 1000 -90 0 1.00000 1.00000
RP 0 361 1 1000 -90 45 1.00000 1.00000
EN
```

The new model consists of two dipoles at 90° angles to each other. Each has its own source,

and the two sources are 90° out of phase with each other. The antenna differs from those we have examined so far by having in the theta pattern significant vertical and horizontal radiation components. The other models have largely been either so vertical or so horizontal that on a polar plot, one component would overlay the total field pattern and the other would disappear due to its very low values. However, the theta pattern of the turnstile has significant levels of each component and shows to some extent how the components contribute to the total field pattern. Run the model and set up the polar plot facility to show all of the components. The result should resemble **Fig. 9-8**.

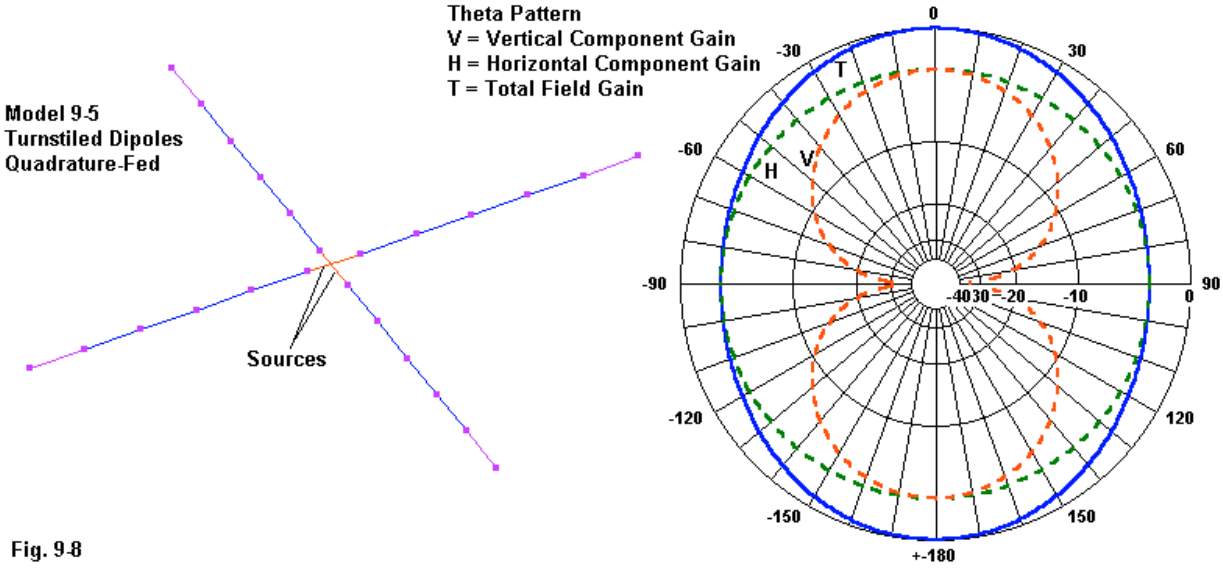

Fig. 9-8

At the -90° and 90° headings, the vertical component shows deep nulls. Hence, the total field line and the horizontal component line converge. At the 0° and 180° headings, the two components have equal gain, and the total field is a complex sum of the two. The radiation pattern table shows the individual component gains as -0.89 dBi, while the total field gain is 2.12 dBi. To perform the addition, first convert the component gain values to relative gain values, as shown earlier. Each component has a relative gain of 0.8147. If we add the 2 gain values, we get 1.6294. Converting that value into dBi requires that we take the log of the relative gain and multiply it by 10, for a result of 2.12 dBi. The total field gain of an antenna is always the complex sum of the gains of its horizontal and vertical components.

Altering XNDA

Many modelers never consciously reach beyond a XNDA setting of 1000 in their RP requests. If we succumb to this temptation, we in fact deny ourselves a good part of the power of the command, even within the restriction in this chapter of using only RP0 or space-wave options. Although we might spend a book covering all of the options, let's at least sample a few to determine if we can derive some useful outputs from our selections.

Open model *9-6.nec*, a model of an axial-mode helical antenna that we encountered in Chapter

4. The model is in NEC-2 form, which both NEC-Win Pro and GNEC can run. This first model retains the XNDA value of 1000, where the initial "1" indicates a request for the radiation pattern in terms of the vertical and horizontal components. Note that there are two RP commands, each identical except for the phi angle that forms the axis for the pattern. **Fig. 9-9** provides a view of the antenna above its perfect ground along with the vertical, horizontal, and total gain patterns taken at each of the listed phi angles.

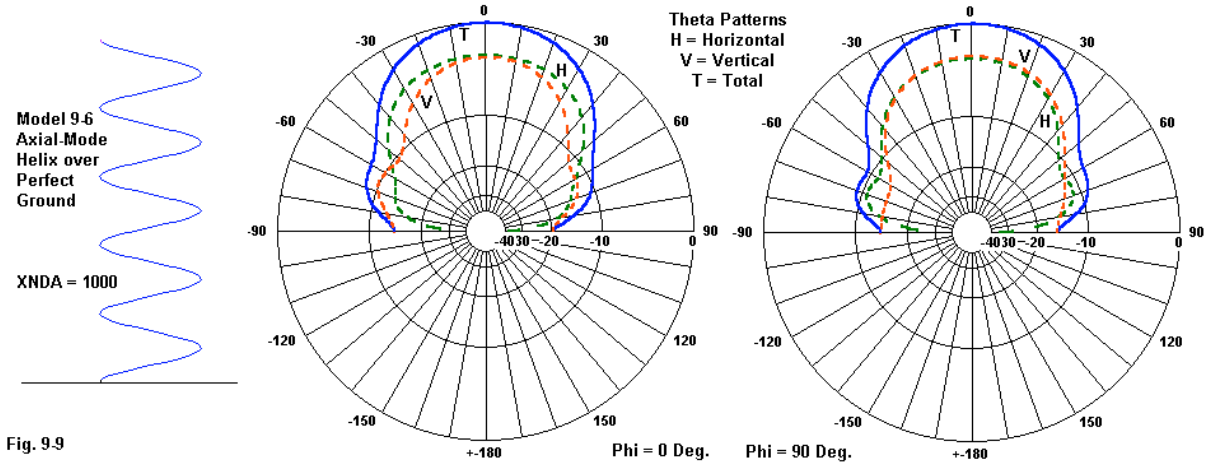

Fig. 9-9

If we look toward the zenith of the plot, we can find the relevant gain values in the NEC output file. If we examine the numbers for 0° in the first theta plot, we find a vertical gain of 5.87 dBi, a horizontal gain of 5.68 dBi, and a total gain of 8.78 dBi. As before, the component gains add through the procedure outlined to the total gain.

Now open model *9-6a.nec*, which contains only one change. In each RP command, XNDA is altered to 0000, indicating a request for radiation patterns using the major and minor axes plus the total gain. For all forms of radiation, the ratio of E_Θ to E_Φ will be other than 1 unless the radiation is circularly polarized. Classical texts often set the ratio to run between 1 and infinity, but NEC uses values between 0 and 1, as shown in the radiation pattern table under the heading of axial ratio. The ratio also sets a major and a minor axis to the resulting elliptical graph of values. The major axis will be tilted relative to the reference axis, and this companion value also appears in the radiation pattern table. The major and minor axes of the radiation form components that are as apt to the development of the total field as the more conventional vertical and horizontal components.

For model 9-6a, the axial ratio is 0.934, suggesting nearly circular polarization for the theta angle 0°, with respect to the pattern produced for a 0°-phi angle. Hence, we would anticipate reasonably close values for the major and minor axis gain. The table reports 6.06 dBi and 5.47 dBi for the major and minor axes, respectively. Like the vertical and horizontal components, the major and minor axis components add in the same complex manner to yield the total gain, 8.78 dBi. One result of this exercise is the fact that if all we ever need from a model is the total gain value, then the X setting of the XNDA combination will make no difference. However, for many models for which elliptical polarization is a significant factor, the use of the major/minor axis option may be more productive. For antennas using essentially linear elements, the use of vertical and horizontal components is both convenient and useful.

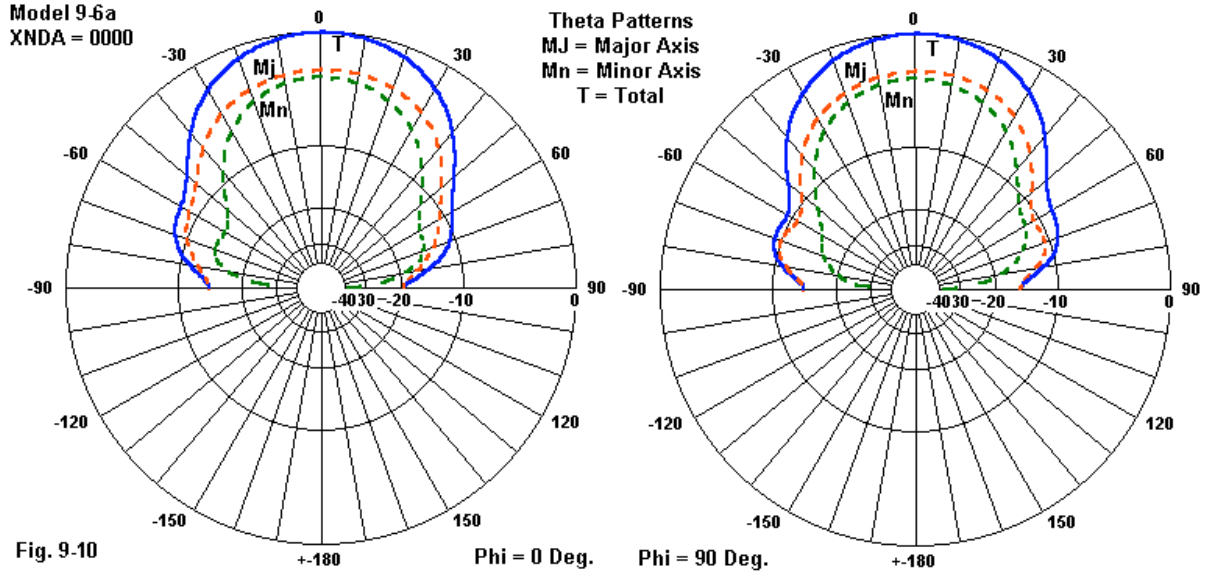

Fig. 9-10 presents the two theta patterns with their axis components. If you compare the total fields for each pattern with those in **Fig. 9-9**, you will find them identical. However, by inspection alone, you can see differences between the component patterns within the overall corresponding theta patterns.

We can also change the XNDA settings to obtain normalized gain data. Let's begin with a small 3-element Yagi. Open model *9-7.nec*, which uses the standard set of XNDA values.

```
CM 3-element Yagi
CE XNDA = 1000
GW 1 21 0 -.249 0. 0 .249 0. .002
GW 2 21 .162 -.227 0. .162 .227 0. .002
GW 3 21 .308 -.217 0. .308 .217 0. .002
GE 0
FR 0 1 0 0 299.7925 1
GN -1
EX 0 2 11 00 1 0.
RP 0 1 361 1000 90 0 1.00000 1.00000
EN
```

Although this model resembles on the surface an earlier Yagi model, it differs by optimizing the front-to-back ratio rather than the operating bandwidth. **Fig. 9-11** shows the outline of the design, along with two seemingly identical free-space phi patterns. When we check the analysis graphic that attaches to each pattern, it shows a gain of 7.82 dBi, with a source impedance in the 25 Ω range.

However, look carefully at the small lines leading from the center of the plot rearward. In the center plot, the line directly opposes the direction of a line from the center of the plot to the point of maximum gain. In the right-hand plot, the rearward line goes off at an angle to the peak of one of the small rearward lobes. The front-to-back values that attach to those lines are 53.2 dB and 26.5 dB, respectively.

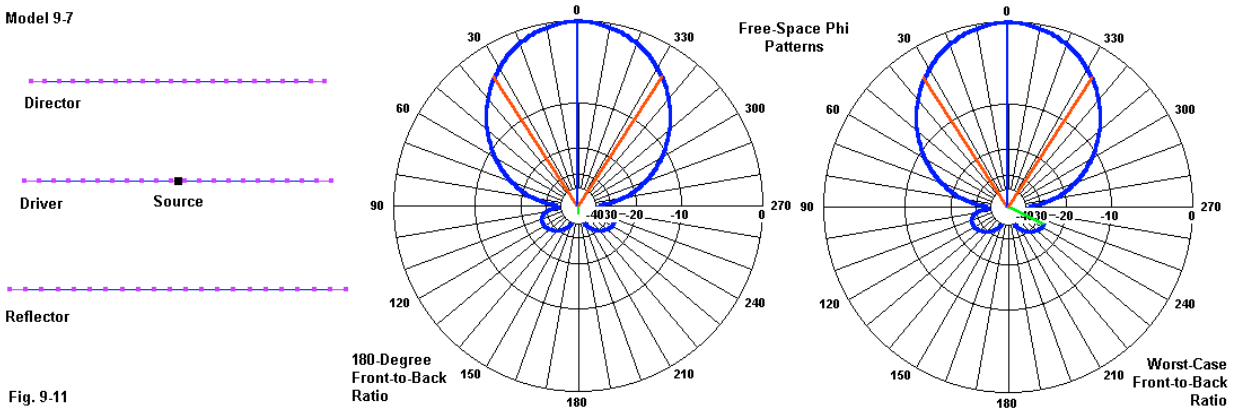

Fig. 9-11

The front-to-back ratio, in its most general sense, is the ratio of forward gain to rearward gain. From the output file radiation-pattern table, we can simply find the maximum forward gain and then subtract the appropriate rearward gain. The open question is which rearward gain from the two rearward quadrants we should use.

Actually, there are three working notions of front-to-back ratio generally current in antenna work:

180-Degree front-to-back ratio: This ratio is simply the difference in gain between the maximum forward gain angle and another angle 180° opposite. Check the radiation table for model 9-7 at 180°. The value for total gain at that heading is -46.0 dBi. 7.82 - (-46.0) dBi = 53.8 dB: this value is the 180-degree front-to-back ratio. However, notice that the point used to derive this number is "dimpled" and there are places in the rear quadrant where the ratio is much less.

Worst-case front-to-back ratio: This ratio uses the maximum gain anywhere in the rear quadrants as the basis for establishing the ratio. In some cases, the side points, as defined by the 90° angle from the maximum forward gain heading, determine where the rear quadrant begins. Between headings of 90° and 270°, the maximum gain values occur at 115° and 116° and repeat at 244° and 245°. The gain value at these points is -18.7 dBi. 7.82 - (-18.7) = 26.5 dBi. This ratio is the worst value that can occur as a front-to-back ratio.

Front-to-rear ratio: To overcome misleading aspects of both 180-degree and worst-case front-to-back ratios, some engineers have adopted the front-to-rear ratio. This ratio is based on averaging the power gain of the antenna over the rear quadrants and using the resulting figure as the basis for a ratio with the forward gain. There is no general standard on exactly how many data points to use or where to locate them. To further confuse matters, some technical writers refer to the worst-case ratio as the front-to-rear ratio.

The plots for model 9-7 show 180° and worst-case front-to-back ratios, both of which are options within the polar plot module in NSI software.

We can arrive at both front-to-back ratios without recourse to post-run calculations by changing the XNDA setting. The second entry (N) controls the normalization of one out of the many gain

values that we can obtain with settings to the other XNDA factors. Since the front-to-back ratio is a function of the total gain, let's set XNDA at 1500 to normalize the total gain. Open model *9-7a.nec*.

```
RP 0 1 361 1500 90 0 1.00000 1.00000 0 0
```

The revised RP command not only shows the new XNDA value set, but also reveals that we must add 2 more entries to it. The maximum gain value for the normalization process goes into position F6 (GNOR). However, to have an F6 entry, we must also fill in F5 (RFLD). Since we do not wish to specify any specific distance value for F5, we enter a zero. However, the zero in F6 is a working value. All normalized gain values will appear as negative values, since the F6 entry converts the maximum value of 7.82 dBi to 0 dB.

Run the model. Then open the NEC output file. You will discover that you have not lost the standard power gain radiation table. Rather, NEC adds a new table of normalized values beyond it. The following samples will establish the front-to-back values that we earlier calculated, although as negative numbers.

```
- - - - NORMALIZED GAIN - - - -
TOTAL GAIN
NORMALIZATION FACTOR = 7.82 DB

- - ANGLES - -      GAIN
 THETA     PHI        DB
DEGREES  DEGREES

 90.00     0.00      0.00        (Maximum gain heading)

 90.00   115.00    -26.49        (Worst-case front-to-back ratio)
 90.00   116.00    -26.49

 90.00   180.00    -53.82        (180° front-to-back ratio)

 90.00   244.00    -26.49
 90.00   245.00    -26.49
```

Although we have not exhausted the possible combinations of XNDA values, these samples may serve to introduce the importance of attending to this portion of the RP command.

Some Custom Patterns

Normalizing the gain values of model 9-7a forced us to put a dummy value into the F5 position, the distance from the coordinate origin to the sampling point. We used a dummy value so that the model output file radiation pattern table would be identical to the one for model 9-7 except for the addition of the normalized value table. However, there is no reason why we should not place a real value there.

Open model *9-8.nec*, and examine the RP line. We shall continue to use the free-space 3-element Yagi as our test model.

```
RP 0 1 361 1000 90 0 1.00000 1.00000 1000
```

The only change relative to model 9-7 is the addition of the last entry, 1000 meters. The entry meets the condition of being well into the far field of the antenna. Run the model and then compare the radiation pattern table to the one that leaves RFLD blank or zero. The first difference that we notice is in the heading.

```
- - - RADIATION PATTERNS - - -
RANGE= 1.000000E+03 METERS
EXP(-JKR)/R= 1.00000E-03 AT PHASE-351.01 DEGREES
```

An RP command without an entry in the RFLD position produces a blank area beneath the radiation pattern heading, because the factor exp(-JKR)/R is not included in the far-field calculations. Next, compare the Ephi values for model 9-7 and 9-8 for the 0° phi heading. The non-specific model yields 1.809E03 peak volts at -1.97°; the model with the 1000-m specification yields 1.809E-03 peak volts at an angle of -352.98°. The voltage is 6 orders of magnitude weaker with the phase angle shifted by the amount in the exponent.

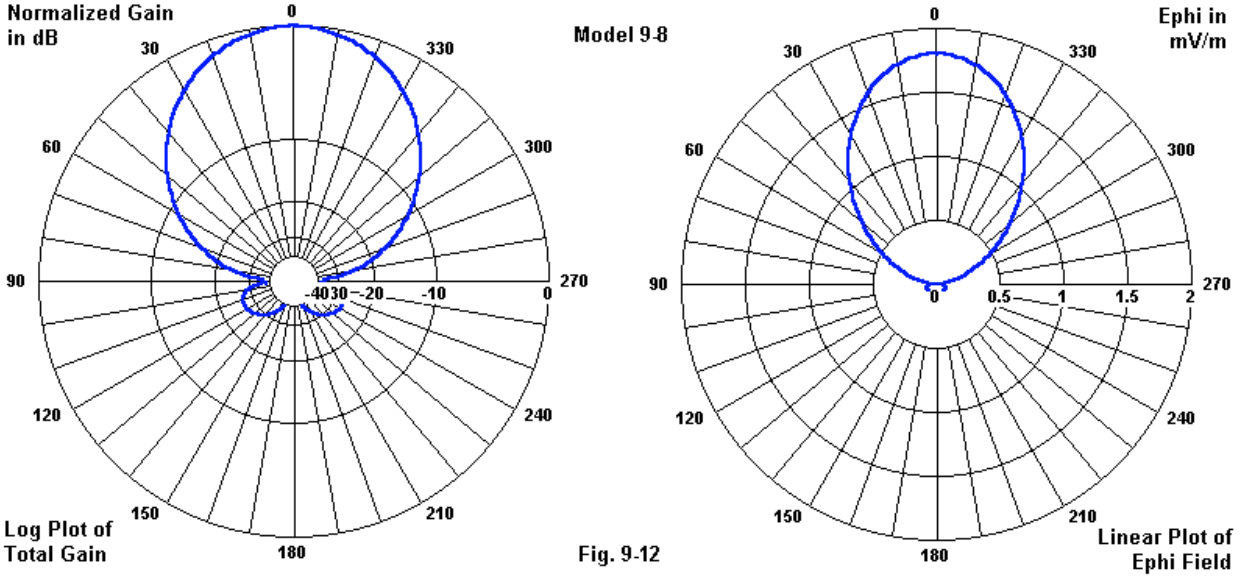

Fig. 9-12

Fig. 9-12 places a normal log plot of the phi pattern along side of a polar plot of the Ephi values for model 9-8. (If you examine the Etheta portion of the radiation pattern table, you will see clearly why that factor has been ignored: all values are in the range E-15 or smaller.) Unlike the gain pattern, for which a log scale is sensible for some purposes, the E-field plot uses a linear scale. Hence, its exact appearance depends on the values selected for the maximum and minimum values: 2 and 0 in this case, where the unit of measure is peak mV/m. In most cases, you may be able to glean more detail from rectangular plots, especially if you set the maximum and minimum values to let parts of the data go off-plot in order to enhance the portion under scrutiny.

There are occasions on which we may wish to set up a gain plot that uses multiple headings for both phi and theta. Open model *9-8a.nec*, which is the same 3-element Yagi in free space.

However, the RP command now shows values for a complete sphere.

```
RP 0 181 361 1000 0 0 1.00000 1.00000
```

To plot a complete sphere, we let the phi entries form complete circles: 361 steps from 0° in 1° increments. Then we set the theta entries to form semicircles from 0° (zenith) in 1° increments for 181 steps. Run the model, but do not attempt to view any patterns, since there will be so many that the polar plot module will overload.

We should note several things about the resulting table. First, although the matrix portions of the calculation did not change, the model took 120 times as long to run as model 9-7, which requested a single phi plot. Second, the file requires about 125 times more output file storage space as model 9-7. Third, as the following lines show, the core processes the file by cycling through all theta values for the first phi angle value, and then proceeds to do the same for the second and succeeding phi angle values.

```
- - - RADIATION PATTERNS - - -

- - ANGLES - -           - POWER GAINS -
THETA     PHI       VERT.     HOR.    TOTAL
DEGREES  DEGREES       DB       DB       DB
   0.00     0.00  -999.99    -2.34   -2.342
   1.00     0.00  -999.99    -2.08   -2.078
   2.00     0.00  -999.99    -1.82   -1.819
   3.00     0.00  -999.99    -1.56   -1.564
   4.00     0.00  -999.99    -1.31   -1.312
   5.00     0.00  -999.99    -1.07   -1.065
```

The RP command that we have just sampled is identical to the one used in the special (3-dimension) surface plot facility. NSI keeps such plots separate in part due to the size of the output files created. The program only stores the file as long as you use the module and then erases the file upon facility closure. Indeed, you may wish to delete the file that you generated.

There is another use for the custom plot request, but it involves a further alteration of the XNDA settings. Open model *9-8b.nec* and examine the RP request.

```
RP 0 181 361 1002 0 0 1 1
```

XNDA now reads 1002. In the A position, a value of 2 is a request for gain averaging, just as is a value of 1. However, the 2-option requests a suppression of the printing of the individual gain values in tabular form. In addition, the theta angle begins at 0° to ensure counting from the zenith downward (rather than beginning at -90° for counting from horizon to horizon). If you run the model--as you should--you will have no data for a polar or rectangular plot. As well, without the need to print the pattern values, the run saves nearly half the total core run time.

```
- - - RADIATION PATTERNS - - -
AVERAGE POWER GAIN= 9.99143E-01
       SOLID ANGLE USED IN AVERAGING=( 4.0000)*PI STERADIANS.
```

The suppression of the individual data points compresses the file size and the run time. More

important, it produces a value for average gain in free space: 0.999143. If you independently run the average gain test on this model, you will find the same reported AGT value, since the model set-up is also the set-up for the AGT test. Note the solid angle entry. If the value in parentheses is not 4.000 for a free-space model, then the RP set-up has an error relative to yielding a proper AGT value.

The NEC-4 core produces an additional line in its average gain report. For model 9-8b, the line is the following.

```
POWER RADIATED ASSUMING RADIATION INTO 4*PI STERADIANS = 8.98949E-03
WATTS
```

This value is simply the average gain times the supplied power, which appears in the power budget immediately above the radiation pattern. The NEC-4 run of the model produces an average gain of .999149, while the supplied power is 8.9972E-03. The product of the two figures is 8.9895E-03. You may perform a similar calculation on the NEC-2 values for model 9-8b.

Let's place the Yagi over a perfect ground and reset the RP command for a hemisphere. Open model *9-8c.nec*.

```
CM 3-element Yagi
CE XNDA = 1002; over ground
GW 1 21 0 -.249 0. 0 .249 0. .002
GW 2 21 .162 -.227 0. .162 .227 0. .002
GW 3 21 .308 -.217 0. .308 .217 0. .002
GM 0 0 0 0 0 0 0 5
GE 0
FR 0 1 0 0 299.7925 1
GN 1
EX 0 2 11 00 1 0.
```

The revised version of the model adds a GM line to lift the Yagi off the ground. Next, it specifies a perfect ground (GN 1). Finally, it revises the RP request so that the theta angles covered run from zenith to horizon and not below. Running the model yields the following average gain entry in NEC-2.

```
AVERAGE POWER GAIN= 1.99827E+00
       SOLID ANGLE USED IN AVERAGING=( 2.0000)*PI STERADIANS.
```

The same model run on NEC-4 produces the following report lines.

```
AVERAGE POWER GAIN= 1.99828E+00
       SOLID ANGLE USED IN AVERAGING=( 2.0000)*PI STERADIANS.

POWER RADIATED ASSUMING RADIATION INTO 4*PI STERADIANS = 1.79292E-02
WATTS
```

First, run the AGT test on your core to confirm a reproduction of the average power gain numbers. Then we can turn to the odd report of radiated power in the NEC-4 report. Note that

over perfect ground, the average power gain uses 2π steradians, but the power radiated uses a value of 4π. Over any ground, the actual power radiated will be half the NEC-4 reported value, or 8.96E-03 watts. For a direct calculation of the radiated power when the model specified a real or a perfect ground, take half the average power value and multiply times the supplied power in the power budget. For the NEC-4 case, the supplied power is 8.97E-03 watts. Half the average power gain is 0.99914. The product of the 2 values is 8.96E-03 watts. You may perform the same direct calculation on the NEC-2 results without reference to a reported average radiated power. Although at the present moment, these calculations may seem to be idle exercises, they will acquire significance in a later chapter in Part C of this volume.

Despite that fact that we have sampled a very wide variety of far-field pattern requests using the RP 0 command, we have not exhausted the possibilities. At most, we have looked at all parts of the command structure with sufficient variations to make us keenly aware of the versatility built into the command. There is much data about a model that we can glean from the command if we take the time to become acquainted with its various parts, along with the resulting NEC output reports for radiation patterns.

Summing Up

The RP0 command is the most basic request for an output table that provides calculated performance data on a modeled antenna. Our initial examination of this command adhered to several restrictions. First, we looked at only space-wave applications of the command. Second, we by-passed a number of NEC-2 options that apply to special ground specifications that we shall meet in a future chapter. Third, we confined ourselves to antennas that use a voltage source applied to one or more segments of the geometry structure. Still, even within these restrictions, the RP command has so many variables that we were able only to sample the range of opportunities.

The structure of the command has several facets. We learned to enter the range of sampling points for 2-dimensional radiation patterns for both theta and phi orientations by specifying the starting angle, the increment between successive angles, and the number of steps or increments to use. Of course a 2 dimensional pattern in either theta or phi requires a single angle in the other angle set to fully define it. As well, there are differences in the set-up for free-space patterns and for patterns over a perfect or real ground. We also noted the caution, especially applicable to theta plots over ground, of using an angle increment sufficiently small to reveal accurately the details of the lobe and null structure of the pattern.

Besides entering the correct angular coordinates for a desired pattern, we also sampled some of the variations in patterns that we may obtain by various combinations of settings in the XNDA entry, where each letter stands for a range of options. We looked at the difference between using horizontal and vertical components of the total field on the one hand and major axis and minor axis components on the other. A sample of the normalization options, including the need to enter a normalization value in the RP command, showed us the additional table that NEC produces for these values. Gain averaging gave us a look ahead at how NEC can perform an average gain test of an antenna under test.

Besides exploring the RP command itself, we also looked at the radiation output table and its relationship to both the RP command and the implementing software graphics. For example, the radiation pattern table contains information on the Ephi and Etheta values, and when we combine this potential with a selected distance in the RFLD position of the command, we may obtain and graph calculated field strengths at the specified distance. Besides the common 2-dimensional theta and phi patterns, we may generate more comprehensive radiation tables for a full sphere in free space and for a complete hemisphere over ground. These potentials also carry with them some cautions. A full sphere of values can give us a 3-dimensional portrait of the antenna space-wave pattern and are necessary for calculation of both average gain and average radiated power. However, they extend core run times and produce exceptionally large output files for storage.

The RP command, even when restricted to space-wave applications, is exceedingly versatile. However, the price of versatility is a requirement to understand the range of variables that the command contains and how to use each one effectively.

10.
Voltage and Current Sources and Frequency Specifications

***Objectives**: We shall explore two commands in these pages. Excitation, especially the voltage source, is necessary to any model and we shall learn how to place and control sources, and even how to convert a voltage source into a current source. The second command necessary to all models is the request for one or more frequencies, and we shall look at both linear and multiplicative sweeps.*

Unless we are only interested in developing wire geometries, we must add some form of excitation (EX) and a frequency request (FR) to give the core enough data from which to calculate segment currents and other important information. Since this part of our work concerns far-field analysis, we shall restrict ourselves to only one of many excitation forms, the voltage source (EX0). However, this form of excitation will prove flexible enough to give us both voltage and current sources. Nevertheless, we shall have to develop some interesting techniques to set the source properly into the model so that it gives us a satisfactory result.

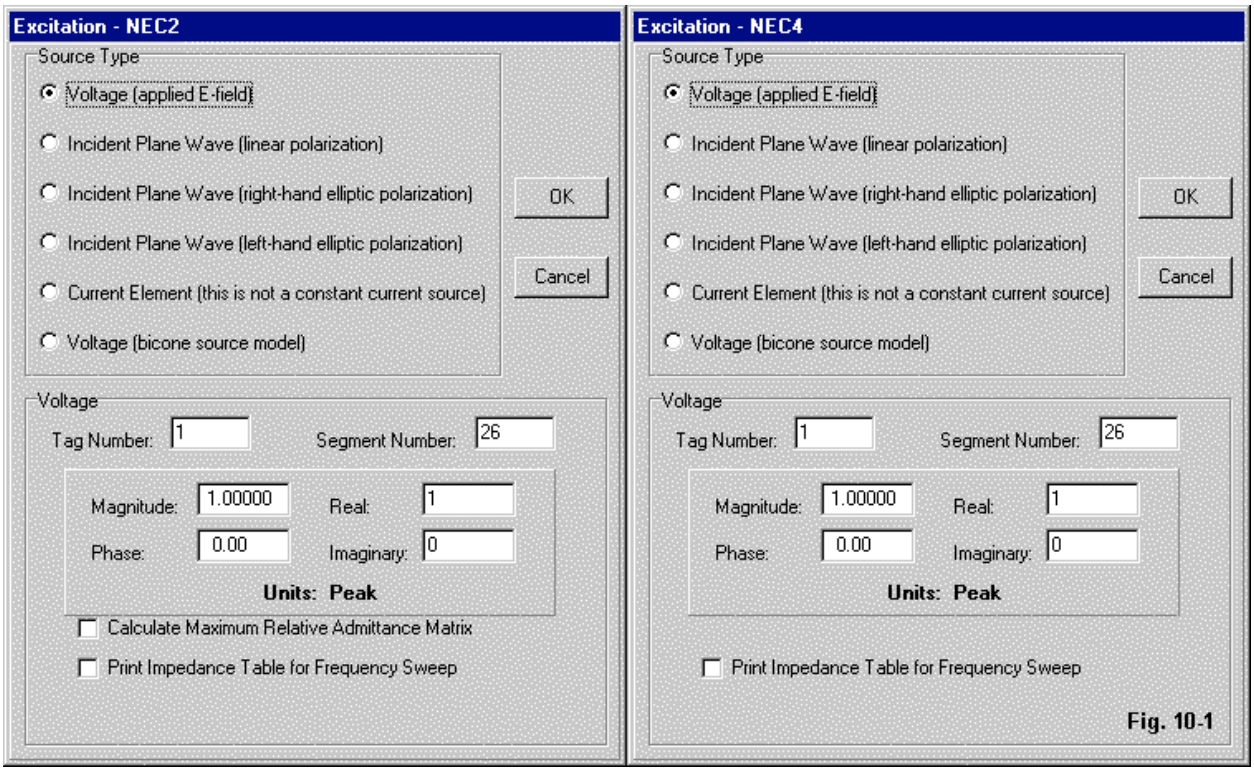

Fig. 10-1 compares the help screens for the NEC-2 and NEC-4 versions of the command. In fact, they are identical. In practice, few modelers made use of the NEC-2 supplementary feature of calculating the maximum relative admittance matrix, resulting in its omission from the NEC-4 version of the command. As well, few modelers use the facility for printing the impedance table,

since the software supplies that data combined with a post-run calculation of the source VSWR relative to a user-selected reference impedance. Besides the voltage source, the second most-used sources are the incident plane wave options. We shall explore the use and structure of these source options in Part C of this volume.

The FR or frequency command has a simple structure. However, learning to use the sweep function built into the command requires some care. Before we leave this chapter, we shall have mastered both linear and multiplicative sweeps.

Voltage Source Placement and Impedance Values

To obtain far-field patterns from an antenna that we have described in the geometry portion of the NEC input file, we must place at least one source somewhere on the structure. The EX command allows us to place a source. If we need multiple sources, we replicate the EX command for as many sources as we require.

```
Cmd   I1    I2    I3    I4    F1    F2    F3    F4    F5    F6    F7
      Type  Tag   Seg.  TBL   ERL   EIM   NORM  ---   ---   ---   ---
            No.   No.
EX    0     1     26    00    1     0
```

The sample command shows in the first line the maximum range of the NEC-4 version. NEC-2 allows only 6 floating decimal positions. However, the EX0 selection requires at most 3 floating decimal positions and normally only 2, since the request for tables is rarely used.

A voltage source normally requires that we specify its position in terms of a tag number and a relative segment number. If we wish to specify the source in terms of its absolute segment number, we place a zero in I2. The second part of the data includes the voltage value as real and imaginary components. If the input data at hand is the voltage magnitude and phase angle, we must pre-convert it into real and imaginary components. As **Fig. 10-1** shows, the software itself allows for either mode of entry, with the proper values inserted into the resulting EX0 command line.

Special Note: All NEC input values for core use are peak volts, not RMS volts. As well, all output voltage and current values are peak values, not RMS values. Independent calculations of any power levels must covert the values to RMS.

You may place a source on any segment of any wire in the wire geometry. For a centered source, you will normally assign the wire containing the source an odd number of segments, since the virtual position of any source is at the center of the segment to which you assign it. The corresponding position for a monopole that touches ground or a ground plane is at the lowest segment of the vertical structure. (For a NEC-4 model with a vertical structure that penetrates the ground, the lowest allowable segment for a source is the first segment above ground.)

Open model *10-1.nec*. Once more, we shall use the simplest possible antennas as examples so that we may focus on the command that we are exploring. Hence, we have a free-space dipole. For most--but not for all--of the exercises in this chapter, the actual patterns produced by the

antenna will be of no interest. More significant to our efforts will be the source impedance reports. Therefore, we shall force execution of the model with an XQ command rather than with an RP command.

```
CM Dipole with odd segments
CE Standard source placement
GW 1 51 0 -.2375 0 0 .2375 0 .001
GE
FR 0 1 0 0 299.7925 1
EX 0 1 26 00 1 0
XQ
EN
```

If we run this model, we may obtain the source impedance conveniently from the software-supplied special table. It will include a 75-Ω SWR value.

```
Input Impedance and VSWR

Frequency      Tag  Seg. Real(Z)   Imag(Z)   Mag(Z)    Phase(Z)  Zo      VSWR
-------------------------------------------------------------------------------
299.790000      1    26  72.402    1.810     72.424    1.432     75.000  1.04
```

Relative to past dipoles that have used the same excitation in free-space, this version shows a slightly different set of impedance values--not significantly different, but enough to be noticeable. Note the number of segment assigned to the dipole: 51 rather than the minimal 11. Hence, we assigned the excitation to segment 26 at the center of this more highly segmented dipole.

It is important to understand from where the software draws the source impedance value. Open the NEC output file and locate the section labeled "antenna input parameters."

```
                    - - - ANTENNA INPUT PARAMETERS - - -

TAG   SEG.    VOLTAGE (VOLTS)         CURRENT (AMPS)         IMPEDANCE (OHMS)
NO.   NO.    REAL        IMAG.       REAL        IMAG.       REAL        IMAG.
 1    26 1.00000E+00 0.00000E+00 1.38032E-02-3.45017E-04 7.24017E+01 1.80971E+00
                                                          ADMITTANCE (MHOS)      POWER
                                                           REAL       IMAG.     (WATTS)
                                                       1.38032E-02-3.45017E-04 6.90160E-03
```

The output entry requires two lines in visible type for easy reading. Even then, it requires careful tracing to understand fully the wealth of data. After locating the source, the line replicates the voltage source information from the EX0 entry. Then follow the calculated current, impedance, admittance, and power at the source segment. The line reveals one of the difficulties involved in parsing a NEC output file for other modes of presentation: the entries beginning with a minus sign have no other separation from the preceding entry on the line.

To convert impedance into admittance--or the reverse--first convert the form into a magnitude and phase angle. To arrive at the power report in watts, convert the current magnitude (derived from the real and imaginary components) to RMS, square the result, and multiply by the real component of the reported impedance. Or, multiply half the square of the current magnitude times the real component of the impedance.

Where the radiation pattern gains (in dBi) and the source impedance are the most critical factors

in an analysis, you may use any value of voltage for the EX0 entry. 1.0 volt peak is a common default value.

Fig. 10-2

Fig. 10-2 shows the structure of our standard model and a simple variation to which we have assigned 50 segments, an even number. If we wish to know the impedance at the element center, which is now a junction of 2 segments, we can place sources on the segments each side of center. If the segments are short enough, the result will be a very close approximation of the single source at the exact center of the element. Open model *10-1a.nec*.

```
EX 0 1 25 00 1 0
EX 0 1 26 00 1 0
```

The extracted lines show the two assignments. Run the model and find the reported source impedances.

```
Input Impedance and VSWR

Frequency      Tag  Seg. Real(Z)   Imag(Z)   Mag(Z)    Phase(Z)
-------------------------------------------------------------
299.790000      1    25  36.217    1.123     36.234    1.776
299.790000      1    26  36.217    1.123     36.234    1.776
```

Since the two sources are in series and on adjacent segments, we may arrive at a single source impedance value by summing the components. The result is 72.434 + j2.246 Ω to which we may compare the single source results of 72.402 +j1.810 Ω. We shall obtain a greater variance among source impedance reports by varying the number of segments in the dipole than we find between these two reports.

Part of the reason for the close proximity of the impedance values that result from two different ways of assigning sources stems from the structure of the model. In this case, we assigned a large number of segments to the 1/2λ dipole, but remained well within even the most conservative limits for the segment-length-to-radius ratio. Hence, the split sources were each very close to the centerline of the dipole. In addition, the current magnitude and phase angle change very slowly in the high-current region of the antenna. Considerably more variation would show itself if the antenna remained center-fed, but was 1λ long. You may raise the frequency entry to 600 MHz to test each of the two models.

Under some circumstances, we may wish to tailor the geometry structure to the source

placement. Consider the three options shown in **Fig. 10-3**.

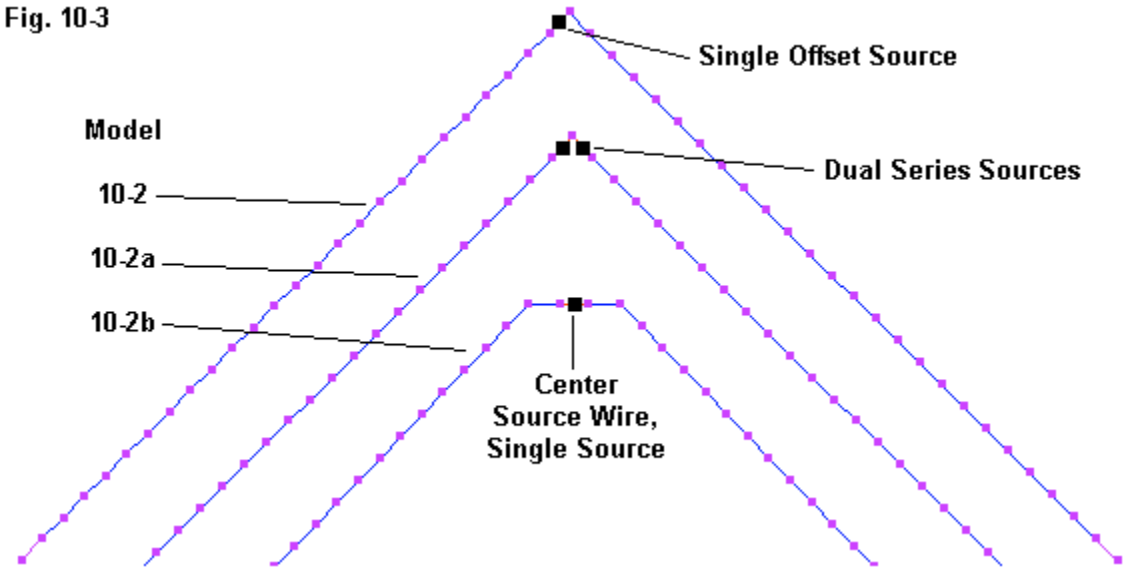

Open model *10-2.nec*, a standard inverted-V antenna at the test frequency. To obtain resonance in the V configuration, the legs are slightly longer than the legs of the dipole as measured from the center outward. The initial model uses a single source placed on one of the two segments that meet at the apex of the V.

```
GW 1 25 0 -.174 -.174 0 0 0 .001
GW 2 25 0 0 0 0 .174 -.174 .001
GE
FR 0 1 0 0 299.7925 1
EX 0 1 25 00 1 0
```

Run the model and confirm the source impedance of 45.1 + j2.8 Ω. Now open model *10-2a.nec*. This version uses the same construction as the first version, but places a source on each of the adjacent segments at the V apex.

```
EX 0 1 25 00 1 0
EX 0 2 1 00 1 0
```

This version of the inverted-V model returns a pair of source impedance values, each of which is 22.55 + j1.1 Ω. Their sum is 45.1 + j 3.0 Ω. The third version of the model is convenient in situations where we might like to alter the angle of the descending wires while retaining a fixed source position. Open model *10-2b.nec*. The model uses a center source wire containing 3 segments to ensure that the segment lengths on each side of the source segment are identical to the length of the source segment itself. As well, the descending legs are segmented so that all segments in the model are as close to identical as feasible. The segmentation data table in the output file tells us that the source wire segments are each 0.00987-m long, while the leg segments are 0.00952-m long.

```
GW 1 24 0 -.174 -.174 0 -.0148 -.01 .001
GW 2 3 0 -.0148 -.01 0 .0148 -.01 .001
GW 3 24 0 .0148 -.01 0 .174 -.174 .001
GE
FR 0 1 0 0 299.7925 1
EX 0 2 2 00 1 0
```

The single source returns an impedance of 43.6 + j2.5 Ω.

The importance of the method of model construction in the third version of model 10-2 appears within a model that we have previously encountered: the dual-band dipole for the 30-meter and 17-meter amateur bands. Open model *10-3.nec* and review the pair of dipoles that meet in the middle. Try to find a position for a single source adjacent to the junction of wires for a source that gives a reasonable impedance report for both 10.125 MHz and 18.108 MHz. **Fig. 10-4** shows us both the initial model and the configuration that we have previously developed as a solution.

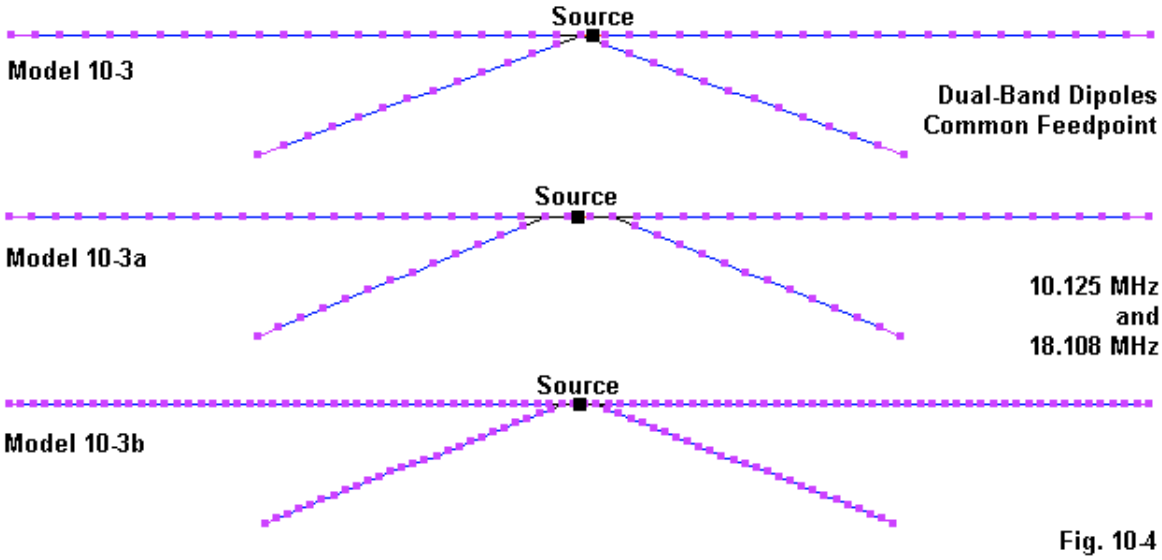

Fig. 10-4

Open model *10-3a.nec*, our initial solution. The model uses 5 wires, with tag 2 representing the center source wire that uses 3 segments.

```
GW 1 23 -7.071 0. 0. -.435 0. 0. .0010262
GW 2 3 -.435 0. 0. .435 0. 0. .0010262
GW 3 23 .435 0. 0. 7.071 0. 0. .0010262
GW 4 13 -4 0. -1.5 -.435 0. 0. .0010262
GW 5 13 .435 0. 0. 4 0. -1.5 .0010262
GE 0
FR 0 1 0 0 18.108 1
GN -1
EX 0 2 2 00 1. 0.
```

First, note the segmentation of the dipole legs. At the higher frequency, segmentation is perhaps double conservative recommendations for the number of segments per half-wavelength (10).

Second, run the model and chart the source impedances for each frequency, along with the AGT value for each band. The following lines present both NEC-2 and NEC-4 values.

Core	Freq. MHz	Impedance R +/- jX Ω	AGT	Core	Freq. MHz	Impedance R +/- jX Ω	AGT
NEC-2	10.125	53.1 + j7.2	1.175	NEC-4	10.125	60.6 - j2.6	1.029
	18.108	27.4 + j9.4	1.151		18.108	30.7 - j8.3	1.020

The model uses segment lengths in each wire that are very close in length. The segment length for the 7.07-m long legs is 0.285 m; for the 4.0-m short legs 0.297 m; for the source wire 0.290 m. Although the AGT scores are quite reasonable, there is some difference between the NEC-2 and NEC-4 values. We might wonder if we can draw them closer to perfect 1.0 values. One route that many modelers use almost instinctively is to add more segments per wire, while maintaining the relative length equality. Open model *10-3b.nec*.

```
GW 1 46 -7.071 0. 0. -.225 0. 0. .0010262
GW 2 3 -.225 0. 0. .225 0. 0. .0010262
GW 3 46 .225 0. 0. 7.071 0. 0. .0010262
GW 4 26 -3.9 0. -1.5 -.225 0. 0. .0010262
GW 5 26 .225 0. 0. 3.9 0. -1.5 .0010262
```

The leg wires double their segmentation density. To compensate, the source wire (GW2) is now shorter, bringing it closer to the length of a center insulator in a physical implementation of the dual dipole. The segment length of the unchanged long legs is now 0.149 m; for the revised 3.9-m short legs 0.152 m; and for the new center source wire 0.150 m. Our question is whether the carefully increased segmentation has effected an improvement in the AGT values. The way to find out is to run the model and chart the results.

Core	Freq. MHz	Impedance R +/- jX Ω	AGT	Core	Freq. MHz	Impedance R +/- jX Ω	AGT
NEC-2	10.125	52.4 - j4.9	1.192	NEC-4	10.125	60.6 - j11.0	1.038
	18.108	30.6 - j3.1	1.203		18.108	35.2 - j13.1	1.034

With models 10-3a and 10-3b, the NEC-4 AGT values are superior to those yielded by NEC-2. However, both cores show a degradation of values with increased segmentation. The point of the exercise is to demonstrate that the methods we might use to place a source in a usable position do not resolve all limitations inherent to the cores. We early noted that wires brought together at acute angles tend to yield less accurate results than linear or right angle wire junctions. The weakness is more severe in NEC-2 than in NEC-4. The problem is mild in this model sequence, but not wholly absent. The difficulty results from the degree of surface penetration of one wire with another at the apex of the angle. Shortening segment lengths places the penetration closer to the centers of the segments forming the acute angle. Hence, adding segments is not the solution to the condition, even if the technique results in a source wire that more closely approximates the physical conditions of implementing the antenna. In the end, we are left with a compromise between the degree to which the model can reflect reality and the conditions of perfect model adequacy. The overall reminder offered by this model sequence is that the conditions governing correct use of the control commands are not independent of the conditions and limitations associated with the geometry portion of a model.

Source placement offers challenges, even with linear wire elements. Consider an off-center-fed half-wavelength element for 3.5 MHz. We shall make it our goal to place the source as precisely as possible at a position that yields a near-resonant impedance of 300Ω. **Fig 10-5** shows us 3 strategies.

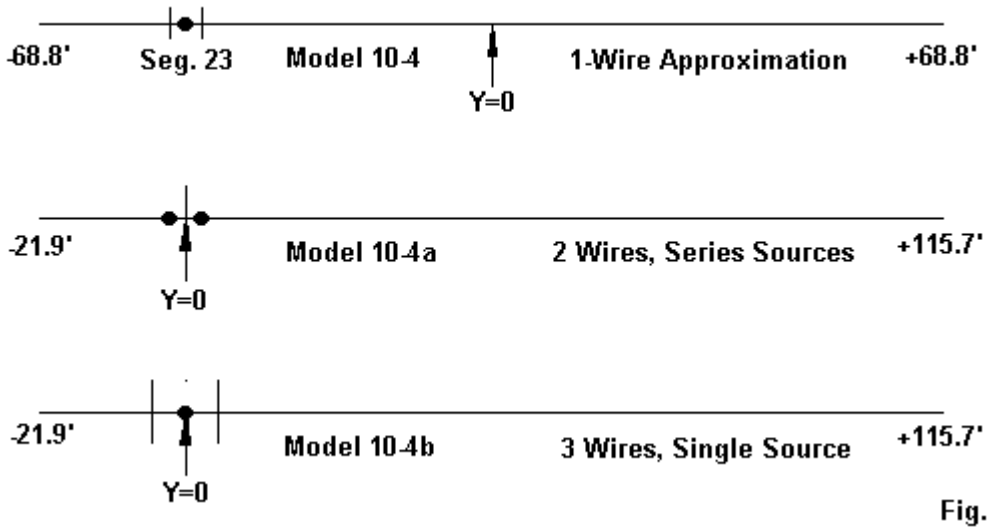

Fig. 10-5

Open model *10-4.nec*. This simplest version of the task sets up a 137.7' wire in free-space centers on the Y = 0 position of the Cartesian coordinate system. With 138 segments, the segment length is about 1' (0.3048 m) per segment. That is many segments for a 1/2λ wire, but the ratio of segment length to radius is close to 148:1 for the AWG #12 wire.

```
GW 1 138 0 -68.85 0 0 68.85 0 .00673

EX 0 1 23 00 1 0
```

The extracted model entries show the structure plus the fact that the model places the source on segment 23 or a little under 17% of the length of the wire counting from the -Y end. Run the model to obtain an impedance of 289.7 + j0.7 Ω. The position is about 10 Ω off the goal. However, if you move the source to segment 22, the result is 313.2 - j3.3 Ω. Hence, without increasing the number of segments in the wire, we have gotten as close to the goal as this technique will permit.

However, we have other techniques available. Open model *10-4a.nec*.

```
GW 1 22 0 -21.9 0 0 0 0 .00673
GW 2 116 0 0 0 0 115.7 0 .00673

EX 0 1 22 00 1 0
EX 0 2 1 00 1 0
```

As the extracted lines show, this model uses the technique sketched in the center of **Fig. 10-5**.

We use 2 wires that meet at Y = 0. We place a source on the segments on each side of the junction. We may now independently adjust the lengths of the short and the long wires until we reach our goal. The 21.9' short end and the 115.7' long end add up to 137.6' for the total wire. The only complication is that we must add source impedance values to determine if we have arrived at the 300-Ω goal. 152.8 - j 2.7 Ω and 147.0 - j1.7 Ω add up to 299.8 - j4.4 Ω. This close approach to the goal does have a reliability question because we are adding series impedances that are not the same.

We may check our work by opening model *10-4b.nec*, a 3-wire version of the off-center-fed wire that corresponds to the bottom sketch in **Fig. 10-5**.

```
GW 1 21 0 -21.9 0 0 -1.5 0 .00673
GW 2 3 0 -1.5 0 0 1.5 0 .00673
GW 3 115 0 1.5 0 0 115.7 0 .00673

EX 0 2 2 00 1 0
```

GW2 is a 3-segment source wire with its center at Y = 0. We use a single source on the center segment and make the segment lengths throughout the 3 wires as similar as feasible. Note that the end coordinates turn out to be the same as in model 10-4a. The reported impedance is 299.7 - j5.5 Ω, confirming the results of the 2-wire technique. Arriving at a set of dimensions that would reduce the reactance further would require adjustment in hundredths of a foot, rather than the 0.1' increment used in this exercise. If further action on the model requires centering the entire wire at Y = 0, you may always invoke the GM command. Although the exercise that we have just performed is far too finicky for any real 80-meter wire antenna design, it may be useful in other modeling tasks. For example, suppose that you wish to track specific off-center feedpoint impedance values in various ways in a large series of models. One or more of the source placement techniques in this exercise might prove useful.

The use of a 3-segment source wire does have limitations, and we may need to employ still other techniques for source placement. Consider the situation shown at the upper left of **Fig. 10-6**. The sketch shows the feedpoint junction region of a 2-element quad beam for 28.5 and 24.94 MHz using a common feedpoint. The quad array is over average ground. Open model *10-5.nec*.

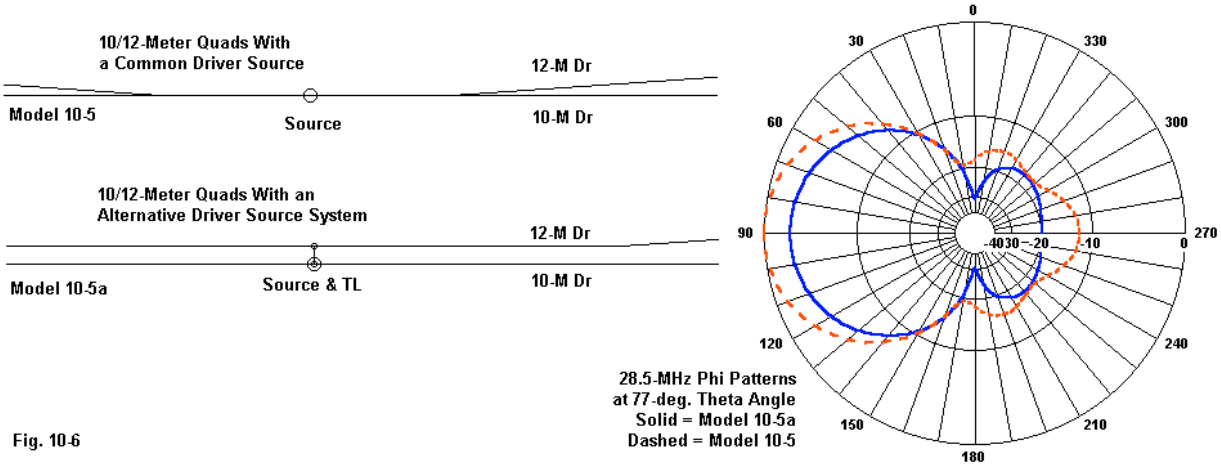

Fig. 10-6

The structure of the elements is complex, especially in the junction of the wires of the drivers (GW3 through GW5, GW11, and GW12). The 10-meter and 12-meter driver wires form extremely acute angles at the center source-wire junctions. If we tabulate the performance results in both NEC-2 and NEC-4, we can get a picture of the modeling problem.

Core	Freq. MHz	Gain dBi	TO Angle Degrees	Impedance R +/- jX Ω	AGT	AGT-dB
NEC-2	24.94	13.22	75	88.0 + j19.4	1.317	+1.20
	28.5	14.07	77	664 + j1750	1.347	+1.29
NEC-4	24.94	12.25	75	109 + j0.9	1.053	+0.22
	28.5	13.06	77	994 + j2274	1.067	+0.28

The disparity of the results as we move from one core to the other suggests that we have a major angular junction problem. Although the NEC-4 results provide seemingly better AGT values, we should wonder if we might develop a better feed system to remove the questions about the sensibility of the initial results. Open model *10-5a.nec*. Examine the wires for each driver in the feedpoint region (GW1 through GW3 and GW11 through GW13). The extract shows the center wires of each group. Note that the 2 AWG #14 wires are parallel but do not touch. In fact, they are 13.7 mm apart.

```
GW 2 3 -.2286 .656844 9.2964 .2286 .656844 9.2964 .0008138

GW 12 3 -.2286 .67056 9.2964 .2286 .67056 9.2964 .0008138
```

The second extract from the model shows a single source, placed at the center of GW2. In place of a direct connection of a second source, the model uses a different technique to arrive at a common feedpoint: a very short transmission line effected by the TL command.

```
EX 0 2 2 00 1 0.
TL 2 2 12 2 300. .003048 0. 0. 0. 0.
```

We shall look into many details of the TL command in a later chapter, but we could not delay its use as another technique to create common feedpoints. The first 4 numerical entries specify the tag and segment numbers that form the terminal ends of the line. The following entry is the assigned characteristic impedance of the line. Next comes the line's assigned electrical length (about 0.01'). The remaining entries are placeholders.

NEC TL-based transmission lines are non-radiating constructs. They do not add to the matrix calculations as they would if we made a transmission line from wires via GW entries. As a result, we may assign any electrical length. We have placed the parallel wires far enough apart that--with parallel segment junctions--they do not create close-spacing problems. Because we wish to simulate a common feed, we have specified the TL length to be almost vanishingly closer: 3 mm. The amount of impedance transformation that would occur on such a short line at the frequencies in question would be minuscule. Hence, TL acts as a virtual short circuit between the terminal points. At the same time, the only remaining angles in the driver wire junctions are extremely shallow, but the wires for each band's driver are close enough to show interactions. The selection of the line characteristic impedance for such a short line is somewhat arbitrary, but the best value is one that approximates a compromise between the impedances anticipated from each individual

line if fed by a dual parallel source system.

The right side of **Fig. 10-6** shows the differences in the 28.5-MHz phi patterns produced by models 10-5 and 10-5a. In addition to this sign that the revised source placement scheme is more adequate, we may also chart the various performance data, again using both cores for comparison.

Core	Freq. MHz	Gain dBi	TO Angle Degrees	Impedance R +/- jX Ω	AGT	AGT-dB
NEC-2	24.94	12.04	75	114 - j22.7	1.002	+0.01
	28.5	12.23	77	129 + j69.4	1.001	+0.00
NEC-4	24.94	12.04	75	114 - j22.8	1.001	+0.01
	28.5	12.22	77	129 + j69.6	1.001	+0.01

Both cores are in exceptionally close agreement and both sets of AGT values are very good. The TL system of effecting a common feed has numerous applications.

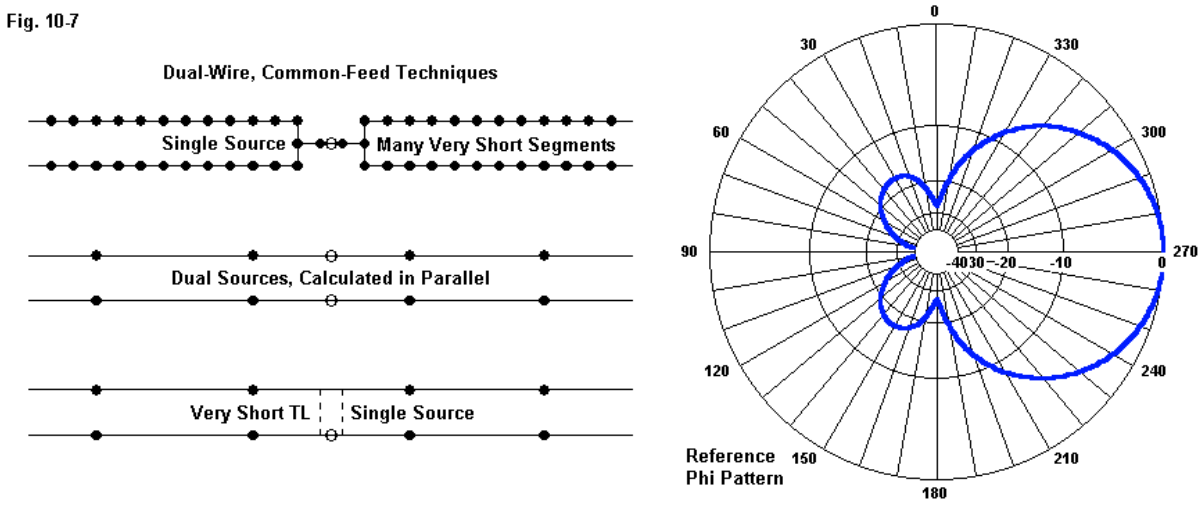

Fig. 10-7 shows another application for the TL workaround for common sources. In this case, we have a 2 element quad beam for 28.5 MHz. The relatively unique feature of this array is that each element is composed of two wires spaced 5.4" (137 mm) apart to simulate in some, but not all, ways a single fat element. The operating bandwidth of the front-to-back ratio and SWR become wider than with a single wire, although the lack of surface area holds the gain lower than with a single fat wire with a diameter about half the distance between the twin wires.

Open model *10-6.nec*. The long fractions in each dimension result from having designed this antenna via equations. Each element uses concentric twin wires. There are cross wires at each corner to ensure equal current distribution between the wires. Model 10-6 uses a total of 646 segments to model the antenna in the manner indicated for the driver at the top left of **Fig. 10-7**. A single source is centered on a 3-segment source wire. The segment length varies from 0.0635 m to 0.0733 m within the structure for maximum accuracy of results.

Next, open model *10-6a.nec*. In this version of the antenna, the segment lengths vary between

0.11 m and 0.12 m, with only 392 segments. The inter-wire connectors limit how short the segments may be. The economy achieved results from using dual or parallel sources at the driver feedpoint rather than bringing the wires together in the model. The center portion of the figure shows the general scheme. As we did earlier, we calculate the parallel "sum" of the source impedance by applying the usual parallel calculation equations to the resistive and reactive portions of the individual source reports.

Finally, open model *10-6b.nec*. This version of the antenna uses the same segmentation as the previous one, but employs a near-zero-length section of transmission line (TL) between driver wires to effect a common connection.

```
EX 0 1 13 0 1 0

TL 5 12 1 13 300 0.0254 0 0 0 0
```

The 300-Ω line is 1" long and runs between tag 5, segment 12 and tag 1, segment 13. (The outer and inner wires have different segmentation levels to align the segment junctions as well as feasible.) Hence, we need only a single source on one of the wires. The performance reports for the 3 versions of the same antenna appear in the following table (using NEC-2 values).

Model	Gain dBi	Front-to-Back Ratio dB		Impedance R +/- jX Ω	AGT	AGT-dB	Adjusted Gain dBi
10-6	6.93	51.15		141.8 + j0.5	0.969	-0.14	7.07
10-6a	7.07	48.75	W1	318.2 - j4.7	0.999	-0.00	7.07
			W5	255.4 - j0.2			
			Sum	141.7 - j0.2			
10-6b	7.07	48.74		141.7 - j0.7	0.999	-0.00	7.07

Despite using extreme care with the geometry of the first version of the array, the AGT score--while acceptable for most purposes--shows a slight deficiency that obscures the equality of gain among all of the antenna versions until we apply the corrective. (The NEC-4 run of the same antenna shows a more nearly perfect AGT and far less of a gain deficit relative to the subsequent versions.) All other values tally well, and there is an extremely tight coincidence of values reported by the dual source and the TL-equipped versions.

Before we depart the subject of constructing and placing voltage sources, we should examine the situation of monopoles. Open model *10-7.nec*.

```
CM Monopole over perfect ground
CE Segmentation and source impedance
GW 1 23 0 0 0 0 0 .2375 .001
GE 1
GN 1
EX 0 1 1 00 1 0
FR 0 1 0 0 299.7925 1
XQ
EN
```

The model sets up a simple 1/4λ monopole with a perfect ground. Although the model shows 23

segments, we shall in fact vary that value from 3 to 23 with a variable increment between steps. See **Fig. 10-8** to see the starting, middle, and ending points of our exploration.

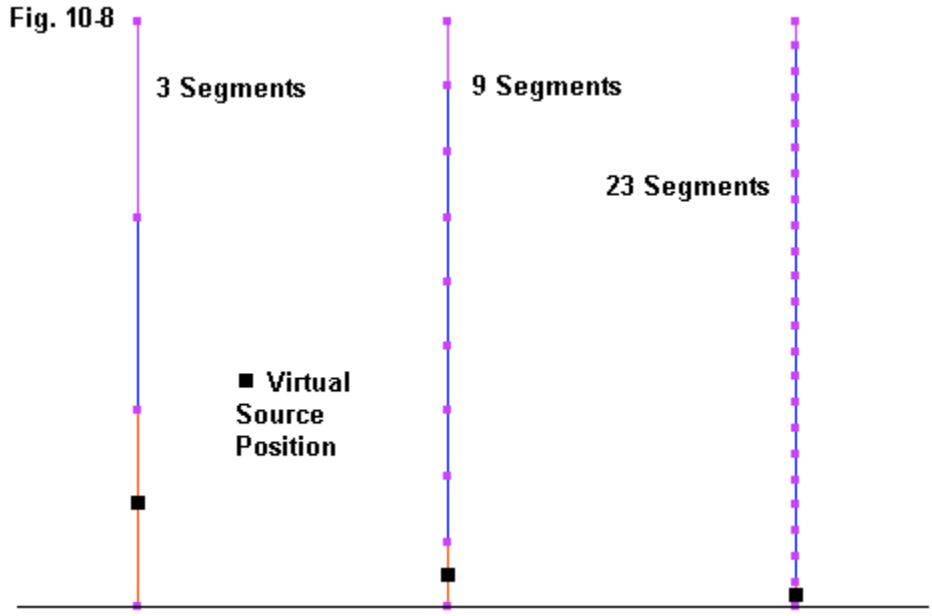

A monopole begins with its source position offset from the physical counterpart (in most cases), because the source segment must be above the ground or Z = 0 position. (Equivalent positions would be on the lowest segment of the vertical wire for an aboveground set of radials and on the segment with one end at Z = 0 for a NEC-4 buried radial system.) Relative to the perfectly reflecting ground of the present model, the source is automatically off center. The impedance and current change very slowly in this region. Still, we should be aware that the number of segments in the monopole will move the virtual position of the source, as suggested by placing the source dot in the figure at the center of the segment to which it is assigned. As a matter of numerical interest, the following table presents the results of changing the number of segments in the monopole. (Because the source assignment is the first segment, you do not need to alter the EX command to replicate the exercise.)

No. Segments	Increase from Previous No.	Impedance R +/- jX Ω
3	--	38.08 + j0.10
5	2	36.65 + j0.53
9	4	36.22 + j0.81
15	6	36.18 + j0.99
23	8	36.21 + j1.10

The table is interesting, not only for its progression of values, but as well for the fact that the source resistance reaches a minimum value at about 15 segments and then turns back upward. Not all of the interesting properties of models have practical significance in terms of antenna construction and testing. Many are relevant as modeling phenomena, with only cautionary implications for analyzing actual antennas.

Source Voltage, Power, and Current

Thus far, we have been concerned with the structure of the EX0 command and the placement of sources on a model to arrive at correct values for the antenna performance parameters, especially the source impedance. We have used a default value of 1 volt peak for all sources, and the phase angle has been 0°. This selection yields values of 1.0 real and 0.0 imaginary for the EX0 command. However, the EX0 command allows us to enter any values for the real and imaginary components of the source value. Where there is only one source on a model structure, the values that we select will not alter the source impedance or the radiation pattern gain values. If we raise the source voltage magnitude, the currents on the segments will rise accordingly and result in the same source impedance. As an idle exercise, you may use model 10-7 and systematically change the real and imaginary values (or, using the EX assist screen, the source voltage magnitude and phase angle) and check the source impedance for each trial.

Nevertheless, there are modeling tasks for which a source voltage of 1.0 at a phase angle of 0° is not appropriate. One application that will appear in a later chapter is the determination of the electrical field of a ground wave at a specified distance from the antenna and at a specified height above ground. We may also need to find out the strength of the electrical field of the space-wave at some specified distance from the antenna and at some theta angle of interest. Both of these applications usually call for the assignment of a certain source power. Let's see how we can easily adjust the source power.

Open model *10-8.nec*. Once more, we have returned to our simple free-space dipole. The RP command is omitted, since we shall be interested for the moment only in the power budget portion of the NEC output report. Run the model and examine the power budget.

```
- - - POWER BUDGET - - -

INPUT POWER   = 6.9676E-03 WATTS
RADIATED POWER= 6.9676E-03 WATTS
STRUCTURE LOSS= 0.0000E+00 WATTS
NETWORK LOSS  = 0.0000E+00 WATTS
EFFICIENCY    = 100.00 PERCENT
```

With a source voltage of 1.0 at 0°, the power supplied to the antenna is 6.9676E-3 watts. You will find the same information in the antenna input parameter section of the report. The following replication splits the 1-line NEC report into 2 lines for easier viewing.

```
- - - ANTENNA INPUT PARAMETERS - - -

TAG   SEG.    VOLTAGE (VOLTS)         CURRENT (AMPS)
NO.   NO.    REAL        IMAG.       REAL        IMAG.
 1     6 1.00000E+00 0.00000E+00 1.39353E-02-2.25275E-05

              IMPEDANCE (OHMS)        ADMITTANCE (MHOS)      POWER
              REAL        IMAG.       REAL        IMAG.     (WATTS)
           7.17602E+01 1.16006E-01 1.39353E-02-2.25275E-05 6.96764E-03
```

The listing shows the assigned source voltage, along with the calculated values for current, impedance, admittance, and power. (Remember to convert the peak values of voltage and/or current into RMS values if you check the power calculation.) For our initial exercises, either the power budget or the antenna input parameters will suffice as an information source, since we need only the power input calculation.

Next, suppose that we wish to set the source voltage to yield a power input to the antenna of 1000 watts. The ratio of the new voltage required to the old one (1.0) will be the square root of the ratio of the new power (1000 watts) to the old power (6.9676E-3 watts). The result is 378.84 volts. (Note that this ratio applies to both peak and RMS volts so long as both the old and the new voltage values are in the same units.) Open model *10-8a.nec*, which plugs this value into the EX0 command.

```
EX 0 1 6 00 378.84 0
```

Run the model and check the relevant output report sections.

```
- - - POWER BUDGET - - -

INPUT POWER   = 9.9999E+02 WATTS
RADIATED POWER= 9.9999E+02 WATTS
STRUCTURE LOSS= 0.0000E+00 WATTS
NETWORK LOSS  = 0.0000E+00 WATTS
EFFICIENCY    = 100.00 PERCENT

- - - ANTENNA INPUT PARAMETERS - - -

TAG   SEG.    VOLTAGE (VOLTS)         CURRENT (AMPS)
NO.   NO.    REAL        IMAG.       REAL        IMAG.
  1     6 3.78840E+02 0.00000E+00 5.27924E+00-8.53433E-03

              IMPEDANCE (OHMS)        ADMITTANCE (MHOS)      POWER
              REAL        IMAG.       REAL        IMAG.     (WATTS)
           7.17602E+01 1.16006E-01 1.39353E-02-2.25275E-05 9.99993E+02
```

The power is 1000 watts. Both the voltage and current have changed, but the impedance and admittance have not.

Just because we have worked out the required voltage for this model to achieve a power input of 1000 watts, do not expect to arrive at the same voltage for every modification of the model that you may make. Consider, for example, model *10-8b.nec*, which adds a simple material load for copper to model 10-8.

```
LD 5 0 0 0 5.8E7
```

Run this model and obtain the power input from the power budget.

```
INPUT POWER   = 6.9487E-03 WATTS
```

The power is slightly lower than for the initial model. You can discover why by extracting the current and impedance numbers from the antenna input parameter data.

```
      CURRENT (AMPS)          IMPEDANCE (OHMS)       POWER
    REAL         IMAG.       REAL         IMAG.     (WATTS)
1.38974E-02 -5.38044E-05 7.19546E+01 2.78574E-01 6.94872E-03
```

Because the impedance at the source has changed slightly due to the addition of mild material loading, the power input will change. Hence, if we now wish to use 1000 watts, we must make a fresh calculation of the required voltage for the EX0 command. Open *model 10-8c.nec* and check the input value used (379.36 volts). Run the model and check at least one of the power input reports.

```
- - - POWER BUDGET - - -

INPUT POWER   = 1.0000E+03 WATTS
RADIATED POWER= 9.9752E+02 WATTS
STRUCTURE LOSS= 2.4959E+00 WATTS
NETWORK LOSS  = 0.0000E+00 WATTS
EFFICIENCY    =  99.75 PERCENT
```

Because we have an almost 2.5-watt power loss in the structure of the antenna, the power efficiency is less that 100%. However, the supplied power is 1000 watts. Now let's move one more step toward a practical application. Suppose that we wished to know the maximum value of electrical field strength at a distance of 1000 m from the antenna, using 1000 watts as the input power. To find the electrical field strength, we would structure the model as in *10-8d.nec*.

```
GW 1 11 0 -.2375 0 0 .2375 0 .001
GE
EX 0 1 6 00 379.36 0
LD 5 0 0 0 5.8E7
FR 0 1 0 0 299.7925 1
RP 0 1 361 1000 0 0 1.00000 1.00000 1000
```

The RP command is a standard phi pattern request with one added entry: an RFLD value of 1000. Run the model and find the radiation pattern values for headings of 0° or 180°. You may note that the far-field gain (2.11 dBi) does not change just because we have elevated power.

```
             ---E (Theta)---          --- E (Phi) ---
  Phi      Magnitude     Phase     Magnitude     Phase
Degrees     Volts/m     Degrees     Volts/m     Degrees
   0.00   0.0000E+000   -351.01   3.1222E-001   -444.24
```

Depending upon the conventions that you use, the Ephi value is 0.31222 V/m or 312.22 mV/m. The phase angle reading from this NEC-2 report is -444.24°. NEC-4 converts these angles to a more conventional -84.22° (the 0.2° angular difference being a function of the core algorithm differences).

Had the pattern been a theta plot along the phi angle of maximum gain, all 360 reports would have been identical. However, the phi pattern is particularly interesting, because it shows the variations in both Ephi and Etheta as we change headings. The antenna is broadside to headings of 0° and 180° with its ends pointed at 90° and 270°. See **Fig. 10-9** for a composite pattern of both electrical fields.

Model 10-8D

Dipole in Free Space at 299.7925 MHz
Power Input: 1000 watts

Antenna Alignment:
Left to Right (90 to 270 Degrees)

Electric Field Strength in mV/m
Solid = Etheta
Dashed = Ephi

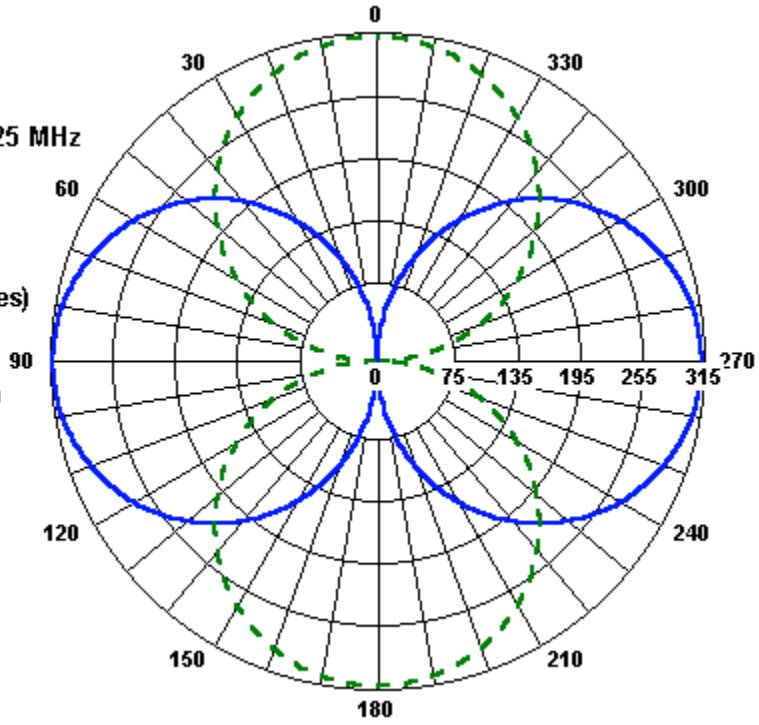

Fig. 10-9

For some types of multi-source phased arrays, voltage sources will not do the job. Such arrays require that each element be fed with a certain current magnitude at a certain phase angle for the array to perform as designed. Although a usable current source for placement on a segment of the array is not an integral part of the NEC core itself, it is possible to create indirect current sources that are perfectly adequate to the task of modeling phased arrays of the type indicated.

The NEC-Win Plus insert in both NEC-Win Pro and GNEC contains a facility to create such arrays automatically. The facility sets up all of the required additions to the NEC input file for current sources. Open model *10-9.nec* to see an example of a 3-monopole phased array over perfect ground.

```
CM 3 monopoles phase fed
CE current sources
GW 1 21 -99.92 0 0 -99.92 0 70.57 0.125
GW 2 21 0 0 0 0 0 70.57 0.125
GW 3 21 99.92 0 0 99.92 0 70.57 0.125
GW 30901 1 9901.0000 9901.0000 9901.0000 9901.0001 9901.0001 9901.0001 .00001
GW 30902 1 9902.0000 9902.0000 9902.0000 9902.0001 9902.0001 9902.0001 .00001
GW 30903 1 9903.0000 9903.0000 9903.0000 9903.0001 9903.0001 9903.0001 .00001
GS 0 0 1
GE 1
GN 1
EX 0 30901 1 0 -0.8387 -0.5446
EX 0 30902 1 0 0.0 1.5
EX 0 30903 1 0 0.9135 -0.4067
NT 30901 1 1 1 0 0 0 1 0 0
NT 30902 1 2 1 0 0 0 1 0 0
NT 30903 1 3 1 0 0 0 1 0 0
FR 0 1 0 0 1 1
```

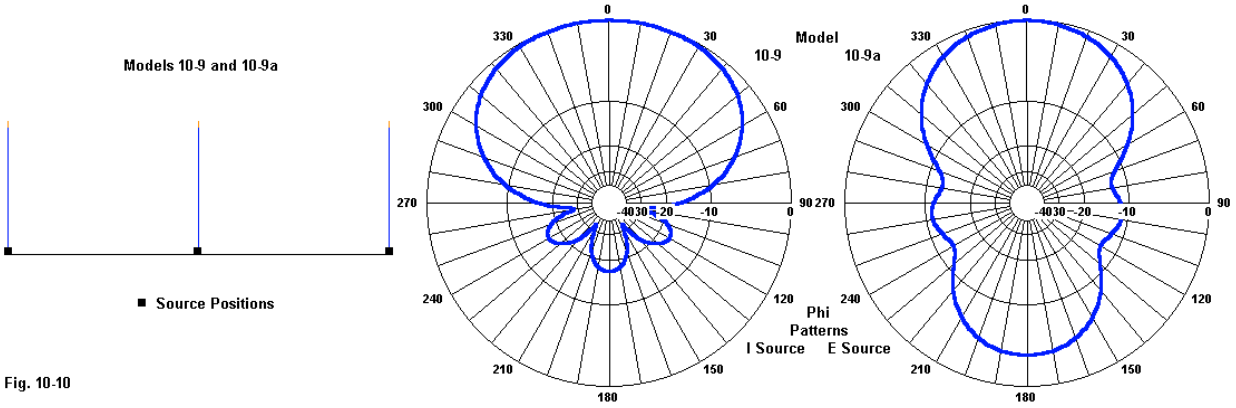

Fig. 10-10

Fig. 10-10 shows on the left the essential structure of the monopole array. The visible monopoles correspond to GW1 through GW3 in the model. The monopoles operate as an endfire array and require the following current sources: rear 1 A @ 123°, center 1.5 A @ 0°, forward 1 A @ -114°. To create the current source, we must once more jump ahead of ourselves and introduce a network (NT) command for each source. A network is similar to a TL transmission line in that it creates a non-radiating addition to the model. As well, the network must run between the former source segment on the model to a new remote wire. The new remote wires are established by the 3 GW entries with very high numbers. (In NSI software, tag numbers above 30,000 are rendered invisible in Necvu so that the main antenna structure will remain centered.)

Note that in the NT command lines, the initial entries specify a remote wire tag number and segment and the original source tag number and segment. Every NT command for a current source is identical in its other specifications to the samples in the model. The 7th numerical entry (Y12 Imaginary = 1) is the only other non-zero entry. The EX0 commands now apply to the remote wires, as indicated by the high tag numbers for the source assignments. Although somewhat opaque due to the need to place real and imaginary components of the source voltage, the values inserted are the ones required as source-segment currents, but shifted 90° for entry. The result is a transformation of the voltage values into current values with a phase shift to normal for the array at the segments marked in the sketch of the array. If we sample the current table in the NEC output report, we shall find the following currents on the base segment of each monopole.

```
FREQUENCY     SEG.  TAG          - - - CURRENT (AMPS) - - -
  (MHz)       NO.   NO.      REAL         IMAG.        MAG.         PHASE
1.000000        1     1   -5.4460E-01  8.3870E-01  1.0000E+00  122.997
1.000000       22     2    1.5000E+00 -1.0401E-14  1.5000E+00    0.000
1.000000       43     3   -4.0670E-01 -9.1350E-01  9.9994E-01 -113.999
```

As a consequence, the array produces the desired pattern, the one at the center of **Fig. 10-10**. The source impedances are as follows: rear 11.9 - j14.7 Ω, center 26.9 + j2.9 Ω, and forward 58.7 + j25.5 Ω. However, the raw NEC core will not directly reveal these values, although you can find them in the antenna input parameters when you know where to look.

```
TAG   SEG.       IMPEDANCE (OHMS)       ADMITTANCE (MHOS)      POWER
NO.   NO.      REAL        IMAG.       REAL        IMAG.     (WATTS)
30901    64 3.32081E-02 4.10055E-02 1.19272E+01-1.47278E+01 5.96365E+00
```

```
30902    65 3.66973E-02-3.89194E-03 2.69468E+01 2.85785E+00 3.03152E+01
30903    66 1.43177E-02-6.22409E-03 5.87427E+01 2.55362E+01 2.93680E+01
```

Because the source voltage on the remote segment is phase shifted, the numerical values for the impedance at the corresponding segment of the physical antenna appear in the admittance columns.

We shall explore the creation of current sources in another example. However, before we leave this one, let's open model *10-9a.nec*. In this version of the same set of monopoles at 1 MHz, we use only voltage sources, each one placed directly on the monopole and given the phase angle that we established for current sources.

```
CM 3 monopoles phase fed
CE voltage sources
GW 1 21 -99.92 0 0 -99.92 0 70.57 0.125
GW 2 21 0 0 0 0 0 70.57 0.125
GW 3 21 99.92 0 0 99.92 0 70.57 0.125
GS 0 0 1
GE 1
GN 1
EX 0 1 1 0 -0.5446 0.8387
EX 0 2 1 0 1.5 0
EX 0 3 1 0 -0.4067 -0.9135
FR 0 1 0 0 1 1
```

This maneuver simplifies the model considerably, but unfortunately produces an entirely different source situation that yields a quite different pattern, the one shown on the right in **Fig. 10-10**. You may explore the reported source impedances to further confirm the fact that none of the monopoles has the correct current magnitudes and ratios to produce the desired pattern.

To obtain a better grasp of how to create a current source, let's use a much simpler example, model *10-10.nec*. We shall find that the elemental dipole is handy for us to create a current source directly, without the aid of an automated system.

```
CM dipole with current source
CE 0 deg at antenna source
GW 1 11 0 -.2375 0 0 .2375 0 .001
GW 2 1 9999 -.005 9999 9999 .005 9999 .001
GE
FR 0 1 0 0 299.7925 1
EX 0 2 1 00 0.00000 1.00000
NT 2 1 1 6 0 0 0 1 0 0
XQ
EN
```

In this case, we create the required dipole (GW1) and add a second remote 1-segment wire (GW2) located too far away from the key element to have any affect on the pattern data. The remote wire is very short, very thin, and never given a material load. Next, we place a network (NT) between the dipole source segment and the remote wire, using the standard set-up of the NT command for a current source. Using the NT assistance screen in the software, as shown on the left in **Fig. 10-11**, will ease the burden of remembering which entry point receives the value of 1 for the Y12 imaginary position. Finally, we add an EX0 command, placing the source on the

remote wire and phase shifting the value by 90°.

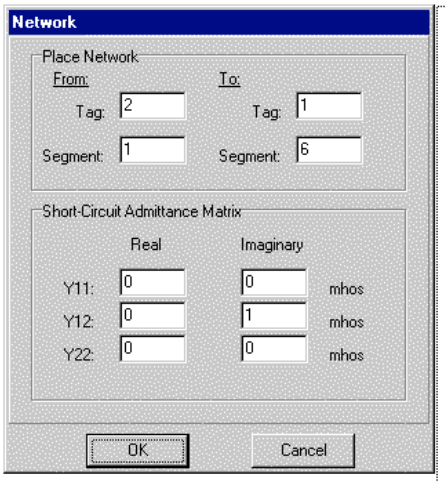

Fig. 10-11

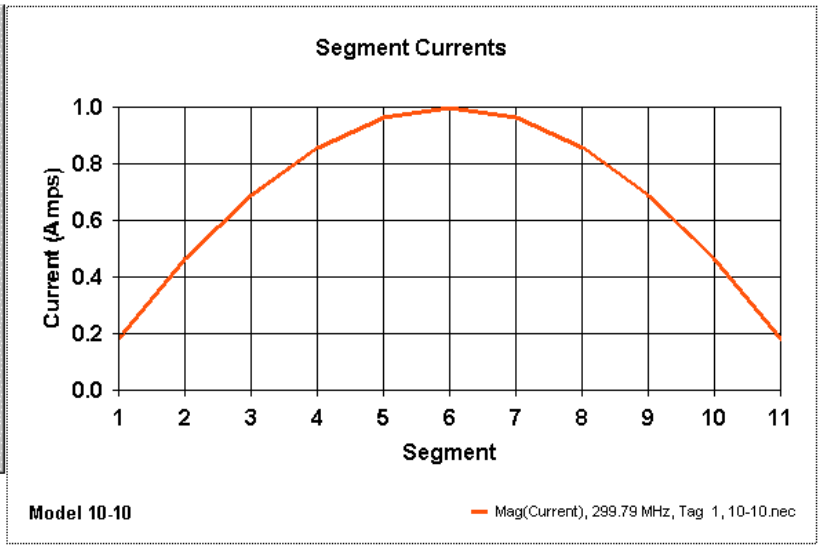

One very significant use of current sources is to allow rectangular plots of the element currents reference to a standard value, such as 1.0. The right side of **Fig. 10-11** shows such a plot for the dipole. Within it, we can instantly and accurately gauge the relative current at any segment within the dipole. With multiple elements, such as in a parasitic array, we may stack the element current lines referenced to a current source of 1 A @ 0° and arrive at a relatively clear picture of the current magnitudes on all segments of all elements at a glance.

To create current source having the correct current phase angle as well as magnitude requires that we keep in mind the need to phase shift the desired value by 90° when we insert the excitation level on the remote wire as a voltage source. Consider the 3 cases shown in **Fig. 10-12**.

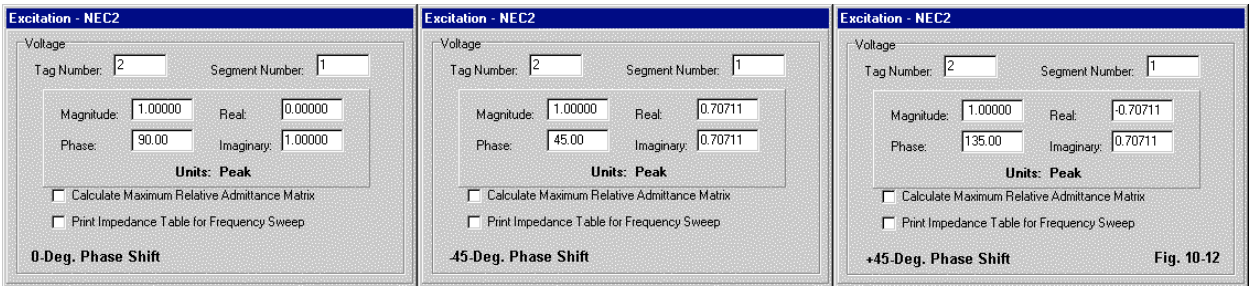

Fig. 10-12

The first case shows the assistance screen for the EX0 command for model 10-10. The magnitude and phase angle entry boxes are the most convenient to use, but note the resultant real and imaginary values of voltage that actually enter the command. If we wish to create a current of 1 A @ -45°, we must enter a voltage of 1 V @ 45°, that is, 90° shifted from the desired phase angle. This source appears in model *10-10a.nec*. To create a +45° phase angle for the current, we must add 90° to the desired angle to wind up with the right-hand entry in **Fig. 10-12**. Model *10-10c.nec* employs this source value.

Run all 3 models and extract the current values for segment 6 of the dipole.

```
Model 10-10
FREQUENCY     SEG.  TAG            - - - CURRENT (AMPS) - - -
  (MHz)       NO.   NO.     REAL         IMAG.       MAG.        PHASE
299.790000      6     1   1.0000E+00 -2.2205E-16  1.0000E+00    0.000
Model 10-10a
299.790000      6     1   7.0711E-01 -7.0711E-01  1.0000E+00  -45.000
Model 10-10b
299.790000      6     1   7.0711E-01  7.0711E-01  1.0000E+00   45.000
```

You may wish to create rectangular plots of the element currents on each of the dipoles and overlay the plots to track their magnitudes as well as their real and imaginary components.

Before departing the subject of current sources, we must discover how to adjust the power level of a current source in order to make sense of field strength readings. If we return to model 10-10, we find that the input power, as shown in the power budget and the antenna input parameter sections of the output file is 3.5880E1 watts for an element source current magnitude of 1 A (peak). The required new current adjustment factor for a power of 1000 watts will be the square root of the ratio of the new power level to the old power level. The square root of 1000/35.88 is 5.2792689. We multiply this adjustment factor value times the old value of the source voltage on the remote wire to arrive at the EX0 line shown for model *10-10c.nec*.

```
EX 0 2 1 00 0.00001 5.27927
```

If we run the model and examine the power budget, we find the following input power entry.

```
INPUT POWER   = 1.0000E+03 WATTS
```

Controlling the source by changing its power level or converting a voltage source into a current source are highly versatile aspects of the EX0 command. In some modeling situations, they may be critical to the task.

Frequency Specifications

In some respects, the FR or frequency command is among the simplest of the entire set of control commands. However, once users pass beyond a request for a single frequency, it becomes the command that usually requires a second try to get right. The command is the same in both NEC-2 and NEC-4.

```
Cmd   I1    I2    I3    I4    F1          F2
      IFRQ  NFRQ  --    --    FMHZ        DELFRQ
FR    0     1     0     0     299.7925    1
```

The sample single frequency request, a part of model *10-11.nec*, shows the structure of the FR command. It has only 4 numerical entries, besides the obligatory zeroes in the unused I3 and I4 positions. The only one of those positions to receive a frequency (in MHz) entry is F1. The other entries control how many frequencies the step will create and at what intervals. For a single

frequency entry, I1 may be either 0 or 1, since it controls the type of frequency sweep where the command requests more than one frequency. I2 requests the number of frequency steps. The number of steps must include the first step, so a minimum value is 1. The last entry (F2) is the increment between steps according to the type of sweep being requested. For a single frequency request, the value may be anything, although values of 0 or 1 are most common.

When I2, NFRQ, is 1, then all self-executing commands will execute, including NE, NH, LE, LH, and RP. However, if NFRQ is greater than 1, NE and NH will not initiate execution, and RP and XQ will execute for the entire set of frequencies only once. Subsequent RP and XQ commands will execute only for the highest frequency in the loop function created by the FR command. Hence, if there are multiple execution commands, the FR command with multiple frequencies must reappear above each one, and NE and NH must have supplementary XQ commands.

Open model *10-11a.nec*. The simple free-space dipole has taken on an 11-step frequency sweep beginning at 250 MHz. 11 steps imply that there will be 10 increments. Hence, with a DELFRQ of 10, the highest frequency will be 250 MHz. Run the model and check the convenient impedance table output from the NSI software.

```
FR 0 11 0 0 250 10
```

```
Input Impedance and VSWR

Frequency      Tag  Seg. Real(Z)   Imag(Z)   Mag(Z)    Phase(Z)   Zo      VSWR
-------------------------------------------------------------------------------
250.000000      1     6  43.301    -155.475  161.392   -74.437   75.000  9.65
260.000000      1     6  48.051    -122.829  131.893   -68.635   75.000  6.23
270.000000      1     6  53.238    -91.048   105.470   -59.684   75.000  3.94
280.000000      1     6  58.907    -59.961   84.055    -45.508   75.000  2.47
290.000000      1     6  65.110    -29.412   71.445    -24.310   75.000  1.55
300.000000      1     6  71.908    0.738     71.911    0.588     75.000  1.04
310.000000      1     6  79.368    30.622    85.070    21.097    75.000  1.49
320.000000      1     6  87.570    60.359    106.356   34.577    75.000  2.10
330.000000      1     6  96.605    90.064    132.076   42.993    75.000  2.83
340.000000      1     6  106.578   119.846   160.381   48.354    75.000  3.65
350.000000      1     6  117.612   149.808   190.460   51.865    75.000  4.53
```

Because model 10-11a requested a type-0 sweep (I1), the steps are linear, with the 10-MHz increment added to the preceding value for each step in the loop. This type of sweep is common for relatively narrow frequency ranges, for example, the end-to-end coverage of an amateur or short-wave broadcast band.

When a sweep must cover much wider portions of the spectrum, you may wish to opt for a type-1 multiplicative sweep. Such sweeps use a multiplier on the preceding frequency for the next step. To calculate the required multiplier for the value of F2, use the following equation:

$$M.F. = \sqrt[N-1]{\frac{f_{HI}}{f_{LO}}}$$

M.F. is the multiplication factor or DELFRQ, f_{HI} is the upper frequency of the sweep, f_{LO} is the starting frequency (F1), and N (I2) is the total number of steps. In most cases, a handy calculator capable of taking x-roots of y is desirable when planning a multiplicative frequency sweep.

Open model *10-11b.nec* and examine the FR entry.

```
FR 1 11 0 0 250 1.0342197
```

The FR command requests another 11-step sweep beginning at 250 MHz. However, the sweep is multiplicative, with a desired termination frequency of 350 MHz. The 10th root of the frequency ratio (1.4) is 1.0342197. In most cases, it pays to enter the F2 value in a multiplicative sweep to excessive decimal places to ensure that the sweep ends at precisely the desired frequency. Run model 10-3b and check the impedance table.

```
Input Impedance and VSWR
```

Frequency	Tag	Seg.	Real(Z)	Imag(Z)	Mag(Z)	Phase(Z)	Zo	VSWR
250.000000	1	6	43.301	-155.475	161.392	-74.437	75.000	9.65
258.550000	1	6	47.338	-127.489	135.994	-69.629	75.000	6.64
267.400000	1	6	51.846	-99.229	111.957	-62.414	75.000	4.45
276.550000	1	6	56.895	-70.608	90.678	-51.139	75.000	2.90
286.020000	1	6	62.571	-41.526	75.097	-33.570	75.000	1.86
295.800000	1	6	68.979	-11.873	69.993	-9.766	75.000	1.20
305.930000	1	6	76.244	18.473	78.450	13.619	75.000	1.28
316.400000	1	6	84.522	49.648	98.025	30.430	75.000	1.87
327.220000	1	6	94.006	81.809	124.618	41.032	75.000	2.62
338.420000	1	6	104.934	115.129	155.775	47.652	75.000	3.51
350.000000	1	6	117.612	149.808	190.460	51.865	75.000	4.53

The start and stop frequencies of this table are identical to the table for model 10-11a. However, all intermediate frequency values differ. Still, if you plot the graph of the impedance or SWR values using a linear X-axis, the curves for the two models will be virtually identical. You may overlay convenient rectangular plots of the two models to verify the results.

In any model that omits the FR command, NEC will default to a single frequency: 299.8 MHz. At this frequency, processed geometry commands in meters are also approximately in wavelengths. However, for maximum control of the model, you should always include an FR command set up the way that you wish the command to operate.

Summing Up

We initially restricted our exploration of the EX or excitation command to EX0, voltage sources placed on one or more segments of the model structure. This source type is the one most commonly used in far-field analyses. However, in the process of looking at source placement, we discovered that the geometry constraints of NEC forced us to look at alternative methods of placing sources.

For sharp corners, where the physical source or feedpoint is the corner itself, we may use one of 3 general methods. Where the segmentation density is high, a single source on one or the other side of the corner may be sufficient. Alternatively, we may use dual or series sources on segments on each side of the junction and then simply sum the two reported impedances. A third alternative involves adding a central source wire with 3 segments, with the source applied to the center segment. This technique ensures that the current on each side of the source segment is

as equal as may be feasible. The technique allows us to use a single source and apply the post-run facilities for impedance and SWR graphing, and its proves equally applicable to angled feedpoint positions and to the precise placement of off-center feedpoints.

There are modeling geometries that may require further special treatment of sources. Most striking are cases of angled wire junctions that will press NEC limits. We may use close spaced parallel source wires and apply dual parallel sources that require post-run calculation of the composite source impedance. Alternatively, we may connect the source positions with an electrically minuscule length of transmission line and feed only one of the terminal segments.

Controlling and manipulating the EX0 entry offers us considerable flexibility when applying sources. For example, we may alter the input power to an antenna within the model by changing the value of the exciting voltage as the square root of the ratio of desired power to the power using an initial value. Setting power levels within a model is very useful to taking field strength readings of various types from the model.

Convenient and sometimes necessary is the development of an indirect current source so that the feedpoint segment of a model has a specified current magnitude and phase angle. The technique requires that, for each current source, we add a remote wire that becomes the new voltage source, along with a simple network connecting the remote wire to the former source segment. The voltage magnitude and phase angle that we enter in the EX0 command for the remote wire must be shifted 90° relative to normal voltage source entries. By examining the antenna input parameters, we discovered how to read out the source impedance at the antenna segment from the data presented.

The FR or frequency command is both necessary and relatively simply to enter. For multiple frequency requests, called sweeps, we repeated reminders concerning the variable way in which self-executing commands operate. As well, we examined the differences between linear and multiplicative sweeps and how to calculate the increment entry for each type.

The exercises in this chapter left us with an incomplete account of the excitation command, a situation that we shall partially remedy in Part C of this volume. As well, our focus on excitation left us with only sketches of the operation of TL and NT commands as they apply to creating and placing sources. We shall remedy that deficiency later in the current part of the volume.

11.
Grounds: Types, Applications, and Specifications

***Objectives**: You will encounter in these exercises 4 types of ground options, a range of ground quality specifications, and two ground description commands (GN, GD) that allow you to set up one or two media. The second medium can use a circular or linear edge. You will also understand the differences between NEC-2 and NEC-4 treatments and the interaction of ground specifications with RP commands.*

Most of the sample models that you have met in these pages are in free-space, one of the allowable ground specifications in a NEC model. In fact, if you omit a ground specification command, the core defaults to a free-space or the "no-ground" condition. Once you go beyond free space and specify a ground, then you must use caution to ensure that all parts of the model are compatible with that ground specification. For example, all wires that you do not wish to touch the ground must use positive Z coordinates in the geometry section of the model. NEC-2 permits a Z = 0 coordinate only for monopoles and similar vertical antennas. NEC-4 permits buried wires so long as there is a segment or a wire junction at Z = 0 for any element passing into the ground. Needless to say, you should have negative Z coordinates only for those wires that you intend to bury.

There are two ground control commands: GN and GD. For every ground specification, you must use a GN command to set the ground quality parameters (conductivity and permittivity). The GD command is a continuation entry that provides a second alternative for specifying a second ground medium, even though, with restrictions, you may place a second medium within the GN command itself. However, you may not use more then 2 media in any model. In addition, NEC-2 and NEC-4 use different overall ground specification systems. For any condition other than a single ground medium specified within the GN command, NEC-2 requires you to select the RP command I1 option that accords with it (values 2 through 6). In contrast, NEC-4 drops the RP command requirements, which places some restrictions on how you may use the GN and GD commands for multiple media.

In addition to the differences in command structure in the two cores, there are two types of real ground calculation systems, the simpler and speedier reflection coefficient approximation (RCA) and the Sommerfeld-Norton method (SN). The latter is slower but much more accurate, especially with respect to wires close to the ground. The increased (and increasing) speed of modern PCs has largely obviated the need for the RCA efficiency advantage, but the RCA system allows some options not available with the SN method.

Finally, the ground specification commands require some familiarity with the method of entering the ground quality parameters: soil conductivity and relative dielectric constant (or relative permittivity). NEC uses these values to form a complex dielectric constant value that affects both the reported source impedance and the reflection calculations that go into the far-field analysis of antenna performance. As a result of all of these variables and variations, we shall have to track the GN and GD commands very carefully.

The GN Command for a Single Ground Medium

A typical single-medium model over ground might look like the following one.

```
GW 1 11 0 -.2375 .05 0 .2375 .05 .001
GE 1
GN 0 0 0 0 13.0000 0.0050
FR 0 1 0 0 299.7925 1
EX 0 1 6 00 1 0
RP 0 181 1 1000 -90 0 1.00000 1.00000
```

The GN or ground parameter command appears simple enough, especially when we learn that some of its entries are placeholders. However, the command holds many surprises when we explore its structure more thoroughly.

```
Cmd   I1    I2    I3    I4    F1    F2    F3    F4    F5    F6
      IPERF NRADL 0     0     EPSR  SIG   (See text for meanings)
GN    0     0     0     0     13    0.005
```

For a single ground medium (including free space), the GN command uses only the entries through F2. The remaining floating decimal places apply to the specification of a second medium within the GN command, and we shall attack that potential later in this exercise set.

I1 has 4 options. -1 sets the free-space condition and requires no further entries in the command. 1 specifies a perfectly reflecting ground (sometimes loosely called an infinite ground, but better abbreviated as a perfect ground to avoid confusion with the free-space condition). Like free space, it requires no further entries in the command.

Both 0 and 2 specify finitely conducting grounds--sometimes called imperfect or "lossy" grounds. The difference lies in the methods of calculation used by the two selections. 0 selects the reflection coefficient approximation (RCA) method of calculation. This system uses equations that calculate rapidly, an important function in the days of much slower computers. However, the approximations have accuracy limitations for wires closer than about 0.2λ from the ground. 2 selects the Sommerfeld-Norton (SN) method of ground calculations that take up to 8 times longer than RCA calculations. However, accuracy remains high for wires as close as $10^{-6}\lambda$ to earth.

I2 applies only to an RCA special feature in which we may specify a number of radial wires for a ground-screen approximation. We shall explore that option late in this chapter. For present purposes, set I2 to 0. As well, I3 and I4 are always 0, since they serve only as placeholders so that the next entries fall within the floating decimal entry positions.

Together, F1 and F2 set the ground conditions in the vicinity of the antenna. For a single medium specification, the conditions extend without limit from the origin of the coordinate system outward. F1 (ESPR) calls for the relative dielectric constant or relative permittivity applicable to the ground in the area. F2 (SIG) requires the ground conductivity in Siemens/meter (S/m), also called mhos/m in older literature.

NEC reports the entered GN data as the antenna environment. The report for our sample line has the following appearance.

```
- - - ANTENNA ENVIRONMENT - - -

FINITE GROUND.  REFLECTION COEFFICIENT APPROXIMATION
RELATIVE DIELECTRIC CONST.= 13.000
CONDUCTIVITY= 5.000E-03 MHOS/METER
COMPLEX DIELECTRIC CONSTANT= 1.30000E+01-2.99807E-01
```

NEC not only reports the entered values of conductivity and permittivity, but also calculates from them a complex dielectric constant used in the ground calculations. However, if you enter I2 as a negative number, then the complex dielectric constant becomes EPSR - j|SIG| without further calculation. Ordinarily, you will enter the conductivity as a positive number.

Each of the types of ground specification has a range of applications most suited to it. Free space, for example, makes a handy vehicle for comparing the performance of antennas of similar or competing types. One restriction in such comparisons is that the main lobes of radiation should peak at the same theta angle, ordinarily 90°. Otherwise, the comparison might not remain valid over real ground.

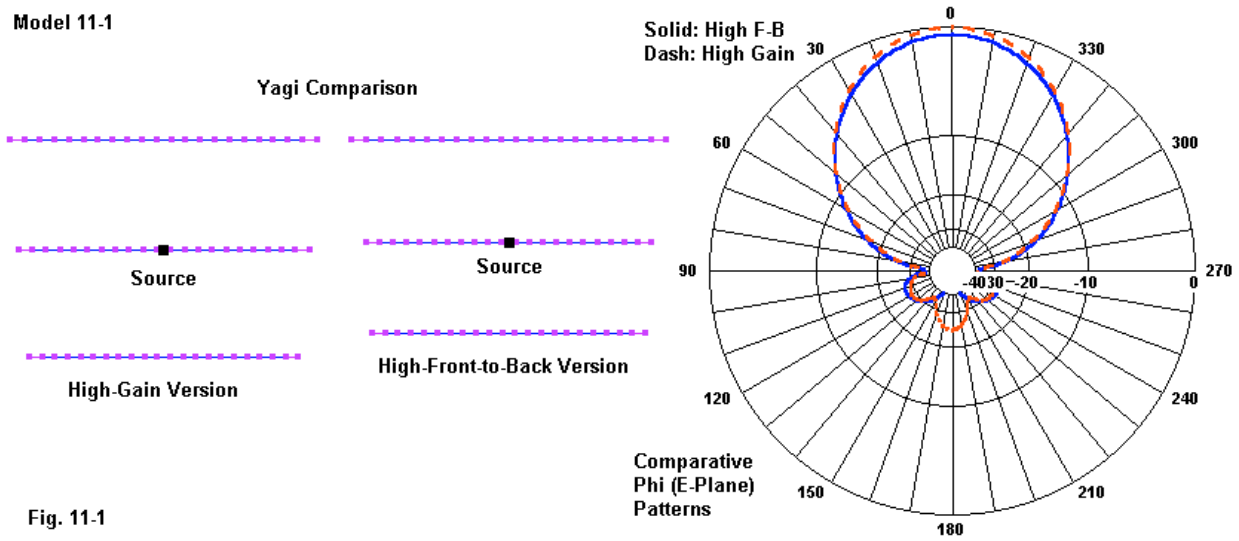

Fig. 11-1

Open model *11-1.nec*. In this model, you will find two independent models of 3-element Yagi arrays, separated by the NX command. **Fig. 11-1** shows antennas on the left the outlines of the two antennas, exactly to scale. By running this model, you will produce two radiation pattern reports that post-processing can combine into an overlaid pair of phi patterns--on the right in the figure. Some of the performance differences are clearly evident. The high-gain version has a free-space gain of 8.36 dBi, compared to the high-front-to-back version's gain of 7.82 dBi. However, the high-front-to-back version has a 180° front-to-back ratio of well over 40 dB, compared to the high-gain value of 24 dB. For some applications, these differences may be significant.

When comparing antennas, we are often interested in the impedance bandwidth of an antenna.

We normally record this in terms of the SWR relative to a reference value and with implied limits of acceptability (for example, a 2:1 SWR ratio). Open model *11-1a.nec*, the same model with frequency sweep requests.

```
FR 0 9 0 0 290 2.5
```

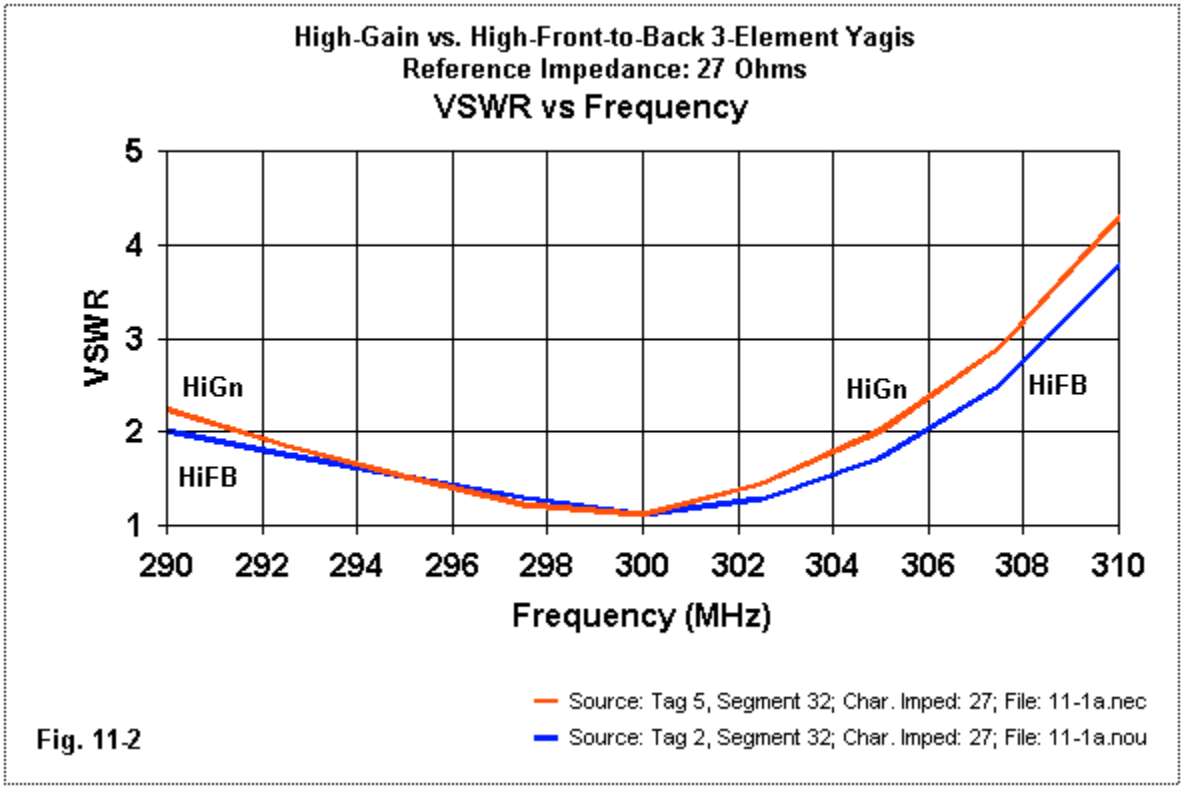

Fig. 11-2

Fig. 11-2 shows overlaid SWR plots keyed to a reference impedance of 27 Ohms (about midway between the resonant impedances of each array at the center frequency). Although model 11-1a will yield that data in the output table, you may need to run model *11-1b.nec* to obtain a separate output file for the second array in order to create the overlaid graph.

For comparisons for monopoles and similar arrays with one end of the structure touching ground, a perfect ground option is often serviceable. Open model *11-2.nec* for a sample of a model monopole specifying a perfect ground.

```
GW 1 15 0 0 0 0 0 .237 .001
GE 1
GN 1
FR 0 1 0 0 299.7925 1
EX 0 1 1 00 1 0
RP 0 181 1 1000 -90 0 1.00000 1.00000
```

Like a free-space GN command, the perfect ground request needs only a single numerical entry to achieve its goal. Because the far-field and impedance calculations employ a perfect image of the given structure, a monopole over perfect ground will replicate fundamental antenna theory

very well. However, it is important not to use the technique with either the RCA or SN ground calculation systems. Their results will be quite unreliable. Open model *11-2a.nec*. The ground specification line uses the RCA ground (I1 = 0) and the values of permittivity and conductivity often classified as "average."

```
GN 0 0 0 0 13.0000 0.0050
```

Run the model and record the maximum gain, TO angle, and source impedance. Do the same for model *11-2b.nec*, which is the same basic monopole over a ground of the same quality, but opting for the SN method (I1 = 2).

```
GN 2 0 0 0 13.0000 0.0050
```

Core	Model	Ground	Gain DBi	TO Angle degrees	Impedance R +/- jX Ω
Both	11-2	Perfect	5.14	90	35.96 + j0.05
NEC-2	11-2a	RCA Average	-0.17	63	30.08 - j615.6
NEC-4	11-2a	RCA Average	-.98	63	27.81 + j3.0
NEC-2	11-2b	SN Average	-1.80	63	48.96 - j199.5
NEC-4	11-2b	SN Average	-1.24	63	45.79 + j5.1

The disparity of the RCA and SN values alone (with the exception of the TO angle) makes the results wholly unreliable. Hence, if a perfect ground will not satisfy the needs of a preliminary comparison of vertical arrays, the final comparisons require modeling of suitable ground radial systems.

We have noted in passing the relative accuracy of RCA and SN ground calculations for wires near to the earth. We may develop a better feel for the divergence by simply modeling a basic dipole over each type of ground, using the same soil quality throughout, and gradually moving the dipole up or down. Open model *11-3.nec*, a dipole 1λ above average ground. The RCA GN entry is identical to that used for the monopole model. Later, open model *11-3a.nec*, which is the same dipole, but over the comparable SN ground. For each dipole, chart the reported gain, TO angle, and source impedance in 0.05λ increments from a height of 0.05λ up to 0.35λ. From past use of this dipole, we know that the free-space gain is 2.12 dBi, with a source impedance of 71.76 + j0.12 Ω.

	RCA Ground			SN Ground		
Height λ	Gain dBi	TO Angle degrees	Impedance R +/-jX Ω	Gain dBi	TO Angle degrees	Impedance R +/-jX Ω
0.05	0.30	0	45.2 + j13.5	-1.49	0	66.6 + j4.2
0.1	3.94	0	46.9 + j13.3	3.22	0	54.8 + j8.2
0.15	5.41	0	58.0 + j20.1	5.23	0	60.1 + j16.3
0.2	5.83	0	70.5 + 20.8	5.82	0	70.5 + j18.5
0.25	5.70	24	80.4 + j15.7	5.74	24	79.7 + j14.6
0.3	5.67	40	85.5 + j7.3	5.71	40	84.7 + j7.0
0.35	5.84	48	85.3 - j1.3	5.87	48	84.8 - j1.2

The performance reports for the two ground calculation systems reach coincidence at about 0.2λ

above ground. Below that level, the RCA system shows ever-higher comparative gains and ever-lower comparative impedances as the antenna approaches the ground. You may wish to perform a similar comparative test using other combinations of permittivity and conductivity for the ground constants.

One of the consequences of the growing inaccuracy of the RCA ground calculation system with horizontal wires near to the ground applies to monopoles using ground radial systems. The rule of thumb is always to use the SN ground method for such systems. Of course, with NEC-2, the entire radial system must be above ground, even if very near to it. When placing such a system near to earth, be certain that the wire specifications do not allow an inter-penetration of the earth (Z = 0) with the surface of the radial wires. Since near-earth radial systems are in wide use to simulate buried radial systems, let's examine a simple model of one and see what results we obtain. Open model *11-4.nec*.

```
GW 1 15 0 0 .002 0 .237 .002 .001
GR 1 8
GW 9 15 0 0 .002 0 0 .239 .001
GE 1
GN 2 0 0 0 13.0000 0.0050
FR 0 1 0 0 299.7925 1
EX 0 9 1 00 1 0
RP 0 181 1 1000 -90 0 1.00000 1.00000
```

The model begins with a single radial and uses the GR command to replicate via rotational symmetry the remaining radials. GW9 is the vertical monopole at the center, with a total length of 0.237 m. The radials have a radius of 0.001 m and a height above ground of 0.002 m, giving us 0.001 m or 0.001λ clearance. Run the model and record the gain, TO angle, impedance, and AGT (free-space) values.

Next, let's see what happens with a buried radial system in NEC-4. Open--if you have the core--model *11-4a-nec4.nec*.

```
GW 1 59 0 0 .237 0 0 0 .001
GW 3 1 0 0 0 0 0 -.004 .001
GW 4 59 0 0 -.004 0 .237 -.004 .001
GM 1 7 0 0 45 0 0 0 4 1 4 59
GE -1 0 0
GN 2 0 0 0 13.0000 0.0050
FR 0 1 0 0 299.7925 1
EX 0 1 59 1 1 0
RP 0 181 1 1000 -90 0 1.00000 1.00000
```

The model uses slightly different construction methods, starting with the monopole that extends 0.237 m above ground. A vertical wire extends from ground down to a depth of 0.004 m so that its end is at Z = 0 and its length is the same as the segments in the monopole (and in the radials). GW 4 creates the first radial. Since rotational symmetry is not pertinent given the order of construction, a GM command creates the remaining 7 radials at 45° intervals.

Special reminder: since the wires penetrate the ground, set GE to -1 so that it does not modify the current expansion.

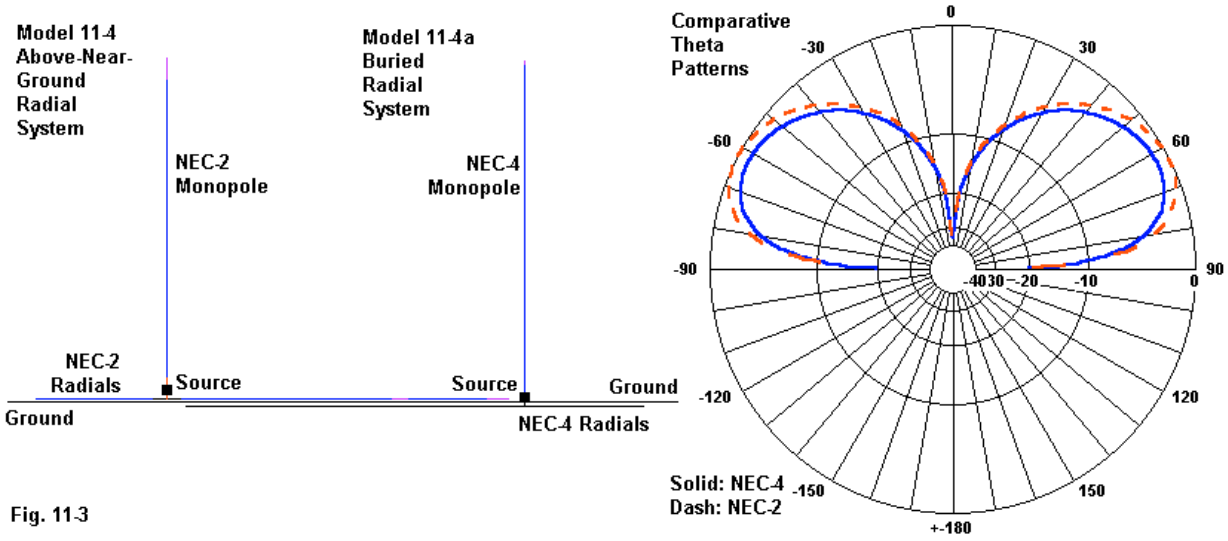

Fig. 11-3

Fig. 11-3 indicates the differences in the model structures. If possible, run the model for the same output data that you recorded for the NEC-2.

Model	Gain DBi	TO Angle degrees	Impedance R +/- jX Ω	AGT	AGT-dB	Adjusted Gain dBi
11-4	0.28	63	32.11 - j3.50	0.958	-0.184	0.46
11-4a	-0.59	62	49.58 - j4.79	1.021	+0.089	-0.68

The differential in the adjusted gain reports is well over 1 dB. In addition, the reported source impedance of the NEC-2 model is below the impedance using a perfect ground despite the use of equal-length monopoles. The above ground model falls short of being an accurate model of the buried radial system that it is supposed to simulate. In contrast, the higher impedance of the buried radial NEC-4 model shows the addition of ground losses to the inherent radiation resistance of the system, and it claims a more modest far-field gain, as illustrated by the comparative theta patterns in **Fig. 11-3**. Within the constraints of continuing investigations of ground properties and their consequences for monopoles with buried radials, the use of NEC-4 and buried radials is recommended for modeling such systems.

So far, we have varied the type of real ground used by the NEC models, but we have used only the ground qualities called "average." The label stems from a list of measured soil characteristics that appeared in "Standards of Good Engineering Practice Concerning Standard Broadcast Stations," *Federal Register* (July 8, 1939), p. 2862. The list has reappeared in several standard sources, such as Terman's *Radio Engineer's Handbook* (p. 709) and *The ARRL Antenna Book* (p. 3-6). NSI software in fact uses a more detailed list drawn from several sources. Both lists appear in the Appendix to this volume. For our present purposes, we need only a few diverse entries, and we may use the older list for our samples. Conductivity is measured in S/m (σ). Permittivity is also called the dielectric constant (ε). Under either name, the value is relative to the value for a vacuum (1.0, by definition) or, in practical terms, for dry air (1.0006). Relative permittivity values are perfectly usable in ground calculations, since the presumed medium for the antenna itself is a vacuum (or dry air).

Soil Description	Permittivity	Conductivity	Label
Salt water	5.0	81	SW
Pastoral, low hills, rich soil, typical from Dallas, TX, to Lincoln, NE	0.0303	20	VG
Pastoral, medium hills, and forestation, heavy clay soils, typical of central VA	0.005	13	Ave
Rocky soil, steep hills, typically mountainous	0.002	13	P
Cities, industrial areas	0.001	5	VP

VG = very good, AVE = average, P = poor, and VP = very poor. Now open model *11-5.nec*, which is the same model that we used previously--a 1/4λ monopole with an 8-radial system 0.002 m off the ground. The model differs only in the GN line.

```
GN 2 0 0 0 5 .001
```

The point of this model is to systematically vary the values of permittivity and conductivity. Note that typical tables may list conductivity first, but the GN command lists permittivity first. Run model 11-5 several times, changing the GN ground quality values with each re-run.

Soil Quality	Gain dBi	TO Angle degrees	Impedance R +/- jX Ω
SW	2.70	73	38.6 + j1.7
VG	0.60	64	33.7 - j1.6
Ave	0.28	63	32.1 - j3.5
P	0.31	63	32.0 - j3.5
VP	-0.70	60	29.9 - j9.4

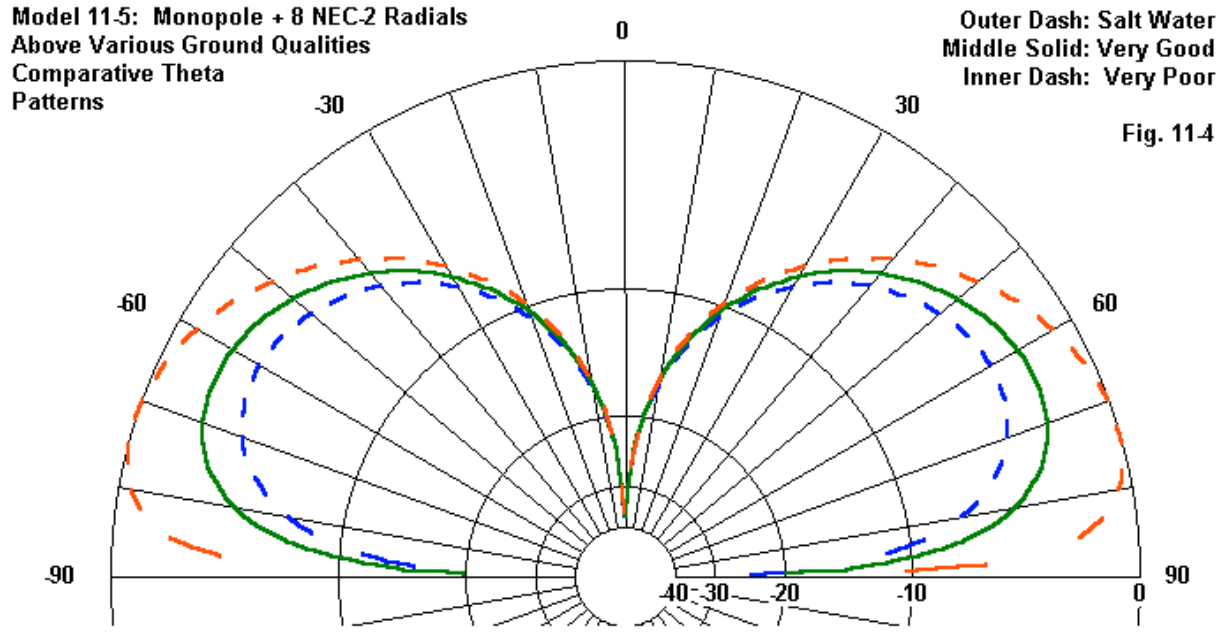

Fig. 11-4 shows selected theta patterns from the list, including the maximum (SW) and minimum (VP) gain values. Between the highest and lowest values, we find almost 3.5 dB differential. However, the curve is not smooth, since poor ground yields a slightly higher gain than the seemingly better average ground. However, the complex relative permittivity used in the calculations is a vector function. NEC-4 yields nearly the very same values for the model with one exception. Salt water produces a slightly lower gain in NEC-4 (2.56 dBi). There is some evidence that the salt-water values more closely approach the limits of reliable results in NEC-4 than in NEC-2. General recommendations suggest that we should not use any values of conductivity and permittivity higher than those of salt water when using the more recent core.

The high variability of both the gain and TO angle of the vertical monopole contrasts to the performance of a horizontal antenna over the same range of ground qualities. Open model *11-6.nec*, a basic dipole placed 1λ above the ground.

```
GW 1 11 0 -.2375 1 0 .2365 1 .001
```

Once more, run the model and change the F1 and F2 values to cover the same ground quality range as for model 11-5.

Soil Quality	Gain dBi	TO Angle degrees	Impedance R +/- jX Ω
SW	8.14	76	68.9 - j9.6
VG	7.72	76	69.8 - j7.3
Ave	7.60	76	70.0 - j6.7
P	7.59	76	70.0 - j6.7
VP	7.18	76	70.8 - j5.1

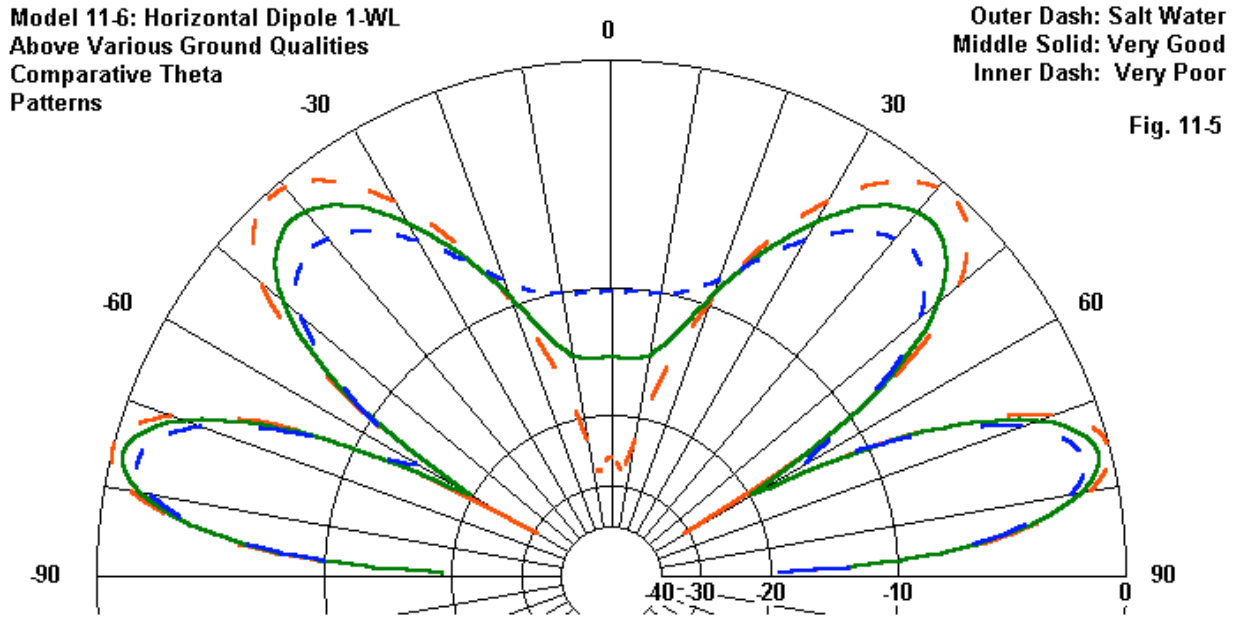

For the same range of ground qualities, the gain varies by under 1 dB, and the TO angle is

constant, as illustrated by **Fig. 11-5**. Although there is little variation in the lowest lobe that defines the TO angle, there is much greater variation in the second lobe upward. Indeed, the better the ground quality, the stronger will be all lobes above the lowest so that over perfect ground, they may be close to equal. You may wish to confirm this condition by changing the GN entry for model 11-6 to perfect ground. Not only does the gain remain within very narrow limits, but so too do the resistive and reactive components of the source impedance. The source resistance varies by less than 1.5 Ω and the reactance varies by 4.5 Ω.

These exercises are designed to acquaint you with the terms and the consequences of the GN command entries when using a single ground medium. However, a single medium is the easy part of the ground story in NEC.

The Second Medium

Mastering the addition of a second medium has two dimensions. The one that we shall not cover--its proper range of applications to real modeling analyses--may in fact be the easier. The first dimension--correctly entering the required data to produce a second medium--has enough convolutions to occupy us for a number of models. The following list enumerates most of the variations and variables.

1. In NEC-2 we may enter a second medium via either the GN command (if we do not specify ground radials for an RCA ground) or on the supplementary GD command.

2. In NEC-2, whichever command we use for the second medium, the inner medium may for a circular cliff or a linear cliff parallel to the Y-axis according to the selection we make in the RP command. RP2 specifies a linear cliff; while RP3 specifies a circular cliff.

3. In NEC-4, the RP command plays no role in the status of the inner medium.

4. In NEC-4, specifying a second medium via the GN command results in a linear cliff only. If we wish a circular cliff, we must use the supplementary GD command.

5. Where the GN and GD formats are compatible, NEC-4 will read a NEC-2 file RP2 or RP3 as RP0. Hence, some NEC-2 dual-medium models are readable in NEC-4--with the linear-cliff restriction.

Before entering into the mysteries of cliffs and second media, let's develop some base-line data. We shall establish a single antenna for all of our variations, a vertical dipole whose source segment is 1λ above ground. Throughout the exercises to follow, we shall use only two levels of ground quality: average soil and salt water. For baseline data, we shall begin with each quality as a single medium. Open model *11-7.nec*.

```
GW 1 11 0 0 1.2375 0 0 .7625 .001
GN 2 0 0 0 13.0000 0.0050
RP 0 181 1 1000 -90 0 1.00000 1.00000
```

GW1 shows the antenna structure, which is constant for all of the models. The GN command

shows average ground values. The RP command is type 0, appropriate to single medium models. Run the model.

Then open model *11-7a.nec*.

```
GN 2 0 0 0 81 5
RP 0 181 1 1000 -90 0 1.00000 1.00000
```

The GN command request salt-water values, and the RP request remains unchanged.

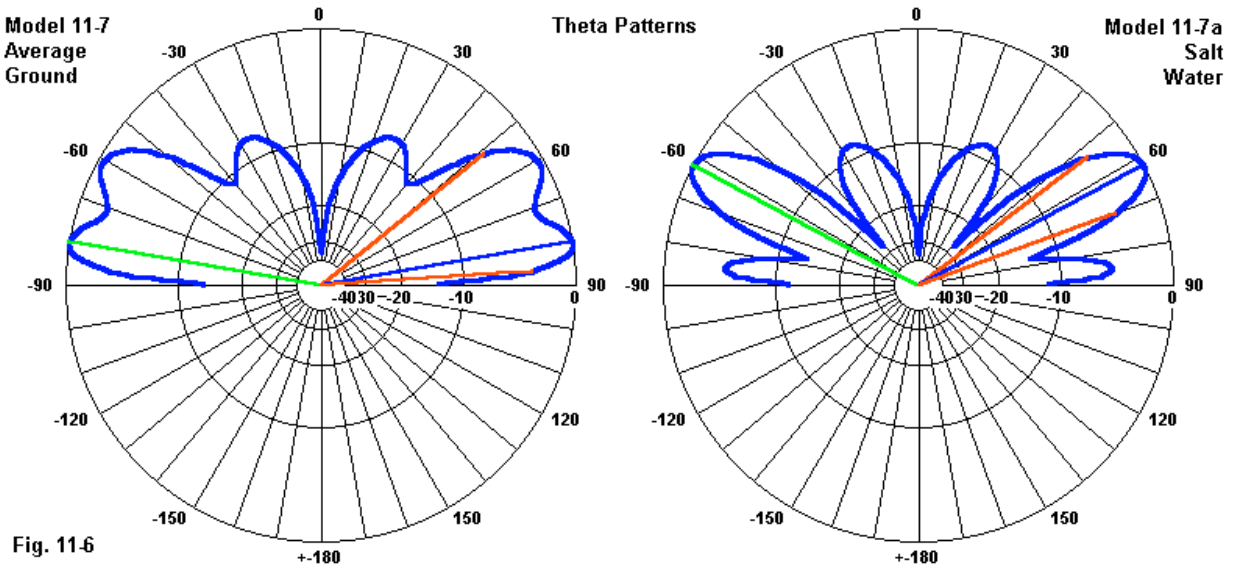

Fig. 11-6

The results for the two models are very different. Over average ground, the elevated vertical dipole has a maximum gain of 3.04 dBi with a TO angle of 80°. The source impedance is 71.1 + j0.2 Ω. Over salt water, the impedance is similar: 70.8 + 0.2 Ω. However, the maximum gain is 5.83 dBi at a relatively high elevation angle of 63°. (Excessive elevation of vertical monopole and vertical dipole systems tend to raise the TO angle beyond the desired range, especially when the ground quality is very high.) The reason for using these soil qualities is that we shall generally be able to identify the effects of a second medium in the resulting theta or phi patterns.

Although the first two models in the 11-7 series are common to both NEC-2 and NEC-4, the next three versions apply only to NEC-2. In all 3 cases, we shall use RP3 radiation pattern requests to specify a circular cliff. We shall begin by requesting the second medium within the GN command.

Cmd	I1	I2	I3	I4	F1	F2	F3	F4	F5	F6
	IPERF	NRADL	0	0	EPSR	SIG	*PER2*	*CON2*	*DIS2*	*CLF*
GN	2	0	0	0	13	.005	81	5	5	0

NEC manuals give no abbreviations for the F3 through F6 entries for a second medium, so I have italicized them to indicate their informal status. We may enter a second medium in the GN command only if I2 (NRADL) is zero. If NRADL has any other entry, the meanings of F3 through F6 change.

F3 (PER2) and F4 (CON2) list the permittivity and conductivity values that apply to the second medium. NEC calculates the source impedance and current distribution based on the ground values within the first medium (F1 and F2), but accounts for the change in values when calculating reflections that become part of the far-field radiation pattern.

F5 (DIS2) sets the distance from the coordinate system origin (X = Y = Z = 0) at which the second medium begins. It is possible to calculate the impedance and current distribution over one medium and the entire far-field radiation pattern over another medium by setting this distance to zero. More normally, we shall set a positive value in the F5 position. For our examples, the distance is 5 m (or 5λ) from the antenna, which is over the coordinate system origin.

F6 (CLF) represents the change of height downward from the initial ground level for the second medium. If the ground is level, F6 is zero. No upward elevation is permitted. We shall use a 5-m drop (entered as a positive value of 5) in the F6 position whenever we desire an actual cliff. However, we may use smaller cliffs to simulate ground slope (using either a circular inner medium or a straight line or linear cliff option). At the other extreme, some modelers obtain a first-order simulation of an antenna atop a tall structure by using a very large cliff value. The transition between media and their heights is abrupt, since NEC does not calculate diffraction effects from the edges formed by second medium entries.

The next 3 sample models all use the same RP command:

```
RP 3 181 1 1000 -90 0 1.00000 1.00000
```

The RP3 command requests a circular boundary for the first medium. If the RP command does not request an I1 value of 2, 3, 5, or 6, the second medium will not register.

Open model *11-7b-nec2.nec*. The GN request is the same one that we used to illustrate the command structure. The command requests a second medium to use salt-water values but to stay at the same level as the inner medium. Run the model and confirm the maximum gain of 2.70 dBi at a TO angle of 60°, with a source impedance of 71.1 + j 0.2 Ω. Because the inner or first medium in all of our further models in the 11-7 series will use the values for average ground, the source impedance will not change. Note that the maximum gain--given this particular combination of antenna position, ground levels, and selected media--is actually lower than the gain for average ground alone.

Next, open model *11-7c-nec2.nec*. In this model, the GN command requests the same medium (average ground) but at a lower height.

```
GN 2 0 0 0 13 .005 13 .005 5 5
```

Run 11-7c and confirm the maximum gain of 6.82 dBi at an 88° TO angle. Now open model *11-7d-ne-2.nec*, which requests both a 5-m cliff and a change of ground quality past the 5-meter radius.

```
GN 2 0 0 0 13 .005 81 5 5 5
```

Confirm the maximum gain of 5.77 dBi at an 81° TO angle.

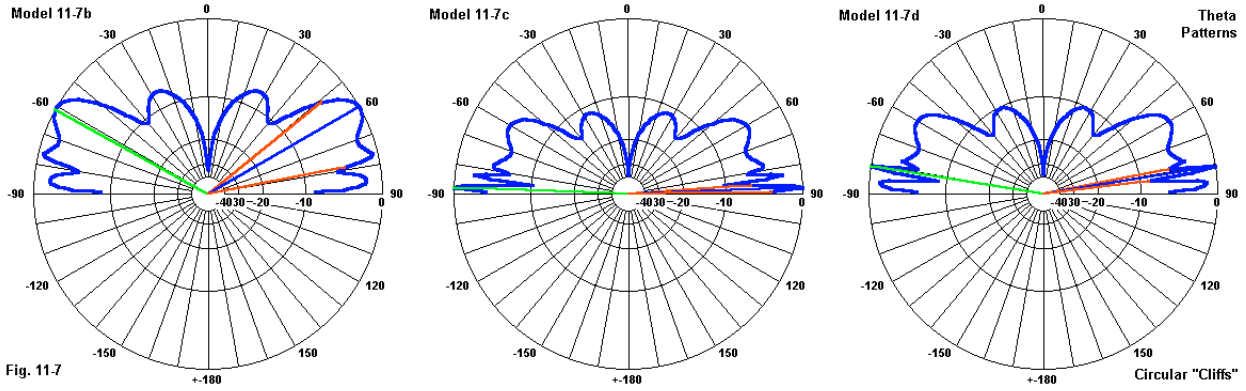

The single value data may be less effective in showing the effects of adding a second medium than the theta patterns in **Fig. 11-7**. Remembering that the gain limit for the first of these three normalized plots is much lower than for the other two, we can recognize that the upper structure of the patterns is relatively unchanged by the second medium. However, terrain changes--in terms of both quality and height--can radically alter the lower structure of the radiation pattern. Because NEC does not calculate diffraction effects, the lobe shifts may be sharper than in reality.

Let's re-run this series but call for a linear cliff. In NEC-2, we achieve this by changing the RP command from I1 = 3 to I1 = 2. Because the effects of the second medium will not apply to the entire horizon, we shall add to the radiation pattern requests a phi pattern at the TO angle recorded in the theta pattern.

```
RP 2 181 1 1000 -90 0 1.00000 1.00000
RP 2 1 361 1000 80 0 1.00000 1.00000
```

Open and run model *11-7e-nec2.nec*, the model corresponding to 11-7b. Note that the maximum gain does not lie in the direction of the second medium, but away from it. The conflict of the reflections from the two media at the same height results in a null region just where the first medium alone would produce a lobe. Perform the same tasks for models *11-7f-nec2.nec* and *11.7g-nec2.nec*. You will discover that the maximum gain and TO angle values are the same as for their counterpart models using a circular boundary between media.

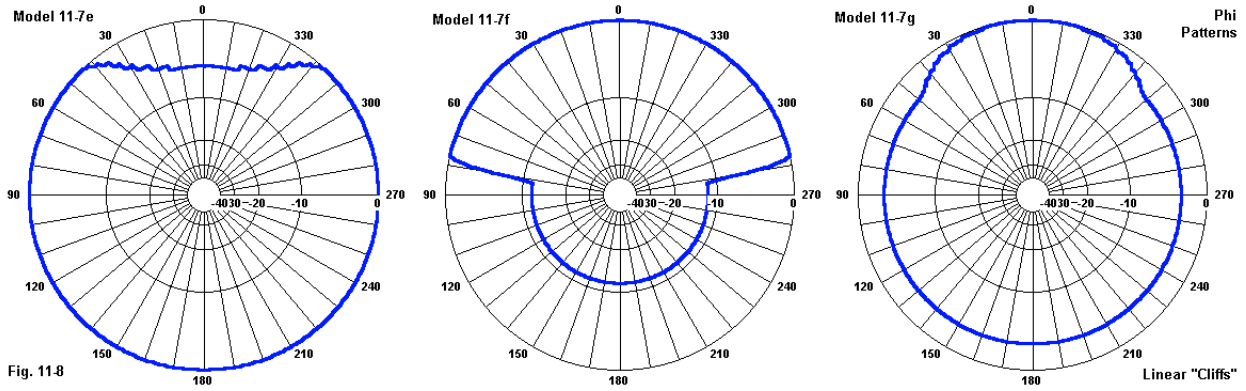

As expected, none of the phi patterns are circular, as they would be for models 11-7b through 11-

7d. Each uses its own TO angle as a reference, so do not expect the patterns to remain constant at all theta angles. Indeed, a full exploration of the "ins and outs" of the patterns would make heavy use of the surface (3-D) pattern facility to find all of the interesting undulations.

Thus far, we have used the GN command to create 2 ground media in NEC-2. We may reformulate the entire sequence of models from 11-7b through 11-7g by using the GD command that provides supplementary ground descriptions. This step would be necessary if NRADL is greater than zero, because the GN entries F3 through F6 would change their meanings. As a general procedure, using GD for the second medium may be advisable as a way of reducing the number of options to remember. A typical pair of GN-GD command lines would have the following appearance.

```
GN 2 0 0 0 13 .005
GD 0 0 0 0 81 5 5 0
```

The GN command now appears identical to a request for a single medium. The entirety of the request for a second medium goes into the GD command.

```
CMD   I1    I2    I3    I4    F1    F2    F3    F4
      0     0     0     0     EPSR2 SIG2  CLT   CHT
GD    0     0     0     0     81    5     5     0
```

In NEC-2 (only), all 4 integer positions take zeroes. F1 through F4 correspond to the F3 through F6 positions of the GN line when used to enter a second medium. ESPR2 and SIG2 are the permittivity and conductivity values, respectively, of the second medium. CLT is the distance between the coordinate system origin and the demarcation between media, whether we use a radial limit (RP3) or a linear limit parallel to the Y-axis (RP2). CHT is the downward height change, entered as a positive number that registers the cliff height.

Run the entire series of models from *11-8b-nec2.nec* through *11-8g-nec2.nec*. Each one corresponds to its similarly numbered model in the 11-7 series. (Hence, 11-8 and 11-8a are missing, since they would not change relative to the 11-7 versions.) Examine and compare the GN-GD commands with the corresponding all-in-one GN commands for the 11-7 series. You should obtain resulting performance parameters and patterns that are identical for each corresponding member of the two series of models.

NEC-4 has some important differences from NEC-2, even thought the GN command entries may look similar. In fact, a 2-media GN command structures has the same meanings as in NEC-2 with one exception.

```
Cmd   I1    I2    I3    I4    F1    F2    F3    F4    F5    F6
      IPERF NRADL 0     0     EPSR  SIG   PER2  CON2  DIS2  CLF
GN    2     0     0     0     13    .005  81    5     5     0
```

If NRADL is zero, then the floating decimal positions have the meanings earlier assigned. However, the only available choices of radiation pattern requests are RP0, the "standard" far-field pattern request and RP1, the ground-wave request. NEC-4 will read the entire sequence of models in the 11-7 series, but it has no way within the GN command of distinguishing between a request for a circular inner medium limit and a linear cliff. By default, NEC-4 will read all second

media included in the GN command as requests for a linear cliff that is parallel to the Y-axis.

To make a selection of cliff types in NEC-4, you must use the GD command.

```
CMD   I1    I2    I3    I4    F1    F2    F3    F4
      ICLIF 0     0     0     EPSR2 SIG2  CLT   CHT
GD    0     0     0     0     81    5     5     0
```

In NEC-4 only, if ICLIF = 0, there is no second medium, although omitting the GD command suffices to achieve this goal unless one includes several execution requests within the same model. If ICLIF = 1, then the boundary is linear at a distance specified in F3 (CLT). If ICLIF = 2, then the cliff is circular with an inner medium radius equal to the value of F3 (CLT).

Open and run models *11-8e-nec4.nec* through *11-8g-nec4.nec*. These models correspond to the NEC-2 versions, with the necessary addition of I1 = 1 to the GD command to inform NEC-4 that the request is for a linear cliff. The radiation pattern requests use the RP0 option for far-field patterns. Do not expect to obtain identical results to the ones that you obtained for the NEC-2 versions of the models. The first version requests a change of ground quality but not of ground height, and its results are very close to the NEC-2 output. Model 11-8f-nec4 shows essentially the same patterns as its NEC-2 counterpart, but with about 0.5-dB lower gain.

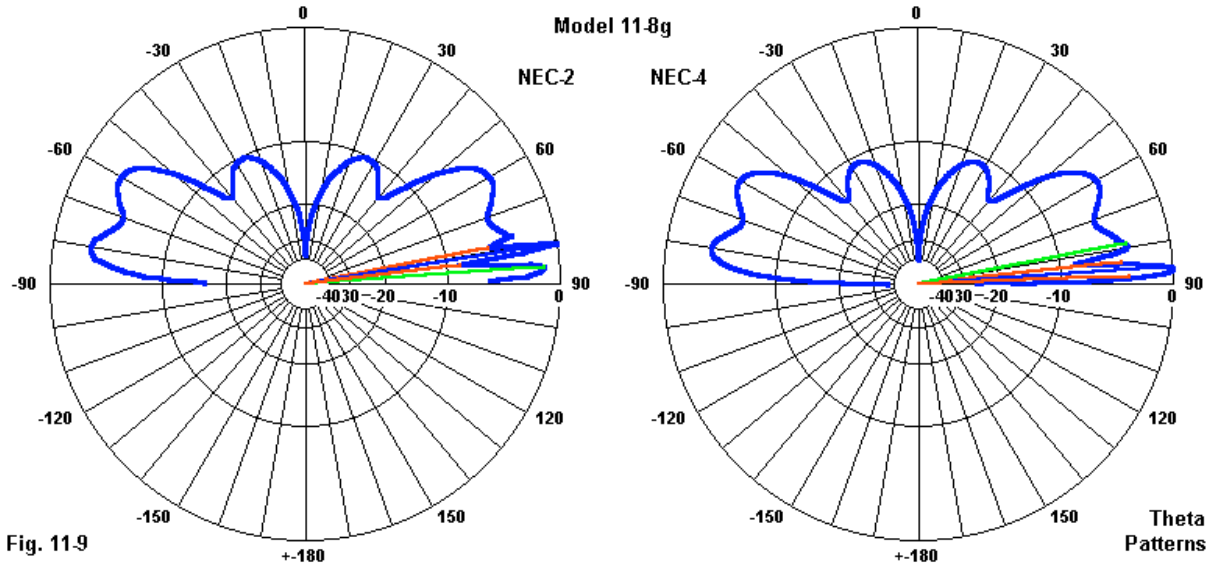

Fig. 11-9

Model 11-8g-nec4 departs most from the NEC-2 version, as revealed in the comparative theta plots in **Fig. 11-10**. Away from the linear cliff, both plots are virtually identical. However, in the direction of the cliff, the 2 cores show different forward lobe structures. The very great differential in the inner and outer medium ground qualities combined with the differences in the core calculation algorithms is the most likely source of the disparity. The NEC-4 core shows a lower main lobe that is near a half-dB stronger than the sharp higher main lobe for NEC-2. However, the weaker lower lobe in the NEC-2 theta pattern does correspond well with the lowest lobe in the NEC-4 pattern. Since neither pattern accounts for diffraction effects of the sharp and high (5λ) cliff, it is likely that the reality of such a situation may yield a third pattern that we cannot show.

The use of the GN and GD commands to set up differential ground conditions and changes in ground height does have limitations.

GN RCA Radials

We have noted that if the GN command's I2 (NRADL) entry is greater than zero, then you must use the GD command to enter a second medium. If NRADL is 1 or more, then the meanings of F3 through F6 change. Let's see what happens to the GN command under these conditions.

```
Cmd   I1    I2    I3    I4    F1    F2    F3    F4    F5    F6
      IPERF NRADL 0     0     EPSR  SIG   RADS  RADW  --    --
GN    0     8     0     0     13    .005  .237  .001
```

I2 shows a request for 8 radials. The single-medium ground quality values go into F1 and F2 as always. However, F3 and F4 have new meaning, with informal italicized headings. RADS is the radius of the screen, or the length of the individual radials in the screen. RADW indicates the radius of the individual wires composing the set of radials.

In NEC-2, the RP command must have an I1 assignment of 4 for a simple set of radials. If there are GN and GD commands requesting both a screen and a second medium, then the NEC-2 RP command must let I1 = 5 for a screen and a linear cliff or let I1 = 6 for a screen and a circular cliff. NEC-4 uses I1 = 0 in the RP command for all these cases, since the type of cliff will be set in the GD command. NEC-4 will read a NEC-2 model with only a screen request by treating the RP4 request as RP0.

The radial screen option in the GN command applies only to the RCA real ground type (I1 = 0) and is not allowable with a request for an SN ground (I1 = 2). The calculations are based upon a modified reflection coefficient, and the resulting source impedance report will be the same as for a perfectly conducting ground (I1 = 1). Despite this limitation, the system is more versatile than simpler ground systems (such as those used with MININEC cores), since it will show differences in far-field patterns due to changes in the ground quality and changes in the number of radials.

Open model *11-9-nec2.nec*.

```
GW 1 15 0 0 0 0 0 .237 .001
GE 1
GN 0 8 0 0 13 .005 .237 .001
FR 0 1 0 0 299.7925 1
EX 0 1 1 00 1 0
RP 4 181 1 1000 -90 0 1.00000 1.00000
```

The GW entry creates a 1/4λ vertical monopole that touches (average) ground. The GN command requests a ground screen with a radius of 0.237 m (the same length as the monopole) with wires having a radius of 0.001 m. The RP4 pattern request acknowledges the desire for a ground screen. Run the model and confirm a gain of 1.02 dBi at a TO angle of 62°. The source impedance is the same as it would be with no screen and a perfect ground: 36.0 + j0.1Ω.

Let's compare these results to the same model, but with 120 radials. Open model *11-9a-*

nec2.nec.

```
GN 0 120 0 0 13 .005 .237 .001
```

Only the GN command entry changes, and then, only in the I2 position. Run the model and confirm the gain as 2.84 dBi at a TO angle of 63°.

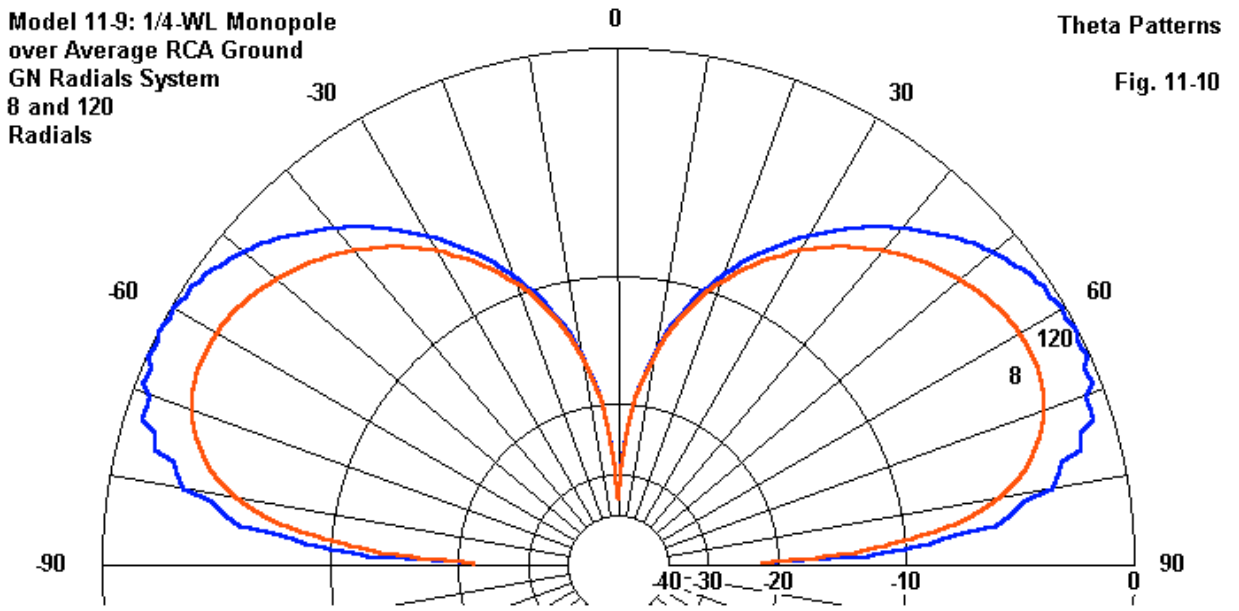

Fig. 11-10 compares two theta patterns, with the inner pattern reflecting a screen that used only 8 radials. However, note the ripple in the lower edges of the pattern for 120 radials. It suggests the limitations of the system. If you are curious, you may run model *11-9b-nec2.nec* and watch the core call out an error for the attempt to run a radial screen with the SN ground method requested. Pattern strength is not the only comparison that we may make between the runs. The 120-radial screen took less than twice the time required for the 8-radial model, and even then, the total time was about 0.1 seconds on a relatively slow PC. The radial screen system does offer speed advantages when making preliminary comparative models involving vertical systems that require radial systems.

NEC-4 runs of the same models yield slightly different gain results: 1.13 dBi for the 8-radial model and 2.62 dBi for the 120-radial model. The small-screen result is higher than for NEC-2, while the large-screen result is lower. You can confirm these values by running models *11-10-nec4.nec* and *11-10a-nec4.nec*, which are modified for that core. Model *11-10b-nec4.nec* will confirm that NEC-4 also provides an error report if the GN command combines a request for an SN ground and a value of NRADL greater than zero.

Before we leave the creation of RCA ground screens, we might well ask how well the reported values correlate to performance reports from a NEC-4 buried radials system for essentially the same monopole. An earlier model (11-4a-nec4) employed 59 segments per long wire (element and radials) to ensure model adequacy in the transition through the Z = 0 level. If we try to use

that model, a version with 120 radials will have around 7000 segments. However, we can shrink the model size and retain relatively good model adequacy by using length-tapering techniques. Open model *11-11.nec*. Because this model creates buried wires, it is for NEC-4 only.

```
CM Monopole with buried radials
CM 8 radials; tapered elements
CE
GW 1 1 0 0 -.004 0 0 0 .001
GW 2 1 0 0 0 0 0 .004 .001
GW 3 10 0 0 .004 0 0 .237 0
GC 2 0 0 .001 .001 .004 .1
GW 4 10 0 0 -.004 0 .237 -.004 0
GC 2 0 0 .001 .001 .004 .1
GM 1 7 0 0 45 0 0 0 4 1 4 7
GE -1 -1 0
GN 2 0 0 0 13.0000 0.0050
FR 0 1 0 0 299.7925 1
EX 0 2 1 0 1 0
RP 0 181 1 1000 -90 0 1.00000  1.00000
EN
```

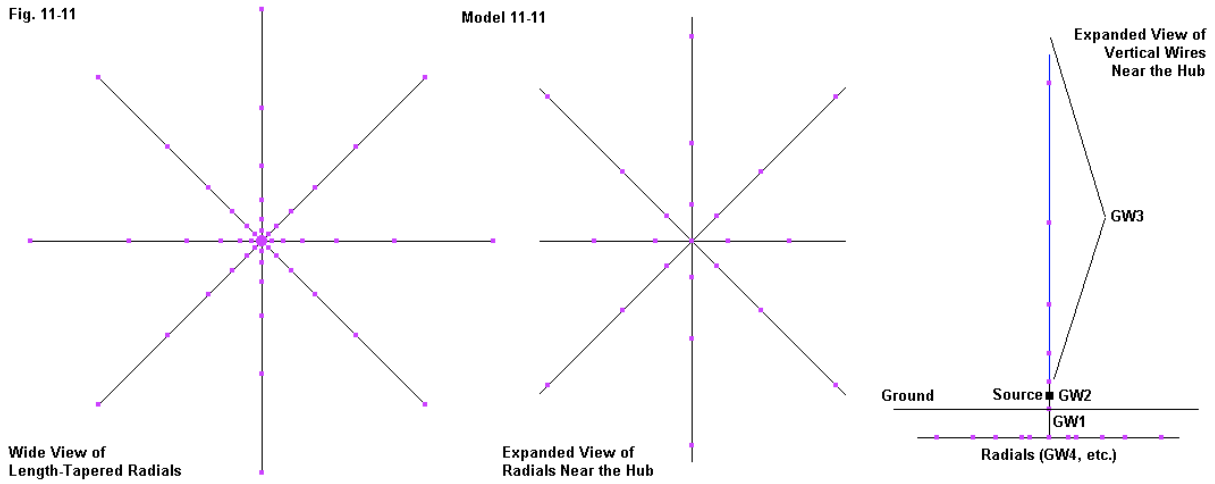

Fig. 11-11 helps to set the geometry structure in place. GW1 is the wire connecting the source wire (GW2) to the radial hub. Both GW1 and GW2c are the same length: 0.004 m. GW 3 creates the remainder of the vertical structure. It requests 10 segments, but the following GC tapering command overrides that value and produces 7 segments ranging in length from 0.004 m at the bottom to 0.1 m at the top. This tapering scheme ensures that the segment adjacent to the source wire is the same length as the source wire. GW4 and the following GC command set up the first radial, again with segments lengths that taper from 0.004 m at the hub end to 0.1 m at the tip. The GM command replicates radials 7 more times. Note that it specifies the actual segment limits of the GW-GC set-up pair, not the 10 segments originally requested in the GW4 entry. Of course, for a set of buried radials, we use the SN ground method. The model requires only 65 segments.

To arrive at 8 equally spaced radials, the GM command used a rotation angle of 45°. Open model

11-11a.nec, also a NEC-4-only model. This one requests 120 radials.

```
GM 1 119 0 0 3 0 0 0 4 1 4 7
```

The only differences in the new version of the model occur in the GM command. It requests 119 copies of the master radial (GW4 + GC) at a 3° rotational increment. Of course, the total number of segments in the model rises, but only to 849. Both the 8-radial and 120-radial models produce AGT scores close to 1.02 and very close to each other, giving confidence in the reported differential of maximum gain.

The following table compares the reports of the RCA screen models to those of the buried radial models, using NEC-4 reports for both.

RCA Radial Screen--Model 11-10/10a

# Radials	Gain dBi	TO Angle degrees	Impedance R +/- jX Ω
8	1.13	62	36.0 + j0.0
120	2.62	63	36.0 + j0.0
ΔGain	1.49		

Buried Radials--Model 11-11/11a

# Radials	Gain dBi	TO Angle degrees	Impedance R +/- jX Ω
8	-0.69	62	49.2 - j8.3
120	0.73	62	31.5 - j13.4
ΔGain	1.42		

The similarity of the gain differentials between small and large radial systems suggests that the RCA ground screen system is quite suitable for preliminary comparisons of vertical arrays that employ radials. The run-speed savings are considerable, even on high-speed PCs. However, for fine tuning a design or determining the trends in the source impedance, the SN method with actual buried radial wires remains vital to modeling efforts.

Summing Up

The GN command is a versatile entry point for specifying both the type of ground environment that we need and for entering appropriate ground quality specifications. The free-space or no-ground condition proves useful for comparing relevantly similar antenna structures with their main lobes in the same vertical and horizontal direction. The perfectly reflective ground is better suited to vertical monopoles and similar structures that contact the ground for direct comparison. However, if we need to analyze the performance over a real ground, then we need to select between the reflection coefficient approximation (RCA) and the Sommerfeld-Norton (SN) method. The former calculates very rapidly, but proves inaccurate as horizontal wires draw closer than about 0.2λ to the earth. While slower to calculate, the SN method yields highly accurate results with wires as close as 10^{-6}λ to the earth. Neither system of real-ground calculation permits the omission of a ground radial structure for antennas touching the ground. However, in NEC-2, any radial ground system must be slightly elevated above ground. Only NEC-4 allows direct modeling of a buried radial system.

The GN command has three major functions. 1. It specifies the type of ground and the ground quality parameters (permittivity and conductivity) for a single ground medium. 2. It allows specification of a second medium in terms of its parameters, its starting point relative to the origin of the coordinate system, and the amount, if any, by which the second medium is lower than the

first. 3. Alternatively to item 2, the GN command can specify a ground medium and a set of ground-screen radials having a specified length and wire radius for use only with the RCA ground calculation system. In NEC-2, you must use RP I1 entries 2 through 6 to cause execution of anything but a single medium and to distinguish between linear and circular cliffs. In NEC-4, no RP special entry is required, but the GN command second medium entry will be interpreted as a linear and not a circular cliff.

You may enter a second medium through the use of the GD supplementary ground description command. If the GN command requests a radial system, then you must use the GD command for a second medium. In NEC-2, the GD command does not specify the linear vs. circular cliff alternatives, since the RP command performs that function. In NEC-4, selection of the circular cliff requires the use of a GD command, which has entry options for both cliff types.

The radial ground screen entries, usable with the RCA ground calculation system, simulate with simplified approximations user-selected radial systems. Calculations are extremely fast, and the range of resulting reported gains generally reflects the gain range reported by buried radial systems in NEC-4. However, the source impedance is always the value calculated over perfect ground, and the gain reports are individually over-optimistic. Hence, the system is useful for rapid preliminary comparisons, but requires more refined modeling methods for more precise results.

NEC-4 removes some of the potential for error that exists in the NEC-2 implementation of the GN and GD commands by removing the need for using special entries in the RP command. However, in either core, the ground commands offer considerable flexibility to those who master the variables associated with their use.

12.
Mathematical and Wire Transmission Lines

***Objectives**: These notes will examine both the special TL command, with its ability to model 2-wire transmission lines operated in the transverse electromagnetic mode (TEM), and modeling parallel transmission lines using wires, that is, GW commands. We shall learn of unique potentials for each type of transmission-line model as well as limitations for each type.*

Both NEC-2 and NEC-4 include a special facility for generating non-radiating, mathematical transmission lines between two wires. The TL command governs the creation, placement, and properties of the lines. With the TL facility, we can create a large number of standard configurations, including straight lines, shorted and open reactive stubs, and multiple series, parallel, or series-parallel combinations. As well, we shall encounter a few non-standard applications for such lines. The lines will be "frequency-nimble," that is, they will require no modification as we change the frequency of operations for a model.

TL-based transmission lines have limitations that will lead us to create physical parallel transmission lines composed of parallel GW and related geometry command wires. Such lines are limited in their own ways by the general constraints on NEC geometry. However, for many applications in which TL lines are not applicable, these lines often serve very well. We shall even be able (in NEC-4) to develop transmission lines that simulate a velocity factor.

Both types of lines allow only 2-wire systems, although in principle, you might be able to model larger transmission-line systems with physical wires. They operate in the most basic TEM mode, i.e., the transverse electromagnetic mode. We shall confine our work to these lines, since they will present challenges enough for this chapter.

TL Command Fundamentals

Introducing a transmission line into a model requires at least two wire segments in the GW portion of the model. Every TL command must specify a termination for both ends of the line. Since every transmission line has a characteristic impedance, we must also know that value. Finally, we must either know the electrical length of the line or be willing to accept the NEC calculation of the straight-line distance between the centers of the segments to which the line connects.

```
CMD      I1    I2    I3    I4    F1    F2    F3    F4    F5    F6
         TAG1  SEG1  TAG2  SEG2  ZC    TLEN  Y1R   Y1I   Y2R   Y2I
TL       1     6     2     1     70    0.5   0     0     0     0
```

The integer entries in the command line specify the two ends of the line in terms of their tag numbers and segment numbers. If either tag number is zero, then the segment number refers to the absolute segment number assignment found in the segmentation data table in the output

report. You may recall an early caution about the possibility of intentionally assigning to a GW or similar entry a tag number of zero. The TL command is an example of why such a practice may result in modeler confusion as to which segment holds the terminal of a transmission line. Geometry entries in most cases should assign tag numbers greater than zero so that zero-value tag entries in a control command can unambiguously result in references to absolute segments.

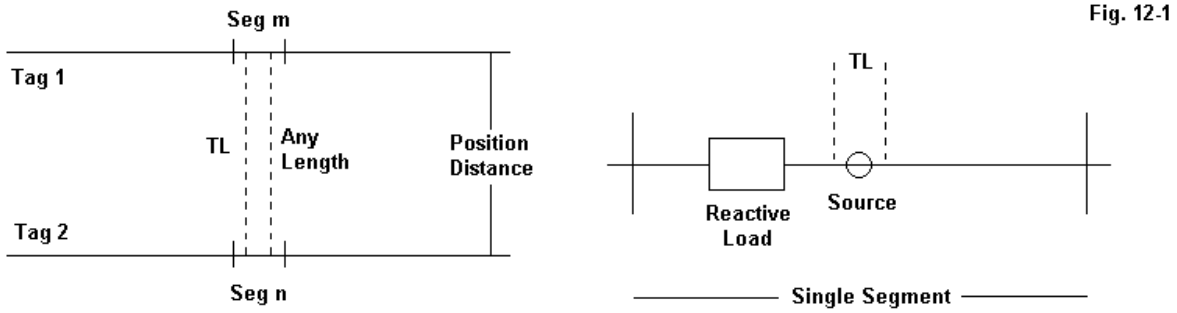

Fig. 12-1

The left portion of **Fig. 12-1** reveals the general set-up for a TL entry. F1 (ZC) gives the line a characteristic impedance. If you enter ZC as a negative number, the minus sign reverses the TL connections at end 2, equivalent to giving a parallel feedline a single half twist along its length. The F2 entry specifies the electrical length of the line in meters, regardless of the unit of measure used in the geometry section of the model. (Since all control commands occur after the use of the geometry scaling command (GS), any control command requiring a dimension will use meters as the unit of measure.) If you enter zero as the value of TLEN, NEC will calculate and use the straight-line distance between the segments representing the line's terminations. If you wish to specify a virtual zero-length line, you must enter a tiny value, such as 1E-10. The line length that you enter under F2 will be the electrical length of the line, regardless of the physical or positional distance between the two terminating points.

The consequences of these entries are numerous. First, the TL entry does not internally handle the velocity factor of a line. The velocity factor is the ratio of the physical length to the electrical length based on the line construction. Velocity factor values are 1.0 or less, so that a line is electrically as long or longer than the physical length of the line. In all cases, the modeler must pre-calculate the electrical length of the line in use, using either general table values, manufacturer specifications for a specific line, or actual measurements of the velocity factor. The more critical the modeling analysis, the more relevant it becomes to actually measure the velocity factor, since the actual value may vary considerably from the value listed in specification sheets or general tables.

In many modeling exercises, you will vary the electrical length of the line within the model until you reach an acceptable value. In such cases, you may then back-calculate the physical length from the known or presumed velocity factor. In other cases, you may have an assigned physical length and then calculate the electrical length. For such exercises, NSI software provides a user convenience demonstrated by the right side of **Fig. 12-2**. The left-side entry shows the direct entry of the electrical length. Note that the resulting velocity factor is always 1.0. However, the right side shows the entry of a physical length and a velocity factor supplied by the modeler. The program then performs the requisite calculation for you.

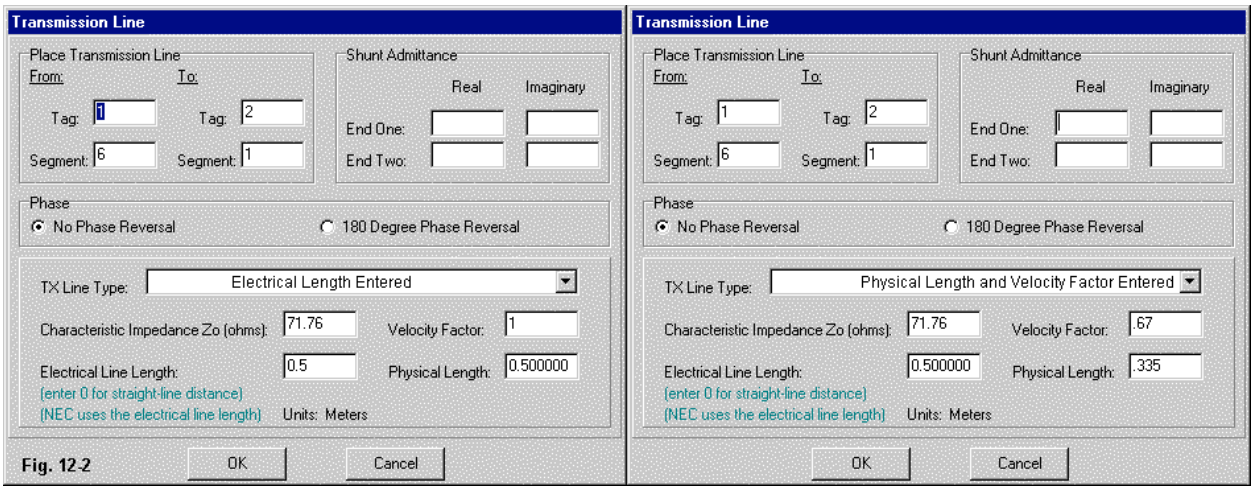

Fig. 12-2

In the sample command and in **Fig. 12-2**, there are blank boxes for the end-1 and end-2 shunt admittance values. Simple applications of a transmission line extending between two wires of the structure geometry rarely call for entries in these boxes or on the line. You may indicate an absence of shunt admittance value by leaving these entries blank or by inserting zeroes in all 4 places. If you wish an entry in only one of the places--for example F5 (Y2R, the real component of a shunt admittance at end-2 of the line, as indicated by the TAG2, SEG2 entry)--then you must insert zeroes in the preceding places. Otherwise, the program will close up the line and treat the initial blanks as a single space, moving the entry to F3.

The real (conductance) and imaginary (susceptance) values of shunt admittance require conversion in advance, if you are initially working with impedance (resistance and reactance) values. In addition, if you start with a series combination of those values, you must convert them to the equivalent parallel or shunt combination. Since the applications for admittance entries are few and simple in this chapter, we shall examine more useful and complex cases when we explore the use of the NT command.

The proper use of the TL command requires that we remember the chart of series and parallel connections among sources, loads, and networks or transmission lines assigned to the same segment. See the right side of **Fig. 12-1**. Transmission lines and networks are in parallel with a source on the same segment. They are also in parallel with a second transmission line or network terminated on the same segment. Hence, we may create some interesting networks of transmission lines between "actual portions" of the structure geometry. The expression "actual portions" refers to the radiating geometry elements of the model. As we shall see, we may add to these elements some wires whose structure or position places them so that they do not alter the resulting operating parameters of the antenna being modeled.

Equally important is the fact that any reactive load (LD0 through LD4) is in series with the transmission line (and a source, if there is one on the segment). Hence, reactive loads will not load a transmission line end.

One of the major uses for simple transmission line assemblies is to find the effects of a transmission line on the impedance due to a mismatch at the antenna's normal source segment and a remote source at the other end of the line. To see the effects of such a system, let's start

with model *12-1.nec*. We shall not reproduce this standard dipole model, but only record the reported source impedance: 71.76 + j0.12 Ω. Our real target is model *12-1a.nec*.

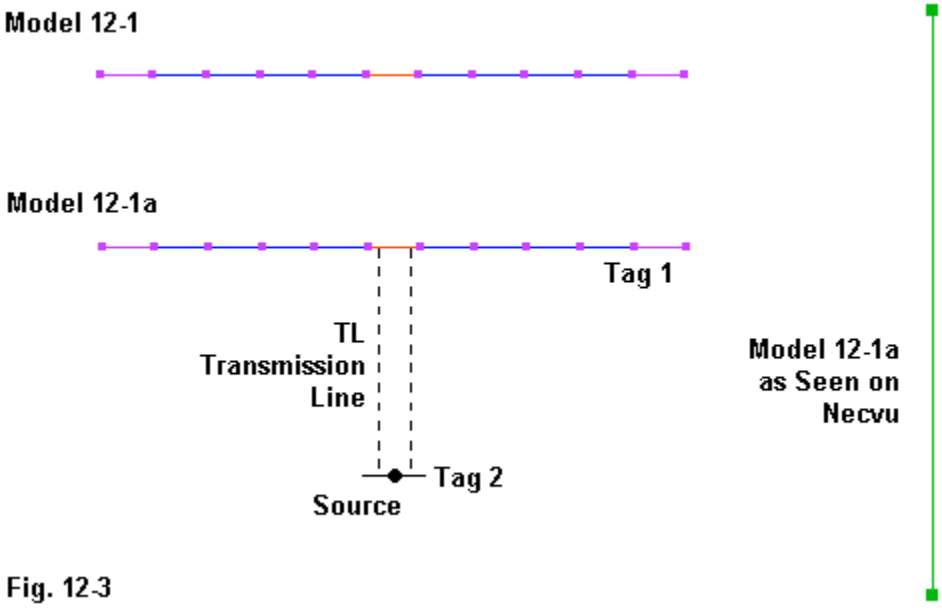

Fig. 12-3

As shown in **Fig. 12-3** and in the extracted lines from the model, we have inserted a transmission line between the normal dipole source segment and a remote wire. The transmission line length is 0.5 m, as specified in the F2 position of the TL command. However, the remote termination wire for the other end of the line has two interesting properties. First, it is as far away from the radiating dipole as may be feasible. It is so far away that the Necvu picture of the system cannot show any dipole detail. Second, the remote wire is very short, thin, and lossless. In fact, had we placed a material load (LD5) on the dipole, we would have omitted it from the termination wire. If the wire were not so remote, we would have set its length to less than $10^{-4}\lambda$ to ensure that the current level due to the interaction matrix is low enough not to disturb the results of adding the transmission line and placing the source on the wire.

```
GW 1 11 0 -.2375 0 0 .2375 0 .001
GW 2 1 0 -.005 9999 0 .005 9999 .0005
GE
FR 0 1 0 0 299.7925 1
EX 0 2 1 00 1 0
TL 1 6 2 1 71.76 0.500000
```

If we run the model, we obtain a source impedance of 71.76 - 0.25 Ω. We obtain this result as a function of several factors. First, we set the characteristic impedance (ZC) of the line to the dipole's original resistive impedance. Second, we set the line length to exactly 1/2λ. Third, all TL-generated transmission lines are lossless. If we wish to account for losses in a TL-based transmission line, we must introduce them as loads on the structure geometry, a tack that may or may not result in an accurate representation of the losses distributed along the length of a transmission line.

Fig. 12-4

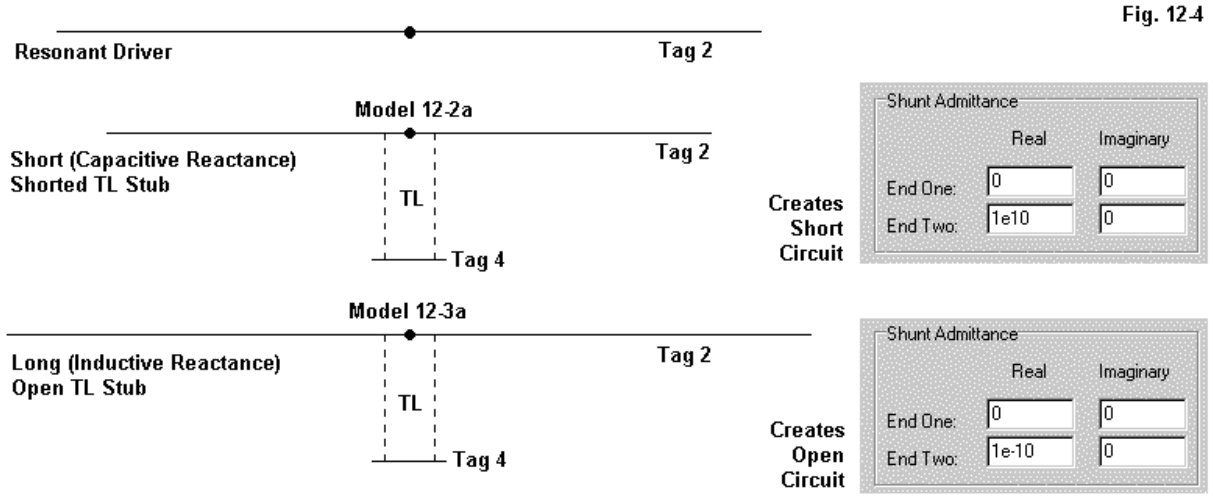

TL-based transmission lines are eminently suited to placing inductive or capacitive reactances in parallel with a source. We may use such lines to create beta matches that effect a match between a lower antenna source impedance and standard 50-Ω coaxial cable. Open model *12-2.nec*.

```
GW 1 21 0 -.249 0. 0 .249 0. .002
GW 2 21 .162 -.227 0. .162 .227 0. .002
GW 3 21 .308 -.217 0. .308 .217 0. .002
```

The model shows a 3-element Yagi, with GW2 as the driver. If we made the driver resonant, the array would show an impedance of about 30 Ω, not an especially good match for the ubiquitous 50-Ω coaxial cable feedline. With the driver dimension shown, the source impedance will be 26.6 - j27.7 Ω. Essentially, we have a 27-Ω resistive impedance and a series capacitive reactance of nearly 28 Ω. The result is a "down-converting" (relative to the source) L-network that lacks a shunt component of the opposite reactance type. In short, we need a shunt inductive reactance of some calculable value, and a shorted transmission-line stub can fill the need.

The following abbreviated table gives some value for series and shunt reactances for the down-converting L-network for a 50-Ω source impedance. Although all values are positive, the series and shunt reactances are normally of the opposite type.

Parameter	Value Combinations for a 50-Ω Source				
R_L	35	25	17	12.5	10
X_S	22.9	25.0	23.6	21.7	20.0
X_P	76.4	50.0	35.4	28.9	25.0

The nearest set of values corresponding to the source impedance is in column 2. Hence, we should expect to need a shorted stub having about j50 Ω inductive reactance across the feedpoint terminals. To obtain the stub length, we may initially use standard equations. X_L is the inductive reactance, Z_O is the characteristic impedance of the line, and *l* is the electrical length of the line in degrees.

$$X_L = Z_O \tan l \qquad l = \arctan\left(\frac{X_L}{Z_O}\right)$$

From the right-hand equation, we can calculate a line length for an arbitrary 300-Ω line and get about 9.46° for j50 Ω inductive reactance. 9.46° is about 0.0263 of a full 360°, which gives us the fraction of a wavelength measure of the stub. Since a wavelength is 1 m, the stub trial length is 0.0263 m. Now open model *12-2a.nec*.

```
GW 4 1 0 -.005 9999 0 .005 9999 .0005

EX 0 2 11 00 1 0.
TL 2 11 4 1 300 .0263 0 0 1e10 0
```

The notable lines appear above. First, we add a remote wire (GW4) to provide the termination of the stub. Second, we leave the source exactly where it was, since the stub is shunted across the source. Finally, we construct the TL command to place a line between the source segment and the new wire. We insert the characteristic impedance and the calculated line length in the F1 and F2 position. However, without further action, the stub will not be a short circuit. At end 2 of the line, on the remote wire, we place a real shunt admittance having a very high value to effect a virtual short circuit. 1E10 S (or mhos) is sufficient. (Some modelers place an imaginary shunt admittance of 1E10 in parallel with the real value, but this is generally unnecessary.) Run the model and obtain a matched source impedance of 55.2 + j3.6 Ω.

Open model *12-3.nec*, the pre-matched version of a driver needing an open stub to effect a match.

```
GW 1 21 0 -.249 0. 0 .249 0. .002
GW 2 21 .162 -.244 0. .162 .244 0. .002
GW 3 21 .308 -.217 0. .308 .217 0. .002
```

The driver is considerably longer than in model 12-2, suggesting that we may obtain an inductively reactance source impedance. Run the model and confirm a source impedance of 34.4 + j24.2 Ω. These values are near the tabulated values for a 35-Ω impedance, suggesting that an open stub having a capacitive reactance of about -j76 Ω might make a good shunt component for the beta match. For an open stub, we also use standard equations:

$$X_C = Z_O \cot l = \frac{Z_O}{\tan l} \qquad l = \arctan\left(\frac{Z_O}{X_C}\right)$$

XC is the only new term, and of course, it refers to capacitive reactance. If we stay with our 300-Ω characteristic impedance, we obtain a line length of 75.7° or 0.21λ. At 299.7915 MHz, this value is 0.21 m. Open model *12-3a.nec* and note the TL command.

```
TL 2 11 4 1 300 .212 0 0 1e-10 0
```

The line terminations, characteristic impedance, and line electrical length are clearly apparent. However, the end-2 shunt admittance has changed. To effect an open circuit, we insert a real shunt admittance value that is exceedingly low: 1e-10. (The equivalent resistance is the inverse of this value.) Now run the model and confirmed the new source impedance as 51.2 - j3.7 Ω.

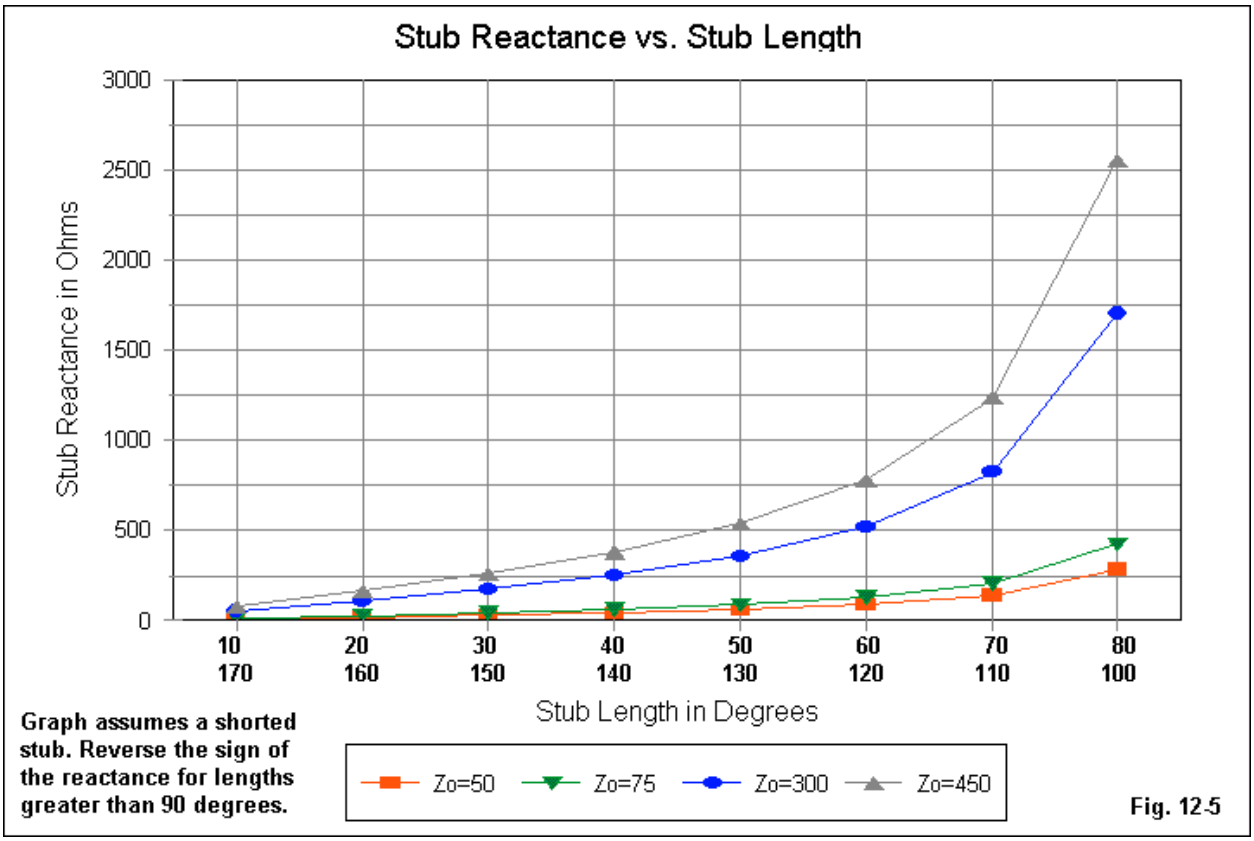

Fig. 12-5

Because stubs are so commonly used in models with the TL facility, I have included **Fig. 12-5** for reference. It lists shorted stub lengths from 0° to 180° and shows the calculated reactance for some of the most-used characteristic impedances. You may reverse the X-axis values to read 80 - 10 and 100 - 170 from left to right for open stubs. Requiring a 75° long open stub for a capacitive reactance of -j75 Ω, compared to a 9° stub for a j50-Ω inductive reactance gives some insight into why shorted stubs are far more common in beta matches than open stubs.

The stub situation, where the line lengths are well under 1/4λ, represents a very good use of the TL facility. Line losses are normally very low at these line lengths, regardless of the real transmission that the model simulates. Hence, modeled values tend to translate easily into physical implementations.

Not all applications of the TL command require the generation of a remote terminating wire. There are numerous element-to-element applications as well, for example, 2-element horizontal phased arrays. Open model *12-4.nec*. The following entries are key to the model.

```
GW 1 15 0 -.233 0 0 .233 0 .001
GW 2 15 -.12 -.256 0 -.12 .256 0 .001

EX 0 1 8 00 1 0
TL 1 8 2 8 -35.00 .214 0. 0. 0. 0.
```

The 2 GW entries describe the elements, with the source on the forward element. The TL entry

runs a 35-Ω transmission line between the centers of the elements, but with a literal twist. Note that the characteristic impedance is negative. The minus sign functions to reverse the connections at opposite ends of the line. For this model, we require no admittance entries.

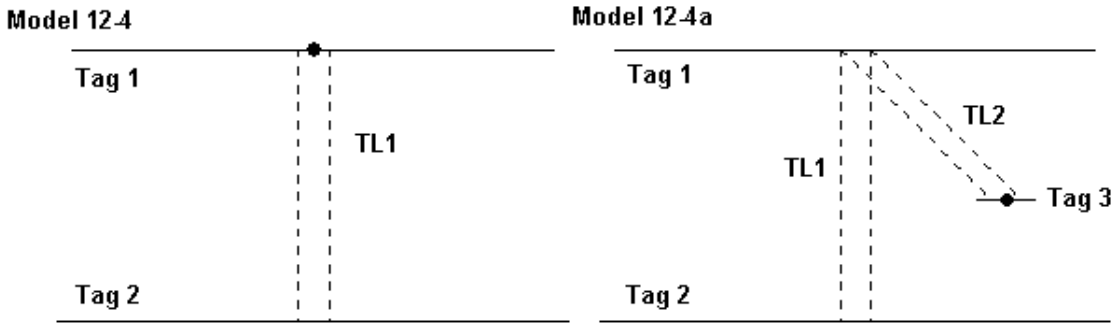

Fig. 12-6

Fig. 12-6 shows the model structure. Run the model to obtain its impedance at the present source location: 25.2 + j5.9 Ω. You may also wish to record the gain and 180° front-to-back ratio to compare with the next variation that we shall create. The source impedance is nearly resonant at a value we might transform to the standard 50 Ω by the use of a 1/4λ matching section. To transform the impedance, we need a line with a characteristic impedance that is the geometric mean of the impedances we wish to match, or

$$Z_O = \sqrt{Z_1 Z_2}$$

Z_O is the characteristic impedance, and Z_1 and Z_2 are the two impedances. The ideal impedance is 35.5 Ω, assuming we had no reactance. Since there is a 35-Ω coax (RG-83), we can use that value in a revision of the model that moves the source to a remote wire and places a new transmission line in parallel with the old feedpoint. The right side of **Fig. 12-6** now describes model *12-4a.nec*.

```
GW 3 1 0 -.001 9999 0 .001 9999 .0005
EX 0 3 1 00 1 0
TL 1 8 2 8 -35.00 .214 0. 0. 0. 0.
TL 1 8 3 1 35 .20
```

The new remote wire terminates the new TL command line. The source is now on GW3. The final length of the ostensible 1/4λ matching section is 0.2 m, since we had reactance at the original feedpoint. Run the model to arrive at the new source impedance of 51.3 - j0.4Ω.

Note that the two TL commands produce lines with seemingly very different functions. The matching line addition seems simply to transform one impedance to another. The original line transform the current magnitude and phase from the common point on GW 1 to a set of values that yields the resulting radiation pattern--which did not change with the addition of the matching section. However, every transmission lines is a continuous transformer of voltage, current, and impedance along its length, where the transformation factor is 1 in all categories for a perfectly matched system.

We may string together any number of TL lines as needed, with shunt or parallel connections at

each junction. Consider **Fig. 12-7** and open model *12-5.nec*.

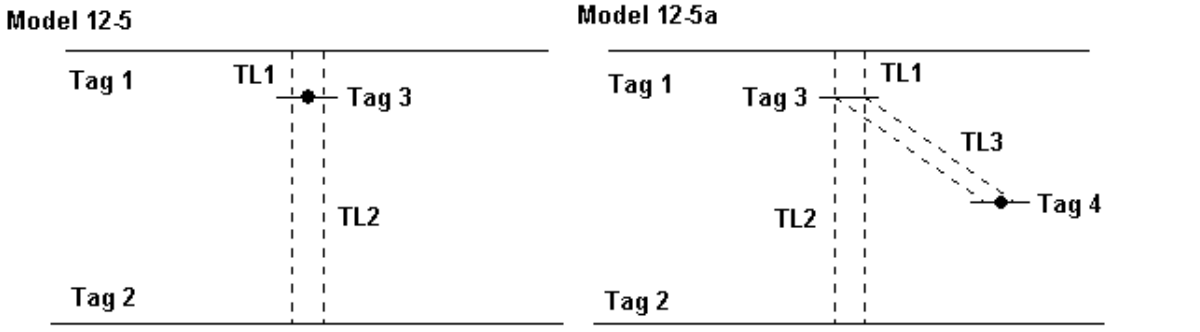

Fig. 12-7

```
GW 1 15 0 -.232 0 0 .232 0 .001
GW 2 15 -.12 -.25 0 -.12 .25 0 .001
GW 3 1 -.02 -.001 0 -.01 .001 0 .0005

EX 0 3 1 00 1 0
TL 1 8 3 1 50.00 .02 0. 0. 0. 0.
TL 2 8 3 1 -50 .2 0. 0. 0. 0.
```

In this case, we have essentially the same elements as in model 12-4, but the phase line system is a bit more complex. Both lines are now 50 Ω, but only the longer line to the rear element is reversed. The two lines meet at a junction formed by GW3. GW3 is placed correctly in the array at the junction position, but is too small to play a significant role in the current distribution that forms the radiation pattern. The total electrical length of the two TL-based lines is 0.22 m, far more than the elements spacing (0.12 m). If the lines had a velocity factor of 0.66, the physical length of the lines together would be 0.14 m, about enough to all for the inevitable bends at junction points. Run the model and obtain the source impedance: 22.2 + j16.2 Ω. Although these values are far from optimal for a perfect 1/4λ matching section, we might try a model having the form of the right side of **Fig. 12-7** and see what happens. Open model *12-5a.nec*.

```
GW 4 1 0 -.001 9999 0 .001 9999 .0005

EX 0 4 1 00 1 0

TL 3 1 4 1 35 .16
```

The key lines are the new GW remote entry on which we place the source (EX0). The 35-Ω transmission line is only 0.16 m long electrically to effect a match. Run the model to confirm the new source impedance: 55.9 - j12.1 Ω at 299.7925 MHz.

Although the new source impedance seems a bit distant from the target 50 Ω, it is not necessarily an undesirable value. Let's assume that we shall operate the antenna over some frequency span for which we wish to have less than a 2:1 SWR ratio relative to a reference impedance of 50 Ω. Open and run models *12-4b.nec* and *12-5b.nec*, both of which request frequency sweeps from 290 to 310 MHz. Overlay the results on a single plot, as in **Fig. 12-8**.

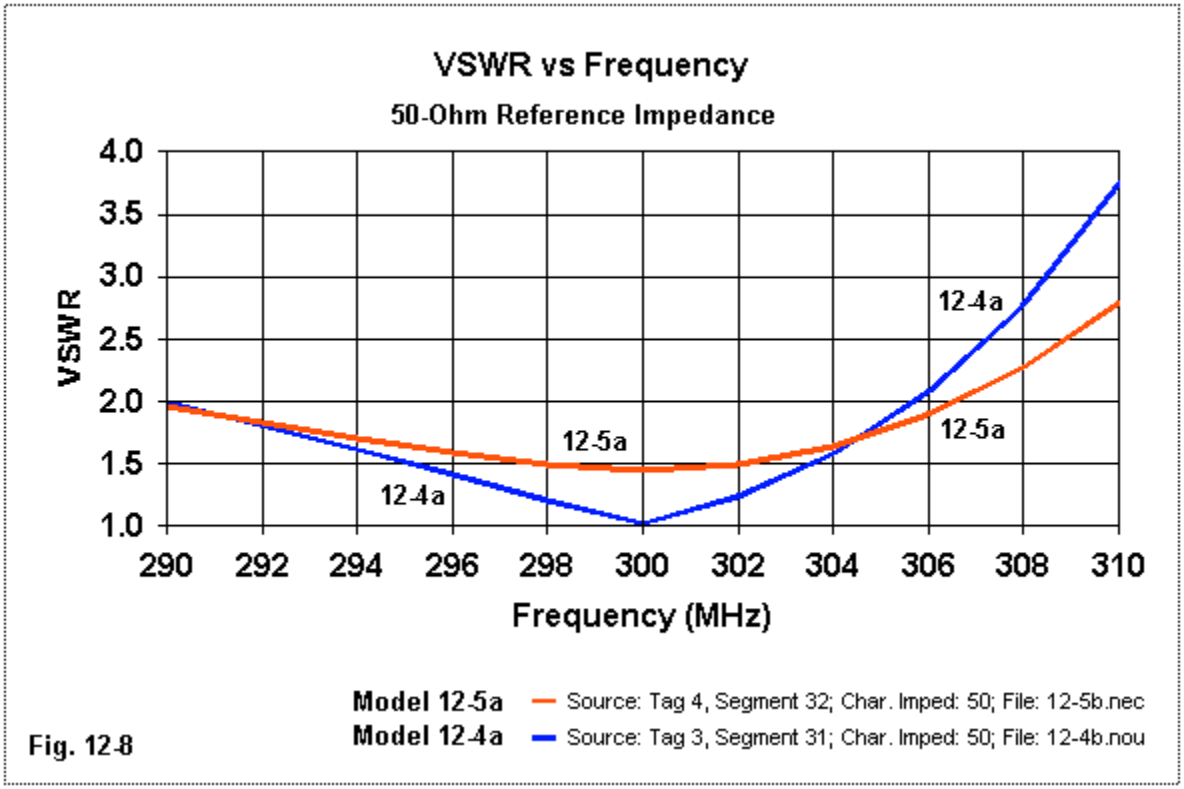

Fig. 12-8

Model 12-5a/b does not reach a perfect 1:1 SWR value, but its 2:1 operating bandwidth is a bit wider than the one for model 12-4a/b. What we call 1/4λ matching sections are more versatile than the precision equation seems to allow, and we can discover some of that flexibility by using the TL facility within NEC.

Perhaps the most ideal model for the use of TL-based transmission lines is the log periodic dipole array (LPDA). Designed by a set of equations, these very wide-band arrays consist of many elements, with each pair having a reversed phasing transmission line between them. Hence, the array requires only one source, normally at the center of the most forward element. If we had to model the phasing lines via GW entries, we would encounter 3 major problems. First, the segment count for the array would increase by as much as a factor of 3, since each phase-line section consists of two wires. Second, we would have to model each dipole as a pair of wires and likely work out a scheme of offsetting each half in the plane at right angles to the elements. Third, we would encounter major accuracy difficulties, since the element diameter tends to differ radically from the phase-line wire diameter. The result is a very large collection of angular junctions of wires with dissimilar diameters. Except for wire versions of the LPDA, modeling these antennas using GW entries for the phase-line structure is not feasible.

Open model *12-6.nec*, a sample of a relatively high performance LPDA for the 14-30-MHz range. This sample LPDA uses near-ideal design factors ($\tau = 0.955$, $\sigma = 0.18$), and the result is a 66-m boom length and 27 elements. However, each element requires only 1 tag, with the number of segments figured to align their junctions from element to element while using an odd number of segments so that the TL entries will be centered. (For further information on LPDAs, see my 2-volume set called *Quad Notes*.) The TL listing shows the reversed 200-Ω phase lines, with the

EX entry placed on the most forward element.

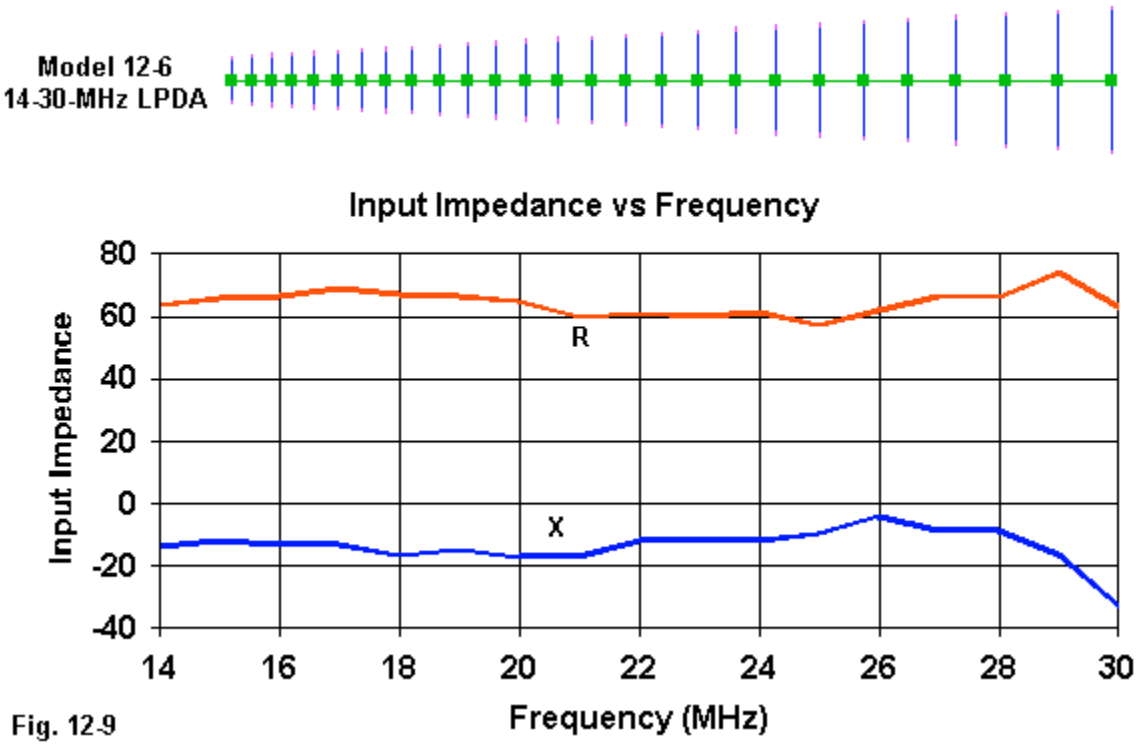

Fig. 12-9

Fig. 12-9 shows an outline of the LPDA proportions. The lower part of the figure provides a snapshot of the relatively stable source resistance and reactance across the operating passband. (The performance from 26 to 30 MHz can be improved by extending the top design frequency and adding further front-end short elements.) You may run the model and examine the phi patterns and impedance values across the passband.

In Chapter 10, we briefly examined the use of a TL-based transmission line with a near-zero length as a means of allowing us to form a single source for wires that we modeled as closely parallel. Now that we have the parameters of using the TL command firmly in hand, let's review that form of sourcing by creating a two-wire dipole with a single central junction and source.

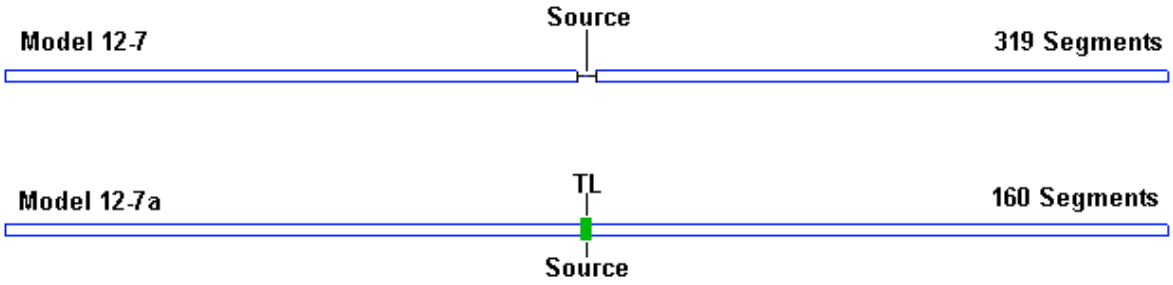

Fig. 12-10

Fig. 12-10 shows two ways of forming the dipole without invoking parallel sources, one on each wire. Open model *12-7.nec*.

```
GW 1 77 0 -.47 .006 0 -.009 .006 .0005
GW 2 77 0 -.47 -.006 0 -.009 -.006 .0005
GW 3 2 0 -.009 -.006 0 -.009 .006 .0005
GW 4 2 0 -.47 -.006 0 -.47 .006 .0005
GW 5 3 0 -.009 0 0 .009 0 .0005
GW 6 77 0 .009 .006 0 .47 .006 .0005
GW 7 77 0 .009 -.006 0 .47 -.006 .0005
GW 8 2 0 .009 -.006 0 .009 .006 .0005
GW 9 2 0 .47 -.006 0 .47 .006 .0005
```

This version of the dipole uses 319 segments in 9 wires, with GW5 describing a center 3-segment wire for the source. The wires are 0.012 m apart, and the segment length is 0.006 m throughout. Run the model and record the impedance value and the AGT value. The frequency is 150 MHz to avoid issues of segment length vs. wire radius. Now examine model *12-7a.nec*.

```
GW 1 79 0 -.47 .006 0 .47 .006 .0005
GW 2 79 0 -.47 -.006 0 .47 -.006 .0005
GW 3 1 0 -.47 -.006 0 -.47 .006 .0005
GW 4 1 0 .47 -.006 0 .47 .006 .0005

EX 0 2 40 00 1 0
TL 1 40 2 40 140 .001
```

This version of the dipole uses only 160 segments, with the number being determined by the required 0.012-m segment length of the end wires. The source is on GW2, with a TL line connecting the centers of the two long elements. Since each wire of the dipole would have about a 140-Ω impedance, that value is the characteristic impedance of the line. However, the value is not critical for a line that is electrically only 1 mm long. Run the model and record the impedance and AGT values

Model	Reported Impedance R +/- jX Ω	AGT	Adjusted Resistive Impedance R Ω
12-7	73.93 + j3.99	0.9668	71.47
12-7a	71.43 - j1.87	1.0002	71.43

The adjusted impedance values closely coincide. However, the smaller model offers a more ideal AGT value because it avoids the need for sharp geometry changes in the high-current region of the structure.

These exercises cover almost (but not quite) all of the salient points for the TL command. You may find other models in the Basic tutorial in Chapter 14 and elsewhere in the volume. Throughout, we have restricted calculations to those absolutely necessary to perform the model construction work. However, for more complete coverage of the mathematics of transmission lines, you may wish to consult a modern basic text, such as *Transmission Lines and Wave Propagation* by Magnusson, Alexander, and Tripathi (1992). Classics, such as *Transmission Line Theory* by King (1955) and *Antennas and Transmission Lines* by Kuecken (reprinted 1996), are equally worth study

Wire Transmission Lines

The TL facility in NEC has one more limitation (besides its restriction to lossless lines) that we have so far not mentioned. All of the models that we have sampled have placed the TL line at the center of a dipole in a position at which the current changed slowly in adjacent segments and the currents on each side of the TL-segment were equal. In this and equivalent situations, the TL lines will register most accurately relative to lines in physical implementations. Using a dipole as an image, the further we move away from the center, the more rapidly the current changes from segment to segment and the more unequal become the currents in the segments adjacent to the TL-segment. As a result, the TL-line becomes less accurate as a representation of a true transmission line.

We can demonstrate the difficulty by comparing ostensibly equivalent models. **Fig. 12-11** shows the test situation.

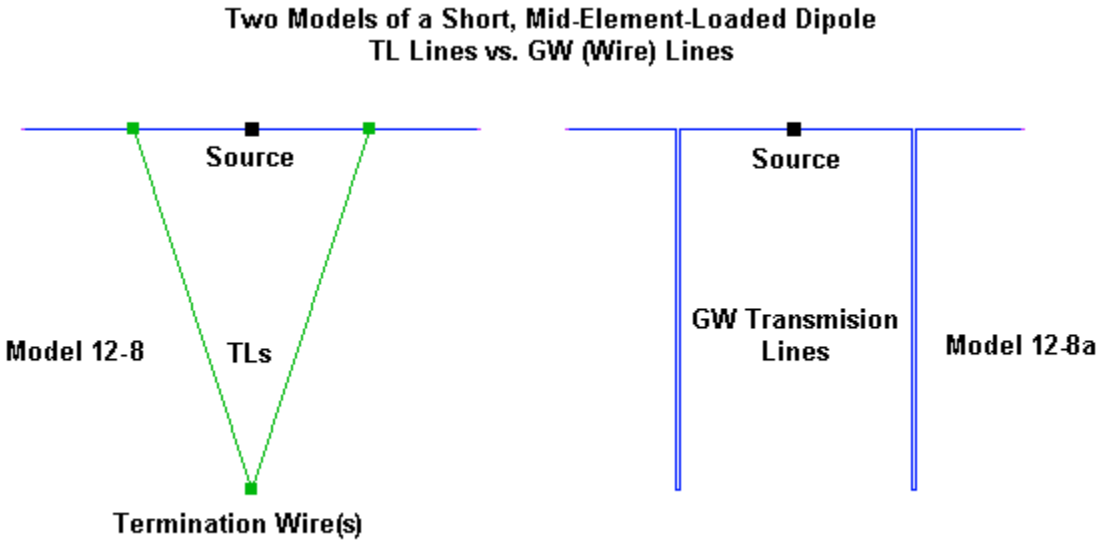

Fig. 12-11

Open model *12-8.nec*.

```
GW 1 101 0 -.2 0 0 .2 0 .001
GW 2 2 0 -.001 -.425 0 .001 -.425 .005
GE
FR 0 1 0 0 150 1
TL 1 25 2 1 157 .425 0 0 1e10 0
TL 1 77 2 2 157 .425 0 0 1e10 0
EX 0 1 51 00 1 0
```

The model shows a short dipole that is loaded by shorted transmission lines near the center of

each leg. The TL position is precisely noted: the segment inner Y coordinate is (+ or -) 0.10099 m and the outer Y-coordinate is (+ or -) 0.10495 m. Independent calculations of a transmission line with a line spacing of 0.00396 m and a diameter of 1 mm produce a characteristic impedance of about 157 Ω. The required electrical length of the TL-line to produce resonance is 0.425 m. Run the model to confirm the source impedance: 18.74 - j1.64 Ω.

The model demonstrates a useful technique when you have multiple stubs. You may create a single remote wire with as many segments as you have lines to remotely terminate. Simply terminate each TL-stub on a different segment. The lines will not interact. To confirm this, open model *12-8a.nec* and run the model to find the same source impedance. This version of the model uses separate TL termination wires.

The significant part of this test situation appears in model *12-8b.nec*.

```
GW 1 24 0 -.2 0 0 -.10495 0 .001
GW 2 107 0 -.10495 0 0 -.10495 -.425 .001
GW 3 1 0 -.10495 -.425 0 -.10099 -.425 .001
GW 4 107 0 -.10099 -.425 0 -.10099 0 .001
GW 5 51 0 -.10099 0 0 .10099 0 .001
GW 6 107 0 .10099 0 0 .10099 -.425 .001
GW 7 1 0 .10099 -.425 0 .10495 -.425 .001
GW 8 107 0 .10495 -.425 0 .10495 0 .001
GW 9 24 0 .10495 0 0 .2 0 .001
```

The new version of the model uses GW constructs for both the horizontal dipole and for the transmission lines, as shown on the right in **Fig. 12-11**. Each GW-based parallel transmission line has a spacing of 0.00396 m and uses a wire diameter of 2 mm. Each stub is 0.425 m long. Run the model to ascertain the source impedance: 29.45 + j1005.65 Ω. The stubs are much too long to bring the antenna anywhere close to resonance.

The GW-based stubs show a large current magnitude differential on the dipole segments at their upper terminations: 1.7E-3 on the inside and 0.65E-3 on the outside. In contrast, the segments adjacent to the TL-based stubs show only a small differential: 5.5E-2 on the inside and 5.3E-2 on the outside. The TL-stubs cannot show the effects of having unequal currents in the legs of the stubs. The GW-based stubs do so automatically.

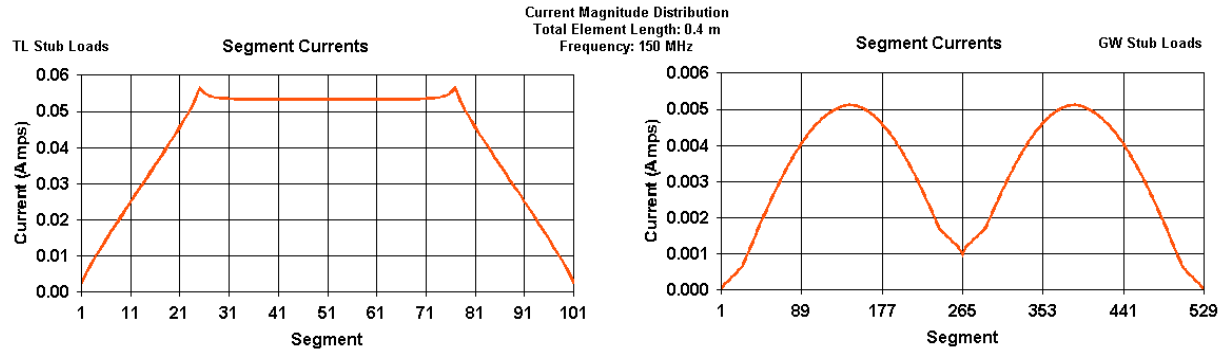

Fig. 12-12 Model 12-8 Model 12-8b

Fig. 12-12 shows the current magnitude graphs for both models. They give very different portraits of the current distribution when we place transmission lines in regions where the current changes. (The key is the curve and not the specific values on the Y-axis, which are functions of the different impedances of the two models.) To the degree that the current magnitude at corresponding points on the stub legs is not the same, the stub also acts as part of the wire forming the length of the dipole. Hence, the stub as a loading element needs to be much shorter than the TL version would suggest, since it is--in effect--loading a longer wire.

The basic rule, then, is that you should use a TL-based transmission line only where the currents on the segments adjacent to the TL-segment are equal or very close to equal. Where TL-based lines are not applicable, you should use, if possible, GW-based wire lines.

There are two types of 2-eire transmission lines in popular use: coaxial cable and parallel transmission lines. Each has its own equation for calculating the impedance in a vacuum or dry air.

$$Z_O = 276 \log\left(\frac{2S}{d}\right) \qquad Z_O = 138 \log\left(\frac{D}{d}\right)$$

Z_O is the characteristic impedance, S is the center-to-center spacing of the wires of a parallel line, and d is the wire diameter. When used with the coaxial cable equation on the right, d is the outer diameter of the inner wire, while D is the inner diameter of the outer wire. These equations are less precise formulations of more accurate versions, but useful for general guidance.

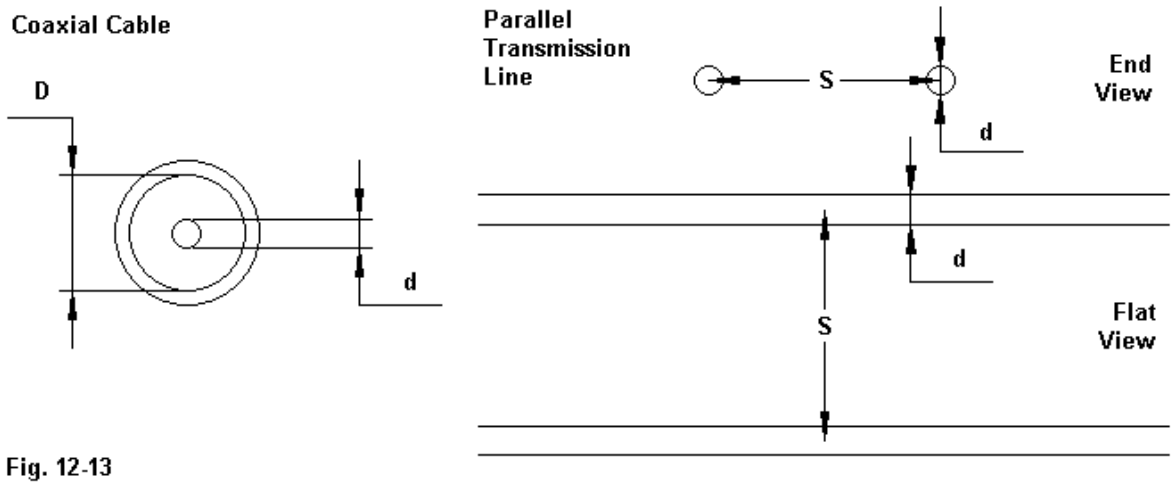

Fig. 12-13

Fig. 12-13 suggests why coaxial cables defy most attempts to model using GW entries. In contrast, as the wire stubs on model 12-7b suggest, we may model parallel transmission lines is a relatively straightforward manner. The major restrictions are fundamental to all NEC modeling. The wires require close attention to the segment-length-to-wire-radius ratio. Excessively close spacing can also lead to errors, even where the segment junctions of the parallel wires are perfectly aligned. The wires in the transmission line should have the same radius as the wires in the antenna to avoid errors resulting from angular junctions of wires with dissimilar radii. These restrictions rule out many modeling efforts, for example, using parallel line to phase large-

diameter tubular elements of an HF array. However, numerous applications remain.

In all cases, you should check your calculated line impedance against a model of them, using a test model similar to the one shown in **Fig. 12-14**. Open model *12-9.nec*.

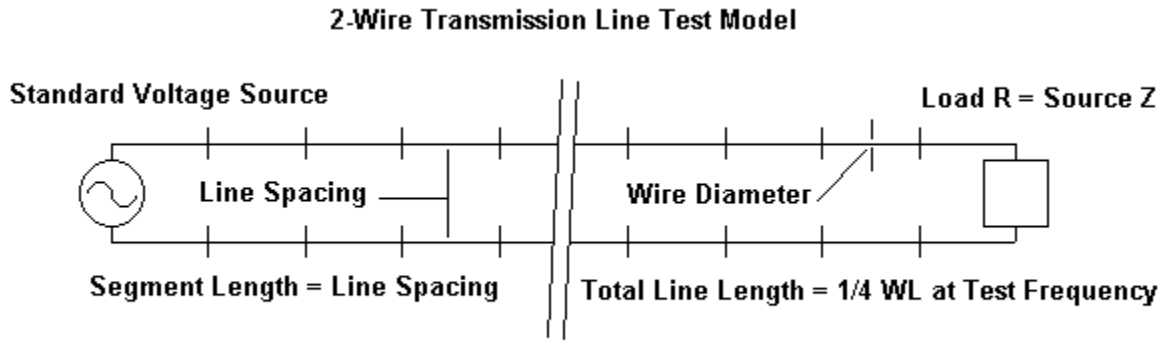

Models 12-9, -9a, -9b, -9c **Fig. 12-14**

```
GW 1 126 -.00198 0 0 -.00198 .499655 0 .001
GW 2 126 .00198 0 0 .00198 .499655 0 .001
GW 3 1 -.00198 0 0 .00198 0 0 .001
GW 4 1 -.00198 .499655 0 .00198 .499655 0 .001
GE
FR 0 1 0 0 150 1
EX 0 3 1 00 1 0
LD 0 4 1 1 197.75 0 0
```

The test model is set to 150 MHz and uses the same dimensions as the stubs in model 12-8b. The line length is 1/4λ at the test frequency, carried out to more than useful decimal places. At one end of the line, place a load (LD0, LD1, or LD4) showing only a resistance. At the other end of the line, place a standard voltage source (EX0). Run the model through several iterations until the source impedance and the load resistance are the same. If you run this model in NEC-2, you will obtain for a load resistance of 197.75 Ω a source impedance of 197.759 - j0.001 Ω.

Because the line spacing is so tight, we should likely use a more accurate equation for the characteristic impedance of parallel lines in a vacuum or dry air.

$$Z_O = 120 \cosh^{-1}\frac{S}{d} = 120 \ln\left(\frac{S}{d} + \sqrt{\left(\frac{S}{d}\right)^2 - 1}\right)$$

The meanings of the terms in the equation are the same as in the simpler version. However, this equation calculates a characteristic impedance of 156.6 Ω, whereas the simpler equation yield about 164 Ω. Wherever the characteristic impedance is about 200 Ω or less, use the more accurate equation.

The model shows an impedance that is over 40 Ω higher than the calculated value. Using the AGT value (0.952) to adjust the impedance provides a figure of 188.17 Ω or about 32 Ω higher than calculated. Since the maximum gain of the modeled assembly is in the -45 to -48 dB range,

the utility of the AGT for adjustments may be questioned. Nevertheless, even with lossless wire, modeled impedance values tend to be higher than those calculated. The length of the cross wires is insufficient to account for the difference, since similar figures emerge from using models with 5/4λ lines.

As the line spacing widens and the characteristic impedance increases, the differential between the modeled line impedance and the calculated impedance decreases. Open model *12-9a.nec*. This line uses 100 MHz as a test frequency, with 2-mm diameter wire and a 40-mm separation between wires. The calculated characteristic impedance is 442.28 Ω, with only about 0.1 Ω difference between the simple and complex equations. If you run the model, you will obtain a source impedance of 476.5 + j0.005 Ω, about 34.2 Ω higher than calculated. Adjusting for an AGT value of 0.977 yields 465.56 Ω, still over 23 Ω higher than calculated.

A similar line in model *12-9b.nec* uses English measures: 1.367" spacing with AWG #14 (0.0641" diameter wire). I selected the dimension to yield a 450-Ω line. Calculations yield 450.3 Ω. Run this model to confirm an impedance of 484.348 +/- j0.000 Ω on NEC-2. (Actually, different computers may yield slightly different values for almost any NEC calculation, usually in the 4th or further significant digits.) Due to the 14-MHz test frequency, this model requires a considerably higher segment count than either of the preceding ones. However, the differential between the modeled and calculated impedance values is almost identical to the values that emerged from model 12-9a, and the impedances are similar. So, too, are the AGT values, as you may confirm from running the test on the latest model.

The models use parallel long wires that run in the same direction. This practice allows you to more easily determine that for any given point along the wire, the currents are equal in magnitude and opposite in phase. For example, the current table returns the following values for the first segment in each of the parallel wires.

```
SEG.  TAG           - - - CURRENT (AMPS) - - -
 NO.  NO.   REAL         IMAG.        MAG.         PHASE
  1    1   -2.1866E-02  6.8294E-05  2.1866E-02   179.821
132    2    2.1866E-02 -6.8294E-05  2.1866E-02    -0.179
```

Clearly, the magnitudes are equal and the phase difference is 180°.

Let's add material loading to the wires of model 12-9b and obtain the situation of model *12-9c.nec*.

```
LD 4 4 1 1 485 0
LD 5 0 0 0 5.8E7 1
FR 0 1 0 0 14 0
```

All wires have the conductivity of copper (about 5.8E7 S/m in the LD5 entry), and even before running the model, we notice a slight change in the load (LD4). If you run this model, you should obtain a source impedance of 485.034 - j1.411 Ω. The short line shows a very slight (insignificant for any practical case) change in impedance with a remnant capacitive reactance. These values indicate one of the advantages of using GW-based parallel lines. In contrast to the lossless lines of TL-based transmission lines, GW-based lines show losses.

In NEC-2, we are generally restricted to creating lines with a single velocity factor: 1.0. However,

NEC-4 has a command that can allow us to create lines with a velocity factor of less than 1.0. Let's see how. Open model *12-10-nec4.nec*. This model sets up a transmission line similar to the one used in model 12-9c, except that the line is now 1.5λ long at 14 MHz. Since the model has nothing special about it, it will run in NEC-2. However, for consistency, a NEC-4 run with the 450-Ω resistive load produces an impedance of 450.98 + j 1.30 Ω with the copper wire lines. The line remains an "air-dielectric" line.

Very commonly used lines in all services employ various insulating materials between the wires, as suggested by the samples in **Fig. 12-15**. Even simple insulating rod separators can reduce the velocity factor of a line by a few points. The vinyl-covered lines tend to have velocity factors ranging from 0.80 to close to 0.90, based on the attempts to reduce the amount of material in the region directly between the wires, where the fields are most intense.

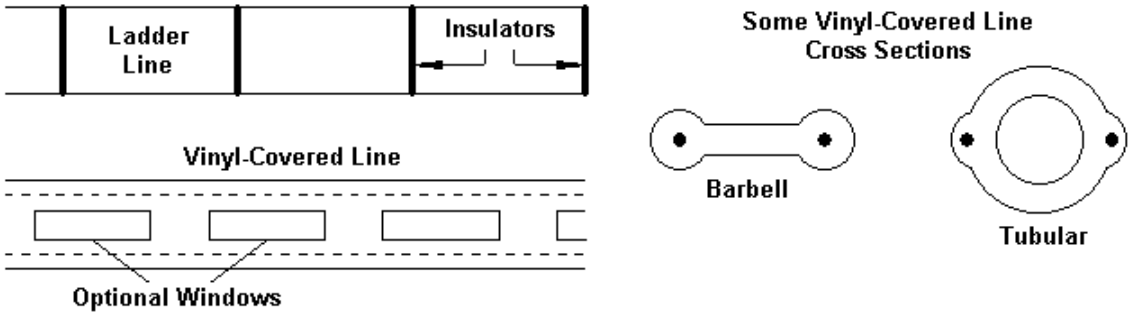

Some 2-Wire Parallel Transmission Lines

Fig. 12-15

We cannot with NEC facilities simulate the exact shapes of the insulating materials. However, we can in NEC-4 add insulating sheathing to the wires. We shall examine the overall structure of the command in more detail in a later chapter, but for now, the assistance screen and the diagram will illustrate how we set up the insulating sheathing via the IS command. See **Fig. 12-16**.

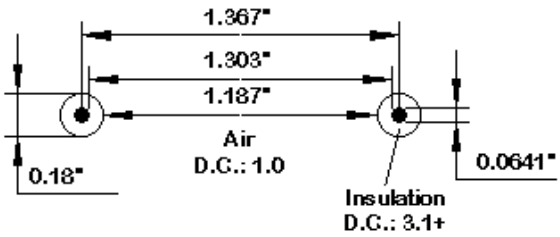

A Sample Simulation of a 450-Ohm, 0.9-VF Parallel Transmission Line

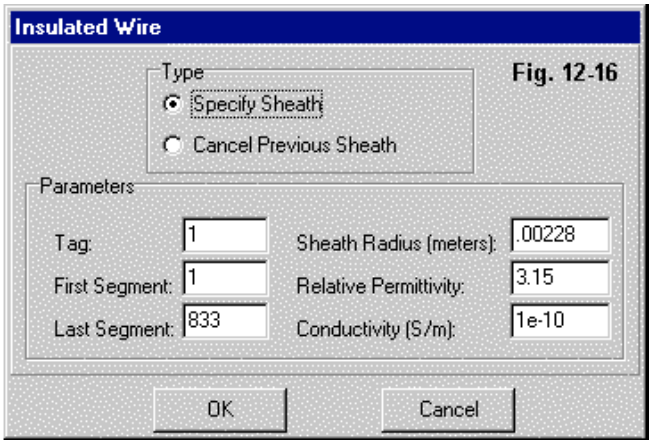

Fig. 12-16

The outer sheath radius does not agree with the 0.9" radius on the left part of the figure, since the IS control command must have all entries directly in meters. Open model *12-10a.nec* and note

the two IS command lines.

```
IS 0 1 1 833 3.25 1e-10 .00224
IS 0 3 1 833 3.25 1e-10 .00224
```

The lines differ from those in **Fig.12-16** because there is no single set of values that will produce a desired velocity factor. Examine the GW lines, one of which appears below.

```
CM cu wire + .9 VF via IS cards GW 1 & 3

GW 1 833 0 0 0 0 0 1138.13 .03205
```

The model seeks to calibrate a set of values for the dielectric constant and sheath radius for insulation that will yield essentially the same line as in model 12-10, but with a 0.90 velocity factor (VF). So we set the line length to 90% of the value in the air-dielectric model and then work with values of sheath thickness and dielectric constant until we arrive once more at a source impedance of 450 Ω using the resistive load of 450 Ω. As we work with permittivity values in the typical plastics range, a table such as the following one emerges.

Insulated Sheath Radius and Permittivity Values for a 450-Ohm, 0.90-VF Line

Sheath Radius		Relative	Source Impedance
Inches	meters	Permittivity	(R+/-jX Ohms)
0.09	0.002286	3.1	452.431 - j 0.967
0.09	0.002286	3.15	452.462 + j 0.461
0.0882	0.002240	3.25	452.437 - j 0.617
0.088	0.002235	3.25	452.430 - j 1.033
0.088	0.002235	3.3	452.456 + j 0.237
0.0878	0.002230	3.3	452.446 - j 0.186
0.0866	0.00220	3.4	452.442 - j 0.342
0.0858	0.00218	3.5	452.454 + j 0.153

You may run the model using any of the combinations to confirm the values. Note that the source impedance continues to increase beyond the value that resulted from moving from perfect wire to copper wire. The additional change in the characteristic impedance of the line that alters the source impedance at near-resonance is the dielectric constant of the region between the wires. As suggested by the left portion of **Fig. 12-16**, the region is a complex function of the air between the sheaths and the sheaths themselves. As well, the dielectric constant not only affects the velocity factor of the line, but as well the characteristic impedance of the line. The full form of the equation for calculating the characteristic impedance of a parallel line is

$$Z_O = \frac{120}{\sqrt{\varepsilon}} \cosh^{-1}\frac{S}{d} = \frac{120}{\sqrt{\varepsilon}} \ln\left(\frac{S}{d} + \sqrt{\left(\frac{S}{d}\right)^2 - 1}\right)$$

The term ε is the permittivity value for the area within which the fields exist. By adding the sheaths, we reduced the characteristic impedance of the line as well as achieving a velocity factor of 0.90.

If we need a lower value for the velocity factor (for example, 0.8), we shall discover that the required IS entry--keeping the conductivity constant at 1E-10 S/m--requires nearly a doubling of

both the sheath radius and the relative permittivity. For our sample line with a VF of 0.8, a radius of 0.0039 m (0.1535") and a permittivity of 7.0 yielded a source impedance of 454.316 - j 0.353 Ω. The new source value continues to climb by another 2 Ω. However, the doubling is not quite linear, since we obtained resonance with a 0.90 VF with a permittivity of 3.5 and a sheath radius of 0.00218 m (which would have yielded, if doubled, 0.00436 m).

Indeed, the non-linearity shows more clearly if we take the wire radius into account, since it is the sheath thickness--and not simply its outer radius--that is effective in establishing a given velocity factor. The thickness of the 3.5-permittivity sheath for a 0.90 VF was 0.00137 m, while the thickness of the 7.0-permittivity sheath for a 0.80 VF is 0.00309 m. Nevertheless, the exercise does provide some guidance in the development of lines with any desired velocity factor by an iterative (or trial-and-error) method within the modeling software.

Being able to assign velocity factors to parts of antenna structures that employ sheathed transmission lines as a part of their construction adds some flexibility to modeling. Consider the antenna shown in **Fig. 12-17**, which employs transmission line sections as part of the radiator and as part of the collinear coupling system.

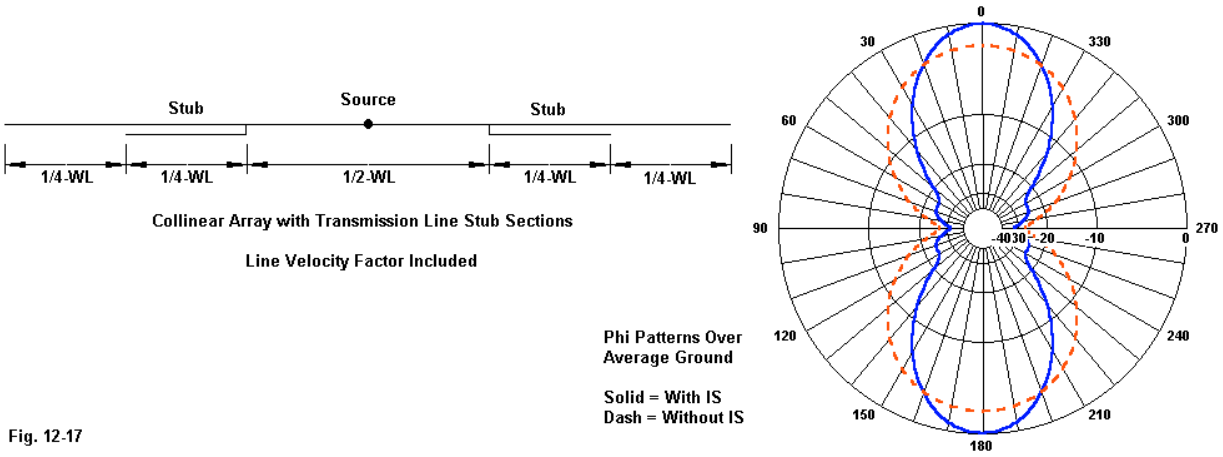

Fig. 12-17

Model *12-11-nec4.nec* models the antenna without sheathing the stub sections. Run the model to obtain a gain of about 7.98 dBi at the TO angle. The gain is similar to that of a simple 1/2λ dipole at the same height above average ground. The right side of the figure shows the pattern as a dashed line. However, the design called for stubs having a velocity factor of 0.9. Open model *12-11a-mec4.nec*. This model adds insulated sheathing only over the stub wires.

```
IS 0 2 1 145 3.5 1e-10 .00218
IS 0 4 1 145 3.5 1e-10 .00218
IS 0 6 1 145 3.5 1e-10 .00218
IS 0 8 1 145 3.5 1e-10 .00218
```

The IS commands include both of the parallel wires in each stub section of the antenna structure. If you run this model, you will obtain a gain at the TO angle of about 9.93 dBi, that is, a 2-dB increase. As well, the half-power beamwidth has decreased from 70° to 42°. The solid-line pattern in **Fig. 12-17** shows the improvement sought by the designer.

The use of the IS command to sheath transmission line wires with insulating materials having a specified thickness and dielectric constant does not directly model the lines. Instead, it simulates the lines by employing a round sheath. The combination of sheath and air between the wires modifies the velocity factor of the line. In all such models, we presume that equivalent changes in velocity factor will yield equivalent changes in characteristic impedance. Within the range of sampled variations, the table of modeled results tends to confirm the presumption. However, for highly critical modeling tasks, one may wish to perform test measurements on the materials used in a given structure to arrive at the best combination of sheath thickness and dielectric constant to replicate both the characteristic impedance and the velocity factor in the model.

In cases where a TL-based transmission line is unsuitable--either by way of its absence of loss or its position in an antenna structure--parallel-wire transmission lines can be highly serviceable. Unfortunately, it is not feasible to simulate coaxial cables, even apart from the structural differences. Air-dielectric parallel lines approach wire inter-penetration at about 80 Ω, and the close-wire limitations of NEC suggest that wider spacing and higher impedances are necessary for accurate modeling. Despite these limitations, wire models of transmission lines have numerous applications in models. Adding insulation to the line wires increases the flexibility of these modeling aids. For advanced models, it may be possible to physically model transmission lines having more than 2 wires.

Summing Up

Modeling transmissions lines within NEC has two distinct directions. By virtue of the TL command, the use of non-radiating lines is perhaps the more common and familiar. Every TL-based line requires two designated termination segments. You must also specify the characteristic impedance of the line and its electrical length. Optionally, you may request normal or reversed connections, with the latter simplifying the process of installing many types of element phasing within an antenna structure. Additionally, you may specify at either end of the line real and imaginary shunt admittance values. For creating shorted and open transmission line stubs, these entries are crucial, since a load applied to a termination wire segment will fall outside of and in series with the transmission line.

Because TL-based lines are in parallel with sources and other TL-based lines, they offer a considerable number of diverse applications. By the use of very short intermediate wires to serve as terminations, we can gang lines to create such structures as Regier series connections, match-line-and-stub assemblies, and combinations of phasing and matching systems. Since a TL-based line is mathematical only with no consequences like those of geometry entries, they can vastly simplify the modeling of complex arrays such as LPDAs.

Nevertheless, TL-based lines have some major interrelated restrictions. They are accurate only where the currents on segments adjacent to the TL-segment are equal, and they cannot show the effects of lines that play a part in the radiation pattern of an antenna. Mid-element loading stubs play a role in the current distribution on the element of which they are a part, and TL-lines cannot show this effect. Other antennas make use of transmission lines as collinear couplers that also play a role in the overall current distribution. For cases such as these, we need to use GW-based transmission lines wherever the line impedance permits.

Parallel transmission lines have a minimum characteristic impedance that generally falls above the impedance of most coaxial cables. NEC's close-wire constraints also limit the simulation of low-impedance lines. As well, the coaxial structure may play a role in a structure in ways that a parallel line cannot emulate.

NEC typically shows a higher impedance for a given parallel wire situation than independent calculations for the lines. The wider the line spacing relative to the wire diameter, the closer that modeled lines draw to calculations. Of course, junctions between wire-based transmission lines and antenna wires must have the same diameter. Nonetheless, wide-based parallel lines have numerous applications in modeling efforts. In NEC-4, the ability to simulate velocity factors other than 1.0 gives an added dimension to such work.

13.
Impedance Loads and Their Limitations

***Objectives**: You will examine in this chapter the LD command and the many types of loads that you may create with it. Besides mastering the command's structure, you will also look at a number of basic applications ranging from setting wire conductivity to using antenna "traps." You will also discover some of the limitations associated with impedance loads.*

The LD command offers you a wide variety of loading possibilities for any antenna structure, ranging from setting the conductivity of each wire within the structure geometry to creating complex RLC loads. There are multiple ways of subdividing the LD command possibilities. One way is to contrast purely resistive loads with loads having complex impedances. Another division contrasts "spot" loads applied to a specific segment to distributed loads that apply values in terms of so many load units per unit of length.

Because the LD command is so flexible, we shall devote our initial work to mastering the command structure for its many functions. Then we shall turn to applications of relatively simple loads, such as those we might use to adjust the electrical length of a given physical antenna length. LD loads are also applicable to the modeling of RLC traps, although using them effectively in models requires some special cautions. Throughout, we shall have to make some external calculations both when entering loads into the model and when converting one kind of load to another.

Like TL commands, LD commands do not add anything to the geometry commands that describe the antenna structure. Instead, LD entries are non-radiating loads based on mathematical adjustments to the interaction matrix output. Therefore, the solenoid inductors and standard capacitors that we presume to lie behind an LD entry have no physical form. This fact sets some limitations to the proper use of loads in a model and to the accuracy of results that fall outside the range of recommended use.

The LD Command Format and Entries

Th LD command has a seemingly straightforward form consisting of 4 integer entries and only 3 floating decimal entries. In its most general form, it has the following appearance, but with no numerical entries as a sample.

```
Cmd   I1      I2      I3      I4      F1      F2      F3
      LDTYP   LDTAG   LDTAGF  LDTAGT  ZLR     ZLI     ZLC
```

There are 6 possibilities for the I1 or LDTYP entry. The next three entries allow the user to specify the tag number and the first and last segment numbers of the structure that the load will affect. These entries alone carry a number of cautions.

The load types are as follows:

-1	Shorts or nullifies all previous loads, normally used following an XQ command.
0	Series RLC load, with the elements in basic units (Ohms. Henries, and Farads).
1	Parallel RLC load, with the elements in basic units.
2	Series RLC load, with the elements in basic units per meter.
3	Parallel RLC load, with the elements in basic units per meter.
4	Complex impedance load, expressed as resistance and reactance in Ohms.
5	Wire conductivity in S/m (or mhos/meter) (for NEC-2)

In order to discover how the remaining entries vary, we shall begin with our standard test dipole at 299.7925 MHz. Open model *13-1.nec* and run it to record the free-space gain and the source impedance: 2.12 dBi, 71.760 + j0.116 Ω. We shall use excessive precision in recording values in order to make some comparisons among values that emerge as we introduce loads.

To nullify previous loads, we need only enter the LD command followed by a -1. Thus we can by-pass this option and turn to more definite load implementations. Let's begin with a type 5 load that specifies the wire conductivity. Open model *13-1a.nec* and examine the LD entry.

```
Cmd   I1      I2      I3      I4      F1      F2      F3
      LDTYP   LDTAG   LDTAGF  LDTAGT  ZLR     ZLI     ZLC
LD    5       1       1       11      5.8E7
```

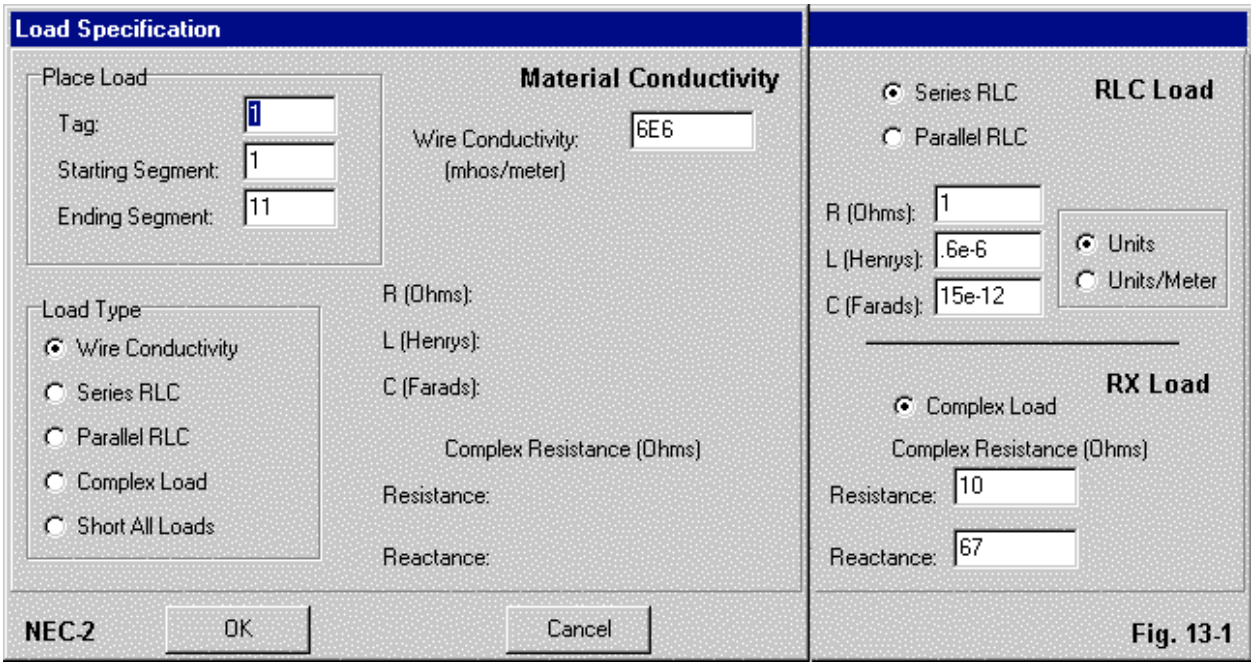

The left portion of **Fig. 13-1** shows the complete entry assist screen in NSI software, with the wire conductivity selected. The value inserted is the bulk conductivity, which NEC adjusts for the wire structure and frequency of the model. The 6E6 entry value applies to a model that we shall soon meet. The right side of the figure shows how the screen appears when we wish to enter LD0 through LD4 loads.

In NEC-2, the LD5 entry only uses the F1 entry to specify the material conductivity of the selected wire or wires. The Appendix contains a table of some materials commonly used in antenna structures, including some that we may press into service, even if they are not highly recommended. The F1 value is for copper. Run the model to obtain the gain and source impedance: 2.11 dBi, 71.995 + j0.279 Ω. Numerically, the losses associated with copper wire, including skin effect relative to the wire radius and frequency, appear in the slightly lower gain and slightly higher source impedance. However, the difference makes no practical difference relative to the initial model that used lossless wire.

The most variable aspect of the entry occurs among the integer entries. We might have achieved the same goal of assigning the prescribed conductivity to all dipole segments with the following 3 variations of the LD5 command.

```
Cmd   I1      I2      I3      I4      F1      F2      F3
      LDTYP   LDTAG   LDTAGF  LDTAGT  ZLR     ZLI     ZLC
LD    5       1       1       11      5.8E7
LD    5       0       0       0       5.8E7
LD    5       1       0       0       5.8E7
```

If I2 specifies a tag number greater than zero, then the following two values--each greater than zero--set the first and last relative segment numbers to which the command applies. When I3 and I4 are greater than zero, I4 must be equal to or greater than I3, with one exception. If I4 is zero, then it takes on the value of I3.

If I2 = 0, then the following I3 and I4 entries refer to absolute segment numbers. If I3 and I4 both are zero, then the load request applies to all segments in the model. If I2 specifies a tag that is greater then zero, then the load request applies only to that tag. If the following I3 and I4 command are both zero, then the command applies to all segments with the specified tag number in I2.

In most cases, you have more than one way to correctly specify the range of segments to which an LD command applies. The ability to specify a tag number of zero to employ absolute tag numbers suggests that you should use zero as an assigned tag number with caution. In most cases, you may avert later confusion by avoiding the practice.

Wire conductivity does have more than a minuscule affect on antenna performance. Open model *13-1b.nec* and look at the LD5 entry.

```
LD 5 1 1 11 1.39E6
```

The new conductivity is for type 302 stainless steel. Run the model and obtain the new gain and source impedance values: 2.05 dBi, 73.032 + j1.164 Ω. As we decrease the wire conductivity, the gain goes down and the impedance goes up, since we are adding resistive losses to the structure's radiation resistance. If you check the output report power budget, you will find that efficiency has dropped to 98.39%. Of course, for many applications, the ruggedness of stainless steel makes the 1.61% power loss a worthy exchange.

The listed permeability of stainless steel is 1.0008, suggesting that it would have negligible effect

on the performance of the material as a dipole at the test frequency. However, not all ferrous and similar materials fare so well. If you have NEC-4, open model *13-1c-nec4.nec*. Once more, examine the LD5 command.

```
LD 5 1 1 11 6E6 200
```

NEC-4 adds a second floating decimal value for relative permeability. If the relative permeability is 1, you may omit the number. However, this model uses general values that appear in some listings for steel. The conductivity is a bit above the value for stainless steel, and the permeability number is high. Run the model and obtain the gain and source impedance: 1.67 dBi, 80.375 + j7.249 Ω. However, despite the reduction in gain, the power budget reports an efficiency of 99.23%, a bit higher than the value for stainless steel.

Now open model *13-1d.nec*, a version of the same model without the permeability entry. Hence, this model will run in NEC-2.

```
LD 5 1 1 11 6E6
```

The NEC-2 version of the model returns these gain and impedance numbers: 2.09 dBi, 72.365 + j0.621 Ω. The efficiency is 99.23%. NEC-2 cannot show--in the absence of an entry provision for permeability--the effects of that phenomenon on antenna performance when the value is very significant. You may wish to vary the NEC-4 version of the model to create curves relating antenna performance to various permeability values that might form a reasonable range for available antenna materials.

"Lumped" or "Spot" Impedance Loads

Impedance loads encompass type LD0 through LD4. They acquire the informal labels "lumped" or "spot" from the fact that in most cases, they represent the insertion of lumped components--namely resistors, inductors, and capacitors--at specific locations or segments of the structure geometry. It is possible to assign to a specific segment more than one load, and the loads will act in series with each other. Hence, it is legitimate to add a load of the lumped type to a wire conductivity load that might apply to all segments of the structure in question. **Fig. 13-2** surveys the load types available.

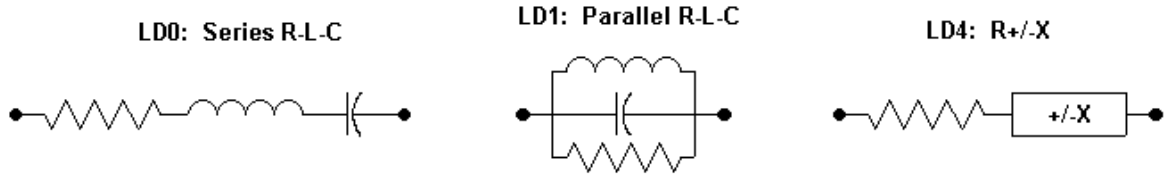

Fig. 13-2

We shall begin our exploration with LD4 loads for 2 reasons. First, they have a singular form in the LD command line. Second, they are somewhat easier to use when searching for a set of values that will yield a certain model outcome. Open model *13-2.nec*. Once more, we have our

resonant dipole with lossless wire, but with the addition of an LD4 load.

```
Cmd   I1      I2      I3      I4      F1      F2      F3
      LDTYP   LDTAG   LDTAGF  LDTAGT  ZLR     ZLI     ZLC
LD    4       1       6       6       1       100
```

The command assigns the load to the center segment of the dipole, where it acts in series with the source. F1, ZLR, specifies the real impedance or resistance, while F2, ZLI, specifies the imaginary impedance or reactance. Zero entries mean either zero resistance or zero reactance, as appropriate. Since the entered value is positive, we have inductive reactance. Run the model to obtain the gain and new source impedance: 2.06 dBi, 72.760 + j100.116 Ω. Note that, relative to the source impedance values produced by model 13-1, the new impedance adds the 1 Ω resistance to the source resistance and the j100 Ω reactance to the source reactance.

One of the benefits of dealing with an LD4 complex impedance load is that we can easily establish (or calculate) the load Q, since Q is simply the reactance divided by the resistance. The test set-up has a Q of 100. The disadvantage of a complex impedance load is that the values are fixed. If we perform a frequency sweep for the model, the load components will not change their reactance value as the frequency changes, in the manner of real lumped components. This condition is not shared by LD0 through LD3 loads in which we specify components in terms of resistance, inductance, and capacitance. NEC will calculate the correct impedance to use at each sampled frequency in a sweep loop. Hence, if we wish our load to be frequency nimble, we must convert its form.

LD0 specifies a series combination of resistance, inductance, and capacitance. Open model *13-2a*, which calls for an LD0 load.

```
Cmd   I1      I2      I3      I4      F1    F2          F3
      LDTYP   LDTAG   LDTAGF  LDTAGT  ZLR   ZLI         ZLC
LD    0       1       6       6       1     5.3088e-8   0
```

Although the integer positions remain unchanged (except for the I1, LDTYP entry), the floating decimal positions have changed their meaning, as indicated by the help screen in **Fig. 13-1** and by the entry values. F1, ZLR, still lists the resistance. F2, ZLI, lists the inductance, while F3, ZLC, lists the capacitance. In any series or parallel load (LD0 through LD3), a zero for either F2 or F3 represents a missing value. This point is especially important for capacitance entries, where an open circuit is not the desired consequence for a missing value. If you wish to enter a capacitance having a very high capacitive reactance, enter a very low value of capacitance, e.g., 1E-99.

As forewarned, value conversion takes a bit of hand-calculator work, using standard equations. If we had capacitive reactance to convert to capacitance (or the other way around), we would use one of these equations:

$$X_C = \frac{1}{2\pi f C} \qquad\qquad C = \frac{1}{2\pi f X_C}$$

Since we have an inductive reactance to convert to a value of reactance, we use the right-hand equation of the inductive pair:

$$X_L = 2\pi f L \qquad L = \frac{X_L}{2\pi f}$$

The equations appear in basic form because all NEC RLC load entries use basic units: Ohms, Henries, and Farads. The calculator gives us an inductance value of 5.3088E-8 H for the series inductor, resulting in the LD0 entry that we used as a sample. Run the model and obtain the gain and source impedance: 2.06 dBi, 72.760 + j100.115 Ω, precisely the same values (within rounding limits) as the LD4 model gave us.

While we are exercising our conversion skills, we might as well convert the series RLC load into an LD1 parallel RLC load. This move requires that we call into play the standard series-to-parallel equations:

$$R_P = \frac{R_S^2 + X_S^2}{R_S} \qquad X_P = \frac{R_S^2 + X_S^2}{X_S}$$

If we apply these equations to the series values in model 13-2a, then we obtain a parallel equivalent resistance of 10001 Ω and a parallel equivalent inductance of 5.3094E-8 H. Now we are ready to open model *13-2b.nec*.

```
Cmd   I1       I2       I3       I4       F1       F2          F3
      LDTYP    LDTAG    LDTAGF   LDTAGT   ZLR      ZLI         ZLC
LD    1        1        6        6        10001    5.3094e-8   0
```

Almost nothing changes as we move from an LD0 to an LD1 load, except, of course, for the numerical values of the floating decimal positions. However, in this case, the inductance entry is significant. If we had a capacitive circuit with no inductor, we would enter a zero for a missing value. If we wish a near short-circuit condition created by an extremely low value of inductive reactance in parallel with the other components, enter a very low inductance such as 1E-10 (or smaller). Treat the resistance entry similarly. When we run this model, we obtain the gain and source impedance: 72.760 + j100.115 Ω. By now, the values call for no comment.

Let's quickly do a replacement on the LD1 entry, setting the R and L positions to zero and entering a capacitance value of 10 pF in the parallel load. Open model *13-2c.nec*.

```
LD 1 1 6 6 0 0 10e-12
```

The zeroes in the F1 and F2 (R and L) positions do not mean short circuits, but only missing values. Run the model and obtain the gain and source impedance: 2.12 dBi, 71.760 - j52.972 Ω. The gain returns to "full" value because we no longer have a resistance in the load. The result is equivalent to an infinite (or indefinitely large) Q.

If we wished to replace the LD1 load with an LD0 load, we would normally have to employ the standard parallel-to-series conversion equations:

$$R_S = \frac{R_P X_P^2}{R_P^2 + X_P^2} \qquad X_S = \frac{R_P^2 X_P}{R_P^2 + X_P^2}$$

However, the absence of resistance simplifies the calculation to yield the same value of capacitor. Open model *13-2d.nec*.

```
LD 0 1 6 6 0 0 10e-12
```

Except for a change of LDTYP, the line is the same as before, as are the output values: 2.12 dBi, 71.760 - j52.972 Ω.

Open model *13-2e.nec*, which performs one last conversion of the RLC loads into an RX or complex impedance load (LD4).

```
LD 4 1 6 6 0 -53.088
```

Note the reactance entry. Because, and only because, we have the load set on the same segment as the source, we can by-pass the usual calculation of the required reactance and simply subtract the original source reactance (+0.116 Ω) from the source reactance in the LD0 and LD1 models to arrive at -53.972 - (+0.116) = -53.088 Ω. However, you may convert the 10 pF by the usual method and end up with the same result. Of course, the model returns the same reports: 2.12 dBi, 71.760 - j52.792 Ω.

These exercises do not intend to challenge modeling skills so much as they aim to develop a certain familiarity with entering, converting, and otherwise manipulating loads within the boundaries of the LD command. We have overlooked LD2 and LD3 loads, the series and parallel loads that employ resistance, inductance, and capacitance per meter. These loads tend to have special uses, and we shall explore some of them in a later chapter.

Let's instead probe at least a couple of applications of the loads that we have examined in detail. An overlooked aspect of LD spot loads is that any of the 3 forms that we have used allow us to insert a resistance into the antenna structure on any segment we specify. Consider the quandary set up in **Fig. 13-3**.

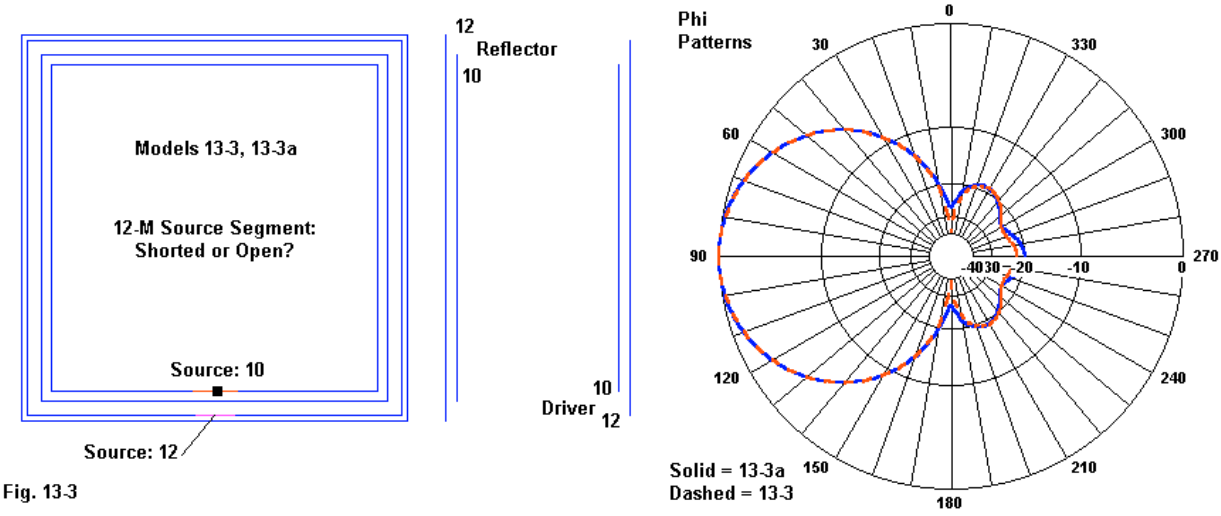

Fig. 13-3

On the left, we have 2 views of a two-band 2-element quad beam for 24.94 and 28.5 MHz. The array uses separate feed points to isolate one band from the other. Because the frequencies are so close together, the 12-meter driver is not much larger than the 10-meter reflector. When operating on 10 meters (28.5 MHz), should the 12-meter (24.95 MHz) driver loop be shorted to

form a complete loop or left open circuited at the source segment?

We may resolve the issue by trying the model both ways. Open model *13-3.nec*, which shows the entire model set up for use on 28.5 MHz. The 12-meter source would normally go on tag 9 at the center. Without a source at that point, the wire is continuous, forming a complete loop. Run the model and obtain the usual performance data: free-space gain 7.33 dBi, 180° front-to-back ratio 21.49 dB, source impedance 59.7 - j0.7 Ω.

To model the 12-meter driver loop as having an open circuit at the normal source position, we need only introduce a purely resistive load having a very high value. Open model *13-3a.nec* and examine the new LD entry.

```
LD 4 9 5 5 1e10 0
```

The complex impedance load (LD4) places at the 12-meter driver center (tag 9, segment 5) as high resistance (1E10 Ω). We could have achieved the same goal with either of the 2 following LD entries:

```
LD 0 9 5 5 1e10 0 0
LD 1 9 5 5 1e10 0 0
```

Run the model and record the typical data: 7.37 dBi, 19.62 dB, and 94.1 - j9.3 Ω. As shown in **Fig. 13-3**, the effect on the radiation pattern is small. However, there is a significant change in the source impedance. The next step after uncovering the difference is a user decision.

Although purely resistive loads are common and simple, purely reactive loads are perhaps fictional. **Fig. 13-4** shows partial equivalent circuits of common solenoid inductors and standard lumped capacitors. Capacitors have some degree of leakage resistance across their dielectrics in parallel with the capacitance. As well, their leads show some inductance, although we generally absorb that factor within the geometry of a model. Indeed, capacitor leakage itself is so small that the capacitor Q tends to be 1000 or more. Hence, capacitive loads tend to ignore resistance--for better or worse.

Fig. 13-4

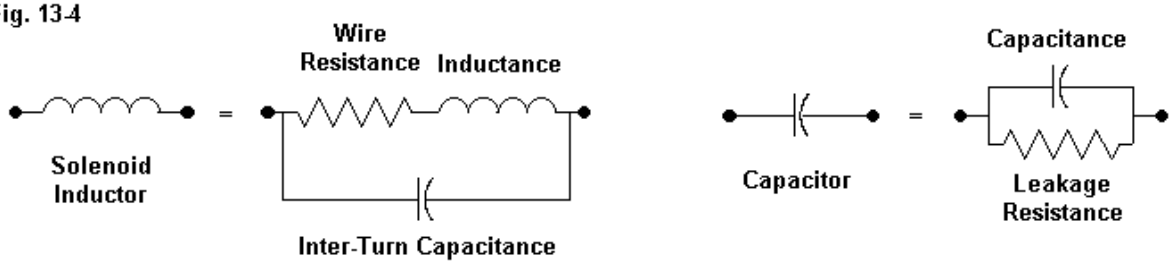

By comparison, inductors have properties that we should not ignore. The series resistance of an inductor tends to limit is Q. Under ideal conditions, coils may have Qs up to about 600 or so. However, on elevated elements, the need to reduce wind loading tends to yield smaller diameter and longer coils, sometimes within aluminum shields. Such coils rarely hit Qs of 300, with the 200 to 250 range being more common at HF. As well, solenoids have a measurable inter-turn capacitance that will produce a self-resonant coil at some predictable frequency. However, if we

operate a solenoid inductor well below its self-resonant frequency, we may usually ignore the capacitance in the model. But we may never ignore the series resistance.

Open model *13-4.nec*. The antenna is a shortened monopole 15 meters high at 2.997925 MHz with a perfect ground for simplicity. The initial model has no load. Run the model and confirm the output numbers: 4.91 dBi gain, 10.537 - j272.236 Ω. We might normally expect a full-size 1/4λ monopole to show between 5.18- and 5.20-dBi gain over a perfect ground, but the model is only 60% of full-size.

For the remainder of this series of exercises, we shall use an LD4, resistance-reactance load. We shall not change frequency, and the complex impedance load will make the calculation of Q very easy. Our quest is to explore the effects of Q on the performance of the antenna as we add a base inductor to bring the antenna to near resonance. **Fig. 13-5** shows the general antenna structure on the left.

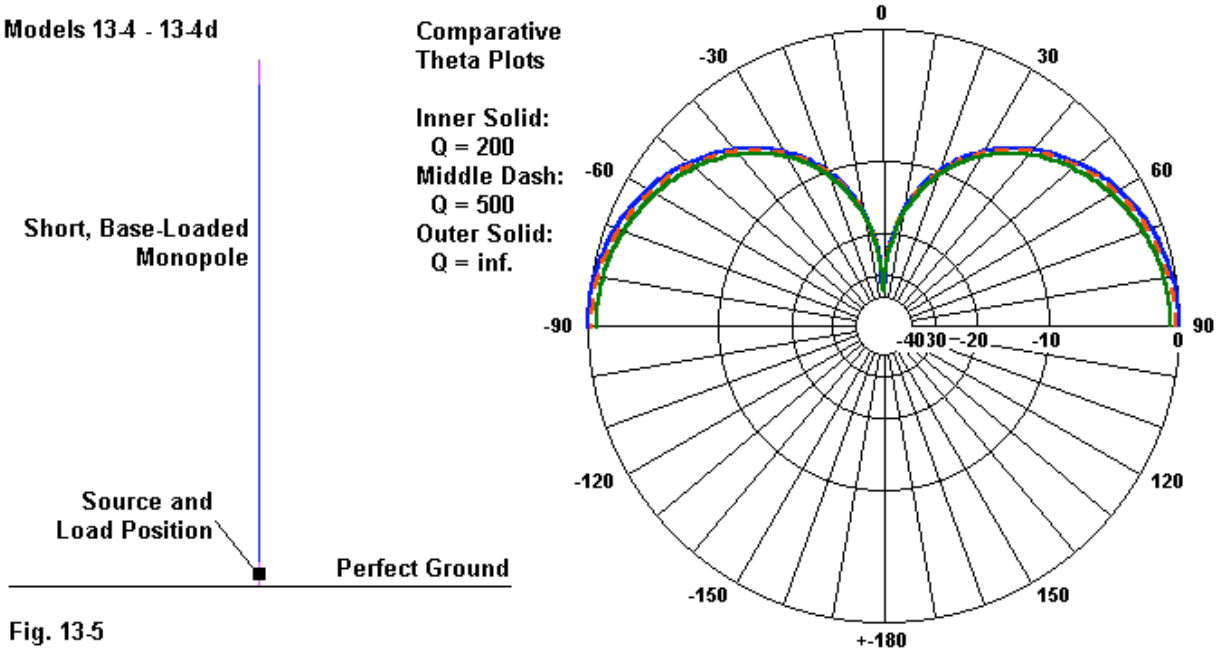

Fig. 13-5

The loadless initial model gives us the reactance that we need to include in an LD4 placed on segment 1, which is also the source segment. With an initial source reactance of -j272.236 Ω, we need a corresponding inductive reactance to bring the source impedance to a purely resistive value. Open model *13-4a.nec*.

```
LD 4 1 1 1 0 272.236
```

Since the resistance is zero in the load, the inductor specified by the reactance has an infinite Q. Hence, we should not be surprised by the output values: 4.91 dBi, 10.537 +/- j0.000 Ω. The power budget still reports 100% efficiency, since we have no losses associated with the structure or networks in the model. However, if we specify a finite Q, matters change. Open model *13-4b.nec*, which assigns a Q of 500 to the load. For the reactance used, the required series resistance is 0.544 Ω.

```
LD 4 1 1 1 .544 272.236
```

A mere half-Ohm of resistance in the base-loading coil lowers the gain by over 0.2 dB: 4.69 dBi, 11.081 +/- j0.000 Ω. Note that the half-Ohm in the coil also shows up in the resistive component of the source impedance.

If we lower the Q to 200, we must place 1.361 Ω in series with the reactance, as in model *13-4c.nec*.

```
LD 4 1 1 1 1.361 272.236
```

The results show a further lowering of the gain and an increase in the source resistance: 4.38 dBi, 11.898 +/- j0.000 Ω. In all, we have lost over 0.5 dB in the progression from infinite Q to a Q of 200, as shown in the overlaid theta plots to the right in **Fig. 13-5**. According to the power budget portion of the output file, the efficiency has dropped to 88.56%.

As one final maneuver, let's find out how large the base inductor needs to be by converting the LD4 load into an LD0 series RLC load. At the test frequency for this model, we need a 14.443-µH coil, as shown in model *13-4d.nec*.

```
LD 0 1 1 1 1.361 1.4453e-5 0
```

The gain remains at 4.38 dBi, and the source impedance is 11.898 + j0.008 Ω. The last variation results from rounding in the conversion procedure. You may for practice convert the LD0 load to an equivalent LD1 load. As well, you may also add an LD5 material conductivity load to the entire monopole to see what various values do to both the gain and the source impedance.

A number of monopole users believe that moving the loading coil to a higher position will significantly improve performance by the shortened system. We are now in a position to test that notion by comparing a base loaded version of the monopole with a mid-element version, both coils using the same value of Q. See **Fig. 13-6** for the general set-up.

The base-loaded version of the antenna is similar in all respects to the models with which we have been working. The monopoles use 21 segments to place both the source and the load reasonably close to the ground. However, model *13-5.nec* uses a Q of 300, resulting in a series resistance of 0.90745 Ω.

```
LD 4 1 1 1 .90745 272.236
```

We may interpolate output values by comparing the Q-500 and Q-200 models from the preceding series of base-loaded monopoles, or we may run the model and obtain better numbers: 4.55 dBi, 11.445 +/- j0.000 Ω. The power budget reports a 92.07% efficiency.

Let's place the mid-element loading inductor on segment 10 working up the monopole. This position is just below the true center of the element. To find a value of inductive reactance that brings the monopole to resonance, we shall have to proceed iteratively, that is, by trial and error. For each adjustment of the reactance, we must also change the resistance to hold the Q at 300. You may modify model 13-5 to go through the process, or you may open model *13-5a.nec*.

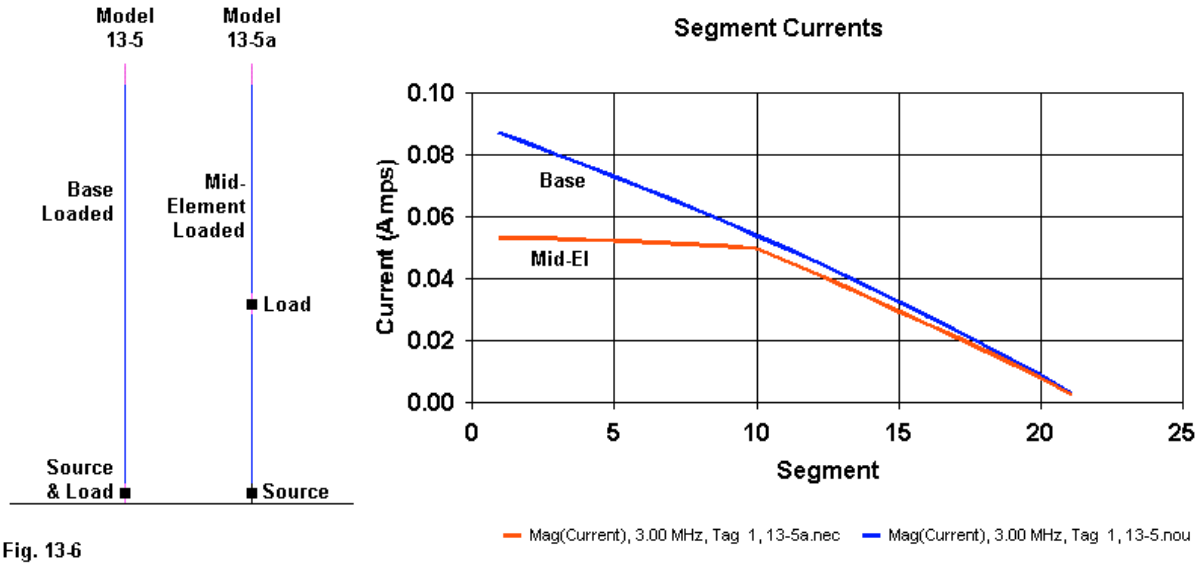

Fig. 13-6

```
LD 4 1 10 10 1.5581 467.42
```

First, examine the output numbers: 4.59 dBi, 18.791 - j0.008 Ω. The efficiency is 92.68%. We have gained 0.04 dB over the base-loaded model. To understand why, look at the second important feature of the model: the required values of resistance and reactance to bring the antenna to near resonance. The reactance is nearly double that of the base-loading coil, requiring a proportionately higher resistance to maintain the Q of 300. Hence, for monopoles of the same length, coil losses are higher for a mid-element loading coil relative to those of a corresponding base-loading coil.

The right side of **Fig. 13-6** shows comparative segment currents. If we had placed the base-loading coil on Segment 2, we would have seen a higher segment-1 current level, since the current "knee" occurs at the loading element. The mid-element version shows the knee clearly. Since we used a constant 1-volt source, the peak current levels are a function of the source impedance and are not indicators of relative performance. In fact, the source impedance of the mid-element version of the monopole may be its better claim to use over base-loaded versions. The source impedance of model 13-5a is nearly double that of model 13-5, reducing the percentage of power converted to heat by mechanical connections that do not appear in the model. On the other side of the coin, we may construct durable base-loaded models in most, but not all, cases.

Traps

So far, we have worked with simple loads. That is, once we place an LD0 or LD1 RLC load on an element, we need do no further work. We may frequency sweep the model, and NEC will provide the correct reactance for each frequency step. The resistance remains a constant. Since the load does not specify the solenoid construction, there is no effective way to estimate such matters as skin effect. For most purposes, this situation produces satisfactory results.

However, we have not yet dealt with traps. Traps are parallel resonant circuits that we use to operate dipoles and other arrays on multiple frequencies. We tune the trap at or just below the lowest frequency used by the inner or higher-frequency portion of the antenna. At the lower frequency range, the trap acts like a loading reactance--with an associated resistance--in the overall antenna length. At the higher frequency, one can with considerable distortion picture the circuit as "trapping" the current so that it cannot flow to the overall antenna tips--hence the name. However, traps are more complex than this introductory account reveals.

Fig. 13-7

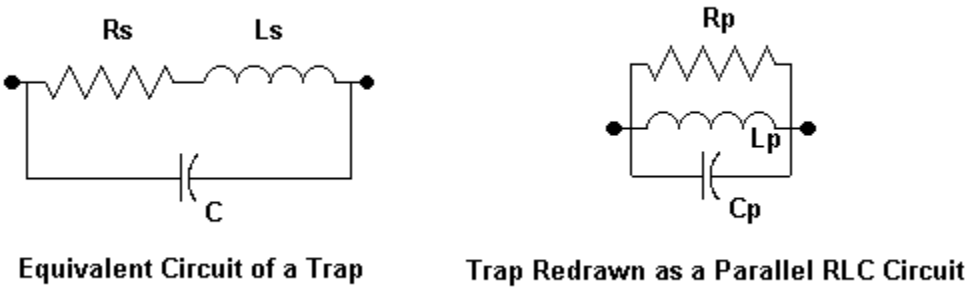

Fig. 13-7 shows the equivalent circuit of a common trap. The left side of the figure shows the key elements, omitting some of the less significant factors. The key ingredients are a series resistor and inductor representing a coil with a finite Q, along with a capacitor in parallel with the series circuit to form a parallel resonant circuit at some design frequency. We cannot directly enter this type of circuit into the NEC LD command. We must first convert the series circuit (Rs-Ls) into its parallel equivalent to obtain a parallel combination, shown schematically on the right. We can work with the purely parallel circuit.

To see what is involved for a complete analysis of a trap element, let's use the diagram in **Fig. 13-8**. The models that follow will use the dimensions shown with elements that are 1" in diameter (radius: 0.0416665'), with the lengths--as shown--in feet.

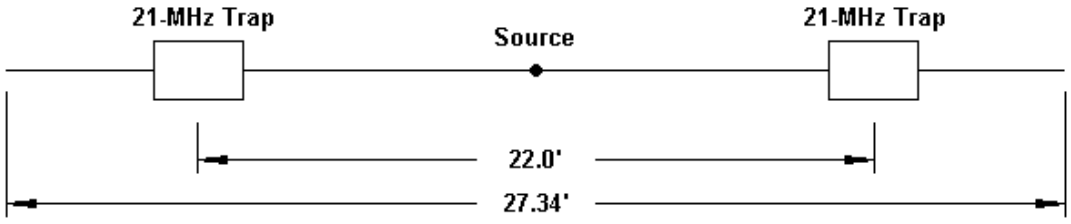

Fig. 13-8

Models 13-4, 13-4a, 13-4b

```
GW 1 8 0 -13.67 0 0 -11.3 0 0.0416665
GW 2 1 0 -11.3 0 0 -10.8 0 0.0416665
GW 3 41 0 -10.8 0 0 10.8 0 0.0416665
GW 4 1 0 10.8 0 0 11.3 0 0.0416665
GW 5 8 0 11.3 0 0 13.67 0 0.0416665
GS 0 0 .3048
```

The wire structure for the dual-band dipole has 5 tags. The functions of the center section (GW3) and the end sections (GW1, GW5) are obvious. GW2 and GW4 hold the loads that represent the traps. This system tends to equalize segment lengths roughly throughout the model. Segment lengths vary from 0.144 m to 0.160 m. More significantly, having separate tags for the loads allows ready identification of the load positions and easy adjustment of the inner and outer lengths of the overall element.

The initial figuring of the traps as parallel loads for LD1 command entries requires that we know the resonant frequency for the circuit, and at least some of the circuit values. We shall operate the dual-band antenna at 14.1 and 21.1 MHz. The inductor is a 3.3-µH coil with a measured Q of about 235. By the standard equation, we can find the inductive reactance. However, we must know the trap resonant frequency. Ordinarily, we design traps to be resonant at or just below the lowest frequency of operation on the upper band. If we set our trap at 21.0 MHz, the inductive reactance is j435.4 Ω. Since the Q is 235, the series resistance of the coil is 1.853 Ω. We can use the capacitive reactance equation to calculate the capacitor, which will be about 17.41 pF to provide the matching reactance for the coil at 21.0 MHz.

We need to convert the series resistance and reactance values into parallel equivalents, again, using equations that appeared earlier in this chapter. The parallel resistance for the trap at its resonant frequency is 102,325 Ω. The parallel reactance is j435.4 Ω, which will return a parallel coil of 3.3 µH. Open model *13-6.nec* and examine the LD1 commands.

```
LD 1 2 1 1 102325 3.3E-6 17.405E-12
LD 1 4 1 1 102325 3.3E-6 17.405E-12
```

Note that the frequency for this version of the model is set to the trap frequency. Its output values are a free-space gain of 2.04 dBi, with a source impedance of 69.9 - j 15.9 Ω. However, we do not intend to operate that antenna at the trap frequency, but at 21.1 MHz. To determine the parallel values at the operating frequency, we need to take a few steps. First, we shall find the inductive and capacitive reactance of the inductor and capacitor at the operating frequency. We may return to basic equations, or we may take this shortcut:

$$X_{LB} = X_{LA}\frac{F_B}{F_A} \qquad X_{CB} = X_{CA}\frac{F_A}{F_B}$$

X_{LA} and X_{CA} are the reactance values at the resonant frequency, F_A, and X_{LB} and X_{CB} are the values of reactance at the new frequency, F_B. For operation at 21.1 MHz, we obtain an inductive reactance of j437.5 Ω and a capacitive reactance of - j433.4 Ω. The required parallel reactance of this combination we may call X_{NET}, which we may determine from this equation:

$$X_{NET} = -\frac{|X_L|\ |X_C|}{|X_L| - |X_C|}$$

Note that the equation uses the absolute values of the reactances, not their originally signed values. For our test model at 21.1 MHz, the net or parallel reactance is - j45,829 Ω, although we do not have to enter that value, since we shall use the values of inductance and capacitance, 3.3 µH and 17.41 pF, respectively.

The parallel resistance for X_{NET} can be derived approximately from the parallel resistance at resonance using this equation:

$$R_{PB} = R_{PA}\left(\frac{F_B}{F_A}\right)^{1.5}$$

R_{PB} is the parallel resistance at the new frequency, F_B, and R_{PA} is the parallel resistance at the resonant frequency, F_A. By raising the ratio of 21.1 over 21.0 to the 1.5 power--using the X^Y function of a hand calculator--we find a new parallel resistance of 103,057 Ω.

We may plug these values into the LD1 commands in a version of our model dual-band antenna for 21.1 MHz, model *13-6a.nec*.

```
LD 1 2 1 1 103057 3.3E-6 17.405E-12
LD 1 4 1 1 103057 3.3E-6 17.405E-12
```

If we run the model, we obtain a gain of 2.05 dBi and a source impedance of 71.8 - j8.1 Ω. The model is well within dipole specifications for 21.1 MHz, although by lowering the resonant frequency of the trap further, we might have obtained an impedance that is a bit closer to the 50-Ω value of the most common coaxial cables. The efficiency report is 97.97%.

We wish to operate the antenna at 14.1 MHz as well. For this operation, we shall need to modify the test model. This version of the model will have loads that approximate the values seen at the lower frequency, well below the trap's resonant frequency. We must recalculate the parallel combination of resistance and reactance that applies to the new frequency. At 14.1 MHz, the reactance of the 3.3-µH coil is about j292.4 Ω, and the reactance of the capacitor is about -j648.5 Ω. Using the same two equations as we did for 21.1 MHz, we obtain for 14.1 MHz a parallel or net reactance of j532.2 Ω and a parallel resistance of about 56,297 Ω. Of course, we shall use the values of inductance and capacitance that we started with, namely, 3.3 µH and 17.41 pF in the parallel R-L-C load, but with the new parallel resistance value.

Open model *13-6b.nec*, which sets up the loads for the new 14.1-MHz frequency.

```
LD 1 2 1 1 56296.6 3.3E-6 17.405E-12
LD 1 4 1 1 56296.6 3.3E-6 17.405E-12
```

If we run the model, we obtain a gain of 1.82 dBi with a source impedance of 68.3 + j9.5 Ω. In part the lower gain stems from the fact that the element is physically shorter than a full-size dipole for 14.1 MHz (about 34'). As well, the power budget returns a 94.57% efficiency. In a parallel circuit, Q is the resistance divided by the (unsigned value of the) reactance, or in this case, 56297/532.2 = 106. The value is somewhat lossier than the value we might obtain considering the coil alone. In fact, the entire trap must be considered at every frequency of use, and we cannot assume that on frequencies below the resonant frequency of the trap that the coil alone determines the effects upon the antenna's performance.

Fig. 13-9 shows the current magnitude curve for the antenna on each operating frequency. Again, the ultimate height of the curves depends on the source impedance values, which differ. However, the key elements in the curves relate to the trap region. At 21.1 MHz, the current drops to a very low level at the traps and is relatively insignificant from those points outward. At the lower operating frequency, we find the typical element-load knee in the current curve. However, current distribution continues to the element ends.

Fig. 13-9

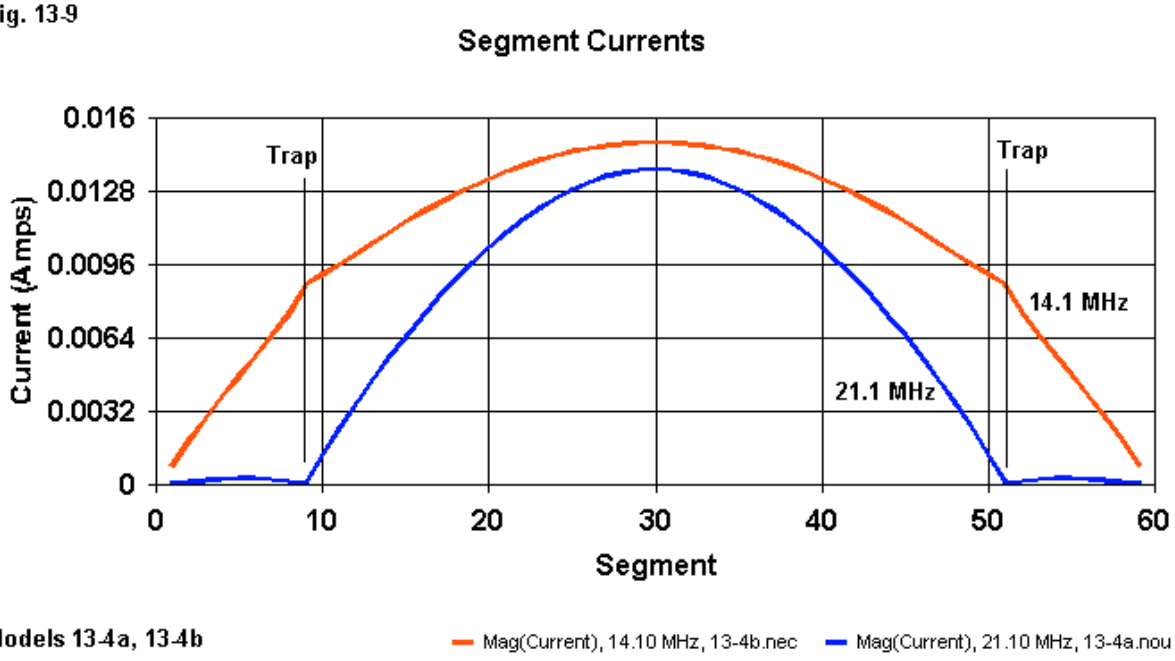

In some ways, the degree of precision of the trap output data is related to more general questions of accuracy with respect to loads placed at some distance from the region in which the current changes slowly from one segment to the next. In our test model, the load is distant from the source on 20 meters, and from **Fig. 13-9**, we know that the current is changing fairly rapidly. Hence, the mathematical loads at the trap points will not calculate as accurately as closer in toward the source, and the inductor wire may have at least some affect on the total antenna length. Therefore, when working with trap antennas, allow considerable adjustment capability when moving from your model to the physical antenna.

LD Limitations

Because LD0 through LD4 loads are non-radiating modifiers to the interaction matrix, they lack physical properties other than those assigned by the command entry. Hence, they have limitations on their accuracy, depending on where we place them within the geometry. For maximum accuracy, spot or lumped loads require that the segments adjacent to the one on which we place them have equal currents. This condition occurs only at the center of dipoles and similar elements and is most closely approximated within the high current portion of an antenna element. Elsewhere on the element, the rate of current change (or voltage change) from one segment to the next creates inaccuracies that are proportional to that rate of change. Demonstrating this fact wholly within NEC models is difficult for capacitance, since we cannot easily replicate a capacitor's physical structure. However, reasonably well-designed inductor models can show the problem.

A pure inductor requires that each end be at the same current magnitude. When placed within the radiating structure of an antenna in a region where the current changes from one segment to the next, an inductor acts as an inductor to the degree that the currents are equal and as a part of

the antenna element to the degree that they are unequal. Consequently, in a region of changing current magnitudes, the inductance called for by an LD load to achieve some specific condition, such as resonance, will be higher than the value required by a physically modeled inductor. The latter has wire within it that contributes to the antenna length and thus needs less inductance to achieve the specified condition.

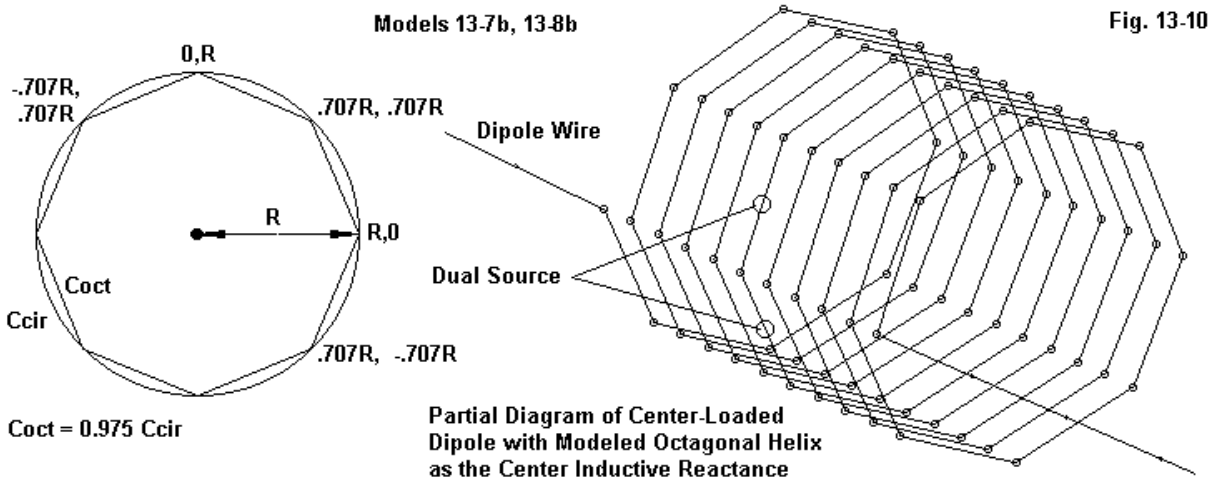

To model a physical inductor requires a test frequency that is low enough to allow significantly large inductors as loading elements. At the same time, the frequency must be high enough so that the spacing between turns is many times the wire diameter to avoid close-spaced wire limitations. As well the antenna wire and the inductor wire must have the same radius (or diameter). **Fig. 13-10** shows the parameters of concern for a center-loading coil constructed from AWG #14 (0.0641" or 2.4 mm diameter) wire. We shall use an octagonal simulation of a circular coil so that the segment lengths within the coil are close to the segment lengths within the antenna wire. Since the coil will have an even number of turns, when used for center loading, we shall need dual or series sources for an exact center feedpoint.

We need only a general formula for calculating the required turns, diameter, and inductance of the coil. The simpler form of the Wheeler equation will work well.

$$L(\mu H) = \frac{d^2 n^2}{18d+40l}$$

L is the inductance in μH, d is the coil diameter, n is the number of turns, and l is the coil length in the same unit of measure as the coil diameter. Since the total length of wires used in the modeled octagonal inductor will be about 2.5% shy of the wire in the calculated circular inductor, we need no more fully refined equation. Each inductor will use 10 turns and be about 345 mm long, with the radius adjusted to achieve a required inductance.

Next, we need a subject antenna into which we may insert either an LD load or our physical inductor. For all tests, a half-length 7.15-MHz dipole will meet the need. The overall length will be 10.48 m and use (in the LD-loaded versions) 91 segments. Each segment will then be about as long as the segments in the physical inductor.

We can begin with a center-loaded version of the dipole, as shown at the top in **Fig. 13-11**.

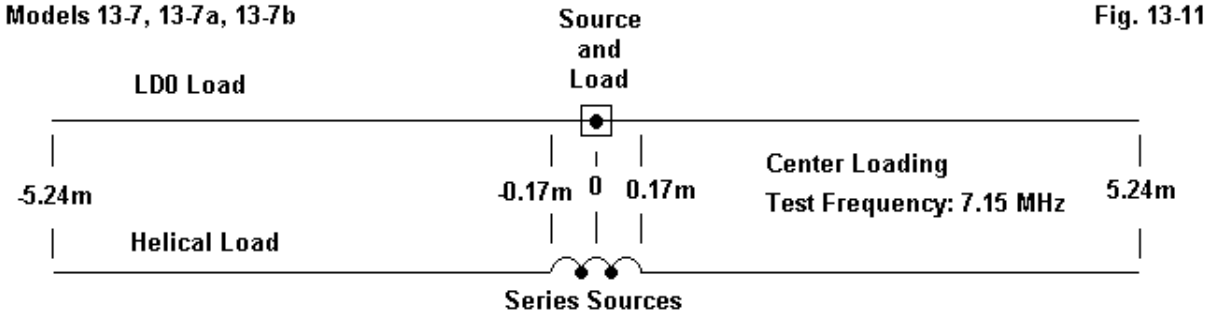

Open model *13-7.nec*.

```
GW 1 91 -5.241112 0 0 5.241112 0 0 .0016317
GE
EX 0 1 46 00 1 0
FR 0 1 0 0 7.15 1
LD 0 1 46 46 0 18.5e-6 0
RP 0 1 361 1000 90 0 1.00000 1.00000
```

The simple center-loaded dipole model initially places an LD0 series load on the center segment. The load has an infinite Q for an inductance of 18.5 µH. Run the model and retrieve standard performance data: 1.85 dBi gain, 13.19 - j1.95 Ω source impedance.

Open model *13-7a.nec*, the same model, but with a Q of 300, as indicated by the addition of a 2.77-Ω resistance to the LD0 entry.

```
LD 0 1 46 46 2.77 18.5e-6 0
```

Run the model and obtain the performance data: 1.11 dBi, 15.96 - j1.95 Ω.

Step three involves model *13-7b.nec*, which replaces the center segments of the wire with the physical loading coil. However, the 18.5-µH coil proved to be too large, so the diameter shrank to a value that produced a 16.6-µH inductor. The linear element segment length is 0.115 m while the coil segments measure 0.108 m. There are 168 segments in the total model. The following small extracts from the model sample the last lines of the geometry and the simple control commands.

```
GW 80,1,.164084,0.,-.141224,.168402,.099822,-.099822,.0016317
GW 81,1,.168402,.099822,-.099822,.17272,.141224,0.,.0016317
GW 82,44,.17272,.141224,0.,5.241112,0.,0.,.0016317
GE 0
FR 0,1,0,0,7.15
GN -1
EX 0,41,1,0,1,0.
EX 0,42,1,0,1,0.
```

Note the dual sources, which require that we add the two reported feedpoint values to arrive at the correct source impedance: 10.07 + j0.17 Ω. The reported gain is 1.58 dBi, but the AGT value is 0.938 or -0.28 dB. Hence, the adjusted gain value is 1.86 dBi.

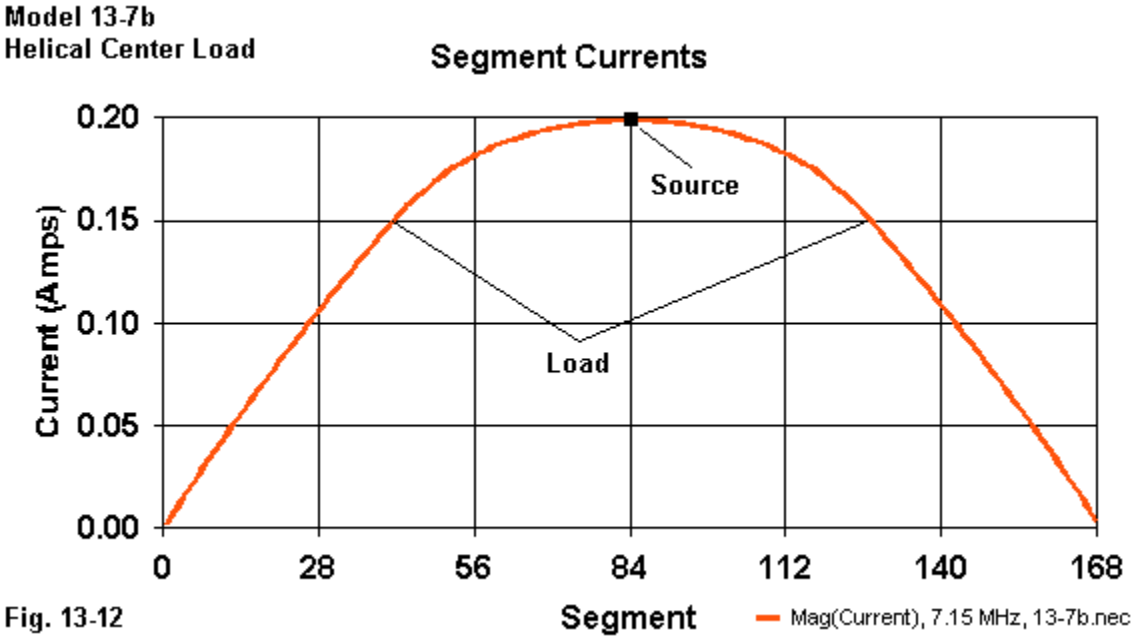

Fig. 13-12

Fig. 13-12 shows the current magnitude along the model on a segment-by-segment basis. The region between the "load" indicators represents the segments used by the coil in the center 345 mm of the total 10-meter wire length. The linear wire begins at a current level that is only about 75% of the peak current at the sources.

Model *13-7b.nec* assigns the material conductivity of copper to the entire structure.

```
LD 5 0 0 0 5.8e7
```

The gain drops to 1.28 dBi, with a source impedance of 10.78 + j0.86 Ω. Comparing this result to the LD version at a Q of 300 suggests a similar Q value for a copper loading coil of the dimensions used.

Models 13-8, 13-8a, 13-8b

Fig. 13-13

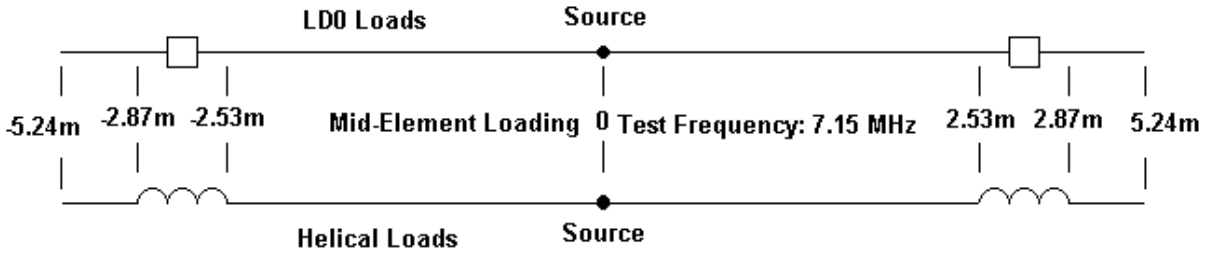

If we retain the same basic 7.15-MHz wire antenna, there will be points near the middle of each leg at which we may place an LD0 load equal to the center load and obtain resonance with the

new pair of inductive loads. **Fig. 13-13** shows the schematic representation of the situation. If we use a 5-wire model, we may place the loads at the centers of the indicated 3-segment wires. Later, we can replace the 3 segments directly with our physical inductor. Open model *13-8.nec* and note the GW and the LD0 entries that employ the same 18.5-µH inductor as the center loaded model, but as a pair of mid-element loads.

```
GW 1 20 -5.241112 0 0 -2.87274 0 0 .0016317
GW 2 3 -2.87274 0 0 -2.5273 0 0 .0016317
GW 3 45 -2.5273 0 0 2.5273 0 0 .0016317
GW 4 3 2.5273 0 0 2.87274 0 0 .0016317
GW 5 20 2.87274 0 0 5.241112 0 0 .0016317

LD 0 2 2 2 0 18.5e-6 0
LD 0 4 2 2 0 18.5e-6 0
```

Run the model and obtain the results: 1.87 dBi, 26.71 - j3.01 Ω. Performance is similar to that of the center-loaded model with an infinite Q, but with a higher source impedance. Model *13-8a.nec* is the same structure, but with Q-300 loads.

```
LD 0 2 2 2 2.77 18.5e-6 0
LD 0 4 2 2 2.77 18.5e-6 0
```

The results are a gain of 1.11 dBi and an impedance of 31.83 - j3.13 Ω. Performance is not noticeably better than the corresponding Q-300 center-loaded model, but the impedance is higher.

The next step is to replace GW2 and GW4 with inductors that will fill the space left by the missing 3 segments left and right of the source position. Model *13-8b.nec* provides the missing parts, resulting in a model with 245 segments. The segment lengths run between 0.099 m and 0.118 m to provide a reasonably close match among segment lengths in the various portions of the model. Initially, the model uses lossless wire throughout, making it equivalent to the LD0 model with infinite Q.

When we worked with the center-loaded dipole, we replaced an 18.5-µH LD0 inductance with a calculated physical inductor of 16.6 µH. If LD0 loads were accurate away from the dipole source position, we should do no worse in terms of the reduction in inductance in the physical coil model. However, to bring the present antenna to resonance with mid-element physical indictors required coils having a calculated inductance of 14.3 µH. The drop in the required resonating inductance is a result of the fact that having the physical coil wires present in the model allows them to perform their non-inductance function of contributing to the overall antenna wire length. This function becomes more pronounced the farther we move away from the high current region of the element.

Run the model to obtain 1.88 dBi and 23.17 + j1.74 Ω. Then open and run model *13-8c.nec*, the all copper version of the same antenna. Interestingly, there is less drop in gain for the mid-element physically loaded model than for the copper-wire center physically loaded antenna: 1.65 dBi with a source impedance of 25.05 + j3.02 Ω.

The physical mid-element loads also show an interesting current magnitude progression, as

evidenced in **Fig. 13-14**, which portrays the currents in model 13-8b. The rise in current at the start of mid-element loads also showed itself in mid-element physical transmission line loads, for example in model 12-8b in the preceding chapter.

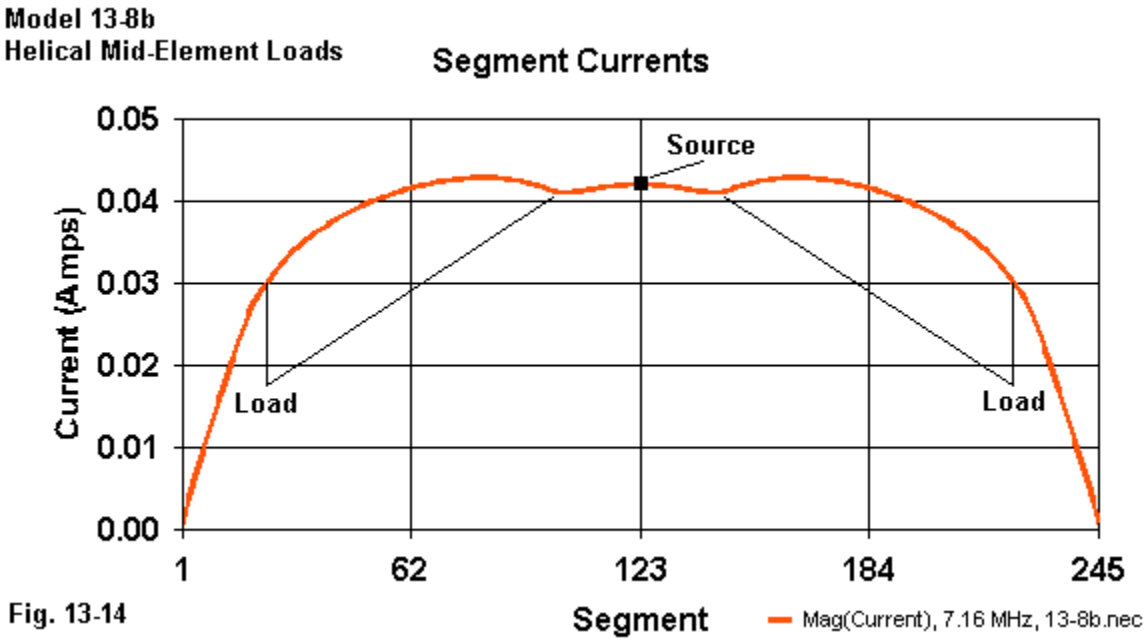

Fig. 13-14

Although physical inductors are impractical in many modeling situations, it often pays--especially in the VHF and UHF ranges--to use them in lieu of the simpler LD inductive loads. Consider the common UHF collinear antenna consisting of a 1/4λ monopole with a 5/8λ top section and a separation to effect collinear coupling. To achieve a combination of correct phasing between the sections and an impedance match so that the base shows a 50-Ω impedance, designers use an inductive section about 1/8λ long. The inductance is tailored to handle the combination of matching and phasing tasks.

Let's develop a pair of models for such an antenna, perhaps set to 435 MHz. We may use 3.175-mm (1/8") diameter aluminum as a reasonable material throughout. Neither the upper or the lower sections of the antenna will be exactly the lengths specified in the generalizations we make about the design, since each length requires adjustment to achieve a near-resonant condition at 50 Ω.

Open model *13-9.nec*. This model uses an inductance of 0.329 μH to effect the matching and phasing condition. To simulate the fact that the section extends for nearly 1/8λ, we distribute the full load in 3 equal individual loads on GW2's 3 segments.

```
LD 0 2 1 1 1. 1.0976E-7 0.
LD 0 2 2 2 1. 1.0976E-7 0.
LD 0 2 3 3 1. 1.0976E-7 0.
```

The remainder of the model is typical monopole construction. However, the outline of the system

appears at the far left of **Fig. 13-15**. The positions of the 3 loads are evident, and the source segment is just above the horizontal ground plane wires, which are 2λ above average ground.

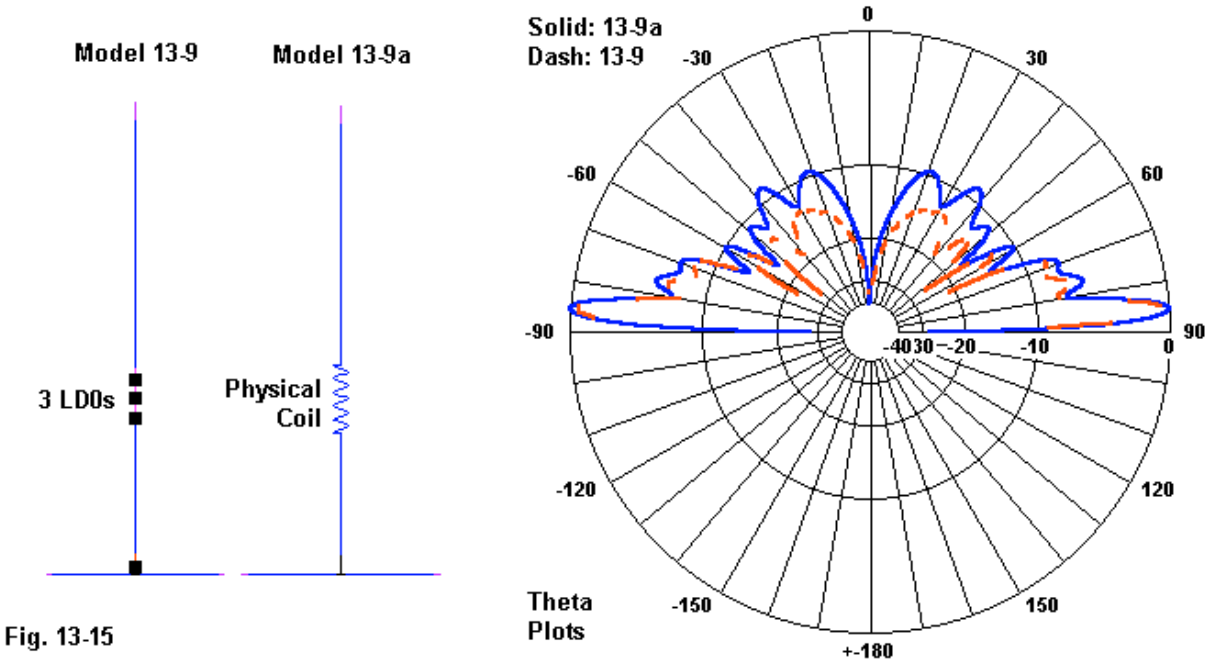

Fig. 13-15

Run the model and obtain a gain of 7.23 dBi at a TO angle of 85°. The reported source impedance is 50.0 - j1.6 Ω.

Open model *13-9a.nec*, which replaces GW2 and its LD0 loads with a physical inductor calculated to fill the space with 0.33 µH. The second outline in **Fig. 13-15** shows the configuration. Top and bottom vertical wires are adjusted to effect a final match among all parts. The gain of this assembly is 7.65 dBi at a TO angle of 86°, with a source impedance of 48.1 + j7.4Ω.

The differences between the models do not show themselves clearly until we overlay the theta patterns on the right side of **Fig. 13-15**. The lowest lobes show little difference between the two versions of the antenna. However, the model using the physical coil shows--as we should have expected--slightly stronger higher lobes due to the fact that the model has a small but not quite insignificant horizontal dimension in the coil structure.

The limitations of LD loads, then, are not confined to the accuracy of the load values they indicate. Even where the loads are accurate, their inability to show with precision (in some, but not all cases) the radiation patterns of antennas in which we use them in place of physical inductors can limit the degree of precision of the full range of data that we draw from models.

Summing Up

The LD command offers us the potential for adding non-radiating loads to a model's structure geometry. The most ubiquitous of the load types is LD5, the material conductivity value that we

can apply from a unit as small as a single segment to the entire structure. NEC-4 adds a permeability entry for use with magnetic materials. The Appendix contains a list of typical antenna materials, along with their bulk conductivity values.

LD4 loads allow us to insert lumped or spot loads on the segment or segments of our choice, usually to simulate loading elements in an antenna. The LD4 version of the load calls for values of resistance and reactance. This load is especially handy for trial-and-error determination of the correct values to achieve some specified operating condition, such as resonance. However, these values remain fixed and are not frequency nimble during sweeps.

Depending on the nature of the load, we may convert the LD4 load to either an LD0 series RLC load or to an LD1 parallel RLC load. Since the loads call for values of inductance and capacitance, they will change their reactance values with frequency and provide a more accurate performance portrayal over a frequency span. We must remember to fill missing values with zeroes, and if we wish an actual zero value, we should use a very small number instead.

LD loads often require some external calculation, as in the case of traps, which consist of a series resistance-inductance combination in parallel with a capacitor. The trap is a good example of a circuit that changes not only its reactance with frequency, but as well its effective parallel resistance (and also its Q). Hence, for some LD entries, a hand-calculator becomes a good companion to NEC.

LD0, 1, and 4 loads have limitations associated with their status as elements that are not part of the structure geometry. They are most accurate when placed on segments such that the current on adjacent segments is just about the same magnitude. They become less accurate as we place such loads in regions where the current is changing rapidly from one segment to the next. As well, for some applications, LD loads may obscure elements of the radiation patterns produced by the structure of their physical counterparts.

Despite their limitations, LD loads are indispensable adjuncts to NEC models. The more familiar we become with both their potentials and their limitations, the more effectively we may use them in our models.

14.
Networks and Some of Their Applications

***Objectives**: The much-neglected NT command offers you another non-radiating function that has many potential applications, once you master at least a few practical steps in implementing 2-terminal port values. In addition to seeing some of the potential for NT, you will also learn a way of implementing some kinds of networks that are frequency nimble.*

The NT command allows you to implement 2-port networks in a model using non-radiating methods, much like the TL command. In fact, the TL command is a specialized implementation of more general networks. However, use of the NT command presumes a basic mastery of handling short circuit admittance matrix parameters. As a result, the command has little general use among the total body of those using NEC.

Short circuit admittance matrix parameters and their calculation from more conventional antenna parameters is a subject well beyond the scope of this volume. However, there are a number of applications of NT networks that admit of some approximations and hence some short cuts in the calculation procedure. They will suffice to allow us to illustrate the fundamental uses of the command, as well as its entry structure. Once the basic elements of NT applications become apparent, supplemental study of short circuit admittance matrices will likely ensue.

One limitation of the NT command is that by using admittance values, it is frequency specific. There are alternative procedures by which you can add a network to a model using LD0 or LD1 loads. While subject to some constraints, such networks are frequency nimble; that is, they permit frequency sweeps with accurate results across the sweep span.

The NT Command and Some Simple Applications

The NT command will let you perform easily some difficult modeling tasks, such as placing a loading element in parallel with a source or creating a parallel connection between segments on different wires within a model. It also allows you to incorporate extremely complex networks into a model so long as you can reduce them to the short circuit admittance parameters required by a 2-port network. In virtually all cases, the command is less troublesome than calculating the values to fit its entry positions. The question facing the modeler who has not previously used networks is not so much understanding the command entries as it is in knowing what entries to make in the floating decimal positions.

The command structure itself is very straightforward. As the sample line below shows, the integer entries specify the specific tag and segment numbers between which we connect the network. In some cases, one of the tags will be a remote wire, and occasionally, it will serve as a "place-holder" to terminate the network. However, there are many applications in which both wires will be active parts of the structure geometry.

```
CMD   I1    I2    I3    I4
      TAG1  SEG1  TAG2  SEG2
NT    2     1     1     6

            F1       F2       F3       F4       F5       F6
            Y11R     Y11I     Y12R     Y12I     Y22R     Y22I
            5.8e-5   -7.3e-3  -5.8e-5  1.7e-2   5.8e-5   -4.8e-3
```

The floating decimal entries call for port values according to the standard 2-port labeling. See **Fig. 14-1**.

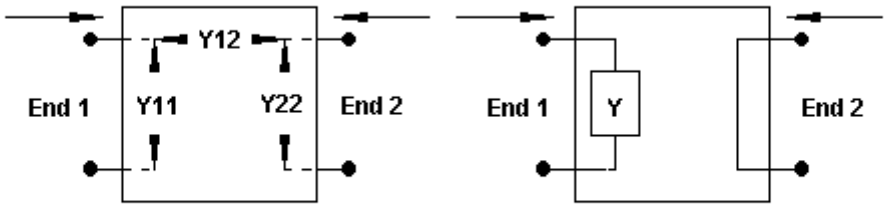

Fig. 14-1

End 1 corresponds to tag 1-seg1, and end 2 to tag 2-seg2. Since the entries that go into the network are usually non-symmetrical, it is important to keep the ends straight. In the sample to the right, we wish the Y element to be in parallel with the assigned tag and segment. Therefore, we must assign its value to the Y11 real and imaginary component positions in the command and be certain that I1 and I2 specify the segment to which the Y element is parallel.

Y11 is the short circuit input admittance, expressed in terms of real and imaginary components. In other contexts, we might call the real component the conductance (G) and the imaginary component susceptance (B). Both use Siemens or mhos as the unit of measure, and they are the inverse of resistance and reactance, respectively. Hence, admittance (Y), also measured in mhos is the reciprocal of impedance (Z). Y22 is the output short circuit reverse-transfer admittance, as indicated by the arrow in the sketch. Since each port has balanced currents, the net current transferred between port 1 and 2 is zero. Hence, Y12 does not represent a physical connection between ports. Rather, it is the short circuit transfer admittance. Since the matrix is symmetric, it is unnecessary to specify Y21, since the forward transfer admittance and the reverse transfer admittance are equal. Y12 and Y22 are also specified in terms of real and imaginary components.

Besides being specific to an assigned frequency, multiple NT entries must be grouped together. You may intermix them with TL commands, but the group must have no other commands separating the members of the group. Intervening commands other than NT or TL will result in the next TL or NT entry destroying previous NT and TL commands. If your NEC core does not employ auto dimensioning, you must set the parameter MAXNET high enough to include the total number of NT and TL commands to be used in the model. For most models, this setting is trivial. However, there may be a large number of driven elements in an array, each with a current source. Since each current source invokes a network, some assemblies may require a very high number

of NT commands.

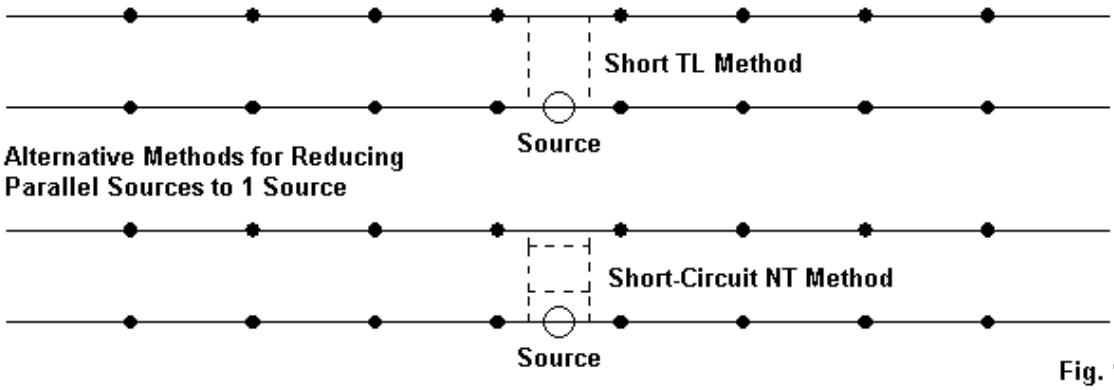

Fig. 14-2

In Chapter 10, we examined a technique for creating parallel sources, but requiring only 1 source assignment. By using a very short transmission line, we effected a virtual short circuit between the specified segments, but with the connections in parallel with the source. The technique proves useful when close space wires might yield inaccuracies if drawn to a single source wire due to very small angles between wires at the junctions. See **Fig. 14-2** and open model *14-1.nec*. These lines show the excitation and transmission line commands for the parallel-wire dipole.

```
EX 0 2 40 00 1 0
TL 1 40 2 40 140 .001
```

The reported source impedance of the dipole is 71.427 - j1.873 Ω. For comparative purposes, the impedance report has far more decimal places than practical applications would require. Now let's suppose that we would like to create the virtual short circuit between wires using the NT command. Like TLs, NTs are in parallel with sources and in series with loads on the same segment.

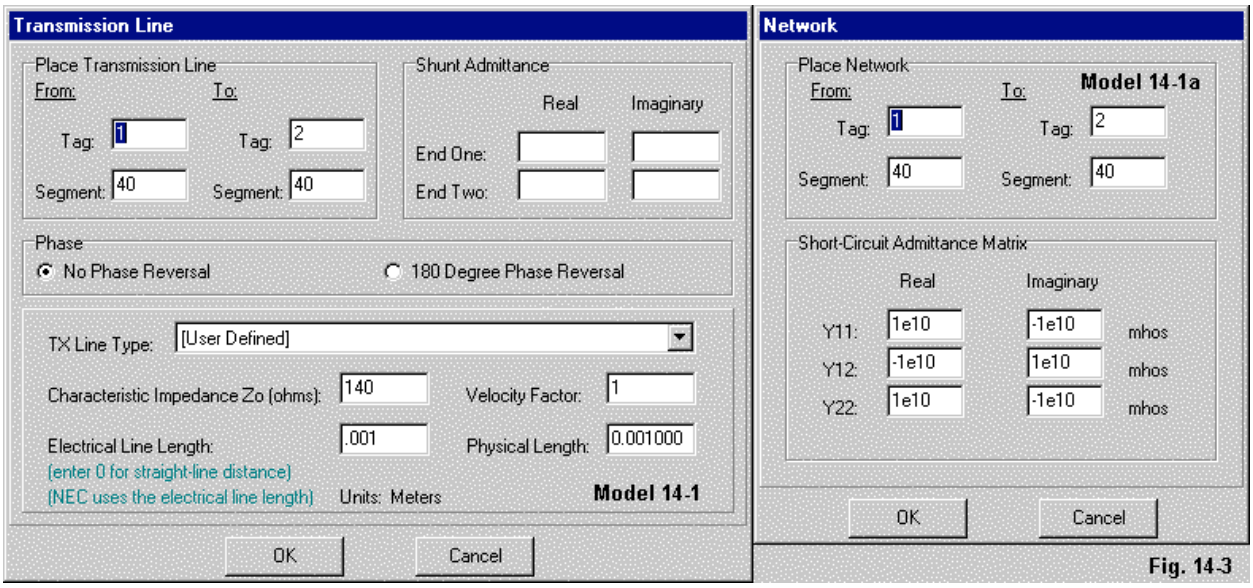

Fig. 14-3

Fig. 14-3 compares the entry assist screens for the required TL and NT entries. The TL entry uses a very short length: 1 mm. By using an electrical length entry as short as 1e-10, the impedance specification would have become wholly arbitrary. Now open model *14-1a.nec*.

```
EX 0 2 40 00 1 0
NT 1 40 2 40 1e10 -1e10 -1e10 1e10 1e10 -1e10
```

Creating a virtual short circuit with an NT command is seemingly complex, but once you have the formula, you may copy it as many times as you need it. In fact, there is a pattern to the entries. Let us set the conductance of the connecting wire (G) to 1e10 and the susceptance (B) to the same value. To create a short circuit with these initial values, we need to set the admittance matrix of the NT command as follows.

Parameter	Real		Imaginary	
Y11	+G	1e10	-B	-1e10
Y12	-G	-1e10	+B	1e10
Y22	+G	1e10	-B	-1e10

We shall later see that this entry set views the short circuit as a special form of a PI network translated into admittance matrix entries. For the moment, we may simply memorize the form--of course, after running the model and confirming that it yields the correct source impedance: 71.430 - j1.868 Ω. Both the TL and NT versions of the parallel-wire dipole return free-space gain values of 2.13 dBi. You may also wish to examine the currents on various corresponding segments of the model to establish their virtual identity.

A second relatively simple use of the NT command that we have already encountered appears in Chapter 10: the current source. Open model *14-2.nec*, a basic dipole with a current source.

```
CM dipole with current source
CE 0 deg at antenna source
GW 1 11 0 -.2375 0 0 .2375 0 .001
GW 2 1 9999 -.005 9999 9999 .005 9999 .001
GE
FR 0 1 0 0 299.7925 1
EX 0 2 1 00 0.00000 1.00000
NT 2 1 1 6 0 0 0 1 0 0
XQ
EN
```

In this case, we create the required dipole (GW1) and add a second remote 1-segment wire (GW2) located too far away from the key element to have any affect on the pattern data. The remote wire is very short, very thin, and never given a material load. Next, we place a network (NT) between the dipole source segment and the remote wire, using the standard set-up of the NT command for a current source. Using the NT assistance screen in the software, as shown on the left in **Fig. 14-4**, will ease the burden of remembering which entry point receives the value of 1 for the Y12 imaginary position. Finally, we add an EX0 command, placing the source on the remote wire and phase shifting the value by 90°.

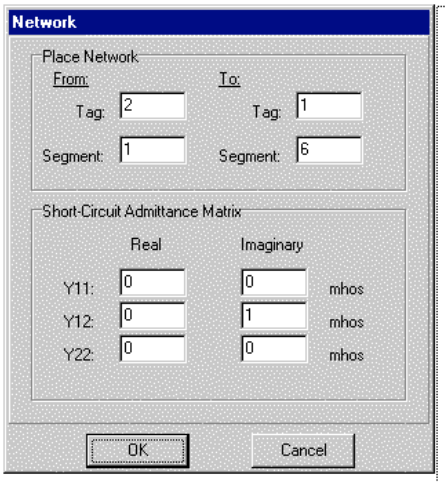

Fig. 14-4

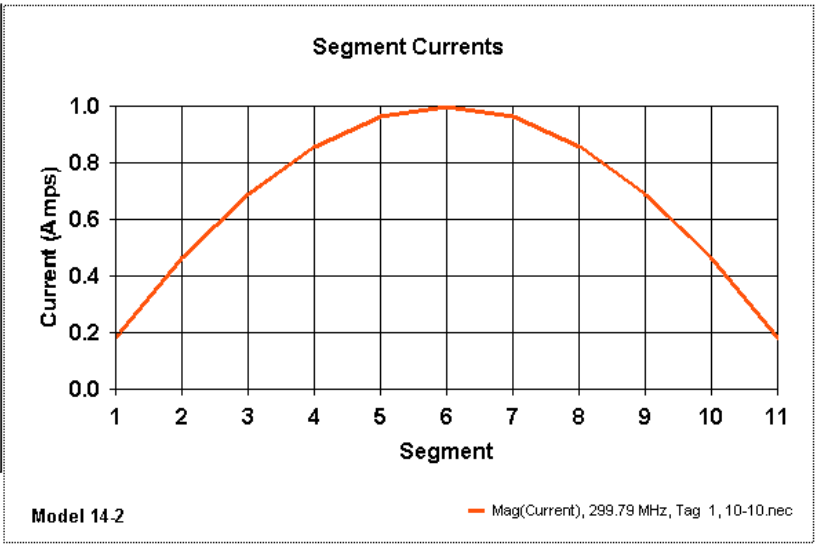

By entering a Y12-imaginary value of 1.0 mho in the network, we obtain a 90° phase shift in the current at the element relative to the phase of the voltage at the source on the other side of the network. As well, whatever value the source shows as its voltage will appear at the other side of the network on the element as the current value. The technique of "forcing" current values is widely used in phased array design, but here, it functions to provide a current source with a known value at the true feedpoint of the antenna. One very significant use of current sources is to allow rectangular plots of the element currents reference to a standard value, such as 1.0. The right side of **Fig. 14-4** shows such a plot for the dipole.

For easy extraction of the required data that applies to the antenna feedpoint (in contrast to the model source on the remote wire), we must learn how to "read" the data. The first key output report entry is the antenna input parameters, shown below for our current-source dipole.

```
- - - ANTENNA INPUT PARAMETERS - - -

TAG    SEG.     VOLTAGE (VOLTS)          CURRENT (AMPS)
NO.    NO.     REAL         IMAG.       REAL         IMAG.
  2     12   0.00000E+00 1.00000E+00 -1.16117E-01 7.17602E+01

           IMPEDANCE (OHMS)          ADMITTANCE (MHOS)       POWER
           REAL         IMAG.        REAL         IMAG.     (WATTS)
         1.39353E-02 -2.25490E-05 7.17602E+01 1.16117E-01 3.58801E+01
```

1. The phase-shifted voltage value--1.0 v imaginary--is the real current level at the element feedpoint. You may verify this from the current table for segment 6.

```
SEG.   TAG            - - - CURRENT (AMPS) - - -
NO.    NO.       REAL         IMAG.        MAG.         PHASE
 6     1      1.0000E+00  -2.2205E-16   1.0000E+00     0.000
```

2. The impedance at the element feedpoint appears as an admittance (and its inverse appears as an impedance). If you recall the standard dipole model, its impedance with a voltage source is 71.76 + j 0.12 Ω, the value that now appears under the admittance entry.

3. The power report is accurate for the current-source model. Hence, by the technique of power adjustment shown in Chapter 10, we would adjust the imaginary voltage value as the square root of the ratio of new power to old to arrive at the correct source for the desired power level. A value of 5.279 volts imaginary will yield a 1000-watt power level.

The NT command also offers us the potential for having one more alternative way to perform a specific task. Open model *14-3.nec*, a simple 3-element Yagi designed for 14.175 MHz and using 1" (0.025 m) aluminum elements.

```
GW 1 101 -5.292 0 0 5.292 0 0 0.0125
GW 2 50 -4.947 3.024 0 -0.049 3.024 0 0.0125
GW 3 1 -0.049 3.024 0 0.049 3.024 0 0.0125
GW 4 50 0.049 3.024 0 4.947 3.024 0 0.0125
GW 5 101 -4.786 6.049 0 4.786 6.049 0 0.0125
```

The elements employ a high segmentation density, with the driver element (GW2 - GW4) subdivided. The left side of **Fig. 14-5** shows the evolution of the element, along with the first alternative that we shall use in our quest to match the antenna to a 50-Ω feedline. However, run this pre-match version of the antenna to obtain its "natural" source impedance: 23.42 - j24.59 Ω. The reported antenna gain is 7.84 dBi with an AGT value of 0.99977, indicating a very adequate model and accurate output reports (as always, within the limits of the AGT test).

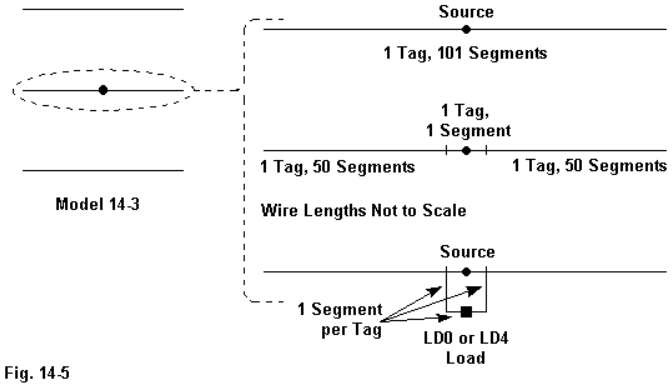

Fig. 14-5

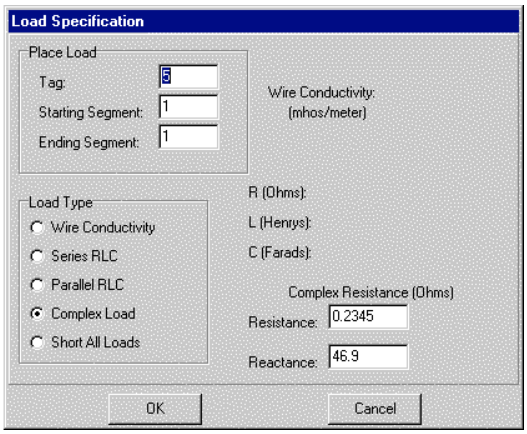

Our matching goal has several options, but we shall choose to add a beta match. The beta match is a version of an L-network with down conversion from the source (50 Ω) to the load. This system requires a series impedance element on the load side of the network, already in place in the form of the capacitive reactance of the source. The other element of the network consists of a shunt reactance of the opposite type (relative to the series reactance) on the source side of the network. To achieve this goal, we need to be able to place a load in parallel with the source. However, LD loads appear in series with the source and thus are not applicable.

One tactic that we can use is to create a physical structure to give a parallel position for the load. The last part of the sketch in **Fig. 14-5** shows a way to accomplish this feat. By using 1-segment wires around the 1-segment source wire, we create a box. Since the wires are short, they contribute very little to the radiation pattern. However, they provide a place for the desired shunt reactance. Open model *14-3a.nec* and examine the additional wires for the box. Note that they

place the box at right angles to the plane of the antenna, although an in-line orientation would work as well. The new wires appear between the original drive entry and the director, which is now GW8. As well, the final end of the driver (GW7) follows the box structure. Excitation remains on GW3.

```
GW 3 1 -0.049 3.024 0 0.049 3.024 0 0.0125
GW 4 1 -0.049 3.024 0 -0.049 3.024 0.098 0.0125
GW 5 1 -0.049 3.024 0.098 0.049 3.024 0.098 0.0125
GW 6 1 0.049 3.024 0.098 0.049 3.024 0 0.0125

LD 4 5 1 1 0.2345 46.9
```

The required value for the shunt element derives from standard L-network equations:

$$\delta = \sqrt{\frac{R_{High}}{R_{Low}} - 1} \qquad X_S = \delta R_{Low} \qquad X_P = \frac{R_{High}}{\delta}$$

The term δ is the loaded Q of the network and derives from the high and low resistance values at the circuit terminals. The required series reactance is δ times the low resistance and appears in series with it. The shunt or parallel reactance is of the opposite type from the series reactance and is the high resistance divided by δ. There are numerous utility programs available for calculating the required values. By using the natural source resistance and the feedline characteristic impedance to determine δ, we discover that the existing series capacitive reactance is almost precisely what the equations calculate. Hence, we need only calculate a corresponding shunt or parallel reactance: 46.9 Ω inductive. Based on experience, we may assign the shunt element a Q of about 200. The final values appear in the LD4 entry for model 14-4a.

Run the model to obtain its performance values: 7.86 dBi gain, 57.58 + j1.51 Ω impedance, 1.008 AGT, 0.036 AGT-dBi, and an adjusted gain of 7.82 dBi. The AGT value shows that the wire box has a small affect on model adequacy, and the adjusted gain value suggests that the box also has a small affect on performance of the driver. The fact that we did not arrive at precisely 50 Ω impedance is a measure of how far off from ideal the series reactance is, as well as the affects of the wire box. Perhaps one of the chief advantages of this system of adding a parallel load is that it allows the simulation of inductors (in contrast to beta hairpin assemblies). By converting the load to a type 0 using the same series resistance, but an inductance of 0.527 μH, the model becomes perfectly frequency nimble, with accurate output values for frequency sweeps across the operating passband.

Although subsequent alternative shunt loads will not require the driver scheme used for the box version, we shall retain it so that the core model remains constant in all of our trials. Open model *14-3b.nec* to see a version of the antenna using a technique that we met in Chapter 12 when exploring transmission lines. This model employs a standard shorted transmission line stub calculated to provide the required reactance. Then, we trimmed the stub to a length that yielded the most satisfactory source impedance.

```
GW 6 1 1.001 1.001 1.001 1 1 1 0.000322

TL 3 1 6 1 600 0.262584 0 0 1e10 1e10
```

GW6 provides the remote termination wire for the shorted stub. The TL command specifies a 600-Ω line with a length of 0.263 m, simulating an open or ladder line stub assembly. Run the model to obtain its output reports: 7.84 dBi gain, 49.23 - j0.005 Ω impedance, 0.999 AGT. The near-ideal value of AGT requires no gain report adjustment, and the gain value coincides with the report from the pre-matched model. Although the TL line cannot show losses within it, they should be negligible. Like the use of an LD0 load in the box model, this version of the beta-matched Yagi is also frequency nimble.

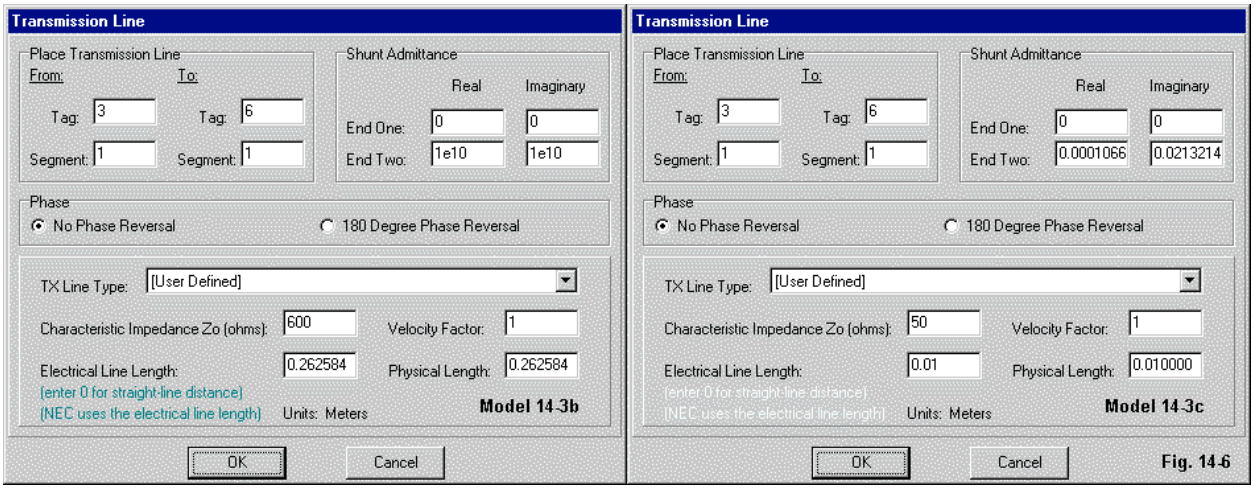

Fig. 14-6 shows the assist screen for the TL stub in the model that we just examined. However, it is not the only way in which we might use the TL command to effect a parallel load on the Yagi source segment. The right side of the figure shows an alternative set of entries. Open model *14-3c.nec*. You will note that the geometry remains unchanged from model 14-3b. However, the TL line reflects the values shown in the figure.

```
TL 3 1 6 1 50 0.01 0 0 0.0001066 -0.0213214
```

As a special form of a network, the TL command allows the use of shunt admittance values at either end of the line for various simulation purposes. In this case, instead of using a stub, we specify a very short line length. The line is so short that no significant transformation of voltage, current, or impedance can occur. On the "far" end of the line, we insert the shunt admittance equivalents of the series values of resistance and reactance that we need for the match. The real component of an admittance (Y) is conductance (G), and the imaginary component is susceptance (B). Since the conversion requires converting a series impedance into a shunt or parallel admittance, we may use these equations:

$$G_P = \frac{R_S}{R_S^2 + X_S^2} \qquad B_P = -\frac{X_S}{R_S^2 + X_S^2}$$

The subscripts "S" and "P" indicate series and parallel values, respectively. Using the original values of the required impedance for a coil with a Q of 200, we convert 0.2345 + j49.6 Ω to 1.066E-4 - j2.132E-2 mhos. These values go on end 2 of the line.

Run the model for its reports: 7.82 dBi gain, 48.98 - j0.32 Ω impedance, 0.999 AGT. The resistive component of the impedance is slightly low because we did not adjust the coil reactance

for a closer approach to 50 Ω before converting the reactance to a susceptance. The limitation of this method of creating a beta match is that it is frequency specific and does not yield highly accurate values in a frequency sweep.

We are not quite done with our beta matched Yagi. We have painlessly slipped into the realm of admittances, and so we might as well create the parallel matching element using the NT command. Open model *14-3d.nec* and examine the NT command that replaces the TL commands.

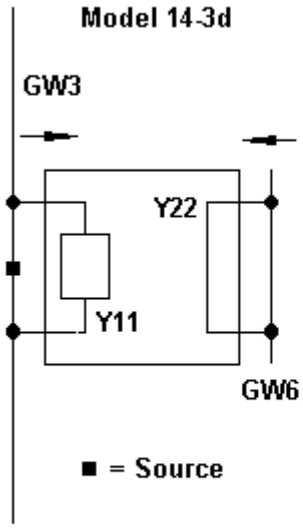

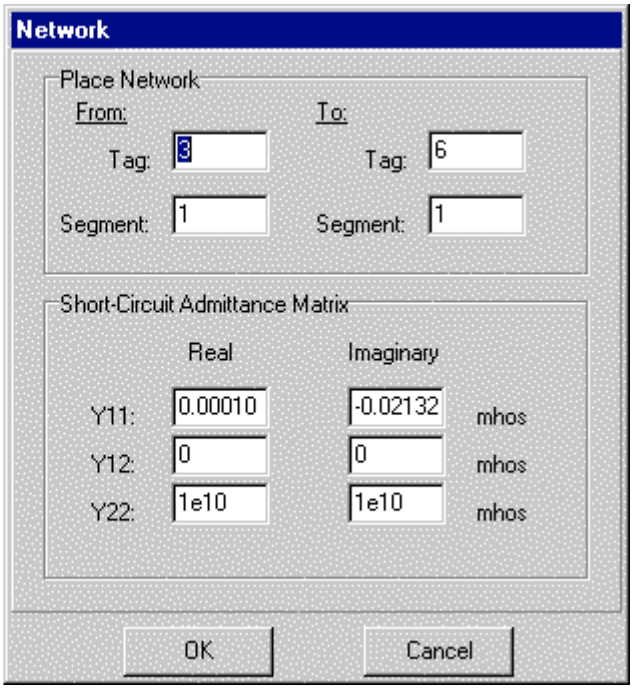

Fig. 14-7

To place a load in parallel with a source on a specific segment, we may use the system shown in **Fig. 14-7**. We place the shunt admittance values on the end of the network connected to the target segment. These are the Y11 values, which are identical to those used for the short-TL version of the model. Y12 remains blank, as indicated by the zero entries. The other end of the network requires a short circuit, normally created by the use of very high values of real and imaginary admittance for Y22. The network short circuit adds nothing to the structure geometry of a model, and so the short-circuited end of the network may connect to any wire without affecting antenna performance. Since GW6 is left over from the TL models, we used that 1-segment wire as the network terminus.

Run the model for its reports: 7.82 dBi gain, 48.98 - j0.01 Ω impedance, 0.999 AGT. The reduced reactance results from not having a 0.01-m line between the source segment and the load. Since we are using admittance values (comparable to using impedance values in an LD4 load), the model is frequency specific. Its chief advantage lies in the place it occupies in our progression of beta-matched models. Hopefully, by revealing its relationship to other techniques that we may use to achieve relatively the same goal, the function and nature of NT networks is somewhat clearer.

Some Slightly More Complex Networks

We have so far examined uses of the NT command that we can easily copy. However, the power of the command rests upon an understanding of 2-port networks and transfer functions, most specifically, short-circuit admittance parameters. The limitation of the NT command is that it permits only passive networks (without active components, such as amplifiers), since Y12 = Y21. However, virtually any passive network can be analyzed in 2-port terms.

In this set of exercises, using models in the 14-4 series, we shall look at 3 examples of the NT command used to simulate simple matching networks: 2 L-networks and a PI. We shall also make use of certain short cuts to simplify the calculations. The approximations will be close enough to the results of complete calculations to yield highly usable model outputs.

The premise for these models will be our faithful friend, the dipole at 299.7925 MHz. Open model *14-4.nec* and run it to find the reported source impedance: 71.760 + j0.116 Ω. Suppose that we wish to transform this impedance to 50 Ω resistive. Although the problem is trivial in practical terms, it will serve our needs very well.

Consider an L-network consisting of a series inductive reactance on the source side and a shunt or parallel capacitive reactance on the load side. We have an up-converting network with minimal components. Using a utility program, we find the calculated series inductance as 0.018 μH and the shunt capacitor as 4.9 pF. See **Fig. 14-8** for the network configuration.

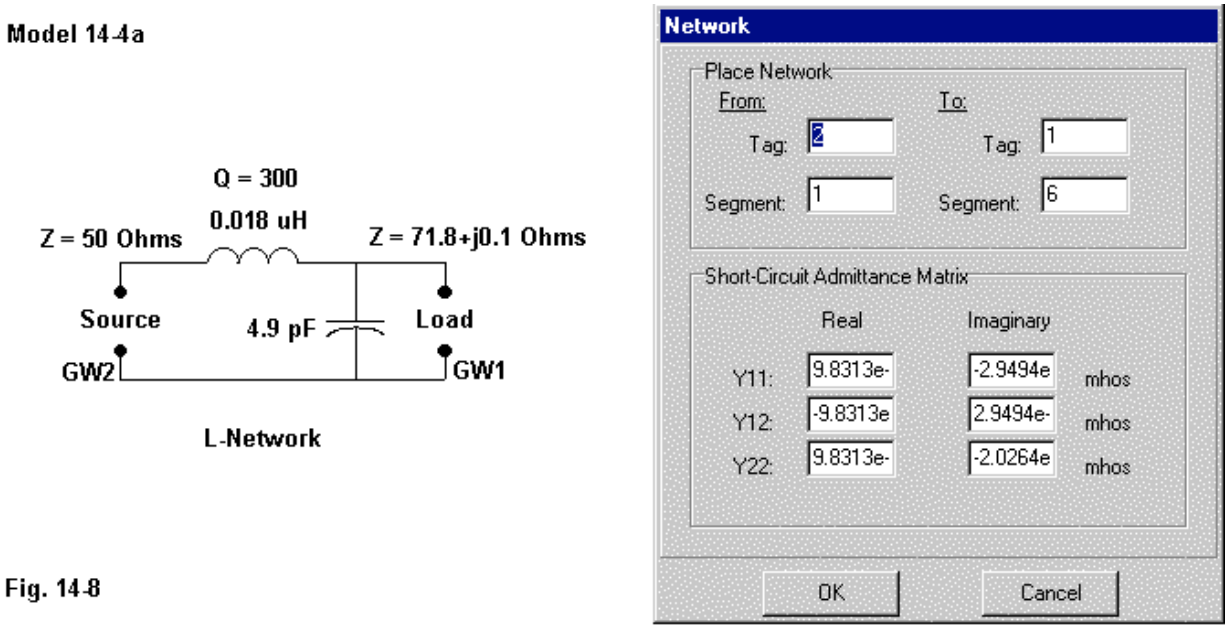

Fig. 14-8

The first step is to create a new wire (GW2) for the new source position. This wire may be short, thin, lossless, and remote. Then we need to create an NT 2-port network to simulate the L-network in short-circuit admittance terms. Open model *14-4a.nec* and examine its elements.

```
GW 1 11 0 -.2375 0 0 .2375 0 .001
GW 2 1 0 -.01 -.2 0 .01 -.2 .0005
GE
FR 0 1 0 0 299.7925 1
NT 2 1 1 6 9.8313e-5 -2.9494e-2 -9.8313e-5 2.9494e-2 9.8313e-5 -2.0264e-
2
EX 0 2 1 00 1 0
XQ
EN
```

The L-network that we shall use--along with the following examples in this series--make certain assumptions that will simplify our work. First, the Q of the network inductors will be 300. Second, the Q of the network capacitors will be so high that we may neglect it entirely. These two assumptions are common and usually harmless at HF but may require revision as we carry capacitors into the VHF and UHF ranges.

We need admittance figures that we may then convert into entries for Y11, Y12, and Y22 in the NT command. We may easily enough calculate the reactances of the given components: j33.9 Ω for the series inductor and -j108.3 Ω for the shunt capacitor. However, these values are generally useless. We might as well directly calculate the admittance of the components from the inductance and capacitance values directly.

$$B_C = 2\pi FC \qquad B_L = -\frac{1}{2\pi FL} \qquad G = \frac{|B|}{Q}$$

Most texts caution against such procedures, preferring the conversion equations shown earlier to arrive at shunt conductance and susceptance values. However, we may use these simplified calculations because we have set the capacitor conductance to a range that has no effect on the values at all, and the Q of 300 will leave the value of coil susceptance unchanged using the standard conversion technique. The susceptance values reverse signs that would attach to impedance values since they will substitute for properly converted shunt admittance values. In all cases, wherever more elaborate and therefore more precise techniques are readily available, use them. As well, use complete calculations wherever the analysis is critical.

Hence, the susceptance of the coil is -1.1302E-1 S. Because the coil Q is 300, the conductance is 9.8313E-5 S. The susceptance of the capacitor is 9.2299E-3 S.

For a series-inductor PI network--and the L network forms an incomplete PI for our purposes--the following simplified entries give us the required values of the NT entries. The p1 subscript indicates the shunt capacitor that is not present and hence is zero in the L circuit. P2 indicates the load-side shunt capacitor, which would have zero conductance in a down-converting L network. S indicates the series component.

Parameter	Real Component	Imaginary Component
Y11	Gp1+Gs	Bs + Bp1
Y12	-Gs	-Bs
Y22	Gp2+Gs	Bs + Bp2

Applying these formulas to the simplified calculations for the components gives us entry values of the following order.

Parameter	Real Component	Imaginary Component
Y11	9.8313E-5	-2.9494E-2
Y12	-9.8313E-5	2.9494E-2
Y22	9.8313E-5	-2.0264E-2

These are the values that appear on the NT entry screen on the right side of **Fig. 14-8**. When setting up the screen and the NT command, be certain that the "from" wire (tag1, seg1) corresponds to the correct end of the L network so that Y11 registers as the source terminals and Y22 as the load terminals.

To find out if our L network is correctly designed and the conversion to short-circuit admittance matrix parameters is successful, run the model and obtain the new source impedance: 50.097 + j0.658 Ω. One of the advantages of using NT to formulate matching networks that transform the source impedance to a desired value is that we obtain a measure of the losses in the network due to its finite Q. We purposely set the losses within the dipole at zero. The power budget shows a network loss of 2.25E-5 watts, giving the overall antenna-plus-network a 99.77% efficiency.

We may apply essentially the same analysis to an L network composed of a series capacitor and a shunt inductor. Using the same matching problem, we now require a series capacitor of 16.1 pF and a shunt inductor of 0.058 μH. Once more, the inductor Q is 300. **Fig. 14-9** shows the overall set-up of such a network, along side the NT entry screen.

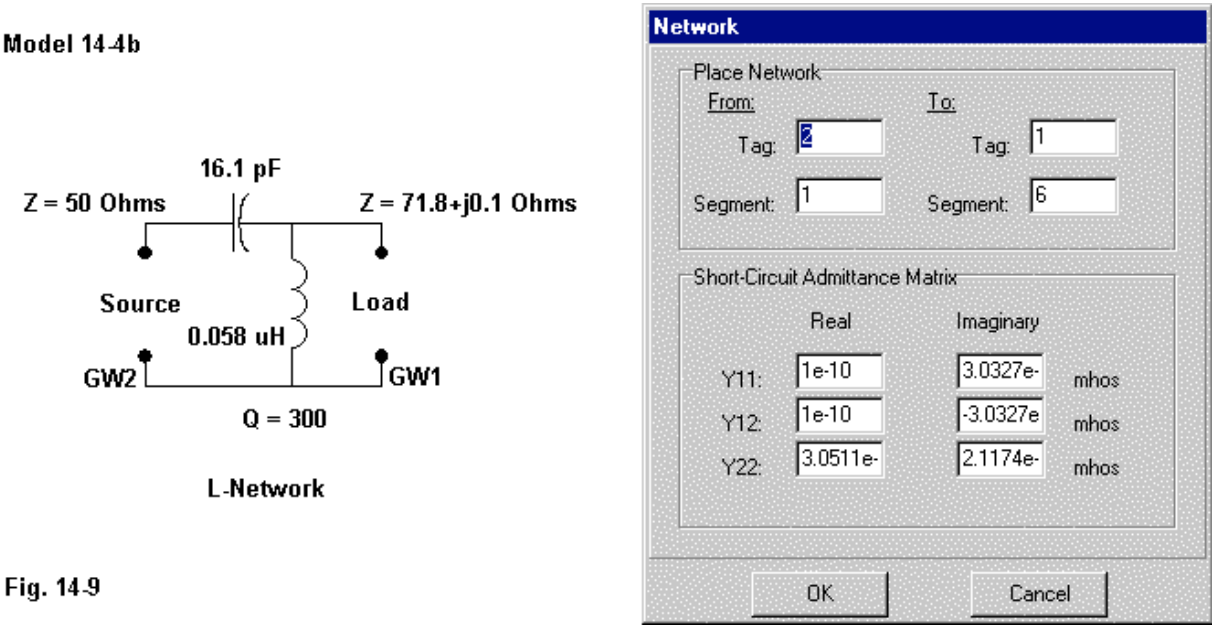

Fig. 14-9

Open model *14-4b.nec*. It is identical to the preceding model except for the NT command.

```
NT 2 1 1 6 1e-10 3.0327e-2 1e-10 -3.0327e-2 3.0511e-5 2.1174e-2
```

We shall use the same calculating scheme to arrive at the susceptance values for the components. The series capacitor yields 3.0327E-2 S, while the inductor shows -9.1532E-3 S. Since the Q is 300, the coil conductance is 3.0511E-5 S.

Parameter	Real Component		Imaginary Component	
Y11	Gp1+Gs	1E-10	Bs + Bp1	3.0327E-2
Y12	-Gs	1E-10	-Bs	-3.0327E-2
Y22	Gp2+Gs	3.0511E-5	Bs + Bp2	2.1174E-2

Because the values of real admittance in Y11 and Y12 are so small, the signs do not matter at all. Once we have installed these values in the NT command, we may run the model to obtain the matched source impedance: 50.010 - j0.342 Ω. The reported efficiency is 99.78%, indicating slightly less loss in this configuration, despite the use of a larger inductance and hence a larger series resistance within it for a Q of 300.

As a final step in this exercise, we may also use a full PI network to effect a match between the dipole and a 50-Ω feedline. The PI will have shunt capacitors surrounding a series inductor, as shown in **Fig. 14-10**.

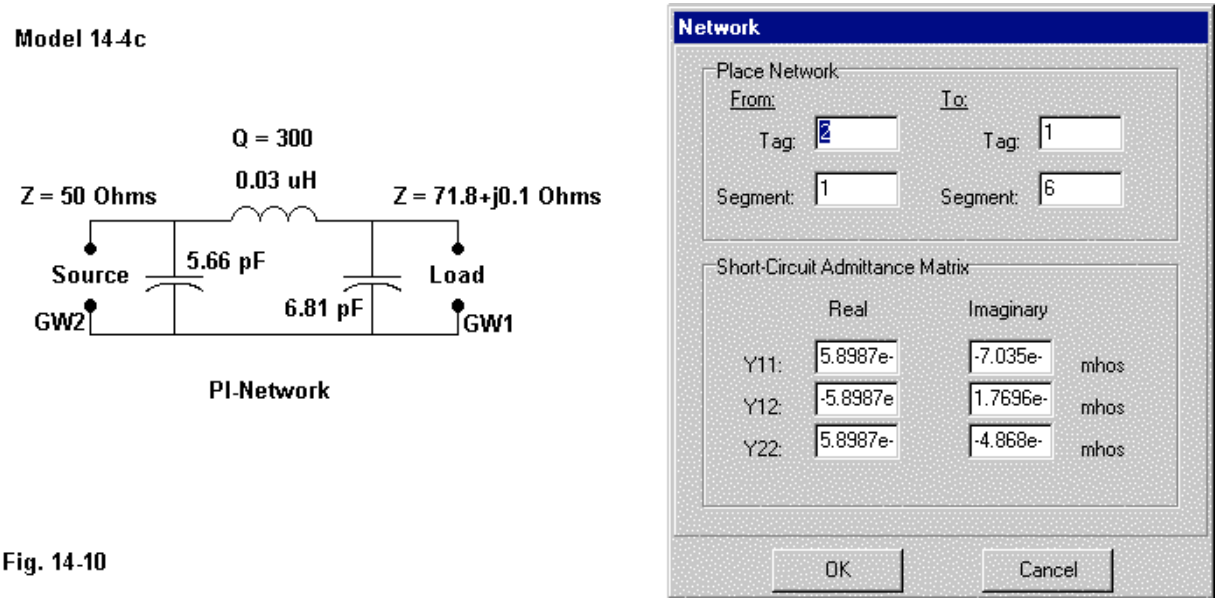

Fig. 14-10

The source-side capacitor is 5.66 pF, while the load-side capacitor is 6.81 pF. The inductor is 0.03 μH. The corresponding values of susceptance are 1.0661E-2 S for Bp1, 1.2828E-2 S for Bp2, and -1.7696E-2 S for the series inductor. With a Q of 300, the conductance is 5.8987E-5 S. With these values in hand, we can arrive at usable entries for the NT command in model *14-4c.nec*.

```
NT 2 1 1 6 5.8987e-5 -7.035e-3 -5.8987e-5 1.7696e-2 5.8987e-5 -4.868e-3
```

We arrive at the entry values using the same simplified procedures as for the L networks.

Parameter	Real Component		Imaginary Component	
Y11	Gp1+Gs	5.8987E-5	Bs + Bp1	-7.035E-3
Y12	-Gs	-5.8987E-5	-Bs	1.7696E-2
Y22	Gp2+Gs	5.8987E-5	Bs + Bp2	-4.868E-3

Run model 14-4c to obtain a source impedance report: 50.139 - j0.426 Ω. However, with a network loss of 4.81E-5 watts, the efficiency of the antenna and its network has dropped to 99.52%. Although not significant in practical terms, the efficiency decrease verifies the fact that 2-element matching networks, such as the 2 versions of the L network, are inherently more efficient than 3-element networks, such as the PI, when we maintain the same component Qs throughout.

From the values that have appeared for the incomplete (L) and complete PI networks when converted to entries for Y11, Y12, and Y22 in the NT command, it should be clear that the short circuit is simply a special case. Review model 14-1a. Now imagine a PI network in which the values of B and G are all indefinitely large, that is, 1E10. Then the formation of the short-circuit between the two sides of the 2-port network becomes clear.

The simplifications in the procedure for calculating the shunt admittance values and for converting those values into 2-port parameters works well enough in non-critical applications of PI networks. You may use standard conversion equations found in many texts to convert T networks into PI networks and continue to use the simplified calculations. However, for more complex circuitry, you should perform a full step-by-step set of calculations, since small deviations have a habit of accumulating rather than canceling out.

The model 14-4 series has been designed to provide an initial experience in using the NT command with 2- and 3-element passive networks. However, all NT commands are frequency specific. Unlike LD0 and LD1 loads, they do not change with frequency in a sweep, but remain as fixed as LD4 loads. If we wish to perform a frequency sweep and obtain usable results, we must turn to a technique for modeling networks--such as the L or the PI, that does not invoke the NT command and that does make use of either LD0 or LD1 loads to simulate the network components.

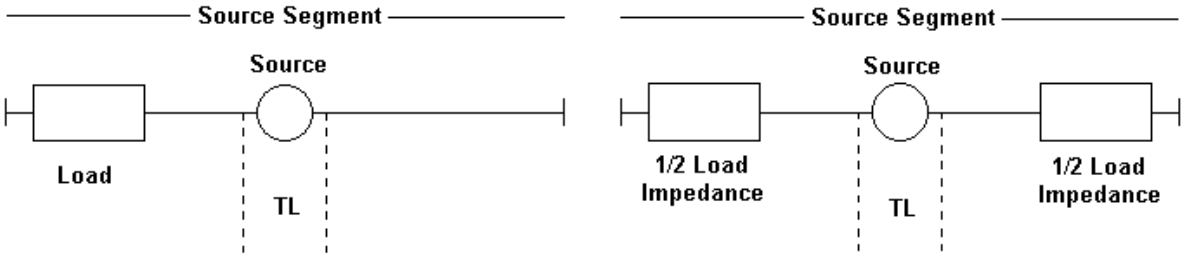

The Common Way to Portray Load, Source, and TL Relationships

Fig. 14-11

An Alternative Way to Portray Load, Source, and TL Relationships

To develop that technique, we should first review a few fundamental relationships among some of the crucial control commands. We are working with EX, LD, and TL commands that we assign to the same segment. The key relationships to note in **Fig. 14-11**, left, are these. First, an LD load is always in series with both a source and a transmission line assigned to the segment. This applies no matter how short the segment or where we may locate it. Second, a voltage source (EX0) always is in series with the segment to which we assign it. In essence, it creates a mathematical gap in the segment and places the assigned source voltage and the resultant current in series with the segment wire. (Hence, any assigned lumped load falls outside the

"gap.") So the source will be in series with any load.

Third, a TL transmission line will be in series with a load and in parallel with a source. All TL transmission lines are non-radiating structures, that is, they are not represented by geometry commands that add to the radiating structure of the model. As well, such lines are lossless. The fact that a TL is in parallel with a source and in series with a load opens the way both to potentials and to limitations.

It is significant to understand that the right side of **Fig. 14-11** is an appropriate reformulation of the left side. For inductive loads added to the source segment, the source and any TL that we may add are mathematically at the center of whatever physical structure we may use to implement them in a real antenna. Therefore, we may assume that the source is at the middle turn of the coil. Likewise, we may physically implement each half of the loading inductance with a shorted transmission line stub and each side of the physical feedpoint. We call such implementations of center loading "linear loads," and they are subject to fields of the antenna itself that may slightly disrupt the equal magnitude but opposite polarity currents we assume for transmission lines. Hence, it is normally most accurate to model linear loads using physical wires rather than the TL facility, which cannot show the influences of the radiated fields.

We are working our way toward a more general solution to the feedline matching and modeling problem. Many of the networks that we physically implement are unbalanced or single-ended. In fact, their names are derived from unbalanced forms of the network: the L, the PI, and the T, to name the most common ones. (Of course, we may create more complex combinations of these networks, such as the PI-L, once common in vacuum tube power amplifiers. However, we must remember that the PI and the T are viewable as simply back-to-back L-networks.)

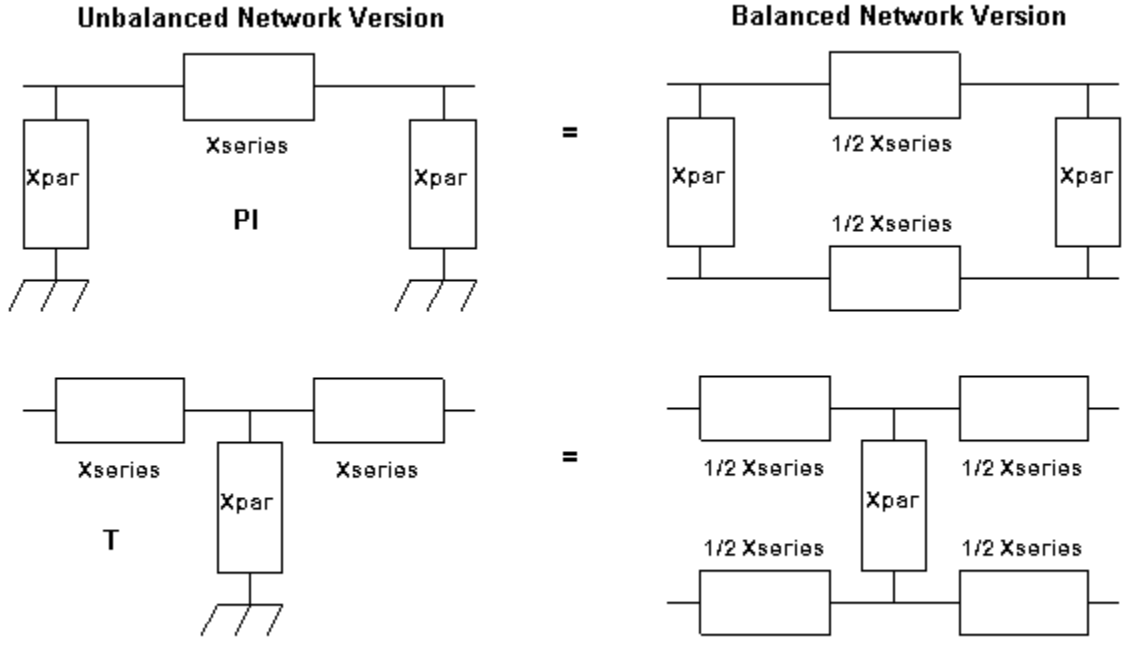

Fig. 14-12 **Equivalent Networks**

As noted in **Fig. 14-12** for the PI and the T unbalanced networks, every single-ended network has a balanced equivalent. We calculate the values using the single-ended equations, which appear in a myriad of utility programs to save us the hand-calculator work. Then, we simply divide the reactances for the series elements in half and place one portion in each of the two lines of the balanced system.

Converting networks into balanced forms relieves us of a major limitation relative to NEC and single-ended networks. An unbalanced network presumes a virtually lossless ground buss to terminate components, as well as a source and a load (the old antenna feedpoint) that also run between the "hot" line and ground. NEC has a limitation in this regard. Simply bringing a wire to Z = 0, except for a perfect ground, will not achieve a virtually lossless interconnection with other wires brought to Z = 0 unless they all terminate at the same point. Two wires connected to a real ground (Sommerfeld or reflection coefficient) at any distance will always show a resistance between the two Z = 0 points. In most instances, this limitation precludes modeling a single-ended network in NEC, except via the NT command, which is not frequency nimble.

A balanced network is independent of any ground connection. We can implement Ls, PIs, and Ts in balanced form without regard to ground and arrive at relatively accurate modeled results. All that we need to do is to figure out how to attach our network to the antenna's former feedpoint. It is a single segment with the former source point at its center, forming two terminals of a 4-terminal network.

The creation of a network using LD0, LD1, or LD4 loads for the reactive components requires that we construct a grid of wires matching the network needs. **Fig. 14-13** shows such a network for a balanced PI network. For the moment, let's concentrate on the wire grid portion of the graphic.

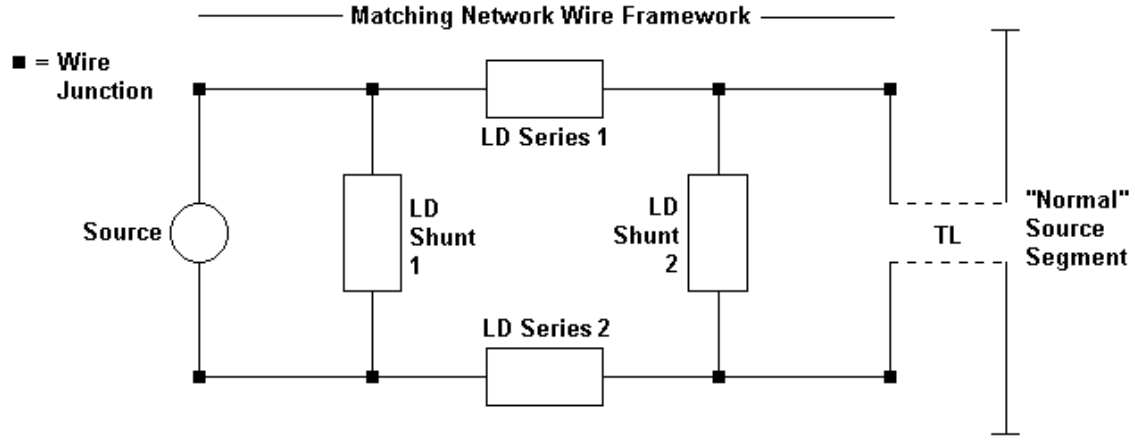

The Matching Network Assembly

Fig. 14-13

Because the network terminating components are shunt reactances, each end of the grid shows a bridge section of only wires connected on one end to a cross wire to which the TL is joined and at the other network end to a bridge wire to which we assign the source. Had we used a balanced Tee network, the "empty legs" of the parallel parts of the wire grid would hold

LD loads, and we would need one less crossing section for shunt or parallel components. An L-network would also be smaller, since we would need only a single pair of series components across from each other and a single shunt component.

The point is to make the wire-grid no larger than it has to be to hold the components and to establish the parallel connection to the grid of both the source (on one end) and the TL (on the other). As well, make the grid as small as possible. By using extremely thin lossless wire for the grid, we can shorten the length of the individual grid wires to the limits of NEC--about .001λ. Each wire in the grid--contrary to the graphic--whether crossing of parallel--should be exactly the same length.

We want the physical structure of the grid to be as far distant as feasible from the antenna wires in the model. However, we want to have the grid as electrically close as is feasible to the former source segment. The TL command allows us to achieve this goal. We may place the grid wires anywhere we wish in terms of the Cartesian coordinates that specify the physical structure. However, the electrical length of the transmission line depends upon the entry that we make for it, regardless of the location of the terminals of the line. We may make the line as short as a millimeter--or less. The shorter the length, the less critical the characteristic impedance of the line. The TL acts like a source in that it creates a series connection to a wire segment. Hence, we may specify only one segment for each end of the TL. (Note: we might have easily used the NT short circuit for the connection between the former source segment and the new wire grid. However, for the sake of not creating confusion, I have used a wholly non-NT system for this exercise. You may, of course, create as many variations as you find productive.)

Let's test the system by matching a near-resonant folded dipole for 28.5 MHz made from AWG #18 wire to a 50-Ω feedline. First, we begin with the folded dipole itself. Open model *14-5.nec*. Examine the structure of the model, since the next step in the process will add a significant number of geometry and control commands to this simple beginning.

```
GW 1 99 -2.4892 0. 0. 2.4892 0. 0. .0005119
GW 2 1 2.4892 0. 0. 2.4892 0. .0762 .0005119
GW 3 99 2.4892 0. .0762 -2.4892 0. .0762 .0005119
GW 4 1 -2.4892 0. .0762 -2.4892 0. 0. .0005119
GE 0
FR 0 1 0 0 28.5 1
GN -1
EX 0 1 50 00 1 0
```

Run the free-space model to obtain the usual performance data: 2.14 dBi gain, 286.705 + j0.651 Ω impedance, 1.00019 AGT. Obviously, we need make no adjustments to the reported gain or impedance. To match this impedance to the 50-Ω line, we may implement a balanced L network within the model. A utility program for L networks shows the required antenna-side shunt capacitor to be 42.4 pF (-j 131.7 Ω) and the required pair of series inductors to be 0.304 μH (+j 54.4 Ω).

We may now create the total model, including the creation of the wire grid for the network. We shall place the network components 1 m from the main folded dipole, but in many cases, more remote positions might be advisable. We shall use 25.4-mm (1") segments for each leg of the

wire grid using lossless wire throughout. A short I-mm, 290-Ω TL will replace the former source and connect the folded dipole to the grid. The source itself moves to the input side of the network. Open model *14-5a.nec* and examine the added structure.

```
GW 5 1 0. -.0254 1 0. .0254 1 .0005119
GW 6 1 0. .0254 1 .0254 .0254 1 .0005119
GW 7 1 .0254 -.0254 1 0. -.0254 1 .0005119
GW 8 1 .0254 -.0254 1 .0254 .0254 1 .0005119
GW 9 1 .0508 -.0254 1 .0254 -.0254 1 .0005119
GW 10 1 .0254 .0254 1 .0508 .0254 1 .0005119
GW 11 1 .0508 -.0254 1 .0508 .0254 1 .0005119
GE 0
TL 1 50 5 1 290 .001
LD 0 9 1 1 0. 2.6E-07 0.
LD 0 10 1 1 0. 2.6E-07 0.
LD 0 8 1 1 0. 0. 4.19E-11
FR 0 1 0 0 28.5 1
GN -1
EX 0 11 1 00 1 0
```

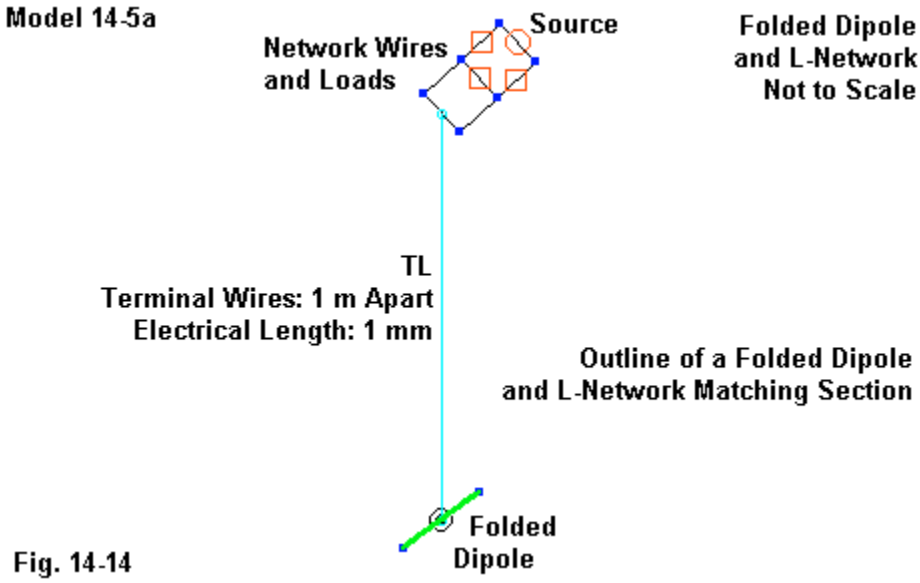

Fig. 14-14

Fig. 14-14 shows the final assembly, but not to scale. A full-size folded dipole would have reduced the network to a dot. Run the model to obtain the revised data: 2.23 dBi gain, 50.231 + j1.412 Ω impedance, 1.021 AGT, 0.089 AGT-dBi, 2.14 dBi adjusted gain. The AGT value tells us that the wire grid network does affect the reported performance values and the overall model adequacy. However, if used with care, it provides a means of obtaining frequency sweep data for the target antenna structure and its matching network.

The system does work--but within limits. Here are some of those limits based on the fact that the wires in the grid will interact with each other.

1. Wire size will make a difference to the results, although the affect tends to be small

compared to some other affects.

2. The TL characteristic impedance for the very short (1-mm) line can vary considerably without significant change in the new source impedance value. Values between 250 and 300 Ω occasioned no change in the reported impedance within the decimal limits shown here. As well, extending the line length from 1 mm to 25 mm also produced no source impedance change.

3. Grid wire length makes a large difference to the adjusted network values to achieve a near-50-Ω source impedance. Doubling the wire length in both directions required 0.24-μH coils and a 40.9-pF capacitor. A second doubling of wire lengths required 0.155-μH coils and a 39.8-pF capacitor. The progression is clear, and the smallest feasible wire grid yields results closest to calculated values.

4. The wire grid presses NEC limits. Hence, it is essential to obtain an Average Gain Test value and to correct the reported system gain accordingly

The sample model does not assign a value of Q to the inductors. However, you may incorporate that value in the LD0 commands applicable to the coils. The exercise models contain a series, 14-a through 14-d, using this same folded dipole, but employing 4 networks and their corresponding NT entries for comparison with Model 14-5a.

The NT method of incorporating networks into models lacks the ability to handle frequency sweeps, but it adds no structure geometry to the model. The wire-grid system just shown sacrifices some accuracy for the sake of those sweeps. Hence, neither is a perfect system for adding practical networks to models. Use each according to the goals of the modeling task.

There is one final practical lesson in the wire-grid network construction: although we have treated geometry and control commands individually to master their basic structures and entries, they actually form a matrix of possibilities for creative modeling when we use them in productive combinations.

Summing Up

Our foray into the NT or network command has been rudimentary, designed mainly to show the basic command structure and a small sample of practical applications. NT networks are 2-port short-circuit admittance parameter networks that require considerable external calculation in preparation for data entry. If you have prior experience with such networks, then this chapter may be superfluous in terms of getting ready to use it. If you have not yet employed such networks in modeling efforts, then it is likely the chapter will amount to a call for additional studies in other sources.

Like the TL command, to which it is related, the NT command calls for the specification of 2 wire segments to use as terminals for the network. Like transmission lines, the NT network is in series with any loads on the same segment and in parallel with any source on that segment. The data input requires entry of information for Y11, the short-circuit input admittance, Y22, the short-circuit output admittance, and Y12, the short-circuit transfer admittance. We began exploring

applications with the simplest cases: a short circuit to connect two section electrically with a physical connection, an alternative formulation of a load in parallel with a source, and a means of creating a current source from an EX0 voltage source.

We also explored a few basic networks--specifically L and PI networks--to examine the transformation of component information into command entry data. By using simplified calculations, we were nevertheless able to simulate matching circuits between the impedance at an element feedpoint and the presumed source impedance of the system. Since 2-port networks like the one used in the NT command can simulate virtually any passive complex of components, extended uses of the NT facility require the use of full calculations and a knowledge of the procedures for developing the admittance parameters.

Despite their versatility, NT commands are frequency specific. That is, they use values that derive from calculations for a selected frequency. Unlike LD0 and LD1 loads, they do not produce accurate information within a frequency sweep for frequencies other than the design frequency. However, there are methods of adapting the LD0 and LD1 loads to wire-grid structures to permit the incorporation of frequency-nimble networks into models. They have limitations stemming from the need to balance two needs: the goal of having minimum influence on the radiation from the model's structure and the necessity of remaining within basic wire-length vs. radius constraints. Nevertheless, the alternative techniques of incorporating networks within antenna models are serviceable in numerous applications.

Throughout this chapter, we have used the term "network" to indicate two different orders of electrical entities: the series-parallel combinations of components whose names emerge from the component configurations--L, PI, T, etc.--and the 2-port admittance parameter network that forms the basis of the NT command. The more we learn of the inter-relationships between these two orders of networks, the more creative our modeling may become in the future.

Part C
Special Outputs, Control Commands, and Techniques

1. The Control Command Input Entries or "Cards" introduced in this Part:

Command	*Command Name*	*Notes*
CP	Maximum Coupling	Conditions differ in NEC-2/-4
EK	Extended Thin Wire Kernel	NEC-2 only
EX*	Structure Excitation	continued
IS	Insulated Wire	NEC-4 only
JN	Junction Charge Distribution	NEC-4 only
KH	Interaction Approximation	NEC-2 only
LD*	Impedance Loading	continued
LE, LH	Near Electric or Magnetic Field along a line	NEC-4 only
NE, NH	Near Electric or Magnetic Field	
PL	Data Storage for Plotting	NEC-4 only
PQ	Charge Densities on Wire Segments	NEC-4 only
PS	Print Electrical Length of Segments	NEC-4 only
PT	Print Control for Current on Wires	Form differs between NEC-2/NEC-4
RP*	Radiation Pattern	continued
UM	Upper Medium Parameters	NEC-4 only
VC	Voltage-Source End Caps	NEC-4 only

A star (*) indicate that in this Part, the command will receive the promised further coverage.

2. The Plan:

As we move into the final set of chapters in this volume, we shall grow ever more aware that we cannot easily exhaust the ways in which we can glean useful information from the NEC output report. Even the seemingly simple entry called the "Power Budget" provides important data by comparing the power supplied to the antenna by a source with the power radiated by the structure as a function of all resistive losses within the antenna. The result is the power efficiency. However, we shall also meet another measure--the radiation efficiency--a figure that will account for losses due to the ground as well as losses within the structure itself.

Next, we shall look at a pair of seemingly disparate commands: LD5 (material loading) and IS (insulated sheath). Only LD5 is available in NEC-2. The insulated sheath command is available only in NEC-4. We shall explore a method of simulating sheathed wires through another LD command within NEC-2.

We did not exhaust the data that we may obtain from the radiation pattern (RP) command with requests for far-field patterns. For example, we may also request ground-wave patterns with all field components. As well, we may perform post-run operations to obtain additional information, such as left-hand and right-hand circular gain values.

The NEC core contains commands for obtaining near-field data. NEC-2 and NEC-4 contain standard electrical and magnetic near-field data in the NE and NH commands, but NEC-4 adds another pair of commands: LE and LH. These requests analyze near fields along a projected line, and one may even add to the line and change its direction in a multiple-request model.

All of the output requests that we have so far examined may use a voltage source (EX0). NEC is also capable of providing receive data in the form of segment currents and gain values. The technique requires the use of incident plane wave sources, either linear or elliptical (EX1 through EX3), combined with requests to print current data in specific forms via the PT command. NEC-4 adds further output options to the version of the PT command used in NEC-2.

Each core contains a number of special purpose commands, some in common and some that are core-specific. NEC-2 contains two unique commands that reflect its fundamental algorithms and the state of computer speeds when it emerged. EK invokes an extended thin wire kernel command to yield more accurate results when the segment-length-to-radius ratio becomes small. KH invokes a timesaving approximation algorithm when elements of the geometry are separated by more than a specified distance. In both cores, you may request a printout of the charge density for the wire segments (PQ) or the maximum coupling between any pair of specific segments in a model (CP). NEC-4 includes a command to include "end caps" (VC) on segments holding voltage sources and impedance loads, which may increase accuracy when the segment-length-to-radius ratio is small. As well, NEC-4 offers the JN command to switch between its normal method of determining the distribution of charge in basis functions and the method used in NEC-2. Finally, NEC-4 includes the PS command to print out the electrical length of wire segments, useful for wires within a lossy or insulating medium, for example, when using the UM or upper medium command.

The last chapter is a brief tutorial on how to model with equations using the NEC cores. The NEC input file cannot recognize equations. However, the NSI insert, NEC-Win Plus, contains full spreadsheet abilities to create models using variables and assigning values to those variables via constants or equations. The results are directly transferable to the basic NEC program as a set of resultant numerical entries for a core run. As well, the equation-based models can be saved within the program for future use and modification.

The array of commands, techniques, and models that we survey in this final set of exercises does not exhaust the capabilities of NEC. However, they carry us well beyond the limitations of entry-level programs, expanding both what we may model and the data that we may derive from models. Further steps depend upon the creativity of the modeler with respect to both the input model and the output data, as well as his or her deeper understanding of the manner in which the NEC cores perform their calculations.

15.
Power Information: Power Efficiency vs. Radiation Efficiency

***Objectives**: In these exercises, you will become very familiar with what the power budget output report can and cannot tell us about antenna performance. In the process, you will learn how to distinguish power efficiency from radiation efficiency. You will learn how to obtain a radiation efficiency report by using the RP command to derive something other than a radiation pattern.*

This chapter does not focus upon any single control command. Instead, it will examine parts of the NEC output report. Initially, we shall look at the power budget to gain some familiarity with its parts: input power, structure losses, network losses, radiated power, and power efficiency. As we wander through these elements in the report, we shall have the opportunity to review and use a number of control commands that we explored in Part B. Some of the key ones will by the LD command, using several of its options, the NT command, and the EX0 command.

We shall be alert to what levels of power and efficiency loss result from various aspects of a model, especially lumped or spot loads, material loading, and networks. We shall also examine the effects of wire radius or surface area on power losses. We can even use frequency scaling of models to demonstrate the consequences of skin effect on models.

We shall also distinguish power efficiency from radiation efficiency. NEC figures the former directly in the power budget report. However, we must set up the RP0 command in a special way to arrive at a report value that we can translate into a value of radiation efficiency. By examining a series of simple models, we can gauge how well NEC tracks actual antenna performance, at least in broad outlines.

The power budget qualifies as a special output only because we so often ignore it on the way to gathering information on gain, beamwidth, bandwidth, and source impedance. Few modelers ever try to obtain a radiation efficiency value, even though they regularly wonder about that aspect of antenna performance. By focusing our attention on these matters in a concentrated set of exercises, we may use these NEC resources more regularly and more effectively.

The Power Budget and Power Efficiency

The power budget portion of the NEC output report seems to attract only limited attention by most modelers. Once we have obtained information on the radiation pattern and the source impedance, all other available data seems somewhat irrelevant. Little could be further from the truth. Current values can give us antenna performance insights that otherwise might elude us. Frequency sweep data provides more than one measure of the antenna's operating bandwidth. We have also examined a number of special purpose reports that supply important information. The power budget is one of those reports, once we learn to use it effectively.

One of the reasons why the power budget evades regular use is that it has no single control command that affects its variations. Rather, it is a set of information that results from the use of numerous other commands. As we acclimate ourselves to the report, we shall have the opportunity to review a number of the control commands that we met in the preceding part of this volume. By using these commands in a series of models, we can not only uncover the structure of the power budget, but as well we can review many of the control commands and see how they integrate to yield the overall performance of an antenna.

The power budget itself is a model of simplicity.

```
- - - POWER BUDGET - - -

INPUT POWER   = 2.1582E+01 WATTS
RADIATED POWER= 1.9937E+01 WATTS
STRUCTURE LOSS= 1.5818E+00 WATTS
NETWORK LOSS  = 6.2787E-02 WATTS
EFFICIENCY    =  92.38 PERCENT
```

A fully packed power budget contains 5 entries. The input power is a function of the values that we set into the EX0 command and the impedance on the source segment. We can find the relevant figures within the antenna input parameters, as in this sample from the same model.

```
- - - ANTENNA INPUT PARAMETERS - - -

   TAG   SEG.     VOLTAGE (VOLTS)          CURRENT (AMPS)
   NO.   NO.     REAL         IMAG.       REAL         IMAG.
     2    22  4.31636E+01 3.72538E+01 5.71420E-01 4.96555E-01
           IMPEDANCE (OHMS)         ADMITTANCE (MHOS)          POWER
          REAL          IMAG.       REAL         IMAG.        (WATTS)
          7.53167E+01 -2.53931E-01 1.32771E-02 4.47639E-05 2.15816E+01
```

Because voltage and current are peak values, the power is 0.5 (I^2R) or 0.5(E^2/R). Essentially, you must obtain the voltage or current magnitude by the vector sum of the real and imaginary components and then use only the resistive portion of the impedance. The radiated power is what is left after subtracting all losses within the antenna model itself--without regard for any losses occasioned by the ground or the medium through which the radiated signal passes. Efficiency is simply the ratio of radiated power to input power, expressed as a percentage.

The power budget divides losses into two types: structure loss and network loss. A simple series of models will show us from what parts of a model the losses come and how they accumulate. As a baseline model, let's begin with one that has no losses. We shall use a shortened free-space dipole. At the center of each dipole leg, we shall insert an inductive load sized to bring the dipole to near resonance. Both the loads and the wire will have no resistance. Open model *15-1.nec*.

```
GW 1 21 0 -.15 0 0 .15 0 .001
GE
FR 0 1 0 0 299.7925 1
EX 0 1 11 00 1 0
LD 4 1 5 5 0 364
LD 4 1 17 17 0 364
```

The portions of the model reproduced in the text establish the key "no-loss" features of the model. **Fig. 15-1** shows the outline of the small assembly. The figure also provides a reference pattern that will hold good for all versions of the model that we shall run. The key to knowing that the pattern shape applies to the variations will be the half-power beamwidth, indicated by the lines forming a wedge in one lobe.

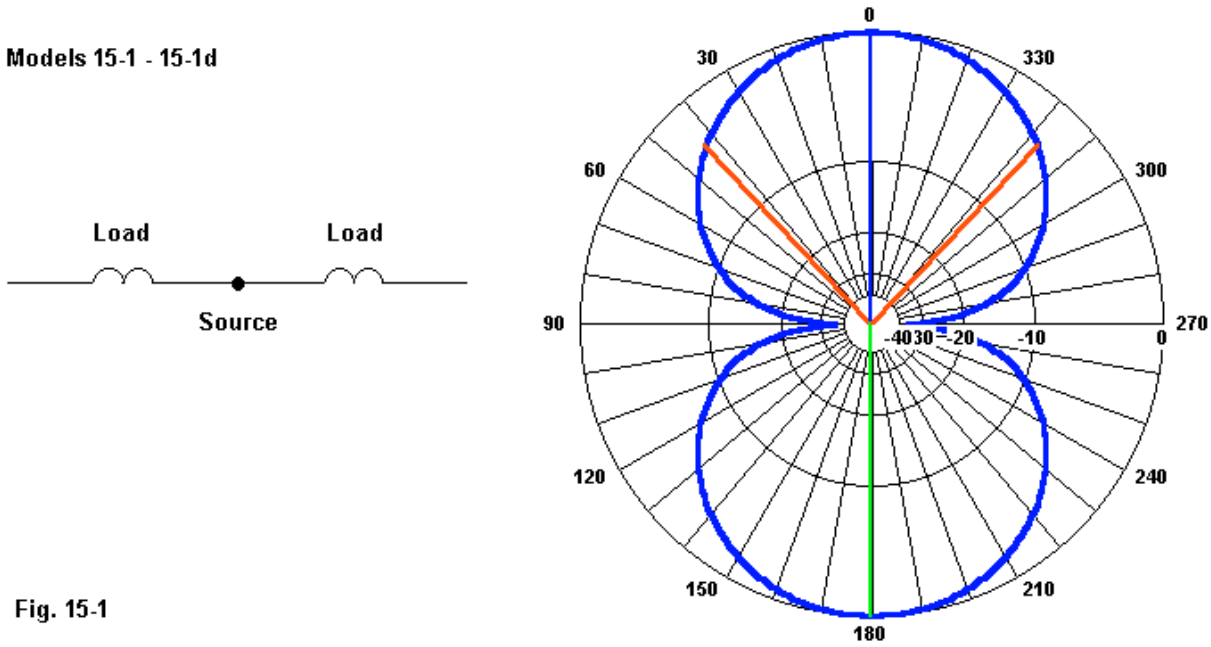

Fig. 15-1

For each version of this assembly, we shall keep a 1-line table of values. For the lossless model, we obtain the following results.

Impedance R +/- jX Ω	Gain dBi	Beam-width deg	Input Power watts	Structure Losses watts	Network Losses watts	Radiated Power watts	Efficiency %
39.876-j0.339	1.93	86	1.2538E-2	0	0	1.2538E-2	100.00

The impedance, gain, and beamwidth come from the usual report sources, while the remaining figures replicate the data in the power budget.

```
- - - POWER BUDGET - - -

INPUT POWER   = 1.2538E-02 WATTS
RADIATED POWER= 1.2538E-02 WATTS
STRUCTURE LOSS= 0.0000E+00 WATTS
NETWORK LOSS  = 0.0000E+00 WATTS
EFFICIENCY    = 100.00 PERCENT
```

Now let's begin adding losses. The first step is to open model *15-1a.nec*, where we add a wire material load (LD5) with the value of copper (5.8E7).

```
LD 5 0 0 0 5.8e7
```

All other parts of the model remain unchanged. If we run the model, we end up with this table.

Impedance R +/- jX Ω	Gain dBi	Beam-width deg	Input Power watts	Structure Losses watts	Network Losses watts	Radiated Power watts	Efficiency %
40.027-j0.202	1.91	86	1.2491E-2	4.4945E-5	0	1.2446E-2	99.64

LD5 losses appear in the structure-loss column and are very small, given the high conductivity of copper. However, the loss is measurable as a loss and affects both the antenna's efficiency and gain. As well, we can see the effects of using a material with losses in the increase in the source resistance. A lossy material also yields a slight velocity factor to the wire, electrically lengthening it relative to its physical length. The effect is numerically noticeable, but of no practical significance whatsoever with the radius of the conductor used here. The input power has a new value, relative to model 15-1, because the source impedance has changed.

Next, let's remove the LD5 command and return to a perfect conductor. However, let's give the inductive mid-element loads a finite Q: 200. Now open model *15-1b*, and examine the LD4 entries.

```
LD 4 1 5 5 1.82 364
LD 4 1 17 17 1.82 364
```

Each LD4 load now consists of 1.82 Ω resistance in series with the required inductive reactance of j364 Ω to bring the element to near resonance. Our table now has new values.

Impedance R +/- jX Ω	Gain dBi	Beam-width deg	Input Power watts	Structure Losses watts	Network Losses watts	Radiated Power watts	Efficiency %
42.888-j0.550	1.61	86	1.1656E-2	8.2056E-4	0	1.0836E-2	92.96

The mid-element loads with a Q of 200 have had a far more profound affect on the source impedance and the gain than the material load. The structure losses, which include all losses due to LD entries, are 18 times the losses due to using copper wire. Hence, the overall efficiency drops to just under 93%.

Next, let's employ both copper wire and inductors with a Q of 200. The LD entries of model *15-1c.nec* have the following form.

```
LD 5 0 0 0 5.8e7
LD 4 1 5 5 1.82 364
LD 4 1 17 17 1.82 364
```

Before we examine the resulting table of values from the various parts of the output report, including the power budget, let's enter a caution. Intuitively, we might guess that the values that we find would be the sum of the values for the individual losses. As a first-order approximation, this maneuver is generally satisfactory. However, the numbers will not add up so simply, since the performance of the antenna is as much a function of the current distribution along its total length as it is a set of report numbers. Hence, we can expect to see a small bit of variance.

Impedance R +/- jX Ω	Gain dBi	Beam-width deg	Input Power watts	Structure Losses watts	Network Losses watts	Radiated Power watts	Efficiency %
43.039-j0.414	1.60	86	1.1616E-2	8.5392E-4	0	1.0762E-2	92.65

The resistance on the segments containing the loads is the series combination of the inductor resistance (LD4) and the copper resistance (LD5). The structure impedance portion of the report indicates this fact with a note:

```
NOTE, SOME OF THE ABOVE SEGMENTS HAVE BEEN LOADED TWICE - IMPEDANCES
ADDED
```

We have used an LD4 (R-X) load for the mid-element inductors. We might have as easily selected an LD0 series R-L-C load. At 299.7925 MHz, the required inductance for a reactance of 364 Ω is 1.9324E-7 H. Open model *15-1d.nec* and examine the new LD0 entries.

```
LD 5 0 0 0 5.8e7
LD 0 1 5 5 1.82 1.9324e-7 0
LD 0 1 17 17 1.82 1.9324e-7 0
```

For this revision, we have retained the copper material conductivity entry so that we may directly compare the new table with the one immediately preceding it.

Impedance R +/- jX Ω	Gain dBi	Beam-width deg	Input Power watts	Structure Losses watts	Network Losses watts	Radiated Power watts	Efficiency %
43.039-j0.419	1.60	86	1.1616E-2	8.5392E-4	0	1.0762E-2	92.65

As expected, there are no differences between the tables (except for a 0.005-Ω change in the source reactance due to not carrying out the values to enough digits). However, for some tasks, the use of LD entries using inductance and capacitance values makes the model frequency nimble, that is, amenable to accurate output reports when calling for multiple frequencies in the FR command. Let's revise models 15-1c and 15-1d to see what happens. Open models *15-1c1.nec* and *15-1d1.nec*. Each model is like its counterpart except for the FR command.

```
FR 0 21 0 0 290 1
```

The frequency request now includes 21 steps to give us a linear sweep between 290 and 310 MHz. Run both models and then compare the results. Above and below 300 MHz, we see a growing divergence in the performance reports, no matter which portion of the output report we examine (except for the segmentation report). In fact, model 15-1c uses the same reactance at all 21 frequencies: 364 Ω. However, for an inductance of 1.9324E-7 H, the reactance at 290 MHz will be 352.1 Ω and at 310 MHz, the reactance will be 376.4 Ω. One of the most graphic ways to illustrate the effects of the gradually changing reactance is to compare SWR curves for the two models, as in **Fig. 15-2**. Failure to change the reactance in the inductors with changes in the frequency produces impedance reports that are far enough off the mark to give a visibly erroneous and overly optimistic impression of the antenna's operating bandwidth. The line labeled LD0 is closer to reality. The disparity approaches a 50% over-estimation of bandwidth

using LD4 loads.

Fig. 15-2

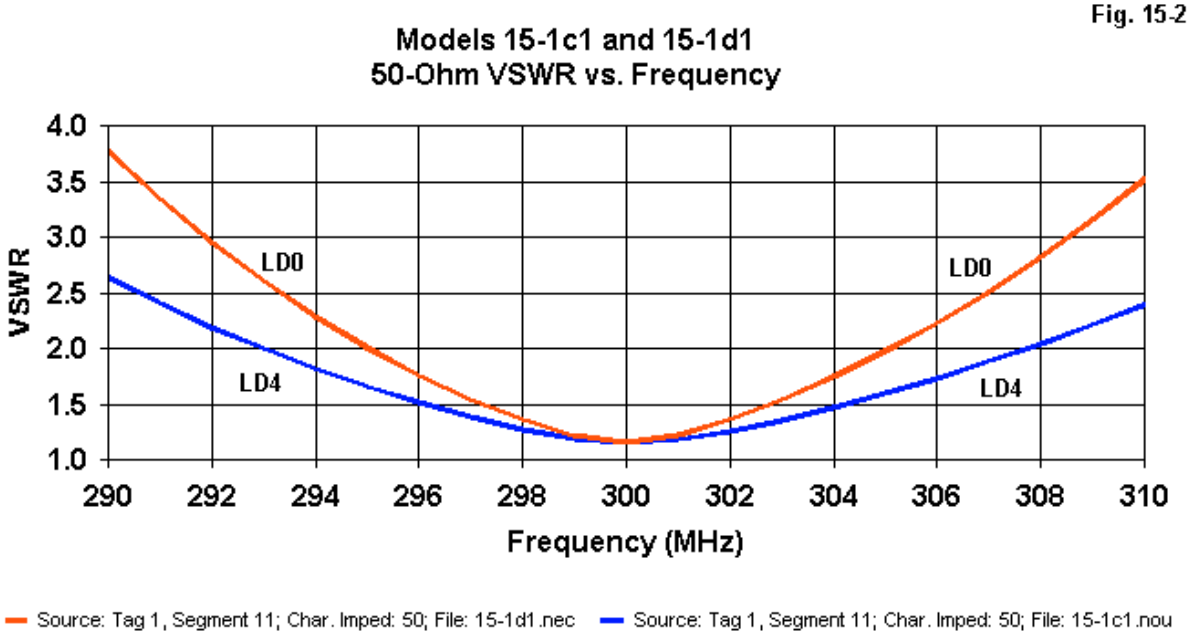

None of the power budgets that we have examined on the way to filling in our tables has shown any value other than zero in the network loss column. The reason is simple: we have not used an NT command in any of the models. Model 15-1d contains both LD5 and LD0 commands to produce a source impedance of 43.039 - j0.419 Ω. Let's use an external utility program to calculate an L network to match the impedance to a presumed 75-Ω feedline. Then, we may calculate the values for an NT 2-port network to go between the former feedpoint on GW1 and a new feedpoint on a new wire: GW2. **Fig. 15-3** shows the general outline of the new model and the down-converting L circuit that uses a series inductor and a shunt capacitor on the source side of the network. We may use the calculation short cuts that we learned in the preceding chapter to develop usable values for the NT command.

Model 15-2

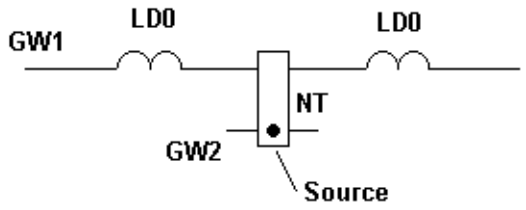

Antenna Model Outline

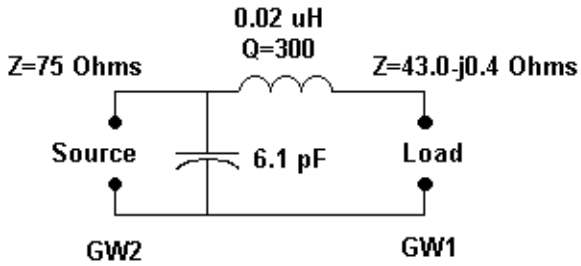

Impedance-Matching Network

Fig. 15-3

First, we obtain the susceptance of the individual components. The 6.1-pF capacitor gives us

1.1490E-2 S, while the 0.020-µH yields -2.6544E-2 S. Since the inductor has a Q of 300, the simplified calculation of coil conductance is 8.8481E-5 S.

We may next plug these values into the procedural formulas used in the exercises in Chapter 14, remembering that the shunt capacitor is the input-side parallel component.

Parameter	Real Component		Imaginary Component	
Y11	Gp1+Gs	8.8481E-5	Bs + Bp1	-1.5054E-2
Y12	-Gs	-8.8481E-5	-Bs	2.6544E-2
Y22	Gp2+Gs	8.8481E-5	Bs + Bp2	-2.6544E-2

Open model *15-2.nec* and examine the NT entry.

```
NT 2 1 1 11 8.8481e-5 -1.5054e-2 -8.8481e-5 2.6544e-2 8.8481e-5 -2.6544e-2
```

Run the model and obtain the same types of reports that we have used throughout to make up a performance and power budget table.

Impedance R +/- jX Ω	Gain dBi	Beam-width deg	Input Power watts	Structure Losses watts	Network Losses watts	Radiated Power watts	Efficiency %
75.317-j0.254	1.58	86	6.6386E-3	4.8658E-4	1.9314E-5	6.1327E-3	92.38

There are several directly comparable numbers, relative to the results we obtained in model 15-1d. The gain has dropped a mere 0.02 dB. (The beamwidth has remained a constant 86° for all of the models in these series, telling us that only field strength has changed, but the basic operation of the antenna has not been altered by the addition of various resistive loads.) The efficiency has dropped a further quarter of a percentage point, which seems reasonable in light of the very small network loss.

However, without some further manipulation of numbers, we cannot compare the actual entries in the power budget categories between this model and the pre-network version. Because the source impedance has changed, the constant 1-volt (peak) excitation voltage will not yield inherently comparable power values. In Chapter 10, we examined ways of altering the excitation voltage to arrive at values that we more directly compare.

For example, we may set a specific power level simply by finding the voltage level that yields that power level as the input power in the power budget. The square root of the new power divided by the old power gives us a multiplier for the excitation voltage. Suppose that we wish to use a 100-watt level in order to read out the power losses as direct percentages of the input power. The old power (model 15-2) is 6.6386E-3 watts. 100 divided by the figure is 1.5063E4, and its square root is 1.2273E2. Let's use that value in model *15-2a.nec* and examine the resulting EX0 command.

```
EX 0 2 1 00 1.2273e2  0.00000
```

Run the model and create a new table. When comparing the values to those in the preceding table, notice especially what remains constant.

Impedance R +/- jX Ω	Gain dBi	Beam-width deg	Input Power watts	Structure Losses watts	Network Losses watts	Radiated Power watts	Efficiency %
75.317-j0.254	1.58	86	9.9994E1	7.3292E0	2.9091E-1	9.2374E2	92.38

Notice that the source impedance, the gain, the beamwidth, and the efficiency values have not changed. However, we can now directly read that the structure losses amount to 7.33% of the input power, while network losses are only 0.29% of the input power. Of the original 100 watts, the antenna radiates 92.37 watts (allowing always for a 1-digit ambiguity in the least significant digit).

While we are gathering data for the table, let's divert ourselves and examine the current on the center of the short loaded dipole, that is, GW1, segment 11.

```
SEG.  TAG          - - - CURRENT (AMPS) - - -
 NO.  NO.   REAL         IMAG.        MAG.         PHASE
 11    1  1.6295E+00 -1.4064E+00  2.1525E+00  -40.797
```

To produce a current magnitude of 1.0 A on this center segment, we need to lower the excitation voltage. Since the impedance will not change, we can use the ratio of the desired current to the existing current to arrive at a new multiplier for the excitation voltage. The new current will be 0.46458 of the old value. Since the existing EX0 voltage is 1.2273E2, the replacement voltage will be 5.7017E1 volts.

Suppose that we also wish the phase angle on this segment to be 0°. The present phase angle is -40.797°. To move it toward zero, we must move the source voltage phase angle by an equal amount. Hence, we need a phase angle of 40.797° in the EX0 command.

The NSI assistance screens will permit you to enter the excitation voltage either as a magnitude and phase angle or as the real and imaginary components of the excitation voltage. However, manually entering the values into the EX0 command line requires the real and imaginary values. Of course, the real component is the magnitude times the cosine of the phase angle, while the imaginary component is the magnitude times the sine of the phase angle. So if we enter these values into the model, we obtain the EX0 entry of model *15-2b.nec*.

```
EX 0 2 1 00 43.16356 37.25380
```

The resulting table is interesting, but is not our primary target in this exercise. The key change lies in the current for segment 11.

Impedance R +/- jX Ω	Gain dBi	Beam-width deg	Input Power watts	Structure Losses watts	Network Losses watts	Radiated Power watts	Efficiency %
75.317-j0.254	1.58	86	2.1582E1	1.5818E0	6.2787E-2	1.9937E1	92.38

```
SEG.  TAG          - - - CURRENT (AMPS) - - -
 NO.  NO.   REAL         IMAG.        MAG.         PHASE
 11    1  9.9999E-01  2.2635E-07  9.9999E-01    0.000
```

The revised excitation allows us to produce with great ease tables and graphs of the current magnitude on each segment of the main element of the model. The Y-axis gives us an easy way to read the relative current at any point along the element, as in **Fig. 15-4**.

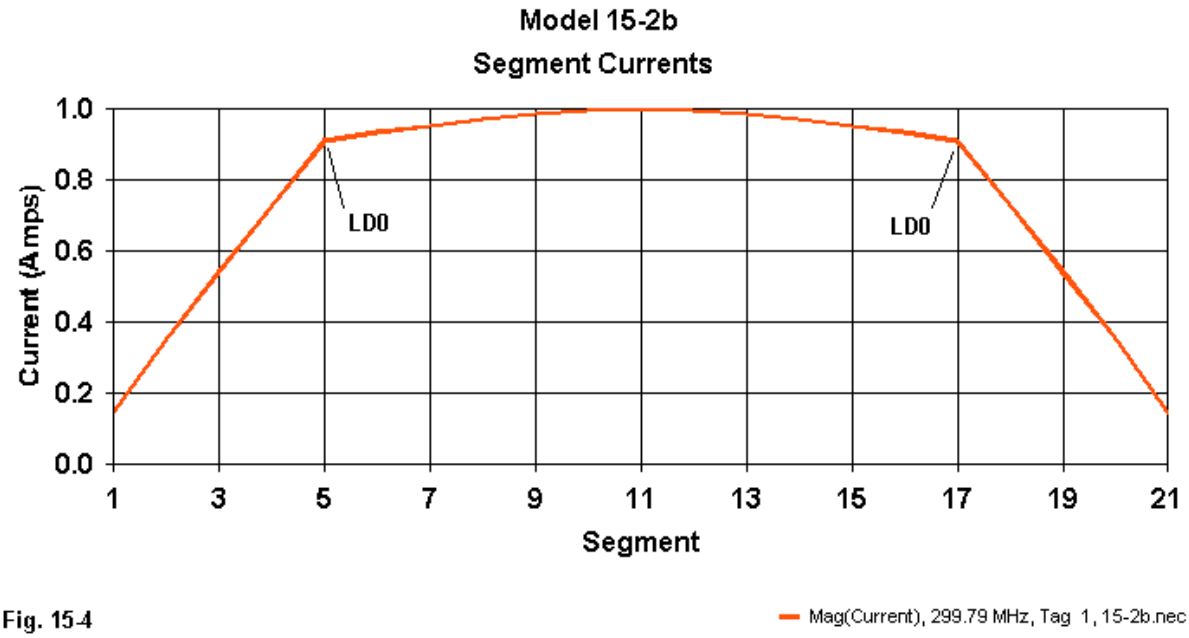

Fig. 15-4

Using the power budget information in concert with other NEC output data gives us considerable flexibility in generating output reports and graphics that permit easy interpretation of the results by those who have less than a solid familiarity with NEC processes. Data that we cannot clearly communicate is very often data that is lost.

So far, we have looked at a series of models in which all structure losses appear on the element containing the voltage source. It is not necessary for loss factors to appear on a driven element if the element on which they do appear plays a significant role in the interaction matrix. Consider a 22-element Yagi. Open model *15-3.nec*, outlined with an E-plane pattern in **Fig. 15-5**. The array is for the center of the amateur 2-meter band (146 MHz) and uses 4.75-mm (3/16") diameter elements. However, the initial model has no structure losses. Run the model and build one of our standard tables.

```
CM 22-el OWA Yagi 146 MHz
CE
GW 1 21 -0.58674 -0.04826 -0.6096 0.58674 -0.04826 -0.6096 0.0023813
GW 2 21 -0.58674 -0.04826 0.6096 0.58674 -0.04826 0.6096 0.0023813
GW 3 21 -0.5194301 0 0 0.5194301 0 0 0.0023813
GW 4 21 -0.50165 0.2233164 0 0.50165 0.2233164 0 0.0023813
GW 5 21 -0.4699135 0.3421513 0 0.4699135 0.3421513 0 0.0023813
GW 6 21 -0.4613642 0.6446176 0 0.4613642 0.6446176 0 0.0023813
GW 7 21 -0.4622487 1.034345 0 0.4622487 1.034345 0 0.0023813
GW 8 21 -0.4598902 1.559092 0 0.4598902 1.559092 0 0.0023813
GW 9 21 -0.44704 2.19682 0 0.44704 2.19682 0 0.0023813
GW 10 21 -0.43561 2.9464 0 0.43561 2.9464 0 0.0023813
```

```
GW 11 21 -0.42672 3.72364 0 0.42672 3.72364 0 0.0023813
GW 12 21 -0.41783 4.53136 0 0.41783 4.53136 0 0.0023813
GW 13 21 -0.40894 5.334 0 0.40894 5.334 0 0.0023813
GW 14 21 -0.40894 6.1722 0 0.40894 6.1722 0 0.0023813
GW 15 21 -0.39116 7.0104 0 0.39116 7.0104 0 0.0023813
GW 16 21 -0.38608 7.8486 0 0.38608 7.8486 0 0.0023813
GW 17 21 -0.381 8.6868 0 0.381 8.6868 0 0.0023813
GW 18 21 -0.37084 9.525 0 0.37084 9.525 0 0.0023813
GW 19 21 -0.36576 10.3632 0 0.36576 10.3632 0 0.0023813
GW 20 21 -0.36068 11.2014 0 0.36068 11.2014 0 0.0023813
GW 21 21 -0.36068 12.065 0 0.36068 12.065 0 0.0023813
GW 22 21 -0.34798 12.7508 0 0.34798 12.7508 0 0.0023813
GS 0 0 1
GE 0
EX 0 4 11 0 1. 0.
FR 0 1 0 0 146 1
RP 0 1 361 1000 90 0 1 1
EN
```

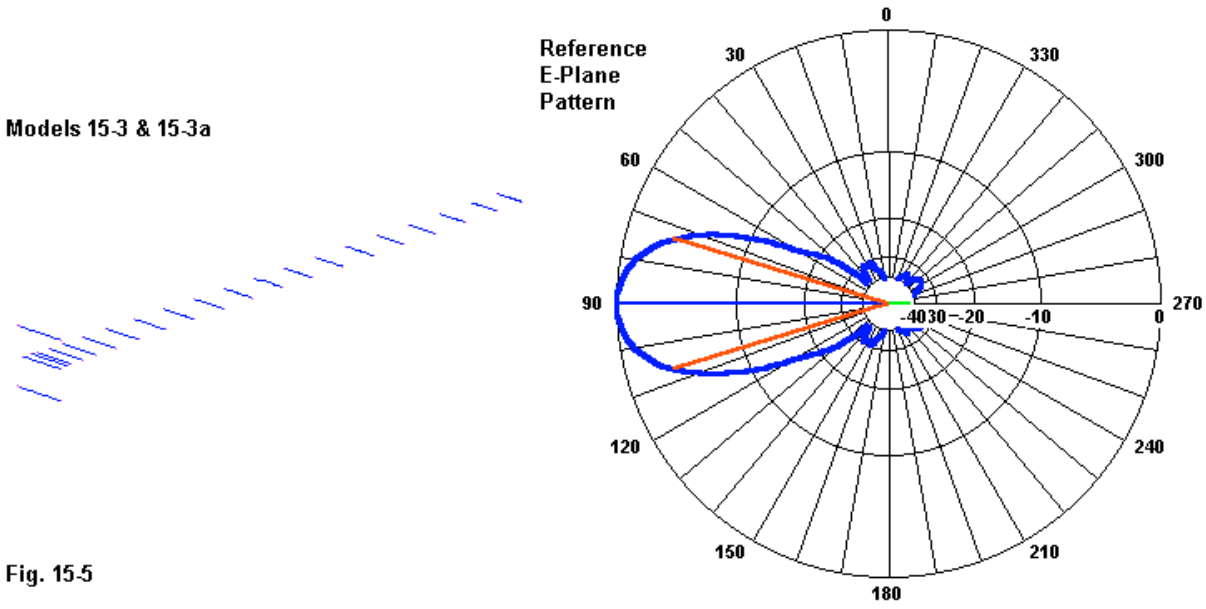

Fig. 15-5

Impedance R +/- jX Ω	Gain dBi	Beam-width deg	Input Power watts	Structure Losses watts	Network Losses watts	Radiated Power watts	Efficiency %
48.354+j6.060	15.80	34	1.0180E-2	0	0	1.0180E-2	100.00

Next, add an LD line, making all of the elements aluminum, using a conductivity value of 2.5E7. The result will by model *15-3a.nec*. Once more build a table.

Impedance R +/- jX Ω	Gain dBi	Beam-width deg	Input Power watts	Structure Losses watts	Network Losses watts	Radiated Power watts	Efficiency %
48.387+j6.057	15.71	34	1.0174E-2	2.1402E-4	0	9.9600E-3	97.90

For a single element, the loss of efficiency due to a moderately good conductor material is roughly 0.5%. The value shown by the Yagi (97.9%) shows the effect of having material losses in every element, although the losses are far lower than 0.5% per element. Of course, except for the driver and first director elements, the remaining elements exhibit lower current magnitudes. As well, the gain loss between the perfect and lossy element versions of the array are comparable to the efficiency loss: roughly 4 to 5 times the loss we saw for a single element, even though the array has 22 elements total. The source impedance change when moving from a lossless to a lossy element is only about the amount that we expect in a single-element array. Parasitic element arrays, then, do increase losses, because every interactive element operates with less than a lossless environment. However, those losses do not add in any linear fashion.

In the short exercise on parasitic arrays we neglected to account for the ratio of the radius of the element to a wavelength. In fact, the 146-MHz array was not too far off the ratio used in the shortened dipole: 0.001λ for the dipole and 0.000974λ used in the Yagi. The element radius is a measure of the element surface area for unit of length, since the wire circumference is 2πr. We can develop a sense for what surface area means to power losses with any material by running a series of sample dipoles that increase their radius by a fixed multiplier.

We shall run our samples by increasing the wire radius by a factor of 10 between runs, as indicated by **Fig. 15-6**. For any step (a) in the process, the next step (a+1) will use a radius that is 10 times the value used in step a. For each step, we shall change the dipole length to approach resonance for a version of the antenna with no losses. Each step will have 2 parts: one sampling the antenna with no losses and the other sampling it with the conductivity of aluminum (2.5E7). All of the models in the series are at 299.7925 MHz.

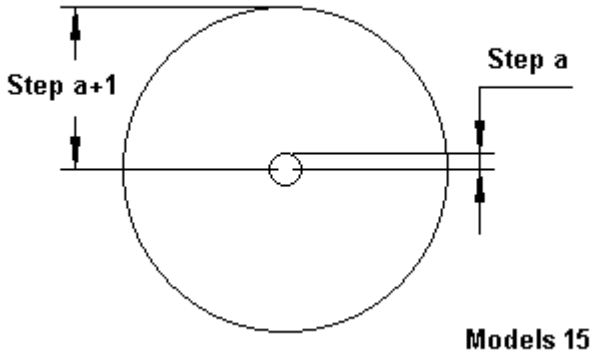

Fig. 15-6 Models 15-4 - 15-4c

Successively open models *15-4.nec* and *15-4-1.nec*. The models use the same wire length and represent the thinnest wire in the series: 0.00001-m radius. The first of the pair is lossless, while the second is aluminum. After extracting data for gain, source impedance, and power efficiency for both antennas, move on to the remaining models in the series: *15-4a.nec* through *15-4c1.nec* and extract similar information. The models use successively fatter wires: 0.0001 m, 0.001 m, and 0.01 m.

Once you have accumulated the information on each model, you may create a table to display and compare the resulting numbers.

Model	Wire Radius m	Material	Source Impedance R +/- jX Ω	Gain dBi	Length m	Power Efficiency %
15-4	0.00001	---	72.291+j0.179	2.13	0.488	100
15-4-1		aluminum	110.288+j20.036	0.34	"	66.29
15-4a	0.0001	---	72.097+j0.410	2.13	0.484	100
15-4a-1		aluminum	75.059+j2.976	1.96	"	96.25
15-4b	0.001	---	71.760+j0.116	2.12	0.475	100
15-4b-1		aluminum	72.056+k0.364	2.11	"	99.62
15-4c	0.01	---	73.094+0.105	2.13	0.4492	100
15-4c-1		aluminum	73.128+j0.126	2.12	"	99.96

Note that all of the lossless versions of the dipole yield the same gain and efficiency. They also show very similar source impedance values. However, the aluminum versions of the dipoles show rising efficiency levels as we increase the surface area of the conductor. As the efficiency rises, so too does the gain. As the gain goes up, the source impedance decreases toward the level of the counterpart lossless version of the model.

You may repeat this type of experiment for any frequency using any range of element diameters that might be relevant to a task. You will discover that there is a wire diameter (or radius) beyond which the gain does not increase and the source impedance does not decrease to any degree that may be significant to the task. Since the curve is smooth, although not linear, the precise point at which you judge that further radius increases are unwarranted will be task specific.

The effect of surface area on the performance of an antenna element has two facets: the surface area itself and the consequences of skin effect. NEC, of course, incorporates skin effect into its calculations. Skin effect is the increasing RF resistance of a wire of any fixed material with increasing frequency due to the decreasing depth into the wire at which current flows. The skin depth decrease is proportional to the square root of the frequency increase. Hence, the effect is not a straight-line frequency function.

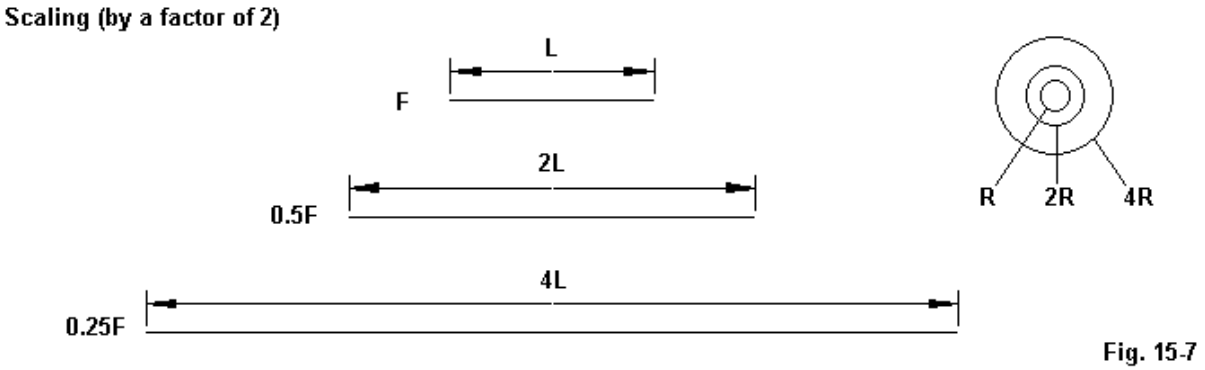

Fig. 15-7

One way to sample the effect with antenna models is to scale a model by the inverse ratio of the frequencies, as suggested by **Fig. 15-7**. The figure uses 2 steps, each scaling by a factor of two (for ease of illustration). As the frequency decreases by the inverse of the scaling factor, both the element length and the radius increase by the factor itself. Since antenna performance depends

upon the inter-relationship of the element length and the element radius, we must scale both factors to achieve a correctly scaled new model. If the antenna used multiple elements, we would also scale the distance separating them.

For our exercise, we shall begin with a near-resonant lossless dipole. Open model *15-5.nec*. Then examine models *15-5a.nec* and *15-5b.nec*. Only the scaled entries for each appear below.

Model 15-5:
```
GW 1 11 0 -0.2375 0 0 0.2375 0 .001
GE
FR 0 1 0 0 299.7925 1
```
Model 15-5a:
```
GW 1 11 0 -2.375 0 0 2.375 0 .01
GE
FR 0 1 0 0 29.97925 1
```
Model 15-5b
```
GW 1 11 0 -23.75 0 0 23.75 0 .1
GE
FR 0 1 0 0 2.997925 1
```

Run each model. The power budget will show 100% efficiency, a gain of 2.12 dBi, and a source impedance of 71.760+j0.116 Ω. Our scaling has been accurate, and the perfect conductor selection is truly lossless.

To each model, let's add just 1 new entry: an LD5 specification of aluminum (2.5E7).

```
LD 5 0 0 0 2.5e7
```

Open models *15-5-1.nec*, *15-5a-1.nec*, and *15-5b-1.nec*. Each model represents its associated model with the addition of a material conductivity for the wire. With this addition, we can sample the effects of the changing skin depth. You may create a table to record the results of running each model.

Model	Frequency MHz	Gain dBi	Source Impedance R +/- jX Ω	Efficiency %
15-5-1	299.7925	2.11	72.056 + j0.134	99.62
15-5a-1	29.79725	2.12	71.854 + j0.194	99.88
15-5b-1	2.979725	2.12	71.790 + j0.141	99.96

As we decrease the frequency, the skin depth increases and the added resistance due to skin effect decreases. As a result, the efficiency increases as the frequency decreases. At the highest frequency, the efficiency has decreased to a level that shows up in the last digit of the gain value. In addition, as we decrease frequency, the source impedance recorded for the aluminum models approaches the value shown by all 3 lossless models.

There are innumerable other exercises that you can create to grow even more familiar with the power budget output report and the relationship of its numbers to other parts of the NEC output data. However, before we leave the matter of power efficiency, there is another type of efficiency that we need to investigate--radiation efficiency.

Power Efficiency vs. Radiation Efficiency

Power efficiency, as reported in the power budget section of the NEC output report, gives us a measure of the effect of structure and network losses on the power radiated by the antenna. However, the power efficiency does not give us a sense of how efficiently an antenna operates within its environment. Antenna models presume (in the absence of a second ground medium) a flat or level ground as far as the eye can see and beyond, and the only objects taken into account are those that appear within the model structure geometry. However, even with these limitations, we need a different measure to determine the radiation efficiency of an antenna. In some circumstances, these antenna environment limitations may also become an advantage, since one may compare antenna radiation efficiencies under conditions in which all "other" things are equal.

To obtain radiation efficiency, we need to set up a request for a radiation pattern. The required call is an RP0 (far field) that sets the XNDA entry to either 1001 (if we wish the pattern data to appear in the output report) or 1002 (if we are interested only in the required information for calculating the radiation efficiency). There are two cases of note: free space (no ground) and all other cases having a ground that may range from perfect to very lossy (using either the refection coefficient or Sommerfeld ground systems). We set up the RP0 request to fairly sample the sphere or hemisphere at reliably constant intervals in degrees. So the two possible lines will look something like the following ones:

Free Space @ 5° intervals :

```
RP 0 37 73 1002 -90 0 5 5
```

Over any ground @ 5° intervals:

```
RP 0 19 73 1002 -90 0 5 5
```

In both cases, we have suppressed the printing (to file) of the radiation pattern. However, one may use this data for generating a surface or 3-D pattern for the antenna model in question. The angles follow the phi and theta conventions.

The 5° interval may not always be sufficient to track precisely the pattern undulations of a given far-field pattern. In such cases, one may reduce the interval for both phi and theta to 2° or even 1°. The number of steps for theta (37 for free space) and phi (73 for free space) will increase accordingly, reaching 181 and 361, respectively, for 1°intervals. However, it will be rare that we need a value for radiation efficiency that approaches that level of precision.

We must calculate the value of radiation efficiency. We base what amounts to a super-simple calculation on the data the emerges when we set the final digit of XNDA to 1 or 2, both of which request "gain averaging." The raw data line has the following appearance at the end of the RP0 request portion of the NEC output report.

```
AVERAGE POWER GAIN= 4.99152E-01
                SOLID ANGLE USED IN AVERAGING=( 2.0000)*PI STERADIANS.
```

First, examine the solid angle data. For free space, the value within (--) will be 4. If that is the case, the radiation efficiency will be the value of the average power gain * 100 % and will be a

percentage. In this report, which applies to the case of a hemisphere created over any ground type, the value in (--) is 2. For all such cases, the radiation efficiency is the (average power gain / 2) * 100 %. Since the reported power gain is 0.4992, the radiation efficiency is 24.96% (using at least 1, if not 2, too many decimal places for most purposes).

There are some short-cuts to arrive at the desired average power gain for patterns of known symmetries. However, on modern computers, using the RP0 calls shown will not create delays for most model runs. Our case study models will not tax any known computer.

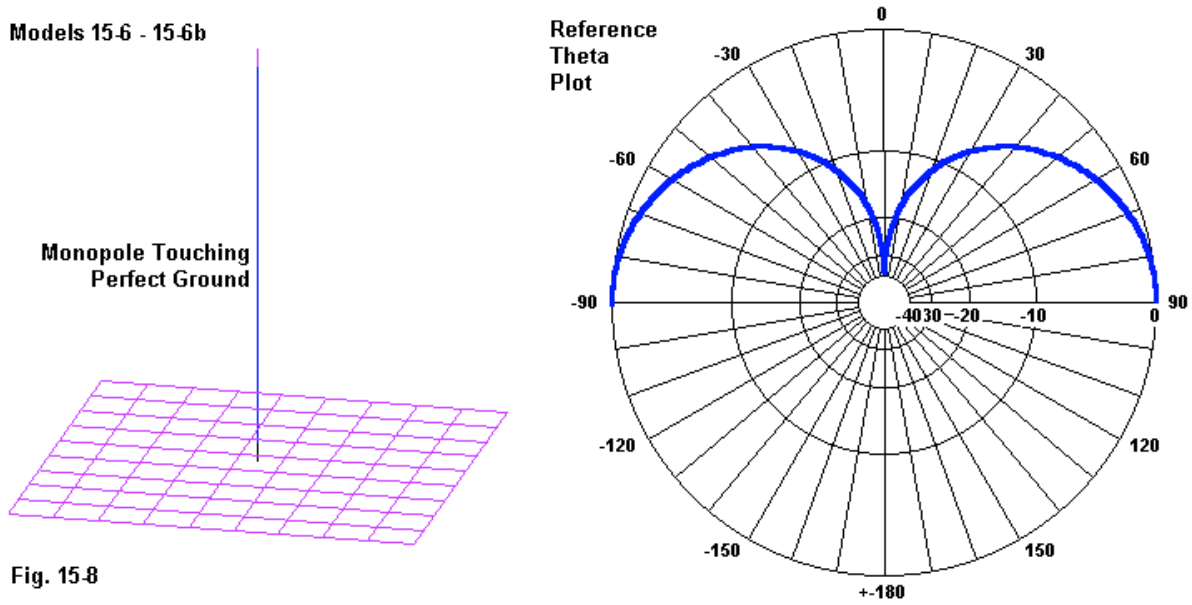

Fig. 15-8

Fig. 15-8 shows the essentials of a simple 1/4λ monopole over and in contact with a perfect ground. Open model *15-6.nec*, the first step on our way to obtain the radiation efficiency. The model uses perfect AWG #12 wire in a 28.5-MHz monopole cut to provide near resonance. If we run the model, with its standard theta-pattern request, we obtain the pattern on the right with a 5.15-dBi gain figure. The reported source impedance is 36.115 + j0.535 Ω and the efficiency--with a lossless conductor and no loads or networks--is 100%.

To derive a radiation efficiency value, let's alter the RP0 request for 5° increments. Open model *15-6a.nec*.

```
RP 0 19 73 1002 -90 0 5.00000 5.00000
```

Since XNDA = 1002, we are requesting averaging, but with a suppression of printing the radiation pattern data. Hence, the output report for this antenna is quite small, with the relevant line in NEC-2 giving us the following information.

```
AVERAGE POWER GAIN= 1.99896E+00
                SOLID ANGLE USED IN AVERAGING=( 2.0000)*PI STERADIANS.
```

Since we are working with a half shell (2π steradians), we simply divide the average power gain

by 2 to arrive at a radiation efficiency of 0.99948 or 99.948%. Running the same problem with a material conductivity and a lossy ground on NEC-4 may yield a slightly different result, but nothing that impinges on accuracy when we reduce the reports to a practical level of precision. NEC-4 yields the following report lines.

```
AVERAGE POWER GAIN= 1.99896E+00
                  SOLID ANGLE USED IN AVERAGING=( 2.0000)*PI STERADIANS.
POWER RADIATED ASSUMING RADIATION INTO 4*PI STERADIANS =
                                                    2.76691E-02 WATTS
```

The radiation efficiency using the NEC-4 report is the same for our perfect wire monopole and perfect ground case. NEC-4 adds an additional line to the output: the power radiated assuming a perfect sphere. Since we are using a half-sphere, the radiated power will half the listed value or 1.3835E-2 watts, a value that coincides well with the radiated power shown in the power budget. More precisely, it coincides with the listed radiated power in the power budget times the calculated efficiency for the antenna.

We have used 5° increments for our sample. We may revise the model to let us obtain a sampling at 1° intervals to see if there is a significant difference in the results. Open model *15-6b.nec* and review the RP0 request. Then run the model in NEC-2 and obtain the average power gain report.

```
RP 0 91 361 1002 -90 0 1.00000 1.00000

AVERAGE POWER GAIN= 1.99957E+00
                  SOLID ANGLE USED IN AVERAGING=( 2.0000)*PI STERADIANS.
```

Dividing the reported average power gain by 2 gives us 0.999785 or 99.9785%. The difference from the 5° report is too small to hold anything but academic interest.

Since we cannot place the simple monopole over a real ground, let's turn to a different model. See **Fig. 15-9** and open model *15-7.nec*.

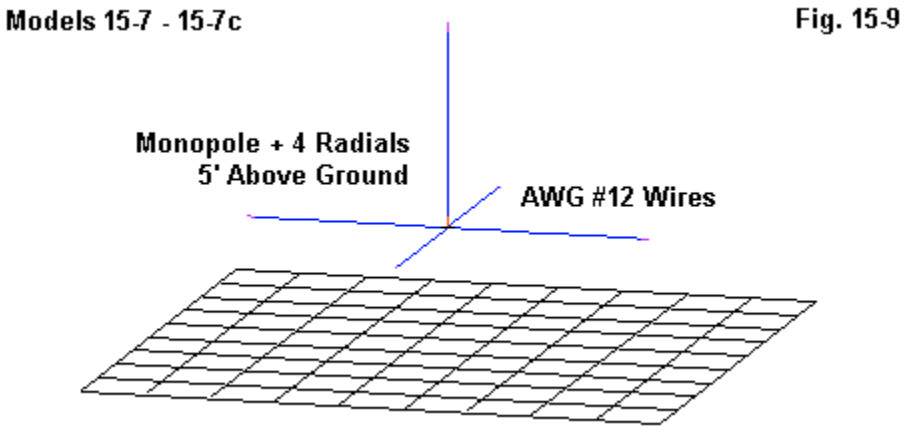

The model uses a monopole with 4 radials trimmed for near resonance at 28.5 MHz, with the

radials initially 5' above perfect ground. All elements use AWG #12 wire, starting with perfect conductors. Running this model gives us 100% power efficiency. However, the average power gain information tells us a different story.

```
AVERAGE POWER GAIN= 1.93898E+00
```

Calculating the radiation efficiency, we obtain a mere 96.949%. Perhaps there is something about the radiation pattern that requires a tighter increment. Open model *15-7a.nec*, which uses the RP0 request for 1° steps. Run this model and obtain the average power gain report.

```
AVERAGE POWER GAIN= 1.93957E+00
```

The power efficiency remains 100%, but the radiation efficiency becomes 96.9785%, which is not significantly different from the 5°-increment report. The more correct reason for the reduction in radiation efficiency relative to the simple monopole in contact with a perfect ground lies in the relationship of the radials to the ground.

If we add a material conductivity load (LD5) to the 5° model, we shall find corresponding reductions in both the power efficiency and the radiation efficiency. Open model *15-7b.nec* and review the addition.

```
LD 5 0 0 0 5.8e7 0
```

Running this version of the model yields the following average power gain report.

```
AVERAGE POWER GAIN= 1.91215E+00
```

The radiation efficiency is now 95.6075%, to go along with a power efficiency of 98.67%, a differential of just over 3%, similar to the differential using a perfect conductor.

We may complete our introductory survey of the monopole with 4 radials by changing the ground from perfect to an SN average ground, while leaving the elements copper. Open model *15-7c.nec* and examine the change. Then run the model and obtain the average power gain.

```
GN 2 0 0 0 13 .005
```

```
AVERAGE POWER GAIN= 5.68933E-01
```

The radiation efficiency shrinks to 28.4467%, which is normal for a monopole and radials only about 0.15λ above a lossy ground. As well, the power efficiency decreases to 98.53%. The tiny reduction in power efficiency is largely due to the fact that the ground has also shifted the source impedance by a very small amount.

In an earlier chapter, we examined the differences between base-loaded and mid-element-loaded short monopoles from the perspective of gain. We found little difference, although the mid-element version of the model used had a higher source impedance. We can perform a similar experiment from the perspective of radiation efficiency by starting with a shortened version of the monopole used in model 15-7. Our options appear in **Fig. 15-10**.

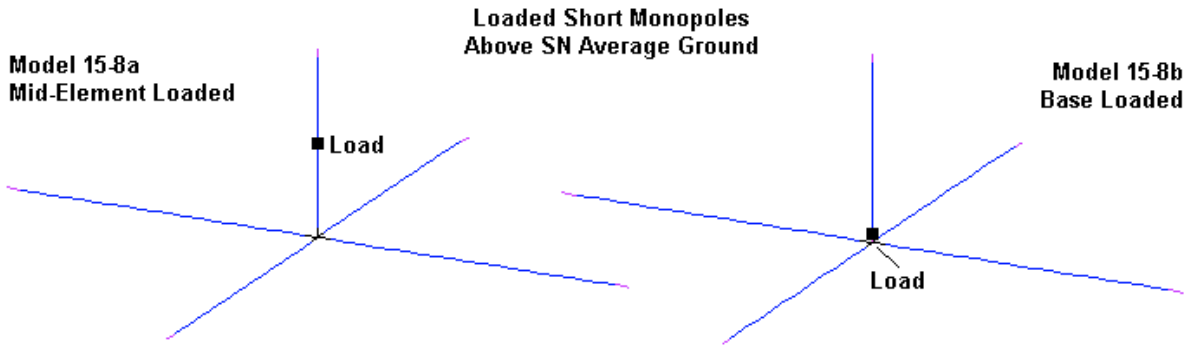

Fig. 15-10

Before loading the element, let's examine model *15-8.nec*, the short copper monopole 5' above average ground with full-length radials. Running the model shows a source impedance of 6.317 - j323.672 Ω and a power efficiency of 97.04%. The efficiency is down slightly from the value associated with the corresponding full-length monopole model. Interestingly, the average power gain report shows the following value.

```
AVERAGE POWER GAIN= 5.71572E-01
```

The radiation efficiency is 28.5786%, which is numerically (but not practically) higher than the value for the full-size monopole. However, our main use for the value is to compare it with loaded monopoles, and we can begin with a mid-element loaded model, *15-8a.nec*. The load assumes a Q of 300.

```
LD 4 1 11 11 1.89 568
```

From the NEC output report, we obtain a source impedance of 13.119 - j1.648 Ω. The power efficiency drops all the way to 85.04% due to the series resistance of the load.

```
AVERAGE POWER GAIN= 4.91889E-01
```

The radiation efficiency is 24.5945%. Note that the radiation efficiency did not decrease as much as the power efficiency, relative to the unloaded version of the short monopole. If we replace the mid-element load with a base load, again with the Q at 300, we obtain model *15-8b.nec*.

```
LD 4 1 21 21 1.06 318.05
```

As expected, the source impedance remains very low: 7.377 - j5.622 Ω. The power efficiency drops further to 83.10%.

```
AVERAGE POWER GAIN= 4.89439E-01
```

Despite these decreases, the radiation efficiency is 24.4719%, scarcely less than for the mid-element loaded monopole. These monopole results coincide well with those we obtained in an

earlier chapter, when we focused on monopole gain values. We have at least a sense of NEC's internal consistency.

We would be remiss if we did not examine the radiation efficiency of at least one horizontal antenna. Consider **Fig. 15-11**.

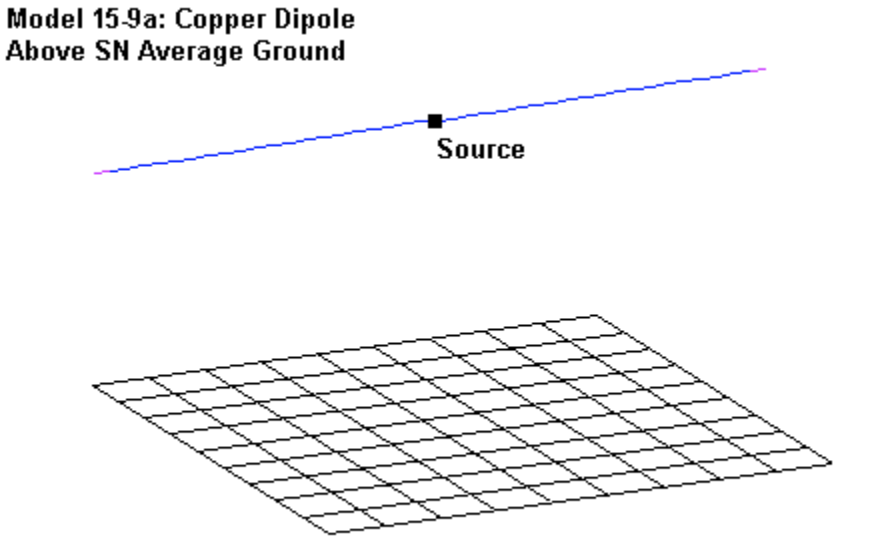

Fig. 15-11

The first step is to look at the antenna in free space. As model *15-9.nec* shows, we have a simple copper dipole, with the units in inches. The key command is the RP request for a complete sphere. With a 5° increment, we need 37 theta steps and 73 phi steps.

```
RP 0 37 73 1002 0 0 5 5
```

The impedance is 72.230 - j1.318 Ω, and the power efficiency is 99.22%.

```
AVERAGE POWER GAIN= 9.92175E-01
                SOLID ANGLE USED IN AVERAGING=( 4.0000)*PI STERADIANS.
```

Since a sphere covers 4π steradians, we may use the average gain report without adjustment, except for the decimal displacement to arrive at a percentage: 99.2175%. Note the coincidence between the power and radiation efficiencies.

Now open model *15-8a.nec*, which places the same antenna over average ground and reverts to a half-shell RP0 request. The antenna is at 35', about 1λ above ground. The impedance changes to 69.888 - j5.952 Ω, and the power efficiency is 99.20%.

```
AVERAGE POWER GAIN= 1.48112E+00
```

The radiation efficiency is 74.056%, typical for horizontal antennas above lossy ground.

Summing Up

The exercises in this chapter have focused on questions of power and efficiency relative to NEC models. The power budget is the chief source--but not the only source--of information about antenna power. The input power is a function of the excitation voltage and the source impedance calculated by NEC for the model. From this input power, we must subtract structure losses, that is, power lost from the resistive components of all LD loads, including both lumped and material conductivity loads. We must also subtract network losses for any model containing an NT entry. The remaining power is the radiated power.

The ratio of radiated power to input power is the basis for the NEC calculation of power efficiency. In addition to this measure of efficiency, we may also calculate the radiation efficiency from the average power gain. To obtain the average power gain, we establish a fair sampling of a free space sphere or of a hemisphere over any type of ground, whether perfect or lossy. We use the RP0 command with the XNDA entry set to either 1001 or 1002, with the latter suppressing the print out of the radiation pattern details. We then derive the radiation efficiency directly from the reported average power gain for a free-space sphere or from half the reported average power gain for a hemisphere over ground.

The basic focus of this chapter allowed us to review a number of the control commands that we met in Part B of this volume. Especially important were the various uses of the LD and NT commands. We also used the occasion to manipulate the source (EX0) voltage to obtain specific input power levels and specific current levels on segments of interest in the structure geometry. The end result was a set of exercises illustrating how the control commands integrate into a package that both modifies a basic model and requests various kinds of information that may be useful to a modeling task.

16.
Material Loads, Wire Insulation, and Work-Arounds

***Objectives**: This set of exercises will introduce the modeling of insulated and other wires exhibiting a velocity factor. We shall meet the NEC-4 insulated sheath (IS) command and discover a way to simulate the command within NEC-2. In addition, we shall explore some situations that require us to accumulate data from a series of related models and use external methods of coalescing the information.*

Mastering the modeling of insulated wires is very straightforward in NEC-4. The effort will introduce us to the concept of a wire's velocity factor, the ratio of the physical length of wire and its electrical length. Once we have met this concept, we shall discover that it appears in many guises, even with bare wires.

The first step in the process will be to complete our exploration of the material load or LD5 command that is common to both NEC-2 and NEC-4. We shall specifically look at the effects of using different values of conductivity for essentially the same antenna wire. The results will show that under the influence of material loading, that is, having a finite conductivity, the properties of the antenna change and it acquires a small but determinate velocity factor.

Once we insulate the wire, the conductivity and permittivity of the insulation create even more noticeable velocity factor values. Given a high resistivity, common to most insulating materials used, the insulation thickness or sheath depth and the permittivity of the material will constitute the key factors controlling the properties of the insulated wire in antenna applications. Once we have mastered the entry of the requisite data in the NEC-4 IS command, we can not only survey some of the critical effects, but as well incorporate into our general modeling practice the creation of physical transmission lines having a velocity factor.

NEC-2 lacks the IS command. However, we shall discover a usable work-around in the form of distributed loading (LD2 and LD3), aspects of the LD command that we by-passed when we examined that command in Part B of our work. With some external calculation, we can distributively load a wire to virtually any level of insulation that we wish. A hand calculator and a spreadsheet notebook are but two of the ways in which we can shorten the work required by the preliminary calculations.

The exercises in this chapter will differ from the standard sort of modeling that we have done in the past. In most exercises, we searched individual models for performance values in the NEC output report. Once we had tabulated them, our work was finished. In the exercises in this chapter, we shall use selected performance data as a start rather than an end. We shall transfer the data to other vehicles, such as spreadsheets, in order to bring together significant information and to graph, tabulate, and otherwise manipulate the results. Although modeling software tends to have quite powerful tabulating and graphing tools, our work does not end with them. In many instances, NEC outputs are only the beginning of our interests in the data produced by antenna models.

Material Loads and Antenna-Wire Velocity Factor

In the preceding chapter, we had occasion to explore the consequences of using antenna wires with a finite conductivity. However, our examination was perfunctory in the sense that we used only a single example of wire conductivity out of the total range of values that we encounter in common antenna materials. The appendix to this volume provides a list of materials and reference values of conductivity and permeability.

NEC-2 allows only for the entry of the conductivity in the LD5 command.

```
Cmd   I1      I2      I3        I4        F1        F2      F3
      LDTYP   LDTAG   LDTAGF    LDTAGT    ZLR       ---     ---
LD    5       0       0         0         6.0e7
```

For our work, I1 will be 5 throughout the chapter to indicate that we are using a material load. More precisely, NEC is calculating the internal impedance for a finitely conducting round wire. I2 may indicate the tag number of the wire that we are loading, followed by the first and last relative segments included in the loading. However, if I2 is zero, then the segment specification uses absolute segment numbers. If both I3 and I4 are zero, then the load applies to all segments of the specified tag number. If I2 is also zero, than the load applies to all segments of the model.

In NEC-2, we may only enter a value of conductivity, as indicated by the F1 entry. However, in NEC-4, we may also enter in F2 a value of permeability.

```
Cmd   I1      I2      I3        I4        F1        F2      F3
      LDTYP   LDTAG   LDTAGF    LDTAGT    ZLR       ZLI     ---
LD    5       0       0         0         6.0e7     1
```

For non-ferrous materials, we either enter a value of 1 or leave the entry blank. Since most of the materials used for antenna wires are non-ferrous, we may omit the F2 entry. We briefly examined the effects of having a significant permeability in an earlier chapter.

Our present interest in antenna materials lies in the effects of various levels of conductivity on the performance of the selected wire as a radiator. Due to surface area considerations, we cannot ignore the radius of the wire in our considerations. However, we shall focus on the level of conductivity, using a range of values that reflects what we might encounter with real materials. On the next page is an extract from the longer table that appears in the appendix. The values shown are for very general guidance only, since they come from standard reference compendia. In any critical situation, you should always use the most accurate data for the material in question.

Since we wish to perform only a demonstration, we need not use the exact values for any specific materials in our exercises. So long as we select a high value that is close to the best in the list and a low value close to the worst in the list, we shall satisfy our exercise needs. As well, we shall be able to select values that step downward in a specified increment. Our goal is to be able to coalesce the accumulated data in a reasonable manner.

Material	Resistivity Ohms/meter	Conductivity Siemens/meter	Permeability
Pure Silver	1.62E-08	6.17E07	1.0
Copper	1.72E-08	5.80E07	1.0
6061-T6 Aluminum alloy	4.10E-08	2.50E07	1.0
Zinc	6.0E-08	1.67E07	1.0
Phosphor Bronze (4% Sn, 0.5% P, rest Cu)	9.4E-08	1.06E07	1.0
Tin	1.14E-07	8.77E06	1.0
Lead	2.19E-07	4.57E06	1.0
Stainless Steel (type 302)	7.20E-07	1.39E06	1.00008

We shall begin each model sequence with a perfect or lossless wire to set a standard for comparison. Given the values in the list of common antenna materials, we may choose a conductivity of 6.0E7 as the high value. If we select other values that are each 1/3 of the preceding value, then we end up with 2.0E7, 6.67E6, and 2.22E6 as the remaining values for a relatively short exercise.

```
GW 1 11 0 -.242 0 0 .242 0 .0001
GE
FR 0 1 0 0 299.7925 1
EX 0 1 6 00 1 0
RP 0 1 361 1000 90 0 1.00000 1.00000
```

The perfect-wire model above is the heart of our initial exercise. The test frequency is 299.7925 MHz, and the wire radius is 0.0001 m. This value is also 0.0001λ, which is relatively thin, but not as thin as common wire sizes used for HF antennas.

For each succeeding model in the sequence, we shall add an LD5 entry, such as the sample used to review the entries. In each case, we shall adjust the Y1 and Y2 entries of GW1 to bring the model to resonance, defined here as a source reactance of under +/-j1 Ω. We may carry the task out using either a reasonable number of decimal places in the Y coordinates, or we may extend the series as long as possible to reach a higher standard, such a +/-j0.1 Ω. Our work requires only the milder standard. For each model, we shall change the LD5 entry by one increment in the series and then re-resonate the antenna. Finally, we shall record the free-space gain, the element length, and the source impedance.

Sequentially open model *16-1.nec* through model *16-1d.nec*. Run each model and record the data. Your table should resemble the following one.

Model	Conductivity S/m	Length m	Gain dBi	Source Impedance R +/- jX Ω
16-1	Perfect	0.4840	2.13	72.097 + j0.410
16-1a	6.0E7	0.4834	2.02	72.729 + j0.409
16-1b	2.0E7	0.4830	1.94	74.980 + j0.509
16-1c	6.67E6	0.4822	1.80	77.183 + j0.360
16-1d	2.22E6	0.4810	1.55	81.353 + j0.534

The maximum differential among the reactance values is well under 0.2 Ω, indicating a fairly precise grouping in which the resistance values are highly comparable. We may notice a continuous rise in the source resistance as the conductivity decreases. With that same conductivity decrease, we find corresponding decreases in both the element length and the dipole gain.

Before we reach any conclusions about the sequence, let us repeat it, using a wire radius of 0.001 m (or 0.001λ). To achieve resonance with this wire, which we may variously categorize as either mildly thin or moderate in thickness, we shall have to adjust the wire length. Open models *16-2.nec* through *16-2d.nec*. Successively run each model and record the same data that we picked up from the first series of models. Then produce a correlative table.

Model	Conductivity S/m	Length m	Gain dBi	Source Impedance R +/- jX Ω
16-2	Perfect	0.4750	2.12	71.760 + j0.116
16-2a	6.0E7	0.4748	2.11	71.863 - j0.098
16-2b	2.0E7	0.4746	2.10	71.914 - j0.355
16-2c	6.67E6	0.4744	2.09	72.067 - j0.527
16-2d	2.22E6	0.4742	2.06	72.406 - j0.522

We have allowed a greater variation in the reactance values for 2 reasons. First, reducing the range would have required more decimal places for the Y coordinates. Second, the resistance changes so little that further refinement of the reactance was not justified. The table shows the same general trends as the first one, but with far smaller increments of change in any category: element length, gain, or source resistance. We must remember that the conductor in this set of models has a radius that is 10 times larger than the one used in models that yielded the first data set.

Although simple tables are often useful for data comparison, we may often enhance our perceptions of the data by the use of graphics. Since the modeling software does not contain facilities for making the comparisons, we may transfer the data to a simple spreadsheet with graphic capabilities.

Model	Radius	Load	Length	Gain	Resistance	VF
16-1	0.0001	Perfect	0.484	2.13	72.097	1
16-1a		6.0E7	0.4834	2.02	72.729	0.99876
16-1b		2.0E7	0.483	1.94	74.98	0.997934
16.1c		6.67E6	0.4822	1.8	77.183	0.996281
16-1d		2.22E6	0.481	1.55	81.353	0.993802
Model	Radius	Load	Length	Gain	Resistance	VF
16-2	0.001	Perfect	0.475	2.12	71.76	1
16-2a		6E+07	0.4748	2.11	71.863	0.999579
16-2b		2E+07	0.4746	2.1	71.914	0.999158
16-2c		6670000	0.4744	2.09	72.067	0.998737
16-2d		2220000	0.4742	2.06	72.406	0.998316

Now we are positioned to create some comparative graphs, such as **Fig. 16-1**, which compares

the gain progressions of the 2 series of models.

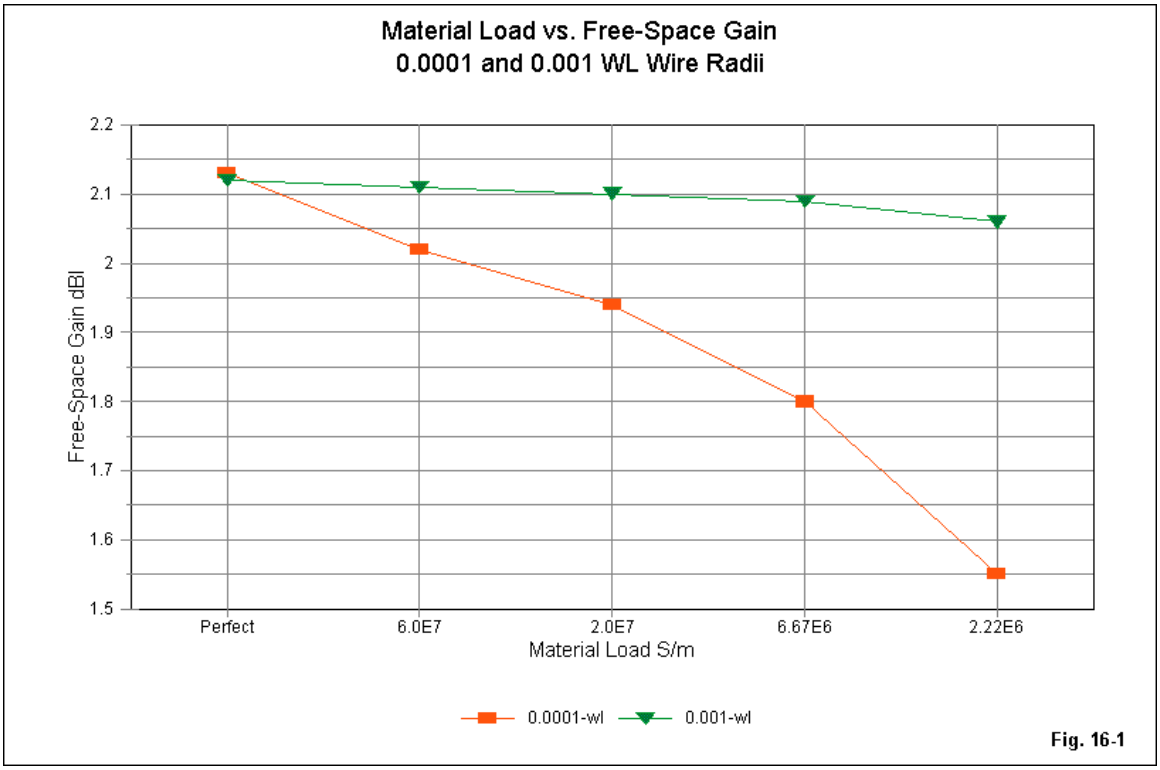

Fig. 16-1

Several features become clearer in the graphical comparison than they might otherwise be in a simple tabular progression. First, there is a slight step-effect in the line from the perfect wire to the first conductivity value. The step results from the fact that the ratio of conductivity between the steps is not 3:1. Second, the gain curve shows an almost precipitous increase in slope between the last two values in the sequence. Finer gradations and a continuation of the graphed values would help to refine the slope of the curve. However, the curve does suggest that, even for the fatter wire, there may be a practical limit as to the resistivity of a conductor suitable for general antenna use. Besides using a smaller increment between models and adding values at the low end of the conductivity range graphed, you may also enter models with intermediate radii to gauge the rate of change per radius step.

In reverse fashion, the curves for the resonant source resistance replicate the properties in the gain graph. As shown in **Fig. 16-2**, the thinner wire increases in source resistance as the conductivity decreases. The effect is virtually proportional to the gain decrease for both curves. Once more, there is a larger increase between the last two steps in both curves than between the preceding steps.

As the conductivity decreases, the required length for a resonant dipole also decreases. Its curves would replicate that shape of the gain curves for both wire radii. However, there is another measure that we may calculate for the change in element length: a provisional velocity factor that takes the ratio of resonant length at any conductivity to the resonant length of a lossless wire of the same radius. See **Fig. 16-3**.

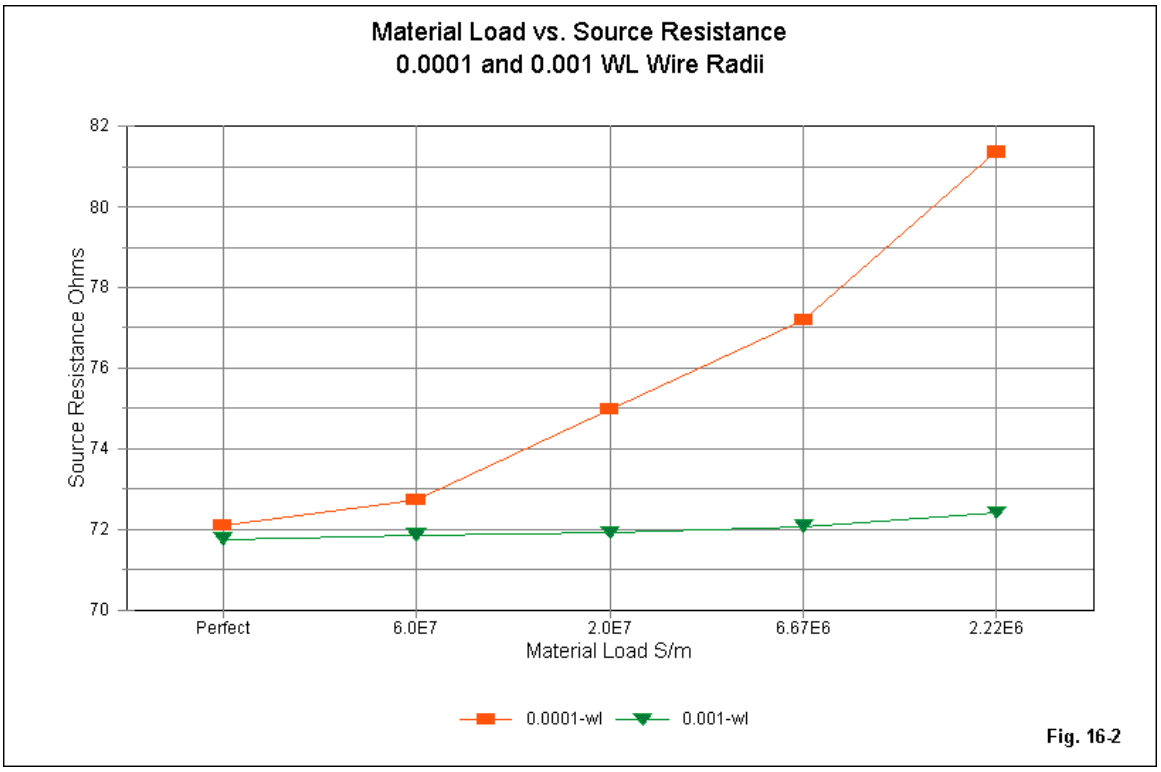

Fig. 16-2

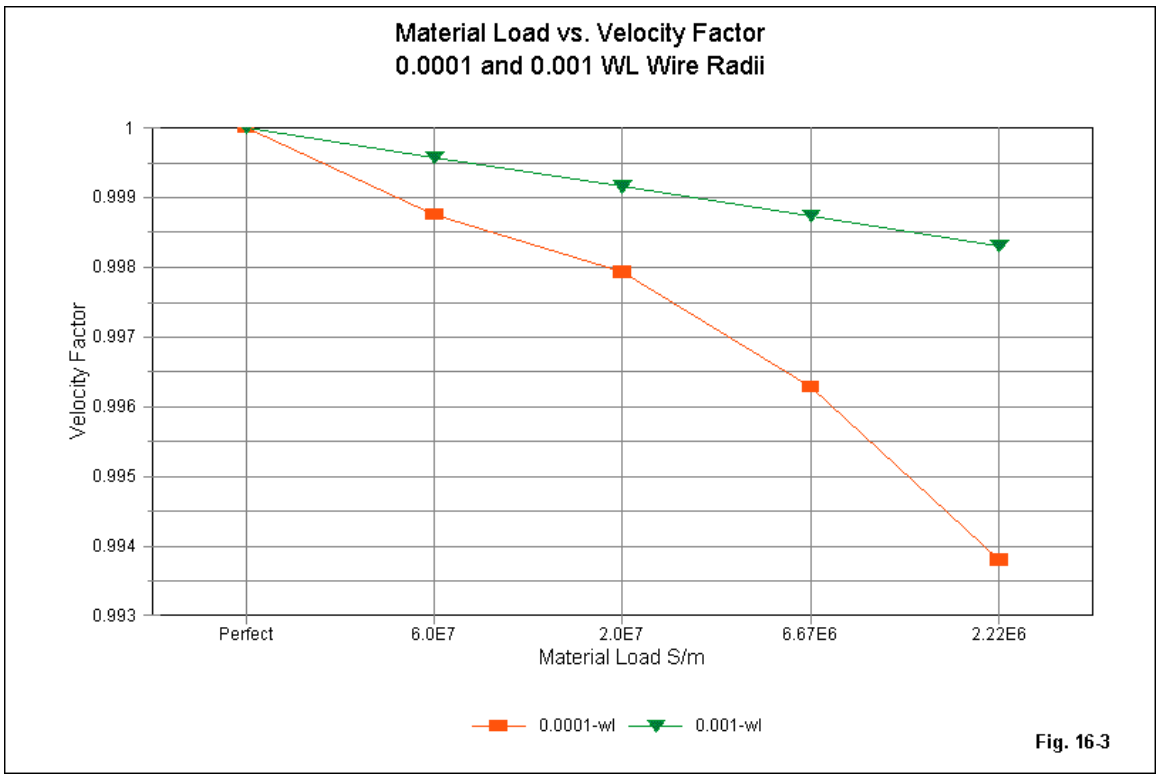

Fig. 16-3

The provisional velocity factor omits the electrical length of a half-wavelength in order to avoid

confusions occasioned by standard end effects of the wire. The values shown in the graph represents only the effects of decreasing conductivity. These values generally accord with the use of the concept of velocity factor when applied to an antenna wire, rather than to a transmission line. The concept is important when insulated wire is the antenna conductor of choice. In these cases, the resonant (or otherwise required) length of the insulated wire relative to a bare wire of the same conductor radius generally defines the velocity factor assigned to the material.

To supplement this exercise, you may conduct additional or other explorations of the effects of conductivity on round wire radiators over any span of wire radii or conductivity values you wish. As well, you may explore further manipulations permitted within your spreadsheet or other calculating instruments, including regression analysis to develop smooth curves for all variables.

The NEC-4 IS or Insulated Sheath Command

NEC-4 contains a special control command for specify an insulated sheath (or a set of insulated sheaths) around the wire (or wires) of a model. NEC-2 lacks the command, so the following exercises apply to the later core only. The command is a model of simplicity.

Cmd	I1	I2	I3	I4	F1	F2	F3
	I1	LDTAG	LDTAGF	LDTAGT	ESPR	SIG	RADI
IS	0	1	1	21	1.25	1E-10	.0015

The I1 entry is normally 0 to specify a new IS entry. The remaining integer commands follow the same rules as those for LD commands. The sample shows a specific tag and range of segments within it to receive the sheath treatment. However, if all three entries had been zero, the command would apply to all segments in the model, and the ITAG zero entry would force the command to use absolute segment numbers. ESPR enters the permittivity (relative dielectric constant) of the insulating material, while SIG records the conductivity of the insulation (S/m). RADI records the radius of the sheath and must be in meters, since control commands are not subject to scaling in the manner of geometry commands.

Often the data for an insulating sheath will list its thickness rather than the total wire + sheath radius or diameter. **Fig. 16-4** shows the relationships involved in calculating the sheath radius when you know its thickness and the wire radius or diameter. The sheath radius (SR) is simply the wire radius (WR) plus the sheath thickness or depth (SD), converted to meters, if the initial terms use other units of measure. In all cases, for the IS command to function, the sheath radius must be greater than the wire radius.

The right side of **Fig. 16-4** shows the GNEC entry assistance screen. The values shown are taken from the sample line used to sort out the command entries. The only unusual option on the screen is to cancel a previous sheath command. This option, as in numerous other control commands, places a -1 in I1. Although not much used in modeling practice, the command is handy when a model contains multiple runs of the core. By judiciously using the command, you may obtain multiple runs of the same wire using different values (including none) of the variables within the IS command.

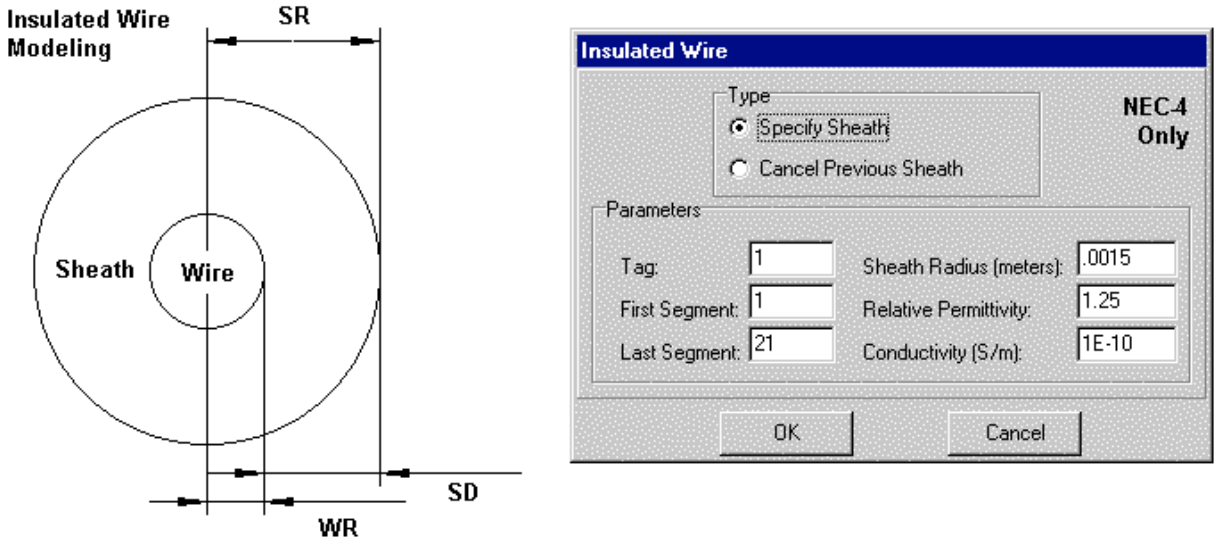

Wire Radius (WR) + Sheath Depth (SD) = Sheath Radius (SR)

Fig. 16-4

To sample the IS command, let's employ a free-space copper dipole at 30 MHz, using a length of under 5 m and a diameter of 2 mm (0.07874"). We shall vary the length in some models to bring the dipole to resonance within the usual standard. However, we have many variables to track: the sheath radius, the permittivity, and the conductivity. Let's see if we can eliminate at least one of them.

Open model *16-3.nec*.

```
CM 30 MHz wire dipole
CM Conductivity test
CE
GW 1 21 0 -2.416 0 0 2.416 0 .001
GE 0
IS 0 1 1 21 3 1 .003
EX 0 1 11 0 1 0
LD 5 1 1 21 5.8001E7
FR 0 1 0 0 30 1
RP 0 1 360 1000 90 0 1 1
EN
```

The IS command shows a somewhat strange entry: a conductivity of 1. That entry represents the last of a string of conductivity values ranging from 1E-10 to 1 in increments of 10:1 per step. The dipole length, the permittivity, and the sheath radius will not change. Our goal is to see whether changing only the conductivity--using a reasonably high value of permittivity and a fairly thick sheath--will have a significant effect on antenna performance. Our gauge will be the source impedance of the dipole.

Run model 16-3 the required number of times and create a table, spreadsheet or graph of the results. The antenna is intentionally long so that we can examine changes in both the resistance and the reactance. See **Fig. 16-5**.

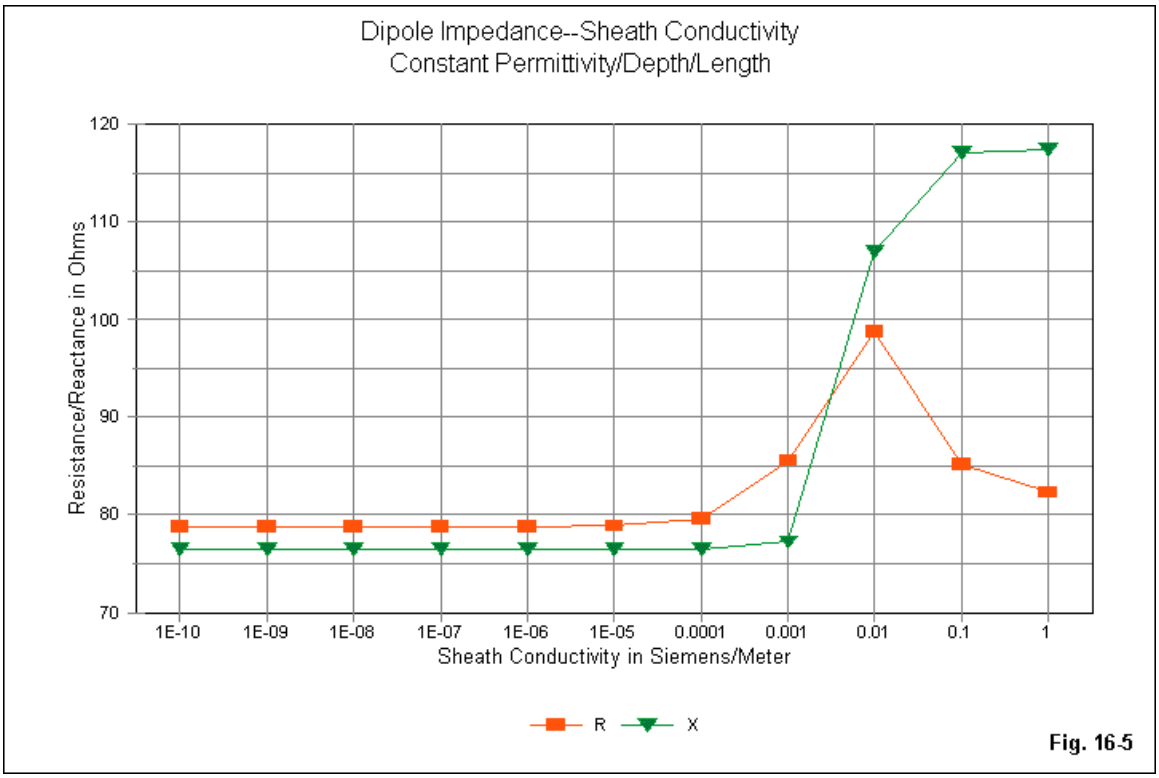

Fig. 16-5

The resistance and reactance remain virtually unchanged for conductivity values between 1E-10 and 1E-5. At the high end of that region, the resistance begins a slow rise, while the reactance does not show a perceptible change until the conductivity is 1E-3. Since most wire insulating materials have a conductivity that is closer to 1E-10 S/m than to 1E-5 S/m, we will be justified in further sampling of the IS command to use a constant for the conductivity entry, perhaps 1E-10 S/m.

The appendix lists a number of plastic and non-plastic insulating materials, along with listed values of relative permittivity taken from standard references. The following list is an extract from the appendix. The values hold well above 100 MHz, some up to 900 MHz. The list does not include materials used for very thin coatings, sometimes called enameled wires.

Material	**Relative Permittivity ε**
Cross-linked polystyrene	2.58
Polycarbonate (PC)	2.96
Polyethylene	2.26
Polyethylene terephthalate (PET)	2.98
Polyisobutylene	2.23
Polypropylene (PP)	2.55
Polystyrene (PS)	2.55
Polytetrafluoroethylene (PTFE--Teflon)	2.1
Polysulfone (PSU)	3.2
Polyvinyl-chloride (100%)	2.85

The general range of wire insulation permittivities used today runs from about 2 to 3. Using the 2-mm-diameter 30-MHz free-space dipole as a basis, our task will be to find the effects of different permittivity values and sheath depths on antenna performance. To simplify the problem, the wire radius will be 1 mm throughout the sequence of models. In addition, we shall test 3 depths of sheath: 0.5 mm, 1.0 mm, and 2.0 mm. The corresponding sheath radii are 0.0015 m, 0.002 m, and 0.003 m. For each of the three set-ups, we shall systematically vary the permittivity from 1.0 to 3.0 in 0.25 steps.

Open and examine models *16-4.nec*, *16-5.nec*, and *16.6.nec*. The initial IS entry for each model appears below.

Model 16-4:

```
IS 0 1 1 21 1 1e-10 .0015
```

Model 16-5:

```
IS 0 1 1 21 1 1e-10 .002
```

Model 16-6:

```
IS 0 1 1 21 1 1e-10 .003
```

Each dipole begins with a length of 4.832 m, despite having a variable-thickness sheath. The reason for the common length is that the permittivity value of 1.0 is also the value of a vacuum or dry air, the natural NEC environment. Hence, regardless of the sheath depth, it acts just like air at the initial value.

Run the models through the steps. For each new permittivity value, adjust the dipole length so that it is resonant within +/-j1 Ω of remaining reactance. Then create a table, spreadsheet, or graph of the results. It should resemble the following spreadsheet extract. As a start, you may refer to models *16-4a.nec*, *16-5a.nec*, and *16-6a.nec*. These models show the model inputs needed for the second step in each progression.

IS	Insulated Sheath Card as an Indicator of the Effects of Insulation on an Antenna Wire								
	Dipole: 30 MHz, 2mm (0.002 m or 0.07874") diameter copper conductor								
TH=0.5 mm; Radius=1.5 mm							0.5 mm	1.0 mm	2.0 mm
Perm	1	1.25	1.5	1.75	2	2.25	2.5	2.75	3
Res FQ	30	29.8	29.69	29.6	29.53	29.48	29.44	29.41	29.39
DP Length	2.416	2.4	2.391	2.383	2.378	2.374	2.371	2.368	2.366
Wire VF	1	0.9934	0.9897	0.9863	0.9843	0.9826	0.9814	0.9801	0.9793
Zres	72.536	71.665	71.238	70.794	70.552	70.355	70.215	70.052	69.961
TH=1.0 mm; Radius=2.0 mm									
Perm	1	1.25	1.5	1.75	2	2.25	2.5	2.75	3
Res FQ	30	29.69	29.47	29.31	29.2	29.13	29.05	28.98	28.93
DP Length	2.416	2.391	2.373	2.36	2.351	2.345	2.339	2.333	2.33
Wire VF	1	0.9897	0.9822	0.9768	0.9731	0.9706	0.9681	0.9656	0.9644
Zres	72.536	71.262	70.306	69.618	69.172	68.915	68.605	68.256	68.142
TH=2.0 mm; Radius=3.0 mm									
Perm	1	1.25	1.5	1.75	2	2.25	2.5	2.75	3
Res FQ	30	29.5	29.17	28.91	28.74	28.6	28.49	28.39	28.3
DP Length	2.416	2.375	2.348	2.328	2.313	2.302	2.292	2.284	2.278
Wire VF	1	0.983	0.9719	0.9636	0.9574	0.9528	0.9487	0.9454	0.9429
Zres	72.536	70.405	69.046	68.029	67.275	66.754	66.235	65.829	65.551

The line labels should be reasonably self-explanatory. Res. FQ means the resonant frequency of the dipole before reduction to a length that is resonant at 30 MHz. DP Length is the 30-MHz resonant length, listed as a half-length. Wire VF means the velocity factor of a resonant insulated dipole relative to a bare wire. Zres is the resistive impedance of the dipole at 30-MHz resonance.

Although we might easily develop a myriad of graphs from this data and other information that we can extract from the NEC output file, let's focus on just two for now. First is the velocity factor of the wire. See **Fig. 16-6**.

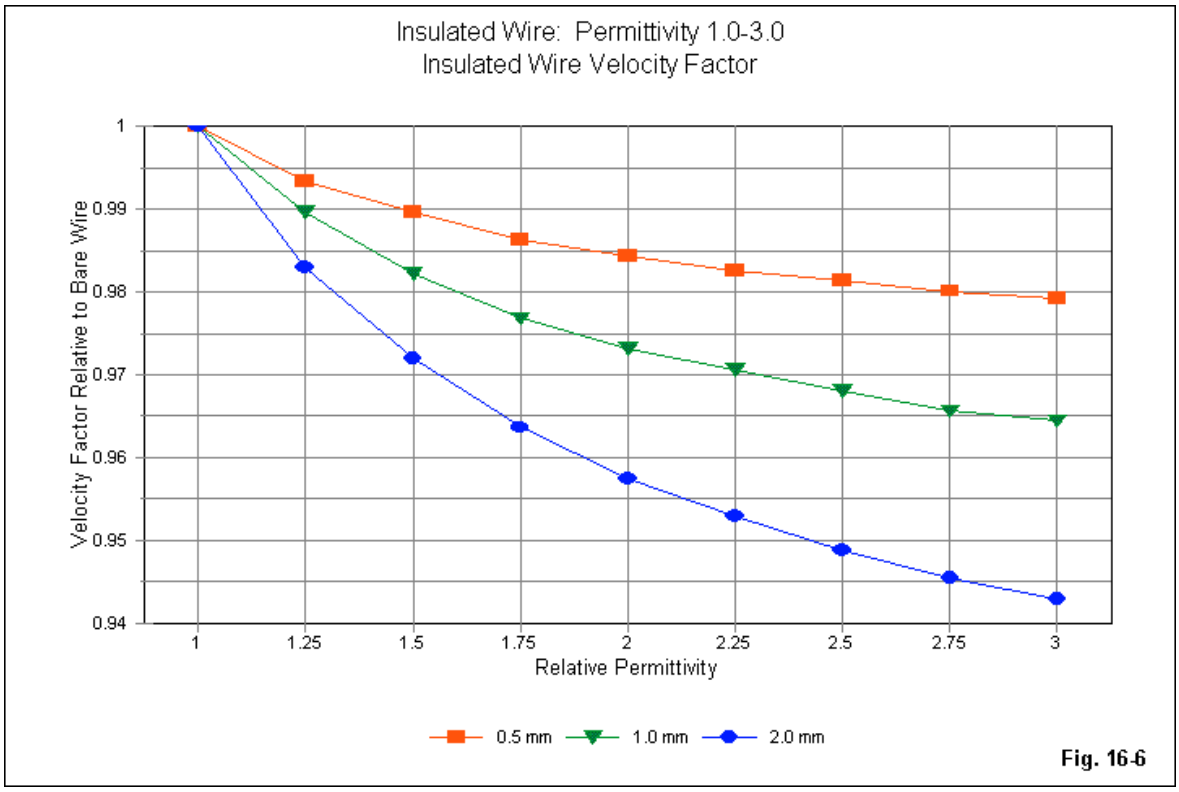

Fig. 16-6

The square markers indicate the thinnest insulation depth, which is still 50% of the wire radius. If we make the insulation vanishingly thin--such as is the case with enamel wires and aluminum wire, tubing, and rods with their natural aluminum oxide coating--the value of permittivity would make little difference. Even high values of permittivity would have negligible effect on the required length of wire relative to a truly bare wire.

Using the highest permittivity value and the thickest insulation, the velocity factor is about 0.943. All other velocity factors are closer to 1.0. The range of velocity factors aligns well with experience-based advice to wire antenna builders to reduce an antenna element length 3% to 5% if the wire is insulated.

The resonant impedance of wires with varying material loads showed a rising set of curves. The total effect was small, although numerically noticeable and systematic. The resonant impedance changes caused by adding an insulating sheath completely override those increases in value. The required element length decreases for each increase in permittivity value or sheath depth reduces

the resonant impedance by a significant amount, as shown in **Fig. 16-7**.

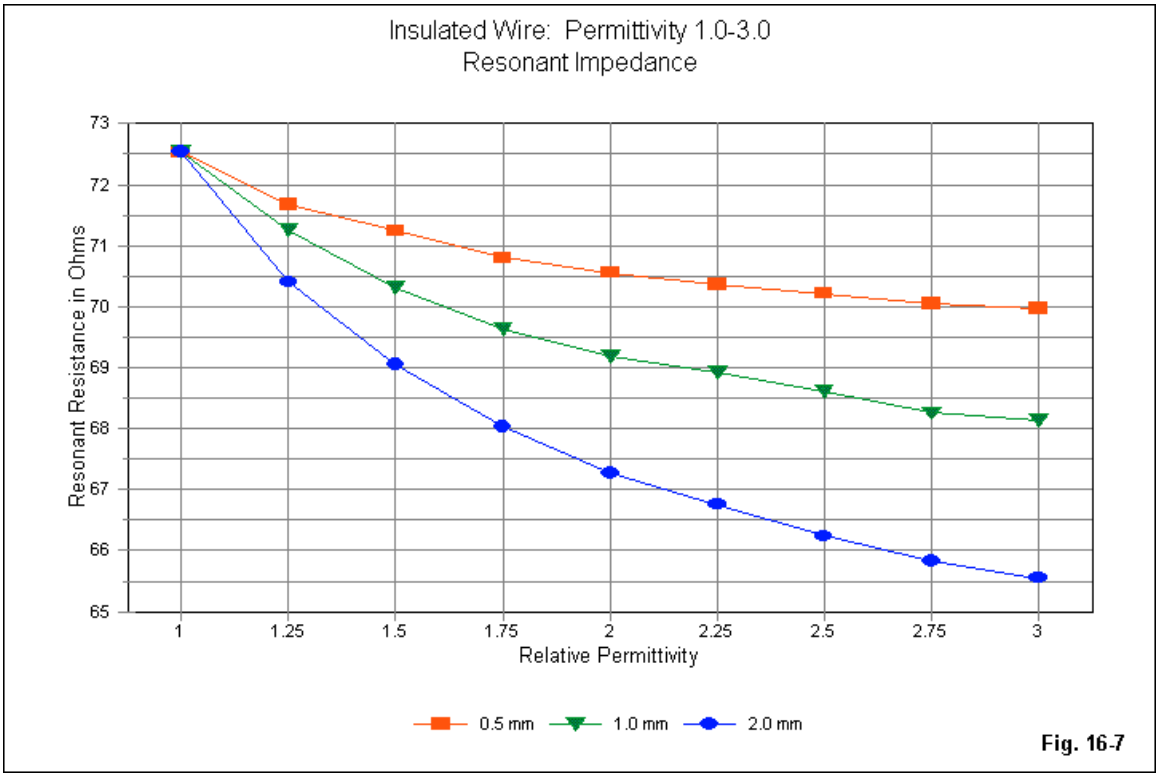

Fig. 16-7

Notice that the curves for the decrease in resonant impedance are congruent with the curves for the velocity factor. As well, these curves would also match curves for the required 30-MHz resonant dipole length.

From exercises like these, tailored to a specific task, you may learn a great deal about the behavior of insulated wires in antenna applications. A number of insulated wires especially designed for such applications have appeared in recent years in answer to the need for wire that is less subject to weathering and associated corrosive effects.

As we learned in Chapter 12, the IS command also has an application in modeling physical transmission lines, that is, lines made up of GW entries rather than TL entries. As a review of that material, but with new models, let's consider a 600-Ω open wire line. We shall use 2-mm diameter (0.001-m radius) wire for the line. Calculations report a required center-to-center spacing of 0.1489 m for the wires (about 5.86"). As we did in the earlier chapter, we shall set up a 1.5λ line as a test bed. The line will be that long electrically and physically. Since the segment length of the source wire and the load wire will be 0.1489-m long, we shall require 101 segments at the 30-MHz test frequency to approximate that segment length in the parallel long wires. (The actual segment length will be 0.14841 m, well under a 1% difference.) **Fig. 16-8** shows the outline of our model.

Most tables list the velocity factor of such lines as 0.92, using generic construction with periodic spacers along the length of the line to effect proper separation. Normally, such values emerge

from test measurements made on commercial products. As shown in the figure, our model has no spacers and the 2-mm diameter wires do not match the wire size used in U.S. lines. Hence, we shall assume a velocity factor of 1.0 for the modeled line.

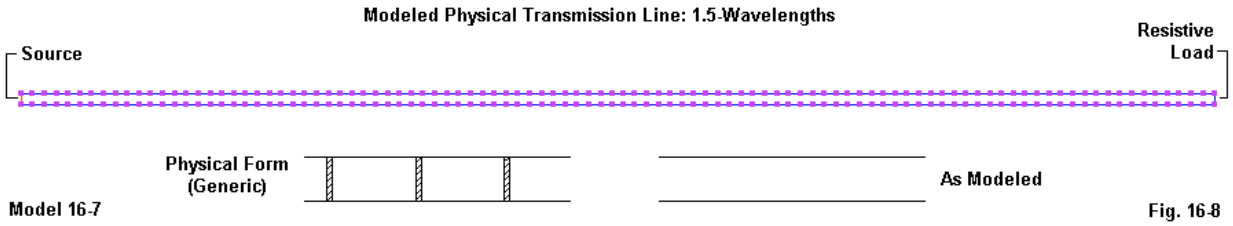

Our initial step will reveal another limitation of modeling physical transmission lines, especially as the spacing between lines becomes significant. Our earlier 450-Ω line used a spacing of 34.67 mm (1.367"), only about 23% of the spacing between the wires of the new 600-Ω lines. As a consequence of the wide line spacing, the cross wires at each end introduce a noticeable inductive reactance into the system so that a purely resistive load of 600 Ω results in an erroneous source impedance. However, we may add a corrective capacitive reactance to the load and bring the source impedance back to expectations.

Open model *16-7.nec*.

```
GW 1 101 0 0 -.07445 0 14.98962 -.07445 .001
GW 2 101 0 0 .07445 0 14.98962 .07445 .001
GW 3 1 0 0 -.07445 0 0 .07445 .001
GW 4 1 0 14.98962 -.07445 0 14.98962 .07445 .001
GE
FR 0 1 0 0 30 1
EX 0 3 1 0 1 0
LD 4 4 1 1 600 -11
XQ
EN
```

The construction of this free-space model is conventional. The only notable exception is the addition of -j11 Ω reactance to the load. Run the model to obtain a source impedance of 599.395 - j0.020 Ω. If we remove the reactance from the load, the impedance report becomes 600.631 + j10.919 Ω. The affect of the removal on the resistive portion of the impedance is evidence that the wires themselves are contributing to the reactive offset.

The next step is to make the wires copper by adding an appropriate LD5 command to the model. Open model *16-7a.nec*.

```
LD 5 0 0 0 5.8E7 1
```

Using the same corrected load, we still anticipate a slight shift in the source impedance due to the material load. NEC does not disappoint us: 599.812 + 0.468 Ω. Now we are ready to add in some IS commands to arrive at a desired velocity factor. In the transmission-line chapter, we learned that there is no single combination of permittivity and sheath depth that will yield a specified velocity factor. So let's add a few specifications to the task. First, the insulation will be

Teflon, which has a permittivity of 2.1 according to reference sources. Second, our target velocity factor is 0.95. Now we need only to reset the model length to 95% of its initial value and probe for the sheath radius that will bring the line back to a 600-Ω source impedance.

Open model *16-7b.nec*.

```
GW 1 96 0 0 -.07445 0 14.24 -.07445 .001
GW 2 96 0 0 .07445 0 14.24 .07445 .001
GW 3 1 0 0 -.07445 0 0 .07445 .001
GW 4 1 0 14.24 -.07445 0 14.24 .07445 .001
GE
FR 0 1 0 0 30 1
EX 0 3 1 0 1 0
LD 4 4 1 1 600 -11
LD 5 0 0 0 5.8E7 1
IS 0 1 1 96 2.1 1e-10 .0025
IS 0 2 1 96 2.1 1e-10 .0025
XQ
EN
```

The notable features of the model begin with the new length of the parallel wires: 14.24 m. Along with the reduction in length comes a reduction in the number of segments for the long lines: 96. The segment length within the long lines is 0.14833 m, again well within 1% of the 0.1489-m cross wires. We retain the reactively compensated load (LD4). We add two IS commands, one for each long wire. The entries show the permittivity of 2.1. The selected sheath radius is 0.0025, indicating a sheath depth of 0.0015 m (1.5 mm). If we run the model on NEC-4, we obtain a source impedance of 600.241 - j1.083 Ω.

Remember that the use of insulated wires is normally a pure simulation of the transmission line, a substitute for the construction actually used. Even if we employed Teflon coated wires for our transmission line, we would still need periodic spacers to maintain the line spacing in any application. Hence, the actual velocity factor would be lower in the projected physical implementation of the model.

Our entire foray into the IS command has necessarily used NEC-4, since the command does not exist within standard NEC-2 cores. However, all is not lost using the earlier version of NEC.

A NEC-2 Work-Around for Insulated Wires

In Chapter 13, we passed over LD2 and LD3 loads. We are now in a position to make use of these loads and their particular characteristics as we work toward a way to incorporate insulated wires within NEC-2 models. LD2 loads call for series R-L-C values exactly as did LD0 loads. Likewise, LD3 loads call for parallel R-L-C values in the same manner as LD1 loads. What differentiates the new loads from the more familiar pair is that the units of measure are not simply Ohms, Henries, and Farads. Rather, they are Ohms/meter, Henries/meter, and Farads/meter. Hence, the new loads are suitable for distributed use along a wire or a designated portion of a wire. The load applies to every segment covered by the integer entries, and NEC distributes the load according to the length of each segment.

If we ignore resistance for our purposes, we may create an element in which each segment is inductive or capacitive according to the load value we specify. To sample this phenomenon, let's begin with model *16-8.nec*. This model is a simple copper wire dipole similar to the ones used in the NEC-4 exercises involving insulated wires.

```
GW 1 21 0 -2.416 0 0 2.416 0 .001
GE 0
EX 0 1 11 0 1 0
LD 5 1 1 21 5.8001E7
FR 0 1 0 0 30 1
RP 0 1 360 1000 90 0 1 1
EN
```

If we run the model, we obtain a source impedance of 72.537 + j0.180 Ω. The impedance is the baseline against which we shall compare results from the remaining models in this sequence. Open model *16-8a.nec* and notice the LD2 entry.

```
LD 2 0 0 0 0 1e-7 0
```

The entry places a distributed load of 0.1 μH/m over every segment in the model. Run the model to obtain the source impedance: 75.619 + j47.883 Ω. Obviously, the load has made the antenna electrically longer than its physical length, resulting in a significant inductive reactance in the source impedance. For reference, open model *16-8b.nec*. It has the same load, but in parallel form. However, without other components in the load, the source value will turn out to be the same as for the LD2 version.

```
LD 3 0 0 0 0 1e-7 0
```

Now open model *16-8c.nec*, which uses an LD2 load with a capacitance of 1.0 nF. We use a high value of capacitance to introduce only a small amount of capacitive reactance.

```
LD 2 0 0 0 0 0 1e-9
```

The model returns a source impedance of 59.227 - j227.228 Ω. The antenna is now electrically short by a sizable amount relative to its physical length. Running the corresponding LD3 version of the model, *16-8d.nec* returns the same impedance.

```
LD 3 0 0 0 0 0 1e-9
```

For many applications, we are not concerned with a segment-by-segment analysis of the load accuracy relative to a physical implementation. Rather, we are concerned only to arrive at a value of loading that will achieve a certain simulation goal. In our case, we shall be seeking values of inductance for LD2 loads that will simulate the effects of insulating sheaths on antenna wires. If the relevant performance data matches what we would achieve in NEC-4 using the IS command, then the substitution will be successful.

To arrive at a reasonable correlation, we may use the data that we acquired from the models in the 16-4 through 16-6 sequence, all of which used the NEC-4 IS command. Each model used a wire radius (WR) of 0.001 m in a 30-MHz copper free-space dipole. The differences among the

models involved the depth of the sheath (SD): 0.0005 m, 0.001 m, and 0.002m. The resulting sheath radii (SR) were 0.0015 m, 0.002 m, and 0.003 m, respectively. We shall replicate these models in NEC-2 by dropping the IS commands and introducing a single LD2 command that specifies an inductance of the correct size to achieve the same goal.

If we had both NEC-2 and NEC-4 on hand, we could easily do the job by replacing the IS commands and introducing LD2 commands for each adjusted resonant dipole. We would change the value of inductance required until the dipole again showed resonance within the usual standard where the reactance is less than +/-j1 Ω. In fact, the following table (in part) performs just that task. See the lines marked Zres-repl and A:L/m Zres-repl means the source resistance at resonance for the direct replacement of IS by LD2 in NEC-4, while A:L/m means the LD2 inductance value used where the listed values is multiplied by E-7. The required values center around 1E-7 H.

NEC-2 Insulation using LD2			L/m values x E-7		DP Length = 1/2-length in m			FQ=30 MHz	
TH=0.5 mm; Radius=1.5 mm									
Perm	1	1.25	1.5	1.75	2	2.25	2.5	2.75	3
DP Length	2.416	2.4	2.391	2.383	2.378	2.374	2.371	2.368	2.366
Zres-repl	72.536	71.665	71.238	70.794	70.552	70.355	70.215	70.052	69.961
A:L/m	0	0.185	0.293	0.393	0.452	0.503	0.54	0.577	0.603
Zres-calc	72.537	71.605	71.142	70.681	70.425	70.244	70.081	69.92	69.832
B:L/m	0	0.171	0.289	0.377	0.444	0.499	0.543	0.581	0.613
TH=1.0 mm; Radius=2.0 mm									
Perm	1	1.25	1.5	1.75	2	2.25	2.5	2.75	3
DP Length	2.416	2.391	2.373	2.36	2.351	2.345	2.339	2.333	2.33
Zres-repl	72.536	71.262	70.306	69.618	69.172	68.915	68.605	68.256	68.142
A:L/m	0	0.295	0.515	0.677	0.793	0.867	0.945	1.022	1.06
Zres-calc	72.537	71.185	70.155	69.43	68.957	68.683	68.363	68.011	67.895
B:L/m	0	0.304	0.506	0.66	0.778	0.873	0.951	1.017	1.073
TH=2.0 mm; Radius=3.0 mm									
Perm	1	1.25	1.5	1.75	2	2.25	2.5	2.75	3
DP Length	2.416	2.375	2.348	2.328	2.313	2.302	2.292	2.284	2.278
Zres-repl	72.536	70.405	69.046	68.029	67.275	66.754	66.235	65.829	65.551
A:L/m	0	0.49	0.83	1.088	1.285	1.435	1.57	1.68	1.76
Zres-calc	72.357	70.291	68.832	67.74	66.933	66.367	65.818	65.391	65.096
B:L/m	0	0.491	0.83	1.081	1.276	1.431	1.559	1.667	1.759

However, the exercise would be superfluous if we had access to NEC-4, since we might have simply used the IS command. However, each section of the table has two extra lines marked Zres-calc and B:L/m. Zres-calc refers to the source resistance that results from a calculation of B:L/m by a means that is independent of NEC-4. The equation that we shall use is a modification of an initial formulation by Alexander Yurkov that required the use of the sheath radius as the wire radius. The present reformulation allows the entry of the wire radius in the standard way and also avoids the use of negative values of inductance in the LD2 load for thin, low-permittivity insulation.

$$L/m = 2E\text{-}07 \left(\sqrt[12]{\frac{R}{r} \cdot \varepsilon} \right) \cdot \left(1 - \frac{1}{\varepsilon} \right) \cdot \ln\left(\frac{R}{r} \right)$$

R is the sheath radius, and r is the wire radius, where both are in millimeters (a necessary step for usable values of the natural logarithm). L/m is the required inductance per meter, and ε is the relative permittivity of the insulation. Although the equation appears a bit formidable, there are reusable intermediate results that simplify the actual calculation. For example, you may prepare a table of likely values of ε and hence of the term (1 - 1/ε). Similarly, you may set up tables for the ratio of R to r. Actual calculations then amount to a simple process of picking and multiplying.

The last 2 lines in each section of the data table result from NEC-2 models and therefore show very slightly different figures from the NEC-4 runs. However, in terms of the required inductance per meter, the two are hardly distinguishable, as shown in **Fig. 16-9**.

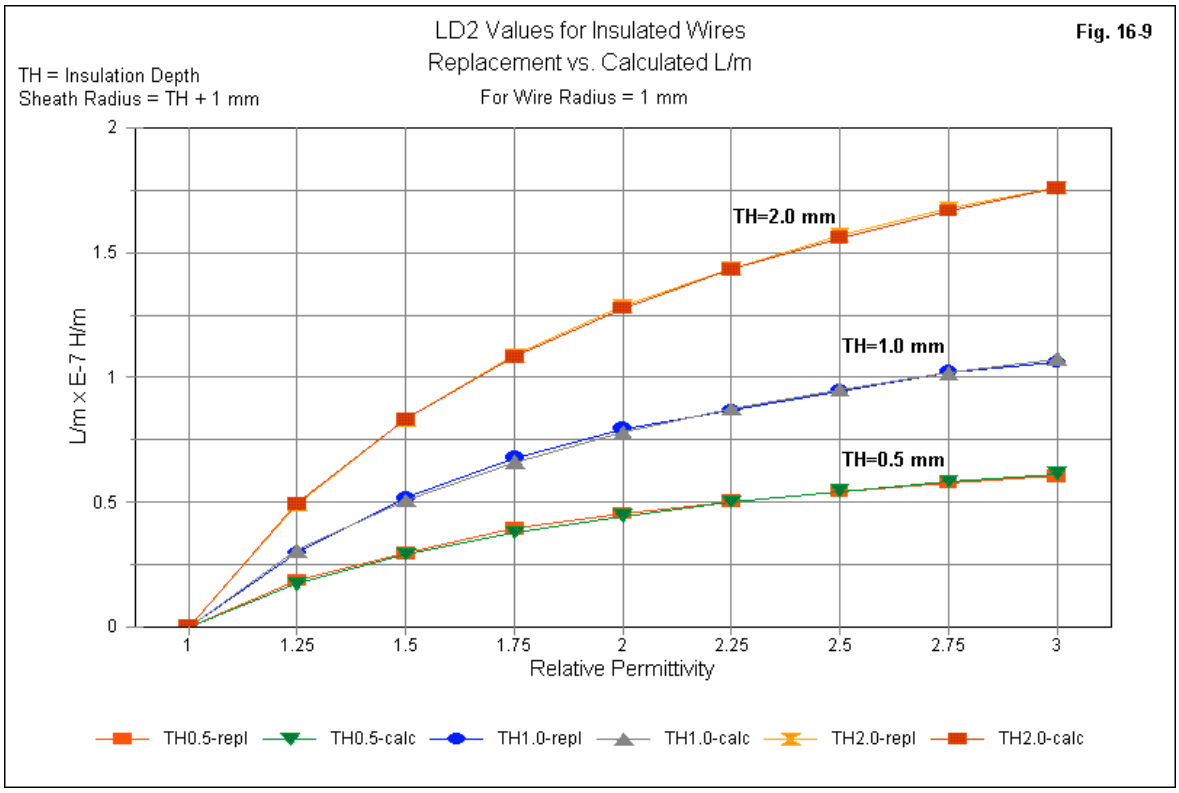

You may replicate the NEC-2 work by opening and running models *16-9a.nec* through *16-9h.nec*, *16-10a.nec* through *16-10h.nec*, and *16-11a.nec* through *16-11h.nec*. The series of models covers all steps of each insulation thickness. You may also use these models in NEC-4 and even replace the LD2 loads with the appropriate IS commands to complete the suggested work for the earlier series of models (16-4, 16-5, and 16-6). Each model includes the adjusted dipole length to arrive at a resonant source impedance.

There is a small but noticeable difference between the source impedance values reported for the NEC-4 IS replacements (and for the original NEC-4 IS-based models) and the calculated versions using NEC-2. **Fig. 16-10** presents curves for the replacement and calculated models as run on NEC-4 and NEC-2, respectively. The largest difference, however, is well under 0.5 Ω, a difference that is unlikely to have any practical significance for most design and analysis efforts.

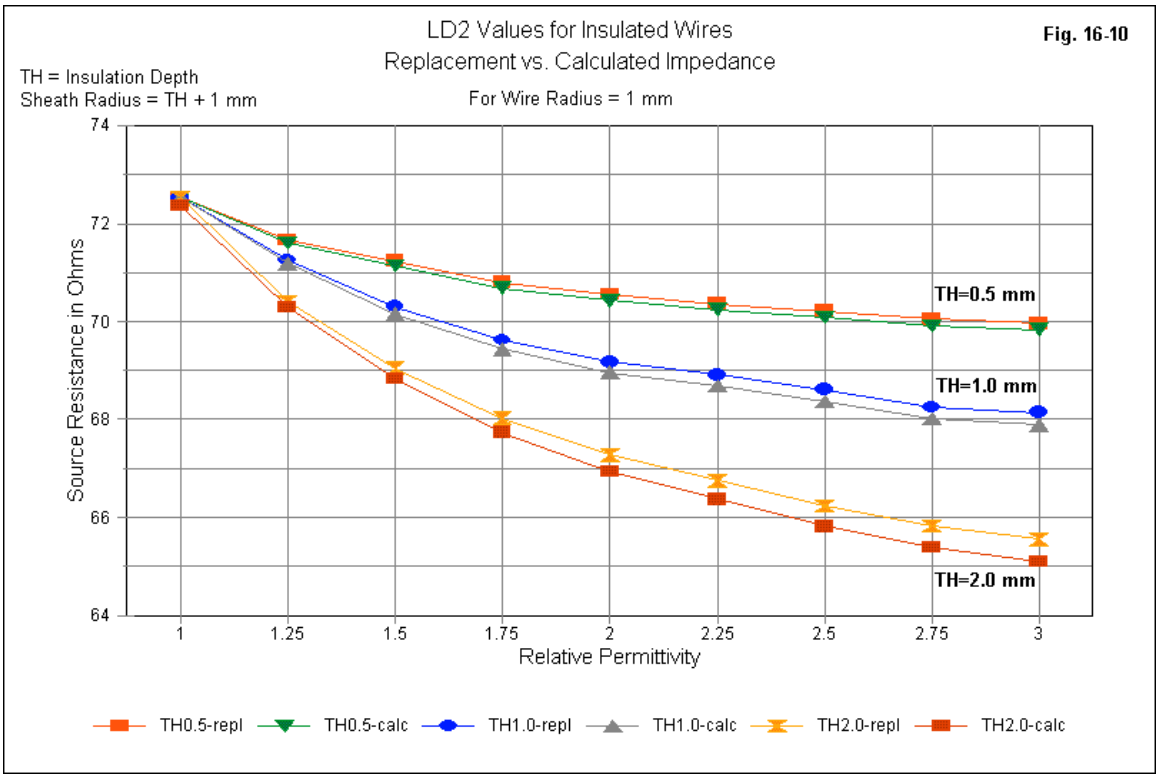

For all practical purposes, then, use of the LD2 load permits us to create the equivalent of insulated wires within NEC. The wires will have the same velocity factor as wires using the IS command in NEC-4. As well, the resulting NEC-2 antenna structures will show just about the same performance as their NEC-4 counterparts.

Every work-around is subject to limitations. This one is no exception. The equation for setting up the LD2 values that replace the values in an IS command is calibrated only to a permittivity of 3.0 and is likely good for some specified range of slightly larger values. Its range of insulating sheaths very likely covers all practical cases for wire antenna use in the HF and lower VHF ranges. The wire size used in the exercise (2-mm diameter) is intermediate between the most popular U.S. antenna wires sizes: AWG #14 (0.0641" or 1.63 mm) and AWG #12 (0.0808" or 2.05 mm). However, use of the equation outside the suggested range remains uncertified.

You may be tempted to apply the technique to coaxial cables used as antenna wires. Many of these antennas attempt to transfer the velocity factor of the cable as a transmission line to its application as a radiating element. Whatever the correctness of transferal in individual cases, modeling these antennas using the LD2 technique or the IS technique may go astray if the section of line involved acts as both a portion of the radiating surface and as a transmission line. Some designs incorporate such lines as part of the antenna's overall length and as phasing stubs or traps. Since the line used is a coaxial assembly consisting of a small tube or cylinder with a central wire, NEC will not likely be able to simultaneously model the transmission line and radiating wire functions of the coaxial cable. As suggested in **Fig. 16-11**, NEC may be able to model such cables used solely as insulated fat wires, that is where both ends are shorted or an open end occurs only at the far end of an element.

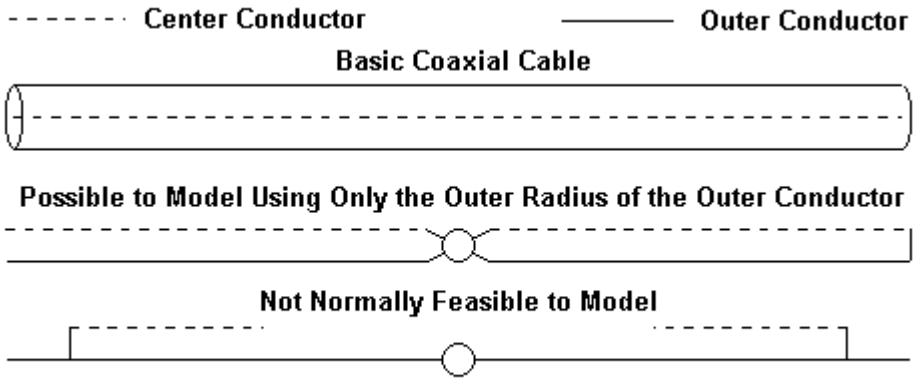

Fig. 16-11

Nevertheless, the NEC-2 work-around for the absence of an IS command remains a valuable tool for the analysis of more ordinary antennas composed of insulated wires.

Summing Up

The commands that we have examined in this chapter include the LD5 material loading or conductivity entry, the IS or insulated sheath command within NEC-4, and the LD2 and LD3 distributed load commands. The concept of antenna-wire velocity factor formed the central theme as the ratio of the resonant length of a loaded or insulated wire to a lossless or bare wire that is also resonant. To examine the antenna properties relevant to its velocity factor required that we transport data from many models to an external calculating or graphing facility, such as a spreadsheet. Although the particular focus of these exercises may have only narrow relevance, the general practice of coalescing bodies of model data will prove both common and necessary.

Our look at the LD5 command completed work begun in an earlier chapter by surveying the range of conductivity values of typical materials used in antenna construction. For any given wire size, the rate of performance decrease with the decrease in conductivity is not linear. Rather the rate of decrease climbs as the conductivity decreases. As well, the thinner the wire as a fraction of a wavelength, the greater the effects of a decreasing conductivity.

Loaded or "lossy" conductors show a small velocity factor relative to a lossless wire. More dramatic is the velocity factor of an insulated wire relative to a bare wire. NEC-4 is able to show this phenomenon clearly by use of the IS or insulated sheath command. To use the command, we must enter the radius of the sheath or insulation, which must be higher than the radius of the wire itself. As well, we enter values of conductivity and permittivity, although for most modern wire insulation materials, the conductivity can be a reasonably arbitrary low value, such as 1E-10. In the main, the combination of insulation thickness and its permittivity are the main controlling factors that require a physical length reduction relative to a bare wire with the same properties. The requirement to shorten the antenna physically also reduces the resonant feedpoint impedance of an insulated wire. This use of the IS command is applicable not only to radiating wires, but as well, to physically modeled transmission lines.

Although NEC-2 does not have the IS command, we can simulate insulated wires by use of the LD2 or LD3 command. These loading commands employ resistance, inductance, and capacitance units of measure per meter, and therefore are useful in distributing a level of loading across a span of segments, for example, the entire length of an antenna elements. By calculating the correct value of inductance per meter, we can create the same velocity factor in a wire that we meet with a corresponding combination if insulation permittivity and sheath thickness. Like all work-arounds, the technique has limitations. However, for many practical problems, it is very usable.

17.
Special Radiation Pattern Data

***Objectives**: Our return to the RP command will focus on three types of outputs. One is the full free-space sphere or the hemisphere over ground, useful for surface and gain-averaging plots. Second is the RP1 command for ground waves. The last is a sample of data that we can develop in post-core-run calculations to yield special pattern information.*

In Part B, Chapter 9, we gave extended treatment to the RP0 command. However, we did not exhaust all of the potential of that command. There are a number of items worth reviewing, along with some other matters that we may draw together into a more cohesive picture. For example, the 3-dimensional surface plot, the calculation of radiation efficiency, and the average gain test all share some common features when invoking the RP0 command. So we shall begin our work by reviewing and extending what we have already done.

We specifically omitted the RP1 version of the command. (NEC-2 has a large number of RP options, since the second ground medium is tied to the RP request. However, NEC-4 reduces all options to the RP0 far-field request and the RP1 ground wave request.) We shall not only see how to enter that command and to read its output, but as well, we shall learn something of its special features.

Not everything that we can learn from an antenna model appears in the NEC output report. Further post-run processing of data is possible to formulate data in other and possibly more useful ways. As a sample of what we can do, we shall examine the calculation of circular polarization power-gain components that are useful for dissecting the patterns of axial-mode helices and other antenna producing circular or elliptical polarization.

Special Far-Field Output Data

Reviewing the far-field command begins with the structure of the command itself.

```
Cmd   I1    I2    I3    I4    F1      F2    F3    F4    F5    F6
      I1    NTH   NPH   XNDA  THETS   PHIS  DTH   DPH   RFLD  GNOR
RP    0     1     361   1000  90      0     1.00  1.00  (NU)  (NU)
```

When used as a request for a normal phi or theta pattern, the command calls for a series of specifications: a pair of initial bearings (THETS and PHIS in degrees), a pair of increments between successive bearings (DTH and PTH in degrees), and the number of steps in each coordinate sequence (NTH and NPH). Although the initial angle and the increment between angles may use decimal entries, the number of steps must be an integer. The far-field distance in meters (RFLD) is optional and useful only when we need a calculated value for the electrical field at a specific location. GNOR, the gain normalization level other than the maximum value in the

pattern, is a special purpose call.

Open model *17-1.nec*, and examine the 2 RP0 requests for this vertical dipole in free space.

```
CM Vertical dipole
CM free space
CE
GW 1 11 0 0 .2625 0 0 .7375 .001
GE
FR 0 1 0 0 299.7925 1
EX 0 1 6 00 1 0
RP 0 361 1 1000 -90 90 1.00000 1.00000
RP 0 1 361 1000 90 0 1.00000 1.00000
EN
```

The first request is for a 360° theta pattern, using a single phi-angle specification (90°). The second request is for a 360° phi pattern using a single theta-angle specification (90°). Note that for each full circle, we specify the result of dividing the circle (360°) by the selected increment plus one more step. The goal is a pair of 2-dimensional plots, each of which covers a selected circle of the pattern sphere presumed to surround the antenna. **Fig. 17-1** shows the antenna in all of its simplicity, along with the resulting patterns.

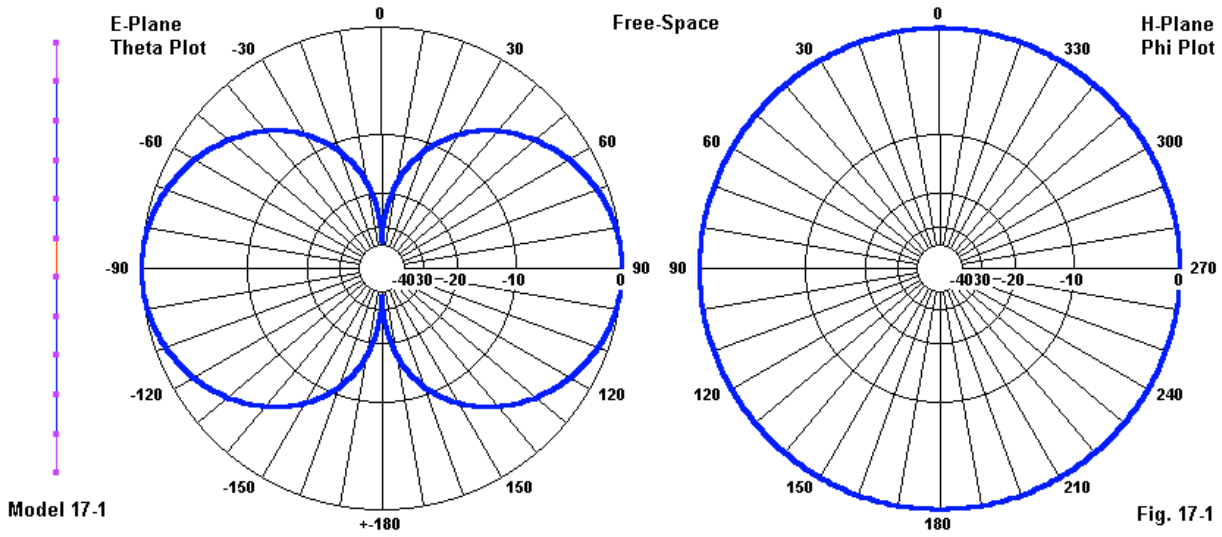

Since the dipole is vertical relative to a presumed ground, the theta plot presents the E-plane pattern, while the phi plot gives us the H-plane pattern. We may produce as many of these patterns as we wish. In practical terms of software limitations, it is usually wise to use successive commands for each 2-dimensional plot that we wish. For an array with a complex radiation pattern, we may take numerous "cuts" using as many theta or phi patterns as may satisfy the need. If we need frequency sweeps, we must re-introduce the multi-frequency FR command prior to each RP command.

Over ground, we make small but critical amendments to the phi and theta pattern requests to arrive at our patterns. First, no theta pattern can extend below ground, forcing us to a half-circle

plot. Second, there will be no phi pattern at the horizon (theta = 90°). Instead, we normally take an interest in some angle above the horizon, perhaps the take-off angle or a specified angle of propagation in the HF range. Open model *17-1a.nec*, the same antenna using an SN average ground.

```
GN 2 0 0 0 13.0000 0.0050

RP 0 181 1 1000 -90 90 1.00000 1.00000
RP 0 1 361 1000 76 0 1.00000 1.00000
```

The GN command shows the ground specifications. The first RP entry requests a theta pattern with 181 1° steps, enough to go from one horizon to the other. The second RP command asks for a phi pattern for the full circle, but at a theta angle of 76° (that is, 14° above the horizon). **Fig. 17-2** shows the results of our entries. Again, we may make as many requests as we wish to make, so long as we observe the frequency-sweep loop limitations.

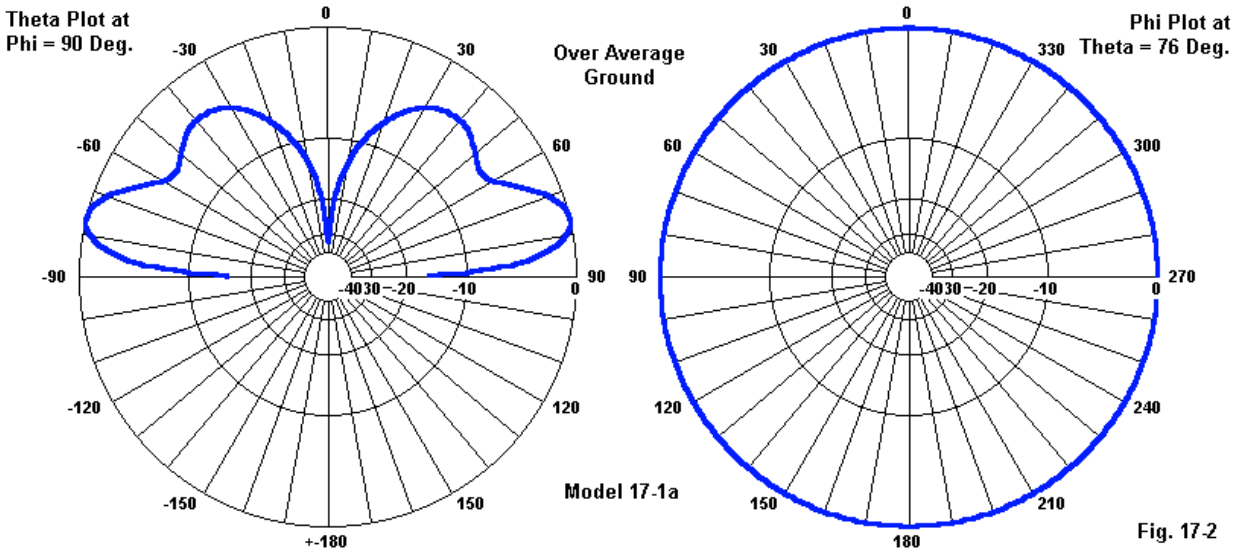

Fig. 17-2

There is no rule within NEC that forbids us from requesting multiple theta angles and multiple phi angles within the same RP request. Open model *17-2.nec* for a sample.

```
RP 0 91 361 1000 0 0 1.00000 1.00000
```

Model 17-2 is the same vertical dipole over the same ground as in model 17-1a. However, the RP0 command now requests a full hemisphere of pattern samples, with 91 theta angles and 361 phi angles. Run the model. First, examine the radiation pattern data section of the NEC output report. Note that NEC runs all of the requested theta angles at the first phi angle, then all of the theta angles at the second phi angle, etc. The result is a mass of information occupying 90% of the report. Selectivity has advantages when ordering the output information.

Next, request a polar plot. At this point you will encounter a practical software limitation. The polar plot facility in GNEC and NEC-Win Pro can handle up to 100 simultaneous plot requests. However, even for 1 frequency, there will be over 450 pattern possibilities. If you perform a

frequency sweep, multiply the total by the number of frequencies requested.

Nevertheless, the RP0 request shown does have important uses. For example, it is precisely the form used for a 3-dimensional surface plot, as shown in **Fig. 17-3**.

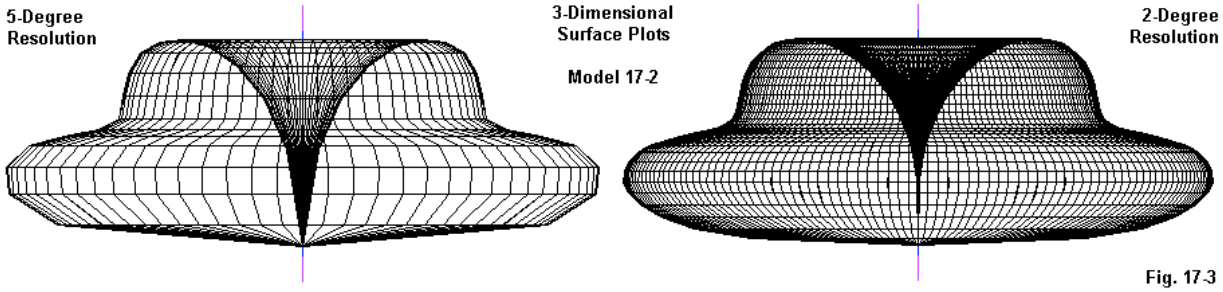

Fig. 17-3

GNEC and NEC-Win Pro delegate the 3-D pattern to a special function. It creates a special temporary file to contain the NEC output data and then deletes the file when you are finished working with the pattern. The graphic also illustrates a special feature of the function: your option to select the increment between steps of the pattern. The 5° option makes virtually every detail of the pattern clearly visible, but at theta angles close to the horizon, the smooth pattern transitions become sharply angular. The 2° option smoothes the angularity, but increases the number of lines so that some plot details may disappear.

The pattern shown is for an antenna above ground, which requires a hemispherical request. For a free-space pattern, we would input the required coordinates for a full sphere.

Above ground RP0:

```
RP 0 91 361 1000 0 0 1.00000 1.00000
```

Free-space RP0

```
RP 0 181 361 1000 0 0 1.00000 1.00000
```

To obtain a radiation efficiency value, we would use the hemispherical RP0 request, as in model *17-2a.nec*. The special feature in this request is the XNDA specification of 1002. Both 1001 and 1002 request gain averaging, but 1002 also suppresses printing of the radiation data.

```
RP 0 91 361 1002 0 0 1.00000 1.00000
```

Run the model to obtain the average power gain: 7.5684E-1. Since radiation efficiency will be half this value times 100, we calculate a radiation efficiency of 37.84%.

The RP0 hemisphere and the RP0 sphere both play roles in obtaining a value for the average gain test. Again, this data emerges from a special function in GNEC and NEC-Win Pro. The command uses the XNDA = 1002 entry. Normally, the version of the model run under the test function also adds a PT command set to -1 in order also to suppress the printing of currents. In large models, data printing suppression can shorten the core run time needed to produce a value.

The average gain test or AGT has some special features. It is a measure of model adequacy based on the fact that an ideal model, when free of resistive losses, will radiate all of the input

power. Hence, the average power gain in free space will be 1.0 and the average power gain over a perfect ground will be 2.0. To perform the test, the special function sets all resistive loading to zero, no matter the type of LD entry in which resistance appears. The result is a model whose radiation depends entirely on the structure geometry (with all of the constraints upon segmentation and its relationship to wire radius, as well as other known sensitive condition). Inadequate models may yield average power gains either above or below the ideal value.

Run the AGT test using the perfect ground option and 1° increments to set up the RP0 request that we have been using. The AGT or average power gain value is 1.99358. You may modify the model itself to arrive at your own NEC output report value for the same test by changing the ground type to perfect and by ensuring that XNDA is 1002. The model has no losses other than the initial ground specification.

Besides power data, we may derive from RP0 commands information on the electrical field. The required modification that we must make to our continuing vertical dipole model is to add an RFLD entry to specify a distance from the coordinate system origin, the presumed approximate location of the antenna. Open model *17-3.nec* and examine the RP0 request.

```
RP 0 181 1 1000 -90 90 1.00000 1.00000 100
```

The last entry calls for a distance of 100 meters from the origin. The distance must be well into the far field for accuracy, which is not a concern at the test wavelength of 1 m. Regardless of the units used in setting up the geometry, the RFLD entry must be in meters.

Run the model, but do not bother with the radiation pattern electric field information at this time. Most such information is useful only when we set the excitation to a certain level, for example, 1000 w. Hence, for this run, the data of interest is the input power: 7.25764E-3 w. If we take the square root of the ratio of the 1000-w desired power to the current power for a 1-volt source, we can arrive at the required excitation voltage: about 371.2 volts peak. Open model *17-3a.nec* and look at the EX0 command. We now wish to know the electric field strength at a distance of 100 meters for a source power of 1000 watts.

```
EX 0 1 6 00 371.19617 0
```

Run the model and examine the electric field information. Because the antenna element is vertical relative to the ground, The Ephi values are all too small to show a value greater than 0. However, the Etheta voltage values vary as the theta angle changes. The highest value occurs at the take-off angle (theta = 76°): 3.0357E0 peak volts/meter. You may wish to modify the model, using a variety of distances for RFLD and a variety of excitation power levels. However, save the original model 17-3a, because we have one more task for it.

You may plot electric fields within GNEC and NEC-Win Pro as rectangular graphs. The model requested a full 180° theta pattern, so such a graph would give you a view of the electric field strength at every theta angle, where -90° represents one horizon and +90° represents the other. Examine **Fig. 17-4** and project the curves onto the theta pattern in **Fig. 17-2** or in **Fig. 17-3**. As a passing matter, although perhaps not insignificant, note the relatively high values of electric field strength at the take-off angle as far away from the antenna as 100 meters with a commonly used power level: 1000 watts.

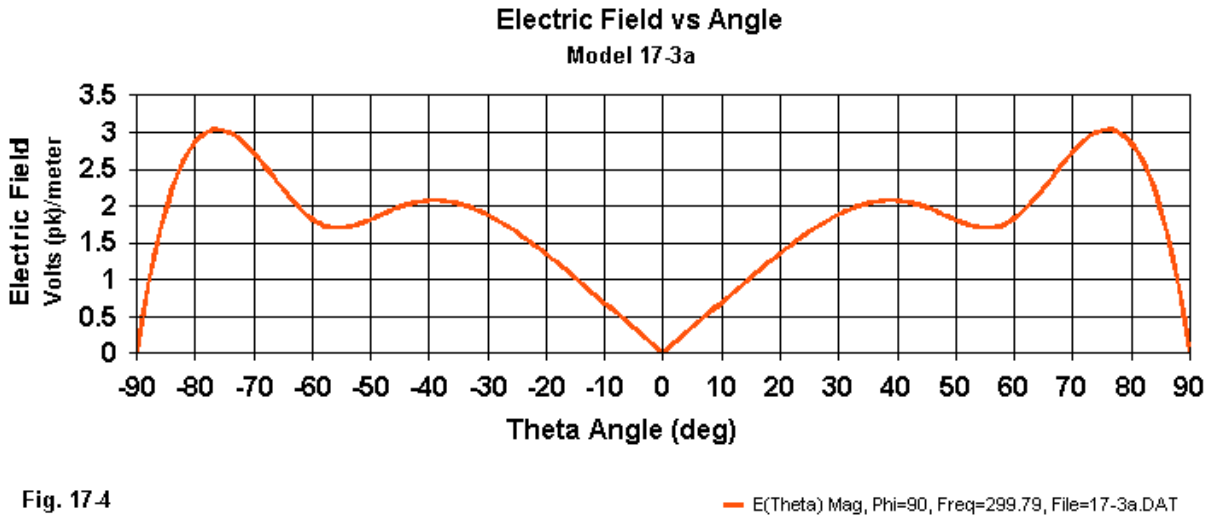

Fig. 17-4

Our review of the RP0 command allowed us to draw together several ordinary and special uses of the command when we set it up for a full sphere (in free space) or hemisphere (over ground). Our quick review of the RFLD entry has not been superfluous, since that feature will be integral to our next set of exercises involving the RP1 or ground wave option. So too will be setting a standard power level for comparative data.

The RP1 Command Option

When used for ground wave analysis, the RP command changes the meaning of some of its entries.

```
Cmd   I1    I2    I3    I4    F1      F2    F3    F4    F5    F6
      I1    NTH   NPH   XNDA  THETS   PHIS  DTH   DPH   RFLD  GNOR
RP    0     1     361   1000  90      0     1.00  1.00  (NU)  (NU)
                                z                       ρ
RP    1     1     37    0000  0       0     1.00  10.00 100   (NU)
```

The example compares a rather ordinary far-field request with a ground wave entry. The phi entries maintain their meanings. NPH is the number of phi steps; PHIS is the starting phi angle, and DPH is the increment between phi angles. However, the theta entries change their orientation. Instead of registering theta degrees, they measure distances in the X-Y plane, beginning at Z = 0. Hence, they create a cylinder whose radius is defined by the RFLD entry, always in meters from the coordinate system origin and designated ρ. Then, THETS records the starting height above zero (designated z) and may include zero, as it does in this example. NTH is the number of sampling points, beginning with THETS and proceeding straight upward. Since there is only 1 sampling point, DTH--the increment between samples in meters--can be any arbitrary number. The result is a request for ground-wave analysis at a point 100 meters from the coordinate origin at ground level. For ground waves, the first digit of XNDA makes no difference.

Since the distance in the X-Y plane (ρ) and the height above ground (z) work with cylindrical coordinates, the distance that you enter does not record the distance to the observation point unless that point is at ground level. The actual distance to the observation point (d) is the square root of $\rho^2 + z^2$.

To see how the RP1 request integrates into an entire model, open model *17-4.nec*.

```
GW 1 11 0 0 0 0 0 4.85 .001
GE 1
GN 1
FR 0 1 0 0 15 1
EX 0 1 1 00 269.19 0
RP 0 181 1 1000 -90 90 1.00000 1.00000 100
RP 1 1 37 0000 0 0 1.00000 10.00000 100
EN
```

The model is for a 1/4λ monopole that touches a perfect ground at the coordinate center. The model has two RP commands: a far-field theta pattern and an RP1 ground-wave request that uses the 100 meter distance and ground level as the single read-out height for 37 equally spaced readings in the phi plane. The test frequency is 15 MHz, where its wavelength is about 20 meters.

The observation point is about 5λ from the antenna. For highest accuracy, ground wave requests should be more than 1λ away from the source. Ground wave analysis uses far-field approximations plus a surface wave calculation. In other words, the ground wave calculation includes both surface wave and space wave components. As the frequency and the distance increase, the surface wave component diminishes to a level where the only significant component may be the direct (or point-to-point) sky wave. As we shall see, there is also a considerable difference in the ground wave between vertically and horizontally polarized antennas.

Model 17-4 is actually a second-run model. The first run established the source impedance (36.228 + j0.372 Ω) and the associated input power with a 1-v source. However, virtually all ground wave analyses will need a set power level. 1000 w is the value used throughout these exercises. In the version of the model shown, an EX0 voltage of 269.19 v achieves that power.

```
                    - - - RADIATED FIELDS NEAR GROUND - - -

  - - - LOCATION - - -     - - E(THETA) - -      - - E(PHI) - -      - - E(RADIAL) - -
RHO     PHI        Z         MAG      PHASE       MAG      PHASE        MAG      PHASE
METERS  DEGREES   METERS   VOLTS/M   DEGREES    VOLTS/M   DEGREES     VOLTS/M  DEGREES
100.00    0.00    0.00    4.4291E+00   86.57   0.0000E+00    0.00    0.0000E+00   0.00
```

The output report has the form of the 1-line sample shown above. Since the monopole has a symmetrical pattern, all of the remaining 36 lines have the same data, since each observation point is at the same distance from the origin and the same height. Since the monopole is vertical and above a perfect ground, the only entry with a value above zero is Etheta, essentially the vertically polarized electrical ground-wave field strength in peak volts/meter.

For the contrast, let's create a 15-MHz horizontal dipole at 1λ above the same perfect ground. We shall sample the ground wave at ground level at a distance of 100 meters, using 73 points in a half phi circle (since the dipole pattern is the same in the other half circle). Open model *17-5.nec*.

```
GW 1 21 0 -4.88 19.986 0 4.88 19.986 .001
GE 1
GN 1
FR 0 1 0 0 15 1
EX 0 1 11 00 378.837 0
RP 0 181 1 1000 -90 0 1.00000 1.00000 100
RP 1 1 73 0000 0 0 1.00000 2.50000 100
```

The model has one other difference. The dipole requires a source voltage of 378.837 peak volts to achieve a 1000-w input with an impedance of 71.758 + j0.174 Ω.

The output report differs in several important respects from the one for model 17-4. First, the significant readings occur in the Ephi column, since the antenna is horizontally polarized. However, the Etheta readings are not so low as to be unreportable. They are just too low to be significant to the overall field strength 100 meters away at ground level. Second, the Ephi readings change at every new phi angle, in tune with the overall pattern of the dipole, with its bi-directional broadside lobes. Finally, even the strongest field-strength value is many orders of magnitude less than the vertical monopole field strength at the same distance from the antenna.

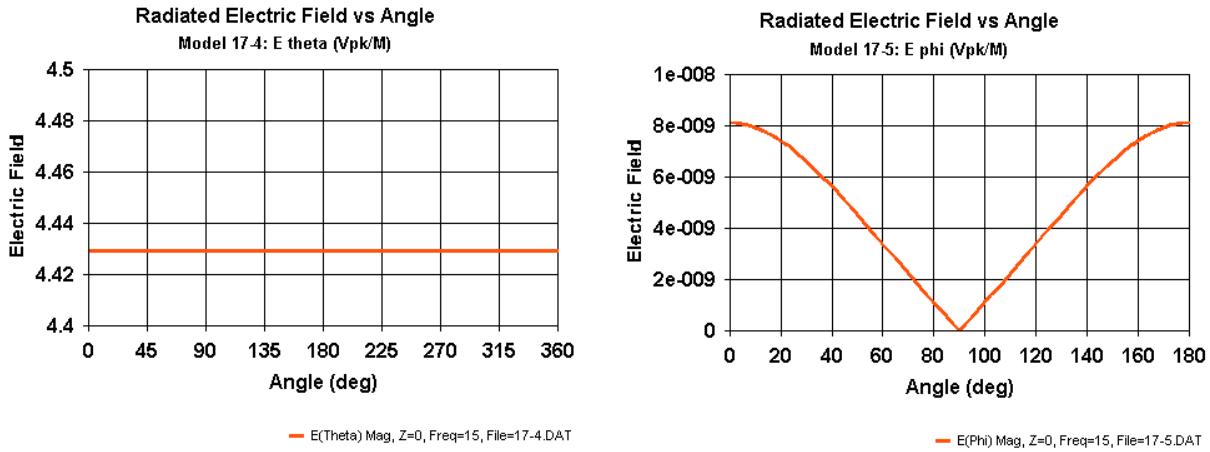

Fig. 17-5 compares rectangular plots of the two test cases. On the left, the full phi-circle plot shows the constant field-strength at about 4.43 peak volts/meter. On the right, the 180° plot tracks the pattern from one lobe peak to the other lobe peak, with virtually zero field strength off the antenna ends. The peak value is about 8.1E-9 peak volts/meter.

If we introduce a real or lossy SN ground to the ground-wave analysis, we must take into account more than just the horizontal and vertical components of the ground wave. As shown at the left of **Fig. 17-6**, we have a radial value to consider, taken along a line from the system origin to the observation point. You may use ρ and z to calculate not only the length of the radial line, but also the angle above the horizon. (Of course, you may also convert that elevation angle into a theta angle by subtracting the elevation angle from 90°.) All three field-strength components have phase angles that may differ from each other. Hence, arriving at a peak value is not a simple calculation. If ρ and z define the cylinder-based observation point, then we may have field strength values along 3 axes that define that point.

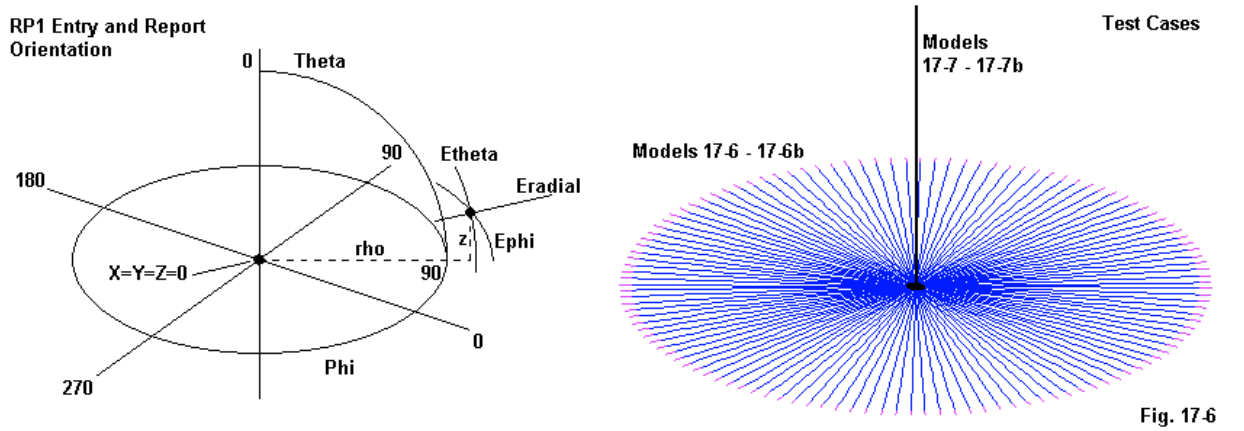

Fig. 17-6

To make a significant example, however otherwise limited, let's move the test frequency to 1 MHz, about the center of the U.S. AM broadcast band. The typical radial field for antennas in this region consists of 120 radials, each about 1/4λ long, although site and engineering considerations may call for other lengths in some cases. Then we have the antenna itself, a 1/4λ monopole with an actual height of 74 m above ground. For simplicity, we shall use 2-mm diameter wire throughout the exercise, however unrealistic that may seem. See the right side of **Fig. 17-6**.

If we work with NEC-2, then our radial system must be placed above ground level. A height of 0.02998 m above ground is 1e-4λ and allows a 3-radius clearance distance for the radial wires. The radials will use 25 segments per wire. We shall also specify three different ground qualities. Very good soil will have a conductivity of 0.0303 S/m with a permittivity of 20. Average soil will use 0.005 S/m and 13 as its values. Finally, very poor soil will enter values of 0.001 and 5 for the ground constants.

Even without the antenna, it appears that we have 3 very large models each with 3000 segments. However, we shall use a short-cut to the required run time by first setting the radials into a model that writes an .NGF file, as we did in Chapter 6. We shall also make use of the rotational symmetry command to create the radials wires, per the work we did in Chapter 5. We might create a single model for all three soil conditions, changing the GN entry with each run. However, for this exercise, examine models *17-6.nec*, *17.6a.nec*, and *17-6b.nec*. The first of the three has the following form.

```
GW 1 25 0 0 .02998 0 74.95 .02998 .001
GR 1 120
GE
GN 2 0 0 0 20 .0303
FR 0 1 0 0 1 1
WG radials-vg
EN
```

The only differences among the 3 models are the GN entries and the file names in the WG command. The use of the combination of GR and WG commands results in two significant savings. First, the run time for the radial file is 10 seconds or less, even on a slow PC. Second, the storage space required for the partial results is only about 1.7 MB, compared to perhaps 140 MB for a radial system created using the GM command or a very large number of GW entries.

Once the NGF files exist, you may use them for any number of antennas atop the radial field.

The second part of the work consists of creating one or more models for the monopole. Once more, we might use a single model and change the file name in the GF command before each new run. However, for reference, we shall use 3 models: *17-7.nec*, *17-7a.nec*, and *17-7b.nec*.

```
GF 0 radials-vg
GW 201 21 0 0 .02998 0 0 74 .001
GE 1
EX 0 201 1 00 277.1 0
RP 0 181 1 1000 -90 90 1.00000 1.00000
RP 1 1 1 0000 2 0 1.00000 1.00000 1000
EN
```

The GF command is the first geometry entry, followed by any additional structures. In this case, we have only the 74-m monopole wire. The tag number is arbitrary, selected to be larger than the largest tag number within the radial field. The RP commands include both a far-field theta request to check the antenna gain and take-off angle and a ground-wave request with ρ = 1000 m and z = 2 m. As with the preceding models in this exercise set, we shall make 2 model runs in order to reset the excitation voltage to a level that gives us 1000 w input power. Each model will display a slightly different source impedance and thus require a unique excitation voltage to maintain equal power input levels. Note that the model does not specify the frequency or the ground conditions, since those commands appear in the model that wrote the NGF file.

Depending upon PC speed, the models require between 1 and 3 minutes of run time. The required run-time is far lower than for models that include all 3021 segments in the same model using no symmetry. Hence, even a double run to set the power level is not a significant delay. The following table summarizes the results of the runs on the sequence of models, where VG means very good soil, Ave means average soil, and VP means very poor soil.

Ground Quality	Gain dBi	TO Angle degrees	Impedance R +/- jX Ω	Etheta peak V/m	Ephi peak V/m	Eradial peak V/m
VG	3.56	74	35.9 + j9.5	4.35E-1	2.76E-14	1.85E-2
Ave	1.76	69	37.9 + j6.3	3.83E-1	9.48E-14	3.96E-2
VP	-0.35	64	35.6 + j2.5	2.82E-1	6.32E-13	6.33E-2

The more familiar gain and take-off angle data follow normal expectations. However, for some soil qualities, the source impedance is lower than the value for a monopole with a perfect ground. We would ordinarily expect at least a slightly higher value, but the elevated radial system cannot incorporate losses from wires in contact with the ground. The less familiar data on the field strength shows the dominance of the Etheta values, with a decrease in strength at the 1000-meter distance that coincides with the worsening soil quality. Note that there is also a radial field strength value well below the level of Etheta, but very much stronger than Ephi.

Although NEC-2's slightly elevated radials are often used to simulate buried radial system, those using NEC-2 can only wonder to what degree they are a satisfactory simulation. Those with NEC-4, of course, can create buried radial systems. Let's run through that exercise, noting mostly how it must differ from the NEC-2 models. The soil conditions will remain the same, resulting in 3 radial models that will write new NGF files. Open models *17-8-nec4.nec*, *18-8a-nec4.nec*, and *18-*

8b-nec4.nec.

```
GW 1 25 0 0 -1 0 74.95 -1 .001
GR 1 120
GE
GN 2 0 0 0 20 .0303
FR 0 1 0 0 1 1
WG bradials-vg
EN
```

The radial system is 1 meter below ground level. Although that depth is lower than most radial systems, it will not make a significant difference to the outcomes at 1 MHz. As well, the radials retain their 25 segments, even though the vertical sections of the array will use a segment length of 1 m. You may wish to develop modified models in this sequence to check whether we obtain any significant changes from using a shallower depth for the radials and whether we need additional segments in the radials. To reduce the total segment count without harming accuracy, you may employ the GC wire-continuation command (chapter 3) to length-taper both the radial and the aboveground monopole wires.

The upper portion of the system appears in model *17-9-nec-4*, *17-9a-nec-4*, and *17-9b-nec-4*.

```
GF 0 bradials-vg
GW 201 1 0 0 -1 0 0 0 .001
GW 202 73 0 0 0 0 0 73 .001
GE -1 0 0
EX 0 202 1 00 287.139 0
RP 0 181 1 1000 -90 90 1.00000 1.00000
RP 1 1 1 0000 2 0 1.00000 1.00000 1000
EN
```

The vertical portion of the antenna consists of two wires. The first connects the hub of the buried radials to the ground level. The second extends the vertical above ground to a height of 73 m. The total vertical length above the radials is 74 m. The excitation is on the lowest segment of GW202. If we run these models, we obtain the following reported values.

Ground Quality	Gain dBi	TO Angle degrees	Impedance R +/- jX Ω	Etheta peak V/m	Ephi peak V/m	Eradial peak V/m
VG	3.19	74	39.1 + j9.1	4.18E-1	5.24E-18	1.78E-2
Ave	1.86	69	38.2 + j9.2	3.90E-1	3.72E-17	4.01E-2
VP	-0.20	64	36.5 + j7.0	2.85E-1	3.51E-16	6.37E-2

The gain range is somewhat smaller with the buried radial model, but not remarkably so, as shown in the comparative patterns in **Fig. 17-7**. All of the source impedance values are higher than for a perfect-ground monopole. In terms of field strength, the most notable effect of using buried radials is the reduction in the Ephi values, although they began and remain nearly insignificant.

These models, of course, are not suitable for deciding any issues. Their purpose is to show how both RP0 and RP1 requests integrate within a single model that also employs a number of other modeling techniques.

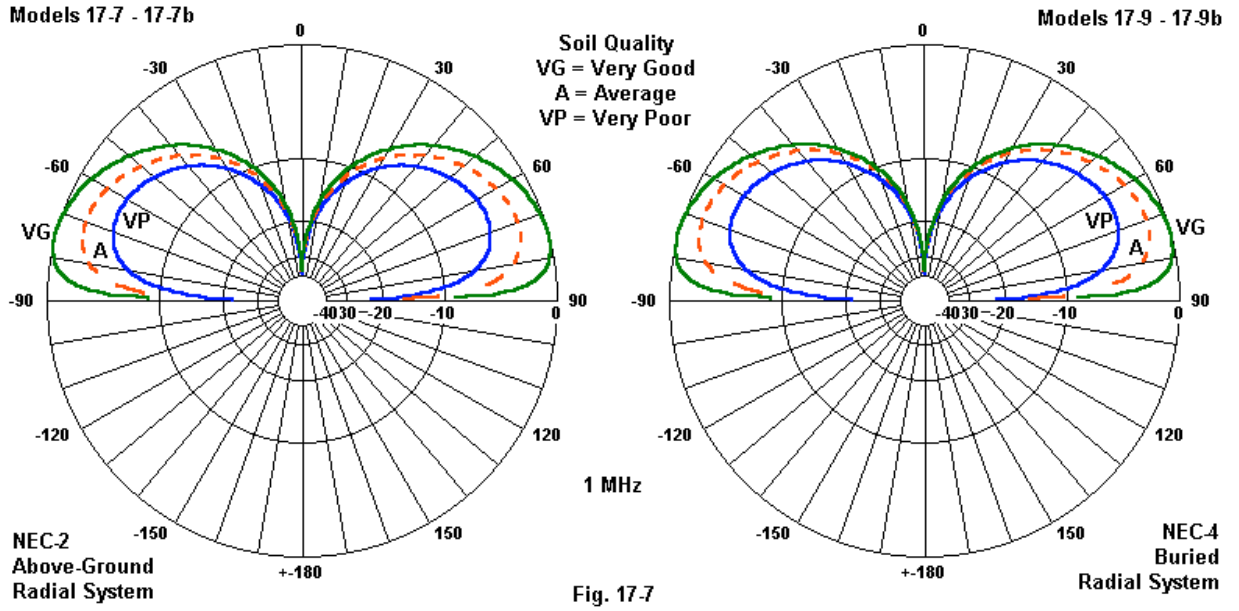

Fig. 17-7

Supplementary Far-Field Data Calculations

In its RP0 or far-field output report, NEC provides a good bit of information. To illustrate, I have extracted a single line from a 180-degree theta (elevation) report for an axial-mode helical antenna.

```
                        - - - RADIATION PATTERNS - - -

 - - ANGLES - -           - POWER GAINS -          - - - POLARIZATION - -
THETA     PHI          VERT.    HOR.     TOTAL       AXIAL      TILT   SENSE
DEGREES   DEGREES        DB       DB       DB         RATIO      DEG.
  0.00    90.00      10.39     3.84    11.261      0.46544     -3.89  RIGHT

          - - - E(THETA) - - -      - - - E(PHI) - - -
         MAGNITUDE     PHASE       MAGNITUDE     PHASE
          VOLTS        DEGREES       VOLTS       DEGREES
         1.00721E+00    -99.56    4.73544E-01    163.94
```

The report line begins with the theta and phi angles for the pattern position. The next three entries are the ones most printed along with polar plots: the power gains in dBi for the total field, the horizontal component, and the vertical component. The component powers add up to the total field power level, however, not by direct addition of dB. Rather, we must first convert the values in decibels into dimensionless power gain, using the standard procedure of dividing the value in dB by 10 and taking the antilog (base 10) of the result. The horizontal gain is 10.94, while the vertical gain is 2.42, for a total of 13.36. The dimensionless power gain of the total field is 13.37, although this simple exercise must allow for rounding of the original double-precision calculation numbers.

The central columns are relevant to elliptically polarized antennas. Although very important to numerous applications involving elliptical polarization, we shall pass over them in this exercise. Basic explanations of the terms "axial ratio" and "tilt angle" appear in many basic college antenna texts. Perhaps the most important function of this data within this exercise is to remind us that even axial-mode helices yield elliptically rather than circularly polarized patterns, where a perfectly circularly polarized pattern would have an axial ratio of 1.0. Although ideally, a linearly polarized pattern would have an axial ratio of zero, NEC will classify a pattern as linear when the minor axis is many orders of magnitude smaller than the major axis so that a practical calculation of the value results in a zero value. Apparently, to avoid excessively large numbers, NEC inverts the classic or textbook definition of axial ratio to "minor axis over major axis."

Relative to the central set of three columns, our interest is in the last entry, the sense. It tells us whether a circularly or elliptically polarized antenna has right-hand (clockwise) or left-hand counterclockwise) polarization. (The terms "clockwise" and "counterclockwise" are apt only if we view the antenna from the source end toward the most forward end.) Since virtually no antenna will produce a pure circularly polarized signal that is only one or the other hand, the sense tells us which pattern will dominate--the left-hand or the right-hand pattern.

Open model *17-10.nec*, using either the NEC-2 or NEC-4 version. Since the calculations to follow are based on the NEC-4 version, we may begin with it.

```
CM General Helix over Perfect Ground
CE
GH 1 100 5 .6959 .191 .191 .0005 .0005 0
GE 1 -1 0
GN 1
EX 0 1 1 0 1 0
FR 0 1 0 0 299.7925 1
RP 0 181 1 1000 -90 90 1.00000 1.00000
EN
```

The third numeric entry on the GH line is positive (and records the number of turns in this NEC-4 version). Hence, the helix formed is a right-hand helix with a dominant right-hand polarization.

The NEC-2 version of the same model uses the following GH entry to achieve the same right-hand polarization.

```
GH 1 100 .13918 .6959 .191 .191 .191 .191 .0005
```

Review Chapter 4 if the differences in entry format are not clear. The key difference is that NEC-4 uses the number of turns as an entry, while NEC-2 uses the spacing between turns.

Fig. 17-8 shows the outline of the helix, along with circularly polarized patterns taken from the NSI Multi-Plot function. These patterns use a linear reference scale, but are normalized to the maximum value for each pattern. Hence, their peak values are very different.

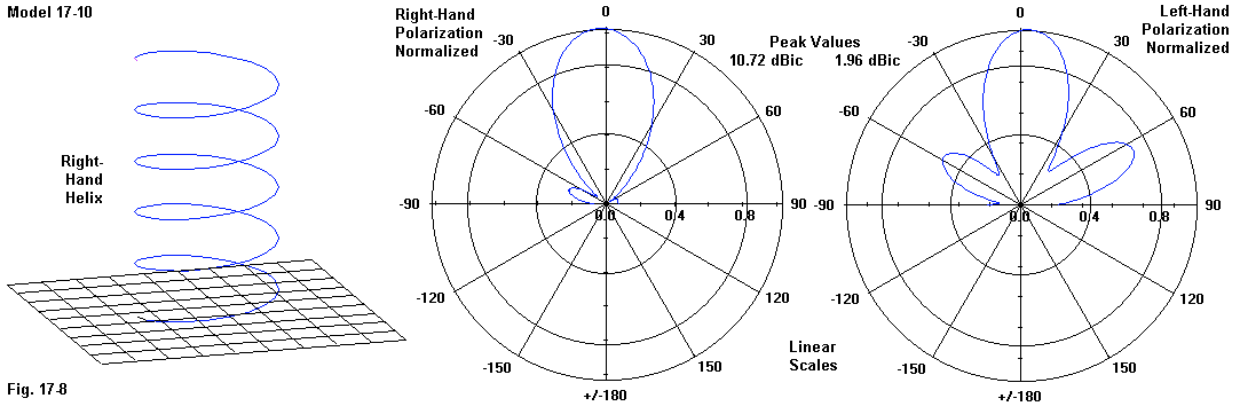

Fig. 17-8

The sample output report line with which we started is for the zenith angle overhead and the helix is pointed straight up. Hence, we might believe that the total field value is the maximum gain. However, because the pattern for the axial-mode helical antenna is a combination of left-hand and right-hand components, the actual maximum total field gain heading is a degree off the zenith or 0°-theta angle heading. The source of the asymmetry is intersection of the helix wire with the ground plane.

We can calculate the pattern values for both the left-hand and right-hand patterns using the previously ignored Etheta and Ephi data. Some implementations of NEC, such as GNEC, NEC-Win Pro, and NEC-Win Plus, already perform these calculations. However, it is useful to understand the calculation of these values, which is a post-core-run process. In order to see how the calculation proceeds, let's repeat the relevant parts of our sample line.

```
  - - ANGLES - -   - POWER GAIN -  POLARIZATION
  THETA      PHI       TOTAL         SENSE
 DEGREES  DEGREES       DB
    0.00    90.00    11.261         RIGHT
                        - - - E(THETA) - - -       - - - E(PHI) - - -
                       MAGNITUDE      PHASE       MAGNITUDE      PHASE
                       VOLTS          DEGREES     VOLTS          DEGREES
                       1.00721E+00    -99.56      4.73544E-01    163.94
```

The procedure begins by taking the real and imaginary components of each value of E (theta and phi). They appear in terms of magnitude and phase angle in the sample line. The steps use spreadsheet notation, since that is the most likely medium for using the equations. However, you may easily translate them into standard algebraic notation.

vetr = EthetaMag * cos(Ethetaphase); theta real
veti = EthetaMag * sin(Ethetaphase); theta imaginary
vepr = EphiMag * cos(Ephiphase); phi real
vepi = EphiMag * sin(Ephiphase); phi imaginary

These initial values are simply intermediate steps. We next must re-combine the collection into units that reflect the polarization of the antenna.

velr = 0.5*(vetr + vepi); left real circular component
veli = 0.5*(veti - vepr); left imaginary circular component
verr = 0.5*(vetr - vepi); right real circular component
veri = 0.5*(veti + vepr); right imaginary circular component

Now we can combine the circular components into values of magnitude by standard "square root of squares" techniques.

elm = sqrt(velr*velr + veli*veli); left magnitude
erm = sqrt(verr*verr + veri*veri); right magnitude

We now have the magnitudes of the left-hand and the right-hand electrical fields in volts (peak)/meter. The move from these voltage magnitudes to pattern data in dBic (dBi circular) requires a few more steps. The following are the calculations required for the conversion.

a. Convert the Total Field Gain into a dimensionless gain measure.

PwrGn = antilog (base 10) (TtlFldGn/10)

b. Square the ratio of the right voltage magnitude (erm) to the left voltage magnitude (elm). This squared ratio is the ratio of the dimensionless power gains for right and left patterns.

RatSq = (erm/elm)^2

The next steps are predicated on the assumption that the sum of the two dimensionless circular power gains is the dimensionless total field power gain.

c. Right Gain and Left Gain are 2 unknowns that are subject to simultaneous equations. Selecting Right Gain first, we obtain the following 2 steps.

GnRt = RatSq * PwrGn/(1 + RatSq)

GnRtdBi = 10 * log(GnRt)

d. Left Gain is simply the power gain minus the right gain (all dimensionless).

GnLf = PwrGn - GnRt

GnLfdBi = 10 * log(GnLf)

For our single sample line of RP 0 reporting, we obtain the following values.

```
Theta     ERM     ELM     Sense   RatSq   PwrGn
0         .7393   .2697   right   7.516   13.369
                          GnRt     GnRtdBic   GnLf     GnLfdBic
                          11.799   10.718     1.570    1.959
```

A spreadsheet or other program can be set-up to handle as many entries as we might need to

encompass a full pattern for the range of angle that we choose. Examine the NEC output report for model 17-10 at 10° increments. Notice that the pattern changes its sense along the selected sampling path. At the horizons, the Etheta values dominate to a degree that allows NEC to classify the pattern as linear. The left-hand and right-hand reversals may be less apparent until we perform the circular pattern calculations on them.

	Values Calculated by the Listed Equations				
Theta	ERM	ELM	Sense	GnRtdBic	GnLfdBic
-90	0.0518	0.0518	linear	-12.367	-12.367
-80	0.1278	0.1105	right	-4.529	-11.916
-70	0.1675	0.1105	right	-2.178	-5.786
-60	0.1226	0.1399	left	-4.891	-3.743
-50	0.0578	0.1226	left	-11.414	-4.891
-40	0.2399	0.0676	right	0.943	-10.056
-30	0.4460	0.0847	right	6.329	-8.100
-20	0.6136	0.1701	right	9.100	-2.045
-10	0.7153	0.2378	right	10.432	0.866
0	0.7393	0.2697	right	10.718	1.959
10	0.6841	0.2611	right	10.044	1.679
20	0.5585	0.2116	right	8.283	-0.148
30	0.3860	0.1287	right	5.072	-4.469
40	0.2057	0.0682	right	-0.393	-9.977
50	0.0635	0.1329	left	-10.605	-4.190
60	0.0274	0.1885	left	-17.890	-1.150
70	0.0506	0.1805	left	-12.578	-1.529
80	0.0486	0.1196	left	-12.924	-5.105
90	0.0574	0.0574	linear	-11.486	-11.486

For the entries sensed as left, the higher gain in the left-hand gain column becomes much more apparent. Of course, the table--or any enlargement of it--becomes suitable for creating a polar or rectangular plot of the two circular components of the overall helix pattern.

As one final exercise, let's see what happens for a helix that is left-handed, as in model *17-11-nec-4* or *17-11-nec2.nec*.

```
CM General Helix over Perfect Ground
CE
GH 1 100 -5 .6959 .191 .191 .0005 .0005 0
GE 1 -1 0
GN 1
EX 0 1 1 0 1 0
FR 0 1 0 0 299.7925 1
RP 0 181 1 1000 -90 90 1.00000 1.00000
EN
```

The only difference between this model and the one that we have previously used is the minus sign in the third entry of the GH or helix-forming line. The negative value for the number of turns creates a left handed helix, as shown in **Fig. 17-9**.

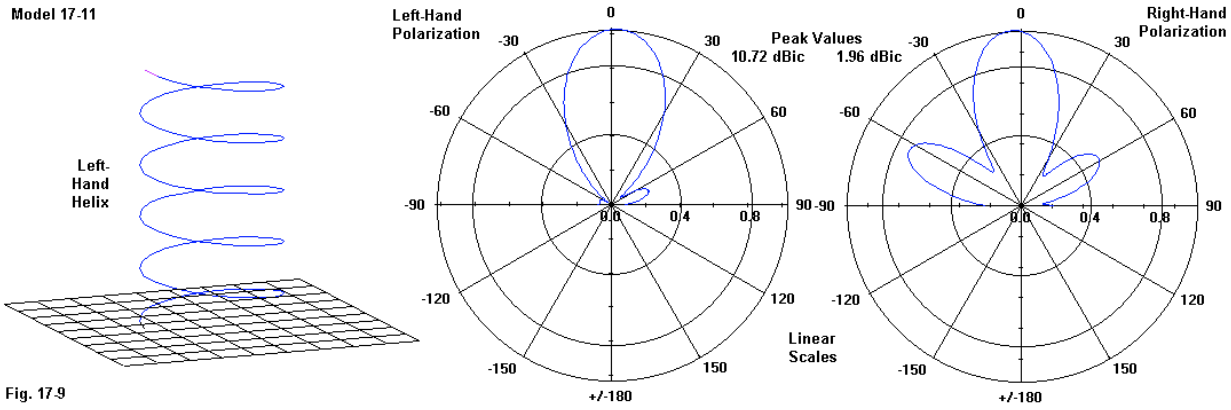

The corresponding NEC-2 GH entry has the following appearance. Note that the required minus sign to create a left-hand helix attaches to the helix length entry.

```
GH 1 100 .13918 -.6959 .191 .191 .191 .191 .0005
```

The sample RP 0 line that corresponds to the one for the previous example appears in the NEC output file.

```
- - ANGLES - -          - POWER GAINS -        - - - POLARIZATION - -
THETA     PHI         VERT.    HOR.     TOTAL       AXIAL      TILT    SENSE
DEGREES   DEGREES       DB       DB       DB         RATIO      DEG.
 0.00     90.00     10.39     3.84    11.261      0.46544     3.89    LEFT
[0.00     90.00     10.39     3.84    11.261      0.46544    -3.89    RIGHT]

        - - - E(THETA) - - -      - - - E(PHI) - - -
        MAGNITUDE     PHASE       MAGNITUDE    PHASE
         VOLTS       DEGREES        VOLTS      DEGREES
        1.00721E+00    80.44    4.73544E-01   163.94
       [1.00721E+00   -99.56    4.73544E-01   163.94]
```

The bracketed entries are from the right-hand helix report. Very little has changed, but the changes make a world of difference. Only the tilt angle and the Etheta phase angle have different numbers. However, those numbers alter the circular polarization calculations.

```
Theta     ERM      ELM      Sense    RatSq    PwrGn
0         .2697    .7393    left     0.133    13.369
                                GnRt      GnRtdBic    GnLf      GnLfdBic
                                1.570     1.959       11.799    10.718

Theta     ERM      ELM      Sense    RatSq    PwrGn
0         .7393    .2697    right    7.516    13.369
                                GnRt      GnRtdBic    GnLf      GnLfdBic
                                11.799    10.718      1.570     1.959
```

The sample output lines are for the left-hand and the right-hand helices in order. The values for the zenith angle show a flip-flop that is not true of the values for the entire pair of left- and right-hand patterns. The pattern on the right sides of **Fig. 17-8** and **Fig. 17-9** show some differences

and are not simple mirror images. Axial-mode helix patterns are not perfectly symmetrical. Since the helixes start in the same place but move the wires in opposite directions, one pattern is a mirror of the other's pattern 90° separated.

Although the NSI Multi-Plot feature calculates the gain in dBic for you, it is always useful to understand from where the numbers come. As well, the exercise may provide further evidence that NEC is not only a calculating engine, but also a data resource from which you may derive a large amount of other interesting information.

Summing Up

We began our further look into the RP command with a review of the essentials of requesting 2-dimensional polar plots. We turned quickly to the RP0 requirements for patterns using a complete far-field sphere in free space or full hemisphere over ground. Besides discovering the required command entries, we also explored what 3-dimensional surface plots, radiation efficiency plots, and average gain test plots had in common and how they differed according to the goals of each task.

When we turned to the RP1 ground wave request, we replaced the theta entries with new cylindrical concerts: ρ or the distance from the origin in the X-Y plane and z or the height above ground. The far-field and surface wave calculations yield electric field values for Etheta, Ephi, and Eradial in peak volts/meter. These values acquire useful comparative significance when we also adjust the excitation to a specific power level. In fact, the exercises stressed the integration of many geometry and control commands into the most efficient models for achieving the desired output.

The NEC output report proved to be less a final report than it is a source of data for additional calculation. Using axial-mode helical antennas, we learned how to use the radiation pattern data to calculate the left-hand and the right-hand components (in dBic) of the total field gain as just one possibility for making further use of the NEC output information.

The exercises in this chapter have provided you with a sampling of ways of treating an antenna model as a fully integrated unit. The process starts with the commands by which we create the geometry and proceeds through the control commands by which we request useful outputs. It does not end with a simple output report and its graphical presentation. Instead, full integration of the modeling process involves the interpretation and manipulation of those outputs to arrive at the most useful data set for a selected task.

18.
Near-Field Analysis in NEC-2 and NEC-4

***Objectives**: Near-field analysis requires us to master Cartesian and spherical techniques of arranging input data in both the NE and NH commands. We shall also examine the nature of the output data, including the calculation of peak values. Finally, we shall look at some unique features of NEC-4's treatment of near fields, including the introduction of the LE and LH commands.*

In the progression from entry-level antenna modeling to more advanced levels, many modelers overlook near-field analysis as an integral and valuable part of NEC's array of tools. The reasons are many, ranging from the limited attention that software implementations of NEC give to such analysis to the multiple and potentially confusing ways of entering required data. In many cases, modelers have too little background in the terms of near-field analysis output to make effective use of the available data.

This chapter is an introduction to NEC's near-field analysis, and certainly not the last word on it. We shall begin with a review of the correlation between the Cartesian coordinate system within which we normally enter wire data and the spherical system used for radiation pattern information. As we shall see, we may enter data in either Cartesian form or spherical form, and determining which form to use requires that we sample a few potential applications. In the process of learning to enter data in spherical form within the commands, we shall also discover an important difference between NEC-2 and NEC-4.

NEC uses the NE command for near electrical fields and the NH command for near magnetic fields. In classic textbook terms, NEC does not calculate near fields alone. Such calculations normally use simplified terms extracted from full field analysis. NEC uses the full field analysis equations. The key difference between a near-field analysis and a ground-wave analysis is usually the distance from the observation point to the antenna structure. Indeed, near-field analysis may sometimes involve intra-structure positions.

The near-field commands have some execution peculiarities that we need to grasp. For a single frequency request, both commands are self-executing, like the RP commands. However, unlike the RP commands, when we request multiple frequencies, we must add execution commands for each near-field request.

The form of the output data--including the calculation of peak field values--is only one of two major ways of expressing the data. NE and NH use Cartesian coordinates to locate the observation points specified in either form of input and calculates values in terms of those coordinates. NEC-4 adds a calculation of peak field values, a feature that NSI software has transported back into the NEC-2 core. Unique to NEC-4 is a second method of calculating near fields in terms of an axial value supplemented by 2 transverse values. The LE and LH commands set up lines of observation points that you may connect into complex patterns that form a continuous series.

Orienting Near-Field Input Data

Effective near-field analysis begins with a naturalized understanding of the correlation between the Cartesian and spherical coordinate systems used within NEC. Without the correlation being completely natural, near-field data entry and the interpretation of output data becomes laborious at best and simply confusing at worst.

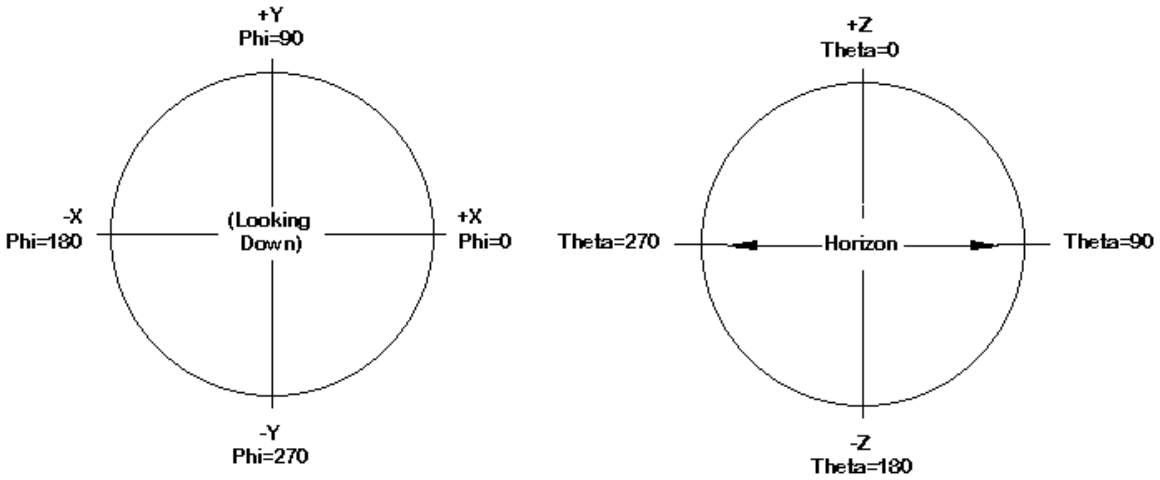

The Correlation of the Cartesian Coordinate System with the Phi-Theta System of Angles

Fig. 18-1

Fig. 1 shows the correlations in 2-dimensional form. The Cartesian X-Y plane corresponds to a spherical phi plane at a theta angle of 90°. When viewed from overhead, the +X-axis points toward a phi angle of 0°. All phi angles increase counterclockwise, with a phi of 90° pointing along the +Y-axis. Note that the input convention represents the Cartesian X-axis as a horizontal line, with the Y-axis using a vertical line. This convention differs from the polar plot convention of placing the 0°-phi heading at the top of the plot page.

The Cartesian Z-axis corresponded to a theta angle of 0° (zenith) in the positive direction, and to a theta angle of 180° in a free-space direction wherein both entries and fields may use the region below the horizon (theta = 90°). An alternative representation of theta angles--especially apt for over any type of ground--is to let the two horizons use values of -90° and 90°. The horizon, of course, is the X-Y plane.

Although there are conventional correlations between the two coordinate systems, the methods of entry differ. Cartesian coordinates require entry in units of measure. With wires, we may use any unit of measure and add a GS command to scale those entries to meters for NEC's calculations. However, the near-field entries are parts of control commands and all Cartesian entries must be in meters. The spherical coordinate entries use a single measured unit: a radius to the observation point. Refinement of the exact point results from adding angular coordinates, using both a phi and a theta angle entry. Because the two near-field commands, NE and NH, permit you to enter

data in either form, it removes the need for external calculation of one form from the other. **Fig. 18-2** contrasts the entry assist screens in NSI software for the two forms of setting up near fields. Except for the command names, the NE and NH commands are identical in format.

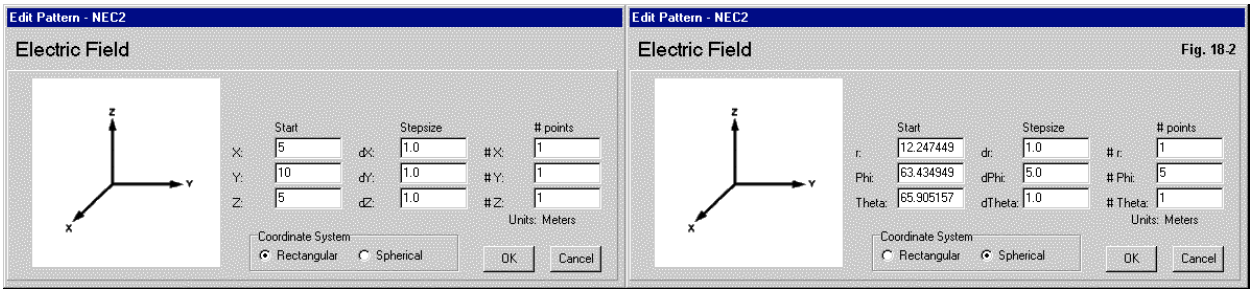

The NE and NH command structures are identical. Let's begin with the Cartesian version of the line and define the meanings of the entries.

Cmd	Type	NRX	NRY	NRZ	XNR	YNR	ZNR	DXNR	DYNR	DZNR
	I1	I2	I3	I4	F1	F2	F3	F4	F5	F6
NE	0	1	1	1	5	10	5	1.0	1.0	1.0
NH	0	1	1	1	5	10	5	1.0	1.0	1.0

NE and NH type 0 commands designate the Cartesian entry system. The remaining integer entries--NRX, NRY, and NRZ--specify the number of observation points in the X, Y, and Z directions, respectively. Each coordinate must have a minimum value of 1 for NEC to yield any near-field output at all. Since we may specify virtually any number of points in each of the 3 directions, we may build as complex a set of points as we might wish, although modesty in this category is usually advisable for ease of interpreting the output tables.

XNR, YNR, and ZNR specify the initial coordinates in meters. DXNR, DYNR, and DZNR specify the increment between points along each axis, again in meters. Since the system increments from the negative toward the positive, the initial values should be the most negative value desired for any set of entries.

In order to input the observation point or points in Cartesian terms, we must know or set the X, Y, and Z coordinates of the point or points. **Fig. 18-3** shows graphically the required information as it relates to setting an observation point. For a specific 1-observation-point example, open model *18-1.nec*. Compare the entries in both the NE and NH commands to the specifications in the 2 circles.

```
CM 1-step, Cartesian coordinates
CE
GW 1 11 0 0 .25 0 0 .75 .001
GE 1 0 0
GN 2 0 0 0 13.0000 0.0050
EX 0 1 6 00 1 0
FR 0 1 0 0 299.7925 1
NE 0 1 1 1 5 10 5 1.0 1.0 1.0
NH 0 1 1 1 5 10 5 1.0 1.0 1.0
EN
```

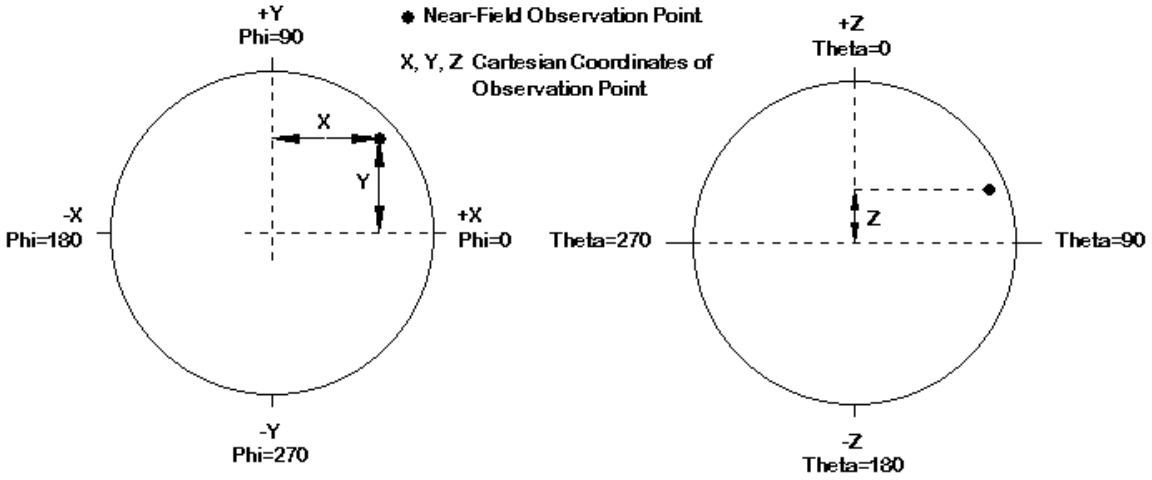

A Near-Field Observation Point Located by Cartesian Coordinates

Fig. 18-3

The model sets up a vertical dipole whose lower end is 1/4λ above an SN average ground. The NE and NH commands use the same entries that we employed in the sample lines. The 3 integer entries are all 1, indicating that we wish only a single point of observation. We define that point as having X- and Z-values of 5 meters and a Y-value of 10 meters. Note that we do not here need a separate execution command, since we are requesting only a single frequency.

Run the model and examine the NEC output file to find both the NE and NH outputs.

```
         **** NEAR ELECTRIC FIELDS ****

       -  LOCATION  -              - PEAK FLD -
   X          Y          Z          MAGNITUDE
 METERS     METERS     METERS        VOLTS/M
5.000000  10.000000   5.000000      4.1105E-02

         **** NEAR MAGNETIC FIELDS ****

       -  LOCATION  -              - PEAK FLD -
   X          Y          Z          MAGNITUDE
 METERS     METERS     METERS          AMPS/M
5.000000  10.000000   5.000000      1.0903E-04
```

I have omitted some of the output data, since our interest for the moment lies in the output table location of the data or observation point in the same terms in which we entered it. We may note in passing that the output field strength is in peak volts/meter for the electric field and peak amps/meter for the magnetic field.

The required information changes slightly if we wish more than 1 observation point within the same NE or NH command. **Fig. 18-4** shows the difference in the entry assistance screens for a single observation point and 5 such points set out in a row parallel to the X-axis. Open model *18-2.nec* and examine the corresponding near field command lines. The model is otherwise identical to model 18-1.

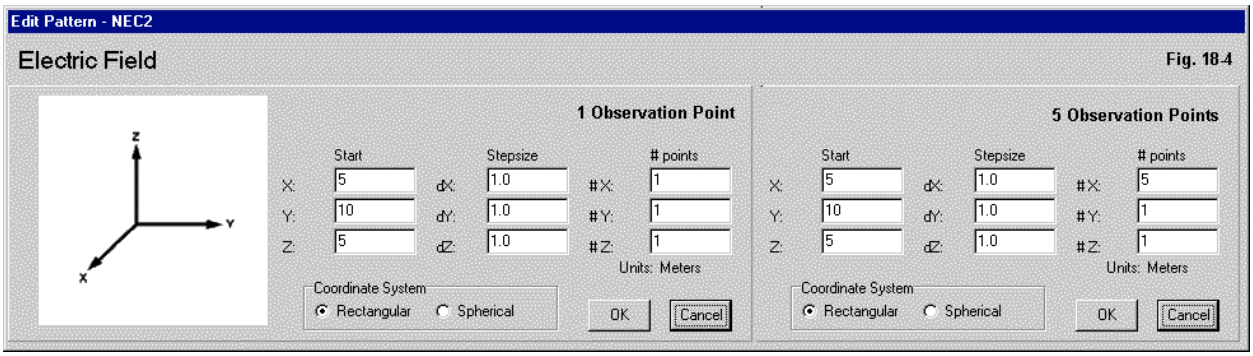


```
NE 0 5 1 1 5 10 5 1.0 1.0 1.0
NH 0 5 1 1 5 10 5 1.0 1.0 1.0
```

Run the model and look at the NEC output file's near-field entries. Only part of the electric field data appears here.

```
         **** NEAR ELECTRIC FIELDS ****

         -  LOCATION  -              - PEAK FLD -
   X           Y           Z          MAGNITUDE
 METERS      METERS      METERS        VOLTS/M
5.000000  10.000000   5.000000      4.1105E-02
6.000000  10.000000   5.000000      4.0987E-02
7.000000  10.000000   5.000000      4.0767E-02
8.000000  10.000000   5.000000      4.0412E-02
9.000000  10.000000   5.000000      3.9900E-02
```

We have our desired 5 observation points, each with a constant Y- and Z-coordinate. The X-coordinate changes in 1-meter increments beginning at the specified 5-meter value.

The NE/NH type 0 input system is only 1 of the 2 possible ways to enter data. The alternative type 1 input system changes the meanings of the command terms.

```
Cmd   Type  NRX   NRY   NRZ   XNR   YNR   ZNR   DXNR  DYNR  DZNR
      I1    I2    I3    I4    F1    F2    F3    F4    F5    F6
NE    1     1     1     1     12.2  63.4  65.9  1.0   1.0   1.0
NH    1     1     1     1     12.2  63.4  65.9  1.0   1.0   1.0
```

The operative terms for the entry of data in spherical terms are the radius, r, along with phi and theta. NRX, NRY, and NRZ still represent the number of points, but in the direction of the radius for X, in the direction of phi for Y, and in the direction of theta for Z, respectively. XNR shows the distance along the radius r in meters for the first observation point. YNR gives the initial phi angle, while ZNR gives the initial theta angle, with both of these values in degrees. DXNR specifies the increment between observation points along the radius in meters. DYNR gives the phi increment and DZNR shows the theta increment, both in degrees.

Special Note: The meanings of the terms just listed apply only to NEC-2. We shall examine NEC-4 spherical coordinate inputs later.

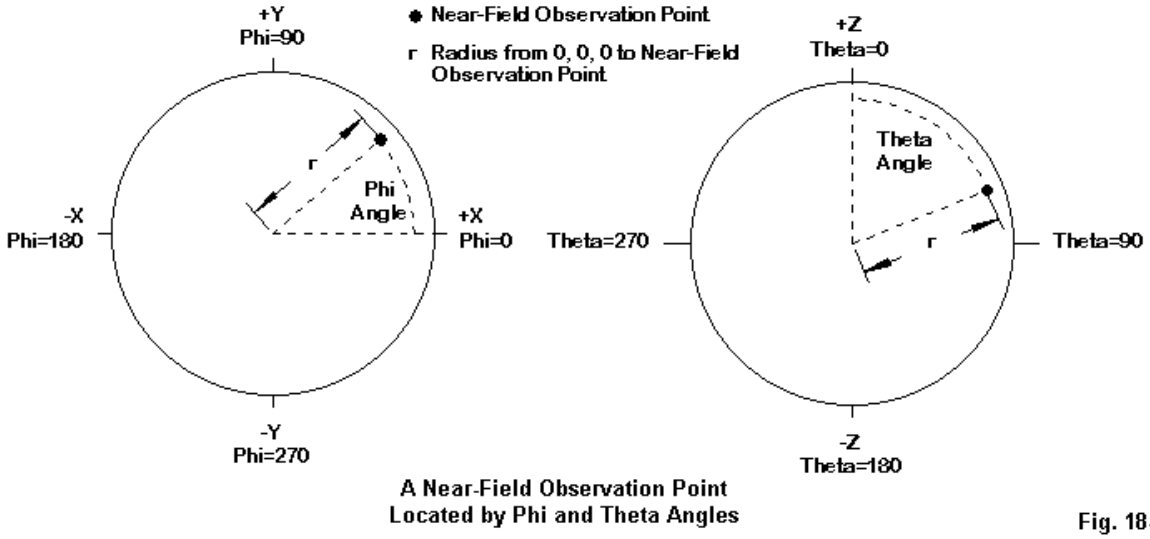

Fig. 18-5

Fig. 18-5 provides graphic orientation to the entry terms just described. For a specific example that uses a single observation point, open model *18-3.nec*. Note that this is a nec-2 model. The NE and NH commands use high decimal values for the entries so that the observation point is the same one that appeared in Cartesian form in model 18-1.

```
NE 1 1 1 1 12.247449 63.434949 65.905157 1.0 1.0 1.0
NH 1 1 1 1 12.247449 63.434949 65.905157 1.0 1.0 1.0
```

Run the model and examine the near field outputs in the NEC output file.

```
         **** NEAR ELECTRIC FIELDS ****

       -  LOCATION  -              - PEAK FLD -
   X           Y           Z          MAGNITUDE
 METERS      METERS      METERS        VOLTS/M
5.000000  10.000000   5.000000      4.1105E-02

         **** NEAR MAGNETIC FIELDS ****

       -  LOCATION  -              - PEAK FLD -
   X           Y           Z          MAGNITUDE
 METERS      METERS      METERS          AMPS/M
5.000000  10.000000   5.000000      1.0903E-04
```

The output table is identical to the one produced by model 18-1. Despite the fact that we entered the observation coordinates in spherical terms, the position shown in the output table will be in Cartesian terms. You may perform the usual vector conversion of the position manually to check the correlation of the input information to the output position in the table.

Just as we did with Cartesian coordinates, we may request multiple observation points within the spherical input system for NE and NH commands of type 1. **Fig. 18-5** shows the difference in the entries for a 1-point and a 5-point request. The NH assistance screens will be identical to the NE

screens shown in the figure.

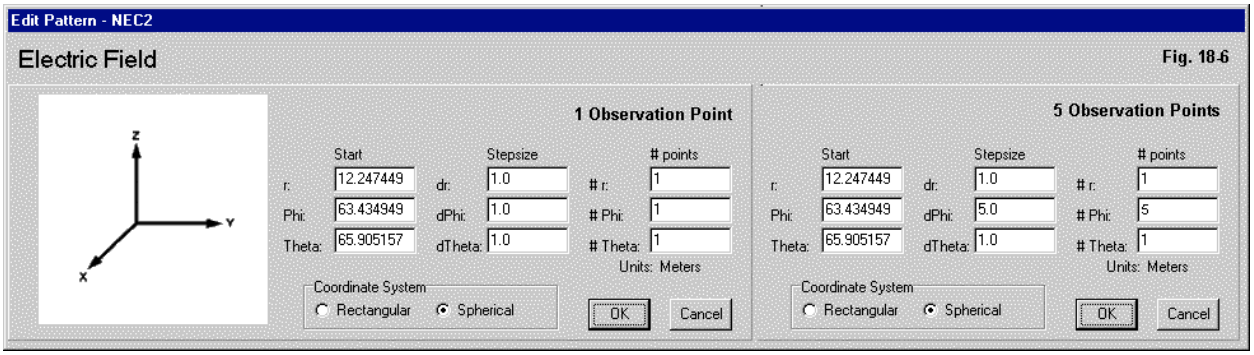

Open model *18-4.nec* to see the NEC input file format for the requested 5 observation points along the phi circle.

```
NE 1 1 5 1 12.247449 63.434949 65.905157 1.0 5.0 1.0
NH 1 1 5 1 12.247449 63.434949 65.905157 1.0 5.0 1.0
```

The near-field commands request 5 points at 5° intervals. To discover where these points land in Cartesian terms, run the model and examine the near-field data. The following lines show only partial data from the electric field portion of the output.

```
      **** NEAR ELECTRIC FIELDS ****

        -  LOCATION  -              - PEAK FLD -
   X          Y          Z          MAGNITUDE
 METERS     METERS     METERS        VOLTS/M
5.000000  10.000000  5.000000     4.1105E-02
4.109416  10.397726  5.000000     4.1105E-02
3.187557  10.716319  5.000000     4.1105E-02
2.241439  10.953354  5.000000     4.1105E-02
1.278262  11.107027  5.000000     4.1105E-02
```

Because we moved the observation points along the phi circle, the radius did not change. Since the distance to each observation point is the same and since the theta angle is constant, all observation points will return the same peak value. However, the Cartesian coordinates for the points after the first one are no longer simple. A 5° step in the phi direction does not correspond to single units of change along any individual axis. Rather, you may note that the X-coordinate shrinks while the Y-coordinate increases. Since the Z-coordinate does not change, you may take the square root of the sum of the squares of the X- and Y-coordinates to confirm that you arrive at the same number for every increment of the observation position.

Special note on NEC-4 spherical coordinate entries: We earlier specified that the system of spherical coordinate entry applied only to NEC-2. NEC-4 reverses the phi and theta entries in all three pairs of entry points relative to those for NEC-2. Open model *18-5-nec4.nec* and examine the NE and NH command lines. The model is identical to the NEC-2 model 18-3. Since the model is for 1 observation point, only the reversal in the initial angles will show, but all 3 pairs in fact are reversed.

Model 18-3: NEC-2

```
   NE 1 1 1 1 12.247449 63.434949 65.905157 1.0 1.0 1.0
   NH 1 1 1 1 12.247449 63.434949 65.905157 1.0 1.0 1.0
```

Model 18-5: NEC-4

```
   NE 1 1 1 1 12.247449 65.905157 63.434949 1.0 1.0 1.0
   NH 1 1 1 1 12.247449 65.905157 63.434949 1.0 1.0 1.0
```

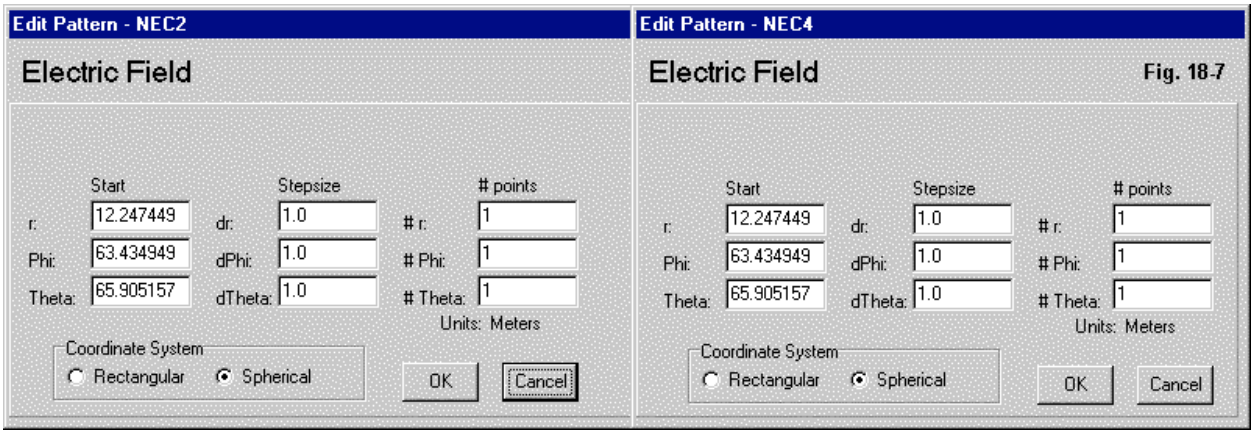

As **Fig. 18-7** shows, there is no difference between the NSI entry assistance screens for NEC-2 and NEC-4. The difference appears in terms of where in the command entry that the screen places each value. If you run models that use spherical input coordinates on the opposing cores, you will simply receive erroneous results, since the cores will each interpret the angles within the individual core instruction set. As well, you may not be well guided in knowing that an error has been made for phi and theta angles that are similar, as in the present pair of models. The algorithm revisions of NEC-4, relative to NEC-2, will yield slightly different results. Because we know from advanced external calculations that the observation point should show up where X = 5, Y = 10, and Z = 5, we can have confidence that we have correctly set the order of entries in the NEC-4 model.

```
         **** NEAR ELECTRIC FIELDS ****

       -  LOCATION  -              - PEAK FLD -
   X          Y          Z          MAGNITUDE
 METERS     METERS     METERS        VOLTS/M
5.000000  10.000000   5.000000      4.2674E-02

         **** NEAR MAGNETIC FIELDS ****

       -  LOCATION  -              - PEAK FLD -
   X          Y          Z          MAGNITUDE
 METERS     METERS     METERS          AMPS/M
5.000000  10.000000   5.000000      1.1325E-04
```

The situation will be far less ambiguous for phi and theta angles that are considerably different and for multiple observation points. If phi and theta angles and their associated but different number of steps are reversed, the coordinates will not appear in the correct places.

Many near-field analyses occur in a context in which we provide the model with a specific power

level. Re-run model 18-1 (which uses Cartesian coordinates for a 1-point near-field analysis) and obtain the power: 4.61192E-3 watts. To arrive at the proper excitation voltage for our standard 1000-watt value (as used in the preceding chapter), we may simply divide the new or desired power by the existing power. The square root of the result (times the old excitation voltage of 1.0) will yield the new excitation voltage: 465.65 peak volts.

Open model *18-6.nec* and examine the EX command (while verifying that all other model details are the same as in model 18-1).

```
EX 0 1 6 00 465.65 0
```

Run the model and obtain the near-field tabular data.

```
         **** NEAR ELECTRIC FIELDS ****

       -  LOCATION  -              - PEAK FLD -
   X           Y           Z          MAGNITUDE
 METERS      METERS      METERS        VOLTS/M
5.000000  10.000000   5.000000      1.9140E+01

         **** NEAR MAGNETIC FIELDS ****

       -  LOCATION  -              - PEAK FLD -
   X           Y           Z          MAGNITUDE
 METERS      METERS      METERS          AMPS/M
5.000000  10.000000   5.000000      5.0770E-02
```

For any near-field data gathered and stored, it is useful to label each preserved output table with the power level used to obtain the information. That information is always available in a full NEC output file. However, the temptation to store individual pieces of the file separately can result in the loss of the power information unless you annotate the stored portion of the full data set.

Near-field analyses have many uses. Coupling between a source antenna and nearby objects or even between elements within the same array makes up one major line of interest. In the far-field zone, we are often limited to modeling a source antenna and a more distant object of interest and then sampling the current induced on the segments of the object. Using the RFLD option within the RP0 command and setting a power level for the source, we can gauge the field strength at the distant object. In the near field, we can determine within the limits of NEC the strength of both the electric and magnetic fields at the position of a closer object. Unlike the far field, wherein the electric field is the only field of interest, the near field has both electric and magnetic fields. Each is initially of equal interest.

In more recent years, interest has grown in the coupling of near fields to organic entities, including human beings. There are two aspects of this interest that have a bearing on the use of NEC and near-field analysis. One aspect is the bio-electronic research efforts trying to determine the level of interaction between radiated fields and organisms. In this regard, NEC can be useful as a preliminary method of calculating the field strength at some distances from the radiating source. However, such studies themselves do not permit conclusions about the health or safety of individuals who come within such fields, since the complexities of organisms do not appear in the NEC calculations. Indeed, most implementations specifically disavow drawing conclusions

concerning whether the field strength from an antenna or other radiating source presents a hazard or unsafe condition.

At the same time, governmental agencies--such as the U.S. Federal Communications Commission and counterpart bodies in other countries--have set field strength or RF exposure standards into the regulations governing radio-wave sources. These standards are comparable to exposure limits for other forms of radiation governed by other agencies. What these regulations share in common is the agency's considered judgment of safety and exposure limits. Any licensed user of significant levels of radio frequency energy must make calculations to demonstrate compliance with the terms of the regulations. In this capacity, NEC calculations are often accepted to satisfy compliance requirements.

For many near-field analyses, which entry system you use--Cartesian or spherical--makes little difference. However, there are some tasks that more naturally fall toward one or the other of the coordinate methods. See **Fig. 18-8** for a pair of uses that more naturally call for Cartesian coordinates than for spherical coordinates.

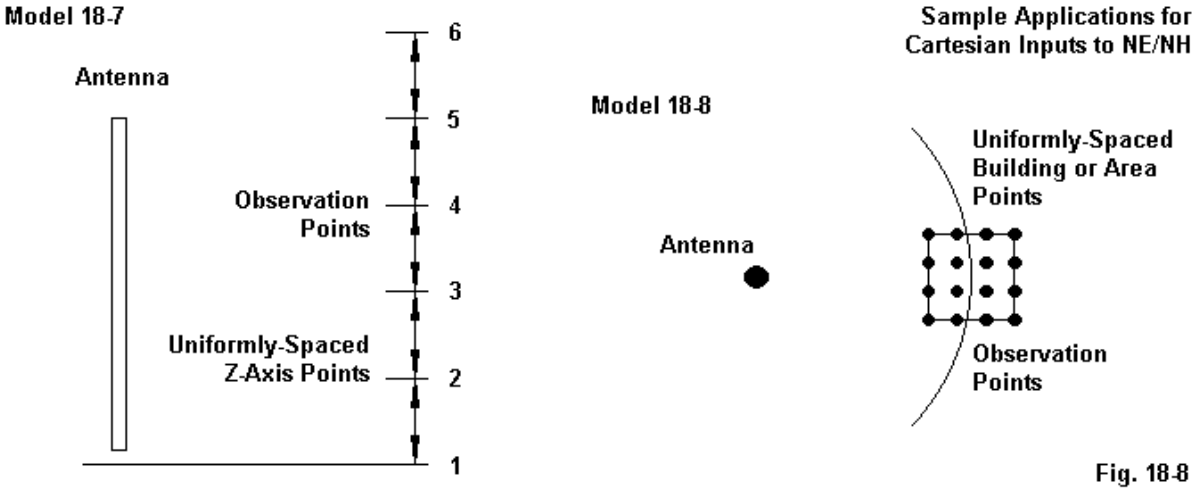

Fig. 18-8

On the left is a call for field strength readings at a specified distance from the antenna, where we may define the distance in terms of X and Y coordinates. The task is to determine at that distance the field strength at several heights that we may define by the Z coordinate. Open model *18-7.nec*.

```
CM 6-step, Cartesian coordinates
CM 1000 watts
CE
GW 1 11 0 0 1 0 0 15.3 .03
GE 1 0 0
GN 2 0 0 0 13.0000 0.0050
EX 0 1 6 00 422.89 0
FR 0 1 0 0 10 1
NE 0 1 1 6 10 0 0 1.0 1.0 3
NH 0 1 1 6 10 0 0 1.0 1.0 3
EN
```

The model places a vertical dipole at 10 MHz 1 m above ground. The top height is just over 15 m. The ground is the usual SN average, and the excitation is set for 1000 w. The NE and NH commands request readings at a distance of 10 m from the antenna (where a wavelength is about 30 m). 6 readings will accumulate along the Z-axis at 3-meter intervals, starting at ground level. Run the model and examine both the NE and NH output tables.

The most significant readings in the electric field table occur in the X and Z columns, while in the magnetic field table, the most significant readings appear in the Y column. For Cartesian entry coordinates only, both GNEC and NEC-Win Pro allow you to graph these results in rectangular plots. The results of that graphing exercise appear in **Fig. 18-9**.

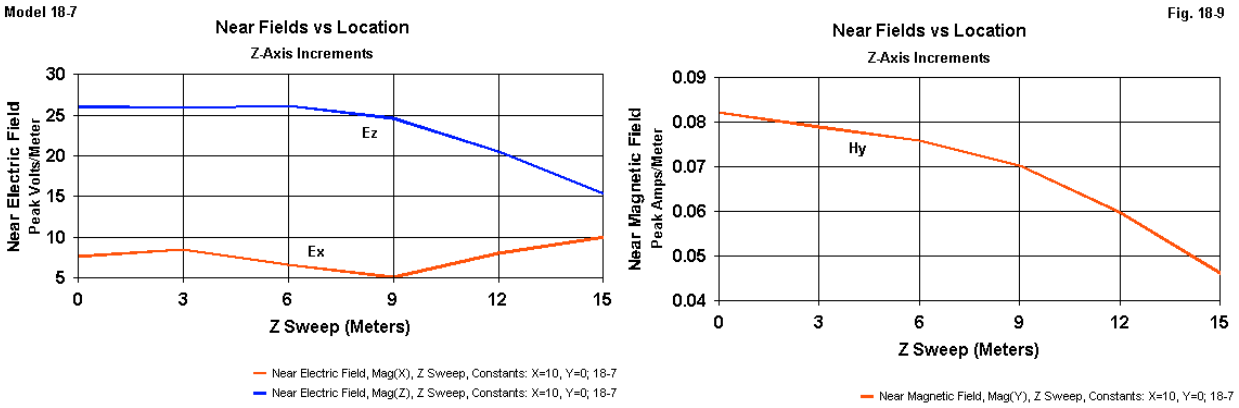

The right side of **Fig. 18-8** shows another task for which Cartesian coordinates are especially apt. Suppose that we have an area or even a non-conductive building constructed in conventional geometric form. We may use Cartesian coordinates to define the area or volume for near field analysis. Open model *18-8.nec*.

```
CM Cartesian coordinates
CM 1000 watts
CE
GW 1 11 0 0 1 0 0 15.3 .03
GE 1 0 0
GN 2 0 0 0 13.0000 0.0050
EX 0 1 6 00 422.89 0
FR 0 1 0 0 10 1
NE 0 4 4 1 10 10 0 3 3 3
NH 0 4 4 1 10 10 0 3 3 3
EN
```

The antenna, ground, and power elements of the model are unchanged from model 18-7. However, the near field commands now request a square area for observation points. In the X and Y directions, beginning at a distance of 10 m along each of those axes, we find a request for 4 observation points. Since the Z-axis requests a single observation point, the entire output will consist of 4 times 4 or 16 data lines. Each point will be 3 m distant from the preceding point, so we shall expect location reports for X and Y that successively read 10, 13, 16, and 19 m.

Run the model and examine the location columns of the output report for either NE or NH.

```
**** NEAR ELECTRIC FIELDS ****

         -  LOCATION  -
     X           Y           Z
   METERS      METERS      METERS
 10.000000   10.000000    0.000000
 13.000000   10.000000    0.000000
 16.000000   10.000000    0.000000
 19.000000   10.000000    0.000000
 10.000000   13.000000    0.000000
 13.000000   13.000000    0.000000
 16.000000   13.000000    0.000000
 19.000000   13.000000    0.000000
 10.000000   16.000000    0.000000
 13.000000   16.000000    0.000000
 16.000000   16.000000    0.000000
 19.000000   16.000000    0.000000
 10.000000   19.000000    0.000000
 13.000000   19.000000    0.000000
 16.000000   19.000000    0.000000
 19.000000   19.000000    0.000000
```

Typical of NEC programming, the near-field analysis first cycles through the X variations at the first Y value and then recycles through them at the second Y value, etc. Had there been more than 1 Z position, the X-Y procedures would be repeated for each Z value. This demonstration is simply to give you correct expectations relative to the order of operations as NEC develops the near-field table.

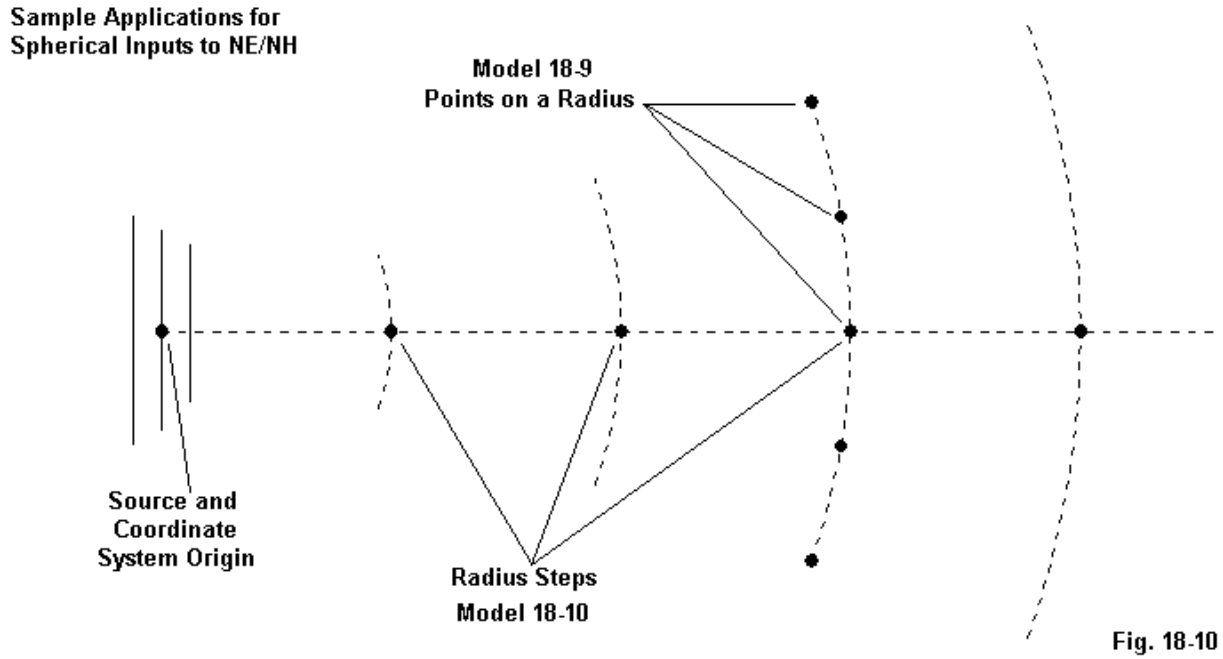

Fig. 18-10

Just as some applications call for Cartesian coordinate entries in the NE and NH commands, other applications find spherical coordinates to be the more apt entry system. **Fig. 18-10** provides

a pair of examples. Note that both examples assume that the source of the array is at the origin of the coordinate system. Open model *18-9.nec* for the first example (in NEC-2 format).

```
CM 3 el Yagi; 1 wl above ave gnd
CM spherical coordinates
CM constant radius. phi increments
CE
GW 1 21 -7.466 -4.517 29.9793 7.466 -4.517 29.9793 0.018
GW 2 21 -7.129 0 29.9793 7.129 0 29.9793 0.018
GW 3 21 -6.708 5.223 29.9793 6.708 5.223 29.9793 0.018
GS 0 0 1
GE 1
GN 2 0 0 0 13. .005
EX 0 2 11 0 223.75 0.
FR 0 1 0 0 10 1
NE 1 1 37 1 10 90 76 1 5 1
NH 1 1 37 1 10 90 76 1 5 1
RP 0 1 361 1000 76 0 1.00000 1.00000
EN
```

The antenna is a 3-element Yagi for 10 MHz, with the source at the center of GW2. The array is 1λ above SN average ground, and the power is 1000 w. An RP0 phi plot request at the take-off angle (theta = 76°) will allow you to reference the near-field readings to the far-field data. Each near-field request specifies a radius of 10 m, using a theta angle of 76°. There will be 37 phi points at 5° intervals, beginning with a heading of 90°. Since the model extends the elements along the X-axis, phi = 90° represents a gain maximum heading, and the remaining points will cover 180° so that the last report corresponds to a heading of 270°. (Since the pattern will be symmetrical, we have no need to cover the remaining part of the phi circle.) Run the model and examine the output tables.

Since the reported Z coordinate is constant, you may verify that each observation point lies on the correct radius by a simplified calculation. The square root of the sum of the squares of the X and the Y coordinates will equal the Y coordinate for the first entry in the table. You may, of course, combine that calculation with the Z coordinate and arrive at a 10-m radius. Unlike models that have used a vertical dipole, the more complex array produces a different set of near-field values for each phi heading. That result, of course, forms a good reason for using spherical input coordinates, even if NEC shows those locations in Cartesian terms in the output table.

As a variant on the Yagi model, open model *18-10.nec*, also in NEC-2 format. The antenna set-up is the same. Only the NE and NH requests vary from model 18-9.

```
NE 1 5 1 1 5 90 76 5 1 1
NH 1 5 1 1 5 90 76 5 1 1
```

The phi and theta angles do not change and thus request only 1 step. The initial radius is 5 m, and the near field commands request 5 steps at 5-m intervals. Since the theta angle is not 90°, we should not expect to find increments of 5 in the output report. Instead, we should expect that those increments to show up in the vector sum of the reported coordinates. Run the model and examine the near-field tables.

```
        -  LOCATION  -
       X           Y           Z
     METERS      METERS      METERS
   0.000000    4.851479    1.209609
   0.000000    9.702957    2.419219
   0.000000   14.554436    3.628828
   0.000000   19.405915    4.838438
   0.000000   24.257393    6.048047
```

Since X is always zero, the square root of the sum of the squares of the remaining coordinates will confirm the 5-m increments in the radius.

In Chapter 8, we explored the variety of ways in which NEC executes commands that provide calculations. RP commands self execute. However, if we need a frequency sweep or request for multiple frequencies, we must repeat the FR command prior to each new RP command within the same model in order to obtain pattern data for each RP request at each frequency. For models in which we do not need a pattern request--for example, if we only wish to see the segment currents--we may add the XQ execution command to force calculations.

NE and NH are hybrid commands when it comes to executing calculations. The simple rule is that for a single frequency request, NE and NH are self-executing. However, if the FR command requests more than 1 frequency, NE and NH are no longer self-executing. Instead, they require an XQ command for each of them. In addition, if we wish to have results for each near-field command at all frequencies in the FR command, we must repeat that command prior to each NE or NH request. Because the near-field commands are so unique in this regard, let's perform a quick survey of what may result from various missteps.

Open model *18-11.nec*. You will recognize this file as model 18-1 with one important change: the FR command now requests 9 frequencies beginning at 290 MHz and extending to 310 MHz in 2.5-MHz increments.

```
GW 1 11 0 0 .25 0 0 .75 .001
GE 1 0 0
GN 2 0 0 0 13.0000 0.0050
EX 0 1 6 00 1 0
FR 0 9 0 0 290 2.5
NE 0 1 1 1 5 10 5 1.0 1.0 1.0
NH 0 1 1 1 5 10 5 1.0 1.0 1.0
EN
```

Run the model and check the NEC output file for NE or NH results. You will find none, since neither NE nor NH will self-execute with a multi-frequency request. Next open mode *18-11a.nec*. The new file adds an XQ execution command following the near field requests.

```
FR 0 9 0 0 290 2.5
NE 0 1 1 1 5 10 5 1.0 1.0 1.0
NH 0 1 1 1 5 10 5 1.0 1.0 1.0
XQ
EN
```

This version of the produces a full set of outputs for all frequencies, but only for the NH command.

NE will not execute without its own XQ command. Next, try model *18-11b.nec*. The new version gives each near-field command its own XQ command.

```
FR 0 9 0 0 290 2.5
NE 0 1 1 1 5 10 5 1.0 1.0 1.0
XQ
NH 0 1 1 1 5 10 5 1.0 1.0 1.0
XQ
EN
```

If you run the model and review the near-field output data, you will find a complete (all-frequency) set of electric field information, but magnetic field information only for the last frequency in the FR loop, 310 MHz. Now open the final model in the series, *18-11c.nec*. The version now has both FR and XQ commands for each near-field command.

```
FR 0 9 0 0 290 2.5
NE 0 1 1 1 5 10 5 1.0 1.0 1.0
XQ
FR 0 9 0 0 290 2.5
NH 0 1 1 1 5 10 5 1.0 1.0 1.0
XQ
EN
```

The output data set is now complete. We have lingered over this and the other near-field set-up options, variations, idiosyncrasies, and necessities, because they represent the region that most inhibits modelers from employing near-field analysis. Failure to create a good near-field analysis model results in data that may be of little or no use. There are fewer questions on the output side, but perhaps we should spend a little time on them.

Near-Field Output Data and the NEC-4 LE/LH Commands

Perhaps the single most significant question most often raised about near-field output data is what the column headings mean relative to the numbers within them. We have correlated the location portion of the output information to the input coordinates, whether the latter are in Cartesian or spherical terms. However, we must still address the column headings.

```
    -  EX  -            -  EY  -            -  EZ  -          - PEAK FLD -
MAGNITUDE   PHASE   MAGNITUDE   PHASE   MAGNITUDE   PHASE     MAGNITUDE
 VOLTS/M   DEGREES   VOLTS/M   DEGREES   VOLTS/M   DEGREES     VOLTS/M
```

The sample output table line (with the location omitted) comes from an electric field report. The units of measure are in peak volts/meter. The same headings would appear for a magnetic field table, but with peak amps/meter for the unit of measure. Each entry has a magnitude and phase angle, except for the final column that lists the calculated peak field magnitude.

The Ex, Ey, and Ez columns represent the components of the field as calculated in terms of the field strength along each axis line of a Cartesian coordinate system. This system stands in contrast to another method of presenting near field strengths. **Fig. 18-11** contrasts the two systems.

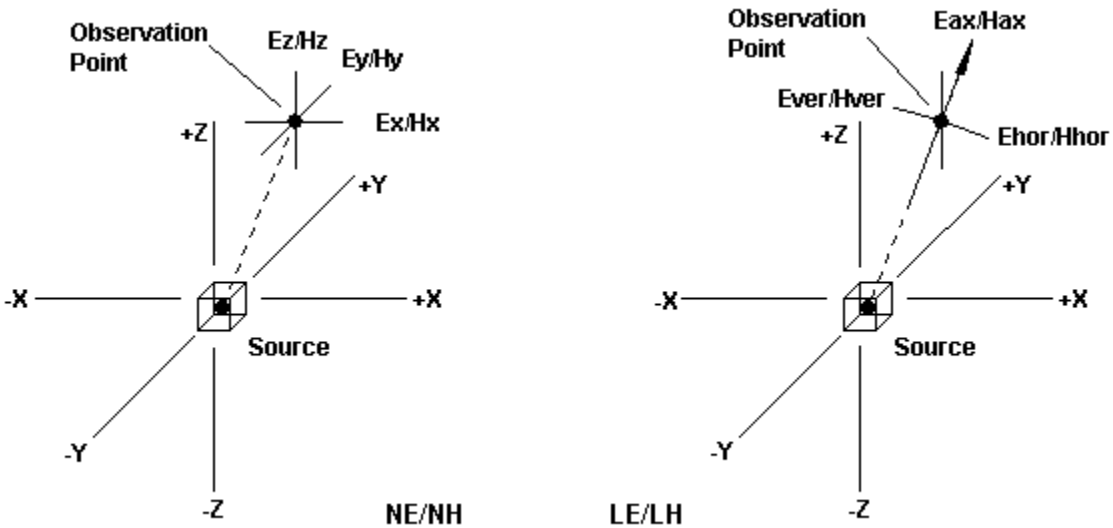

Fig. 18-11

The system on the right--often presented in basic texts--uses the axial field value plus two transverse measures that the diagram calls horizontal and vertical. The system of reporting for the NE and NH command aligns the calculated values with the axes of the coordinate system, as shown on the left. For most purposes, the system provides very usable information. Open model *18-12-nec2.nec*. (Since the model uses spherical input coordinates, you may use model *18-12-nec4.nec* if running the NEC-4 core.)

```
NE 1 16 1 1 0 90 71.565051 .10540932 0 0
NH 1 16 1 1 0 90 71.565051 .10540932 0 0
```

The model uses a constant phi angle, with a carefully selected theta angle and radius increment to produce output locations that step by 0.1 m along the Y-axis and by 0.3333 m along the Z-axis. Hence, the model creates a line of 16 observation points at easily tracked intervals. The free-space vertical dipole then produces electric and magnetic field values. Out of the total report, the following lines replicate just 3 from the electric field.

```
   -  LOCATION  -                          -  EX  -
  X          Y          Z          MAGNITUDE   PHASE
METERS     METERS     METERS        VOLTS/M   DEGREES
0.000000   0.000000   0.000000    0.0000E+00      0.00
0.000000   0.100000   0.033333    1.4134E-12    176.12
0.000000   0.200000   0.066667    4.4330E-13    175.10

                -  EY  -                -  EZ  -        - PEAK FLD -
           MAGNITUDE    PHASE     MAGNITUDE    PHASE     MAGNITUDE
            VOLTS/M    DEGREES     VOLTS/M    DEGREES     VOLTS/M
           0.0000E+00     0.00    1.1000E+01  -180.00    1.1000E+01
           2.7696E-01    -3.88    8.1372E-01   147.91    8.5038E-01
           8.6864E-02    -4.90    3.9984E-01   101.89    4.0066E-01
```

The split-line presentation should not obscure the reference point for the field strength values. The

slight flaw in the model is that the first point lies within the antenna, although NEC-will move it off the antenna by a wire radius.

We shall return to the values for Ex, Ey, and Ez after we examine the peak field magnitude. For purposes of compliance with regulations, many modelers are concerned solely with this figure, but do not know its origin. Let's examine line 3 from the table. If we create a vector sum for Ex, Ey, and Ez, we arrive at a value: 4.0917E-1 peak V/m for the apparent peak magnitude of the electric field. This value does not agree with the listed value: 4.0066E-1 peak V/m. What is wrong is our geometric interpretation of what is essentially a temporal calculation. If the phase angles were identical or if one component dominates, then the simple vector sum would be a good approximation of the peak voltage or current. Otherwise, the peak value will be equal to or less than the result of the geometric calculation. The phase differences among the component values tell us that each reaches its magnitude at a different time during a cycle, and so the calculation of a peak value must take that fact into account.

The actual calculation of the peak value is a multi-step procedure found in the NEC routine called NFPAT. It proceeds approximately as follows. For either NE or NH, for a given field point defined by X, Y, and Z, let

EXM, EYM, EZM = magnitude of EX, EY, EZ (given in peak volts/m or peak amps/m)
EXP, EYP, EZP = phase angle of EX, EY, EZ (degrees or radians)

"E" is a stand-in for either the voltage or the current. There is no difference in the calculation procedures. Next, let's calculate some intermediate terms involving the phase angles, finally arriving at a term called "TP."

$$CP = EXM^2 \cdot \cos(2\,EXP) + EYM^2 \cdot \cos(2\,EYP) + EZM^2 \cdot \cos(2\,EZP)$$

$$SP = EXM^2 \cdot \sin(2\,EXP) + EYM^2 \cdot \sin(2\,EYP) + EZM^2 \cdot \sin(2\,EZP)$$

$$TP = CP^2 + SP^2$$

Now we may include TP in the final calculation involving the squares of the component magnitudes.

$$E_{peak} = \sqrt{0.5\left(EXM^2 + EYM^2 + EZM^2 + \sqrt{TP}\right)}$$

The resulting peak voltage or current reading (called "Epeak") in V/m or A/m is also in peak units.

NEC-4 introduced a new pair of near-field commands in addition to the pair that it inherited from NEC-2. So you have a choice between using the pair that best suits the requirement of the modeling task. (Of course, you have no requirement to use either NE and NH or LE and LH in pairs, and you may use both within the same model.) NE and NH are general abbreviations for near-electric and near-magnetic fields. LE and LH indicate near-electric and near-magnetic fields along a line. The differences between the two systems of calculating near fields may prove useful, not only in understanding the new NEC-4 commands, but as well in better appreciating the terms of the NE and NH output reports.

On the right in **Fig. 18-11** is a similar situation. An observation point has a bearing from the source that is identical to the one on the left. However, the LE and LH command pair request output data along a defined line, in this case, running from the source to the final observation point. The data returned by the request provides electric or magnetic field strength using the axial direction of the line as the primary field component. Also provided are two transverse

components, one horizontal and the other vertical. If we define the axial vector as a-cap, we may let h-cap and v-cap be the horizontal and vertical transverse components, respectively, as roughly represented on the right side of **Fig. 18-11**. The actual vectors use the following equations.

$$\hat{a} \qquad \hat{h} = \hat{z} \times \hat{a} / |\hat{z} \times \hat{a}| \qquad \hat{v} = \hat{a} \times \hat{h}$$

The key entry data for both the LE and LH command are the number of points along the line to use for field strength reports and the starting and ending coordinates of the line. Hence, the pair of commands has the following structure.

CMD	I1	I2	I3	I4	F1	F2	F3	F4	F5	F6
	RSET	NPTS	0	0	X1	Y1	Z1	X2	Y2	Z2
LE	0	16	0	0	0	0	0	0	1.5	.5
LH	0	16	0	0	0	0	0	0	1.5	.5

I1 is called RSET because a value of -1 resets one of the output values (the cumulative line integral) to zero. However, for a new request, I1 normally equals 0. I2 shows the number of equally spaced observation points along the line. Since I3 and I4 have no function, zeroes serve as placeholders pending the start of the floating decimal places. The input system differs from either system used with the NE and NH commands, but is a variant on Cartesian coordinates and similar to the system used in GW entries. F1 through F3 define one end of the line in terms of X, Y, and Z, while F4 through F6 define the other end of the line in the same terms. Unlike GW commands, the units of measure must be meters. **Fig. 18-12** shows the GNEC assistance screens for LE and LH.

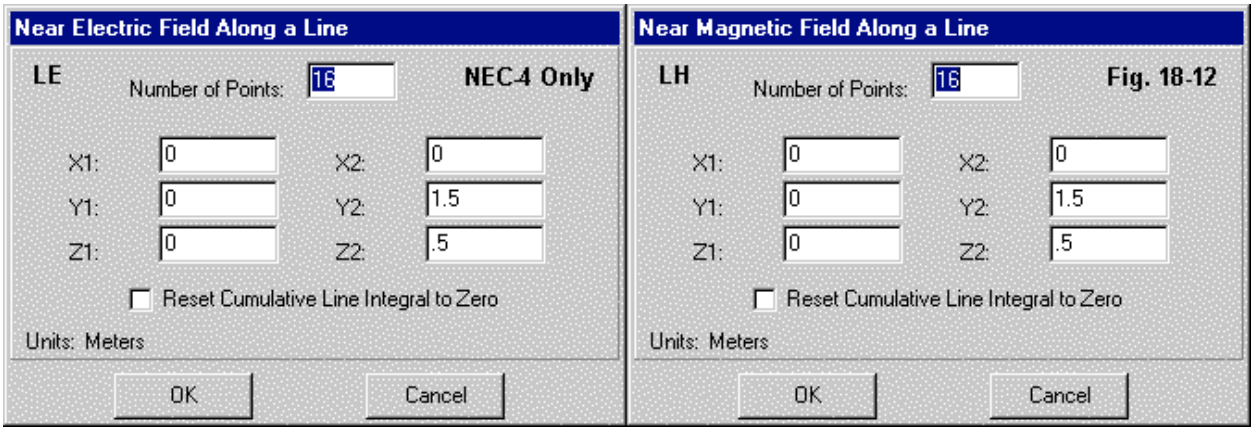

Both of the sample lines request a report using 16 points along a line defined by 0, 0, 0 at end 1 and by 0, 1.5, and 0.5 at end 2. The LE and LH commands use the same execution rules as the NE/NH pair. They will self-execute if there is only one frequency requested. However, for multiple frequencies in the FR command, they require either a following RP or XQ command to execute. As well, if there are multiple near-field requests as well as multiple frequencies, then the FR command requires repetition before each LE or LH command to ensure that data is available for all requests at all frequencies. As well LE and LH are subject to the same ground and boundary conditions as NE and NH.

The safest procedure to obtain controlled results is to ensure that no selected field point falls

within the wires of the antenna, that is, along the segment line or within its radius. If a field point does fall within these confines, NEC will move it an amount equivalent to the wire radius outside the wire in a direction normal to the plane for a reading and along the vector from the source segment to the observation point. Because the results may not include that segment's contribution to the H field or to the radial component of the E field, it is always wise to pre-plan the observation points so that they all fall outside the wire segments of the model.

The preferred ground calculation system for near-field analysis is the Sommerfeld-Norton (SN) system. However, there are restrictions. To minimize errors that tend to appear at very low frequencies, no observation point should be exactly at ground level. In fact, the minimum distance above ground in NEC-2 should be 0.001 wavelength. The reflection coefficient approximation (RCA) system, sometimes called the "fast" ground calculation system, may produce errors in the magnetic field calculations for observation points at some distance from the source. The RCA system does not include surface-wave contributions for this calculation and so may underestimate the field strength.

We may set up a model that is--with respect to the location of observation points--identical to model 18-12. The difference is that we shall employ the LE and LH commands in this NEC-4-only model. Open model *18-13-nec4.nec*.

```
LE 0 16 0 0 0 0 0 0 1.5 .5
LH 0 16 0 0 0 0 0 0 1.5 .5
```

Run the model and obtain the first 3 lines of the electric field report. Compare them with the corresponding lines for model 18-12.

```
          -  LOCATION  -                  - Axial -
   X            Y            Z        MAGNITUDE     PHASE
METERS       METERS       METERS       VOLTS/M     DEGREES
0.0000       0.0000       0.0000     3.4785E+00   -180.00
0.0000       0.1000       0.0333     1.2688E-01     69.64
0.0000       0.2000       0.0667     1.2948E-01     64.35

                          - Transverse1 -          - Transverse2 -
                         MAGNITUDE    PHASE       MAGNITUDE    PHASE
                         VOLTS/M     DEGREES      VOLTS/M     DEGREES
                        0.0000E+00     0.00     1.0436E+01   -180.00
                        0.0000E+00     0.00     8.5015E-01    150.69
                        0.0000E+00     0.00     3.8826E-01    105.77
```

The coordinates of each observation point are the same as for the NE/NH version of the model. However, the electric field strength values are nowhere the same, due to the differences in the way in which each command calculates the field component values. It is possible to have the axial and transverse orientations align with the coordinate system axes. This condition will exist if the axial line lies along one of the axes of the Cartesian coordinate system. Such a condition will normally be exceptional.

Note that within the LE (and LH) report are supplemental data at both the top of the table and the bottom.

```
 Unit Vectors:       X         Y         Z
 Axial       =    0.00000   0.94868   0.31623
 Transverse1 =   -1.00000   0.00000
 Transverse2 =    0.00000  -0.31623   0.94868
```

At the top of the report, we find the axial, horizontal, and vertical vectors that define the components listed as axial, transverse 1, and transverse 2. For each line, the square root of the sum of the squares of the values is, of course, 1.0. You may use the arc-cosine of axial Z value to obtain the theta angle used in the NE/NH version of the model (71.656 degrees). Given that we have a vertical dipole in free space, the zero-readout for the horizontal vector should not be surprising. Since the Axial and transverse2 magnitudes are in phase and since the transverse1 value is zero, you may perform a simple vector addition of the two significant values to obtain a sum of 1.1000E1 peak value. This value matches the peak value for the corresponding line of the NE output report.

```
 Line integral of E       = -1.45652E-01 3.06530E-02 Volts
 Cumulative line integral = -1.45652E-01 3.06530E-02 Volts
```

At the end of the report, we find the line integral of E, as well as a cumulative integral. We may add further LE and LH requests to this model, so that the end of one line is the beginning of the next, as illustrated in **Fig. 18-12**.

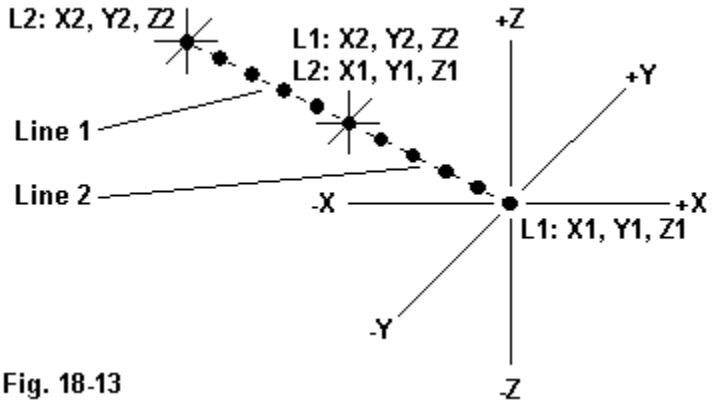

Fig. 18-13

A succeeding line may run in any direction and even return to the series starting point. Each subsequent LE or LH command, as appropriate, will show its own line integral and a new cumulative value. However, the lines must form a continuous string with no breaks; that is, the end-2 coordinates of one line must be the end-1 coordinates of the next line. In addition, the LE and LH commands must form a group with no intervening control commands. For example, open model *18-14-nec4.nec*.

```
LE 0 16 0 0 0 0 0 0 1.5 .5
LH 0 16 0 0 0 0 0 0 1.5 .5
LE 0 16 0 0 0 1.5 .5 0 3 1
LH 0 16 0 0 0 1.5 .5 0 3 1
```

The first set of LE/LH commands is identical to the set in model 18-13. The second set uses the

X2, Y2, and Z2 coordinates of the first line to start the second line as X1, Y1, and Z1. In this simple model, the coordinates simply extend the length for another equal distance. If you run the model, you will discover that the last entry of the first (electric or magnetic) field table is the same as the first entry of the second (electric or magnetic) field table, since they both represent the same point. However, the line and cumulative integrals will change to reflect--in the latter case--the extension of the total line of observation points.

```
Line integral of E       =  2.13307E-03-1.83322E-03 Volts
Cumulative line integral = -1.43519E-01 2.88197E-02 Volts
```

We have only scratched the surface of near field analysis. Our goal has not been to explain near fields and their applications, but to provide an orientation to setting up near-field commands and obtaining the appropriate outputs. The requested output may range from a single point at a single frequency to a 3-dimensional shape full of points, with single or multiple frequency requests. Although some graphic presentation aids are available, tabular data will be the main resource.

Summing Up

Effectively using near-field commands (NE and NH) requires a clear conception of the relationship between the Cartesian coordinate system and the associated spherical coordinate system. The near electric field and near magnetic field commands that are common to both NEC-2 and NEC-4 permit either type of observation point specification within the command. However, since each system uses a different mode of progressing from the initial starting coordinates, you must be careful which system you select in order to obtain the desired pattern of observation points in the output.

Cartesian input coordinates (command type 0) require that you input a set of initial coordinates, each with a specified number of steps and an increment between steps. Spherical input coordinates (command type 1) require that you set a radius along with phi and theta angles to locate the first point. Further points will then be a function either of a number of steps along the radius as measured in meters or of a number of either phi or theta angles measured in degrees. A notable feature of NEC-4, relative to NEC-2, is that the later core reverses the command line positions for phi and theta angles. Regardless of the selected system of coordinate input, the NE and NH output tables will show the locations of the observation positions in Cartesian coordinates.

The NE and NH commands are self-executing only if there is only a single frequency request. Multiple frequency requests require a following execution command for each near field request. As well, if each near-field request requires a data set for each frequency in the multiple-frequency request, then the frequency command must be repeated prior to each near field command.

The NE and NH output data appear as series of field strength readings in peak volts/meter for the electric field and in peak amps/meter for the magnetic field. A NEC-4 feature that has been retrofitted to NEC-2 is the presentation of the peak field strength, which is calculated from the components. The component field strength values are oriented to the Cartesian X-, Y-, and Z-axes.

NEC-4 introduces two new near-field commands: LE and LH for near electric and magnetic fields along a line. The input system for these commands requires specification of the end Cartesian coordinates of a line, along with the number of equally spaced observation points along the line. The output tables present the field strength as an axial value plus 2 transverse values. Hence, for the same observation points that an NE or NH command might generate, the LE and LH component values will differ. An advantage offered by the LE and LH commands is that we may specify additional connected lines to accumulate near field data in selected geometric sequences.

19.
Receive and Scattering Data: Excitation and Data Requests

***Objectives**: Receive and scattering data acquisition will acquaint us with three plane-wave excitation options available within the EX or excitation command: linear, right-hand elliptical, and left-hand elliptical sources external to the antenna. Conjointly, obtaining this data will require that we examine the options of the PT command that controls printing the wire-segment currents.*

Throughout our work in this volume, we have focused on mastering the command structure of NEC to obtain sensible output results within the limits of the program. We have left the theory and mathematics underlying the program to the extensive NEC manuals. The first 2 volumes of the NEC-2 manual constitute essential background against which to explore the program changes made for NEC-4. We shall continue our practical focus as we take some first steps into obtaining receive and scattering data from NEC.

Receiving information requires that we probe into two commands. We must have an external or incident source of energy relative to the antenna structure. The EX command has options that we previously by-passed in Chapter 10. By selecting EX1, EX2, or EX3, we can externally excite the antenna from any angle with linear plane waves, right-hand polarized plane waves, or left-hand polarized plane waves. Each selection allows numerous specifications, including the polarization angle and--for elliptical plane waves--the ratio of minor to major axes. We shall look at both the command structures needed to set the various options in place and some first-order consequences of varying the input data.

NEC also provides a number of provisions for obtaining output data tailored to plane wave excitation. The primary vehicle for useful information with plane-wave excitation is the wire-segment current table. The PT command controls the printing of wire-segment current data and includes both suppression and format changes among its options. We have used the command in some past exercises, but have not fully scoped the numerous options and their applications. In these exercises, we shall perform a more thorough survey of what we can do with the PT command. Of course, we shall give major attention to receive applications.

Finally, the RP0 radiation pattern command does not entirely disappear from relevance when we use plane-wave excitation. The command provides scattering data, that is, information on the relative strength of energy reflected from the antenna or other objects established by the structure geometry. When we provide an antenna with a voltage source (EX0), we are most often interested in complete radiation patterns as captured in 2- and 3-dimensional polar plots. For many applications employing plane-wave excitation, we shall be interested in only part of the data. For example, a radar source may be primarily interested in the energy reflected or scattered back to the source location, although recent developments of aerial and naval techniques may have a high interest in where the remainder of the energy goes. Each potential application will have its own special interests. Our task will be to master the NEC commands that will permit us to obtain the information fitting to interests that we bring to receive and scattering data.

Plane-Wave Excitation: EX1, EX2, and EX3

If you are not acquainted with incident plane-wave excitation, the first item to understand is that these sources do not excite a specific wire segment on the model. Instead, they simulate an external signal source that excites the entire antenna structure. The entry-line structure for them has a number of interesting properties that differ from the line structure of a simple voltage source.

```
Cmd   I1    I2       I3       I4    F1          F2
      Type  # Thet   # Phi    Not   Th angle    Ph angle
            angles   angles   used  to vector   to vector
EX    1     1        8        0     90          0

                               F3          F4       F5    F6       F7
                               Eta         Theta    Phi   Axis     El. field
                               pol angle   step     step  ratio    V/m
                               90          0        45    0        0
```

The sample NEC-4 entry is for a linear plane wave. Hence, F6 is 0 by non-relevance. F7 also has a 0, but that value indicates a default value of 1 V/m. In some problems designed to ferret out coupling potentials among wires, you may use a specific value that closely approximates the value from the source signal at the structure being examined in model form.

Most of the remaining entries define incident plane waves as a calculation loop within NEC (with some properties resembling the loop operation of frequency sweeps using the FR command). In the sample, for the sake of clarity, there is only one theta angle: 90°. This angle is parallel to the plane of the antenna elements. The sample specifies 8 phi-angle (azimuth-angle) steps at 45° increments, thus providing samples evenly spaced in the element plane.

The F3 entry, called Eta (η), under linear polarization is easy to memorize. With a value of 0°, the polarization is in the +/-Z direction--vertically polarized for antennas over ground. If F3 is 90°, the polarization is in the X-Y plane--horizontally polarized for antennas over ground. The sample in free space uses horizontal polarization for simplicity, but there is no restriction against checking results when cross-polarized or with the polarization set to intermediate angles. When using EX 2 or EX 3, elliptical polarization, the entry changes its meaning and defines the major ellipse axis.

Special Note for NEC-2 Users: The structure of the NEC-2 plane-wave excitation entry is slightly different than the NEC 4 entry. It has the following appearance:

```
Cmd   I1    I2       I3       I4    F1          F2
      Type  # Thet   # Phi    Not   Th angle    Ph angle
            angles   angles   used  to vector   to vector
EX    1     1        8        0     90          0

                               F3          F4       F5    F6
                               Eta         Theta    Phi   Axis
                               pol angle   step     step  ratio
                               90          0        45    0
```

Note that the NEC-2 version lacks the F7 floating point entry for the electrical field strength, and the default value of 1 V/m always applies. **Fig. 19-1** shows the differences as they appear on the NSI command assistance screens. Only 1 incident plane wave is allowed at a time (that is, before a succeeding execution step). If excitation types are mixed before a succeeding execution command, then the program will use only the last excitation type encountered.

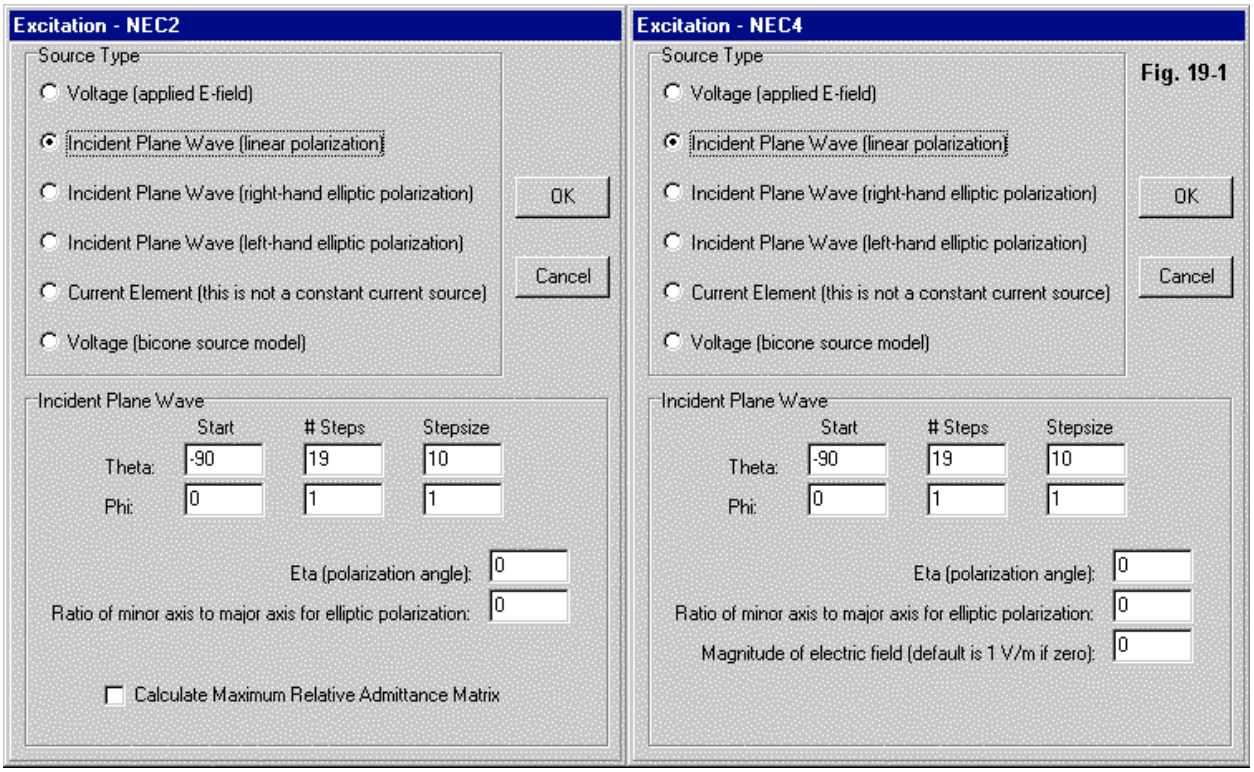

Fig. 19-1

The command line allows you to specify many plane-wave sources of the same type. The sources will be arrayed across the sphere (free space) or hemisphere (over ground) according to your selection of the initial theta angle (F1), the number of theta angles (I2), and the angular increment of each step (F4). You have similar latitude in selecting the initial phi angle (F2), the number of phi angles (I3), and the increment of each step (F5). Because the position of each entry is separated from related entries, the use of the assistance screens offers assurance of developing a correctly structured command line.

The angular position described by the theta and phi entry trios is the source position from which there is a vector toward the coordinate system source. The left portion of **Fig. 19-2** shows the key elements of the vector as it relates to the Cartesian coordinates. For all structure geometries, you should correlate the orientation of the structure and the source of plane-wave excitation in order to be certain that you understand just how the energy source relates to the structure. If the structure extends "forward" along the +X axis, then an initial phi angle of 0° will place the source ahead of the structure (unless the initial theta angle is so low as to place the source overhead). For any analysis, using a modest number of steps and fixing one or the other angular systems at only 1 step will usually result in a much clearer table of output data. Since you may repeat the EX

command and its associated data request commands as many times as you need or wish, you can subdivide the output data into more easily digested chunks.

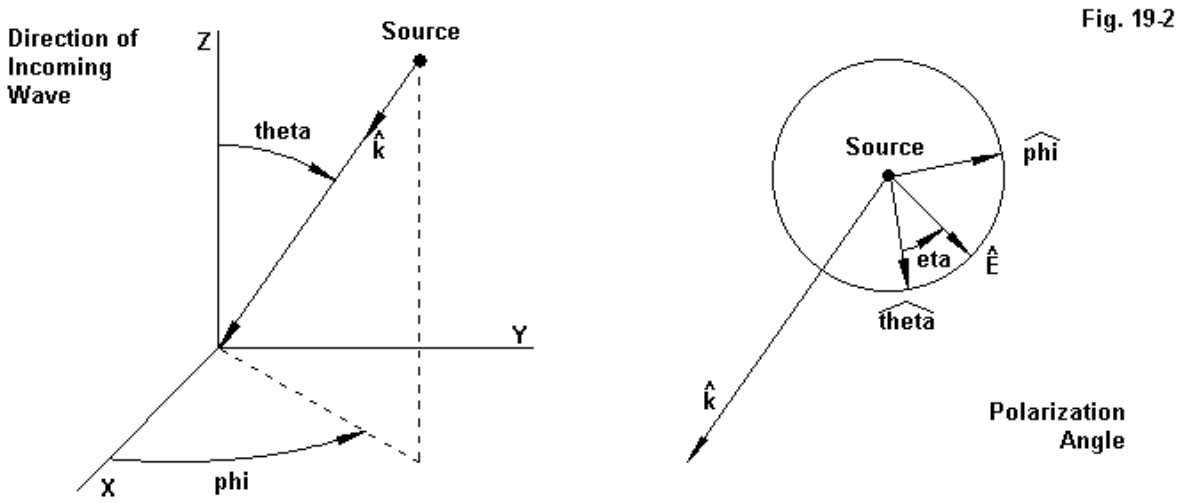

Fig. 19-2

The right side of **Fig. 19-2** shows the relationship of eta (F3) to the theta and phi unit vectors. The polarization angle is the angle between the theta vector and the plane wave. For simple linear polarization (EX1) cases, eta will by 0° to simulate vertical polarization and 90° to simulate horizontal polarization when the source is near the horizon. When using elliptical polarization (EX2 or EX3), F3 specifies the major ellipse axis for the source E-cap. In that case, F6 gives the ratio of the minor to the major axis.

In order to sample some of the options available within the incident plane-wave excitation family, we shall need a sensible output. For that reason, we shall jump ahead of ourselves and employ the PT1 command. This command allows us to print a table of current values for a specified array of segments on a given tag. For all the following samples (except some reference models), we shall use only one segment, the segment on which we would place the source if we were using an EX0 command. The easiest way to grasp the idea is with an example. Open model *19-1.nec*, a standard dipole in free space using a voltage source and request a phi radiation pattern.

```
CM Voltage excitation
CM Horizontal dipole
CE
GW 1 11 0 -.2375 0 0 .2375 0 .001
GE
GN -1
FR 0 1 0 0 299.7925 1
EX 0 1 6 00 1 0
RP 0 1 361 1000 90 0 1.00000 1.00000
EN
```

Run the model and create a plot of the pattern. However, use the rectangular plot facility. Because the receive data very often uses only partial phi and theta scans, very often with wide sampling increments, the rectangular plotting feature is often more useful than the polar plot

feature. You may see just how useful rectangular plots are when you open model *19-1a.nec* and compare it to model 19-1.

```
CM Plane-wave excitation-linear
CM Horizontal dipole
CM phi variation
CE
GW 1 11 0 -.2375 0 0 .2375 0 .001
GE
FR 0 1 0 0 299.7925 1
EX 1 1 19 0 90 0 90 1 20 0
PT 1 1 6 6
XQ
EN
```

The geometry and frequency remain unchanged. However, the EX command requests an incident linear plane wave at theta = 90° (unchanging) and 19 steps of phi angles, beginning at 0° and increasing in 20° steps. The result will be a series of plane-wave sources that circle the dipole. Eta is 90° to simulate horizontal polarization. The PT1 command requests a table of current values, one per source increment, using the center segment of the dipole where we had earlier placed the EX0 voltage source. Run the model and inspect the table.

THETA (DEG)	PHI (DEG)	- CURRENT - MAGNITUDE	PHASE	SEG NO.
90.00	0.00	4.3963E-03	-3.09	6
90.00	20.00	4.0227E-03	-3.04	6
90.00	40.00	3.0631E-03	-2.92	6
90.00	60.00	1.8470E-03	-2.76	6

The extracted lines give you an idea of the data presentation, which includes the theta and phi angles in addition to the current magnitude and phase. You may create a rectangular plot of this data to compare with the radiation plot.

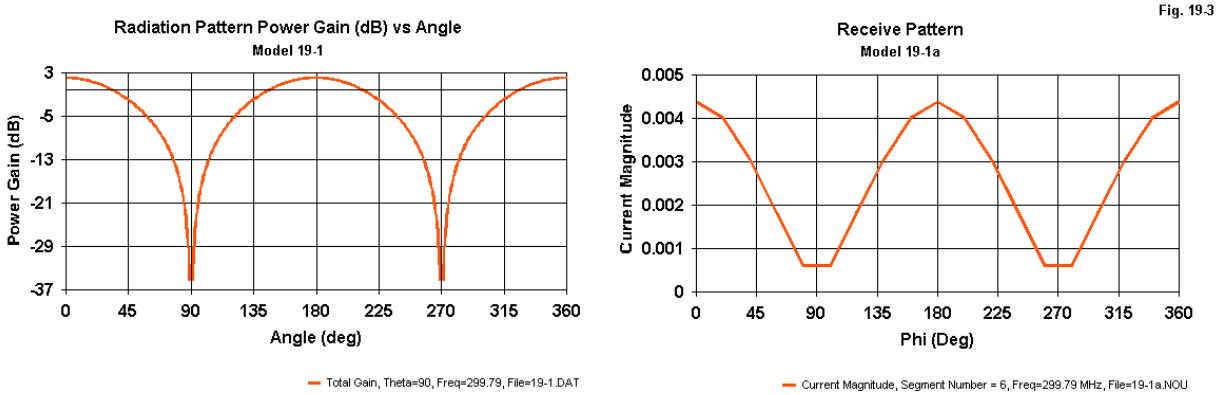

Fig. 19-3 places the graphs side-by-side. The receive data plot has far fewer data points, resulting in straighter lines. As well, a plot of current values differs from a plot of power gain values in dBi, since the dBi scale results from a log of a function that is the square of the current level. With that adjustment, the relationship of the two graphs becomes clear.

Let's alter the dipole by setting it vertically about 1/4λ above an average SN ground. Open model *19-2.nec*, again, a standard form model with a voltage source and a request for a theta radiation pattern. Run the model and save a rectangular graph of the radiation pattern.

```
GW 1 11 0 0 .2375 0 0 .7125 .001
GE 1 -1 0
GN 2 0 0 0 13.0000 0.0050
FR 0 1 0 0 299.7925 1
EX 0 1 6 00 1 0
RP 0 181 1 1000 -90 0 1.00000 1.00000
EN
```

The incident linear plane-wave version of the model is *19-2a.nec*.

```
EX 1 19 1 0 -90 0 0 10 1 0 0
PT 1 1 6 6
XQ
```

In this version, the excitation source undergoes the position change that the first model places in the radiation request. We have 19 steps at 10° intervals beginning with a theta angle of -90°. Run the model and compare the rectangular plot of the currents with the gain plot for model 19-2.

Fig. 19-4

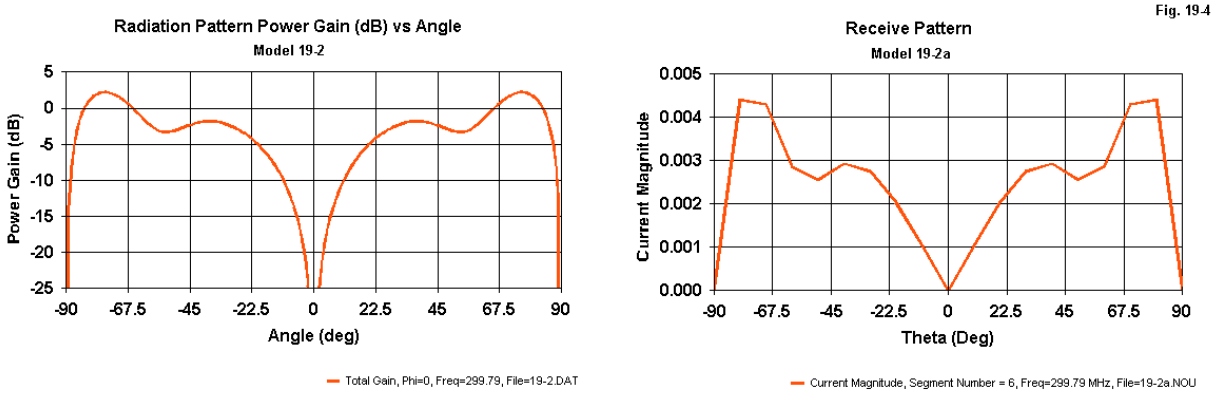

Examine **Fig. 19-4**. If we allow for the facts that the new graph uses 10° steps and is of current rather than power, we can easily see the correlation between it and the radiated power plot. However, both of our dipole models have an ambiguity as to the exact position of the source relative to the antenna structure, since both produce symmetrical patterns. Therefore, let's try the same experiment with a directional antenna. Open model *19-3.nec*, a voltage-source version of a 2-element horizontal Yagi.

```
GW 1 15 0 -0.2303 0 0 0.2303 0 0.001
GW 2 15 -0.1449 -0.2506 0 -0.1449 0.2506 0 0.001
GS 0 0 1
GE 0
EX 0 1 8 0 1 0
FR 0 1 0 0 299.7925 1
RP 0 1 361 1000 90 0 1 1
EN
```

GW2 is the reflector, which is more negative along the X-axis than the forward driver element. Hence, we expect a gain peak toward 0° in a phi plot. Run the model and produce a rectangular plot of the radiation pattern. Next, open the incident linear plane-wave version, model *19-3a.nec*.

```
EX 1 1 37 0 90 0 90 1 10 0 0
PT 1 1 8 8
XQ
```

The plane-wave source uses 37 steps beginning at phi = 0° and proceeding in 10° increments. Compare a rectangular plot of the currents in the PT1 report to the radiation pattern for model 19-3. See **Fig. 19-5**.

Fig. 19-5

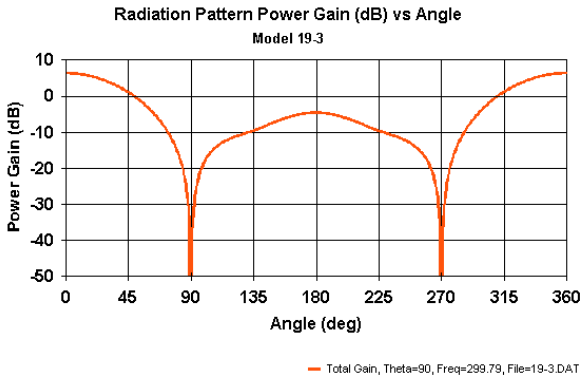

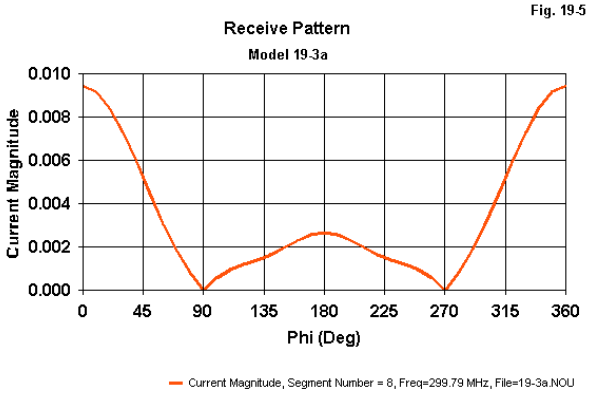

We find that maximum current occurs with the plane-wave source at a phi angle of 0°, that is, in front of the antenna along the X-axis. We may perform the same orientation exercise with a vertically polarized Yagi. This model faces the opposite way on the X-axis, as indicated by the more positive X value for the reflector (GW2). Open model *19-4.nec*, and create a rectangular graph of the requested phi pattern.

```
GW 1 15 0 0 -0.2303 0 0 0.2303 0.001
GW 2 15 0.1449 0 -0.2506 0.1449 0 0.2506 0.001
GS 0 0 1
GE 0
EX 0 1 8 0 1 0  1 10 0 0
FR 0 1 0 0 299.7925 1
RP 0 1 361 1000 90 0 1.00000 1.00000
EN
```

We shall compare the pattern with the current graph for model *19-4a.nec*. This model follows the same model structure as model 19-3a with one exception (besides the wire positions). Note the eta angles in the two models. For the horizontal Yagi, we set eta (F3) at 90°, but for this vertical Yagi, eta is 0°

```
EX 1 1 37 0 90 0 0 1 10 0 0
PT 1 1 8 8
XQ
```

Run the model and create a rectangular plot of currents for comparison. See **Fig. 19-6**.

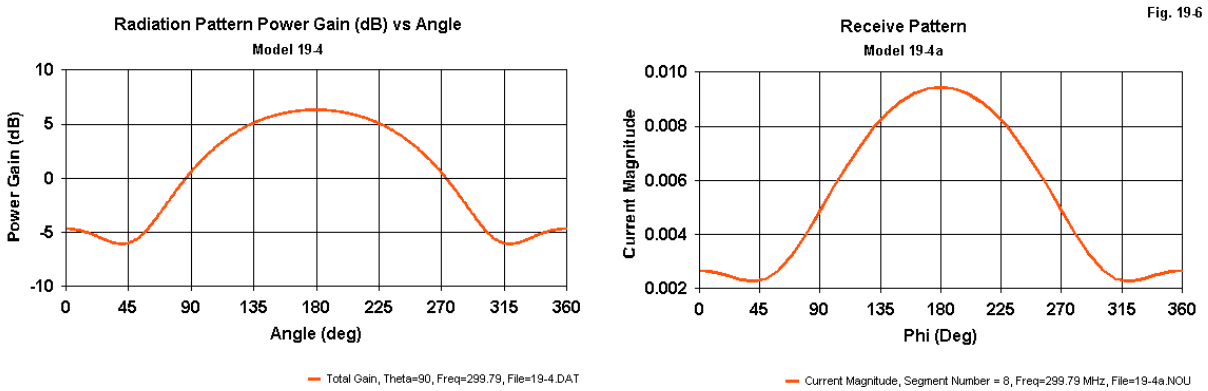

Fig. 19-6

In both cases, we find the highest values of power and of current, respectively, at the 180° mark, coinciding with the beam direction of maximum gain. Note also that the peak gain and current values are similar for both plots to those for the 19-3-model series. The lowest values for models in the 19-4 series do not go as low in those in the 19-3 series, since the H-plane of the beam does not have the deep side nulls of the same beam in the E-plane.

In all of these introductory exercises, we have pre-set eta to the angle that yields linear incident plane waves having the same polarization as the elements. We can see some of the effects of both mild and radical cross polarization by returning first to our horizontal dipole in free space. Open models *19-5a.nec*, through *19-5e.nec*. The first model of the set appears here.

```
GW 1 11 0 -.2375 0 0 .2375 0 .001
GE
FR 0 1 0 0 299.7925 1
EX 1 1 1 0 90 0 0 1 1 0 0
PT 1 1 6 6
XQ
EN
```

Eta is 0° and will progressively grow to 90° through the sequence. Each EX1 command calls for a single linear incident plane-wave source at theta = 90° and phi = 0°, exactly broadside to the dipole. Record the current values for each of the 3 models in a table.

Model	Eta (Deg)	THETA (DEG)	PHI (DEG)	- CURRENT - MAGNITUDE	PHASE	SEG NO.
19-5a	0	90.00	0.00	0.0000E+00	0.00	6
19-5b	22.5	90.00	0.00	1.6824E-03	-3.09	6
19-5c	45	90.00	0.00	3.1086E-03	-3.09	6
19-5d	67.5	90.00	0.00	4.0616E-03	-3.09	6
19-5e	90	90.00	0.00	4.3963E-03	-3.09	6

Note that when the source plane wave is fully cross polarized relative to a strictly linear element, the current at its center segment goes to zero in a free-space model. We likely should see if something similar happens in the presence of ground reflection. Therefore, let's perform the same experiment with our vertical dipole placed over average SN ground. Open in order models *19-6a.nec* through *19-6e.nec* and run the same experiment. The model sample is again the first in the sequence.

```
GW 1 11 0 0 .2375 0 0 .7125 .001
GE 1 -1 0
GN 2 0 0 0 13.0000 0.0050
FR 0 1 0 0 299.7925 1
EX 1 1 1 0 76 0 0 1 1 0 0
PT 1 1 6 6
XQ
EN
```

Note that the single incident plane-wave source uses a theta angle of 76° to coincide with the take-off angle for the antenna when set up (as in model 19-2) with a voltage source.

Model	Eta (Deg)	THETA (DEG)	PHI (DEG)	- CURRENT - MAGNITUDE	PHASE	SEG NO.
19-6a	0	76.00	0.00	4.7167E-03	-139.72	6
19-6b	22.5	76.00	0.00	4.3577E-03	-139.72	6
19-6c	45	76.00	0.00	3.3352E-03	-139.72	6
19-6d	67.5	76.00	0.00	1.8050E-03	-139.72	6
19-6e	90	76.00	0.00	2.4071E-14	40.29	6

Cross polarization at eta = 90° does not drive the current to zero, although very close to it. Of course, propagation effects, including those that affect point-to-point paths, may play a role in further altering the current level at cross polarization.

The examples that we have so far surveyed all use EX1 commands producing linear plane waves. If we wish to sample the elliptical plane-wave sources (EX2 and EX3), we would do well to use a different antenna. Open model *19-7-nec2.nec*, a 5 turn NEC-3 helix over a perfect ground. **Fig. 19-7** shows the outline of the model and its theta pattern as a reference. Knowing that the helix has 5 turns will allow you easily to reformulate the model in case you wish to run it using NEC-4.

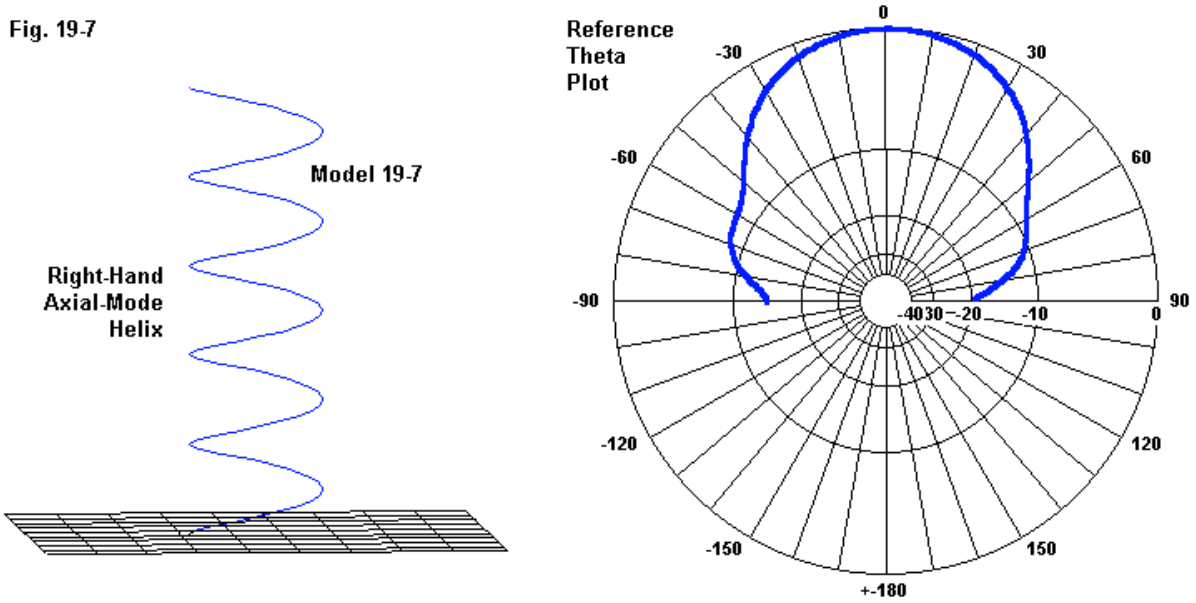

```
GH 1 100 0.2125566 1.0627828 .1591549 .1591549 .1591549 .1591549 .001
GE 1
GN 1
EX 0 1 2 00 1.0 0.0
FR 0 1 0 0 299.7925 0
RP 0 181 1 1000 -90 0 1.00000 1.00000
EN
```

Next open model *19-7a-nec2.nec*. The EX2 command specifies a single right-hand elliptical plane-wave source directly over the helix. The F6 entry specifies a 1:1 ratio for the major and minor axis of the ellipse, the condition for circular polarization. Run this model and record the current information.

```
EX 2 1 1 0 0 0 0 1 1 1
PT 1 1 1 1
```

Next, open model *19-7b-nec2.nec*. Note the one difference: a request for an EX3 source, that is, a left-hand circularly polarized incident plane-wave source. Run this model and compare the current information to the value derived for model 19-7a.

```
EX 3 1 1 0 0 0 0 1 1 1
```

Model	EX	THETA (DEG)	PHI (DEG)	- CURRENT - MAGNITUDE	PHASE	SEG NO.
19-7a	2 (RH)	0.00	0.00	7.8064E-03	174.24	1
19-7b	3 (LH)	0.00	0.00	2.5959E-04	64.41	1

The current ratio is about 30:1. We may run the same experiment using a left-hand helix, as shown in **Fig. 19-8**, the outline and reference theta plot of model *19-8-nec2.nec*. Note the placement of the negative sign in the NEC-2 form of the helix to create the left-hand turn set. If you transform the model for NEC-4, move the negative sign to the proper command entry.

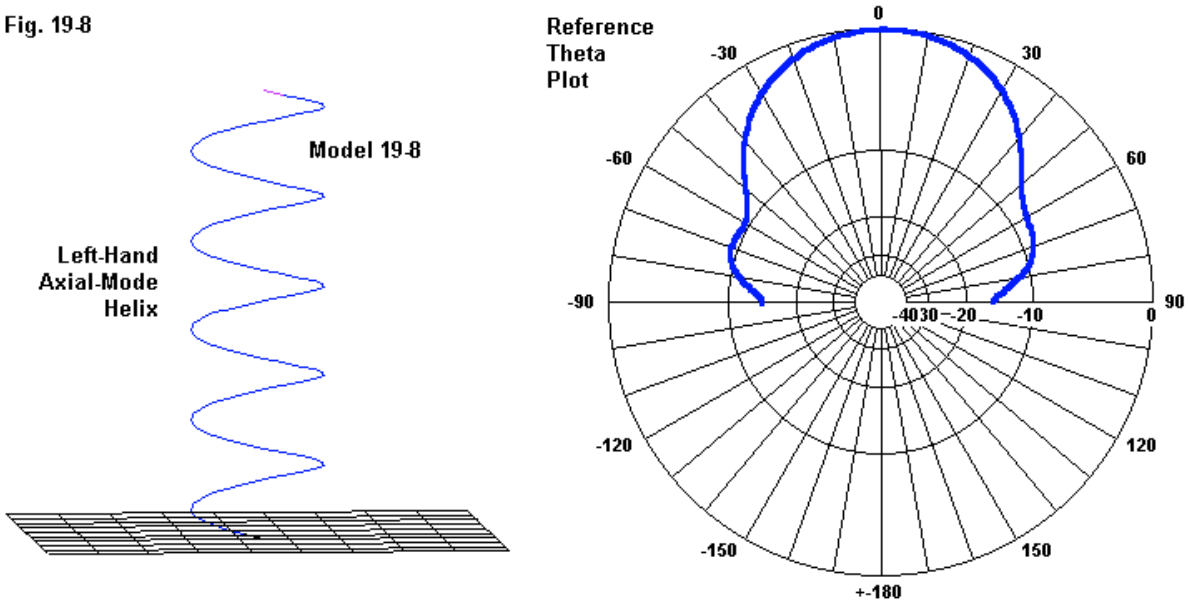

```
GH 1 100 0.2125566 -1.0627828 .1591549 .1591549 .1591549 .1591549 .001
GE 1
GN 1
EX 0 1 2 00 1.0 0.0
FR 0 1 0 0 299.7925 0
RP 0 181 1 1000 -90 0 1.00000 1.00000
EN
```

Next, open models *19-8a-nec2.nec* and *19-8b-nec2.nec*. In each case, note the polarization of the EX command, run the model, and then record the current data.

Model 19-8a

```
EX 2 1 1 0 0 0 0 1 1 1
```

Model 19-8b

```
EX 3 1 1 0 0 0 0 1 1 1
```

Model	EX	THETA (DEG)	PHI (DEG)	- CURRENT - MAGNITUDE	PHASE	SEG NO.
19-7a	2 (RH)	0.00	0.00	2.5959E-04	154.41	1
19-7b	3 (LH)	0.00	0.00	7.8064E-03	84.24	1

With respect to current magnitude, we have a mirror image of the situation for the right-hand helix. Reverse circularity yields a very large change in the current level at the source segment (relative to the voltage-source model).

Command entry F6 permits us to change the ratio of the minor axis to the major axis for elliptically polarized plane-wave sources. Before we leave plane-wave sources, let's systematically vary the ratio, beginning with a 1:1 ratio and reducing the ratio toward zero. The steps will be 1.0, 0.75, 0.5, 0.25, and 0.0, as shown in **Fig. 19-9**. The diagram incidentally shows why circular and linear polarization are special cases of elliptical polarization.

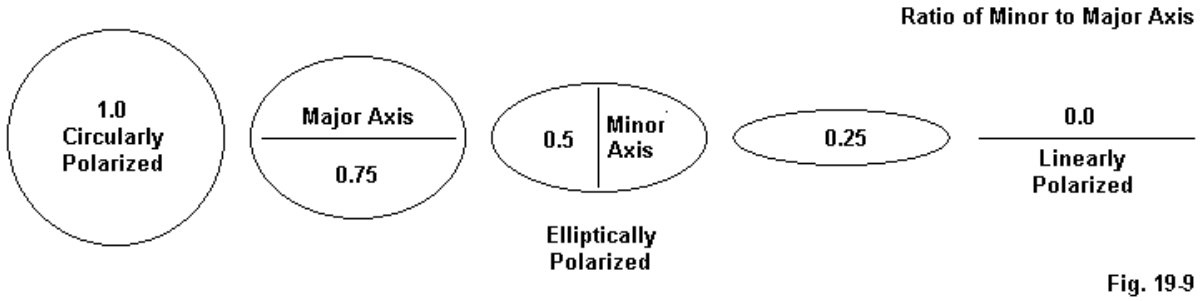

Fig. 19-9

The exercise will use a right-hand helix and a right-hand (EX2) incident plane-wave directly above the helix. Open models *19-9a-nec2.nec* through *19-9e-nec2.nec*. The sample from the sequence is for model 19-9a, which begins with a 1:1 ratio. If you modify the model for use with NEC-4, the fact that there are 5 turns will ease the calculations for entry. NEC-4 will give you an opportunity to change the magnitude of the electric field in the incident wave along the major axis for elliptical polarization by entering a value other than 0 or 1 for F7. The absence of an F7 position in NEC-2 results from the early Fortran limit of 4 integer and 6 floating decimal entries. A number of NEC-4 commands--where different from their NEC-2 counterparts--make use of the additional floating

decimal places that are currently available.

```
GH 1 100 0.2125566 1.0627828 .1591549 .1591549 .1591549 .1591549 .001
GE 1
GN 1
EX 2 1 1 0 0 0 0 1 1 1
FR 0 1 0 0 299.7925 0
PT 1 1 1 1
XQ
EN
```

Run each model in the sequence and create a table of results.

Model	Min/Maj Ratio	THETA (DEG)	PHI (DEG)	- CURRENT - MAGNITUDE	PHASE	SEG NO.
19-9a	1.0	0.00	0.00	7.8064E-03	174.24	1
19-9b	0.75	0.00	0.00	6.8197E-03	173.98	1
19-9c	0.5	0.00	0.00	5.8332E-03	173.64	1
19-9d	0.25	0.00	0.00	4.8469E-03	173.15	1
19-9e	0.0	0.00	0.00	3.8611E-03	172.42	1

As the ratio diminishes, the current magnitude decreases. Between the highest and lowest values, there is a ratio of 2.02:1

There are many other combinations of entry values that we might survey, some especially applicable to specific applications. However, our goal has been more general and more fundamental: to orient you to the required and optional entries in the incident plane-wave excitation commands, EX1, EX2, and EX3. Along the way, we have restricted the output side of the ledger to a single command: PT1. From that command, we were able to extract enough information to show some first-order results of using incident plane-wave excitation.

However, the PT command has many facets and many applications. Many of them are apt to receive data, but others have more general application. So let's examine the output side of the ledger in some detail.

PT: Printing, Suppressing, and Formatting Segment Current Information

Receiving pattern data largely use or depend upon the currents that we find on specific wire segments of the subject antenna. These current levels result from an incident plane wave specified in the EX command. From that basis, we may go on to develop other information, such as scattering data. However, everything focuses on the segment currents.

NEC has a command that controls the printing, suppressing, and formatting of segment current data: PT. The command has many facets, more than half of which apply specifically to receiving pattern tables. In addition, the command has more general functions.

Cmd	I1 IPTFLG	I2 IPTAG	I3 IPTAGF	I4 IPTAGT
PT	2	2	1	11

IP stands for current printing. The first integer entry specifies the PT option.

PT -2: All current printed. This option is the default if PT is omitted altogether.
PT -1: Suppress printing of all wire-segment currents.
PT 0: Current printed for a specified range of segments only.
PT 1: Currents for a specified range of segments printed in a format designed for a receiving pattern using the magnitude and phase of the current.
PT 2: Currents for a specified range of segments printed in a format designed for a receiving pattern using the magnitude and phase of the current, plus a normalized value for the last segment's current.
PT 3: Only the normalized current for a specified segment is printed.

In addition, NEC-4 offers two additional options that do not appear in the original NEC-4 manual.

PT 8: Current printed for a specified range of segments only, using the magnitude and phase of the current. In addition, the data is saved to a file bearing the model file name and the extension .GPT (in NSI software).
PT9: Current printed for a specified range of segments only, using the real and imaginary components of the current. In addition, the data is saved to a file bearing the model file name and the extension .GPT (in NSI software).

IPTAGF and IPTAGT refer to the first and last segments of the range of segments for the tag IPTAG. If IPTAG = 0, then the command uses absolute segment numbers. If IPTAGF = 0, then the current is printed for all segments. If IPTAGT = 0, then its value is the same as IPTAGF.

To examine the kinds of data yielded by the various PT options, we shall need a single antenna design to serve as a continuous thread. Using a single design will permit us to correlate one set of output data with another. Our subject antenna will be a straightforward 6-element Yagi. Open model *19-10.nec*, which uses a typical set-up for a voltage source and a standard radiation pattern.

```
CM 6-el Yagi
CM PT exercises
CE
GW 1 21 0 0.2506 0 0 -0.2506 0 0.0012
GW 2 21 0.1253 0.2472 0 0.1253 -0.2472 0 0.0012
GW 3 21 0.1772 0.2312 0 0.1772 -0.2312 0 0.0012
GW 4 21 0.3207 0.2246 0 0.3207 -0.2246 0 0.0012
GW 5 21 0.4612 0.2246 0 0.4612 -0.2246 0 0.0012
GW 6 21 0.6707 0.2162 0 0.6707 -0.2162 0 0.0012
GS 0 0 1
GE 0
EX 0 2 11 0 1 0
FR 0 1 0 0 299.7925 1
RP 0 1 361 1000 90 0 1 1
EN
```

The key wire segment is GW2, segment 11, the source segment of the driver. Run the model and tabulate the basic information for later reference. **Fig. 19-10** shows the outline of the Yagi along with a reference pattern and some analytical data.

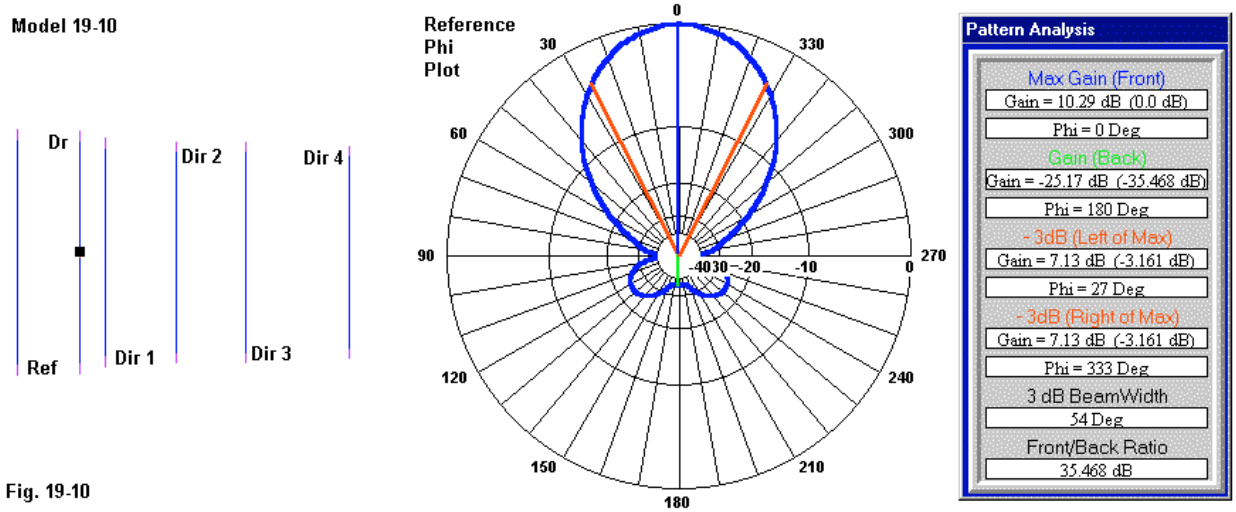

Fig. 19-10

The free-space gain is 10.29 dBi, with a 180° front-to-back ratio of 35.47 dB and a 54° half-power beamwidth. The source impedance is 50.1 + j9.1 Ω.

The model uses no PT command. Under this condition, PT -2 is the NEC default value, and all segment currents appear in the output report. Although this 126-segment model produces a table of reasonable length, the combination of a full current table and a radiation pattern can be weighty. Open model *19-10a.nec* and examine the revisions.

```
PT -2
RP 0 181 361 1001 0 0 1.00000 1.00000
```

The model and its environment remain the same. However, we now specifically insert the PT command with a value of -2. Although superfluous to the model run, the insert of the PT command illustrates the fact that some PT options (-2 and -1) require no tag and segment inputs, since these two options govern the existence or non-existence of a current table in the output report. In addition, the RP0 command requests a full sphere of values, just as the special function for the 3-dimensional surface pattern would request. The only other notable feature of the RP0 command is XNDA, which is set for gain averaging. However, the 1001 value indicates that the entire radiation patterns data will appear in the output report.

Run the model. The pattern derived from it appears in **Fig. 19-11**. More significant than the 3-dimensional surface pattern is the output report. You may scan the report and discover that the current values are identical to those in the output report for model 19-10. In addition, find the file size for the output report. It should be about 7.8 MB.

We can use PT and RP options in concert to shorten the stored report. Let's assume that all we really wish from the model is the average power gain. Both the current details and the radiation pattern details are extraneous to our need. Open model *19-11b.nec*.

```
PT -1
RP 0 181 361 1002 0 0 1.00000 1.00000
```

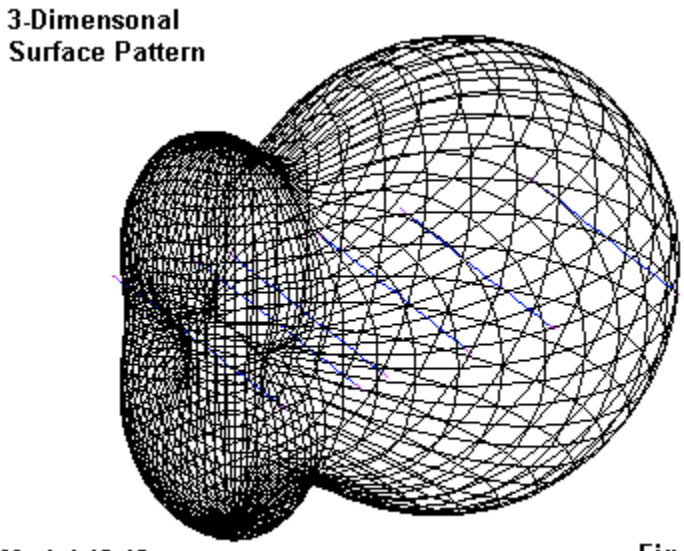

Model 19-10 Fig. 19-11

The model makes 2 revisions. First, it sets PT to -1, the value that suppresses all segment current printing. Second, the RP0 command uses a value of 1002 for XNDA, which requests gain averaging but suppresses the printing of the radiation pattern data. Compare the size of the output file to the one produced for model 19-11a. The new file is only about 19 KB. In many cases, like this one, we may tailor the output report to the needs of the modeling task.

If we need some segment currents, but not currents for every segment of every wire, we may use the PT0 option. From this point forward in the list of PT options, we shall need to specify the tag and segment numbers for which we need current values in the output file. Open model *19-11.nec* and look at the PT command. It requests currents for tag 2 (the driver) beginning with relative segment 1 and ending with relative segment 21 (absolute segments 12 through 22).

```
PT 0 2 1 21
XQ
```

Because the PT command is not self-executing, we require a following XQ command (or either an RP command or an NE/NH command for this single frequency request). Run the model and explore the current portion of the output report.

```
                        - - - CURRENTS AND LOCATION - - -

                    LENGTHS NORMALIZED BY WAVELENGTH (OR 2.*PI/CABS(K))

 SEG.  TAG    COORD. OF SEG. CENTER     SEG.            - - - CURRENT (AMPS) - - -
 NO.   NO.      X        Y        Z      LENGTH      REAL         IMAG.        MAG.        PHASE
   22    2   0.1253   0.2354   0.0000  0.02354    1.9370E-03  -7.7748E-04   2.0873E-03  -21.869
   23    2   0.1253   0.2119   0.0000  0.02354    4.9098E-03  -1.7888E-03   5.2255E-03  -20.018
```

The PT0 option produces a standard-form current table, but only for the requested range of segment. You may return to model 19-10 and compare the sample lines for absolute segments 22 and 23 with the sample lines.

Suppose that the current values of interest are the ones on the center segment of all 6 elements. Since the segments are not contiguous, we shall need 6 PT0 commands. The first temptation is to set them up as in model *19-11a.nec*.

```
PT 0 1 11 11
PT 0 2 11 11
PT 0 3 11 11
PT 0 4 11 11
PT 0 5 11 11
PT 0 6 11 11
XQ
```

Run the model and see what emerges in the output report current section.

```
                        - - - CURRENTS AND LOCATION - - -

                    LENGTHS NORMALIZED BY WAVELENGTH (OR 2.*PI/CABS(K))

  SEG.  TAG     COORD. OF SEG. CENTER      SEG.              - - - CURRENT (AMPS) - - -
  NO.   NO.       X         Y         Z     LENGTH       REAL          IMAG.         MAG.         PHASE
   116    6   0.6707    0.0000    0.0000  0.02059    1.3072E-02  -4.8880E-03   1.3956E-02  -20.502
```

Only the last of the PT commands executes, since each new PT command requires a separate XQ command. To obtain the current reports for all of the designated segments, set up the commands as in model *19-11b.nec*.

```
PT 0 1 11 11
XQ
PT 0 2 11 11
XQ
PT 0 3 11 11
XQ
PT 0 4 11 11
XQ
PT 0 5 11 11
XQ
PT 0 6 11 11
XQ
```

Because NEC will repeat the frequency data for each request, the currents will appear in a series of separate reports. However, NSI software has a current-table function that locates and coalesces the data into a more compact format.

```
SEG.  TAG     COORD. OF SEG. CENTER      SEG.              - - - CURRENT (AMPS) - - -
 NO.   NO.      X         Y         Z     LENGTH       REAL          IMAG.         MAG.         PHASE
  11    1   0.0000    0.0000    0.0000  0.02387    2.7297E-04   9.3095E-03   9.3135E-03   88.320
  32    2   0.1253    0.0000    0.0000  0.02354    1.9318E-02  -3.5149E-03   1.9635E-02  -10.312
  53    3   0.1772    0.0000    0.0000  0.02202   -1.2595E-02  -2.1765E-02   2.5147E-02 -120.057
  74    4   0.3207    0.0000    0.0000  0.02139   -1.3848E-02   7.8738E-03   1.5930E-02  150.377
  95    5   0.4612    0.0000    0.0000  0.02139    1.1965E-03   1.6904E-02   1.6946E-02   85.951
 116    6   0.6707    0.0000    0.0000  0.02059    1.3072E-02  -4.8880E-03   1.3956E-02  -20.502
```

If we wish the current data for a frequency sweep we must take an additional step to ensure that we receive full information for each frequency in the sweep. Open model *19-11c.nec*. The model requests a 5-step sweep starting at 295 MHz with 2.5-MHz increments. The end frequency will be 305 MHz.

```
PT 0 1 11 11
XQ
FR 0 5 0 0 295 2.5
PT 0 2 11 11
XQ
FR 0 5 0 0 295 2.5
PT 0 3 11 11
XQ
FR 0 5 0 0 295 2.5
PT 0 4 11 11
XQ
FR 0 5 0 0 295 2.5
PT 0 5 11 11
XQ
FR 0 5 0 0 295 2.5
PT 0 6 11 11
XQ
```

Because a multiple-frequency request creates a loop, we must repeat the FR command for each PT-XQ combination in order to obtain a full data set. The output table is too large for reproduction, but the NSI current versions lists the current for each element center segment, along with the frequency to which the individual lines apply.

The models in the 19-11 sequence not only illustrate how to work with the PT0 option, but as well, provide guidelines for multiple segment and multiple frequency requests for all of the ensuing PT options. Careful attention of housekeeping details can often be as important as creative antenna structure modeling in the pursuit of full and useful output information.

The PT commands from PT1 through PT9 are all designed for use with incident plane-wave excitation (EX1, EX2, or EX3) and produce tables with a special set of formats. Therefore, let's re-fit our 6-element Yagi model with an EX2 linear incident plane wave and a suitable PT1 command. Open model *19-12.nec*.

```
EX 1 1 37 0 90 0 90 1 10 0 0
PT 1 2 11 11
XQ
```

The model requests a 37-point phi circle at 10° per step at a theta angle of 90°. The PT1 command specifies the center segment of the driver as the only segment for reporting the current magnitude and phase angle. Run the model and examine the format of the PT1 table.

```
THETA      PHI          -  CURRENT  -         SEG
(DEG)     (DEG)       MAGNITUDE    PHASE      NO.

90.00      0.00     1.3239E-02    111.89       32
90.00     10.00     1.2618E-02    109.64       32
90.00     20.00     1.0885E-02    102.87       32
```

Relative to a PT0 table, the PT1 table is free of extraneous information, such as a repetition of the segment location and size information. The first 3 lines of the 37-line table make it evident that the information will be largely self-explanatory. We can obtain similar data by requesting

an EX2 linear incident plane wave that covers a 360° theta circle for the free-space model. Open model *19-12a.nec* and look at the same pair of lines. Note that the eta angle remains 90° since we have not changed the orientation of the antenna elements to the incident plane wave.

```
EX 1 37 1 0 0 0 90 10 1 0 0
PT 1 2 11 11
XQ
```

Run the model and again explore the current report.

```
THETA       PHI           -  CURRENT  -          SEG
 (DEG)      (DEG)       MAGNITUDE     PHASE      NO.

 0.00       0.00      2.6320E-03    -160.74       32
10.00       0.00      2.1821E-03    -114.70       32
20.00       0.00      2.0283E-03     -44.87       32
```

The initial value does not correspond with the first line of the phi pattern table because the new pattern begins at 0° theta or directly overhead. However, the coincidence of current magnitudes is clear from the rectangular plotting of the two patterns in **Fig. 19-12**, where the 0°-phi angle coincides with the 90°-theta angle.

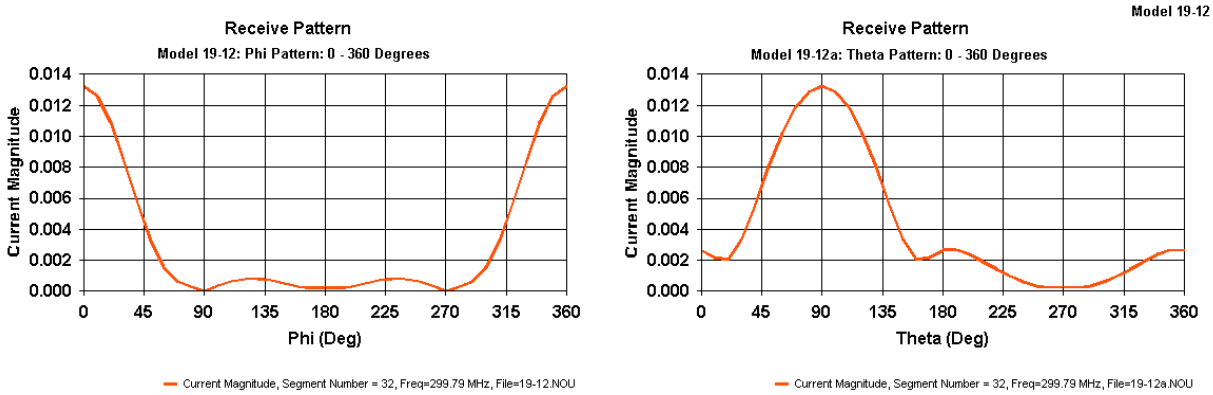

The PT2 option provides the same data as the PT1 selection, plus a second table. In the supplementary table, the current data for the last segment in the selected range is normalized to 1.0. From that information, the second table also includes the relative strength in dB. Open model *19-13.nec* to view the required line changes from model 19-12.

```
EX 1 1 37 0 90 0 90 1 10 0 0
PT 2 2 11 11
XQ
```

```
THETA       PHI           -  PATTERN  -
(DEG)      (DEG)          DB          MAGNITUDE

90.00       0.00          0.00      1.0000E+00
90.00      10.00         -0.42      9.5304E-01
90.00      20.00         -1.70      8.2214E-01
```

The table lines omit the portion of the double current table that replicates what we saw in model 19-12. It lists the first three lines of the second table. Since the first listed angle provides the strongest current reading, its normalized magnitude value is 1.0. Hence, the relative strength in dB begins at 0.0 dB and works downward. Graphing the two situations makes their relationship clearer. In **Fig. 19-13**, the current chart for the 37-point graph is smoother, since the power graph is based on a 20 * log (I1/I2) calculation relative to the magnitude column data.

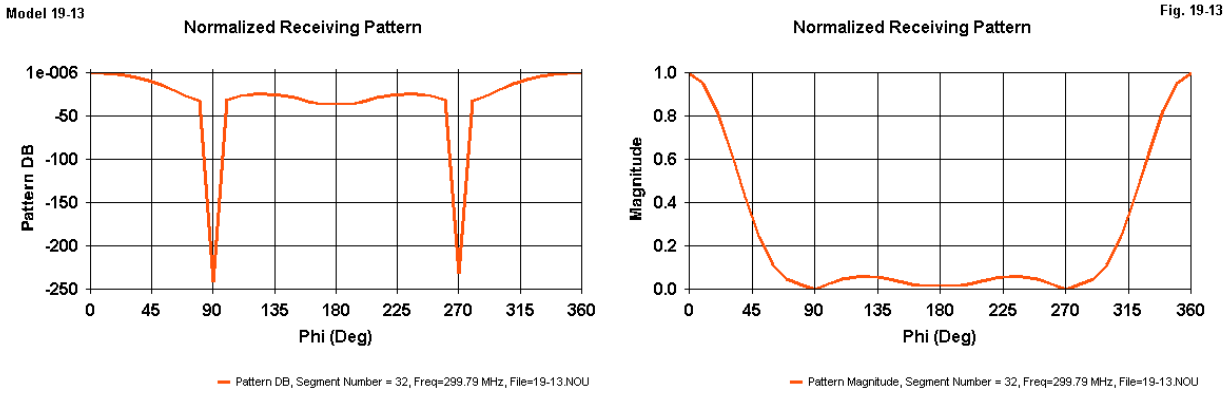

Fig. 19-13

We may wish to compare the receive and transmit graphs. **Fig. 19-14** provides a preliminary comparison. However, for greater precision, we would wish the graphs to use the same number of sampling points and a comparable length for the Y-axis.

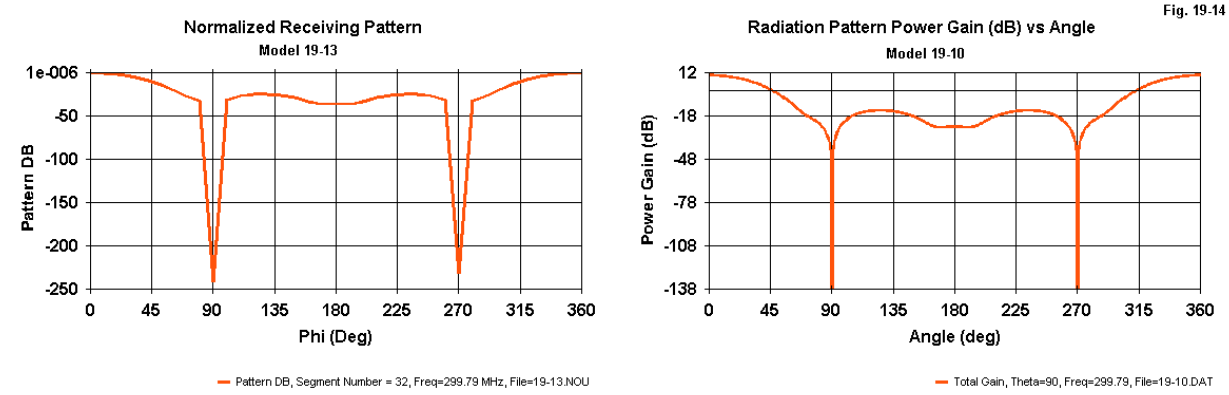

Fig. 19-14

We may also plot the new data in a theta circle by transforming model 19-12a. Open model *19-13a.nec* and compare its PT command to the corresponding line in the earlier example.

```
EX 1 37 1 0 0 0 90 10 1 0 0
PT 2 2 11 11
XQ
```

Like model 19-13, the output report contains 2 tables. The first repeats the data obtained with the PT1 command. The second table contains data for the theta circle in terms of the normalized magnitude of the current and its translation into relative strength as measured in dB.

```
THETA      PHI          -  PATTERN  -
(DEG)     (DEG)         DB          MAGNITUDE

 0.00      0.00      -14.03      1.9880E-01
10.00      0.00      -15.66      1.6482E-01
20.00      0.00      -16.29      1.5320E-01
```

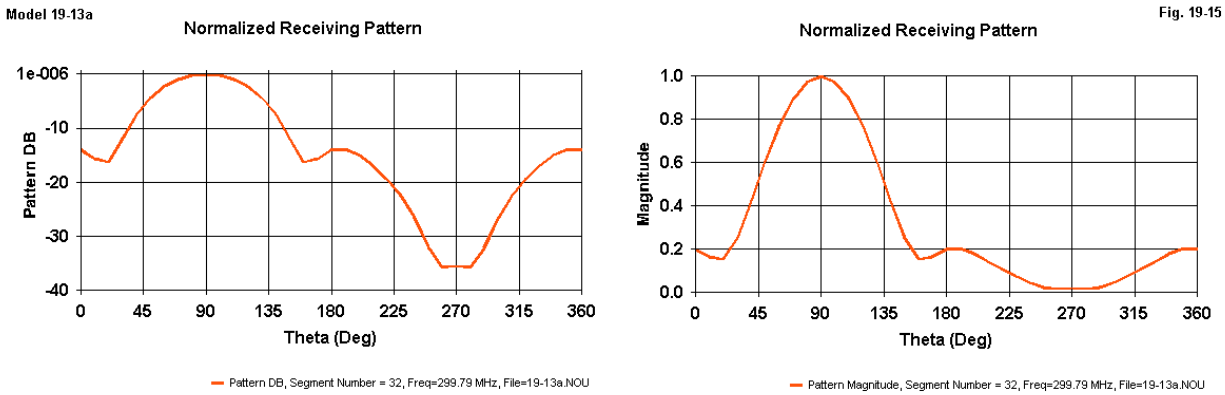

Graphing both sets of values provides a correlation between the normalized values and power values. The theta circle power pattern is smoother because the H-plane plot for a horizontal Yagi does not exhibit the deep nulls that characterize the E-plane pattern.

If we do not need the current magnitude and phase, we may opt for a PT3 command. This request omits the PT1 data and provides the normalized information in the second table of a PT2 command only. It applies only to a single selected segment. If you specify a range of segments, you will obtain data only for the last segment in the series. Model *19-14.nec* illustrates the required entry.

```
EX 1 1 37 0 90 0 90 1 10 0  0
PT 3 2 11 11
XQ
```

Because model 19-14 replicates the EX2 request of model 19-13, the table that it produces shows the same lines as for the earlier model. Hence, we have no new information to display in either tabular or graphic form. For receive information, the selection of PT1, PT2, or PT3 will depend on what data you most need.

NEC-4 contains two supplementary PT command options. Open model *19-15-nec4.nec*. Note the PT8 request. The model uses the EX2 command for a phi ring of incident plane waves.

```
EX 1 1 37 0 90 0 90 1 10 0 0
PT 8 2 11 11
XQ
```

PT8 provides the same tabular output as PT1. The reason that PT8 is available is that it also saves the table to a file for use in other software media for further processing. The filename will be the same as the model itself, but the extension assigned by NSI software is .GPT. Since the

file is in ASCII format, you may locate the file and open it using Notepad or any other word-processing software.

Open model *19-15a-nec4.nec*. Here we have a PT9 request.

```
EX 1 1 37 0 90 0 90 1 10 0 0
PT 9 2 11 11
XQ
```

PT9 also saves the current data to a file. It bears the same file name and extensions as the PT8 request, so you will have to decide which current table you desire. The PT8 table yields current magnitude and phase angle, while the PT9 table provides the real and imaginary components of the current.

```
PT8
THETA      PHI          -  CURRENT  -         SEG
(DEG)     (DEG)       MAGNITUDE    PHASE      NO.

90.00      0.00     1.3239E-02    111.89       32
90.00     10.00     1.2618E-02    109.64       32
90.00     20.00     1.0885E-02    102.87       32

PT9
THETA      PHI          -  CURRENT  -         SEG
 (DEG)     (DEG)         REAL       IMAG.      NO.

90.00      0.00    -4.9352E-03  1.2285E-02     32
90.00     10.00    -4.2418E-03  1.1883E-02     32
90.00     20.00    -2.4235E-03  1.0611E-02     32
```

You may easily confirm that the sample lines contain the same information in 2 different forms.

We have exhausted the PT options, but not the many different circumstances that might call for a receiving pattern. For example, all of the exercise models in this section involved linear incident plane waves. We might easily replace the subject model with the 5-turn helix and re-run everything using EX2 and EX3 elliptical incident plane waves. We may easily construct arrays consisting of elements at some distance from each other. As well, we have throughout used the standard 1 peak volt/meter excitation level. If we have NEC-4, then we may vary this value so that it more closely coincides with the actual anticipated or measured signal strength at the key element in the antenna or array. For any of the PT options, we may vary eta and/or the ratio of the minor to the major elliptical axis in order to explore the consequences or to refine a model to closely fit actual working circumstances.

When we work with paired commands, the number of possible combinations will almost always exceed the space available to test them. However, in these notes, you have all of the materials you need to create further exercise models to increase your familiarity with receive pattern data calculation within NEC. If you have not previously worked with receive data, you may wish to spend as much time on interpreting the data output as on creating it through either these or additional models.

Scattering Patterns

When an object receives energy from an external source, it reflects that energy in ways that depend on the conductivity and shape of the object, as well as the vector of the incoming signal. The pattern of re-radiation is sometimes called scattering. We may determine that pattern by adding an RP0 request to any of the models that we have so far used as exercises. However, many of the objects in which we are interested from a scattering perspective are not antennas. Rather, they are ordinary mechanical objects, ordinarily metallic. Typical objects are motor vehicles, sea craft, and aircraft.

Setting up an example requires 3 steps. First, we must model an object. Because wire-grid structures can involve thousands of segments, we shall follow the NEC Manual lead and use a stick aircraft, with segmentation adjusted to our test frequency of 299.7925 MHz. The left side of **Fig. 19-16** shows the outline of the model. It uses the fattest radius possible that allows the model to remain easily within NEC modeling guidelines.

Second, we need a source. We shall use a linear incident plane wave located in line with the model (theta = 90°) but with a phi angle of 30° to place it at an angle to the fuselage. We shall vary the eta angle from 90° to 45° and finally to 0° to see if that angle makes a difference to the scattering pattern.

Finally, we need to decide at which bearing or bearings to take pattern readings. For much scattering work, a single bearing may be of sole interest. For example, a radar installation often uses the same location for its transmitting and receiving functions. Hence, the vector from the source to the object may require reflection back to the same location. We shall use a phi angle of 30° for our example, but for the sake of curiosity, we shall use a variety of theta angles from 90° to 270°, obtaining radiation pattern readings for the oblique region beneath but offset from the aircraft.

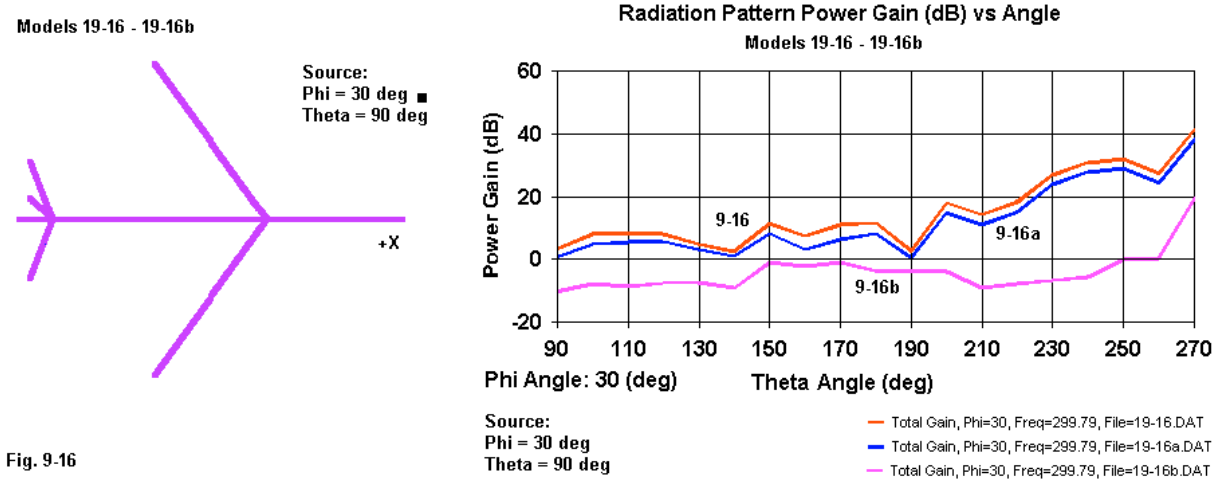

Fig. 9-16

Open models *16.nec*, *16a.nec*, and *16b.nec*. Each model uses the same structure geometry and RP0 request.

```
RP 0 19 1 1000 90. 30. 10.00000 1.00000
```

Run the models and combine the results into a single graph of the total gain, as in the graph to the right in **Fig. 19-16**. Notice first that the left-most value on the graph is the weakest and represents the line of direct return. Re-radiation strength tends to increase as the angle away from the source increases. Of course, the complex structure (even in this simplified model) moderates all generalities. Second, notice that as the eta angle departs from the plane of the craft (excepting its sloping vertical tail) scattering radiation decreases in strength (for the range of values covered here), but even an eta angle of 0° yields a usable return.

In some cases, we may find it more useful to plot the Ephi and Etheta field strengths of the scattered radiation. **Fig. 19-17** provides a view of such graphs for the models that we have just run. Ephi tends to be stronger than Etheta for the simplified structure used as a scattering object. However, both components produce non-trivial field strengths.

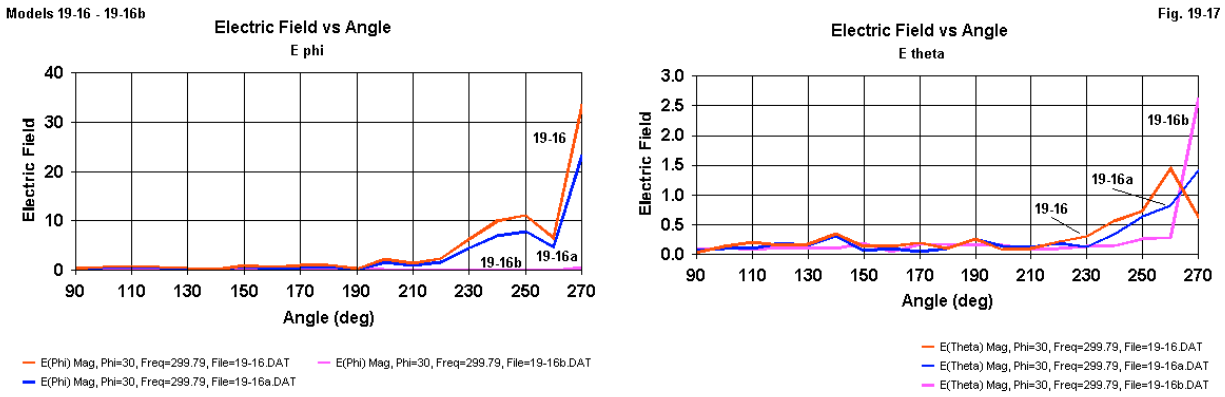

Our goal is simply to introduce the relevance of RP0 commands to receive data modeling. The desired information will be a function of each task, and therefore, so will the range and limits of the radiation field requested. In any case, the parameters for setting up RP0 commands covered in Chapter 9 will serve this effort as well.

Summing Up

In the exercises in this chapter, we examined the modeling requirements for deriving receive data. The necessities include an incident plane wave source external to the antenna structure and a means of tabulating current levels on selected wire segments.

The EX1, EX2, and EX3 options for excitation provide linear, right-hand elliptical, and left-hand elliptical incident plane waves. In NEC-2, the excitation is 1 peak volt/meter, but in NEC-4, you may set the value as desired. The location of the source follows standard phi and theta conventions. For all incident plane waves, you may set the polarization angle, and for elliptical

plane waves, you may set the ratio of the minor to the major axis.

The PT command controls the printing, suppression, and formatting of the output data, namely, the current magnitude and phase or an alternative form of this data. For general use, PT-2 mimics the program default setting that prints all segment currents. Regardless of the type of source, PT-1 suppresses current printing. PT0 allows you to print the current magnitude and phase angle of segment currents over a selected contiguous range. Every PT command must be followed by an XQ command or by a command that is self-executing.

More specifically designed for receive data and plane wave excitation, PT1 lists the magnitude and phase angle of currents over a specified range of segments in a table that tracks the changes in the phi and theta angles of the EX command. PT3 provides current magnitudes normalized to the maximum value over the excitation position limits, but only for a single segment. The PT2 command produces both the PT1 and PT3 tables, but if the magnitude and phase angle information apply to a range of segments, then the normalized data will appear only for the last segment in the specified range. Graphic outputs of the tabulated data permit ready comparisons of both transmit and receive patterns in addition to pattern overlays from variations on a model.

NEC-4 offers two additional options, both of which save the current data to a file. PT8 saves the PT1-type current data in magnitude and phase angle format, while PT9 saves the same data in terms of the real and imaginary components of the current.

The RP0 command does not disappear from relevance with receive data. Rather, it provides scattering pattern information. Although radar applications may focus on the scattering back toward the incident plane-wave source, other applications may take interest in reflected energy for any and all angles relative to the object under investigation.

20.
Miscellaneous Special Commands

***Objectives**: In this potpourri of control commands that we have so far by-passed, we shall briefly note the entry requirements and major reasons for using them. Some commands, such as EK within NEC-2, have sufficient general importance for more extended treatment. Other commands that are common to both cores, such as PQ and CP, will call for more work than those that appear in only 1 of the 2 cores*

In the course of our work, we have overlooked a number of control commands that have varying importance to general modeling work. In this chapter, we shall introduce the commands and provide at least a general orientation to their use. One command, EK, is so important to some work using NEC-2 that we shall give it a larger space and more exercise examples. One of the problems attending this potpourri of control commands is that some are common to both NEC-2 and NEC-4; some appear only in NEC-2; and some exist only within NEC-4. Here is the list of commands that we shall at least touch upon in the following pages.

NEC-2 Only
- EK Extended thin-wire kernel
- KH Interaction approximation range

NEC-2 and NEC-4
- CP Maximum coupling calculation
- PQ Print control for charge on wires

NEC-4 Only
- JN Junction charge distribution
- VC Voltage-source end caps
- PL Data Storage for Plotting
- PS Print Electrical Lengths of Segments
- UM Upper Medium Parameters

Although the EK command is critical to the proper use of NEC-2 wherever the segment length-to-radius value is low, other commands are somewhat superfluous to intermediate modeling, such as KH in NEC-2 or JN and VC in NEC-4. The remaining commands acquire significance according to the needs of the modeling project.

NEC-2 Commands: EK and KH

The NEC-2 EK command is critical to many models. In general, we invoke the EK (extended thin-wire kernel) command whenever we suspect that the segment-length-to-wire-radius ratio is low enough to yield inaccurate results using the standard thin-wire kernel. Implementing the EK command is simple: anywhere after the GE (end geometry) command, we write a new line.

```
EK 0
```

In fact, we can even omit the zero, although if we replace the 0 with -1, then the command returns a model to calculating with the standard thin-wire kernel. The 0-entry line changes the approximation of the electrical field integral equation in the core calculations from the thin-wire kernel to the extended thin-wire kernel.

The information necessary to appreciate the significance of the extended thin-wire kernel in NEC-2 appears early on in the user portion of the manual. "In the thin-wire kernel, the current on the surface of a segment is reduced to a filament of current on the segment axis. In the extended thin-wire kernel, a current uniformly distributed around the segment is assumed. The field of this current is approximated by the first two terms in a series expansion of the exact field in powers of a^a [where a is the wire radius]. The first term in the series, which is independent of a, is identical to the thin-wire kernel, while the second term extends the accuracy for larger values of a. Higher order approximations are not used because they would require excessive computation time."

"In either of these approximations, only currents in the axial direction on a segment are considered, and there is no allowance for variation of the currents around the wire circumference. The acceptability of these approximations depends on both the value of a/λ and the tendency of the excitation to produce circumferential current or current variation. Unless $(2\pi a)/\lambda$ is much less than 1, the validity of these approximations should be considered." One potential arena in which the validity of these approximations may be tested is the modeling of a boom connected directly to the parasitic elements of a Yagi antenna. In practice, the connection or the very close proximity of a boom to the parasitic elements alters the required length of the elements to preserve array performance. However, in NEC-2 and NEC-4--when modeled within the other limitations of the software--the boom has no effect upon the parasitic elements. The result strongly suggests that boom-to-element effects are functions of variations in circumferential currents, which NEC does not take into account.

The NEC-2 manual goes on. "The accuracy of the numerical solution for the dominant axial current is also dependent on [the ratio of segment length to radius or Ls/a]. Small values of [Ls/a] may result in extraneous oscillation in the computed current near free wire ends, voltage sources, or lumped loads. Use of the extended thin-wire kernel will extend the limit on [Ls/a] to smaller values than are permissible with the normal thin-wire kernel." In general, Ls/a must be greater than 8 for errors under 1% using the normal thin-wire kernel. This value amounts to a segment length-to-wire-diameter ratio of 4:1, for programs that input wire thickness as a diameter. The manual notes that "reasonable solutions" have been obtained for the normal thin-wire kernel for Ls/a values down to about 2, with equally "reasonable solutions" for the extended thin-wire kernel for Ls/a values down to about 0.5. However, exact specification of the geometries involved does not appear. Hence, the most general guidance one might give is to use the EK command to implement the extended thin-wire kernel whenever the value of Ls/a goes below 8 (or a segment-length-to-wire-diameter ratio of 4). For straight-wire elements, the limit to Ls/a may be between 2 and 1 for very reliable results.

There are numerous other facets of extended thin-wire kernel implementation noted in the manual. For example, the normal thin-wire kernel is used--even if the EK command is implemented--at wire bends, such as those encountered in closed and nearly closed antenna geometries. Delta, quad, and Moxon rectangle geometries are samples of such antennas. At

bends, the modeler should avoid very small values of Ls/a so that the surface of one wire at the junction does not penetrate into the central region of the other wire, a condition that "generally leads to severe errors."

Why EK is not used in NEC-4: The NEC-4 manual provides a chapter outlining the differences between NEC-3 and NEC-4. Over the range of considerations relevant to the use of EK in NEC-2, NEC-3 is essentially the same as NEC-2--but is different in other respects. In NEC-4, "the thin-wire approximation is now implemented with the current treated as a filament on the wire surface and the boundary condition enforced on the wire axis."

"With the boundary condition enforced on the wire axes, the openings at wire ends should be closed with end caps. This is particularly important when the ratio of segment length to radius is on the order of 2 or less. Wire ends are closed with flat caps in NEC-4, with the current and charge density assumed continuous from the wire onto the cap." NEC-4 also includes optional caps for use with voltage sources with low values of Ls/a. "This approximate treatment was found to be about as effective as the extended thin-wire kernel included as an option in [NEC-2 and] NEC-3. The extended thin-wire kernel option (EK command) has been dropped from NEC-4."

The NEC-4 thin-wire kernel appears at first sight to replicate the extended thin-wire kernel of NEC-2 and NEC-3. Hence, results seemingly should be identical. However, the implementation of wire end caps and other alterations to the solution algorithms for wires tells us otherwise. Rather, expect results to be very close. For relatively thin, straight wires having long segment lengths, where Ls/R is more than 8, there will be almost no difference between NEC-2 and NEC-4, even without implementing the extended thin-wire kernel in NEC-2. For values of Ls/a between 8 and 2, NEC-2 with EK and NEC-4 will normally show very close results. However, as the value of Ls/a passes 2 on its way downward, expect larger differences.

What we have been reviewing are simply the most relevant extracts from the fuller treatment provided by the manuals to cover not only the situation surrounding the EK command, but as well overall core operations. Hence, I fully recommend that every user of NEC-2 or NEC-4 (or even NEC-3) gradually become fully conversant with the provisions of the manuals. They were not written for the purpose of being supplanted by a series of summary statements. Such statements may be useful as the beginning, but are never the ultimate end of understanding both the capabilities and the limitations of the cores.

However, we might pause to go through a pair of small exercises in order to appreciate better the function of the EK command in NEC-2 and how its results compare to identical models using the NEC-4 core.

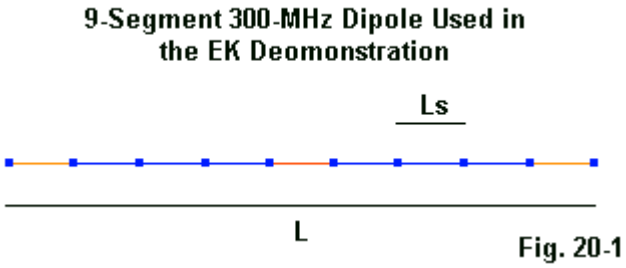

Fig. 20-1

The first exercise involves a simple dipole. **Fig. 20-1** outlines the element. Nothing in the dipole will change except the radius of the one wire that makes up the model. Beginning with a radius of 0.0001 m (0.1 mm), we shall increase the radius until we reach levels that allow us to create segment-length-to-radius values in the range from 4:1 down to 1:1. Since we shall not change the wire length, every increase in radius will carry us theoretically further from the initial resonance of the antenna. This move is intentional, since once we have significant reactance in the source impedance, differences created by running the model under various conditions will become more vivid.

Because we shall begin with a 1/2λ resonant dipole, we should not expect much change in the gain or variation among models with respect to gain. Resonant dipoles change gain only very slowly with changing conditions, a common feature of most simple antennas resonated for a high source current. Therefore, the source impedance values will be our primary window on the differences. We shall run them without the EK command in both NEC-2 and NEC-4, and also with the EK command in NEC-2. Open and run models *20-2a-nec2.nec* through *20-2g-nec2.nec*, the NEC-2 models using the EK command. Then run on NEC-2 and NEC-4 (if the latter is available) models *20-3a.nec* through *20-3g.nec*. Create a table of results.

A Dipole in NEC-4 and in NEC-2 With and Without EK

Constants: Free-Space Environment; Frequency: 300 MHz
Length: 0.4836 m; Segments: 9; Segment Length: 0.5373 m
Ls = segment length; a = radius

Core	*Gain (dBi)*		*Source Impedance (R+/-jX Ω)*
Wire Radius: 0.0001 m		Ls/a: 537	
NEC-4	2.12		72.080 - j 0.001
NEC-2 w/o EK	2.12		72.079 - j 0.002
NEC-2 w EK	2.12		72.079 - j 0.002
Wire Radius: 0.001 m		Ls/a: 53.7	
NEC-4	2.13		75.629 + j16.514
NEC-2 w/o EK	2.13		75.628 + j16.515
NEC-2 w EK	2.13		75.222 + j16.490
Wire Radius: 0.01 m		Ls/a: 5.37	
NEC-4	2.18		91.469 + j32.379
NEC-2 w/o EK	2.18		92.039 + j33.316
NEC-2 w EK	2.18		90.677 + j31.667
Wire Radius: 0.0134 m		Ls/a: 4.00	
NEC-4	2.20		95.680 + j30.113
NEC-2 w/o EK	2.20		97.272 + j32.149
NEC-2 w EK	2.20		94.637 + j30.042
Wire Radius: 0.0179 m		Ls/a: 3.00	
NEC-4	2.22		99.783 + j23.974
NEC-2 w/o EK	2.22		103.832 + j27.652
NEC-2 w EK	2.22		98.657 + j25.572
Wire Radius: 0.0269 m		Ls/a: 2.00	
NEC-4	2.26		102.414 + j 5.134
NEC-2 w/o EK	2.27		114.262 + j 9.213
NEC-2 w EK	2.27		102.410 + j12.229

Wire Radius: 0.0537 m		Ls/a: 1.00	
NEC-4	2.38		51.890 - j46.292
NEC-2 w/o EK	2.43		54.146 - j58.430
NEC-2 w EK	2.47		86.345 - j31.830

Certain results appear incontestable. First, wherever there are differences among the results, the NEC-2-with-EK data are closer to the NEC-4 data than are the data from NEC-2-without-EK. Second, the values for a ratio of segment length to radius of 1.0 are sufficiently variable as not to be able to say which values are more reliable than the others. From the table alone, without external verification, it would even be presumptuous to assert that the NEC-4 values are the most reliable. At all other values, we have much more confidence in the coincidence between NEC-4 and NEC-2-with-EK.

The more difficult question to answer is when to implement the EK command in NEC-2. For Ls/a values above 5.37, the EK command is certainly unnecessary for the dipole. Even at the radius of 0.01 m, the NEC-2 results seem equally separated from the NEC-4 results, although in opposite directions. There is a change when we simply reduce the Ls/a value from 5.37 down to 4.0: the NEC-2-with-EK results are clearly more coincident with the NEC-4 results than NEC-2-without-EK. Hence, a segment-length-to-radius ratio in the range of 6 down to 4 seems an appropriate changeover to the use of EK for NEC-2 users.

Coincidence between NEC-2-EK results and NEC-4 is not always a decisive reason for implementing the EK command in NEC-2. As well, a linear element, such as a dipole, does not exhaust the range of modeling phenomena that we may associate with the use of the EK command.

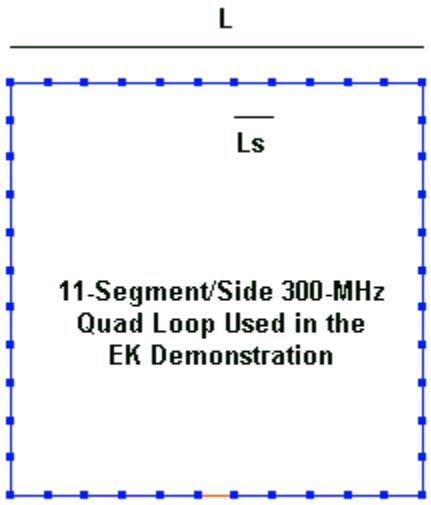

Fig. 20-2

Consider, for example, a simple quad loop, such as the one outlined in **Fig. 20-2**. The EK version of the first model in the sequence that we shall test has the following appearance.

```
CM Quad Loop with EK
CM Ls/R = 241:1
CE
GW 1 11 -0.1324 0 -0.1324 0.1324 0 -0.1324 0.0001
GW 2 11 0.1324 0 -0.1324 0.1324 0 0.1324 0.0001
GW 3 11 0.1324 0 0.1324 -0.1324 0 0.1324 0.0001
GW 4 11 -0.1324 0 0.1324 -0.1324 0 -0.1324 0.0001
GS 0 0 1
GE 0
EK 0
EX 0 1 6 0 1 0
FR 0 1 0 0 300 1
RP 0 181 1 1000 -90 0 1 1
EN
```

The loop is set for 300 MHz, with initial side lengths that are 0.2648 m and 11 segments per side. With the initial wire radius of 0.0001 m, the segment lengths are 0.0241 m. As we increase the radius of the wire, the loop will drift farther from resonance. Since the geometry is closed, the loop will show capacitive reactance as we enlarge the wire (in contrast to the increasing inductive reactance of a straight wire under similar conditions). Open and run the following two sequences of models. In NEC-2 only, use the EK models *20-4a-nec2.nec* through *20-4g-nec2.nec*. For both NEC-2 and NEC-4, use the non-EK models *20-5a.nec* through *20-5g.nec*. Tabulate the results of modeling in NEC-4, NEC-2-without-EK, and NEC-2-with-EK.

A Quad Loop in NEC-4 and in NEC-2 With and Without EK

Constants: Free-Space Environment; Frequency: 300 MHz
Side Length: 0.2648 m; Segments: 11; Segment Length: 0.0241 m
Ls = segment length; a = radius

Core	*Gain (dBi)*		*Source Impedance (R+/-jX Ω)*
Wire Radius: 0.0001 m		Ls/a: 241	
NEC-4	3.30		125.46 - j 1.213
NEC-2 w/o EK	3.30		125.46 - j 1.207
NEC-2 w EK	3.30		125.46 - j 1.207
Wire Radius: 0.001 m		Ls/a: 24.1	
NEC-4	3.29		119.53 - j52.554
NEC-2 w/o EK	3.29		119.58 - j52.323
NEC-2 w EK	3.29		119.58 - j52.322
Wire Radius: 0.0048 m		Ls/a: 5.00	
NEC-4	3.28		106.48 - j86.861
NEC-2 w/o EK	3.26		107.84 - j83.170
NEC-2 w EK	3.26		108.21 - j83.076
Wire Radius: 0.006 m		Ls/a: 4.00	
NEC-4	3.38		108.21 - j83.076
NEC-2 w/o EK	3.25		104.60 - j86.457
NEC-2 w EK	3.25		105.33 - j86.268
Wire Radius: 0.008 m		Ls/a: 3.00	
NEC-4	3.29		95.571 - j97.117
NEC-2 w/o EK	3.20		99.146 - j89.857
NEC-2 w EK	3.22		100.91 - j89.398

Wire Radius: 0.0269 m		Ls/a: 2.00	
NEC-4	3.31		80.679 - j102.15
NEC-2 w/o EK	3.20		87.361 - j92.323
NEC-2 w EK	3.16		93.264 - j90.958
Wire Radius: 0.0241 m		Ls/a: 1.00	
NEC-4	3.32		37.507 - j80.703
NEC-2 w/o EK	3.11		43.091 - j78.095
NEC-2 w EK	2.58		81.412 - j80.556

Variations of both gain and source impedance begin to appear with a segment-length-to-radius ratio of 5:1. Down to a ratio of about 2:1, the pair of NEC-2 results are closer to each other than either is to the NEC-4 result. The most likely reasons for this divergence from the type of results we obtained from the straight dipole are the conditions of the model and how each core handles them. NEC-4 applies its revised algorithm to all segments and junctions of the loop. The simplified thin-wire kernel of NEC-2 also applies to each segment and wire junction. Hence, we expect some divergence of results relative to NEC-4. The EK version of NEC-2 does not apply the extended thin-wire kernel to junctions of wires that are at an angle--the bent-wire case. As a consequence, its reports will coincide with neither NEC-4 nor NEC-2-without-EK.

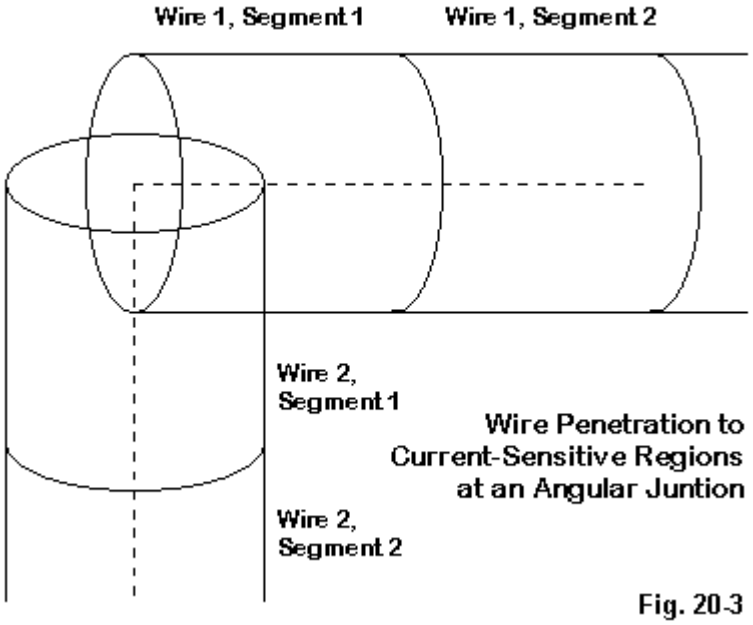

Fig. 20-3

As we increase the wire radius, the surface of one wire at a junction penetrates farther into the central region of the other wire segment forming the junction, as suggested by the simple sketch in **Fig. 20-3**. As the penetration reaches a region where it alters the current calculation, the results grow less reliable. Between ratios of 5:1 and 3:1, we encounter a growing variance among the reports, with no internal guidance as to which report may be the more nearly correct. In just the region that the EK command in NEC-2 provided significant modeling assistance in terms of the accuracy of results, it proves to be of little assistance with closed geometries and other bent-wire configurations without external means of verification.

The use of the EK command with NEC-2 thus finds its best range of uses with straight-wire elements of uniform diameter. For segment-length-to-radius ratios between 8:1 and 2:1, it yields results that are consistent with those emerging from NEC-4.

The second control command that appears in NEC-2 but not in NEC-4 is KH, or "interaction approximation range." The command has a fairly simple structure.

```
Cmd    I1    I2    I3    I4    F1
       ---   ---   ---   ---   RKH
KH     0     0     0     0     7
```

The command sets the minimum separation distance for the use of a timesaving approximation in filling the interaction matrix. The integer entries are not used and receive zeroes as placeholders. F1, RKH, specifies the separation distance in wavelengths. If two segments are separated by more than the value of RKH, NEC-2 calculates the interaction field from an impulse approximation to the segment current, using the field of a current element located at the segment center. The command may appear anywhere after the end of the geometry (GE) and affects all calculations after its appearance.

In the 1980s, when NEC-2 first appeared, CPUs were slow and saving run time weighed heavily in the development of the complex modeling program. The need for the command has dwindled in proportion to the increase in computer speed so that it now has virtually no use. For widely separated elements that nonetheless interact, the use or non-use of the command has no detectable affect on either the run time or the core output. Consider 2 vertical dipoles in free space, only one of which is driven. The dipoles are broadside to each other and 10λ apart, as shown in **Fig. 20-4**. As the pattern shows, the presence of the second dipole has a small but determinate effect on the pattern of the system.

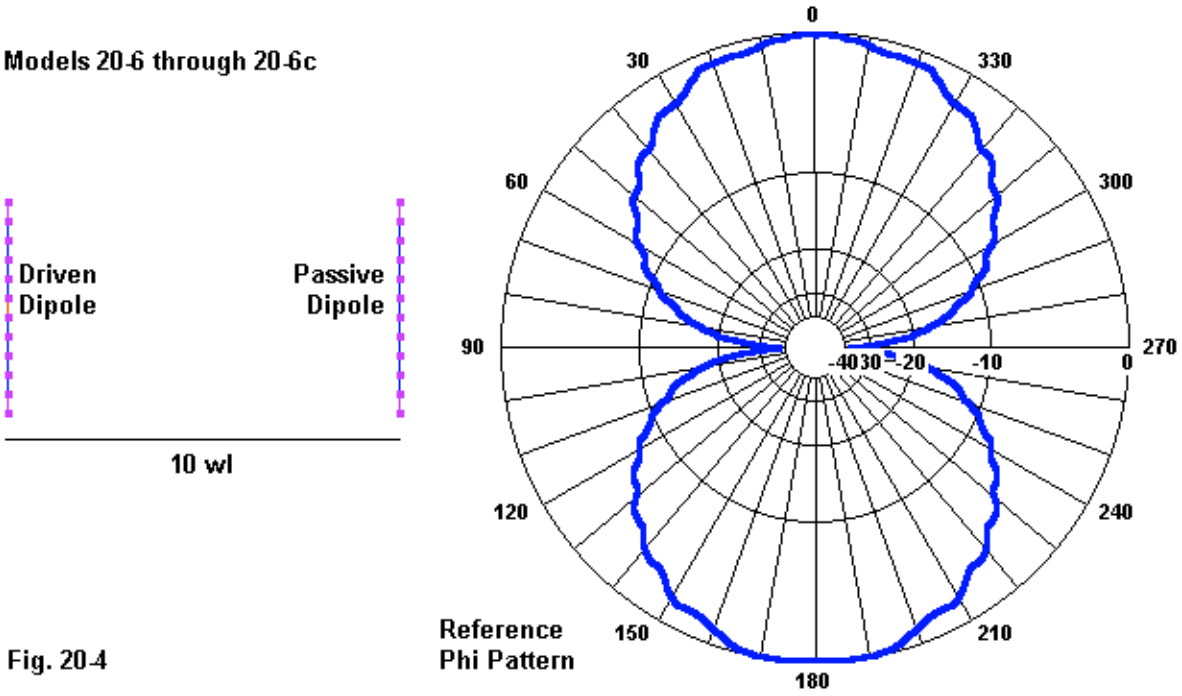

Fig. 20-4

Open and run model *20-6.nec*. The model uses no KH command. The test frequency equates 1 meter with 1 λ. The source impedance is 71.808 + j0.106 Ω, and the system gain is 2.11 dBi maximum. With 1 peak volt excitation, the current on the source segment (GW1, segment 6) is 1.3926E-2 at a phase angle of -0.085°. The corresponding segment on the passive dipole (GW2, segment 6) is 3.6226E-4 at a phase angle of -97.411°. Examine the total output file for the NEC-2 core used by NSI. Following the frequency data in that report, we find the following line for all models not using a KH entry.

```
APPROXIMATE INTEGRATION EMPLOYED FOR SEGMENTS MORE THAN
   1.000 WAVELENGTHS APART
```

Approximate integration uses the default value of 1λ in the absence of a KH command. Hence, the approximation method is enforced for the interactions between the 2 dipoles that are 10λ apart. To discover if the approximation makes a difference to this type of model, let's use the KH command to change the radius from the coordinate system origin at which it takes affect. Open and run models *20-6a.nec* and *20-6b.nec*. The first model reduces the radius to a very small value: 0.1λ. The second increases the radius to a very large value: 1E10λ. The large value for RKH yields result identical to those for the model using the default value that places the boundary between elements. The wide spacing of the 2 dipoles reduces any differences between using RKH values that fall between the elements or outside the boundaries of the wires. However, the small value places the boundary within the limits of the driven element. In this case, we find small changes in the output reports: gain 2.14 dBi, source impedance 71.087 - j7.419 Ω. The segment currents that correspond to those in Model 20-6 are 1.3991E-2 at 5.958° and 3.6221E-4 at -85.292°. Although the differences are not great, perhaps the best guidance available is to place the RKH boundary outside of the structure of any antenna geometry wherein there may be significant levels of mutual coupling.

Commands Common to NEC-2 and NEC-4: CP and PQ

Although the CP and PQ commands are common to both NEC-2 and NEC-4, there are variations between cores for each of them. Since the PQ command has the smaller range of variation, we may begin with it.

PQ prints the charge densities on a specified wire. The entry has the following format.

```
CMD   I1       I2       I3       I4
      IPTFLQ   IPTAQ    IPTAQF   IPTAQT
PQ    0        1        1        11
```

I1 has only 2 possibilities. -1 suppresses the printing of charge densities and is the default condition in the absence of a PQ command. 0 prints the charge densities. Normally, the following integer entries will indicate the tag number, the first segment on that tag, and the last segment on that tag. If I1 through I4 are blank or zeroes, then the program will print charge densities for all segments in the model. If I2 is zero, then I3 and I4 refer to absolute segment numbers. If I4 holds a zero, then its value is the value of I3.

Open model *20-7.nec*. This model will run in both NEC-2 and NEC-4.

```
GW 1 11 0 -.2375 0 0 .2375 0 .001
PQ 0 1 1 11
EX 0 1 6 00 1 0
XQ
EN
```

The lines indicate a single vertical dipole, which is sufficient for this demonstration. PQ requests the charge densities for all segments on GW1. The output will be a list of segments. Each line begins in a form identical to a current table. The segment identification is followed by the location of the segment center and its length. Then comes the charge density in coulombs/meter in 2 forms: the real and imaginary components, followed by the magnitude and phase angle of the charge density. The first 2 lines of a NEC-2 report appear in this way:

```
                              - - - CHARGE DENSITIES - - -

 SEG.  TAG    COORD. OF SEG. CENTER     SEG.          CHARGE DENSITY (COULOMBS/METER)
 NO.   NO.      X        Y        Z      LENGTH     REAL        IMAG.       MAG.        PHASE
    1    1   0.0000  -0.2159   0.0000  0.04318   5.7972E-12  5.6030E-11  5.6329E-11   84.093
    2    1   0.0000  -0.1727   0.0000  0.04318   2.8440E-12  4.3028E-11  4.3122E-11   86.218
```

The NEC-4 report differs in its data by adding two end values, as shown in **Fig. 20-5**.

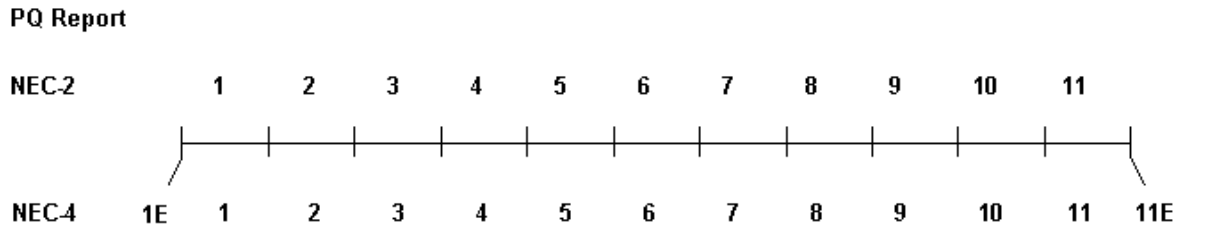

Fig. 20-5

To allow you to correlate lines, we must print the first 3 from the NEC-4 run of the same model. "1E" indicates the first end segment.

```
                              - - - CHARGE DENSITIES - - -

 SEG.  TAG    COORD. OF SEG. CENTER     SEG.          CHARGE DENSITY (COULOMBS/METER)
 NO.   NO.      X        Y        Z      LENGTH     REAL        IMAG.       MAG.        PHASE
   1E    1   0.0000  -0.2375   0.0000  0.04318   7.5218E-12  6.4388E-11  6.4826E-11   83.337
    1    1   0.0000  -0.2159   0.0000  0.04318   5.7951E-12  5.6030E-11  5.6329E-11   84.095
    2    1   0.0000  -0.1727   0.0000  0.04318   2.8425E-12  4.3028E-11  4.3122E-11   86.220
```

The CP command requests a calculation of the maximum coupling between sources on 2 specified segments. The procedure requires that each specified segment be excited with a voltage source (EX0) with the other segment shorted. This step permits the computation of the self and mutual admittances and the level of coupling between segments in dB. In the NSI implementation of the CP command, the assistance screen is identical for both cores and simply requests the integer information.

```
CMD      I1    I2    I3    I4
         TAG1  SEG1  TAG2  SEG2
CP       1     6     2     6
```

If either TAG1 or TAG2 are zero, then the following segment number refers to an absolute segment number. The CP command plays a different role in NEC-2 and in NEC-4. Therefore, models using the command look and operate differently. Open model *20-8-nec2.nec*. The model creates 2 vertical dipoles aligned broadside to each other, as shown in **Fig. 20-6**.

```
GW 1 11 0 -.2375 0 0 .2375 0 .001
GW 2 11 2 -.2375 0 2 .2375 0 .001
GE
FR 0 1 0 0 299.7925 1
CP 1 6 2 6
EX 0 1 6 00 1 0
XQ
EX 0 2 6 00 1 0
XQ
EN
```

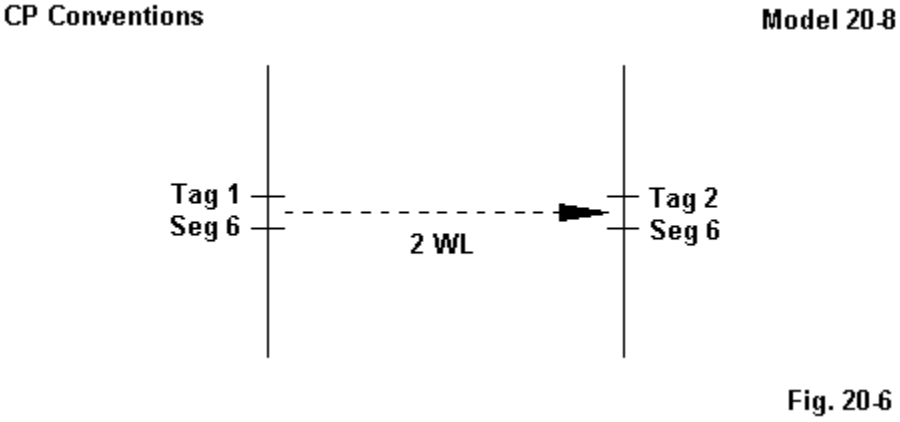

Fig. 20-6

In NEC-2, the CP command specified the 2 segments but does not execute any calculations. Rather, it must await the execution of separate EX0 command for each of the 2 segments in the order specified. Once the required excitation calculations are complete, then CP will direct the reporting of the mutual coupling under the heading of "Isolation Data."

```
                                - - - ISOLATION DATA - - -

    - - COUPLING BETWEEN - -         MAXIMUM              - - - FOR MAXIMUM COUPLING - - -
            SEG.              SEG.   COUPLING    LOAD IMPEDANCE (2ND SEG.)       INPUT IMPEDANCE
TAG/SEG.    NO.    TAG/SEG.   NO.      (DB)        REAL          IMAG.         REAL          IMAG.
1    6      6      2    6     17    -23.884     7.23185E+01  7.59123E-02   7.23185E+01 -7.59123E-02
```

NEC-4 simplifies the required modeling by executing the matrix evaluation and factoring portion of the calculations as soon as the CP command appears. Hence, a NEC-4 request for CP does not require an EX command. Open and examine model *20-8-nec4.nec*.

```
GW 1 11 0 -.2375 0 0 .2375 0 .001
GW 2 11 2 -.2375 0 2 .2375 0 .001
GE
FR 0 1 0 0 299.7925 1
CP 1 6 2 6
XQ
EN
```

The isolation data for NEC-4 uses the same form as the NEC-2 version. As well, the values for maximum coupling and for the load and input impedances are also very similar.

```
                                - - - ISOLATION DATA - - -

    - - COUPLING BETWEEN - -         MAXIMUM              - - - FOR MAXIMUM COUPLING - - -
          SEG.              SEG.    COUPLING    LOAD IMPEDANCE (2ND SEG.)       INPUT IMPEDANCE
TAG/SEG.   NO.    TAG/SEG.   NO.      (DB)        REAL          IMAG.         REAL          IMAG.
1    6     6      2    6    17    -23.883     7.23185E+01  7.82591E-02   7.23185E+01 -7.82591E-02
```

The total NEC-4 report does not contain current data, since the model lacks a separate excitation command. (The NEC-2 version contains 2 current tables, one for each EX0 command.)

The economy of the NEC-4 approach to the CP command shows up as soon as we move beyond the simple situation of model 20-8. Consider the request for mutual coupling in **Fig. 20-7**. The driver (Tag 2) will become the first entry in a pair of CP requests that wish to find the maximum mutual coupling between its center segment and the center segment of the reflector and then the director. Open model *20-9-nec2.nec*.

CP Conventions **Model 20-9**

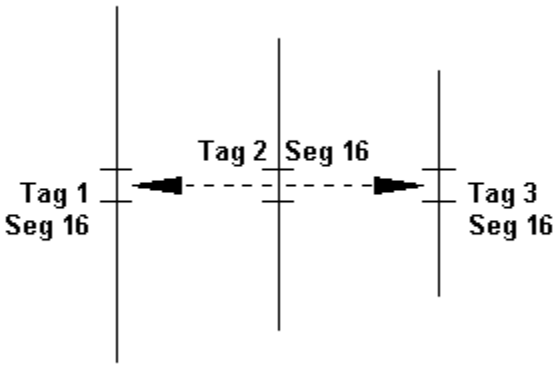

Fig. 20-7

```
GW 1 31 0. -.2434 2. 0. .2434 2. .003175
GW 2 31 .1763 -.2308 2. .1763 .2308 2. .003175
GW 3 31 .3471 -.2134 2. .3471 .2134 2. .003175
GE 1 0 0
GN 2 0 0 0 13.0000 0.0050
FR 0 1 0 0 299.7925 0
CP 2 16 1 16
EX 0 2 16 00 1 0
XQ
EX 0 1 16 00 1 0
XQ
CP 2 16 3 16
EX 0 2 16 00 1 0
XQ
EX 0 3 16 00 1 0
XQ
EN
```

In order to arrive at both values of mutual coupling where Segment 16 of GW2 is the first segment in each pair, we must repeat the EX0 command. (We may group the CP commands to arrive at a single table, but it will contain a number of extraneous lines.) The format shown will produce 4 current tables and two separate isolation data tables.

```
   - - COUPLING BETWEEN - -        MAXIMUM              - - - FOR MAXIMUM COUPLING - - -
         SEG.              SEG.   COUPLING    LOAD IMPEDANCE (2ND SEG.)       INPUT IMPEDANCE
TAG/SEG.   NO.    TAG/SEG.   NO.      (DB)        REAL         IMAG.         REAL         IMAG.
2   16    47      1   16    16     -7.990     6.52275E+01 -5.43423E+01   2.55660E+01 -6.46313E+00

   - - COUPLING BETWEEN - -        MAXIMUM              - - - FOR MAXIMUM COUPLING - - -
         SEG.              SEG.   COUPLING    LOAD IMPEDANCE (2ND SEG.)       INPUT IMPEDANCE
TAG/SEG.   NO.    TAG/SEG.   NO.      (DB)        REAL         IMAG.         REAL         IMAG.
2   16    47      3   16    78     -2.614     2.13959E+01  5.63384E+01   1.59467E+01  2.57385E+01
```

Now open model *20-9-nec4.nec*.

```
GW 1 31 0. -.2434 2. 0. .2434 2. .003175
GW 2 31 .1763 -.2308 2. .1763 .2308 2. .003175
GW 3 31 .3471 -.2134 2. .3471 .2134 2. .003175
GE 1 0 0
GN 2 0 0 0 13.0000 0.0050
FR 0 1 0 0 299.7925 0
CP 2 16 1 16
CP 2 16 3 16
XQ
EN
```

Not only is the model simpler, but so too is the output file. It omits current calculations and yields a pair of isolation data tables that follow one another.

```
   - - COUPLING BETWEEN - -        MAXIMUM              - - - FOR MAXIMUM COUPLING - - -
         SEG.              SEG.   COUPLING    LOAD IMPEDANCE (2ND SEG.)       INPUT IMPEDANCE
TAG/SEG.   NO.    TAG/SEG.   NO.      (DB)        REAL         IMAG.         REAL         IMAG.
2   16    47      1   16    16     -8.023     6.50988E+01 -5.39599E+01   2.57359E+01 -7.17282E+00


   - - COUPLING BETWEEN - -        MAXIMUM              - - - FOR MAXIMUM COUPLING - - -
         SEG.              SEG.   COUPLING    LOAD IMPEDANCE (2ND SEG.)       INPUT IMPEDANCE
TAG/SEG.   NO.    TAG/SEG.   NO.      (DB)        REAL         IMAG.         REAL         IMAG.
2   16    47      3   16    78     -2.604     2.12819E+01  5.70371E+01   1.57867E+01  2.49860E+01
```

In the simple model, the input or first segment impedance was the conjugate match of the load or second-segment impedance. However, the presence of a third element in the Yagi changes the relationship of the input and load impedance values.

NEC-4 Commands: JN, VC, PL, PS and UM

NEC-4 contains a pair of commands that are basically switches to change the way in which certain calculations proceed. Under certain conditions, the two forms will yield differing results. Since we would need an external standard, such as a controlled laboratory experiment, to determine which form of calculation produces the most accurate results, our work will confine itself to demonstrating the difference in output and under what conditions the difference occurs.

The JN command controls the method of calculating the charge distribution at the junction of

wires. The command has no parameters; implement it by simply entering JN as a new command line or add a zero as I1. The I1 position also allows the use of -1 to cancel a previous JN command.

In normal operation (without the JN command activated), NEC-4 employs a method-of-moments solution for the continuity at a wire junction to determine the distribution of charge on the wires. The result is then employed in the current base functions. In NEC-2 (and NEC-3), the charge on a wire with the radius a_j is proportional to $[\ln(2/ka_j)-\gamma]^{-1}$, a condition that does not take into account the proximity of wires at the junction. The JN command allows you to compare results. One condition that yields a considerable difference in results between the two methods of calculation is a change of radius at the junction, as suggested in **Fig. 20-8**.

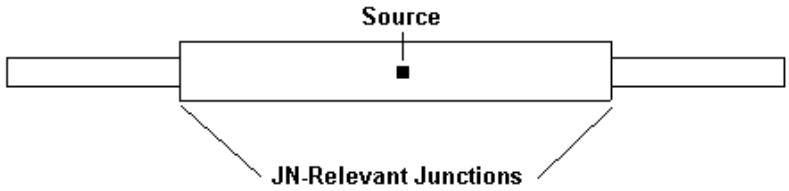

Models 20-10 and 20-10a

Fig. 20-8

Open models *20-10.nec* and *20-10a.nec*, remembering that this pair of models only makes sense when using NEC-4. Note the 2:1 difference in the radii of the center and end sections of the dipole.

```
GW 1 4 0 -.247 0 0 -.12 0 .001
GW 2 7 0 -.12 0 0 .12 0 .002
GW 3 4 0 .12 0 0 .247 0 .001
GE
JN 0
FR 0 1 0 0 299.7925 1
EX 0 2 4 0 1 0
RP 0 1 361 1000 90 0 1.00000 1.00000
EN
```

The only difference between model 20-10a, shown above, and 20-10 is that the latter lacks the JN command line. To determine that there is a significant difference in the output only requires that we obtain from each model the source impedance.

Model 20-10	74.487 + j0.196 Ω	(without JN)
Model 20-10a	76.021 + j15.190 Ω	(with JN)
(Model 20-10)	75.021 + j5.266 Ω	(when run on NEC-2)

The last entry shows that changing a single calculation method is not the entire story with the two cores, since the NEC-2 results are much closer to the standard NEC-4 results than are either to the NEC-4+JN results. Hence, the JN command fits into the category of a demonstration command rather than a command that we should use in the general course of modeling.

A second command that fits into this category is VC, the voltage source end-cap command. As the segment-length-to-radius ratio gets smaller, that is, below about 2:1, the charge distribution on segments containing either a source (EX0) or an impedance load (LD) may become erratic. **Fig. 20-9** shows the general situation.

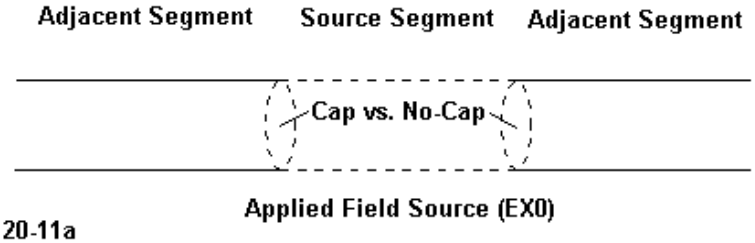

Models 20-11 and 20-11a

Fig. 20-9

The use of end-caps generally corrects the problem. However, if we place a voltage source near the end of a wire, the use of end-caps may create a small error in the effective source voltage. Hence, the use of end-caps is an option exercised by placing the VC command into the model. However, use caution if the source is not at or near the center of the driven element.

Open models *20-11.nec* and *20-11a.nec* within NEC-4. Model 20-11a appears here.

```
GW 1 4 0 -.26 0 0 -.12 0 .01
GW 2 7 0 -.12 0 0 .12 0 .02
GW 3 4 0 .12 0 0 .26 0 .01
GE
VC
FR 0 1 0 0 299.7925 1
EX 0 2 4 0 1 0
RP 0 1 361 1000 90 0 1.00000 1.00000
EN
```

Although the model appears similar to model 20-10, note the increase in the radii of the element sections. The center portion of the dipole shows a 1.7:1 ratio of segment length to radius. To see the difference, we need only run each model.

Model 20-11	97.860 - j0.198 Ω	(without VC)
Model 20-11a	98.896 + j9.904 Ω	(with VC)

A more generally useful command is one that does not appear in the NEC-4 manual: PL. This command establishes files for storing data from the NEC output file, data that we might like to plot. The command is so multi-faceted that we can only sample some of the options, although the NSI GNEC manual describes all of them.

```
Cmd   I1      I2      I3      I4
      IPLP1   IPLP2   IPLP3   IPLP4
PL    3       1       0       3       m20-12-RP0.dat
```

Depending upon the data to be stored, the command may use up to 4 integer values, but for

some data, the file name may directly follow the 3rd integer position. The file name must begin with a letter rather than a number. The latter will confuse the core into believing that the file name is actually an ill-formed numeric entry. NSI's implementation of the command allows you to select any file name, and multiple data storage requests should use different file names, each related to the model file name in some way for future reference.

Open model *20-12.nec*. Note the double PL command. Each PL command in a model must have a following execution command. The second PL entry has a following RP0 request to implement its execution. However, without the XQ command following the first PL entry, that request for data storage would not execute.

```
GW 1 11 0 -.2375 0 0 .2375 0 .001
GE
FR 0 1 0 0 299.7925 1
EX 0 1 6 00 1 0
PL 1 2 0 m20-12-currents.dat
XQ
PL 3 1 0 3 m20-12-rp0.dat
RP 0 1 361 1000 90 0 1.00000 1.00000
EN
```

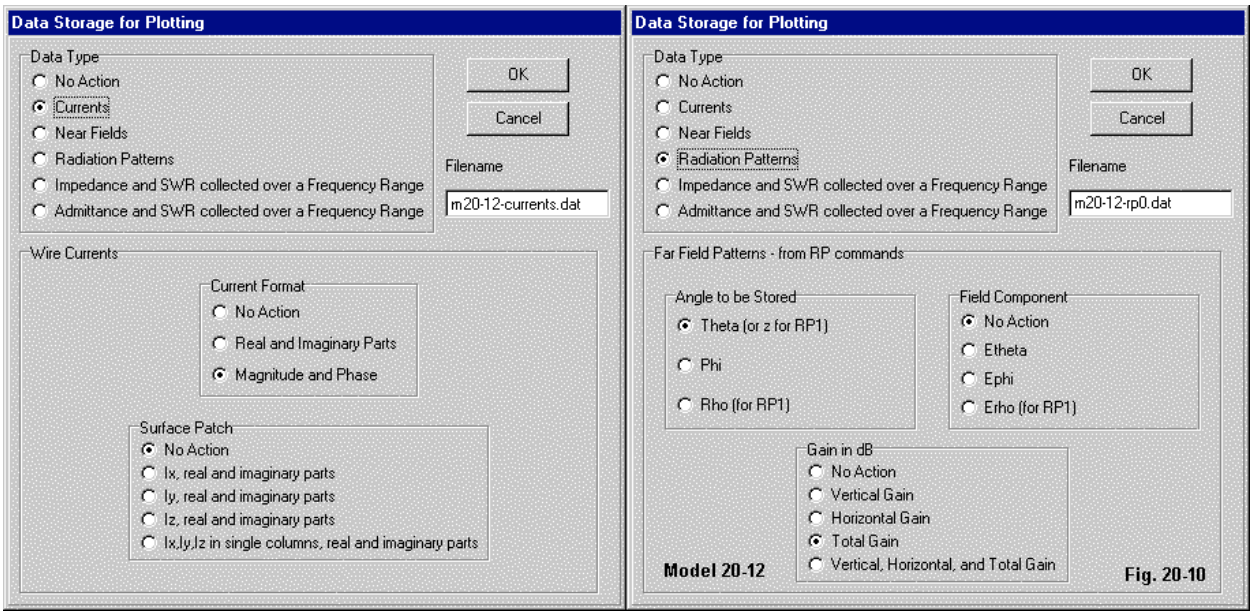

Fig. 20-10 shows the assistance screens for the two PL commands in Model 20-12. For the first command, I1=1 indicates a request for current storage, while I2=2 is a request to store the data in a form using the magnitude and phase angle. I3=0 means that the command takes no action on surface patch data, since none exists. The designated filename follows I3, with no placeholder for I4.

The second PL request involves the storage of data from the RP0 request (I1=3). I2=1 requests saving the phi angle, since that is the changing angle in the RP0 request. I3=0 means that the file will save none of the component information, while I4=3 indicates a request for total

gain in dB. The file name follows I4, when I1=3.

The format of the saved file is simple, indicating the NEC output reference number and the data, all without labels. Hence, you must know and remember what you are saving in order to use it within a plotting program. The following sample lines come from the two files.

From m20-12-currents.dat
```
M802  2.528E-03 -6.319E+00
M802  6.460E-03 -5.468E+00
M802  9.606E-03 -4.486E+00
```

From m20-12-rp0.dat
```
R810  0.000E+00  2.122E+00
R810  1.000E+00  2.120E+00
R810  2.000E+00  2.114E+00
R810  3.000E+00  2.104E+00
```

Open model *20-13.nec*. The assistance screen for the PL request for this near-field analysis appears in **Fig. 20-11**.

```
GW 1 11 0 -.2375 0 0 .2375 0 .001
GE
FR 0 1 0 0 299.7925 1
EX 0 1 6 00 1 0
PL 2 1 4 0 m20-13-NF.dat
NE 0 11 1 1 -5.0 -5.0 0.0 1.0 1.0 1.0
NH 0 11 1 1 -5.0 -5.0 0.0 1.0 1.0 1.0
EN
```

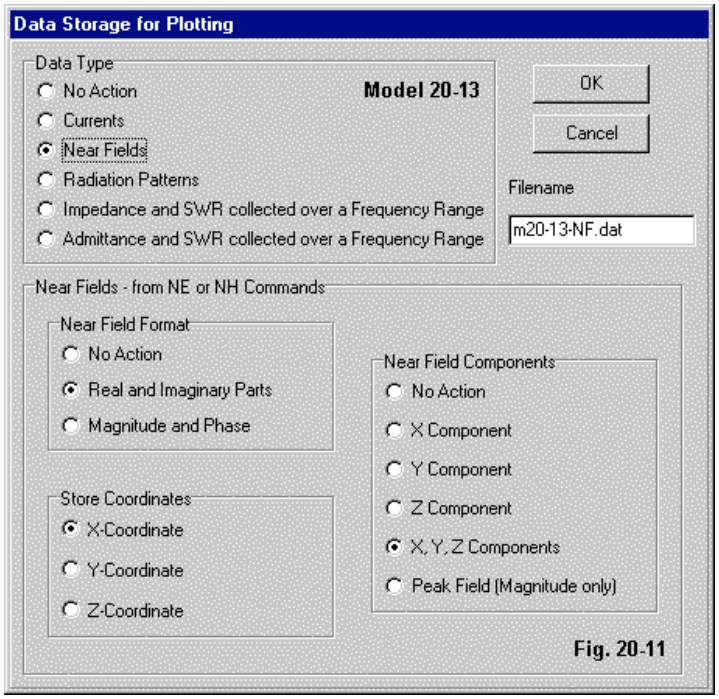

In the PL command, I2=2 is a request to store near-field data. I2=1 designates the data form as real and imaginary parts. I3=4 calls for storage of the X, Y, and Z components of the data, and I4=0 specifies storage of the X-coordinate, since that is the value that changes in both the NE and NH lines. Since the model requests only 1 frequency, both NE and NH are self-executing, carrying the PL request with them.

From file m20-13-NF.dat

```
N808 0.000E+00-2.596E-02 4.828E-02-2.601E-02 3.552E-02 0.000E+00 0.000E+00
N808 0.000E+00-2.771E-02-4.418E-02-2.319E-02-4.680E-02 0.000E+00 0.000E+00
N808 0.000E+00 0.000E+00 0.000E+00 0.000E+00 0.000E+00 9.556E-05 1.708E-04
N808 0.000E+00 0.000E+00 0.000E+00 0.000E+00 0.000E+00 9.699E-05-1.590E-04
```

The sample lines are the last 2 entries for the electric field and the first 2 entries for the magnetic field. The storage file adds no break between data lines and does not label the data blocks. Hence, you must be familiar with the data in order to use the file entries effectively. Note also that there is no space between columns. The apparent blanks simply indicate a positive value to follow.

For some purposes, the NEC-4 data storage facility may prove very useful, especially if the program that uses the data is self-parsing. However, other programs may find some of the NSI tables and formats more useful. (See Chapter 8 for samples.) Having access to both facilities adds flexibility to NEC-4 as implemented in GNEC.

The PS command prints a table of the electrical lengths of the segments, normalized to 1 wavelength. The command is suited to determining the electrical segment of buried wires and those supplied with an upper medium (UM). The calculation of the electrical length of a segment uses a transmission-line approximation to arrive at a wave number from which the program calculates the electrical wavelength. You should use the electrical segment lengths in determining the adequacy of the modeled segments relative to NEC's general boundary conditions.

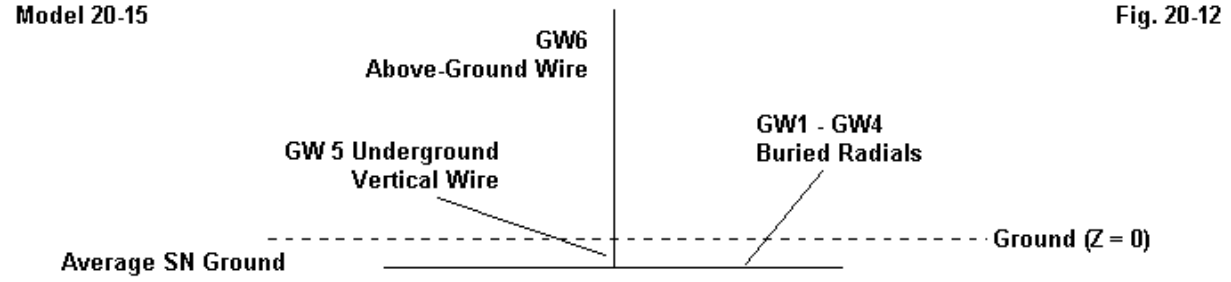

Consider the simple monopole with 4 buried radials outlined in **Fig. 20-12**. GW1 through GW5 are below ground. Their environment is a lossy medium with a conductivity of 0.005 S/m and a relative permittivity of 13, the so-called average ground. GW6, on the other hand, has a medium of dry air or a vacuum. Open model *20-14.nec*, understanding that this model is usable only in NEC-4. Since the PS command has no parameters, we may simply enter the command name to receive the table of electrical lengths. However, always insert the command after the FR line to ensure that the table takes the test frequency into account. For ease of

translating physical and electrical lengths, the model uses the test frequency at which 1 m = 1λ. Run the model, check the segmentation data, and then examine the data for segment lengths and radii.

```
GW 1 10 0 0 -.025 .25 0 -.025 .001
GM 1 3 0 0 90 0 0 0
GW 5 1 0 0 -.025 0 0 0 .001
GW 6 10 0 0 0 0 0 .25 .001
GE -1 -1 0
GN 2 0 0 0 13.0000 0.0050
FR 0 1 0 0 299.7925 1
EX 0 6 1 0 1 0
PS
RP 0 181 1 1000 -90 90 1.00000 1.00000
EN
```

The following lines sample the table from the last entry for a radial through the first 2 segments of the portion of the vertical element that is above ground level.

```
       K  = WAVE NUMBER IN MEDIUM       KS = WAVE NUMBER FOR CURRENT EXPANSION

                              ELECTRICAL LENGTHS NORMALIZED -            WAVE NO. FOR CURRENT EXP.
SEG.     - - METERS - -          BY 2.*PI/CABS(K)       BY 2.*PI/CABS(KS)            (KS)
40   2.500E-02  1.000E-03   9.015E-02  3.606E-03   9.015E-02  3.606E-03   2.2655E+01 -2.6120E-01
41   2.500E-02  1.000E-03   9.015E-02  3.606E-03   9.015E-02  3.606E-03   2.2655E+01 -2.6120E-01
42   2.500E-02  1.000E-03   2.500E-02  1.000E-03   2.500E-02  1.000E-03   6.2830E+00  0.0000E+00
43   2.500E-02  1.000E-03   2.500E-02  1.000E-03   2.500E-02  1.000E-03   6.2830E+00  0.0000E+00
```

Absolute segment 40 is the last radial segment. Absolute segment 41 is the 1-segment vertical wire (GW5) that extends from the radial hub to Z = 0. Absolute segments 42 and 43 are the first two segments of GW6. Since segments 42 and 43 have a medium with a permittivity of 1.0, their normalized lengths are identical to their physical lengths at the test frequency. In contrast, the calculated electrically equivalent lengths of the wire segments in the ground medium are 3.6 times longer than the aboveground segments, and their electrical radii are equally electrically fatter. Finally, note that the wave number that yields these values is later used in the current calculations and has consequences for the remaining values in the output file.

UM is a special command that sets the conductivity and permittivity for the region above ground. A key restriction for the command is that you cannot use the SN ground calculation system (GN2). Hence, for most cases, you must use the RCA ground system. The command itself requires a set of integer placeholders and 2 floating decimal entries.

```
Cmd   I1    I2    I3    I4    F1    F2
      NU    NU    NU    NU    EPSR  SIG
UM    0     0     0     0     20    .03
```

EPSR is the relative permittivity of the upper medium. SIG is the conductivity of the medium in S/m. The specifications for the upper medium use the same types of values found in ground specifications, but apply them to the entire region above ground. In order to see the consequences of specifying an upper medium, let's begin with a normal situation, in which the presumed medium is a vacuum or dry air. We may use an ordinary horizontal dipole 1λ above a relatively poor ground. Open and inspect model *20-15.nec*.

```
GW 1 11 0 -.2375 1 0 .2365 1 .001
GE 1
GN 0 0 0 0 4.5000 0.0010
FR 0 1 0 0 299.7925 1
EX 0 1 6 00 1 0
RP 0 181 1 1000 -90 0 1.00000 1.00000
EN
```

Run the model and obtain the usual output data: gain 7.11 dBi at a theta angle of 76°, source impedance 70.591 - j4.947 Ω. Next open model *20-15a.nec*, which adds a UM command.

```
UM 0 0 0 0 1.0 1E-10
```

If you run this model, you will obtain the same output reports as for model 20-15. The reason is simple. The UM command specifies a conductivity of 1E-10 S/m and a relative permittivity of 1.0, the values that simulate a vacuum. Next open model *20-15b.nec*. This model calls for a conductivity of 0.03 S/m and a relative permittivity of 20, which approximate the properties of very good soil. However, these properties extend from the ground upward, while the relatively poor soil remains intact below ground. Because we are altering the medium in which the dipole exists, we have added a PS command to check the electrical length and radius of the dipole segments. Run the model.

```
UM 0 0 0 0 20 .03
PS
```

The source impedance of the model is 127.224 - j48.395 Ω. However, if you look at the polar plot of the output, you will find nothing within the frame. To discover the reason, examine the overall NEC output report. In the radiation pattern section, you will find gain value of -999.99 throughout. The electric fields (both phi and theta) record nothing but zeroes. For most work with an upper medium other than a vacuum, the gain of the geometric structure holds the least interest.

Next, examine the current table for the model.

- - - CURRENTS AND LOCATION - - -

LENGTHS NORMALIZED BY WAVELENGTH (OR 2.*PI/CABS(K))

SEG. NO.	TAG NO.	COORD. OF SEG. CENTER X	Y	Z	SEG. LENGTH	- - - CURRENT (AMPS) - - - REAL	IMAG.	MAG.	PHASE
1	1	0.0000	-0.9677	4.4810	0.19309	1.2806E-03	5.3575E-03	5.5084E-03	76.557
2	1	0.0000	-0.7746	4.4810	0.19309	3.3221E-04	7.9285E-03	7.9355E-03	87.601
3	1	0.0000	-0.5815	4.4810	0.19309	-2.7313E-03	1.1015E-04	2.7335E-03	177.691
4	1	0.0000	-0.3884	4.4810	0.19309	-2.3008E-03	-8.3310E-03	8.6428E-03	-105.439
5	1	0.0000	-0.1953	4.4810	0.19309	2.9563E-03	-6.3021E-03	6.9610E-03	-64.869
6	1	0.0000	-0.0022	4.4810	0.19309	6.8666E-03	2.6120E-03	7.3466E-03	20.826
7	1	0.0000	0.1909	4.4810	0.19309	2.9563E-03	-6.3021E-03	6.9610E-03	-64.869
8	1	0.0000	0.3839	4.4810	0.19309	-2.3008E-03	-8.3310E-03	8.6428E-03	-105.439
9	1	0.0000	0.5770	4.4810	0.19309	-2.7313E-03	1.1015E-04	2.7335E-03	177.691
10	1	0.0000	0.7701	4.4810	0.19309	3.3221E-04	7.9285E-03	7.9355E-03	87.601
11	1	0.0000	0.9632	4.4810	0.19309	1.2806E-03	5.3575E-03	5.5084E-03	76.557

Compare this table to the corresponding table for model 20-15. In the earlier model, the current magnitude decreases smoothly from the center segment to the end segments. However, model 20-15b shows current peaks near the centers of each dipole leg, suggesting an electrical

structure that is nearly 3/2λ long. The reason for this condition appears in the segment length column. For more specific data, compare the physical segment data with the electrical segment data that results from the PS command.

```
                              - - - SEGMENT LENGTHS AND RADII - - -
                              K  = WAVE NUMBER IN MEDIUM
                              KS = WAVE NUMBER FOR CURRENT EXPANSION

                            ELECTRICAL LENGTHS NORMALIZED -            WAVE NO. FOR CURRENT EXP.
SEG.      - - METERS - -       BY 2.*PI/CABS(K)       BY 2.*PI/CABS(KS)            (KS)
NO.      LENGTH     RADIUS      LENGTH     RADIUS      LENGTH     RADIUS       REAL        IMAG.
  1   4.309E-02  1.000E-03   1.931E-01  4.481E-03   1.931E-01  4.481E-03   2.8127E+01 -1.2623E+00
  2   4.309E-02  1.000E-03   1.931E-01  4.481E-03   1.931E-01  4.481E-03   2.8127E+01 -1.2623E+00
```

Because the physical length equates 1 m and 1λ at the test frequency, you can easily gauge the relative increase in electrical length and radius for each segment--a factor of about 4.5. For this reason you must use care with junctions of wires, especially where the medium changes (at Z = 0). NEC-4 will use the electrical length and radius when performing its current calculations.

In general, the UM command is for special modeling problems and not for general antenna modeling. You may glean a hint of this from the location of the current calculations in the Z-axis for the sample dipole. We placed the dipole 1λ above ground, but the electrical position in the Z-axis is now 4.481λ above ground level.

Summing Up

Of the commands that we have surveyed in this potpourri, NEC-2's EK and NEC-4's PL and PS are perhaps the most important. The PQ and CP commands that both cores share, when needed, are equally significant.

The EK command is vital to obtaining accurate results from NEC-2 models when the segment-length-to-radius ratio is less than about 8:1. Where its results closely parallel the results from models not using the command, no harm accrues from using it. However, as the ratio of segment length to radius approaches and passes 2:1, it becomes a necessary feature of the model. However, the command is not the equivalent of the revised algorithms of NEC-4, since NEC-2 will always treat angular wire junctions using the basic thin-wire kernel rather than the extended version of EK.

NEC-4's PL command provides a very flexible way of storing data in files for later use within plotting and other programs. Its structure is variable, according to the data you wish to store, but the final entry is always a file name and extension suited to both the model and the type of data stored. Whether the file is useful depends upon your ability to remember the meaning of the data stored within it, since the file has no labels or separators. The absence of separators also means that the program that opens the file must be able to parse the columns and rows.

The PS command in NEC-4 is exceptionally valuable in learning the electrical length of segments in media other than a vacuum or dry air. The electrical length--that is, the wave number used to calculate it--also enters subsequent calculations. Hence, we should use the electrical segment length in meeting the NEC boundary conditions for model adequacy. The UM command provides a case in point, since the specification of an upper medium having

significant values for both conductivity and permittivity displaced the electrical position of the wire with respect to the location of currents. The UM command is for special projects and is not allowable with the SN ground calculation system.

The PQ command is perhaps the simplest to use in both cores. It provides the charge density on each segment in coulombs/meter. NEC-4 adds the charge density at the ends of the wire, while NEC-2 lacks this feature.

Maximum mutual coupling data requires the CP command. The outputs of the NEC-2 and NEC-4 versions are identical, but the procedure for obtaining the data differs between the 2 cores. Obtaining the information from NEC-2 requires that you individually excite the segments that are under scrutiny in the order listed in the CP command, with each EX0 entry followed by an execution command. NEC-4 automates the process so that a single execution command in the model (RP, NE, NH, XQ) produces data without need to individually request excitation for the segment specified in the CP command.

Effective use of most of the commands that have appeared in this chapter--along with the commands that we have by-passed altogether in this volume--falls into the realm of advanced modeling. Since they are tied to specific applications, one might require a full text just to sample adequately the good uses to which we might put them.

21.
Modeling by Equation

***Objectives**: The exercises in this chapter will use the NEC-Win Plus insert of NEC-Win Pro and GNEC to introduce some rudimentary aspects of modeling by equation. Beginning with the use of simple variables, the exercises will progress to more complex equations that will define the antenna geometry and permit automated scaling of a design to other frequencies.*

Many types of antenna structures have regular features subject to mathematical treatment in the form of equations. NEC itself has no direct provision for handing such equations that may define the antenna elements in terms of length and diameter. However, the NSI program, NEC-Win Plus contains a full spreadsheet that allows you to set either some or all of the tag-end coordinates and wire diameter as variables. On a related page of the spreadsheet, you may then define the variables with constants or equations. You may even define a variable using the frequency or wavelength of the model, thus permitting automated frequency scaling. The NEC-Win Plus program forms the core of the "insert" of NEC-Win Pro and GNEC.

The NEC input file created by the Plus insert contains only the dimensions calculated by the use of variables and equations. Therefore, if you wish to save the spreadsheet work, you must save the file from within the Plus insert as either an .NWP (NEC-Win Plus) or an .NPI (NEC-Plus Insert) file. The exercises for this chapter are available in both forms, and also as .NEC files to record the input file actually used by the core.

Modeling by equation has a price. All wires must be GW entries only. Therefore, such handy commands such as GM, GX, GC, GR, and GA are not available on the spreadsheet. In some modeling situations, the use of one or more of these commands may be preferable to the use of a model that employs equations. For example, we may create a nearly perfect circle by using the GA command and specifying many segments for the arc. The result requires only one entry--the radius--to modify the circumference. This procedure may for some cases prove to be more economical than the use of the insert to define the same circle in terms of individual wires and variables.

Deciding whether or not to use equations to define the antenna geometry or to use the geometry commands available within the normal NEC input framework requires that we have some feel for modeling by equation. Providing the basics for what modeling by equation involves is our goal in this chapter.

Using Variables

The spreadsheet input screen of NEC-Win Plus and the Plus insert allows you to see, in alternative views of the structure spreadsheet, a. the numbers and equations used to set the values of variables, b. the values that result from those equations, c. the assignment of variables

to the X, Y, and Z coordinates of the model structure, and d. the physical values of the X, Y, and Z coordinates that result from the preceding steps. So for this exercise, I shall make use of Plus to demonstrate a few (but by no means all) of the steps involved in modeling by variables--along with a couple of the advantages that accrue from the practice. Note that the Plus insert uses wire diameter rather than radius to define the element size. However, when updating the NEC input file, the program automatically translates that value into the required radius entry.

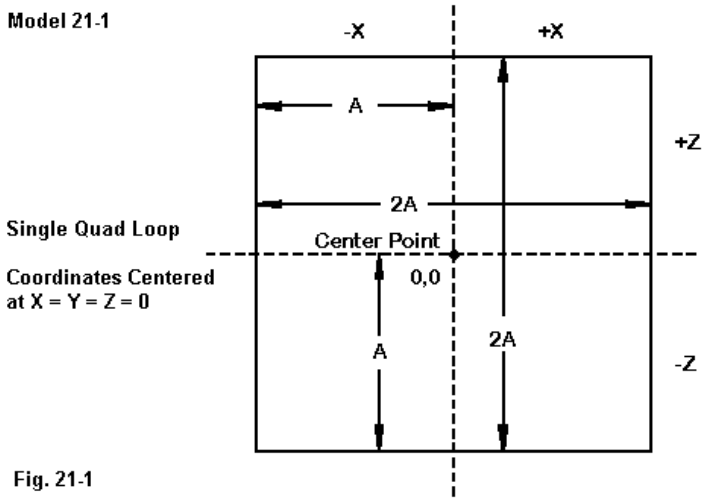

Fig. 21-1

Fig. 21-1 represents our sample antenna--a simple quad loop. For simplicity, we shall begin with a free space model for 300 MHz, composed of #20 AWG (0.032" diameter) copper wire. A square quad loop consists of 4 equal sides. A simplistic approach to modeling by variables might simply let some variable A equal the physical length of a side and proceed from there.

However, when modeling by variables, it pays to do a preliminary inspection of the geometry of the antenna to see if one might obtain a more sophisticated and ultimately more useful selection of variables and values. **Fig. 21-1** shows that a square quad loop can be framed against a center point so that we can take advantage of the Cartesian reference system. The example takes the 2-dimensional square and assigns the horizontal dimension to the X-axis and the vertical dimension to the Z-axis. Initially, Y will always equal zero.

In a free-space model, we can keep the structure centered by using values of A as +/-X and +/-Z values. This will come in handy later when we move the antenna over real ground. For initial purposes, A becomes about 1/8λ long to form the approximately 1λ total loop circumference. For the present, we shall not be concerned with whether the loop should be exactly 1λ long, since that is something we shall discover from our modeling. Unless otherwise specified, the dimensional units for our exercise will be inches.

The first step is to define a variable as 1/8λ long. **Fig. 21-2** shows the Plus equations page, with A defined as W/8. (I shall by-pass the program specific instruction set by which we accomplish this, but it follows standard spreadsheet procedures.) Two other variables are already assigned permanent values: F for the initial frequency (and in this case the only frequency) of test, and W for the wavelength. Note that the wavelength entry has a reference to model parameters. The parameter of relevance here is the conversion factor for changing the modeling units (inches in

this instance) into the NEC core requirement of meters. The result is the wavelength in the unit of choice.

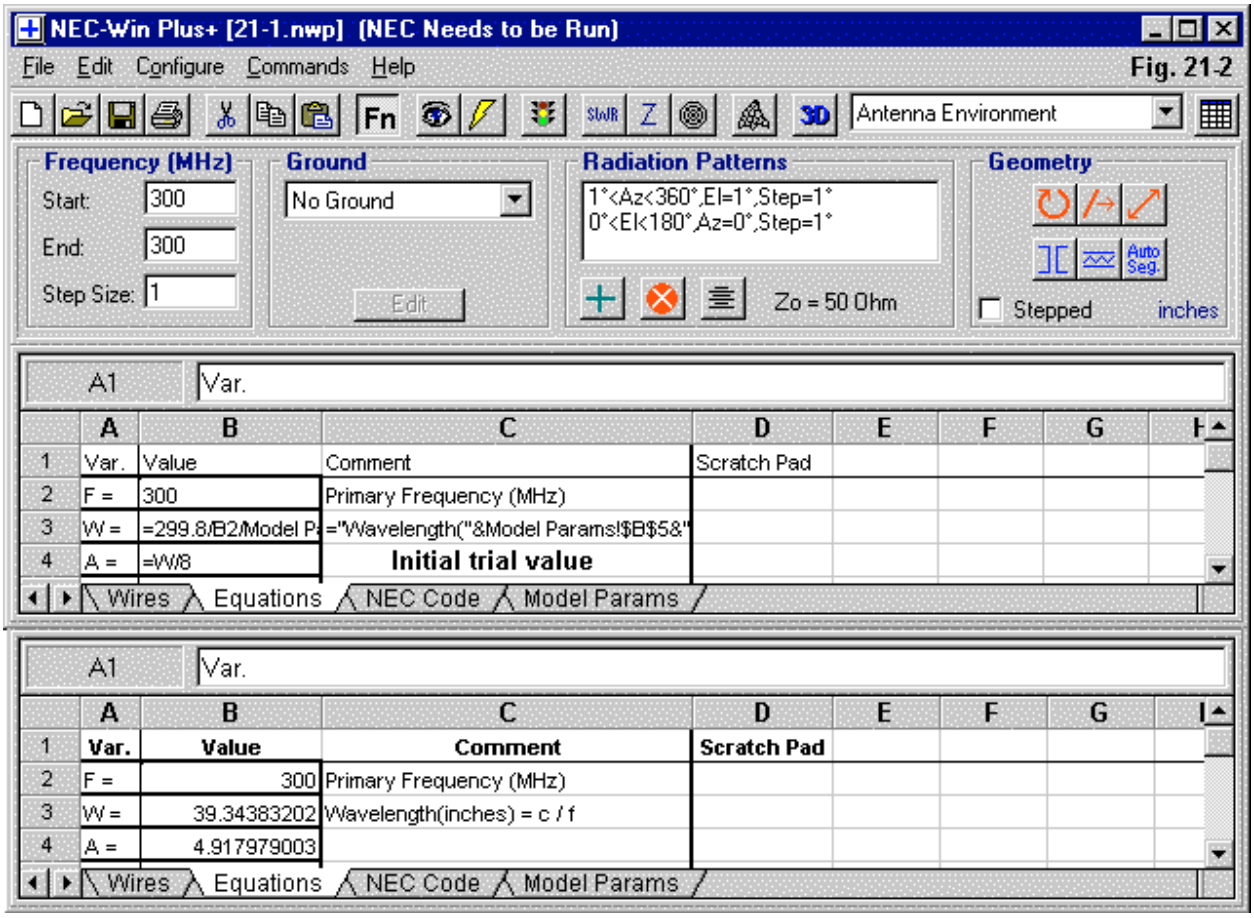

The lower half of **Fig. 21-2** shows the value of A in inches that results from establishing the equation that defines A. At the top of the Plus screen is a button labeled Fn. When highlighted, we see the equations. When dark, we see the values that the equations yield. In this model, we have let A = W/8, whatever the value of W might be. You may also note the header information that establishes this as a free-space ("No Ground") model at 300 MHz. At 300 MHz, A has a value of 4.91797. . ." because a wavelength is 39.34383. . ." long.

We might have defined the value of A in terms of frequency, but that would have required that we confine the units of measure to a single system, or that we define conversion variables. Defining A in terms of the wavelength will give us some versatility later on. The next question is how to set up a structure that makes use of the variable A to set antenna dimensions.

If we go from the equation page to the wires page, as we have in **Fig. 21-3**, we can set up the antenna structure using the variable A. Note the highlighted Fn button--we shall "un-highlight" it in a moment. We construct the quad in the normal manner, but we use values of "=-A" and "=A" instead of the normal numerical values we might otherwise use. Note that the structure parallels the set-up shown in **Fig. 21-1**, using the X- and Z-axes as the dimensional columns, leaving Y at

zero. Many modelers prefer to use the Y- and Z-axes, leaving X at zero. This procedure achieves the same goal, but with the antenna aligned 90° relative to the convention selected for the example. The antenna is constructed sequentially, beginning with the lower horizontal wire, then the right vertical, then the top horizontal, and finally the left vertical. Connections are sequential in order to facilitate an examination of the geometry.

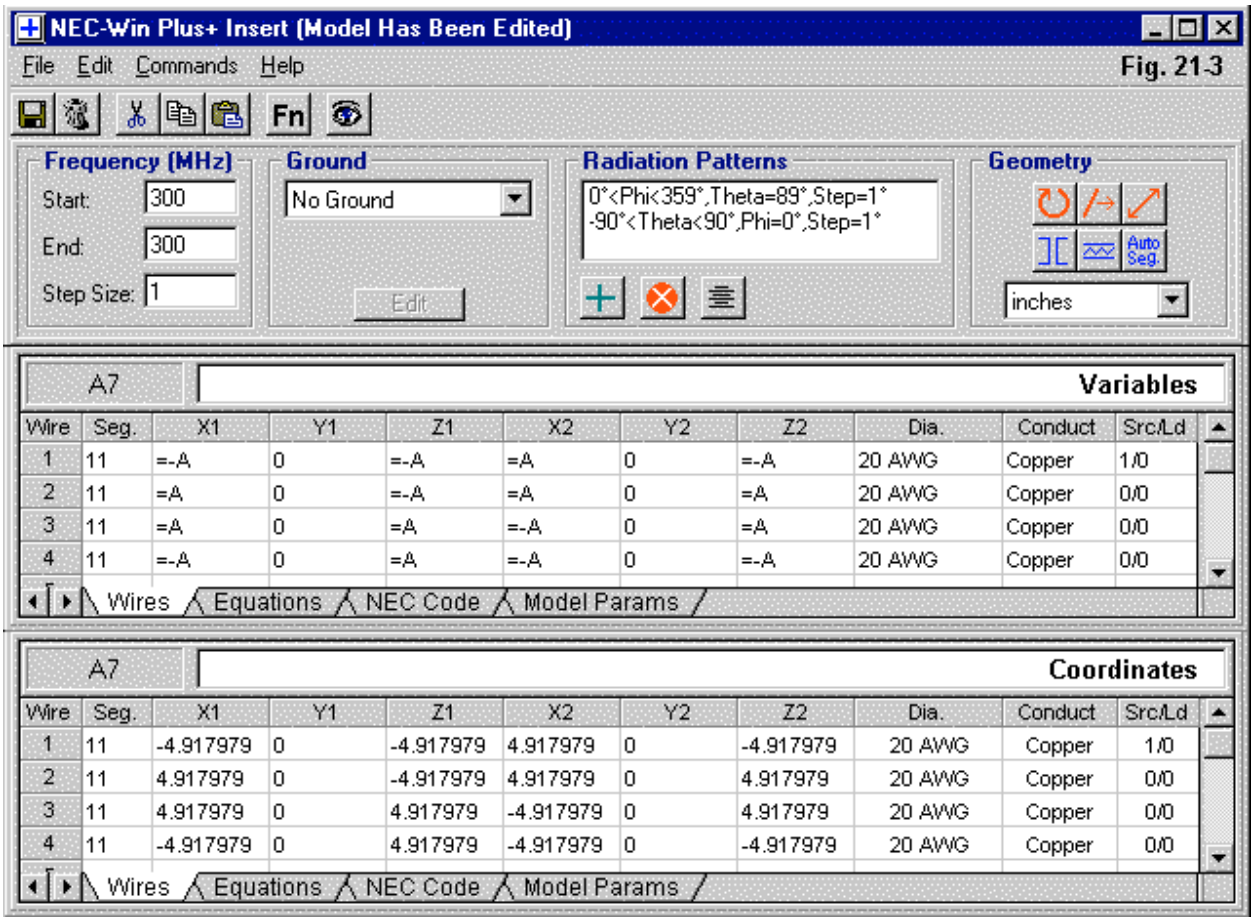

The remaining wire data to the right of the chart is constant for now. The source segment is the center segment of the lower horizontal wire. The conductivity entry of "copper" represents a specific numerical value built into a program table. You may discover that different programs (for proper reasons within the context of each program) may use very slightly different values for the conductivity of any material, mostly varying in the number of decimal places to which the value is carried. As well, Plus allows the selection of AWG wire sizes. AWG #20 has a diameter of 0.0320".

By flipping to the un-highlighted Fn version of the wires page (lower portion of **Fig. 21-3**), we can view the values (in inches, our chosen unit of measure) for the variables in each position of the antenna structure. Perhaps the most difficult facet of this page to which we must grow accustomed is the number of digits in each value. We must remember that NEC programs are essentially calculating machines and do not choose the number of significant digits for us. We must do that according to the task at hand. For building this loop, we might round the figure for A

into 4.92, and then translate that into 4 15/16" for measuring wire. Some other tasks involved in finding the trends in values might relevantly preserve additional decimal places. For now, we can simply accept the calculated value of A and focus on making sure that we have constructed the loop correctly by checking appropriate End-1s and End-2s of each wire.

Open model *21-1* in any of its forms. Use the .NPI form to view the equation pages on the insert. The .NEC form shows what actually forms the NEC input file.

```
CM Model 21-1
CM NEC version
CE
GW 1 11 -4.91797900262467 0 -4.91797900262467 4.91797900262467 0
 -4.91797900262467 0.0159843
GW 2 11 4.91797900262467 0 -4.91797900262467 4.91797900262467 0
 4.91797900262467 0.0159843
GW 3 11 4.91797900262467 0 4.91797900262467 -4.91797900262467 0
 4.91797900262467 0.0159843
GW 4 11 -4.91797900262467 0 4.91797900262467 -4.91797900262467 0
 -4.91797900262467 0.0159843
GS 0 0 .02540
GE 0
```

These lines capture only the model geometry and not the load, excitation, or pattern request commands. Run the model and obtain the usual vital data: free-space gain 3.08 dBi, source impedance 108.7 - j143.7 Ω. Our loop is much too small to be a resonant quad loop for 300 MHz.

Had we entered our coordinate values in terms of individual numbers, we would now be faced with revising each coordinate value by the amount we think might move the quad loop toward resonance. To suggest that this is a time consuming procedure is to make a very serious understatement. We would have to revise 16 values however many times it takes to find a value that allows the loop to be resonant with an Ohm or two. I have found that many modelers enlarge the concept of resonance to encompass many Ohms of reactance, not because the task does not require close tolerances, but because they simply tire of adjusting coordinate values on the wires page. Some programs have shortcuts that permit adjusting junctions and wire groups together, but there are still multiple steps involved--and each becomes an invitation to drop, double strike, or transpose a number along the way.

With our model-by-variable system in place, we shall change the loop dimensions by changing only one number. For this we return to the equation page and look back at **Fig. 21-2**. Where we had entered the value for A as W/8, we shall enter a new value. To make the loop larger, we should choose a smaller value than 8 as the denominator. To keep the story brief, let's replace 8 with 7.43. Had we exercised a preference for multipliers rather than divisors, we might have started with a value of A of W*0.125. Given that choice of equation formulation, to make the loop larger, we need a larger constant. The result would have been W*0.1346 or thereabouts.

The change we just made will make no difference to the version of the wires page that shows the assignment of variables to the coordinates of the structure. So we shall by-pass that version of the wires page and go directly to the bottom of **Fig. 21-4**, the version of the wires page that shows the actual dimensions that result from the revised value for A.

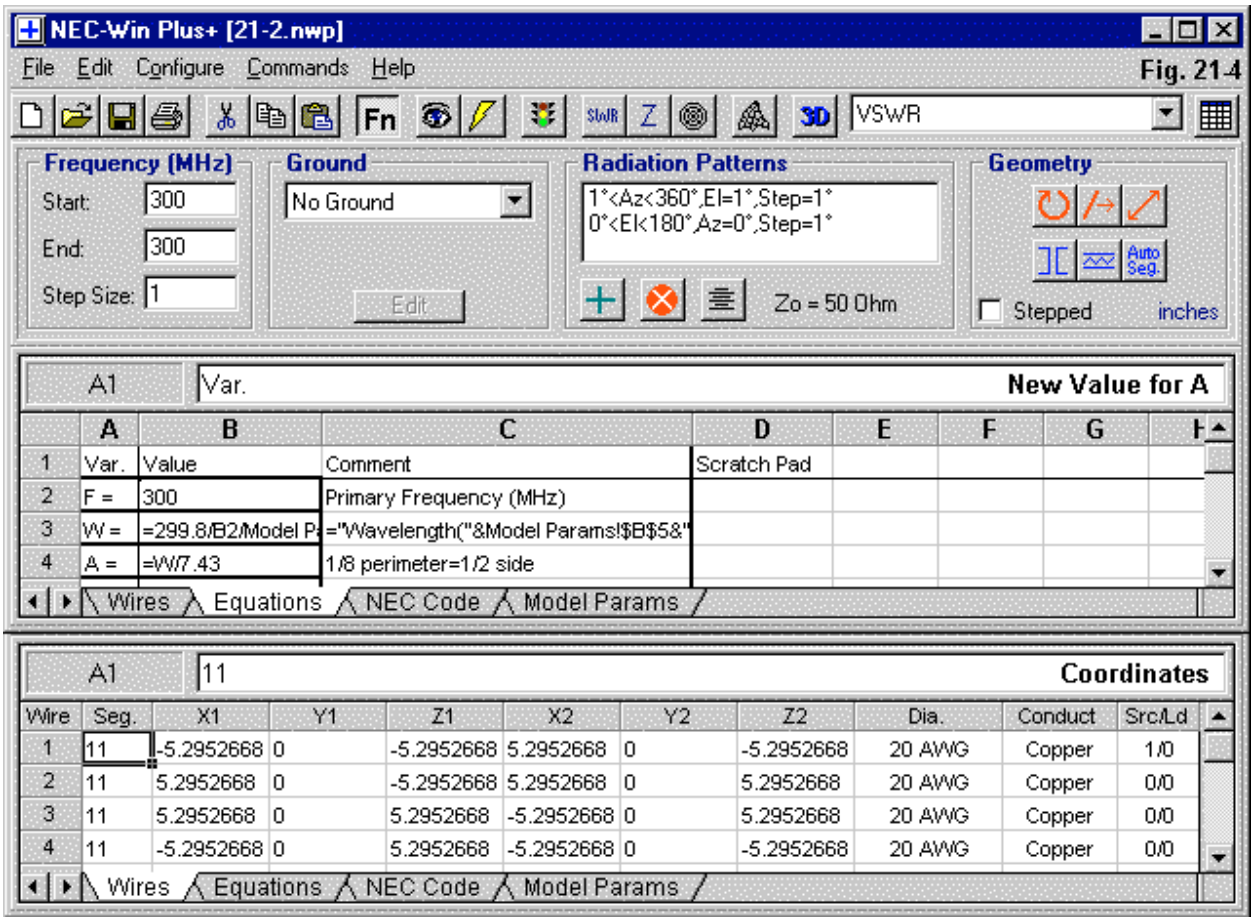

The value for A is now (at 300 MHz) about 5.3, a full 7% larger than the value with which we made our trial start. Each side of the quad is now about 10.6" long. The question is whether we have achieved resonance. So let's run the model once more. Open model 21-2 in any of its forms and run the model. The free-space gain is 3.32 dBi and the source impedance is 128.9 - j0.1 Ω. Our initial task is complete. At this point, we should take a moment to appreciate the time we have saved in creeping up on the resonant dimensions of this simple loop. A little time spent with an initial analysis of the antenna geometry resulted in a much larger amount of time saved in the optimizing process.

There is a limitation on the exercise we have just run. In order to focus on the aspects of dimensional modeling by the use of variables, we let the wire diameter be a constant. In virtually all programs, selecting a wire size from a chart--that is specifying the wire size in AWG values--creates a constant. For some purposes, it is better to make the wire size a variable.

Therefore, let's add a new variable B to our list. We shall make the wire size a function of a wavelength. If we let B = W/1228 (or W*0.000814), we shall have captured the diameter of #20 wire at 300 MHz. We must now go back to the "variables" version of the wires page and replace all of the wire diameter entries with "=B" to put the variable into effect. The end result on the dimensions version of the wires page and the equation page will look like **Fig. 21-5**.

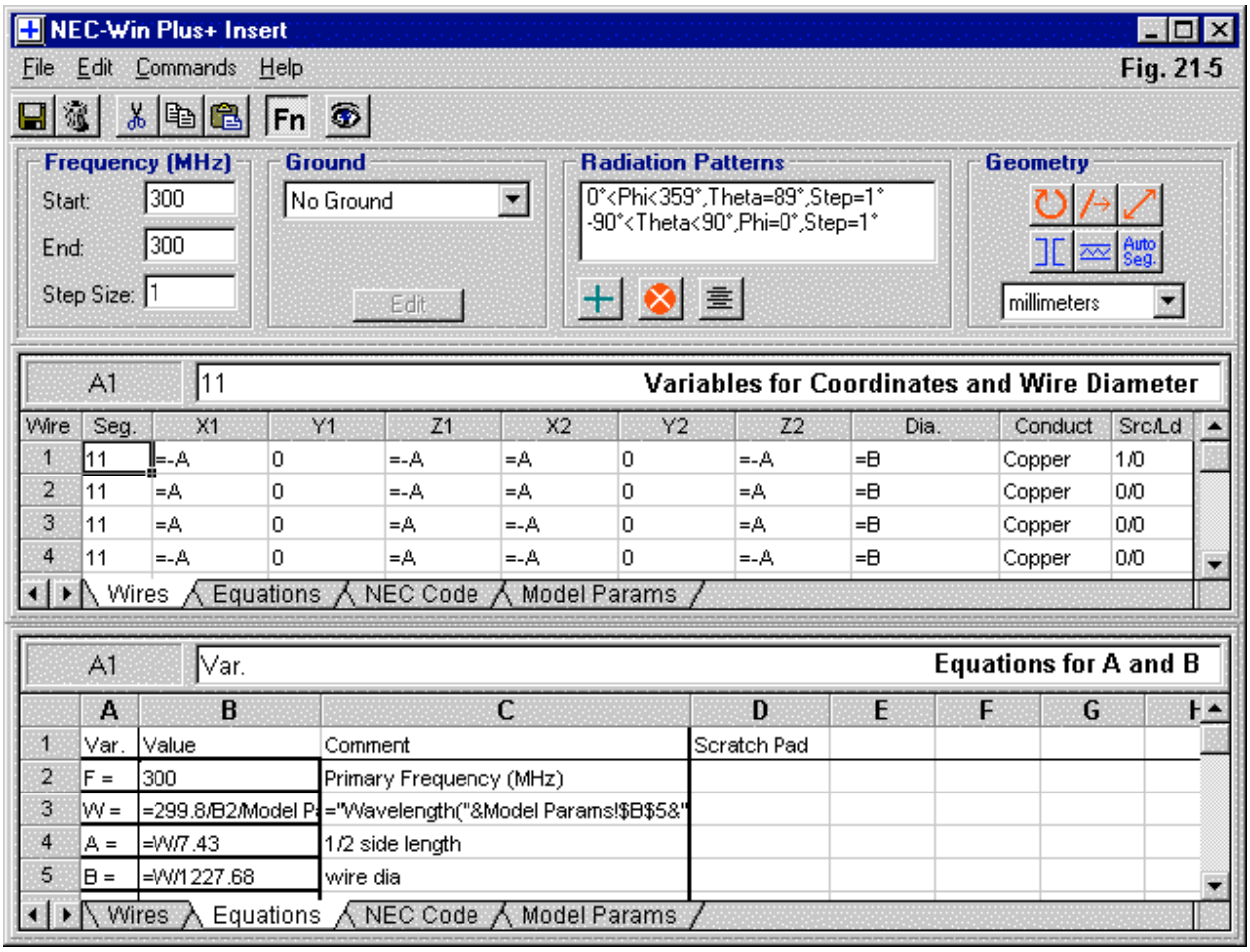

What we gain by making the making the wire diameter a function of a wavelength is a good bit more than the little trouble it took to create the variable and to put it into place on the wires page. Here are just two examples.

1. *Units conversion*: Since we defined all of our physical dimensions as functions of a wavelength, changing the units of measure will automatically change all of the physical values. If we remember from model 21-1, the value for W, a wavelength, included adjustment into the currently selected units of measure by taking into account the adjustment factor for the eventual conversion into meters. Hence, the numerical value of W changes with each change we make in the units of measure. And if we change the value of W, then the values of A and B (the variables in our example) also change to the correct values for the selected unit of measure.

As an experiment, the model shown in **Fig. 21-5** changes from inches to millimeters. Open model *21-3* in any of its versions and run the model. The source impedance is 128.9 - j0.2Ω.

2. *Frequency scaling*: Complete frequency scaling requires that we multiply every dimension of an antenna by the ratio of the old frequency to the new frequency. Hence, if we go lower in frequency, we obtain larger dimensions, and vice versa. There may be a very slight adjustment to be made for differences in skin effect, but if we scale the wire diameter as well as the wire lengths,

we come as close to perfection as is possible.

If we fail to scale the wire diameter, we will find that the antenna at the new frequency may not perform as it did at the old frequency. The greater the frequency jump, the greater the difference in performance, if we simply let the wire size be a constant. For perfect scaling, we must make the wire diameter--like the wire lengths--a function of a wavelength.

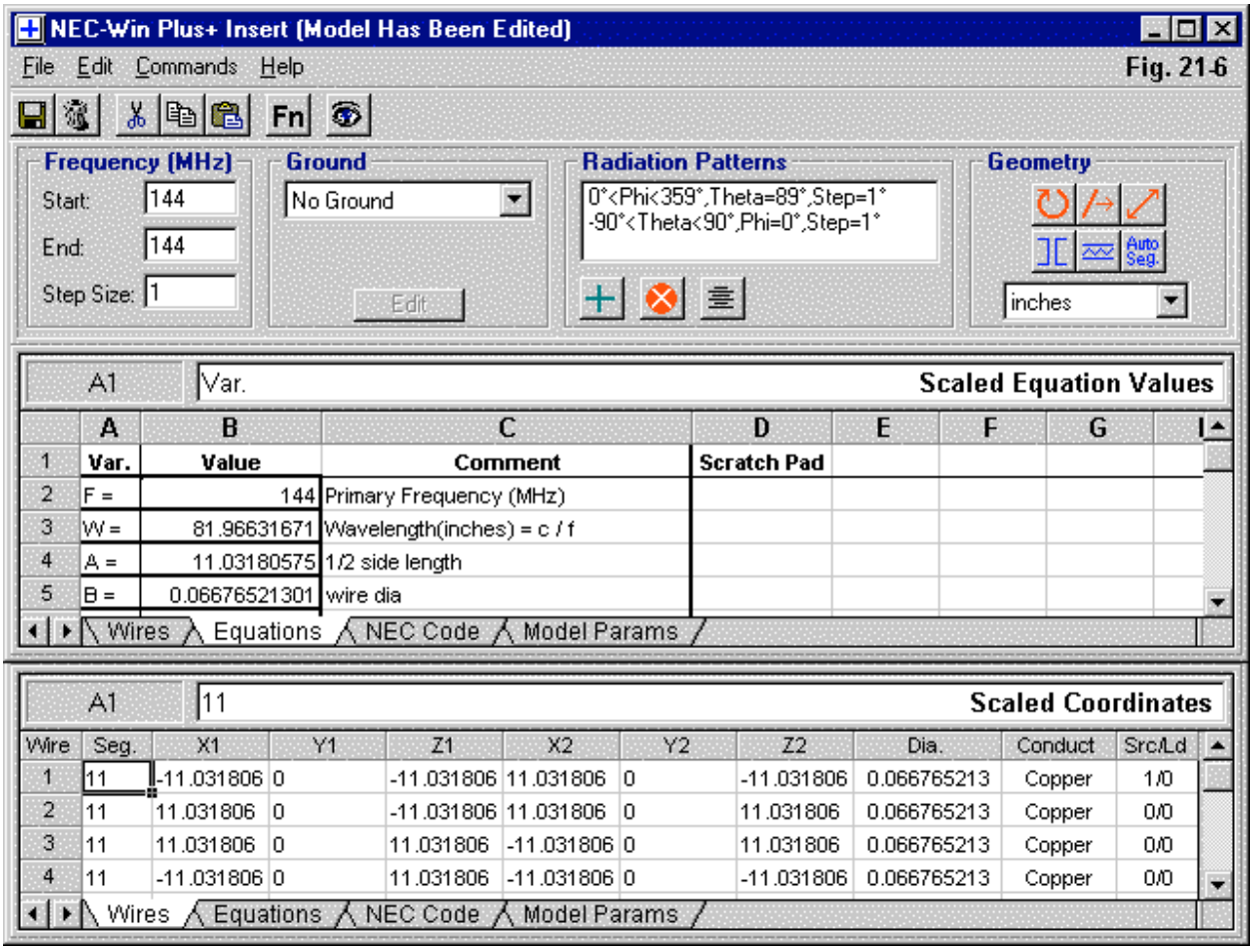

Fig. 21-6 shows the coordinate version of the wires page and the equation page of our quad loop, with dimensions in inches. The only alteration made was to change (at the upper left corner) the frequency. We moved from 300 MHz to 144 MHz. On the equation page, since F changed, so too did W, the length of a wave, and so on through every variable defined in terms of W.

Open model *21-4* and run the model. The source impedance is 128.6 - j0.6 Ω. The slight change in source impedance follows from the use of copper wire with a finite conductivity and a skin effect that varies with frequency. Our new diameter is 0.067", which does not coincide exactly with any AWG value. However, it is close enough to #14 AWG (0.0641") that using this size would likely turn up no measurable differences in loop dimensions--given the variables of physical construction. The exercise does suggest that there is a limit to physically scaling antennas. When the wire diameter reaches unreasonably thin or thick values, it is time to redesign the antenna. If

we scale our 300 MHz loop of #20 wire to 28 MHz, it calls for 0.343" diameter copper wire. This diameter is an unreasonably heavy wire for a quad loop (unless one simulates it with a double strand of thinner wire, spaced to achieve the same resonance with the same loop length).

Conventions and 3-Dimensional Models

Effective and efficient antenna modeling requires more than a random approach. The more systematic we become, the fewer things we have to decide in each modeling task. Not only do we save time, but as well, we are less likely to commit errors in the construction of our models.

The rules of the modeling programs set some boundaries to the ways in which we can proceed. Within those limits, we have a good bit of flexibility. Sometimes, we need to make use of that flexibility and model some special structure in an unusual but correct way. Most of the time, however, we are more likely to speed success in our modeling efforts if we develop some good procedures and stick with them until the special case comes along. I tend to call these procedures conventions. There are several types.

1. *Structural procedures*: Creating a model, wire by wire, is best done by developing certain habits. For example, with linear elements, we can model from left to right or from right to left for each element. Either way permits us to track the currents along the element and easily read other portions of the NEC data output in ways that modeling from the center outward only confuses. However, our linear progressions should always move in the same direction from model to model.

Loop elements, such as the one shown in **Fig. 21-1**, offer us additional opportunities to create conventions in our modeling. Since a loop is a continuous element composed of at least 4 wires, we shall normally encounter fewer confusions and errors if we model the circumference in a regular progression. If the current phase is not a concern, then this progression works well. The figure also shows the loop symmetrically placed around a center point. For initial free-space modeling, one should let the center point be 0,0, so that each dimension of the antenna involves A or -A for each coordinate point. The advantage of this procedure becomes evident as soon as we wish to place a second loop behind or ahead of the first, but to use a different set of dimensions at the same time. The 0,0 center point ensures that each loop is aligned with the next one.

A third facet of structural conventions involves the choice of coordinate axes for various antenna dimensions. The Z-axis handles vertical dimensions automatically. You can place side-to-side dimensions across either the X- or the Y-axis. The unused X- or Y-axis normally becomes the front-to-back axis, if the antenna has more than one element. The goal is to pick one system (according to your modeling goals overall) and to stick with it so long as it serves well.

Fig. 21-7shows a representative set of front-to-back conventions. In this sketch, all elements count their dimensions from the rear of the multi-element array, in this case, the reflector. It is set to zero. Each element will have a distance value that is positive, represented by the variables D and E in the sketch. The advantage of this scheme is that the total front-to-back dimension is always readily available to the modeler. The disadvantage is that distances from the second to the third element must be calculated. For our work in this episode, we shall use the conventions shown in the sketches.

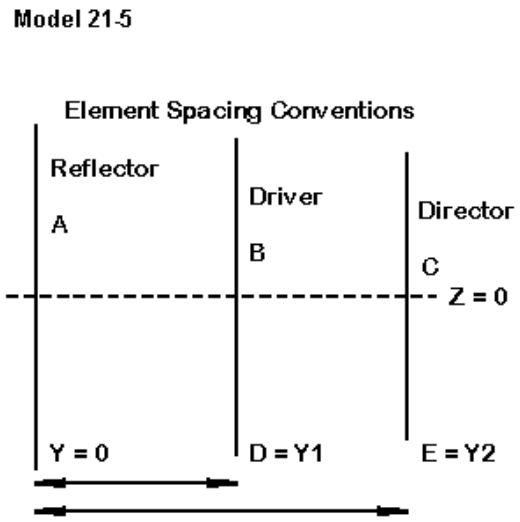

Fig. 21-7

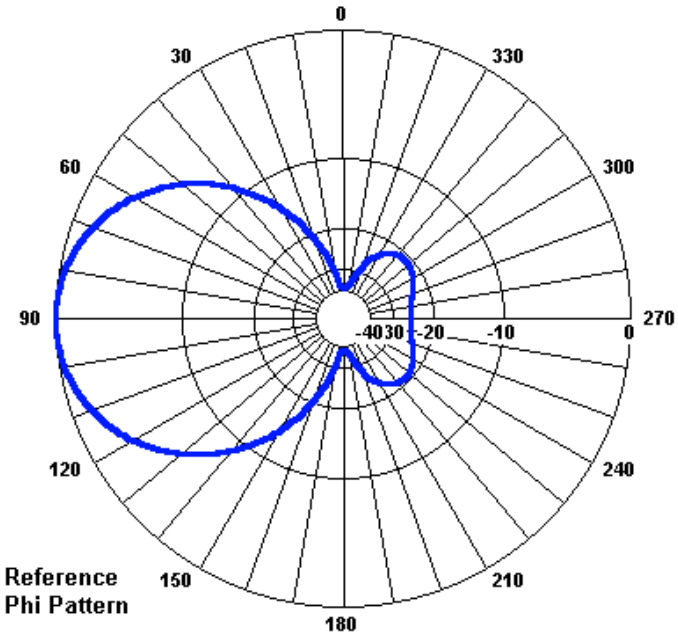

2. *Equation conventions*: When constructing values for the variables out of which you will build the antenna model, give some preliminary thought to the ways in which you will develop the variables. Of course, the simplest system is to simply assign variables a numerical value. This system permits multiple dimensional changes with the change of a single value on the equation page. However, it is limited insofar as it does not permit full scaling of the antenna structure.

Open model *21-5* and examine the Plus insert pages. A reference phi pattern for the finished model appears in **Fig. 21-7**. **Fig. 21-8** shows the equation and variable pages for the model, a 3-element quad beam for 300 MHz using AWG #20 wire, with all dimensions in inches. The equations all relate the antenna dimensions to a wavelength. One might choose to relate them to frequency. Although this latter scheme allows frequency scaling, it does not provide automatic numerical value changes with changes of units. Relating the numeric values to a wavelength provides both facilities. The equations also arrive at the final values by dividing the length of a wave by a certain number. Alternatively, one might have multiplied a wavelength by the reciprocal of the divisor, if that scheme is more efficient for a given modeler.

There are also some conventions at work that logically group the values in the total set. A, B, and C are the variables controlling the reflector, driver, and director wire lengths, respectively. Note that each element has an independent equation related back to W, a wavelength. It is also possible to develop one variable, for instance, the driver, and then to set the reflector and director dimensions as functions of the driver. Since the reflector will be set to zero along the Y-axis, D controls the reflector to driver spacing and E controls the reflector to director spacing. Even within the scheme used to assign values, one might have reorganized these variables. However, consistency from one model to the next reduces confusion and errors. The wire diameter is assigned to H, with G reserved. Since the initial model will be in free space, no height equation is necessary. However, to keep the dimensional variables well grouped ahead of the wire diameter, G is reserved for later use, while the wire diameter moves to H. Later, when we move the model over ground, G will have a value. More importantly, you will be able more easily to correlate the

components of the free-space model to those of the model over ground.

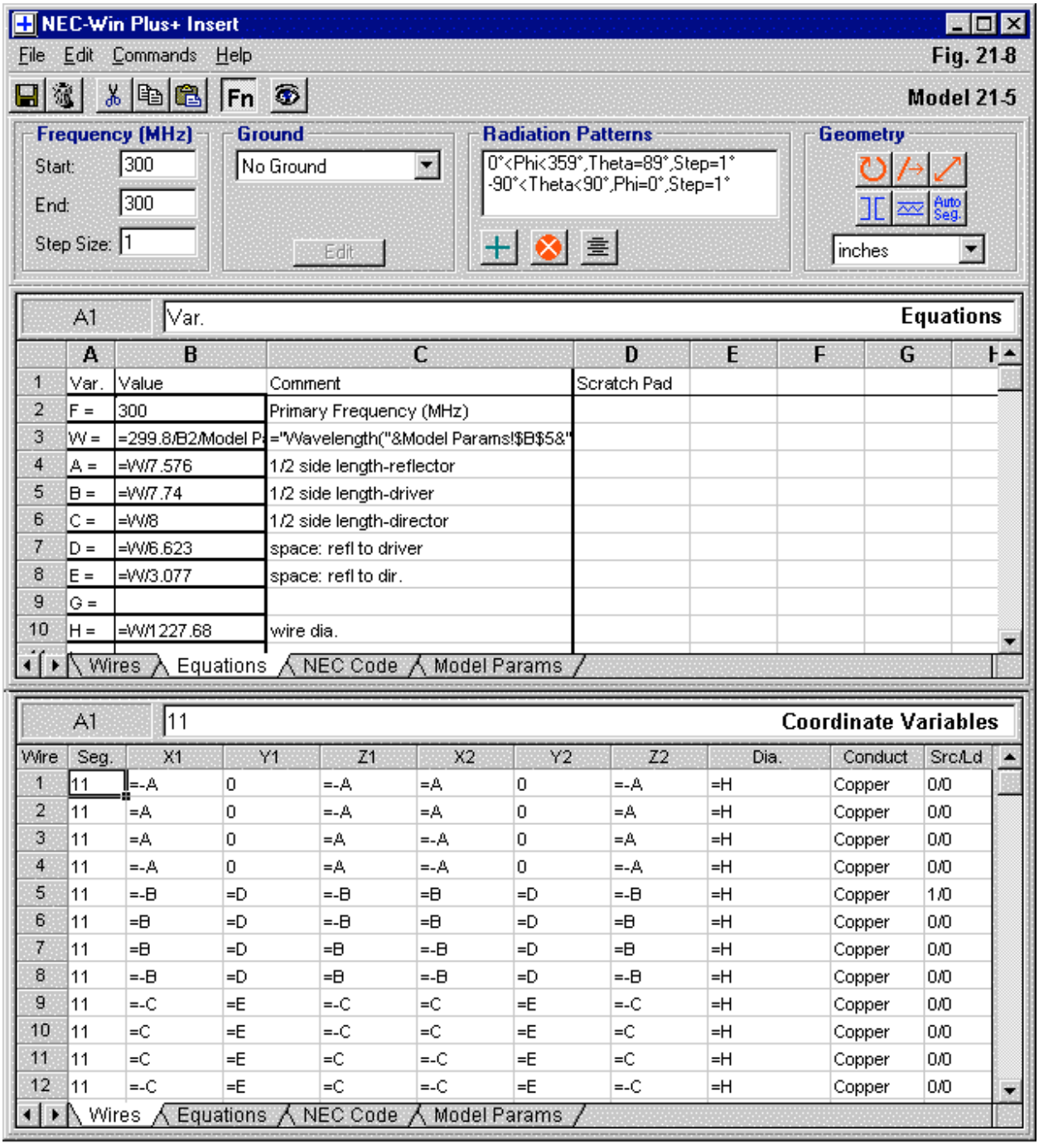

The end result is the use of A, B, and C for dimensions to be placed in the X column, D and E for dimensions to be placed in the Y column, and G for dimensions that go in the Z column. (Since the quad had a vertical dimension to begin with, using A in the Z column is, of course, inevitable.) Wire diameter comes last. No magic attaches to this particular system. It serves to illustrate one of many possible orderly schemes that permit easy reading by both the modeler and others.

The lower portion of **Fig. 21-8** shows how the equation conventions work their way into variable assignments for the individual wires. The Y columns have been assigned the back-to-front dimension. Recording the variables for these distances has the additional benefit of allowing us easily to identify which element is which. The X and Z columns record the variables associated with each of the elements, using the half-lengths of each side of the quad. Note that each element follows identically the same pattern of development around the perimeter of the loop. Consistency of geometric layout is an aid to error detection and to interpreting NEC output data.

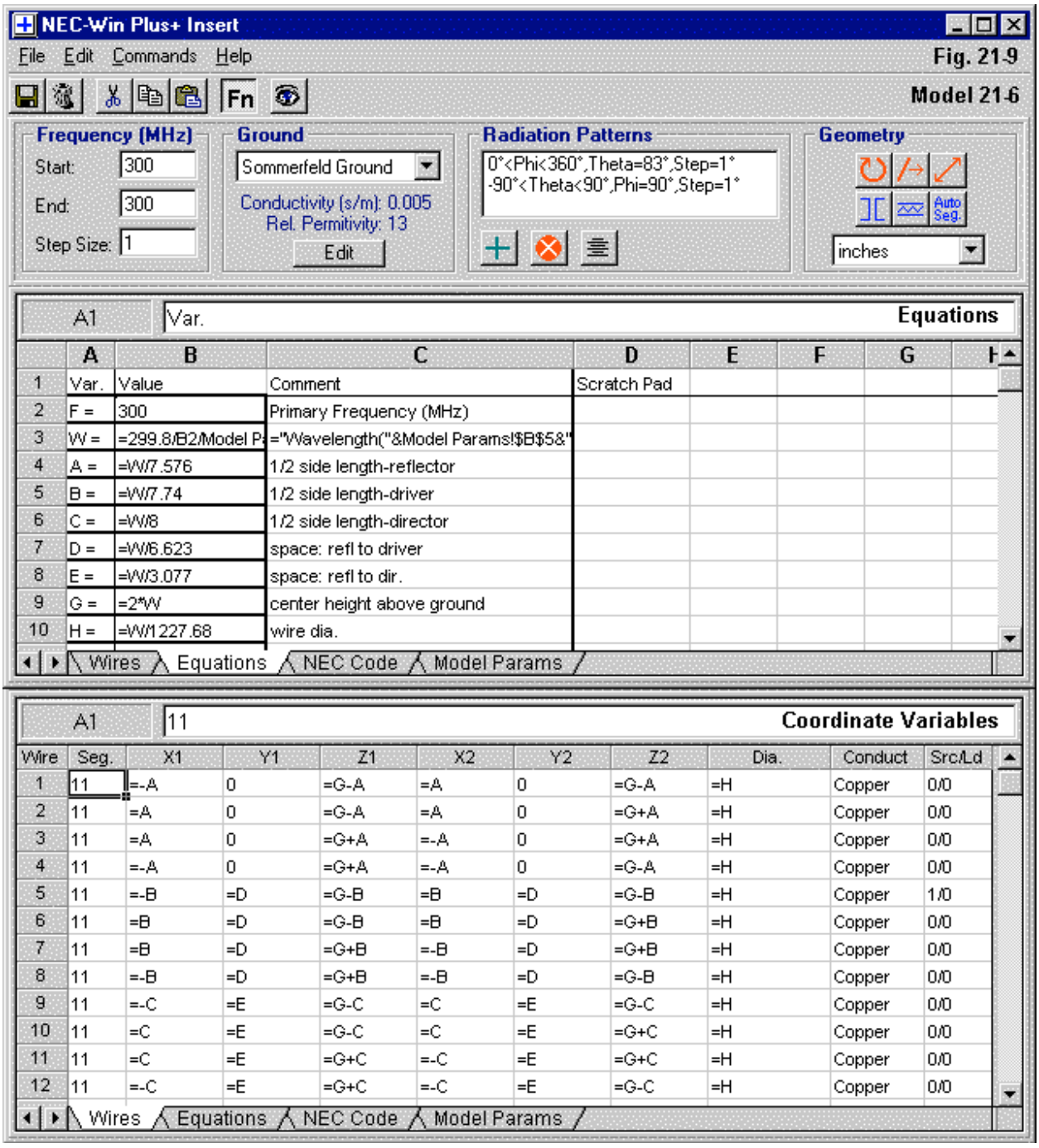

	A	B	C	D	E	F	G
1	Var.	Value	Comment	Scratch Pad			
2	F =	300	Primary Frequency (MHz)				
3	W =	=299.8/B2/Model P	="Wavelength("&Model Params!$B$5&"				
4	A =	=W/7.576	1/2 side length-reflector				
5	B =	=W/7.74	1/2 side length-driver				
6	C =	=W/8	1/2 side length-director				
7	D =	=W/6.623	space: refl to driver				
8	E =	=W/3.077	space: refl to dir.				
9	G =	=2*W	center height above ground				
10	H =	=W/1227.68	wire dia.				

Wire	Seg.	X1	Y1	Z1	X2	Y2	Z2	Dia.	Conduct	Src/Ld
1	11	=-A	0	=G-A	=A	0	=G-A	=H	Copper	0/0
2	11	=A	0	=G-A	=A	0	=G+A	=H	Copper	0/0
3	11	=A	0	=G+A	=-A	0	=G+A	=H	Copper	0/0
4	11	=-A	0	=G+A	=-A	0	=G-A	=H	Copper	0/0
5	11	=-B	=D	=G-B	=B	=D	=G-B	=H	Copper	1/0
6	11	=B	=D	=G-B	=B	=D	=G+B	=H	Copper	0/0
7	11	=B	=D	=G+B	=-B	=D	=G+B	=H	Copper	0/0
8	11	=-B	=D	=G+B	=-B	=D	=G-B	=H	Copper	0/0
9	11	=-C	=E	=G-C	=C	=E	=G-C	=H	Copper	0/0
10	11	=C	=E	=G-C	=C	=E	=G+C	=H	Copper	0/0
11	11	=C	=E	=G+C	=-C	=E	=G+C	=H	Copper	0/0
12	11	=-C	=E	=G+C	=-C	=E	=G-C	=H	Copper	0/0

Examine the final dimensions on the wires page and then return to the NEC form of the model to run it. You should obtain a free-space gain of 9.50 dBi, with a 24.9-dB 180° front-to-back ratio. The source impedance is 28.7 +/- j0.0 Ω.

To place the antenna above a desired ground requires two steps. The first is to define a ground. Model *21-6* shows the selection of the Sommerfeld-Norton ground, using the values for average ground (conductivity = 0.005 S/m; dielectric constant or relative permittivity = 13.0). **Fig. 21-9** shows the equation and variable pages of the revised model. The variable that we earlier reserved is now assigned the value of 2*W, indicating a height of 2λ. However, this entry does not say how we shall implement the height. Let us assume that the 2λ height represents the height of the center of the quad structure. This is a common practice--and a good reason for centering each of the elements of the quad array on the same axis line. Implementing the new height above ground requires some work on the variables. When entering the antenna geometry as a set of variables, we are not limited to single letter assignments. We can enter more complex equations involving those variables. The equations can involve complex functions, but in the present case, we only need simple addition and subtraction involving the variable for the antenna height and the loop dimension variable. Lower wires will be below the value of G and upper wires will be above the value of G. Note that values in the X and Y columns are unaffected: everything we need to modify in order to place the antenna above ground occurs in the Z axis column.

Examine the final dimensions on the wires page. The center of the quad beam is about 6.5' above ground. (Of course, we might have easily change units to meters or millimeters on the equation page.) Because we placed the antenna over ground, the RP0 phi pattern request uses an elevation angle of 7° (theta = 83°). Run the model using the .NEC input file form and obtain the usual data. The gain is 15.10 dBi, with a 180° front-to-back ratio of 24.7 dB. The source impedance is 28.6 - j0.0°.

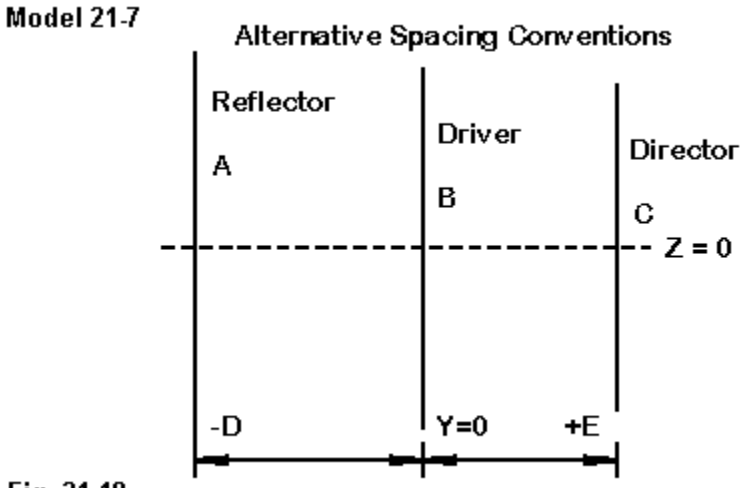

Fig. 21-10

Let's take the original free-space version of the antenna (model 21-5) and look at it in another way. An alternative convention to the one we have used is to set the driver at 0 along the selected front-to-back axis. Then, the reflector will have a negative value and the director (or directors) will have a positive value. A third scheme occasionally used is to set the array in equal distances

forward and behind the zero point. However, this system can only be put in place after the final front-to-back dimension is known. At the same time, we shall let the driver be the central element in another sense. We shall define the length dimensions for the reflector and the director in terms of the driver length. As a final variation, we shall use multipliers rather than divisors to create the equations for the coordinates. **Fig. 21-11** shows the final form of the equation page for model *21-7*.

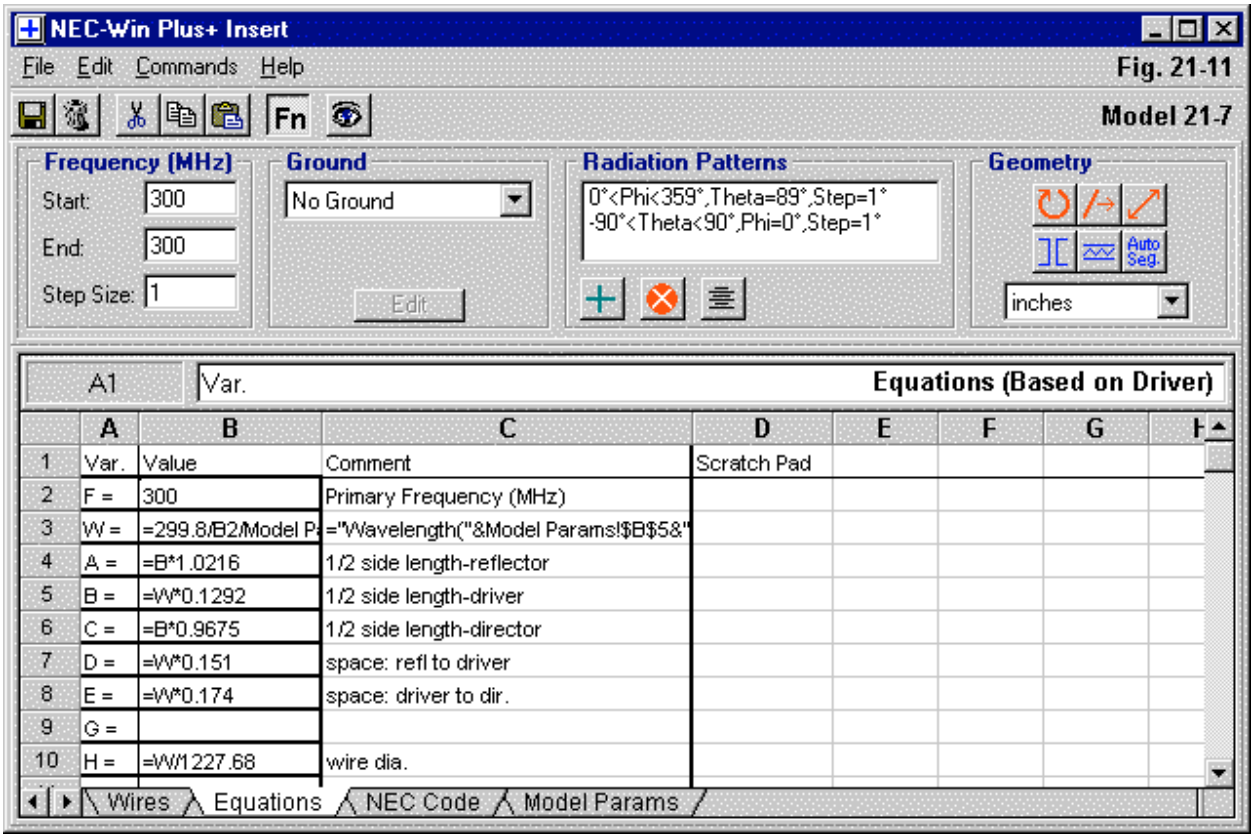

	A	B	C	D
1	Var.	Value	Comment	Scratch Pad
2	F =	300	Primary Frequency (MHz)	
3	W =	=299.8/B2/Model P	="Wavelength("&Model Params!$B$5&	
4	A =	=B*1.0216	1/2 side length-reflector	
5	B =	=W*0.1292	1/2 side length-driver	
6	C =	=B*0.9675	1/2 side length-director	
7	D =	=W*0.151	space: refl to driver	
8	E =	=W*0.174	space: driver to dir.	
9	G =			
10	H =	=W/1227.68	wire dia.	

The changes that we made to the equation page will require some minor alterations to the variable entries on the wires page. Examine that page and then run the model. The free-space gain remains 9.50 dBi, with a 24.8-dB 180° front-to-back ratio. The source impedance is 28.6 +/- j0.0 Ω.

We have not explored all of the permutations and combinations of ways in which we can construct models using variables and equations. The procedure with which you become most comfortable may not coincide with either of the variants that we have explored. However, developing a consistent procedure--except where a specific task may dictate otherwise--will go a long way toward naturalizing the process of modeling in this way. The larger the model, the more crucial it is to adhere to conventions that yield the quickest error detection, the clearest readout of your work, and the greatest ease in modifying the model en route to the perfect antenna.

The equations that we have so far used are simple. There are no rules against using equations that flex the full abilities of the spreadsheet system. As well, spreadsheets have some interesting

attributes in terms of moving and copying blocks of information. We shall next sample a few of those features.

Equations and Blocks

In this part of our work, we shall look at the rudiments of other mathematical techniques used to define variables--leaning especially on a little trigonometry as applied to spreadsheet formulations. In addition, we shall also explore ways to cut long repetitive model-creation tasks down to simple work. Finally, we shall look at when and how to freeze a design that we initially create for frequency-scaling purposes.

Many antenna designs are amenable to trig-treatment. Theoretically, most antenna designs can be handled with trig, since we can transform almost any geometry into a collection of angles and triangles. More realistically, loop antennas--especially triangles or "deltas"--are most apt for trig-treatment. So let's pick one and see what we might do with it.

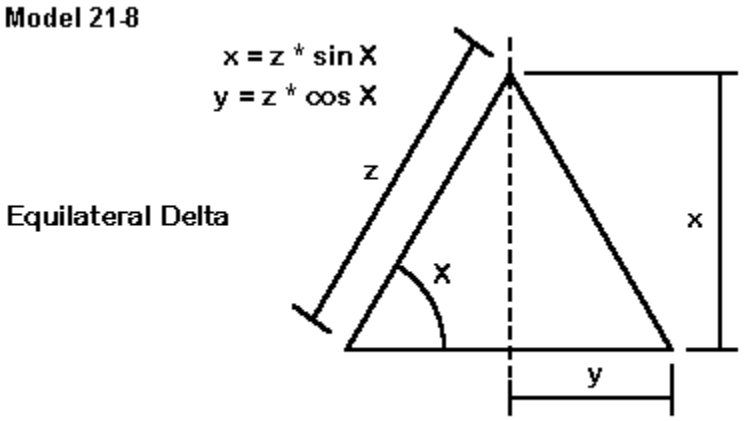

Fig. 21-12

Fig. 21-12 shows a typical equilateral delta, much used on the lower HF bands. The antenna consists of 3 sides of equal length (z). Since the angles of every triangle add up to 180°, each corner angle is 60 degrees. Now we can appeal to basic trig functions to determine the values of +/-y and x so that we can model the antenna within 2 of the 3 Cartesian dimensions that form the basis of model construction in NEC. Note that we have cut the equilateral triangle in half along a vertical line to get two equal right triangles. This conversion makes the calculation of dimensions much easier.

Since a delta loop has a circumference of about 1λ, we know that each side is about 1/3λ long. We also know that the equations for half the base and the overall height shown in **Fig. 21-12** are simple transformations of the basic trig relationships. Now, we can let the spreadsheet equation system of the program help us create a perfectly general delta loop.

Fig. 21-13 shows the equation page for an equilateral delta loop. Open model *21-8*. Nothing seems to correlate with what we have just said. The length of the hypotenuse (A) is not shown as

W/3, but as W/2.84. The loop is larger than a wavelength in circumference, as it was with the quad loops we looked at earlier. Actually, the denominator of the equation for A was derived by resonating the final model--which used #12 AWG copper wire in free space--to a source impedance of 116.8 - j0.4 Ohms at 7 MHz. (For this exercise, we can by-pass absolute generality of design with the wire size specified in terms of a wavelength. However, that option is always open to us.)

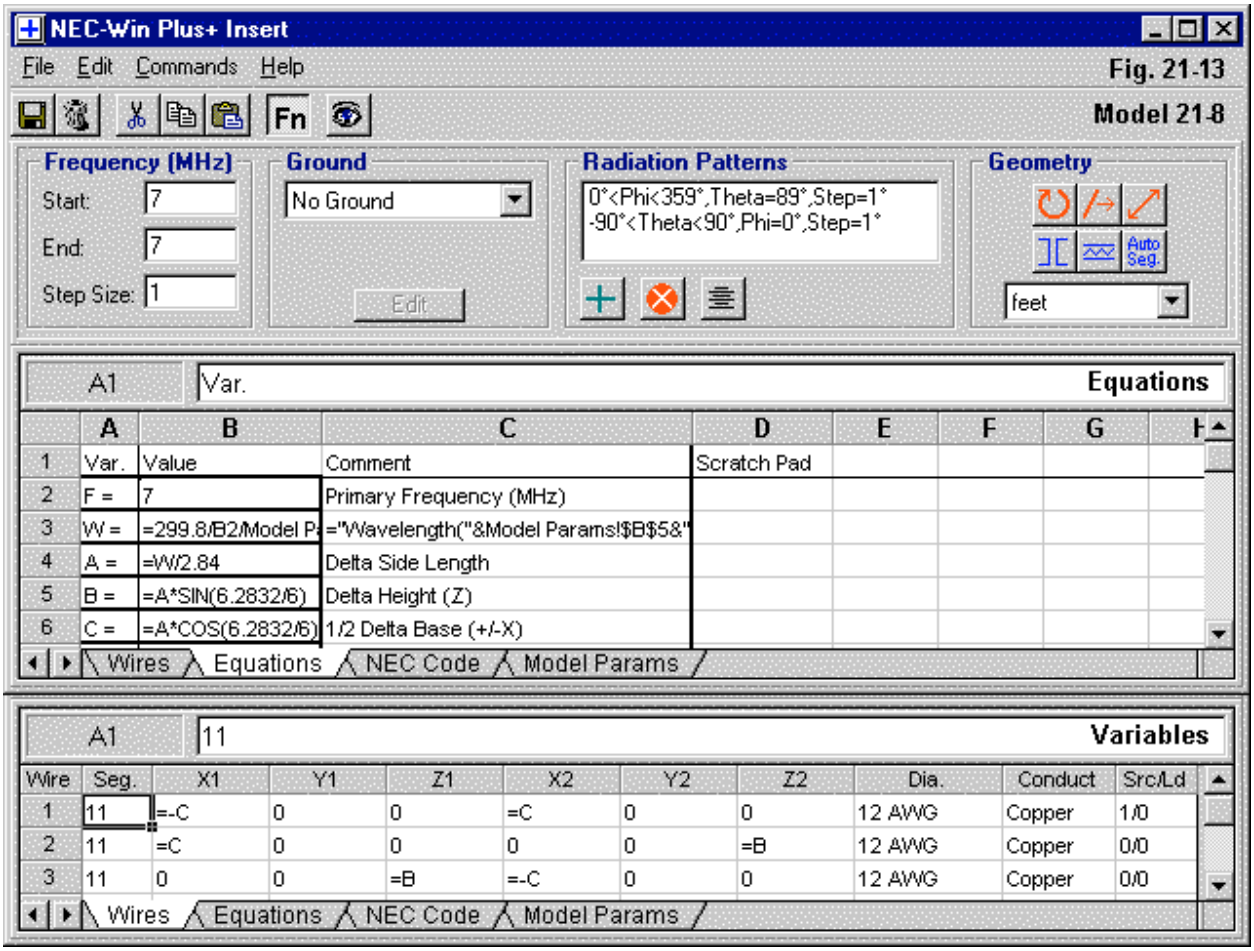

The next deviations from our initial discussion are the equations for B and C, the height and half-base length equations. These variations result from the fact that spreadsheet math is a derivative of Basic, a programming language that does all its angles in radians rather than degrees. To use radians effectively requires that we remember just one fact: a circle has 2*π radians or 360°. Hence, to convert an angle from degrees to radians, we simply divide 2*π by the result of 360/angle, where "angle" is the angle with which we are concerned. Since our equilateral triangle uses an angle of 60°, 360/60 = 6. π is about 3.1416, so 2*π is about 6.2832. Hence, our angle in radians is 6.2832/6. We shall let the spreadsheet finish the calculation, but we know the angle is a little over 1 radian. If you forget to make the conversion into radians, your results will not make any sense at all. As well, you may do some of the conversion calculations on the scratch pad facility available on the equation page.

We can construct our equilateral delta by using the variables we have just defined, as shown in the lower part of **Fig. 21-13**. The baseline of the delta lies along the X-axis (at Z = 0) from -C to +C, with the source centered. The two angled wires go to or from these end points to a common height, B. This is the easiest part of the process.

Sometimes, trig can simplify our equations more than we might initially expect. Consider the right-angle delta, an alternative version of the delta we just explored. We shall retain the same wire size and material, and we shall keep the antenna in free space. Our interest will be in the angles, shown in **Fig. 21-14**.

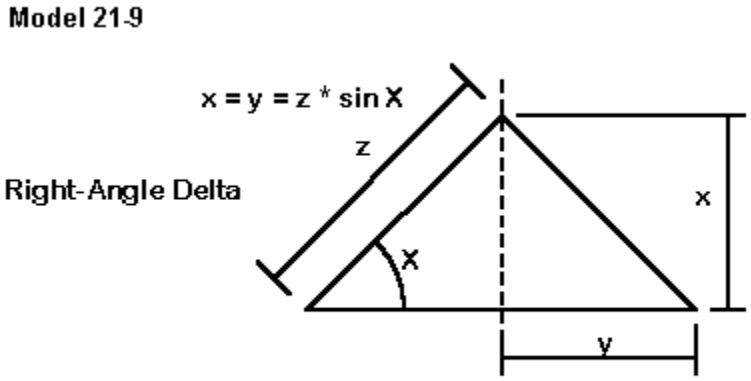

Fig. 21-14

First, let's think about the perimeter of the right-angle delta. If we start with a wavelength, it is divided into three legs, but only 2 of them are equal: z. However, we know that a right triangle has two 45° angles and a 90° angle. The length y is the cosine of angle X times Z. Since the sin of 45 degrees is 0.707, y is .707*z, and the total length of the base is 1.414*z. (We can also use the old right-angle theorem from plane geometry: The square root of the sum of the squares of the two sides of the entire right triangle is the length of the entire base, which is the hypotenuse. The base is still 1.414*z.) So in terms of z, the total perimeter is 3.414*z. In terms of a wavelength, the length of z will be W/3.414 as a starting value.

One of the conveniences of a right triangle is that the sine and the cosine of 45° are both 0.707. Hence, we can define our right-angle delta with only two equations, one to define z in terms of a wavelength and one to define both the lengths x and y. Let's now turn to the equation page of our spreadsheet. Open model *21-9*.

In the top portion of **Fig. 21-15**, we find the final equations for the right-angle delta. Values for the X- and Z-axes appear in the equation for variable B. This follows the same pattern we used earlier in converting from degrees to radians. We recognize the value of 2*π. The denominator of 8 derives from dividing 360° by 45°. The final value for A comes from adjusting our initial denominator of 3.414 until the antenna achieved resonance with a source impedance of 196 + j0.6 Ohms. Once more, for a loop, the final size to give 1-λ resonance will be physically longer than 1λ. The simplification of our set-up also shows up in the variables on the wires page, shown in the lower portion of **Fig. 21-15**.

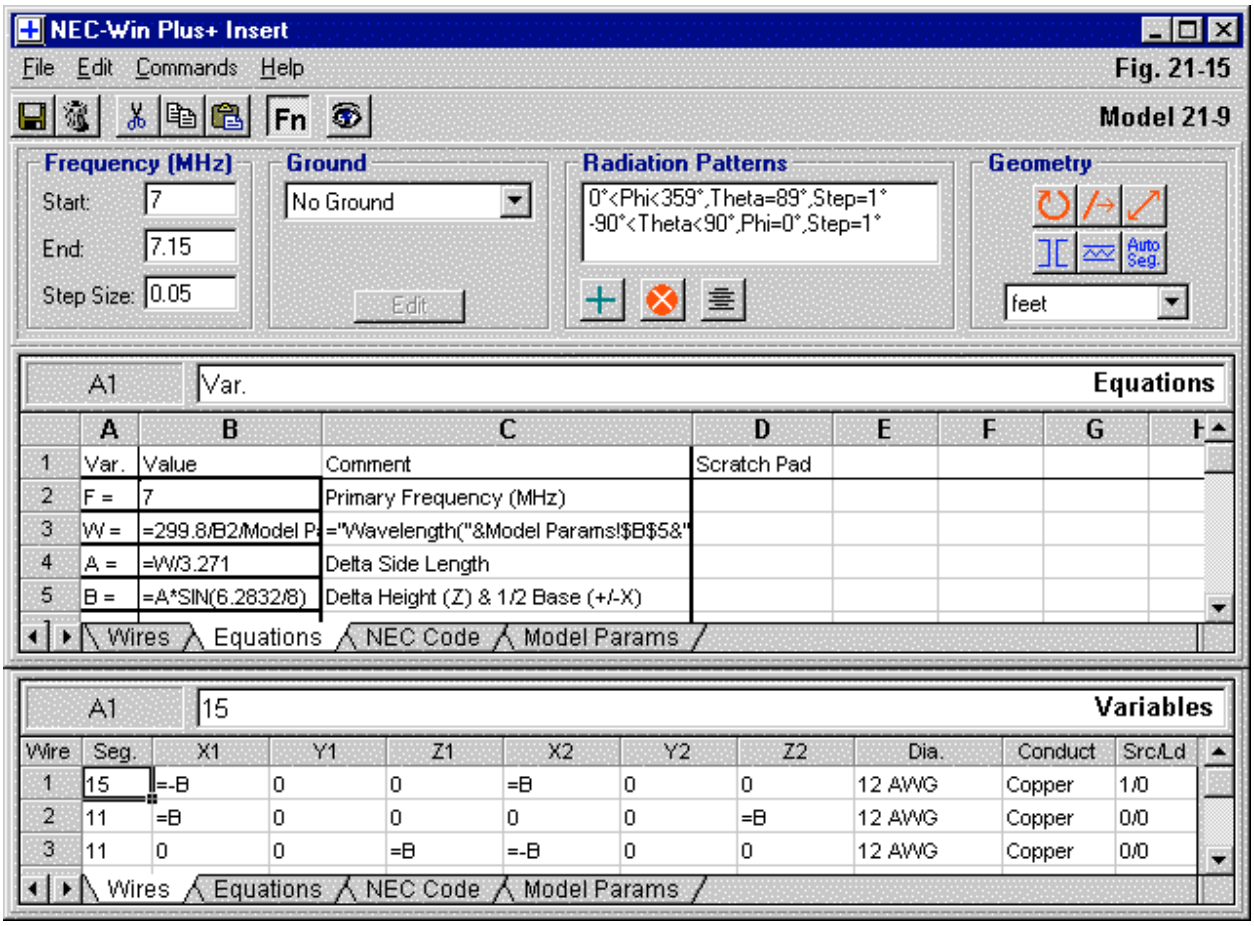

For a right triangle, we only need to set the baseline ends at -B and +B, and the height will be +B. Both deltas use a baseline set at zero on the Z-axis. Should we wish to center the model vertically, using +/-Z values that are the same, we shall have to wait until we know the final physical dimensions, or we shall have to create a further equation for this purpose to the short list on the equations page. For example, we might have defined C as 1/2 the value of B and then specified Z coordinate of the baseline as -C and the peak as +C. Once we start down the road of modeling by equation, we can get as sophisticated as we desire. The key questions are these: Do we need the added fanciness? Will the resulting model be easy to read in the future? For this example, a baseline of zero on the Z-axis will do just fine. If we develop a special need later on, we can adjust the equations. For example, a particular project might set a maximum height. In that case, we can revise the equations to work downward from that height.

We have lingered over the basics of using trig functions in a spreadsheet model-by-equations system to prepare ourselves for larger tasks. The larger task that we shall use as an exercise is the creation of a helical dipole for 10 meters. What we wish to achieve is a helical dipole that is under 10' from end to end for a frequency of 28.5 MHz, using #12 wire. Since we might run into difficulties with the limits of NEC if we wind the helix too tightly, we shall specify a radius of 4".

NEC must create a helix from straight wires. In fact, NEC has the GH command that will

automate the creation of a helix, but that command is not available within the spreadsheet. So we shall have to create the helix manually. The left portion of **Fig. 21-16** shows us an outline of the helical dipole. Almost any representation of a helix made from straight wires will give some visual distortion of what is actually happening to the wire, and **Fig. 21-16** is no exception. However, we can see the straight wire sections of each turn of the helix. Each wire forms part of the circumference and also proceeds part way down the line from one end to the other. Since each wire is the same length, the increment of movement along the total length will also be the same for each successive wire.

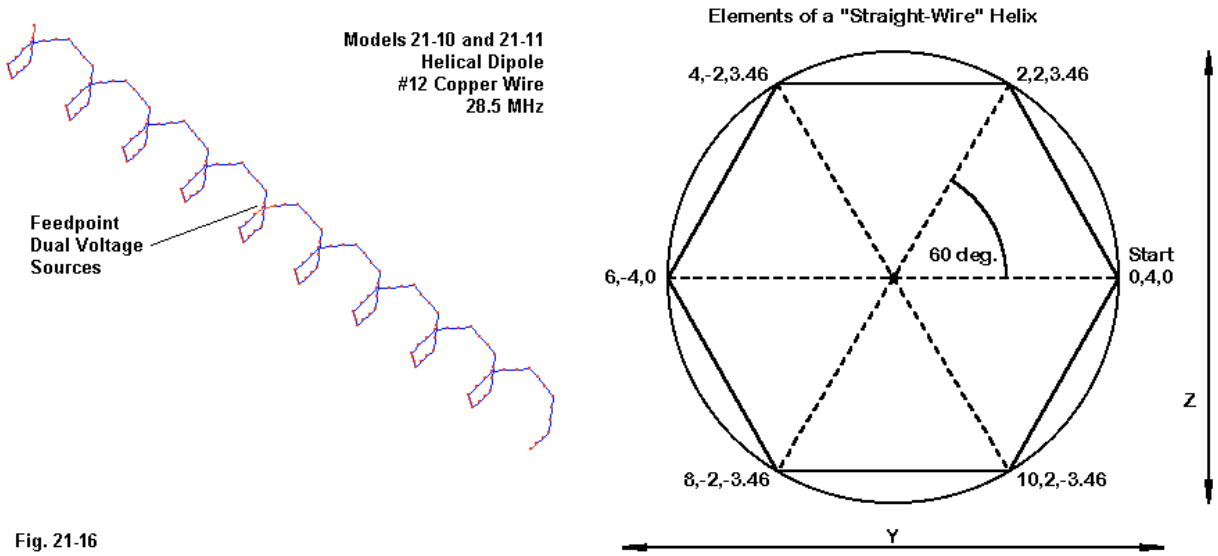

Fig. 21-16

For the example, the total number of wires turned out to be an even number. Hence, we may specify a split feed, using the last segment of one wire (28) and the first segment of the next wire (29). We shall look at the consequences of placing the source in this manner later on. First, we need to figure out how to make up the turns of the helix.

The right side of **Fig. 21-16** shows the cross section of one complete turn of the helix. Since the length of the entire assembly will lie along the X-axis, the turns will be defined for the Y- and Z-axes. The circle shows the true helical shape. For this exercise, we shall use a hexagon as the substitute. An octagon would have been more true to the circle, but the hexagon is more interesting for our purposes. Obviously, when translating the final model into a physical antenna, we would likely discover that a true circular radius a bit under 4" will best capture the model. We may subdivide a hexagon into a collection of equilateral triangles. If we let the radius lie along the Y axis, the first set of X, Y, Z coordinates will be 0, 4, 0, indicating no progress along the length of the antenna, and a peak of +4" on the Y axis.

The angle between successive point of the hexagon is 60°. Therefore, we can use the same subdivisions of each triangle that we used with the equilateral delta. The value of Y for the second point will be half the base, or 2". The height of the triangle will be the sine of 60° (0.866) times the radius, which becomes the hypotenuse of the triangle. The result is 3.46 for the Z-axis. The value of X increases by 2", which is half the radius. Continuing counterclockwise, the values for X increase regularly. However, the values for Y and Z are simple repetitions of the values

already derived, with some sign changes depending on which side of the axis the value falls. Consequently, we can define our helical dipole with very few equations, as shown in the upper portion of **Fig. 21-17**.

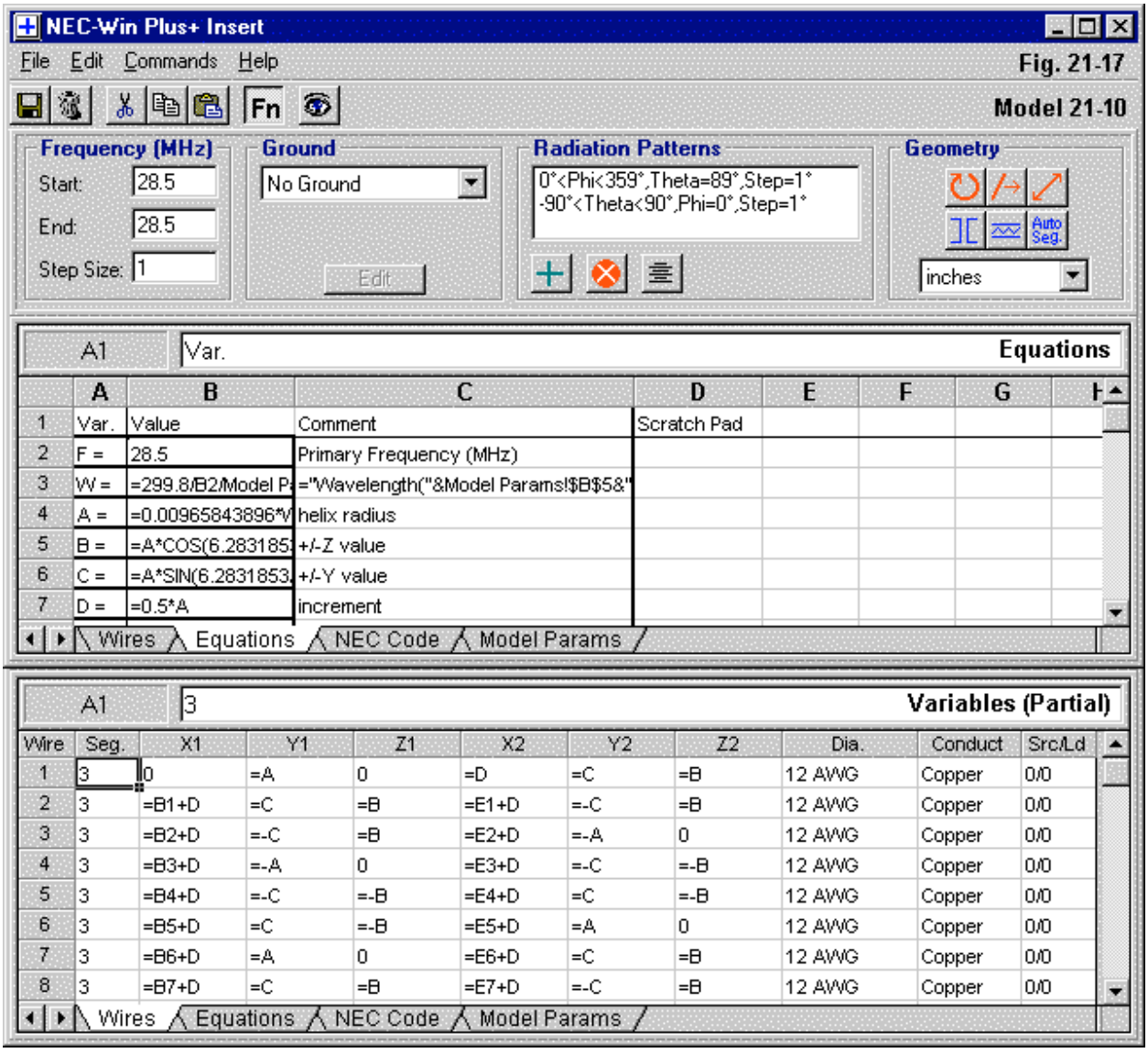

The values used in the equations are fussy beyond belief--simply because I wished the subsequent wires page to have simple numbers. The radius is defined in terms of a wavelength at 28.5 MHz. The extended decimal value is simply what was necessary to get a radius of 4.0000000". Likewise, the value of 2*π is carried out to many significant figures so that the equation shown on the working line (B5) would yield exactly 2.000000". You may truncate these values to practical sizes--if you are willing to live with longer decimals on the wires page. Open model *21-10* and examine the coordinates that result from excessive fussiness on the equation page.

The variables we have just defined complete one turn of the helix. The next question is how we

create the total structure of the entire dipole. The lower portion of **Fig. 21-17** provides a clue to the answer. Note that the Y and Z columns repeat themselves periodically, in fact, every 6 lines. To create the first 6 lines in each column, we manually enter the variables. Then we copy that block of 6 lines in the column and paste them to the next six lines. We can continue to paste until we reach line 54, the last line divisible by 6. The final step is to copy only the first two lines and past them to lines 55 and 56. Of equal ease is the specification of the wire diameter and material conductivity, since each can be selected in a single block operation encompassing all 56 lines of the model.

We have covered every part of the model except the progression of the helix along the X-axis. Here we use another spreadsheet facility. We enter the values of X on line 1. Then we set an equation on line 2 for the X-entries that, in each case, references the first line box and the increment defined by variable D. The values for X1 occur in column B, so the first formula become =B1+D. Likewise, for X2, in the E column, we get =E1+D. The spread sheet knows to read "D" as a variable from the equations page and to read "B1" and "E1" as the values within the cells with those names.

Spreadsheets have a special function that works in the following way. Let's place the heavily outlined box on line 2 and the column with the X1 values, which is B. We can now type CTL-C for "copy." The value goes to what Windows calls the "clipboard." Now, with the mouse, block the entire column from B3 (the next line) down to B56, the end of the model. Next, type CTL-V, which pastes the value on the clipboard to the cells in the block. However, remember that this is a spreadsheet, and the special function is at work. Each new cell value created will have the same form as the original formula: it will use the preceding B line and add D to it for the cell at hand. Hence, the progression of values increases regularly from line 1 to line 56. We do the same for the X2 column, which is column E on the spreadsheet.

Had we wished to keep the precise value within cell B2, we would have had to signal that with a special sign. On this spreadsheet, placing $s (dollar signs) before B and before 2 ($B$2) would have done the job. Other spreadsheets may use other symbols. In the end, the laborious task of manually entering even the simple variables for the model is reduced to about a 5-minute job. As well, we have reduced the potential for entry errors of all sorts. If an error appears, we know to look back to the equation page or to the equations we entered on the variables version of the wires page. Hence, error correction also becomes a short-order task.

If we run model 21-10 at 28.5 MHz, we will obtain two values of impedance, each of which is about 12.68 + j2.69 Ω. The impedance of the antenna for a single feed is simply the sum of the resistances and reactances: 25.5 + j5.4 Ω, which is close to resonance. Although incidental to this exercise, the free-space gain of the helical dipole is 1.74 dBi, about 0.4 dB below a full-length linear dipole for the same frequency. Helical dipoles are certainly usable, but even as open a helix as this one shows losses in dipole use. Had we tightened the increment or shrunk the diameter, we would have seen even lower gain. Nonetheless, the helical dipole has allowed us to create an extensive structure using the equations and variables provisions of a spreadsheet entries page for our model geometry. Other types of equations are certainly possible for other geometries, but the trig relationships we used allowed us to draw out some of the features of spreadsheet use. As well, the long repetitive structure of the helix gave us the occasion to use some of the timesaving features that spreadsheets offer.

Before we close the book on modeling by equations and variables, we have one more question to pose. When is maximum generality too much generality? Suppose we wished to do a frequency sweep for the range from 28 to 29 MHz of the helical dipole we just designed for 28.5 MHz. Models designed by equations and variables are linked to the "Start" frequency (in the upper left corner of any of the screen captures shown). Remember that we defined the variable A in terms of a wavelength and then defined the other variables in terms of the value of A. If we change the start frequency from the design frequency of 28.5 MHz down to 28 MHz, the dimensions of the antenna will change.

To preserve the dimensions of the design we just created, we must "freeze" them. This task involves only one change in the equation page, and the change appears in **Fig. 21-18**.

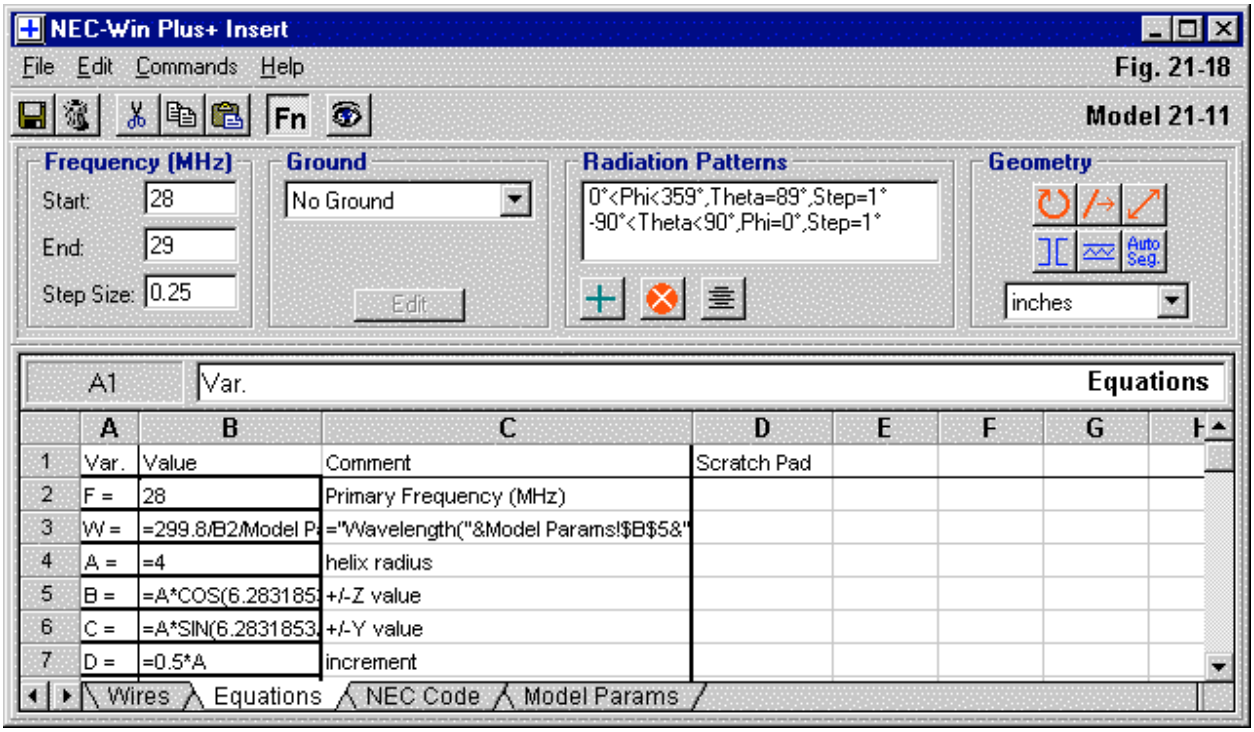

Note that we have changed the value of A from a wavelength-dependent value to a constant. The value of 4 (inches) derives from the dimensions on the wires page that proved successful when we ran the model. Now, all of the other variables depend on the set value of A and are independent of the frequency. At this point, we can set the frequency sweep with a start frequency of 28 MHz, an end frequency of 29 MHz, and any desired interval for the sweep check frequencies.

The upshot of this final move is to note that there are limitations to designing models by equations and variables for maximum generality. For every task, there is an appropriate level of generality somewhere between the maximum and, at the other extreme, specifying each dimension as simply a number on the wires page. It is not possible to specify in advance of knowing the task parameters what the proper level of generality should be. However, with some practice in both "normal" modeling with numbers and modeling with equations and variables, you will gain a sense of the level of generality that works best in each circumstance.

Scratch Pads and Regressions

In our final set of exercises, we shall examine the utility of having a "scratch pad" at our disposal within the equation pages. A scratch pad is simply an area on the spreadsheet in which we may store data and equations that are necessary in the process of deriving the values for the variables that will appear on the wire coordinate page. However, the data and equations in question do not necessarily directly define these variables. In simple models, we may not need the scratch pad, but as models become more complex--either in structure or in the mathematics used to define the structure--reserving variables for use on the wires page and placing supplementary data and calculations on the scratch pad can be very useful.

The other feature of the final 4 models in this chapter is that all of them employ regression analysis to develop models that automatically calculate the dimensions of a given antenna from just 3 user entries on the equation page. The first entry is your selection of the desired unit of measure. The second is the design frequency, and it is independent of the start and stop frequencies that enter the FR command when we update the NEC input file. The final entry is the wire diameter in the preferred unit of measure. In general, the automated designs will yield dimensions that give maximum performance relative to the basic design within 0.5% of optimal for a frequency span of 3 to 300 MHz (and beyond) for wire sizes ranging from 3E-5λ up to about 1E-2λ. At the top of the wire diameter range, the wire radius becomes large relative to the length of the segments in the models.

Regression analysis is a mathematical technique for developing equations that connect the dots of a set of observations. The result is a smooth curve that essentially allows calculated interpolations between the observation points. More than one regression technique exists. The technique used in the sample models employs a version of the following equation:

$$N = K1\ D^4 + K2\ D^3 + K3\ D^2 + K4\ D + K5$$

N is the calculated value for the desired parameters, such as an element length or spacing. K1 through K5 are constants produced by regression analysis. D^4 through D are functions, in this case, of the log of the wire diameter when translated first into a fraction of a wavelength. The sample is for a 4^{th}-order equation, although many acceptable curves result from lower-order equations. We shall need a version of the equation and the set of associated constants for each major dimension of any subject antenna.

The subject antennas are all based on the square quad loop. For any loop within a simple or complex quad antenna, we shall need a side length (or a half-side length). If the antenna has more than one element, we shall need equations for the spacing between elements. A 3-element parasitic quad beam would therefore need 5 equations for a completely automated design.

The sample models that we shall observe provide automated design for quads from 1 to 3 elements. The general outlines of the quads appear in **Fig. 21-19**. The 1-element quad loop is, of course, the simplest case, since the only parameter of optimizing it is to achieve near-resonance. The 2-element quad beam uses a driver and a reflector set for the best compromise of operating bandwidth, front-to-back ratio, and gain, in that order. Like all drivers,

the element with the source segment is near resonance.

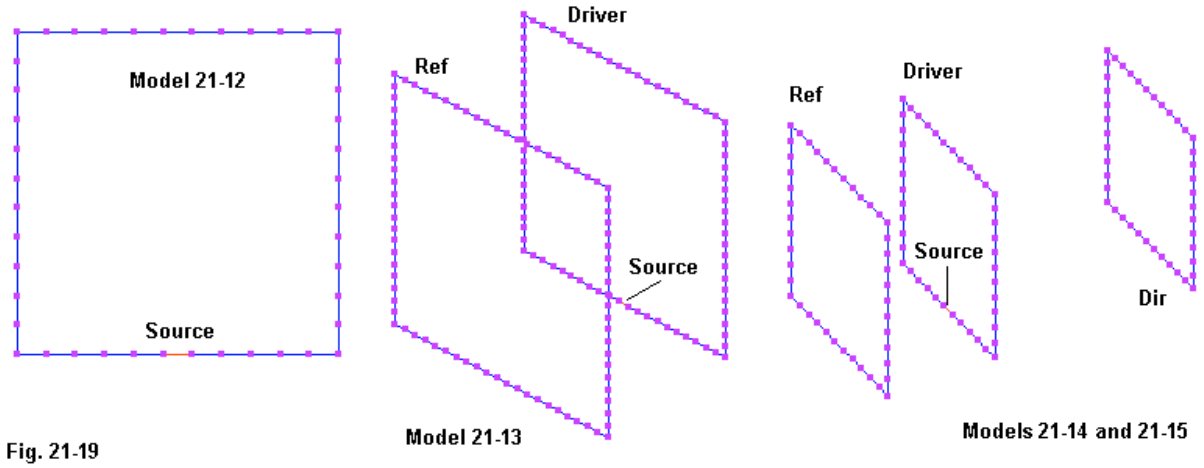

Fig. 21-19

There are two versions of the 3-element quad beam. One places a higher weight on operating bandwidth. For quad beams, the gain curve and especially the front-to-back curve tend to be steeper than the SWR curve. Hence, the operating parameters take precedence over a wide SWR bandwidth. The second version allows a narrower bandwidth in order to derive maximum gain from the array with a front-to-back ratio at the design frequency that roughly matches the ratio for the wide-band version.

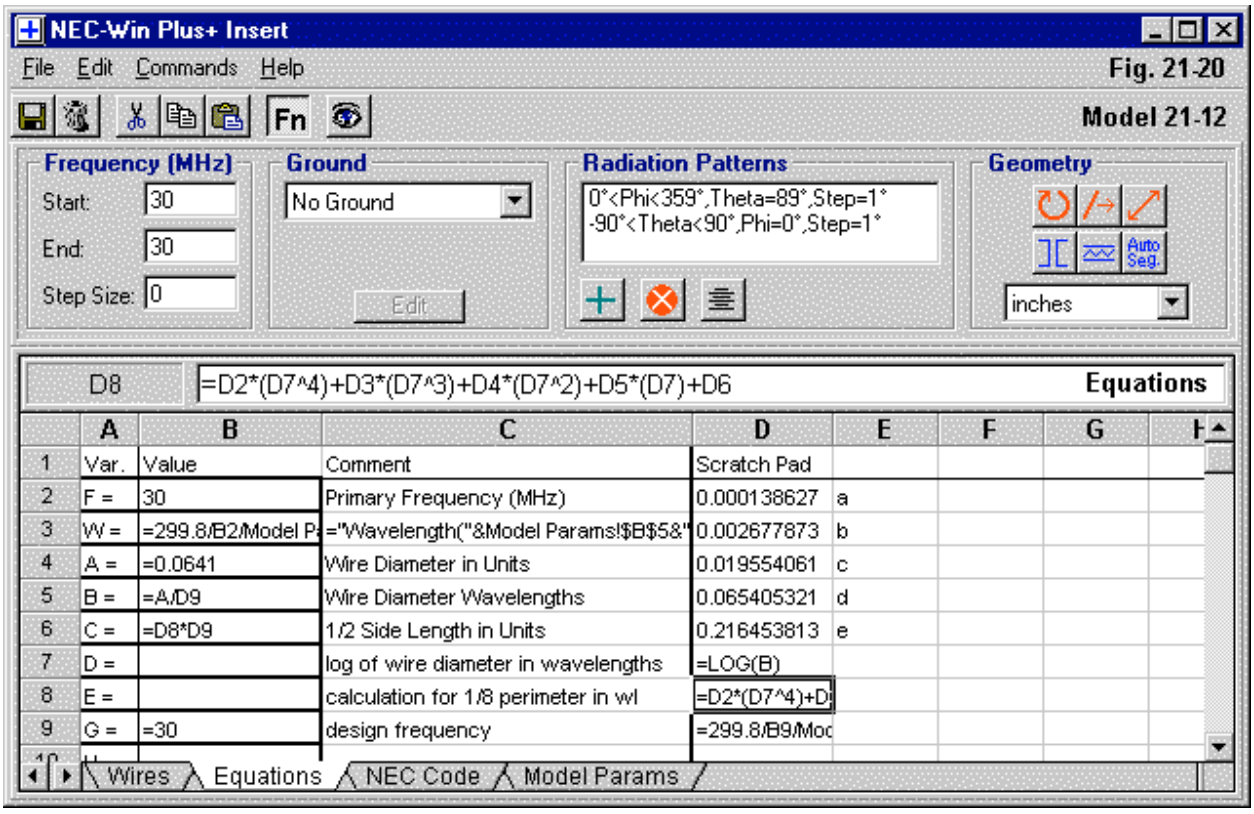

Open model *21-12*. There is a procedural restriction for accessing the Plus insert if it contains equations and variables. Begin with a blank main screen. If necessary, select a new model from the File options to remove the model on the screen. Then open the Plus insert and retrieve the selected model in .NPI format. After altering the Plus insert entries in any desired way, you may save the changes or not, as you choose. You may also update the NEC input screen, creating a NEC input file that you may also save.

However, do not return to the insert from the NEC screen. If you do, you will erase all of the equations, since the NEC file does not contain them. Instead, when you are finished with the NEC version of the model, request a new file and receive a blank screen. Then start the Plus insert and retrieve the desired .NPI file from its directory. For safe storage, you may wish to keep .NEC files and .NPI files in separate directories.

Fig. 21-20 shows the equation screen for the single quad loop. The figure highlights the regression equation used to calculate a half side length. Note that the terms of the regression equation appear in the scratch pad area of the spreadsheet. The only restriction in using these entries is the need to refer to them by their cell names, that is, by reference to the column and line. Since the design frequency is independent of the start and stop frequencies, a number of the variables in column B call for the value of cell D9.

You may revise the model in any way that you desire by changing the frequency (variable G) or the wire diameter (variable A). The wire diameter is in the units of measure selected at the top right of the screen. Then update the NEC screen and run the model after checking the calculated dimensions. The sample files include .NEC models for 3, 30, and 300 MHz (models *21-12a.nec*, *21-12b.nec*, and *21-12c.nec*). Run each model and catalog the results.

Model	Frequency MHz	Gain dBi	Impedance R +/- jX Ω
21-12a	3	3.26	123.3 + j1.2
21-12b	30	3.30	125.2 - j1.0
21-12c	300	3.39	130.5 + j2.9

Since we did not change the wire size, it became thicker relative to a wavelength as the frequency increased. Hence, the gain and impedance rose with frequency.

Open model *21-13* from within the Plus insert. Examine the equation page, shown in **Fig. 21-21**, and the resulting dimensions of the 2-element quad. Optimal front-to-back ratio and operating bandwidth occur with the elements spaced about 0.17λ, with variations according to the wire diameter used for the array. The design model requires 3 regression equations to fully determine the array dimensions for any frequency and wire size within the model's scope.

The figure highlights the equation used to provide a design frequency that is independent of the start and stop frequencies. Note that although the program uses a light-speed constant of 299.8, the design frequency uses the more exact (but not fully exact) reference value of 299.7925. The "parameters" portion of the equation refers to internal functions calculated as a matter of course by the Plus insert program module to relate the unit of measure to the calculation.

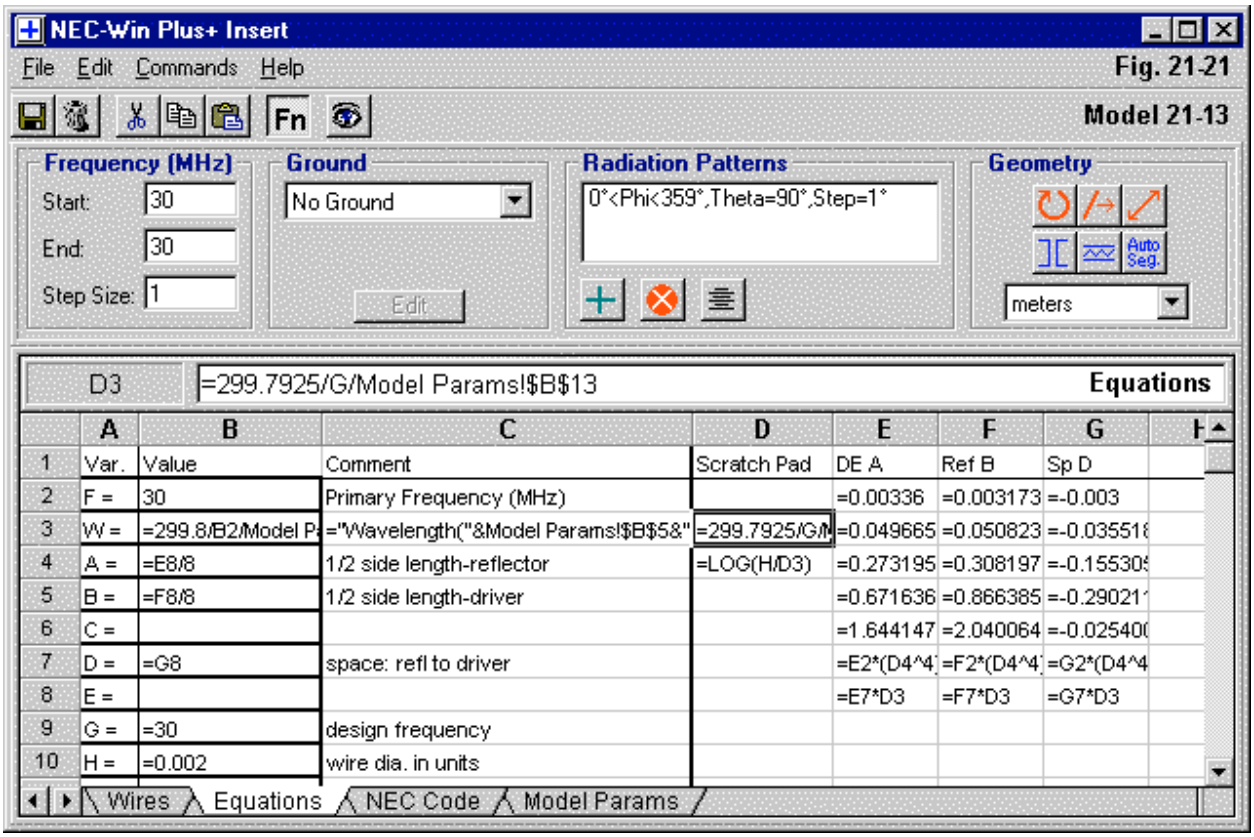

	A	B	C	D	E	F	G
1	Var.	Value	Comment	Scratch Pad	DE A	Ref B	Sp D
2	F =	30	Primary Frequency (MHz)		=0.00336	=0.003173	=-0.003
3	W =	=299.8/B2/Model P	="Wavelength("&Model Params!$B$5&"	=299.7925/G/M	=0.049665	=0.050823	=-0.035518
4	A =	=E8/8	1/2 side length-reflector	=LOG(H/D3)	=0.273195	=0.308197	=-0.155305
5	B =	=F8/8	1/2 side length-driver		=0.671636	=0.866385	=-0.29021
6	C =				=1.644147	=2.040064	=-0.025400
7	D =	=G8	space: refl to driver		=E2*(D4^4)	=F2*(D4^4)	=G2*(D4^4
8	E =				=E7*D3	=F7*D3	=G7*D3
9	G =	=30	design frequency				
10	H =	=0.002	wire dia. in units				

Open and run model *21-13.nec* to obtain representative data on the model at 30 MHz using 2-mm wire. The gain is 7.14 dBi, with a 180° front-to-back ratio of nearly 43 dB. The source impedance is 135.7 + j1.2 Ω. You may wish to change the perfect or lossless wire of the insert model to copper or aluminum to see the effect of the load on the performance and source impedance.

Open model *21-14* within the Plus insert. The wide-band version of the 3-element quad design requires 5 equations to define the dimensions, as shown in **Fig. 21-22**. The figure highlights the first of the regression equations. However, note that the result does not immediately become a value for a variable used in the coordinates. Instead, that value is multiplied by cell D3, which yields the wavelength of the design frequency.

Finally, open model *21-15* within the Plus insert. The 3-element quad uses different equations to define the dimensions of a high-gain version. This version has narrower bandwidth characteristics, and you may wish ultimately to run frequency sweeps of both models 21-14 and 21-15 to compare gain, front-to-back, and SWR curves. **Fig. 21-23** shows the equation page for the new model and reveals difference values for the terms of the regression equations. You may directly compare the values for each cell within the 5 equation columns. Although the frequency and wire size entries have no affect on the regression equations, both models use 30 MHz and 0.0808" (AWG #12) wire.

Find the corresponding .NEC files and run each to compare the performance data in the usual categories.

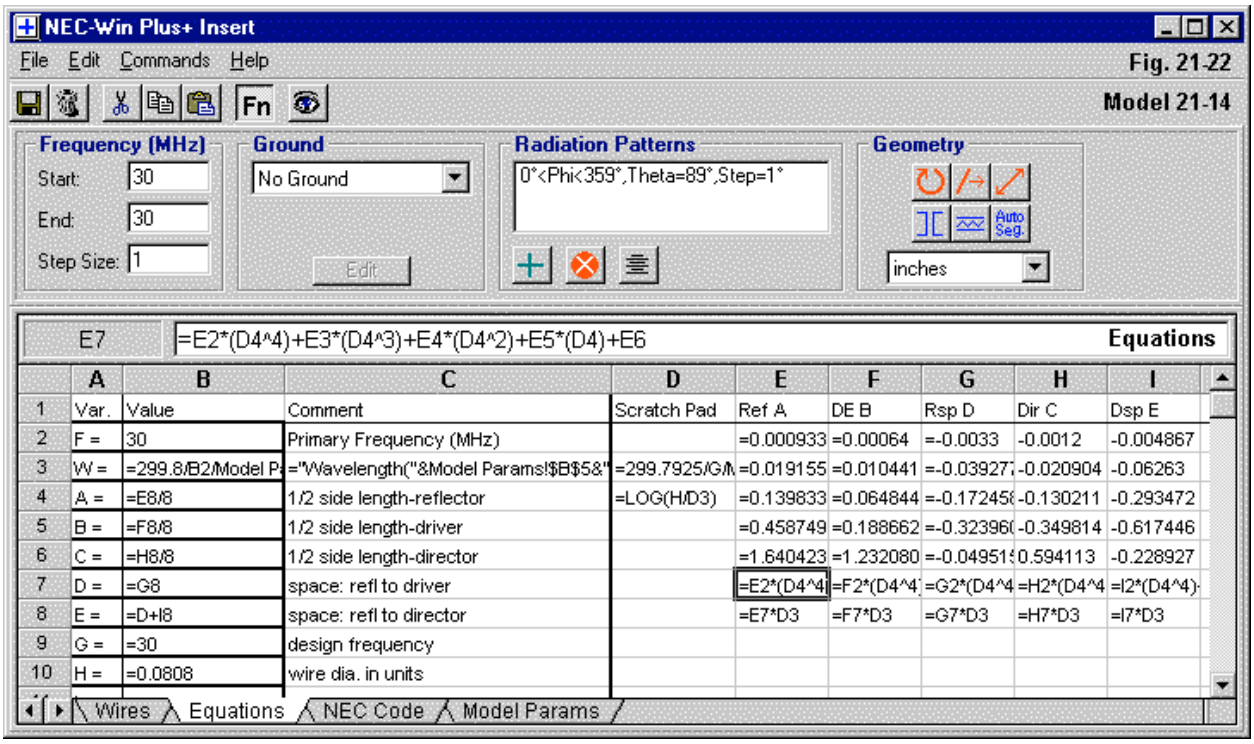

	A	B	C	D	E	F	G	H	I
1	Var.	Value	Comment	Scratch Pad	Ref A	DE B	Rsp D	Dir C	Dsp E
2	F =	30	Primary Frequency (MHz)		=0.000933	=0.00064	=-0.0033	-0.0012	-0.004867
3	W =	=299.8/B2/Model P	="Wavelength("&Model Params!$B$5&"	=299.7925/G/M	=0.019155	=0.010441	=-0.03927	-0.020904	-0.06263
4	A =	=E8/8	1/2 side length-reflector	=LOG(H/D3)	=0.139833	=0.064844	=-0.17245	-0.130211	-0.293472
5	B =	=F8/8	1/2 side length-driver		=0.458749	=0.188662	=-0.32396	-0.349814	-0.617446
6	C =	=H8/8	1/2 side length-director		=1.640423	=1.232080	=-0.04951	0.594113	-0.228927
7	D =	=G8	space: refl to driver		=E2*(D4^4	=F2*(D4^4	=G2*(D4^4	=H2*(D4^4	=I2*(D4^4)
8	E =	=D+I8	space: refl to director		=E7*D3	=F7*D3	=G7*D3	=H7*D3	=I7*D3
9	G =	=30	design frequency						
10	H =	=0.0808	wire dia. in units						

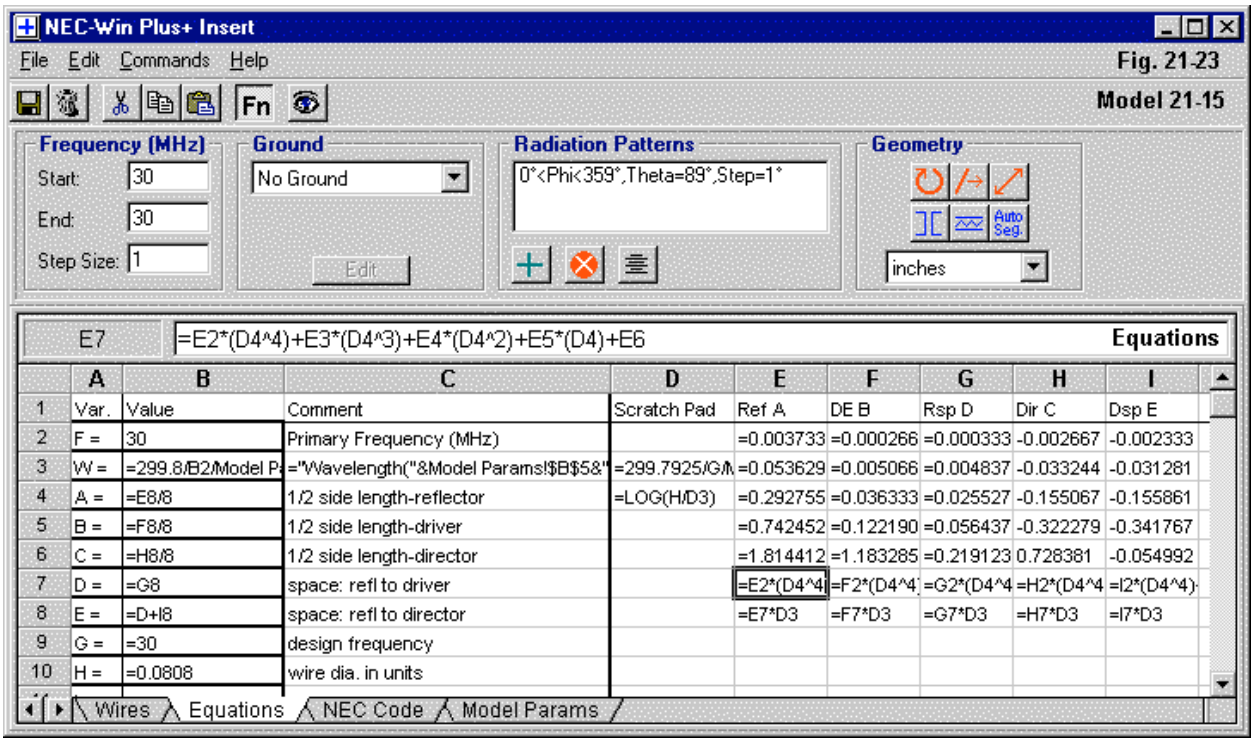

	A	B	C	D	E	F	G	H	I
1	Var.	Value	Comment	Scratch Pad	Ref A	DE B	Rsp D	Dir C	Dsp E
2	F =	30	Primary Frequency (MHz)		=0.003733	=0.000266	=0.000333	-0.002667	-0.002333
3	W =	=299.8/B2/Model P	="Wavelength("&Model Params!$B$5&"	=299.7925/G/M	=0.053629	=0.005066	=0.004837	-0.033244	-0.031281
4	A =	=E8/8	1/2 side length-reflector	=LOG(H/D3)	=0.292755	=0.036333	=0.025527	-0.155067	-0.155861
5	B =	=F8/8	1/2 side length-driver		=0.742452	=0.122190	=0.056437	-0.322279	-0.341767
6	C =	=H8/8	1/2 side length-director		=1.814412	=1.183285	=0.219123	0.728381	-0.054992
7	D =	=G8	space: refl to driver		=E2*(D4^4	=F2*(D4^4	=G2*(D4^4	=H2*(D4^4	=I2*(D4^4)
8	E =	=D+I8	space: refl to director		=E7*D3	=F7*D3	=G7*D3	=H7*D3	=I7*D3
9	G =	=30	design frequency						
10	H =	=0.0808	wire dia. in units						

Model	Freq. MHz	Gain dBi	Front-Back Ratio dB	Impedance R +/- jX Ω
21-14	30	8.86	32.31	75.3 - j0.4
21-15	30	9.44	33.89	54.8 - j1.0

The quad examples illustrate one of the many uses of the scratch pad facility. Not only is it a place to enter reference data, it also serves as an active data pad that the variable equations can routinely reference. The scratch pad data need not be just a series of constants, but may also consist of equations. Indeed, any equation that is not used on the wires page may best be placed on the scratch pad. In addition, we may also use the scratch pad area for identifying notes and labels to ensure that the data we place there today can be interpreted months later. Although these notes have focused exclusively on elements that we may model through the use of equations, we must also remember that none of the requirements and limitations of NEC are set aside in the process. Segmentation, source placement, load placement and type, convergence testing, and AGT testing all remain important concerns to the modeler, no matter how simple or complex the equations of the model.

Summing Up

Modeling by equation within NSI software requires attention to the general requirements of spreadsheets and to the special format used in the Plus insert. We began with the special list of pre-set variables, assigning them values either as constant or as equations. We also learned how to set up the model wires using variables instead of direct numeric entries. In the process, we found out how to simplify the process of frequency scaling by defining the dimensions and coordinates as a function of a wavelength. If modeling by equation becomes a regularly used procedure, then it benefits from the adoption of consistent modeling conventions for both the structure geometry and the formulation of equations.

The next step in the process of mastering the art of modeling by equation involves not just the use of more complex equations, but as well, a growing familiarity with spreadsheet facilities and requirements. For example, some spreadsheets permit direct angular entries in degrees, and some do not. In addition, spreadsheets have special rules that attach to copying and pasting blocks of cells. We used those rules to our advantage in creating a large but repetitive structure.

Finally, we looked at the NSI "scratch pad" area of the spreadsheet to see both its utility and how it differs from the pre-set list of variables in the left-most columns. By a series of models based on regression equations, we learned that the remainder of the Plus insert spreadsheet is not merely a storage area for labels and data, but that it is also an active area for computations that result in the assignment of values to variables.

The notes in this chapter do not exhaust all that may go into a model based upon equations. At best, they serve as an introduction to the process and an alert to the various facets of spreadsheet work that we should master for the most effective use of the facility.

Appendix
Some Useful Data for Antenna Modelers

The following pages contain a potpourri of information useful to antenna modelers. You should perhaps clip or key this appendix, since you are likely to refer often to the data on these pages. Material data is for general guidance and should be replaced by more recent or material-specific information wherever available for critical tasks.

1. Conductivity and Permittivity of Common Ground Conditions
2. Conductivity and Resistivity of Common Materials Used in Antenna Construction
3. Relative Permittivity of Some Common Wire (and Other) Insulating Materials
4. Common Wire Gauges and Associated Diameters in Inches and in Millimeters
5. Some Common Frequency-Wavelength Relationships
6. Frequency Domains
7. Some Common Transmission Lines Values
8. Metric-English Conversion

1. Conductivity and Permittivity of Common Ground Conditions

A Standard Table

The following soil descriptions are commonly used in antenna modeling. Always substitute more precise values wherever known. The table represents an adaptation of values found in *The ARRL Antenna Book* (p. 3-6), which are themselves an adaptation of the table presented by Terman in *Radio Engineer's Handbook* (p. 709), taken from "Standards of Good Engineering Practice Concerning Standard Broadcast Stations," *Federal Register* (July 8, 1939), p. 2862. Terman's value for the conductivity of the worst soil listed is an order of magnitude lower than the value shown here.

Soil Description	**Conductivity in S/m σ**	**Permittivity (Dielectric Constant) ε**	**Relative Quality**
Fresh water	0.001	80	
Salt water	5.0	81	
Pastoral, low hills, rich soil, typical from Dallas, TX, to Lincoln, NE	0.0303	20	Very Good
Pastoral, low hills, rich soil, typical of OH and IL	0.01	14	Good
Flat country, marshy, densely wooded, typical of LA near the Mississippi River	0.0075	12	
Pastoral, medium hills, and forestation, typical of MD, PA, NY (exclusive of mountains and coastline)	0.006	13	
Pastoral, medium hills, and forestation, heavy clay soils, typical of central VA	0.005	13	Average
Rocky soil, steep hills, typically mountainous	0.002	12 - 14	Poor
Sandy, dry, flat, coastal	0.002	10	
Cities, industrial areas	0.001	5	Very Poor
Cities, heavy industrial areas, high buildings	0.001	3	Extremely Poor

The Table Used in NEC-Win Pro and GNEC

The following list of conductivity and permittivity values is drawn from many recent sources and is used as a set of user-selectable entries for ground conditions in GN and GD entries in NSI programs. Users may also enter custom values wherever information on the actual soil conditions is available.

Soil Description	**Conductivity in S/m σ**	**Permittivity (Dielectric Constant) ε**
Poor	0.001	4.5
Moderate	0.003	4
Average	0.005	13
Good	0.01	4
Dry, sandy, coastal	0.001	10
Pastoral hills, rich soil	0.007	17
Pastoral medium hills and forestation	0.004	13
Fertile land	0.002	10
Rich agricultural land, low hills	0.01	15
Rocky, steep hills	0.002	15
Marshy land, densely wooded	0.0075	12
Marshy, forested, flat	0.008	12
Mountainous, hilly (up to about 1000 m)	0.002	5
Highly moist ground	0.005	30
City industrial of average attenuation	0.001	5
City industrial of maximal attenuation	0.0004	3
City industrial area	0.0001	3
Fresh water	0.001	80
Fresh water @ 10° C and 100 MHz	0.001	84
Fresh water @ 20° C and 100 MHz	0.005	80
Sea water	5.0	81
Sea water @ 10° C up to 1 GHz	4.0	80
Sea water @ 20° C up to 1 GHz	4.0	73
Sea ice	0.001	4
Polar ice	0.0003	3
Polar ice cap	0.0001	1
Arctic land	0.0005	3

2. Conductivity and Resistivity of Common Materials Used in Antenna Construction

Normal NEC antenna material entries (Load Type 5) are specified in terms of material conductivity. In the table below, both the resistivity and the conductivity are shown, although each is the simple inverse of the other. In many texts, the unit of measure for conductivity is still specified as "mhos/meter" rather than as "Siemens/meter." Permeability is useful only in NEC-4 LD5 entries. Permeability values, other than 1.0 for non-magnetic materials, may vary widely in actual practice. As well, the conductivity and resistivity of variable alloys, such as brass, galvanizing mixtures, etc., may also vary considerably with small changes. See, for example, the brass and phosphor bronze entries below. All values may also vary with temperature.

Material	**Resistivity Ohms/meter**	**Conductivity Siemens/meter**	**Permeability**
Pure Silver	1.62E-08	6.17E07	1.0
Copper	1.72E-08	5.80E07	1.0
Gold	2.19E-08	4.57E07	1.0
Chromium	2.6E-08	3.85E07	1.0
Pure Aluminum	2.62E-08	3.82E07	1.0
6063-T832 Aluminum alloy	3.25E-08	3.08E07	1.0
6061-T6 Aluminum alloy	4.10E-08	2.50E07	1.0
Zinc	6.0E-08	1.67E07	1.0
Brass ("yellow," 35% Zn)	6.4E-08	1.56E07	1.0
Brass (66% Cu, 34% Zn)	3.9E-08	2.56E07	1.0
Beryllium Copper	8.0E-08	1.25E07	1.0
Iron	9.71E-08	1.03E07	150
Phosphor Bronze (4% Sn, 0.5% P, rest Cu)	9.4E-08	1.06E07	1.0
Phosphor Bronze (5% Tin)	1.1E-07	9.09E06	1.0
Tin	1.14E-07	8.77E06	1.0
Steel (0.4-0.5% C, rest Fe)	1.3E-07 - 2.2E-07	7.69E06 - 4.54E06	200
Lead	2.19E-07	4.57E06	1.0
Stainless Steel (type 302)	7.20E-07	1.39E06	1.00008

3. Relative Permittivity of Some Common Wire (and Other) Insulating Materials

The values listed in the abbreviated table below are for general guidance. The IS (insulated sheath) command requests the relative permittivity and conductivity. However, for most cases, the ionic or electronic conduction of materials used to insulate modern wires is far lower than the level at which conduction becomes a noticeable factor in the performance of the insulated wire (about 10E-7 S/m or higher). Insulating materials are more likely to show effects from a peak in the dissipation factor within a given frequency range of use. Both the conduction and the dissipation of a material will vary with temperature. Values shown in the table are for 100 MHz (where available), although most of the plastic materials listed are stable from 1 kHz through 1 GHz. Values that may change by more than +/-10% across the 1 MHz to 1 GHz range are starred (*).

Material	**Relative Permittivity ε**
Plastics	
Cross-linked polystyrene	2.58
Epoxy resin (Epon resin RN-48)	3.32 *
Phenol-formaldehyde (Bakelite BM 120)	3.95 *
Polycarbonate (PC)	2.96 *
Polyethylene	2.26
Polyethylene terephthalate (PET)	2.98 *
Polyisobutylene	2.23
Polypropylene (PP)	2.55
Polystyrene (PS)	2.55
Polytetrafluoroethylene (PTFE--Teflon)	2.1
Polysulfone (PSU)	3.2
Polyvinyl-chloride (100%)	2.85
Some Non-Plastic Insulating Materials	
Aluminum oxide	8.80
Porclain (dry process)	5.04
Steatite 410	5.77
Titanium dioxide (rutile)	100
Soda-borosilicate glass	4.84
Silica dioxide (100%--fused quartz)	3.78
Butyl rubber	2.35
Gutta-percha	2.47
Silicone-rubber compound	3.16
Douglas fir wood	1.88
Mahogany wood	2.07 *
Ruby mica	5.4
Paper (royalgrey)	2.77 *
Ice (from distilled water)	3.45 *
Freshly fallen snow	1.20
Water (distilled)	78

4. Common Wire Gauges and Associated Diameters in Inches and in Millimeters

Common **AWG** wire size diameters in inches and in millimeters. Although program input pages may permit the entry of wire diameters (or AWG gauge numbers), direct entry on the GW wire card require the radius (1/2 the listed diameter).

AWG Gauge #	Diameter Inches	Diameter Millimeters	AWG Gauge #	Diameter Inches	Diameter Millimeters
1	0.2893	7.348	21	0.0285	0.723
2	0.2576	6.544	22	0.0253	0.644
3	0.2294	5.827	23	0.0226	0.573
4	0.2043	5.189	24	0.0201	0.511
5	0.1819	4.621	25	0.0179	0.455
6	0.1620	4.115	26	0.0159	0.405
7	0.1443	3.665	27	0.0142	0.361
8	0.1285	3.264	28	0.0126	0.321
9	0.1144	2.906	29	0.0113	0.286
10	0.1019	2.588	30	0.0100	0.255
11	0.0907	2.305	31	0.0089	0.227
12	0.0808	2.053	32	0.0080	0.202
13	0.0720	1.828	33	0.0071	0.180
14	0.0641	1.628	34	0.0063	0.160
15	0.0571	1.450	35	0.0056	0.143
16	0.0508	1.291	36	0.0050	0.127
17	0.0453	1.150	37	0.0045	0.113
18	0.0403	1.024	38	0.0040	0.101
19	0.0359	0.912	39	0.0035	0.090
20	0.0320	0.812	40	0.0031	0.080

Common **BSWG** wire size diameters in inches and in millimeters.

BSWG Gauge #	Diameter Inches	Diameter Millimeters	BSWG Gauge #	Diameter Inches	Diameter Millimeters
1	0.3000	7.620	21	0.0320	0.813
2	0.2760	7.010	22	0.0280	0.711
3	0.2520	6.401	23	0.0240	0.610
4	0.2320	5.893	24	0.0220	0.559
5	0.2120	5.385	25	0.0200	0.508
6	0.1920	4.877	26	0.0180	0.457
7	0.1760	4.470	27	0.0164	0.417
8	0.1600	4.064	28	0.0148	0.376
9	0.1440	3.658	29	0.0136	0.345
10	0.1280	3.251	30	0.0124	0.315
11	0.1160	2.946	31	0.0116	0.295
12	0.1040	2.642	32	0.0108	0.274
13	0.0920	2.337	33	0.0100	0.254
14	0.0800	2.032	34	0.0092	0.234
15	0.0720	1.829	35	0.0084	0.213
16	0.0640	1.626	36	0.0076	0.193
17	0.0560	1.422	37	0.0068	0.173
18	0.0480	1.219	38	0.0060	0.152
19	0.0400	1.016	39	0.0052	0.132
20	0.0360	0.914	40	0.0048	0.122

Depending upon the selected units of measure for the input interface, diameters in millimeters may require multiplication by 0.001 for entry in meters and by 0.1 for entry in centimeters. Diameters in inches may require multiplication by 0.0833 (1/12) for entry in feet.

5. Some Common Frequency-Wavelength Relationships

Because the speed of electromagnetic radiation in free space is not exactly 300E6 m/s, more exact measures of wavelength are sometimes required. The following tables present the length of a free-space wave (λ) in both feet and meters for frequencies from 1 to 10 MHz and for the amateur bands between 160 meters and 23 centimeters. Band center-points are the geometric mean frequency within the band. You may interpolate other values from the ones given. For greater precision, you may divide 299.7925 by the frequency in MHz to obtain the wavelength in meters or divide 983.5712 by the frequency in MHz to obtain the wavelength in feet.

Frequency MHz	**λ feet**	**λ meters**	**Frequency MHz**	**λ feet**	**λ meters**
1.000	983.5712	299.7925	8.000	122.9464	37.4741
160 m			9.000	109.2857	33.3103
1.800	546.4285	166.5514	10.000	98.3571	29.9793
1.897	518.4877	158.0351	**30 m**		
2.000	491.7856	149.8963	10.100	97.3833	29.6824
3.000	327.8571	99.9308	10.125	97.1428	29.6091
80 m			10.150	96.9036	29.5362
3.500	281.0204	85.6550	**20 m**		
3.742	262.8464	80.1156	14.000	70.2551	21.4138
4.000	245.8928	74.9481	14.174	69.3926	21.1509
5.000	196.7142	59.959	14.350	68.5416	20.8915
6.000	163.9285	49.9654	**17 m**		
40 m			18.068	54.4372	16.5925
7.000	140.5102	42.8275	18.118	54.2870	16.5467
7.148	137.6009	41.9408	18.168	54.1376	16.5011
7.300	134.7358	41.0675			

Frequency MHz	λ feet	λ meters	Frequency MHz	λ feet	λ meters
15 m			**1.25 m**		
21.000	46.8367	14.2758	222.000	4.4305	1.3504
21.224	46.3424	14.1252	223.495	4.4009	1.3414
21.450	45.8541	13.9763	225.000	4.3714	1.3324
12 m			**70 cm**		
24.890	39.5167	12.045	420.000	2.3418	0.7138
24.940	39.4375	12.0206	434.740	2.2624	0.6896
24.990	39.3586	11.9965	450.000	2.1857	0.6662
10 m			**33 cm**		
28.000	35.1275	10.7069	902.000	1.0904	0.3324
28.837	34.1080	10.3961	914.910	1.0750	0.3277
29.700	33.1169	10.0940	928.000	1.0599	0.3231
6 m			**23 cm**		
50.000	19.6714	5.9959	1240.00	0.7932	0.2418
51.962	18.9289	5.7695	1269.60	0.7747	0.2361
54.000	18.2143	5.5517	1300.00	0.7566	0.2306
2 m					
144.000	6.8304	2.0819			
145.990	6.7373	2.0535			
148.000	6.6458	2.0256			

6. Frequency Domains

Abbrev.	Classification	Frequency Range
VLF	Very low frequencies	10 to 30 kHz
LF	Low frequencies	30 to 300 kHz
MF	Medium frequencies	300 to 3000 kHz
HF	High frequencies	3 to 30 MHz
VHF	Very high frequencies	30 to 300 MHz
UHF	Ultra-high frequencies	300 to 3000 MHz
SHF	Super-high frequencies	3 to 30 GHz
EHF	Extremely high frequencies	30 to 300 GHz

7. Some Common Transmission Lines Values

Modeling transmission lines (TL) requires a knowledge of both the characteristic impedance (Zo) of the line and the Velocity Factor (VF). The TL facility in NEC requests the electrical length of the line in meters, which will always be greater than the physical length of the line for any coaxial cable or parallel line with a VF less than 1.0. NEC does not make use of other parameters of transmission lines, such as conductor size and spacing, capacitance per foot, remnant inductive reactance within the characteristic impedance, or line loss values. The values shown are representative. For more precise values, consult manufacturer specification sheets. Since the actual VF for a given line type varies from batch to batch, bench measurements may be even superior.

The listings on the left are for common "RG-" coaxial cables. The listing is necessarily incomplete. In addition, other types with improved loss, flexibility, or jacket properties are available under specific manufacturer numbers. The listing to the right contains representative figures for "hard lines" and common parallel transmission lines.

RG-#	Zo (Ω)	VF	Type	Zo (Ω)	VF
RG-6	75.0	0.75	Alum. jacket; foam diel.		
RG-8	52.0	0.66	1/2; 3/4; or 7/8"	50.0	0.81
RG-8 foam	50.0	0.78	1/2; 3/4; or 7/8"	75.0	0.81
RG-8A	52.0	0.66			
RG-8X	50.0	0.78	Twin leads		
RG-11	75.0	0.66	75-Ω transmitting	75.0	0.67
RG-11 foam	75.0	0.78	300-Ω flat	300.0	0.82
RG-11A	75.0	0.66	300-Ω tubular	300.0	0.80
RG-58	53.5	0.66			
RG-58A	50.0	0.66	"Window"		
RG-58A foam	50.0	0.78	1/2"	300.0	0.95
RG-58C	50.0	0.66	1"	450.0	0.95
RG-59	75.0	0.66			
RG-59 foam	75.0	0.79			
RG-213	50.0	0.66			

8. Metric-English-Metric Conversion

As a convenience, the following table provides handy conversion factors for changing the units of measure for antenna model dimensions.

From	To	Conversion
Millimeters	Inches	0.03937 x mm
Centimeters	Inches	0.3937 x cm
Meters	Inches	39.3701 x m
Millimeters	Feet	0.00328 x mm
Centimeters	Feet	0.03281 x cm
Meters	Feet	3.28084 x m
Millimeters	Yards	0.001094 x mm
Centimeters	Yards	0.01094 x cm
Meters	Yard	1.0936 x m
Inches	Millimeters	25.4 x in.
Inches	Centimeters	2.54 x in.
Inches	Meters	0.0254 x in.
Feet	Millimeters	304.8 x ft.
Feet	Centimeters	30.48 x ft.
Feet	Meters	0.3048 x ft.
Yards	Millimeters	914.4 x Yd.
Yards	Centimeters	91.44 x Yd.
Yards	Meters	0.9144 x Yd.

Index

The following brief index uses the following two conventions. 1. Only the beginning page for a topic is listed. 2. Command explanations are separately listed (see “Commands” entry).

X

User Notes